

12-18-1959

Spectroscopic Studies of Metal-Cyanide Complexes

Roy L. McCullough

Follow this and additional works at: https://digitalrepository.unm.edu/chem_etds

 Part of the [Physical Chemistry Commons](#)

Recommended Citation

McCullough, Roy L.. "Spectroscopic Studies of Metal-Cyanide Complexes." (1959). https://digitalrepository.unm.edu/chem_etds/131

This Dissertation is brought to you for free and open access by the Electronic Theses and Dissertations at UNM Digital Repository. It has been accepted for inclusion in Chemistry ETDs by an authorized administrator of UNM Digital Repository. For more information, please contact disc@unm.edu.

UNIVERSITY OF NEW MEXICO-GENERAL LIBRARY



A14419 548084

SPECTROSCOPIC
STUDIES OF
METAL-CYANIDE
COMPLEXES

BY

McCULLOUGH

378.789

Un310m

1960

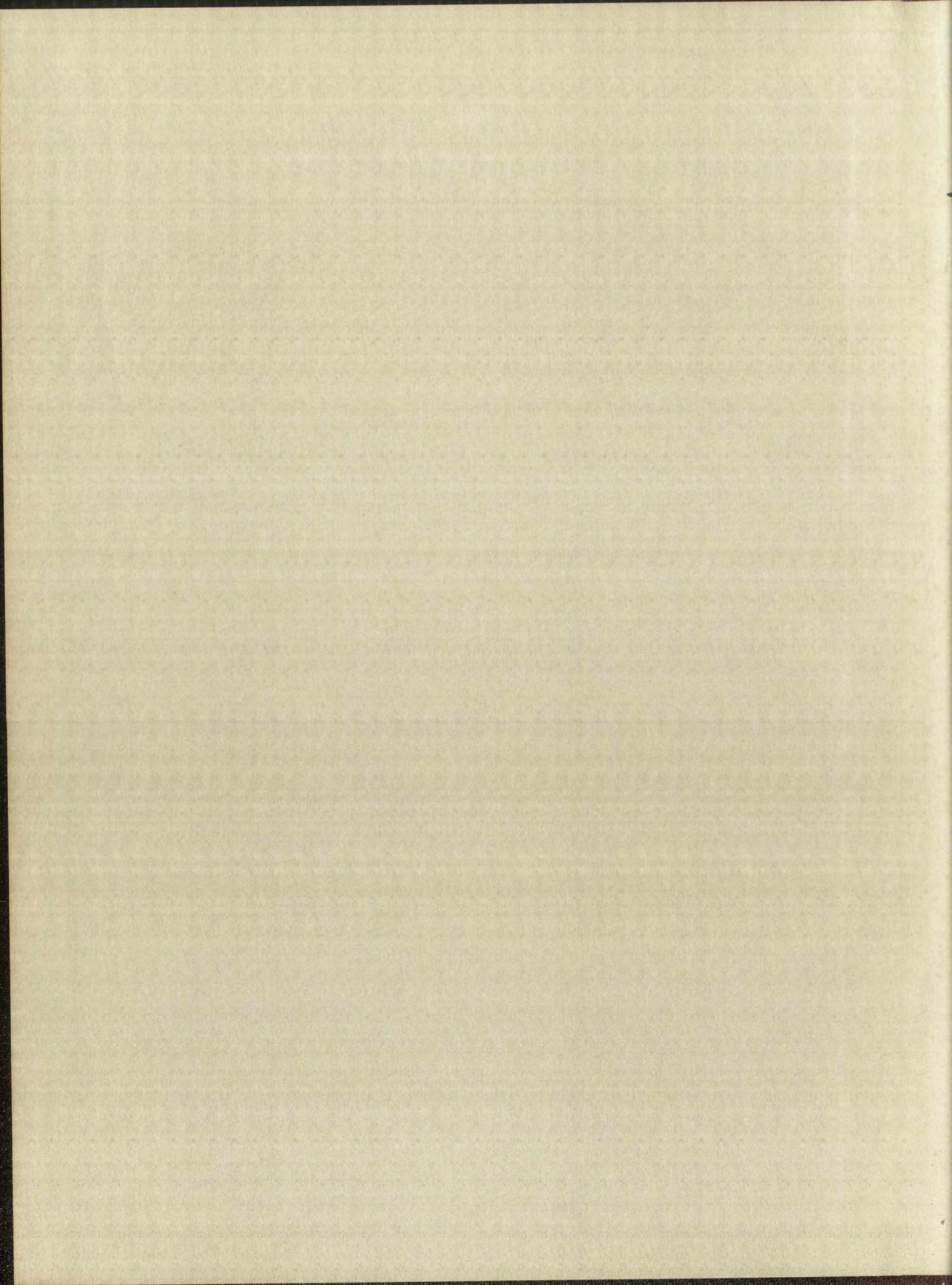
cop. 2

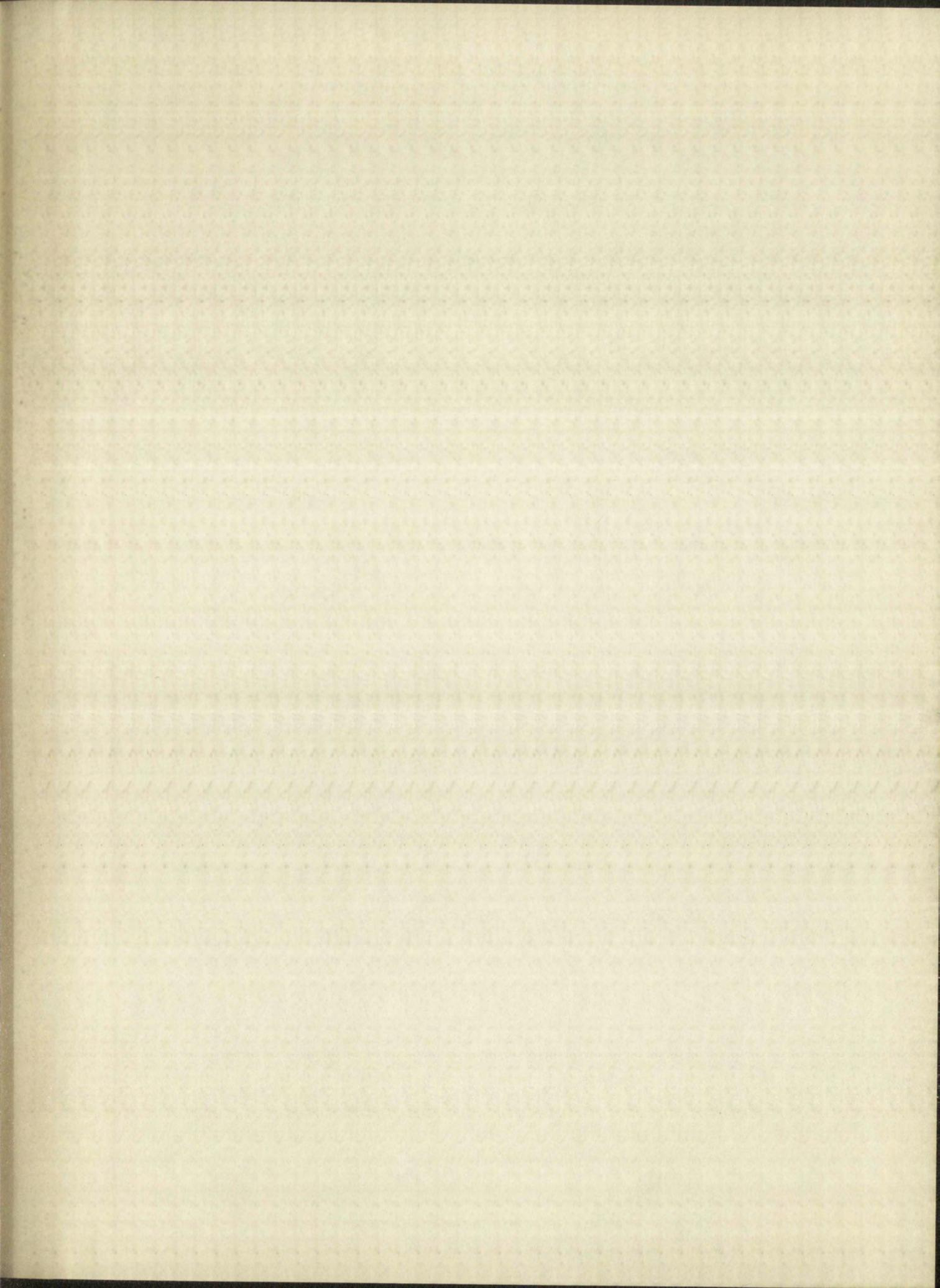
THE LIBRARY
UNIVERSITY OF NEW MEXICO

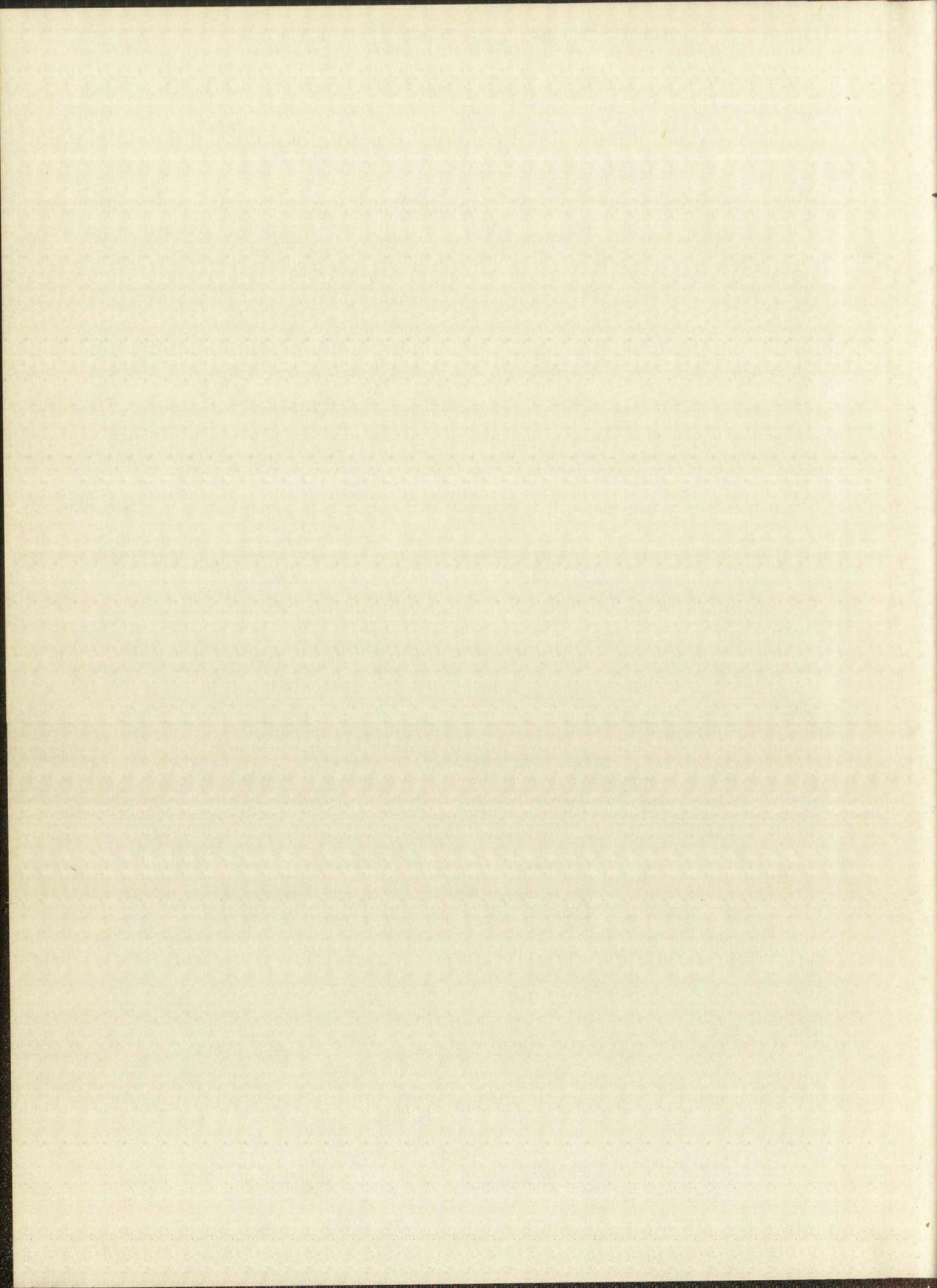


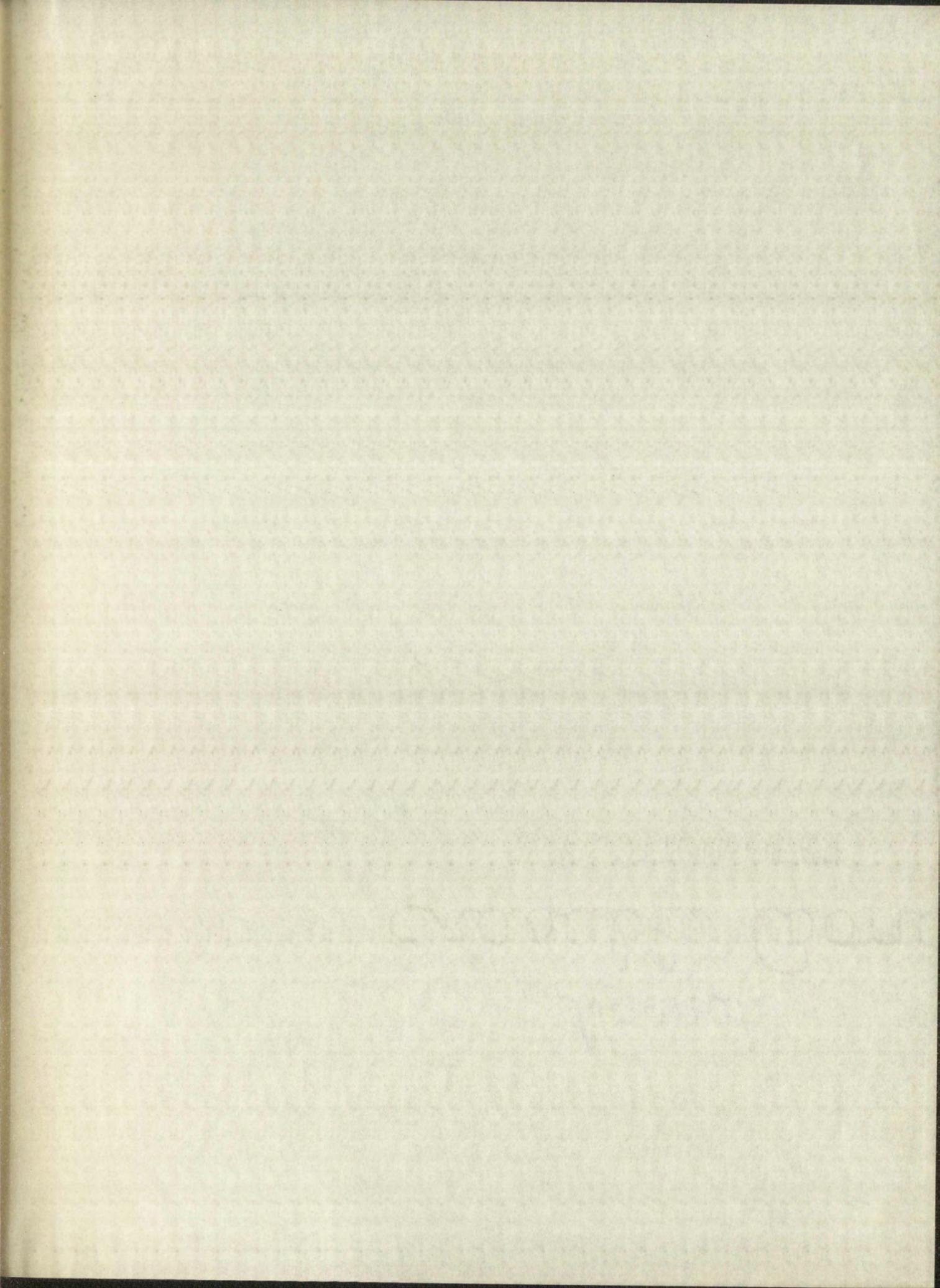
Call No.
378.789
Un310m
1960
cop.2

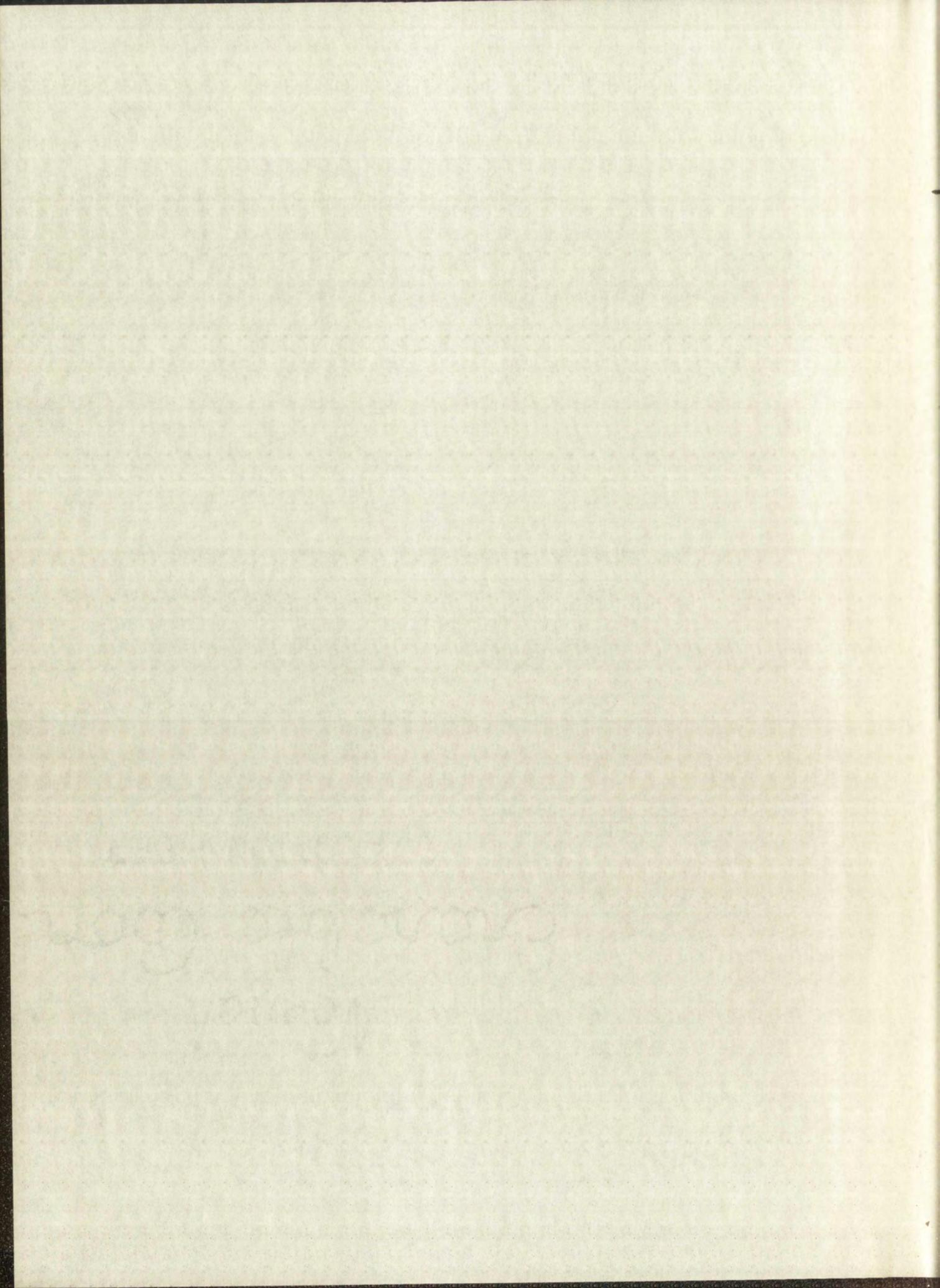
Accession
Number
253459











UNIVERSITY OF NEW MEXICO LIBRARY

MANUSCRIPT THESES

Unpublished theses submitted for the Master's and Doctor's degrees and deposited in the University of New Mexico Library are open for inspection, but are to be used only with due regard to the rights of the authors. Bibliographical references may be noted, but passages may be copied only with the permission of the authors, and proper credit must be given in subsequent written or published work. Extensive copying or publication of the thesis in whole or in part requires also the consent of the Dean of the Graduate School of the University of New Mexico.

This thesis by Roy L. McCullough
has been used by the following persons, whose signatures attest their acceptance of the above restrictions.

A Library which borrows this thesis for use by its patrons is expected to secure the signature of each user.

NAME AND ADDRESS

DATE

MANUSCRIPT STATEMENT

I hereby certify that the above described manuscript is the property of the University of New Mexico Library and is deposited in the Library of the University of New Mexico. I further certify that the manuscript is not to be loaned, sold, or otherwise disposed of without the written consent of the University of New Mexico Library. I further certify that the manuscript is not to be reproduced, copied, or otherwise used in any way without the written consent of the University of New Mexico Library.

The date is

has been made by the following persons: _____

acceptance of the above statement

A library which holds a manuscript for which a statement is expected to receive the amount of said fee

NAME AND ADDRESS

DATE

SPECTROSCOPIC STUDIES OF METAL-CYANIDE COMPLEXES

PART I

INFRARED AND VISIBLE ABSORPTION STUDIES OF CYANIDE
COMPLEXES OF Ni(II) IN AQUEOUS SOLUTION

PART II

AN ANALYSIS OF THE INFRARED VIBRATIONAL SPECTRA OF THE
TETRACYANONICKELATE(II) ION IN THE SOLID STATE

By

Roy L. McCullough

A Dissertation Submitted to the Graduate
Faculty in Partial Fulfillment of the
Requirements for the Degree of Doctor of
Philosophy in Chemistry

The University of New Mexico

1959



This dissertation, directed and approved by the candidate's committee, has been accepted by the Graduate Committee of the University of New Mexico in partial fulfillment of the requirements for the degree of

DOCTOR OF PHILOSOPHY

E. H. Astetter
DEAN

December 18, 1959

DATE

Committee

Glenn A. Crosby
CHAIRMAN

J. H. Richardson

Milton Kahn

J. V. Lewis

R. A. Penman

Llewellyn H. Jones

This dissertation directed and approved by the candidate's
committee has been accepted for the degree of Doctor of Philosophy
of the University of New Mexico in partial fulfillment of the
requirements for the degree of

DOCTOR OF PHILOSOPHY

[Faint, illegible signature]

IN THE DEPARTMENT OF

[Faint, illegible text]

AND THE FACULTY OF THE

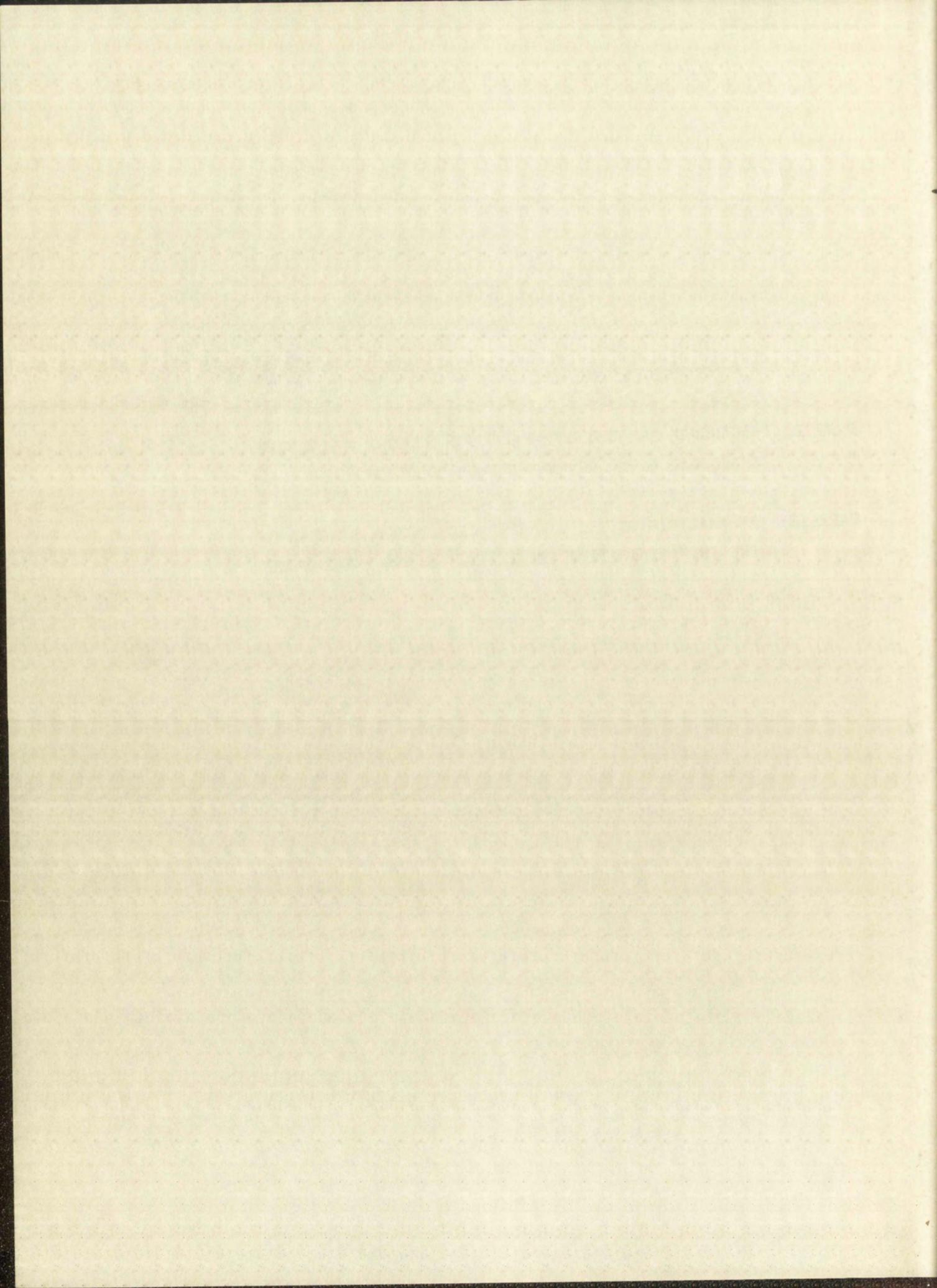
Committee

[Faint, illegible signature]

378.789
Un310m
1960
Cop. 2

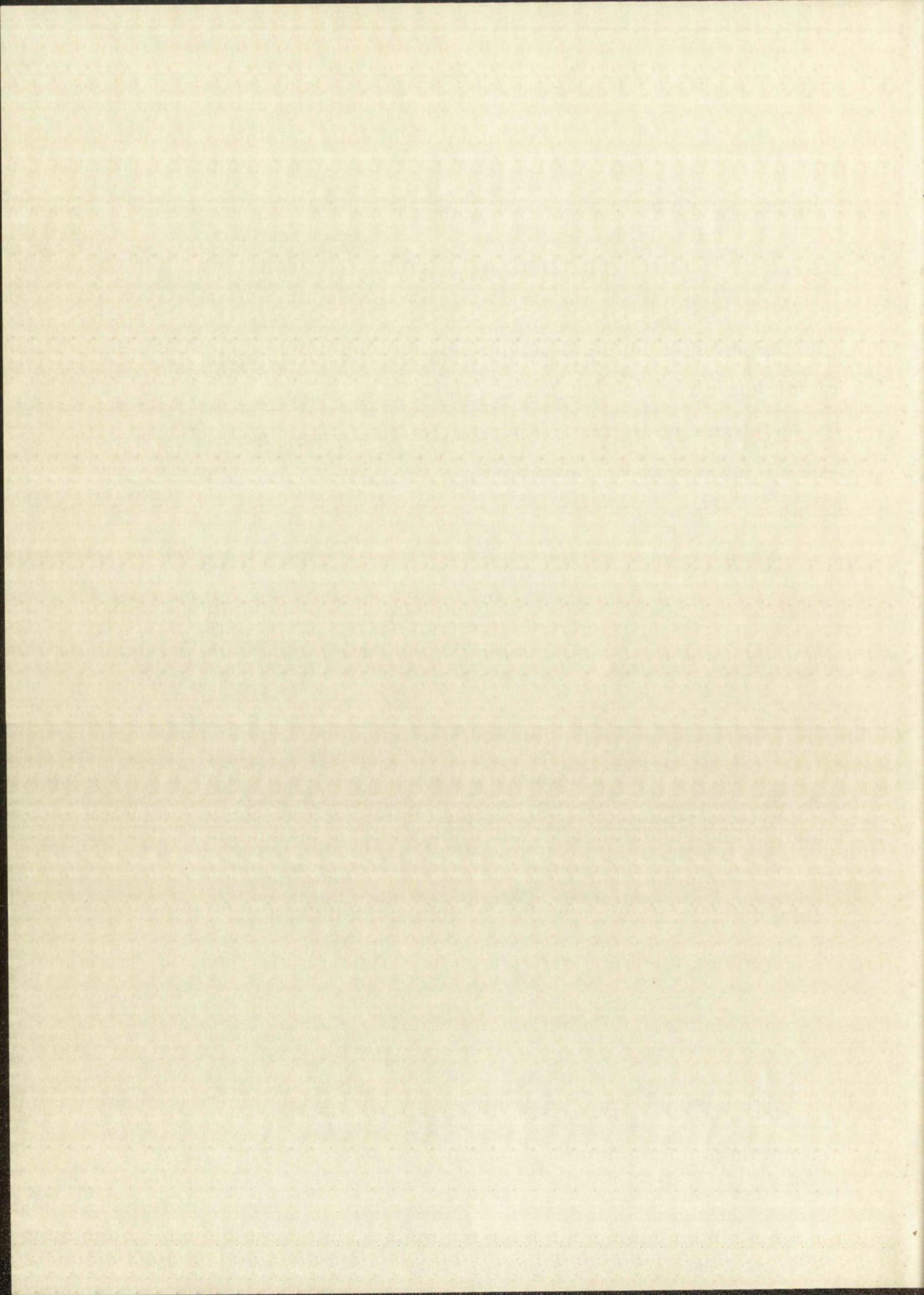
SPECTROSCOPIC STUDIES OF METAL-CYANIDE COMPLEXES

PART I: INFRARED AND VISIBLE ABSORPTION STUDIES OF CYANIDE COMPLEXES OF Ni(II) IN AQUEOUS SOLUTION	Page 1
PART II: AN ANALYSIS OF THE INFRARED VIBRATIONAL SPECTRA OF THE TETRACYANONICKELATE(II) ION IN THE SOLID STATE	66



ACKNOWLEDGMENT

The author wishes to express his thanks to Dr. G. A. Crosby of the University of New Mexico, and to Dr. L. H. Jones and Dr. A. Penneman of the Los Alamos Scientific Laboratory, for the help and guidance given him throughout the progress of this work.



SPECTROSCOPIC STUDIES OF METAL-CYANIDE COMPLEXES

PART I

INFRARED AND VISIBLE ABSORPTION STUDIES OF CYANIDE
COMPLEXES OF Ni(II) IN AQUEOUS SOLUTION

By

Roy L. McCullough

A Dissertation Submitted to the Graduate
Faculty In Partial Fulfillment of the
Requirements for the Degree of Doctor of
Philosophy in Chemistry

The University of New Mexico

1959

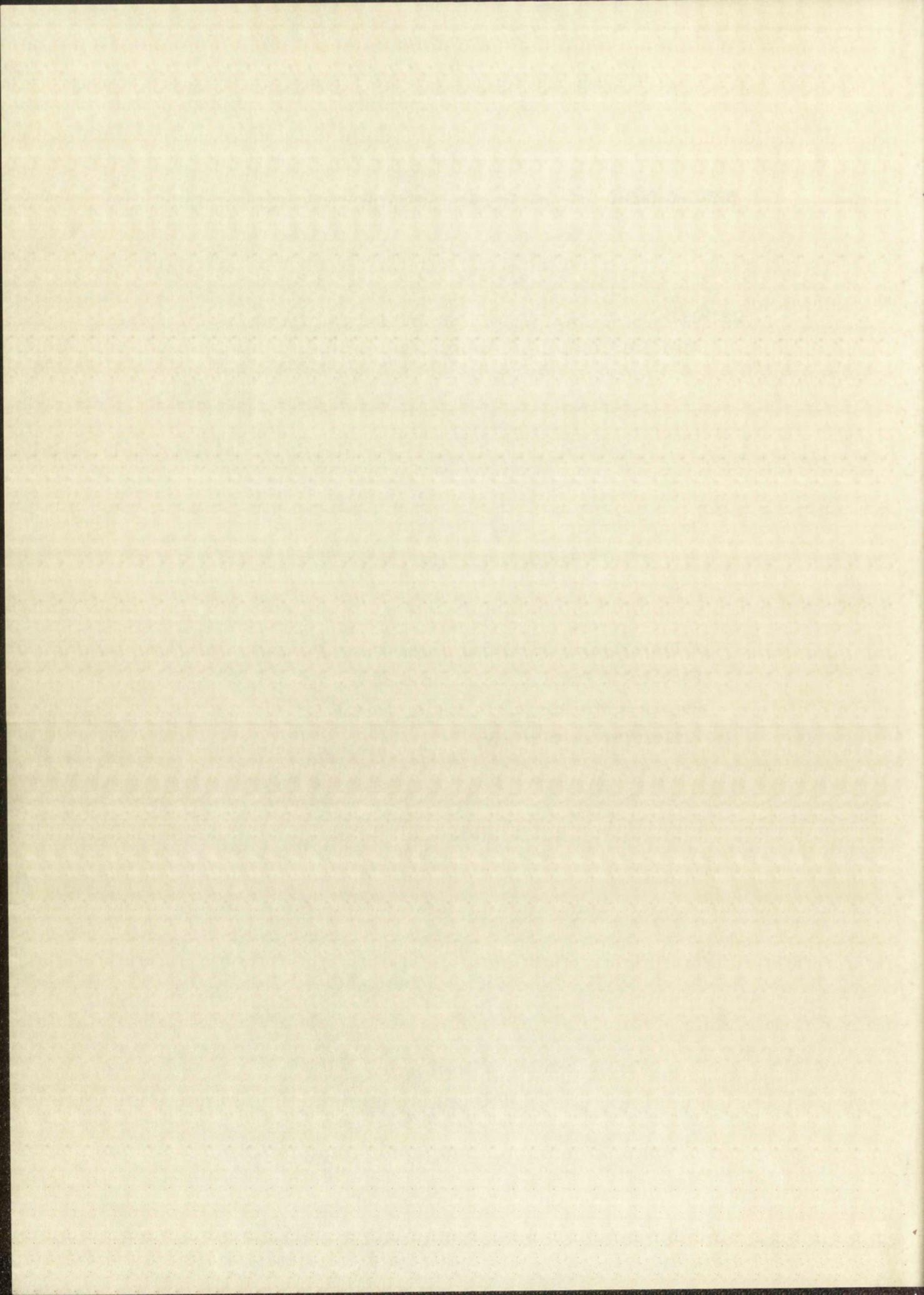
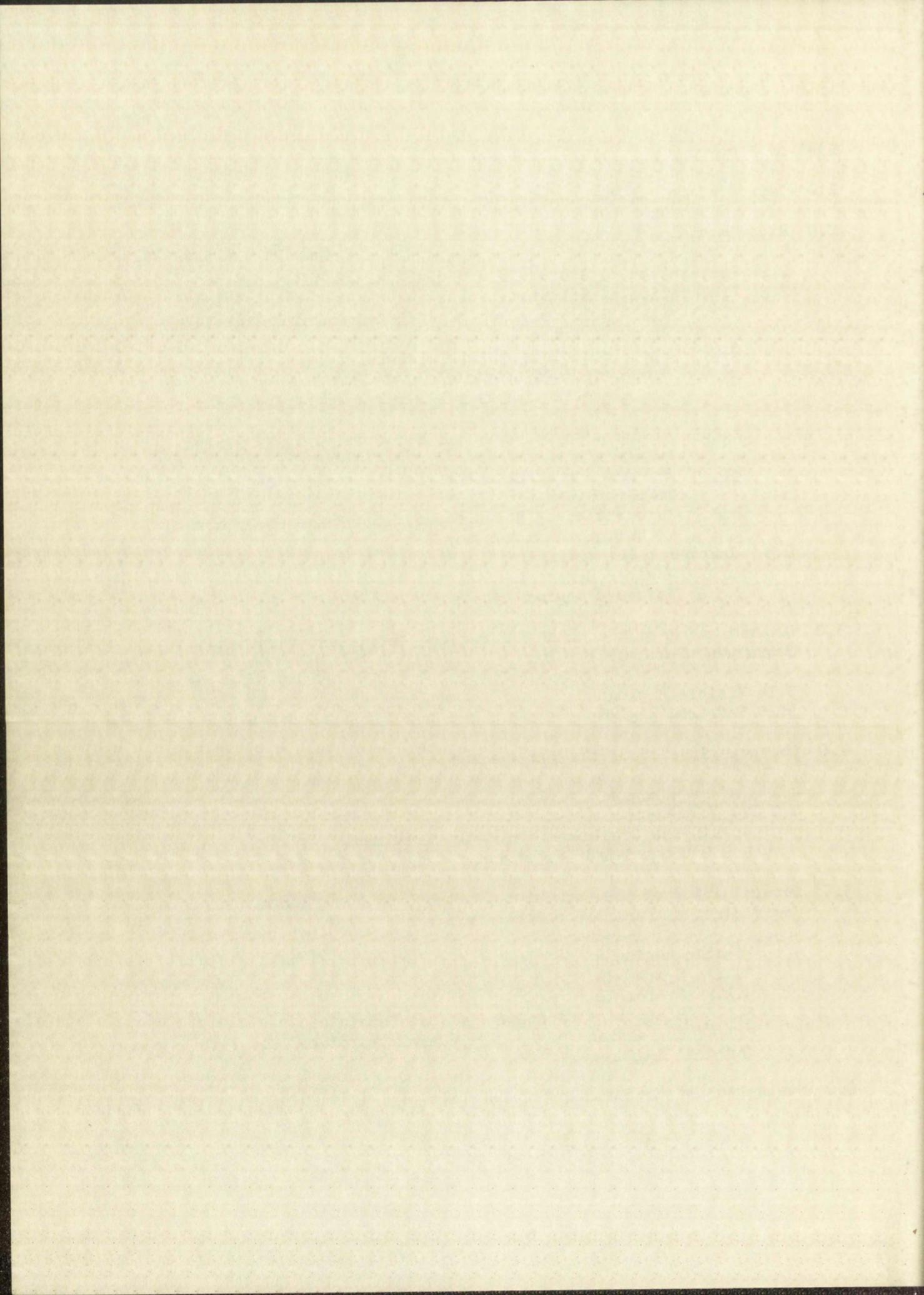
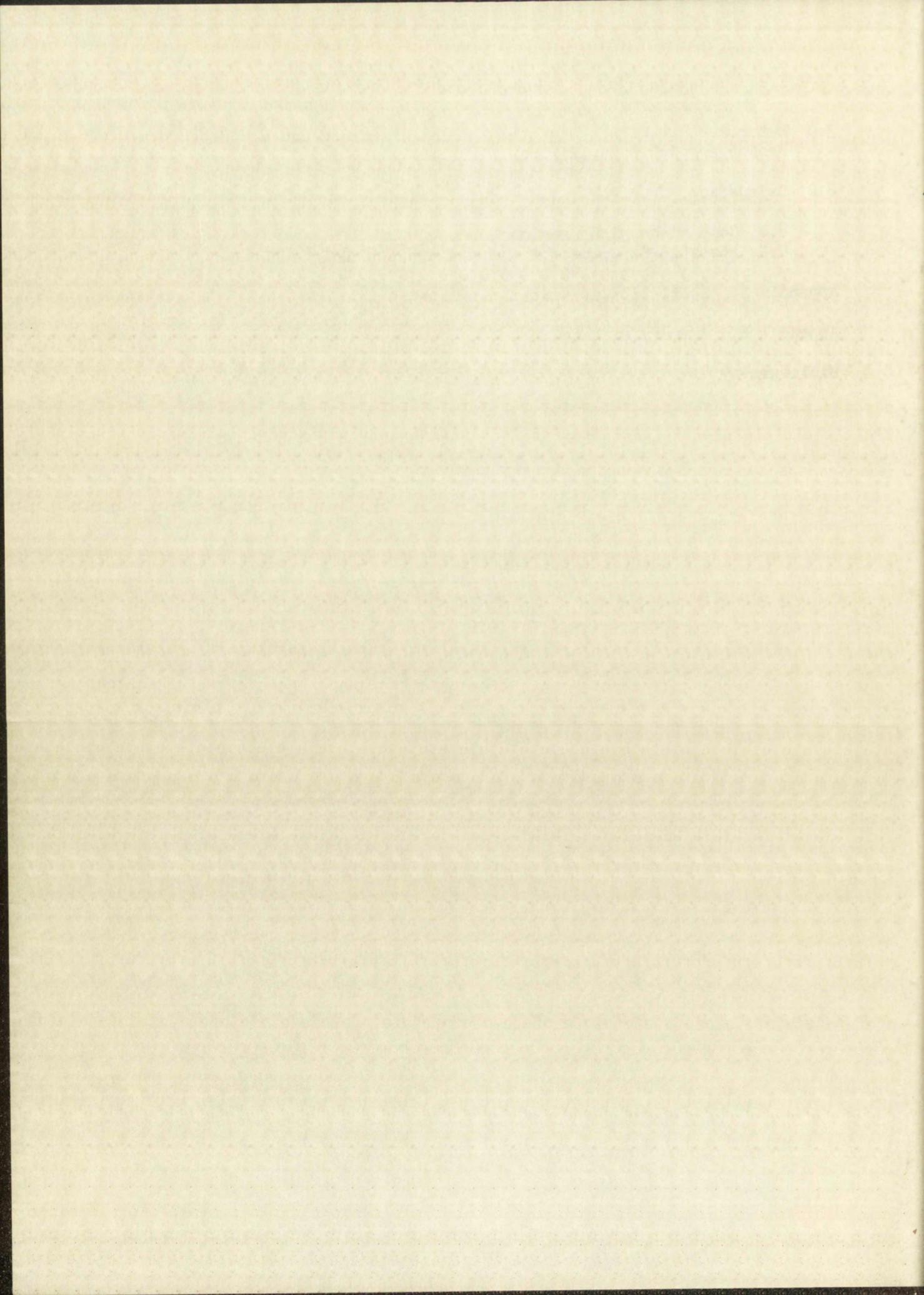


TABLE OF CONTENTS

	Page
List of Figures	iii
1.0 Introduction	1
2.0 Experimental	2
2.1 Preparation of Sodium Tetracyanonickelate(II)	2
2.2 Preparation of Solutions	3
2.2.1 Stock Solutions of Sodium Tetracyanonickelate(II)	3
2.2.2 Stock Solutions of Sodium Cyanide	3
2.2.3 Stock Solutions of Sodium Perchlorate	3
2.2.4 Preparation of Solutions of Sodium Tetracyano- nickelate(II) for the Determination of the Molar Extinction Coefficient	4
2.2.5 Preparation of Solutions for Continuous Variation Method	4
2.2.6 Preparation of Solutions for the System $\text{Na}_2\text{Ni}(\text{CN})_4\text{-NaCN-NaClO}_4\text{-H}_2\text{O}$	4
2.2.7 Preparation of Solutions of High Ratio of Cyanide to Tetracyanonickelate(II)	5
2.3 Absorbance Measurements	5
2.3.1 Visible Region	5
2.3.2 Infrared Region	6
3.0 Determination of the Molar Extinction Coefficient for the Tetracyanonickelate(II) Ion	9
3.1 Visible Region	9
3.2 Infrared Region	12
4.0 Characterization of the New Species	12
4.1 Infrared Region	12
4.2 Visible Region	17
4.2.1 The Continuous Variation Treatment	17
4.2.2 Logarithmic Treatment	22
5.0 Determination of the Formation Constant and Molar Extinction Coefficient of Pentacyanonickelate(II)	29
5.1 Visible Region	29
5.1.1 System I	30
5.1.2 System II	31
5.1.3 Statistical Treatment of the Data	32
5.1.4 Correlation of Species Characterization Data with \bar{K}	40
5.2 Infrared Region	40
6.0 Evaluation of the Enthalpy of Reaction	46

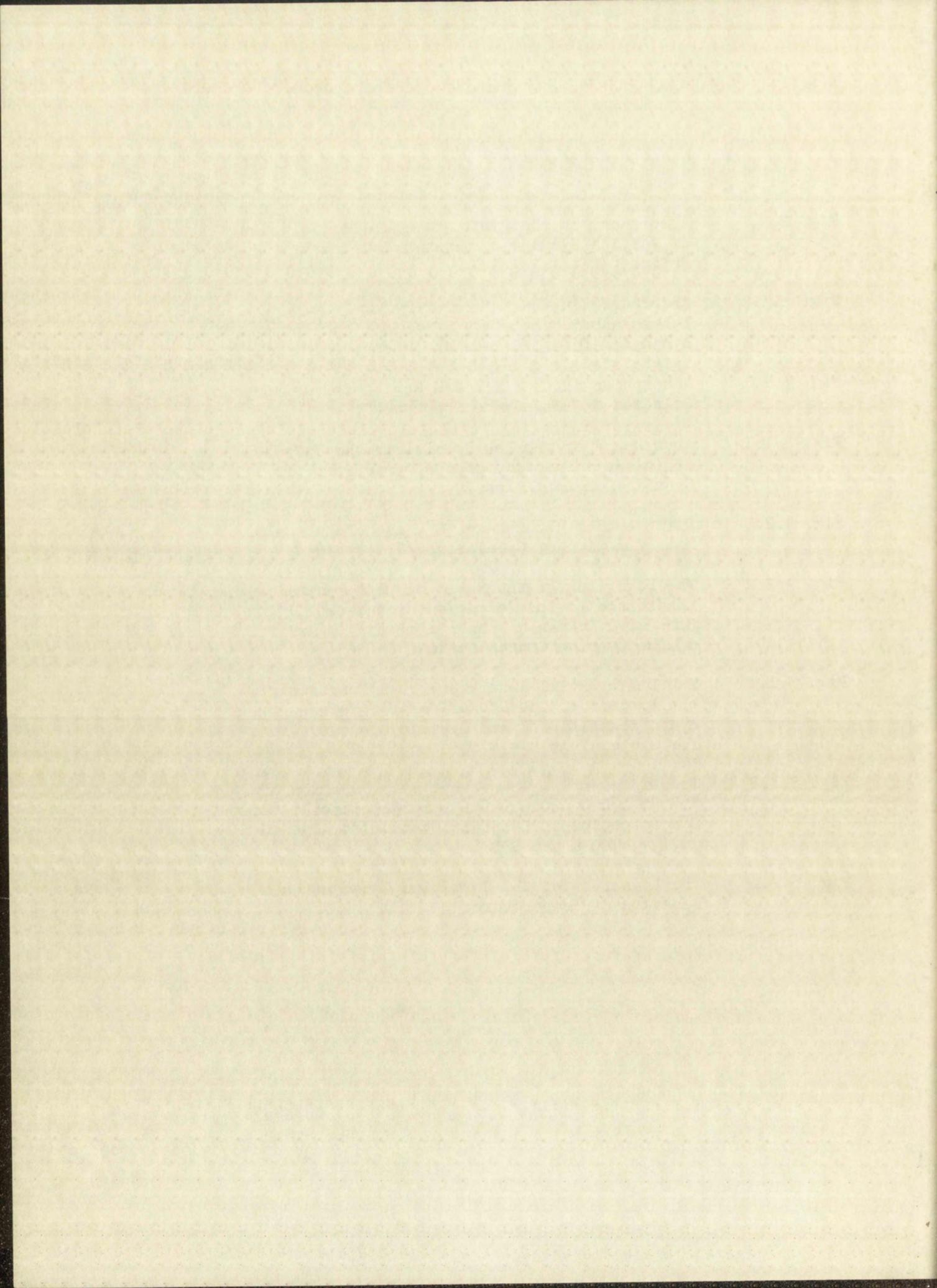


	Page
7.0 Determination of the Magnetic Susceptibility of the Pentacyanonickelate(II) Ion	48
8.0 Discussion	48
8.1 Comparison with Previous Work	48
8.2 Possible Structure of the Pentacyanonickelate(II) Ion	51
Appendix A. Statistics of a Straight Line	52
Appendix B. Summary of Data	56
Bibliography	65



LIST OF FIGURES

		Page
Fig. 2.3.1	Absorbance in the Visible Region for Solutions of Varying Cyanide to Tetracyanonickelate(II) Ratios.	7
Fig. 2.3.2	Absorbance in the Infrared Region Showing Tetracyanonickelate(II), Cyanide, and Pentacyanonickelate(II) Ions in Aqueous Solution.	10
Fig. 3.2.1	Absorption in the Infrared Region for an Aqueous Solution of Tetracyanonickelate(II).	14
Fig. 4.1.1	Absorbance of the New Species in the Infrared Region as a Function of the Stoichiometric Cyanide Concentration.	19
Fig. 4.2.1	Differential Absorbance, D^λ , as a Function of Mole Fraction of Cyanide, b_0/N .	23
Fig. 4.2.2	The Logarithm of the Ratio of Differential Absorbance to the Tetracyanonickelate(II) Ion Concentration as a Function of the Logarithm of the Cyanide Concentration.	27
Fig. 5.1.1	The Differential Absorbance as a Function of the Product of the Stoichiometric Tetracyanonickelate(II) and Cyanide Concentrations for System I at $\lambda = 4700 \text{ \AA}$ and 25.2° .	33
Fig. 5.1.2	The Differential Absorbance as a Function of the Stoichiometric Tetracyanonickelate(II) Ion Concentration at Constant Cyanide for System II at $\lambda = 4700 \text{ \AA}$ and 25.2° .	35
Fig. 6.2.1	The Logarithm of the Formation Constant as a Function of Temperature	49

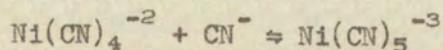


1.0 INTRODUCTION

The existence of the tetracyanonickelate(II) ion, $[\text{Ni}(\text{CN})_4]^{-2}$ has been known for several years and the properties of the hydrated potassium salt are given by Gmelin.⁽¹⁾ Hume and Kolthoff⁽²⁾ as well as Vrestal and Havir⁽³⁾ report that tetracyanonickelate(II) is stable in aqueous solution with a dissociation constant on the order of 10^{-22} . In agreement with these reports, pure solutions of the tetracyanonickelate(II) ion were observed to obey Beer's Law over a wide concentration range. The species $\text{Ni}(\text{CN})_2$ (or $\text{Ni}[\text{Ni}(\text{CN})_4]$)⁽²⁾ precipitates from aqueous solutions if an attempt is made to remove the cyanide ligands from the complex.

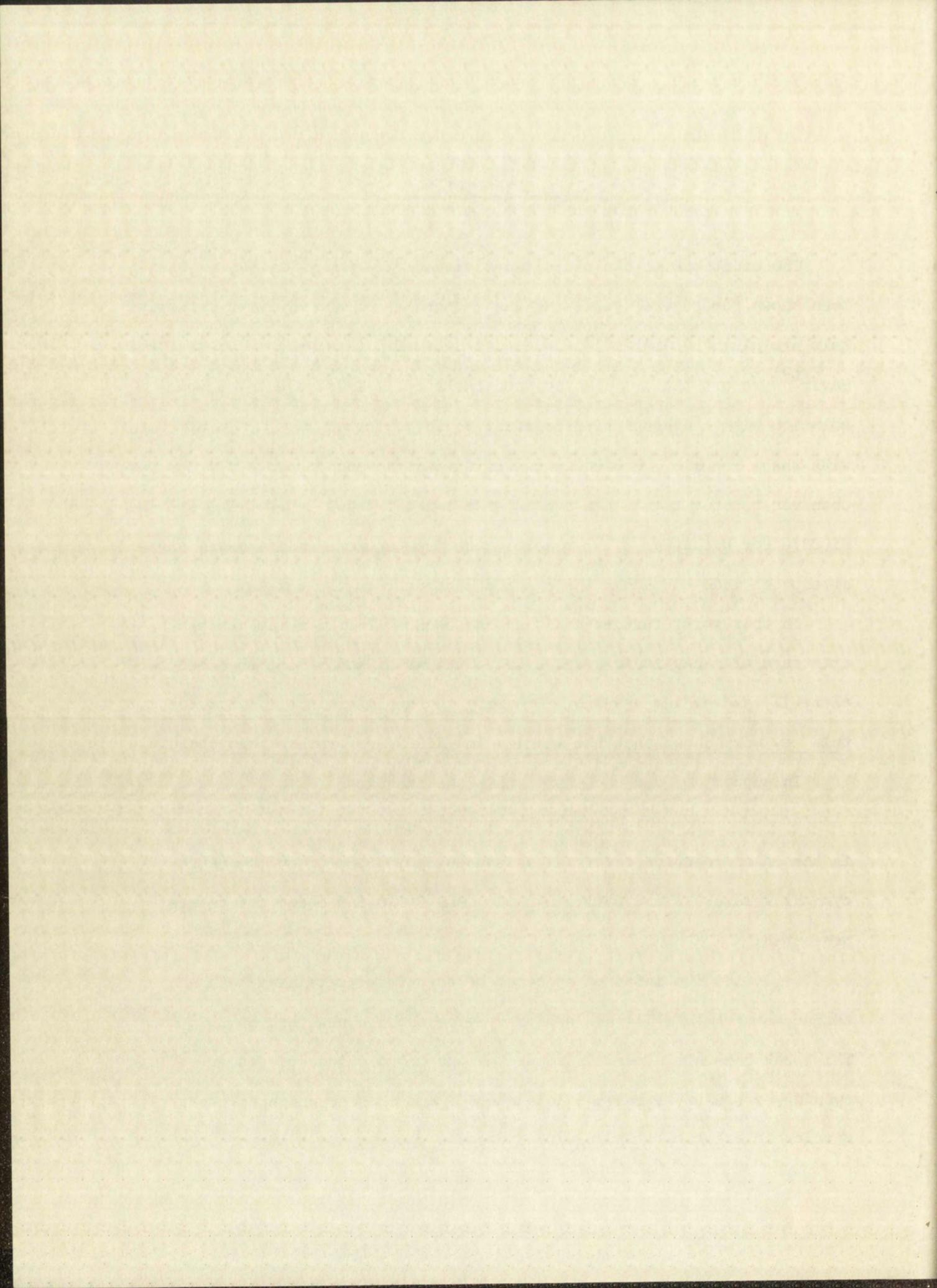
In this work, further evidence has been collected establishing the existence of a new ionic species in solutions of sodium tetracyanonickelate(II) and sodium cyanide. Contrary to the literature,⁽⁴⁾ however, this new work shows that the species is $[\text{Ni}(\text{CN})_5]^{-3}$ rather than $[\text{Ni}(\text{CN})_6]^{-4}$.

In support of our contention that the reaction



is the chief reaction occurring in aqueous solutions of sodium tetracyanonickelate(II) and sodium cyanide, the following observations are presented:

(1) The infrared spectrum of solutions containing both sodium tetracyanonickelate(II) and sodium cyanide shows a new peak at 2108 cm^{-1} . This peak does not appear in separate aqueous solutions of either sodium cyanide or sodium tetracyanonickelate(II) and thus establishes a new species in solution. The new peak becomes progressively larger upon



successive additions of sodium cyanide to an aqueous solution of sodium tetracyanonickelate(II). Concomittantly, the infrared peak characteristic of sodium tetracyanonickelate(II) is observed to diminish with the increase of this new peak, which is a linear function of the cyanide concentrations (see Fig. 4.1.1).

(2) Continuous variation experiments in the visible spectrum (4300 - 4700 Å) indicate the formation of a new species of the composition $[\text{Ni}(\text{CN})_5]^{-3}$.

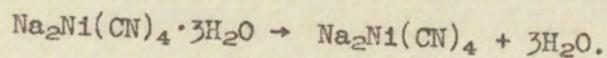
(3) The increase in absorbance in the visible region, when plotted as a logarithmic function of the stoichiometric cyanide concentration indicates the formation of the species $[\text{Ni}(\text{CN})_5]^{-3}$.

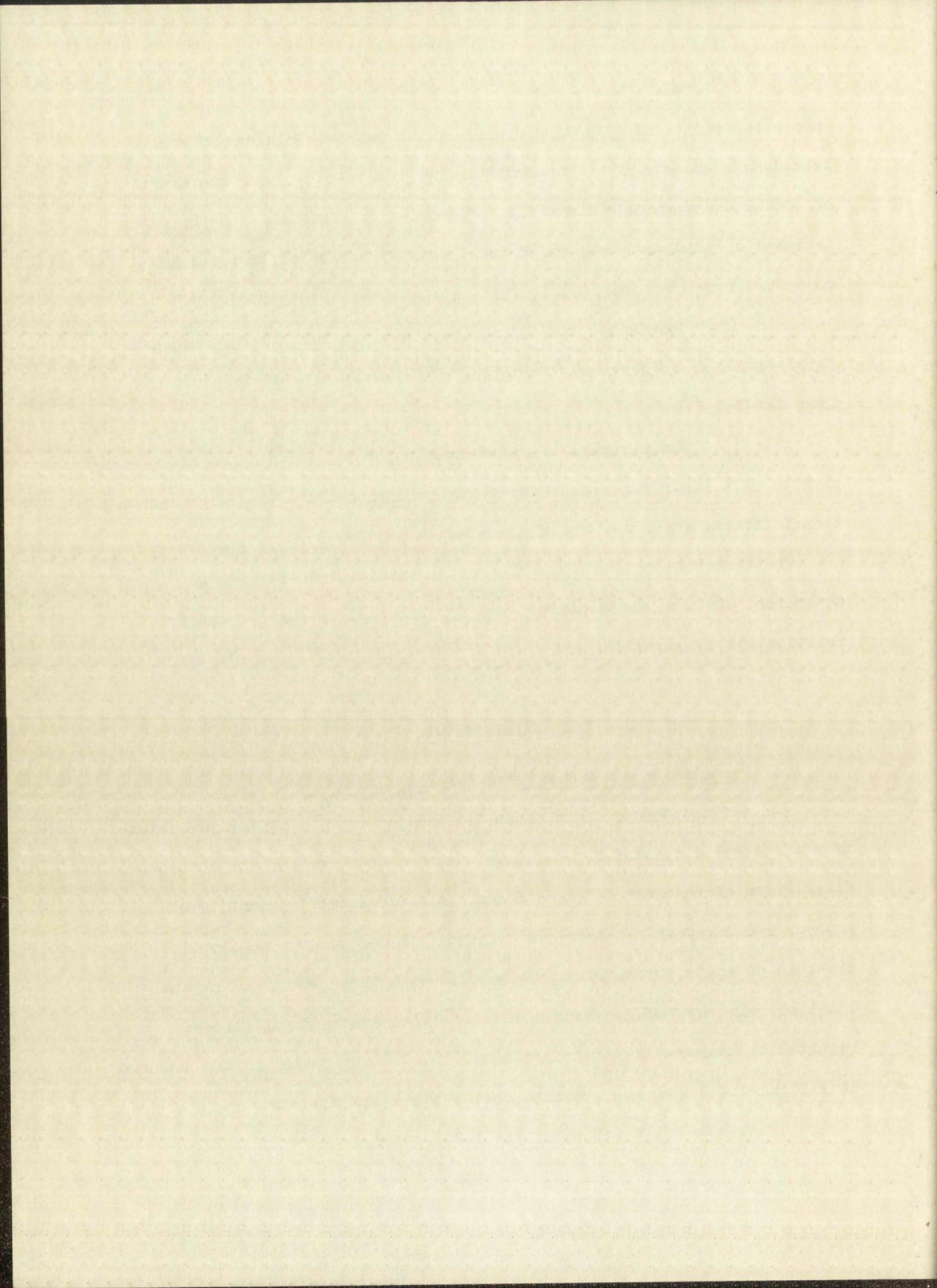
The formation constant for the pentacyanonickelate(II) ion was determined at three temperatures, and from these data, the enthalpy of reaction was obtained.

2.0 EXPERIMENTAL

2.1 Preparation of Sodium Tetracyanonickelate(II)

Sodium tetracyanonickelate(II) was prepared⁽⁵⁾ by the precipitation of nickel dicyanide from a nickel nitrate solution and the subsequent dissolution of the nickel dicyanide with a stoichiometric quantity of aqueous sodium cyanide. Recrystallization yielded yellow, needle-like crystals of sodium tetracyanonickelate(II) with three waters of crystallization. The optical properties of the crystals agreed with those reported by Brasseur and De Rassenfosse.⁽⁶⁾ On dehydration of the material at 110° a weight loss was obtained corresponding to the reaction





Dehydration occurs slowly at room temperature when exposed to laboratory air. A sample of the trihydrate analyzed as 22.69% Ni (calculated value = 22.34%). Evidently, some of the hydrated water was lost during the analysis.

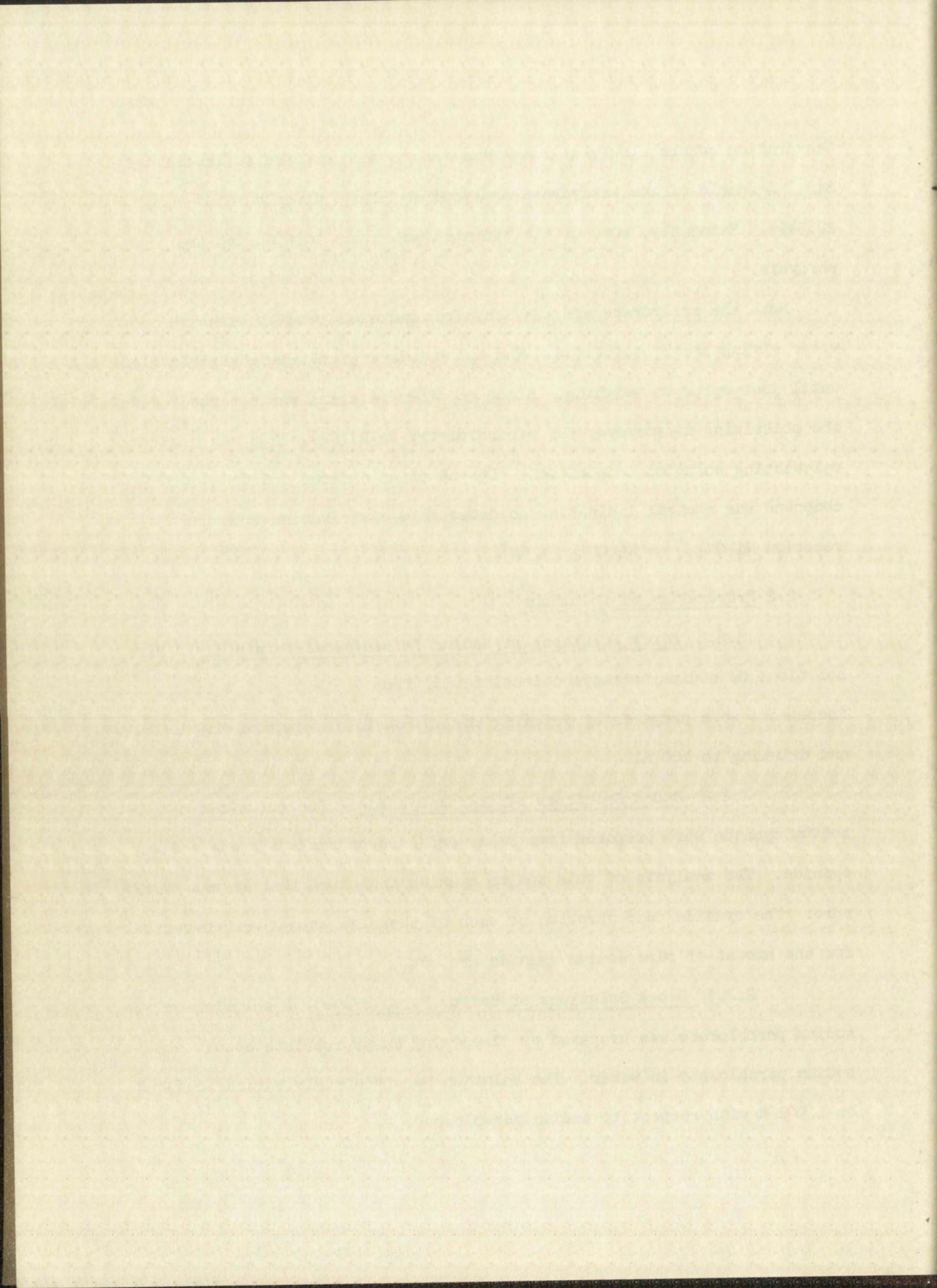
Both the trihydrate and the anhydrous material readily dissolve in water giving clear solutions. The trihydrate crystals were kept bottled until just prior to weighing. Since no other material was detected under the polarizing microscope, the stoichiometry $\text{Na}_2\text{Ni}(\text{CN})_4 \cdot 3\text{H}_2\text{O}$ was used for calculating solution composition. The pH of an aqueous solution of this compound was neutral indicating no detectable contribution from the reaction $\text{Ni}(\text{CN})_4^{2-} \rightleftharpoons \text{Ni}(\text{CN})_3^- + \text{CN}^-$.

2.2 Preparation of Solutions

2.2.1 Stock Solutions of Sodium Tetracyanonickelate(II): Five solutions of sodium tetracyanonickelate(II) from 0.5 M to 0.3 M in 0.05 M increments were prepared by weighing the appropriate amount of $\text{Na}_2\text{Ni}(\text{CN})_4 \cdot 3\text{H}_2\text{O}$ and diluting to 100 ml.

2.2.2 Stock Solutions of Sodium Cyanide: Ten solutions of sodium cyanide were prepared from Baker and Adamson reagent grade sodium cyanide. The analysis of this sodium cyanide indicated that it was 97.02% pure. The cyanide concentration of each of these solutions was corrected for the amount of pure sodium cyanide present.

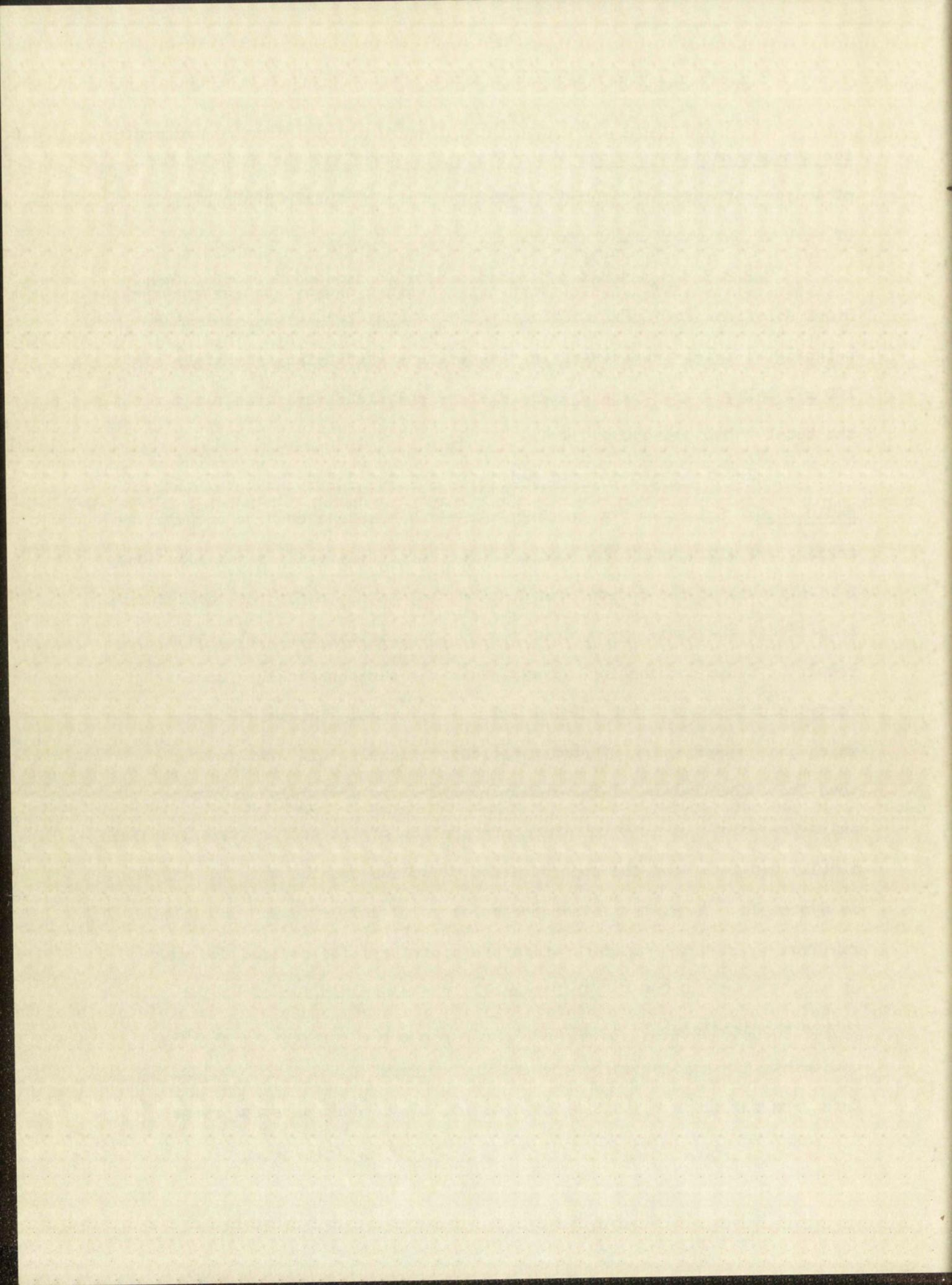
2.2.3 Stock Solutions of Sodium Perchlorate: A solution of sodium perchlorate was prepared by dissolving an appropriate amount of sodium perchlorate in water. The solution was then analyzed and found to be 1.902 M with respect to sodium perchlorate.



2.2.4 Preparation of Solutions of Sodium Tetracyanonickelate(II) for the Determination of the Molar Extinction Coefficient: Five solutions of sodium tetracyanonickelate(II) were prepared by taking 5 ml aliquots of each of the stock solutions and diluting to 25 ml.

2.2.5 Preparation of Solutions for Continuous Variation Method: Stock solutions of 0.1250 M KCN and 0.1250 M $K_2Ni(CN)_4$ were prepared by weighing an appropriate amount of the solids and diluting separately to 100 ml. Aliquot portions of each of these solutions were mixed so that the total volume was maintained at 30 ml.

2.2.6 Preparation of Solutions for the System $Na_2Ni(CN)_4-NaCN-NaClO_4-H_2O$: Solutions for spectrophotometric examination were prepared by taking 5 ml aliquots of the sodium tetracyanonickelate(II) stock solutions, 5 ml aliquots of the sodium cyanide stock solutions, sufficient perchlorate to maintain the ionic strength at ~ 1.34 and diluting to 25 ml. As a result of these combinations, forty solutions were obtained. These forty solutions were then divided into two systems. The solutions in which the concentration of sodium tetracyanonickelate(II) was greater than the concentration of the sodium cyanide were identified as System I, while the solutions in which the concentration of the sodium tetracyanonickelate(II) was less than the concentration of sodium cyanide were identified as System II. In System I the concentration of sodium tetracyanonickelate(II) ran from ~ 0.1 M to ~ 0.06 M, while the sodium cyanide covered the range of ~ 0.03 M to ~ 0.009 M. In System II, the concentration of sodium tetracyanonickelate(II) again ran from ~ 0.1 M to ~ 0.06 M, while the sodium cyanide concentration covered the range of ~ 1.0 M to ~ 0.5 M. Data from solutions containing cyanide ion in the concentration range



0.03 to 0.5 M were not amenable to treatment under the approximations necessary.

The concentration of the sodium cyanide in each of these forty solutions was corrected for hydrolysis using a value of $K_{\text{HCN}} = 4 \times 10^{-10(7)}$.

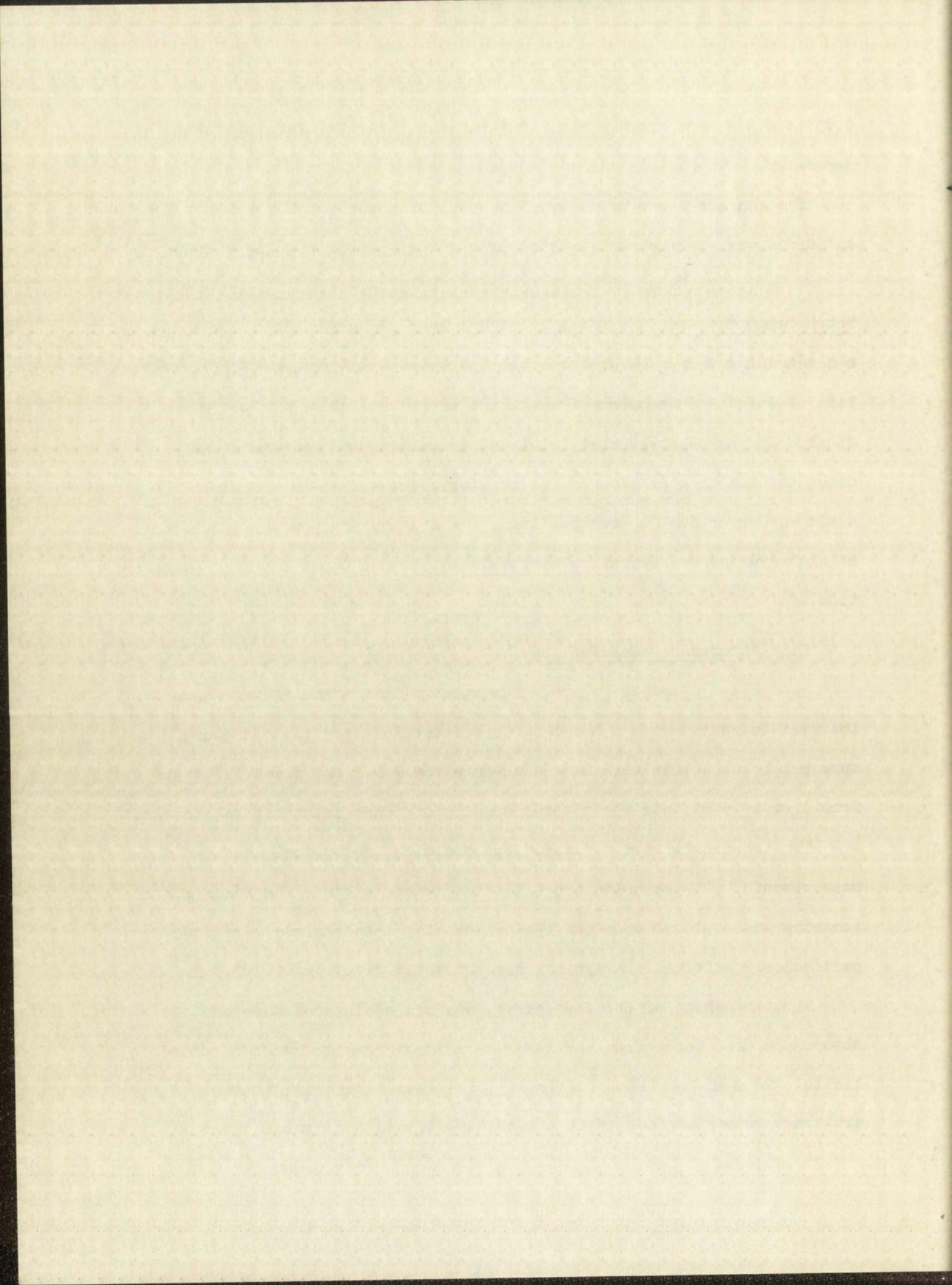
2.2.7 Preparation of Solutions of High Ratio of Cyanide to Tetracyanonickelate(II): Five solutions were prepared with the cyanide concentration very much greater than the tetracyanonickelate(II) concentration by weighing the appropriate amount of the solids and diluting to 25 ml. It was observed that solutions containing sodium cyanide at concentration greater than one molar slowly decomposed on standing. To avoid any error due to decomposition, the observations on the solutions of high cyanide concentration were made as soon as possible after preparation.

2.3 Absorbance Measurements

2.3.1 Visible Region: The spectral measurements were made in the visible region with a Model 14 Cary recording spectrophotometer. The appropriate solutions were placed in Corex cells which varied in length from 1 cm to 5 cm, and the optical density of these solutions was observed.

Two techniques were utilized for obtaining the optical density measurements: (i) scanning and (ii) fixed wave length. The technique of scanning was employed when the optical density measurements were not particularly critical. A typical scan curve is given by Fig. 2.3.1.

From the shape of the scan curve, one can easily see that the absorbance data taken from the lower wave length region would be unreliable. To overcome this difficulty, the wave length was fixed at arbitrary values (4300 Å, 4500 Å, and 4700 Å), and the optical density



was obtained for these wave lengths.

Each Corex cell was observed against a standard cell in this region to obtain a background reading. The optical density measurements were corrected for cell absorption. The solutions of low optical density were run against water; those solutions of high optical density were observed against a solution of known optical density.

The temperature of the solutions was controlled by circulating water, at the appropriate temperature from a constant temperature bath, through the walls of a cell holder. The solutions were placed in Corex cells which were in turn placed in the constant temperature bath. The solutions were allowed to equilibrate for approximately 30 minutes and were then placed in the cell holder. Experiments performed on solutions of comparable volume immersed in the water bath at the appropriate temperatures showed that the solutions reached temperature equilibrium in approximately three minutes.

2.3.2 Infrared Region: The spectra measurements were made in the infrared region with a Model 112 Perkin-Elmer Infrared Spectrometer using a lithium fluoride prism.

Approximately 0.01 ml of an appropriate solution was placed between two calcium fluoride windows separated by an approximately 2 mil tantalum spacer and the spectrum for the solution was obtained. A typical spectrum of a solution of $\text{Na}_2\text{Ni}(\text{CN})_4 \cdot \text{NaCN} \cdot \text{NaClO}_4 \cdot \text{H}_2\text{O}$ is given by Fig. 2.3.2. Separate spectral measurements of the pure solutions characterized the peaks indicated by CN^- and $[\text{Ni}(\text{CN})_4]^{-2}$ as belonging to these species.

The cell length was determined by measuring the thickness of the tantalum spacer and adding $5 \times 10^{-4} \text{ cm}^{(3)}$ to compensate for the solution film between spacer and window.

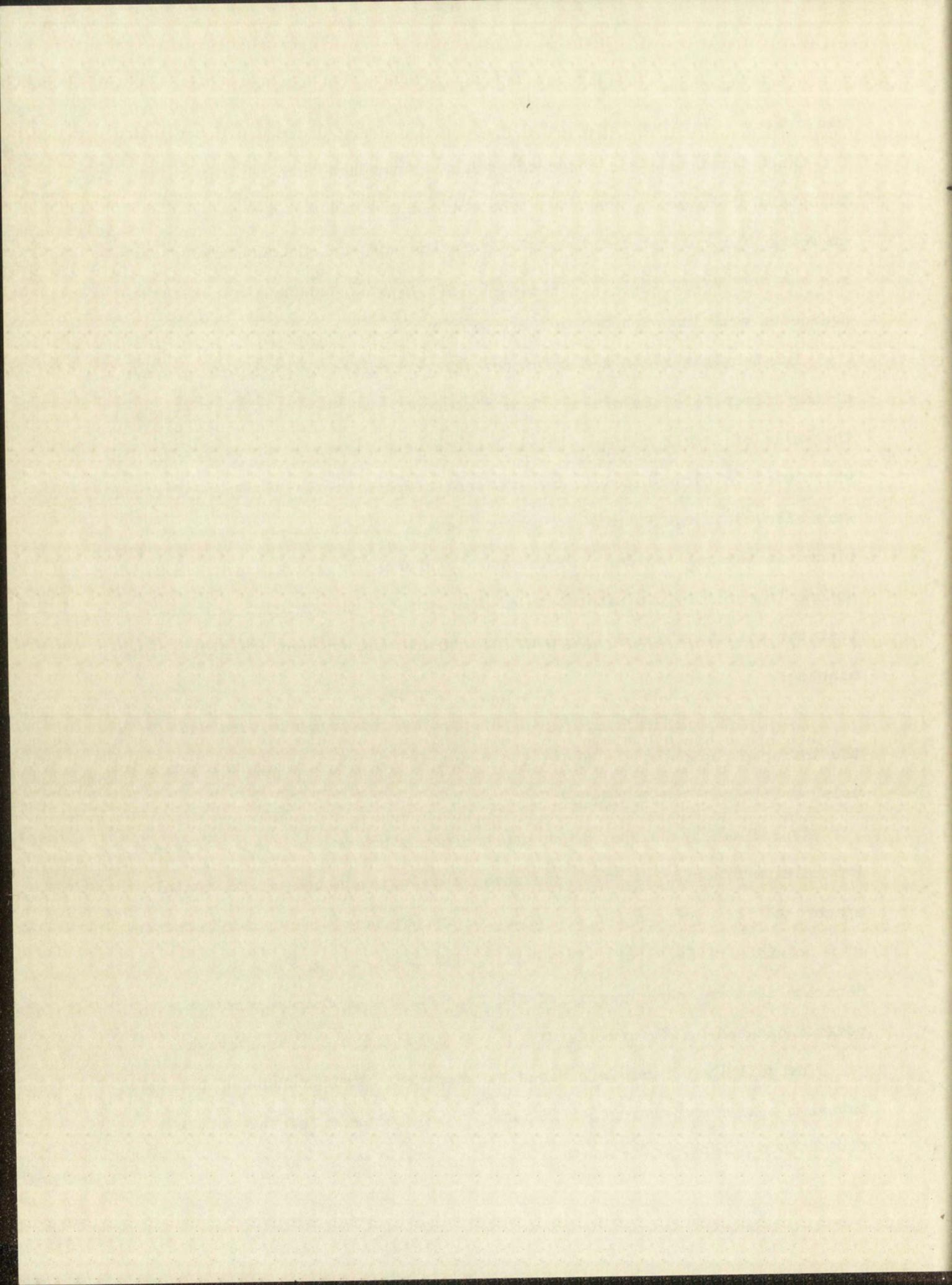
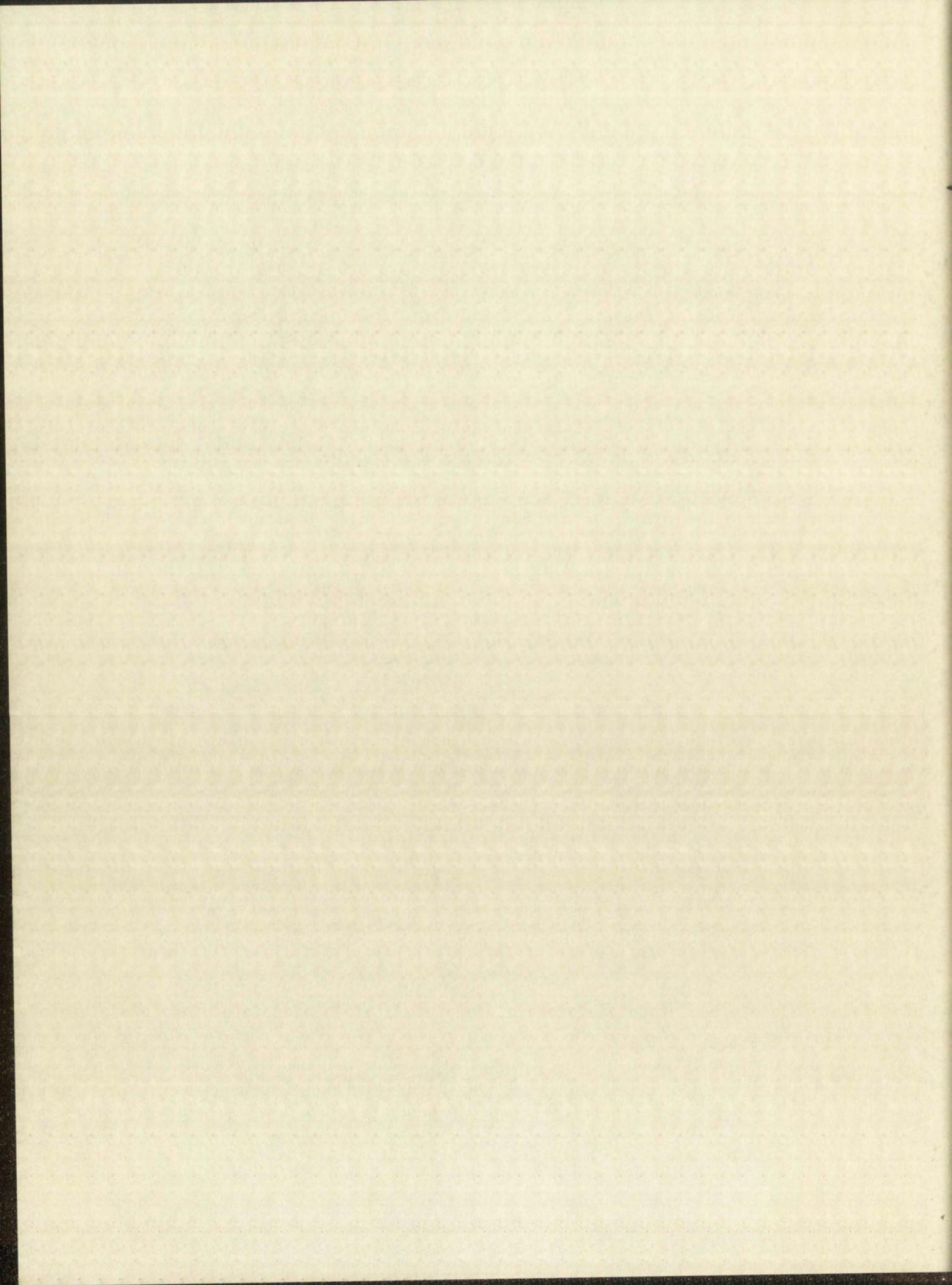
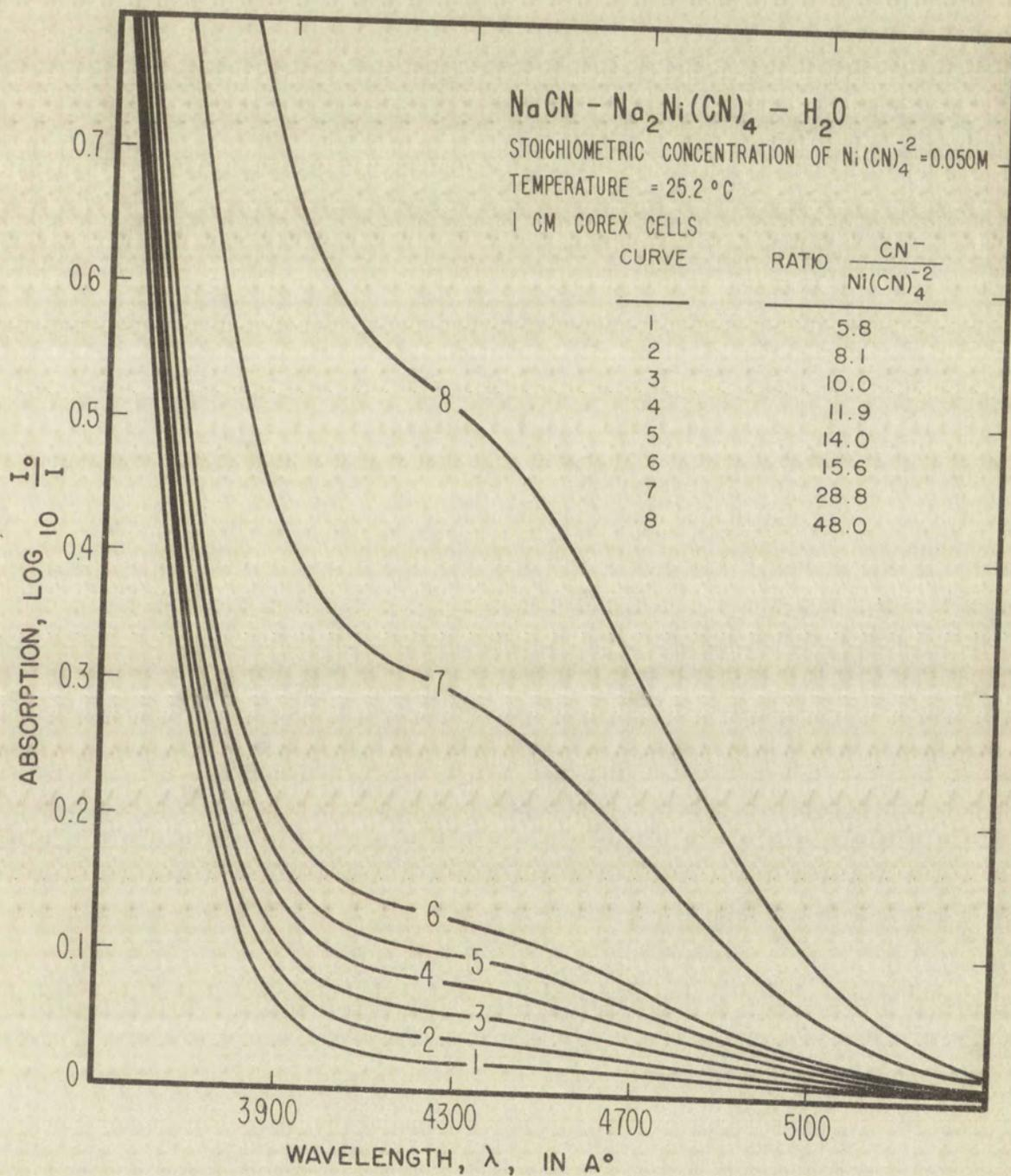
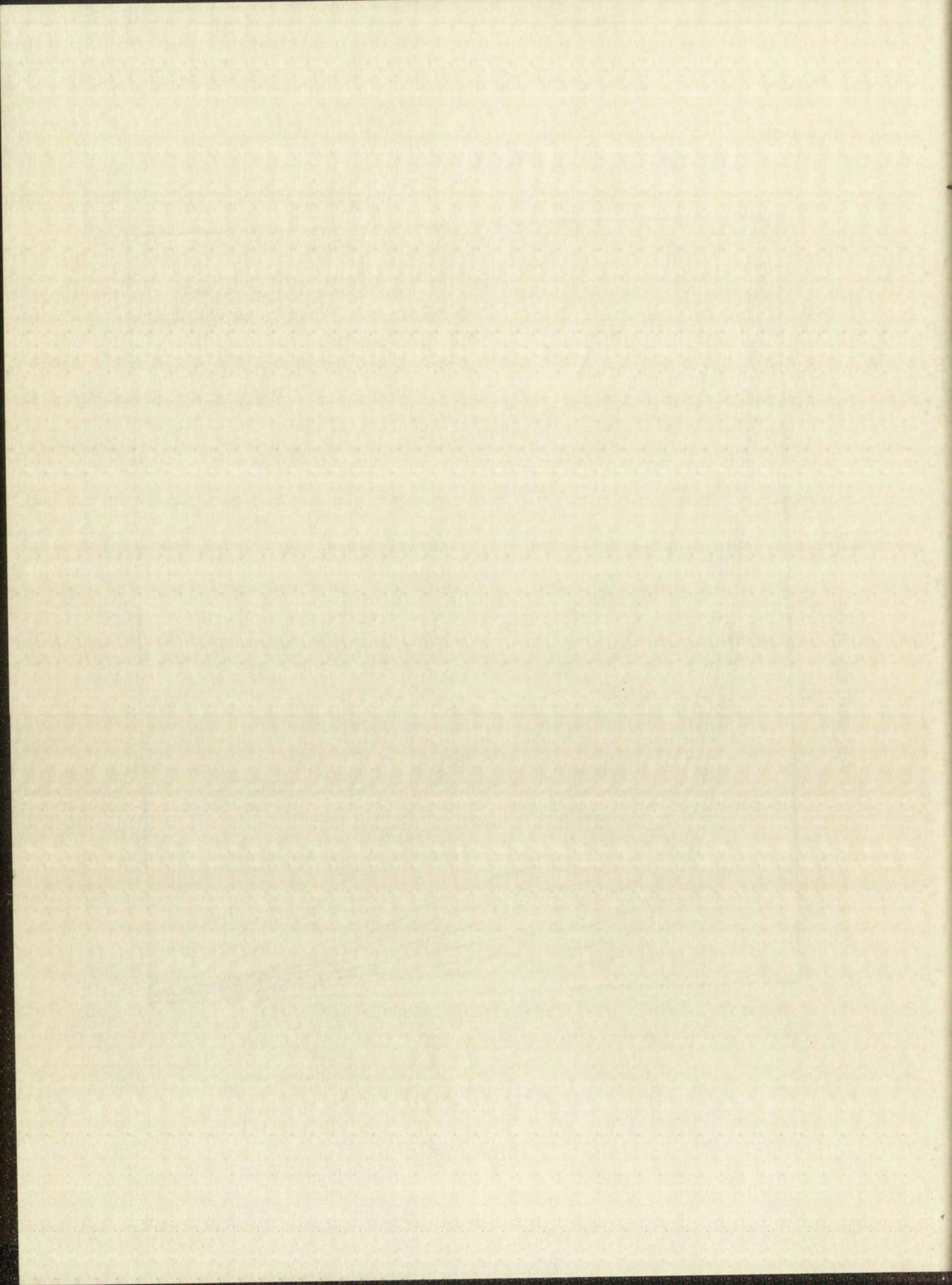


Figure 2.3.1

ABSORBANCE IN THE VISIBLE REGION FOR SOLUTIONS
OF VARYING CYANIDE TO TETRACYANONICKELATE(II) RATIOS







Since the room in which the spectra were observed was at a constant temperature of 25°, the temperature of the solutions was controlled by blowing dry air at 25° through the apparatus. There was some heating of the solutions due to the infrared beam, but this heating effect has been shown to be small⁽⁹⁾ (2-3°) and would be the same for all solutions.

The optical densities measured for the infrared region are, in all cases, those at the frequency of maximum absorption.

3.0 DETERMINATION OF THE MOLAR EXTINCTION COEFFICIENT FOR THE TETRACYANONICKELATE(II) ION

Solutions of different sodium tetracyanonickelate(II) concentrations were examined in the visible region from 4000 Å to 6500 Å at 25.2°. Portions of the same solutions were observed in the infrared region from 2000 cm⁻¹ to 2200 cm⁻¹ at 25°.

The molar extinction coefficient is given by:

$$\epsilon_m^\gamma = \frac{A_m^\gamma}{m_0 t} \quad 3.0.1$$

where: ϵ_m^γ = the molar extinction coefficient of species, m, in the region, γ , of the spectrum (λ for the visible region; ν for the infrared region), in mole⁻¹ liter cm⁻¹; A_m^γ = the absorbance of species m in the γ region of the spectrum, i.e., $\log_{10} \frac{I_0^\gamma}{I_m^\gamma}$; m_0 = the stoichiometric concentration of species, m, in moles per liter.

Equation 3.0.1 was used to calculate ϵ_m^γ for each solution in a given region of the spectrum.

3.1 Visible Region

The values of ϵ_a^λ (where a refers to the species $[\text{Ni}(\text{CN})_4]^{-2}$) and their standard deviation, $S_{\epsilon_a^\lambda}$, for the wave lengths, 4300 Å, 4500 Å,

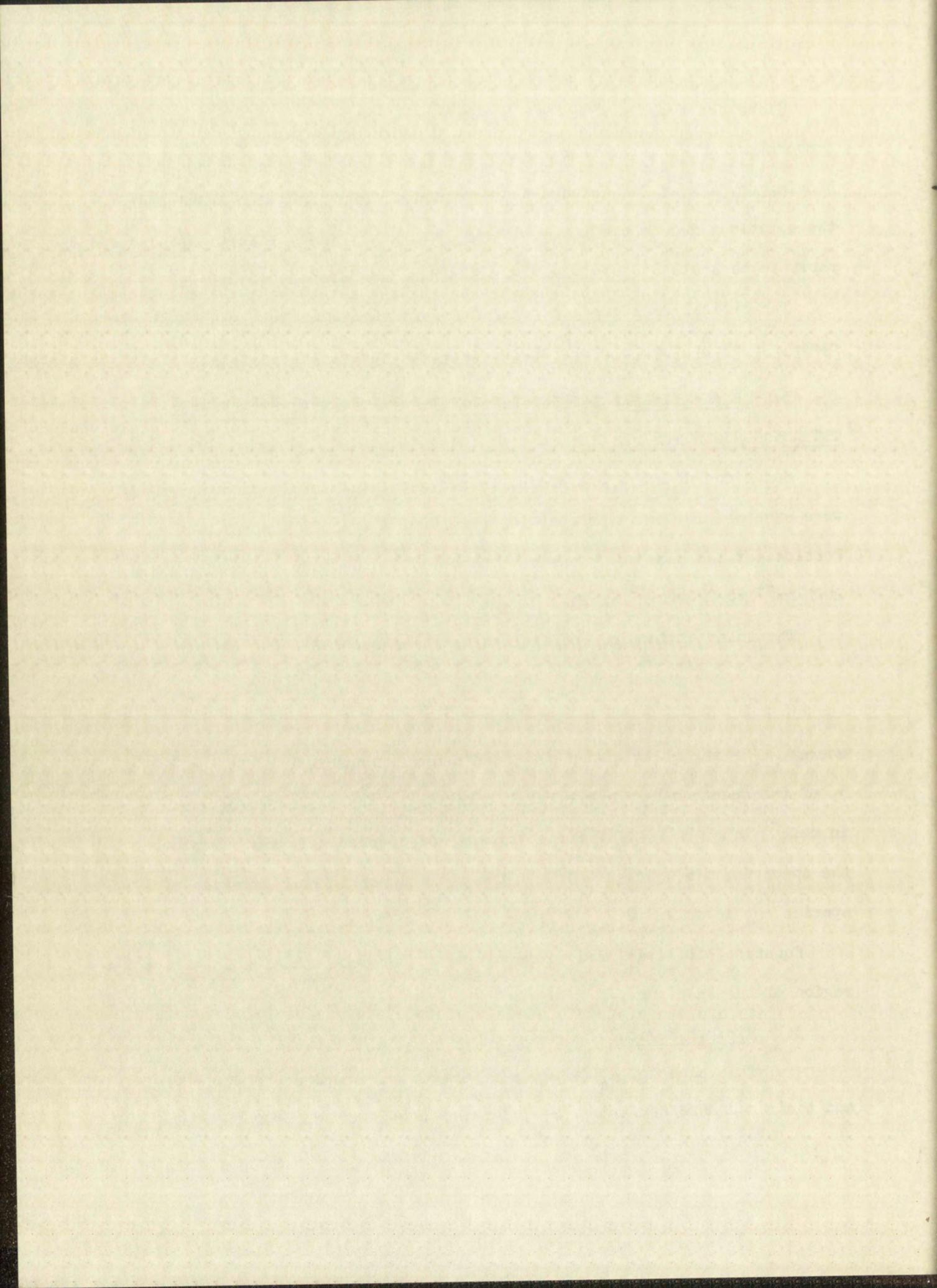
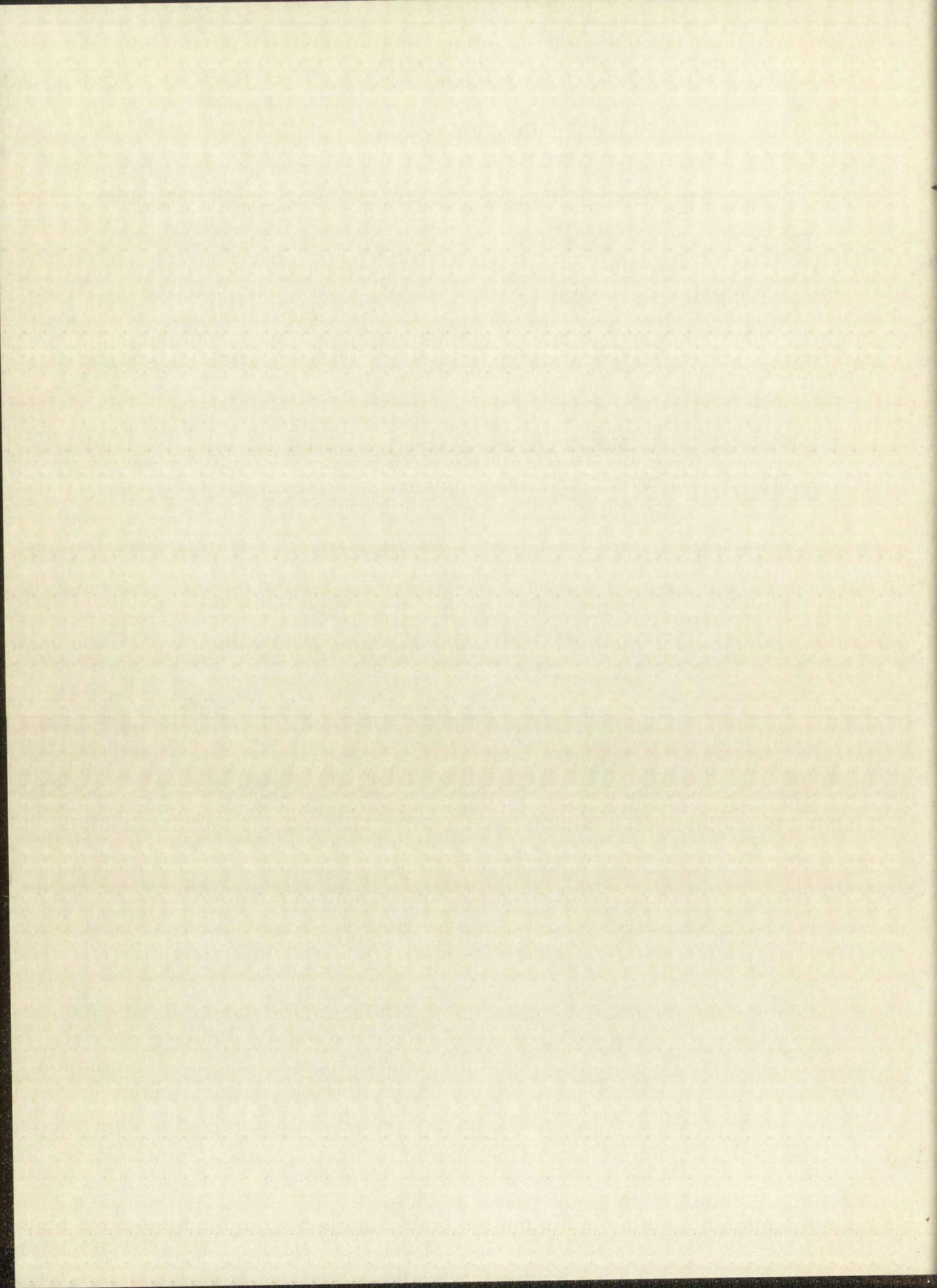
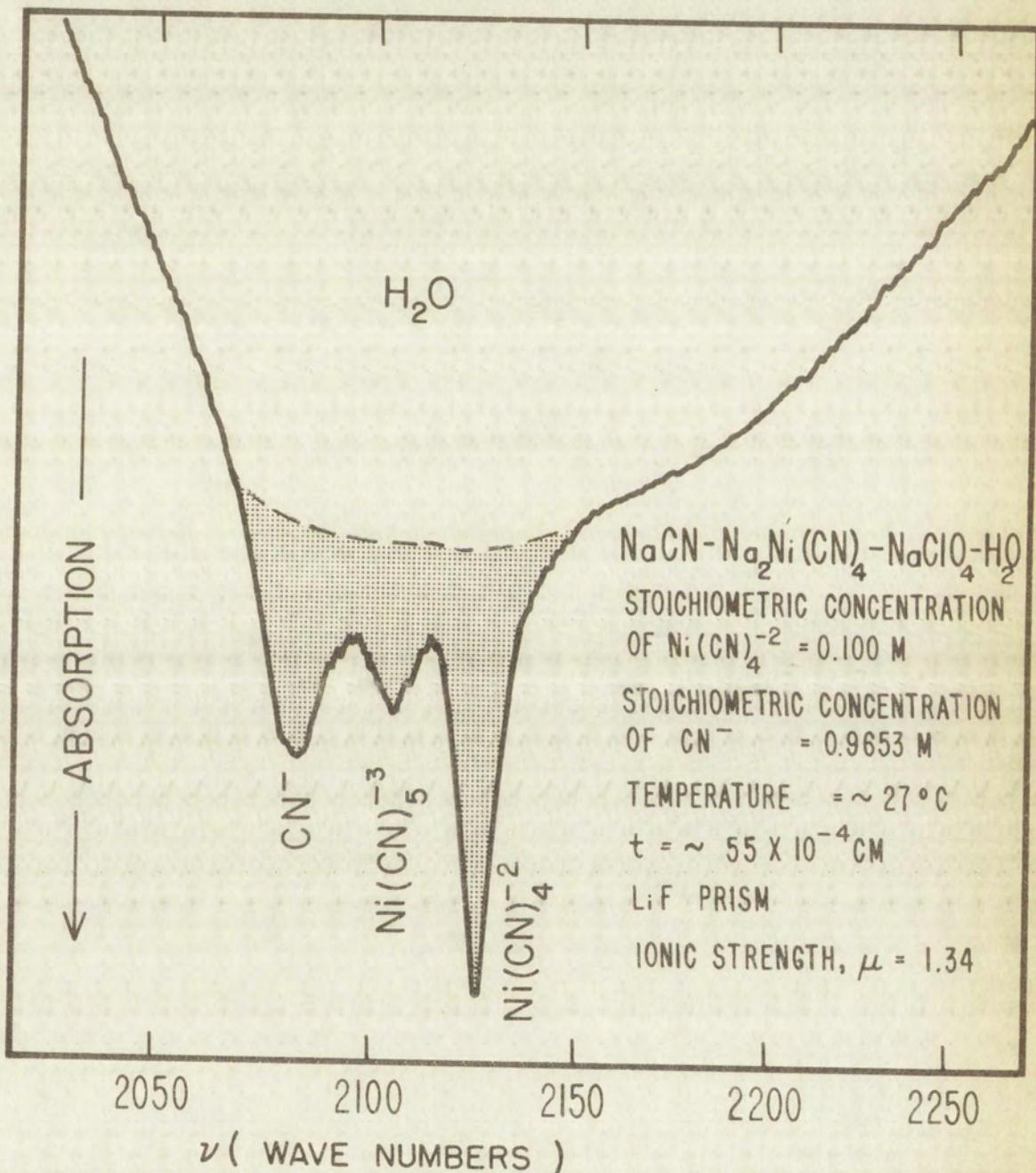
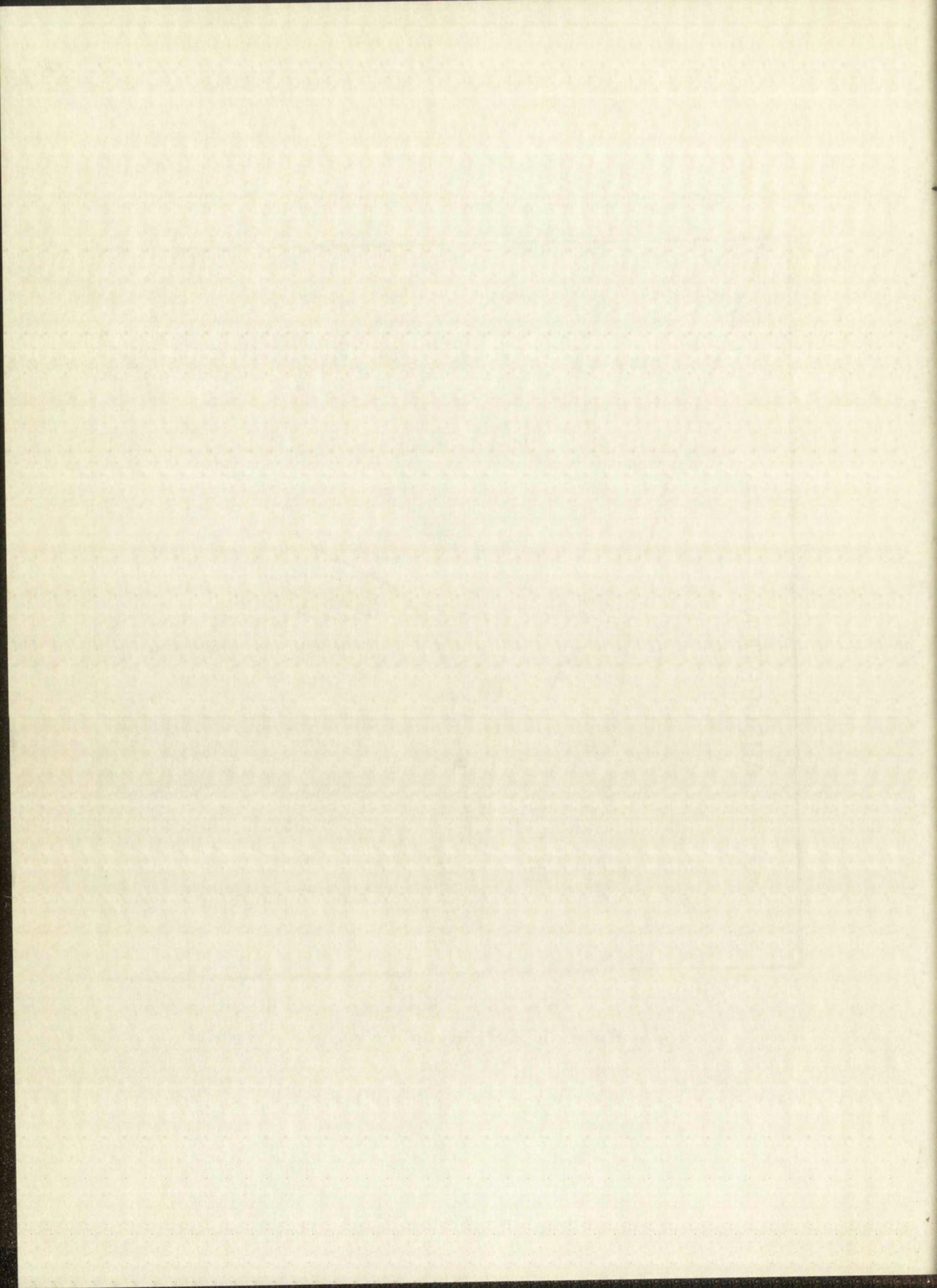


Figure 2.3.2

ABSORBANCE IN THE INFRARED REGION SHOWING TETRACYANONICKELATE(II),
CYANIDE, AND PENTACYANONICKELATE(II) IONS IN AQUEOUS SOLUTION







and 4700 \AA , are given in Table 3.1.1. Two separate measurements were made on solutions of the same concentration.

3.2 Infrared Region

A typical absorption curve for the tetracyanonickelate(II) ion in the infrared region is given by Fig. 3.2.1. The value for the molar extinction coefficient was determined at the frequency of maximum absorption.

Tantalum rings cut from 2 mil sheets were used as spacers. Using a value of $5 \times 10^{-4} \text{ cm}^{(8)}$ as the thickness of the capillary solution film, a total thickness of $55 \times 10^{-4} \text{ cm}$ was obtained for the sample.

The value for $\epsilon_a^{2130 \text{ cm}^{-1}}$ and its standard deviation for the infrared region is given in Table 3.2.1. The large standard deviation may be attributed to uncertainty in the path length arising from variance in the thickness of the tantalum spacers and variance in the pressure applied to the calcium fluoride windows.

4.0 CHARACTERIZATION OF THE NEW SPECIES

4.1 Infrared Region

The strongest piece of evidence supporting the existence of a new species in solutions containing sodium tetracyanonickelate(II) and excess cyanide is the appearance of a new absorption peak in the infrared region. The growth of this new peak with increase of the CN^- concentration should also serve as a clue to the composition of the new complex.

Consider the absorbance of the new species as given by

$$A_c = \epsilon_c t [c] \quad 4.1.1$$

where the c refers to the new species, with the bracketed term representing equilibrium concentration.

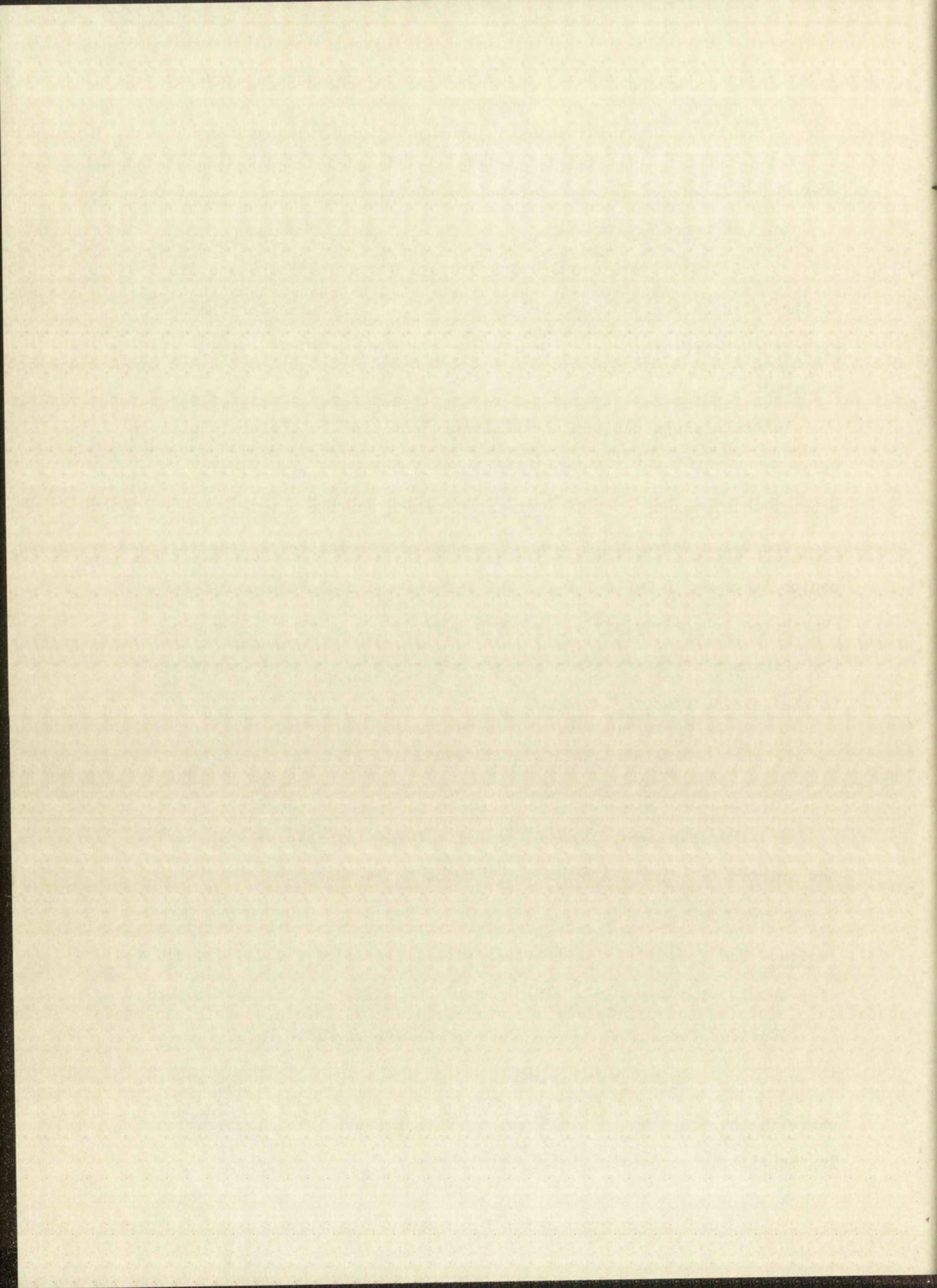


TABLE 3.1.1

THE MOLAR EXTINCTION COEFFICIENT OF THE TETRACYANONICKELATE(II) ION, ϵ_a^λ , AND ITS STANDARD DEVIATION, $S_{\epsilon_a^\lambda}$, FOR THE VISIBLE REGION

$$\epsilon_a^\lambda = \frac{A_{\text{obs}}^\lambda}{a \cdot t}$$

a_0 in moles/l.	4300 Å		4500 Å		4700 Å	
	A_{obs}^{4300}	ϵ_a^{4300}	A_{obs}^{4500}	ϵ_a^{4500}	A_{obs}^{4700}	ϵ_a^{4700}
0.1000	0.905	1.810	0.672	1.344	0.480	0.960
0.1000	0.905	1.810	0.675	1.350	0.483	0.966
0.0900	0.814	1.809	0.606	1.346	0.432	0.960
0.0900	0.820	1.822	0.614	1.364	0.442	0.982
0.0800	0.723	1.808	0.538	1.345	0.385	0.962
0.0800	0.726	1.815	0.545	1.362	0.391	0.978
0.0700	0.632	1.806	0.470	1.343	0.337	0.963
0.0700	0.633	1.808	0.474	1.354	0.340	0.971
0.0600	0.542	1.807	0.402	1.340	0.286	0.953
0.0600	0.544	1.813	0.406	1.353	0.292	0.973
$\epsilon_a^\lambda \pm S_{\epsilon_a^\lambda}$	1.811 \pm 0.005		1.350 \pm 0.008		0.967 \pm 0.009	

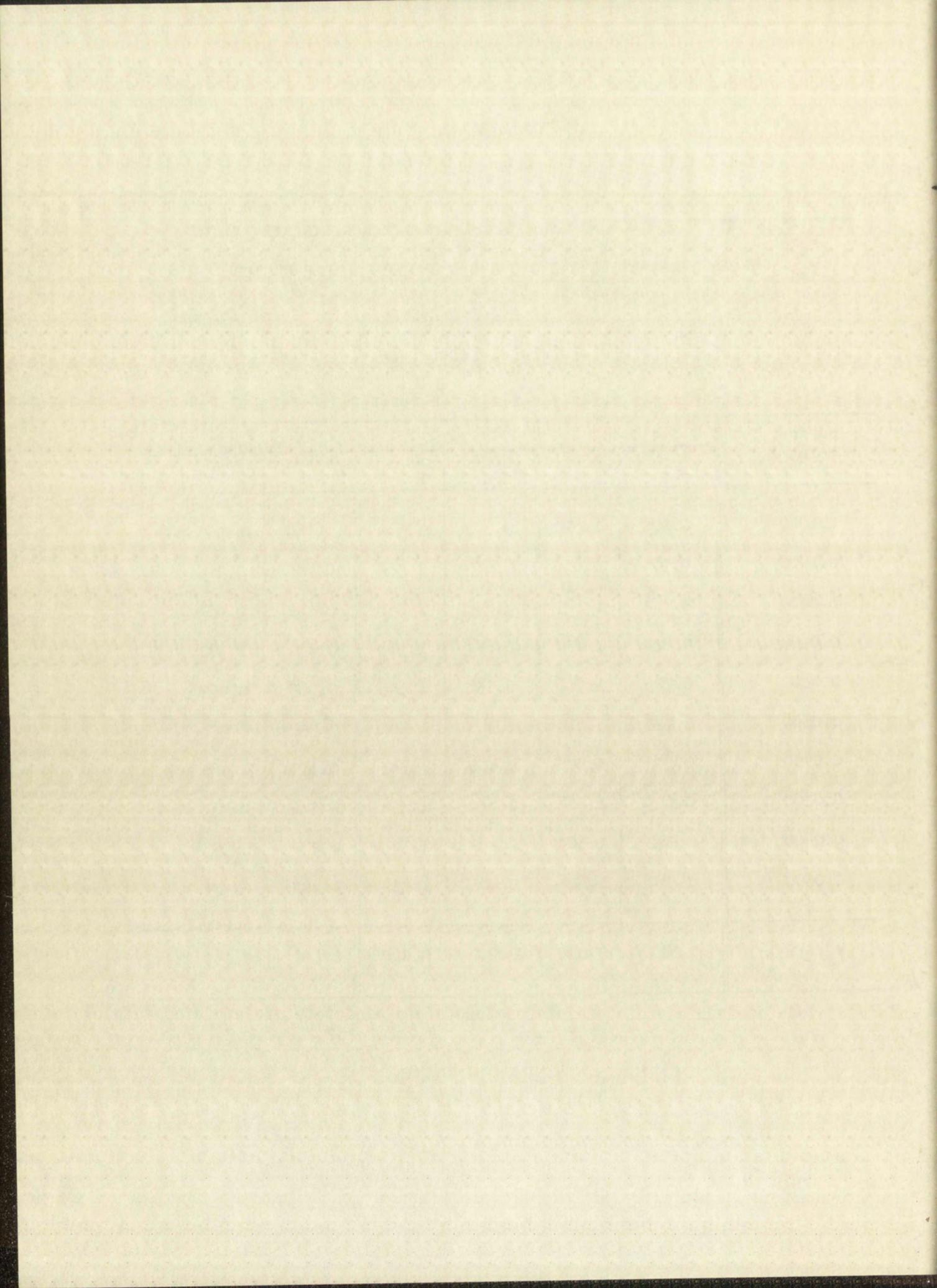
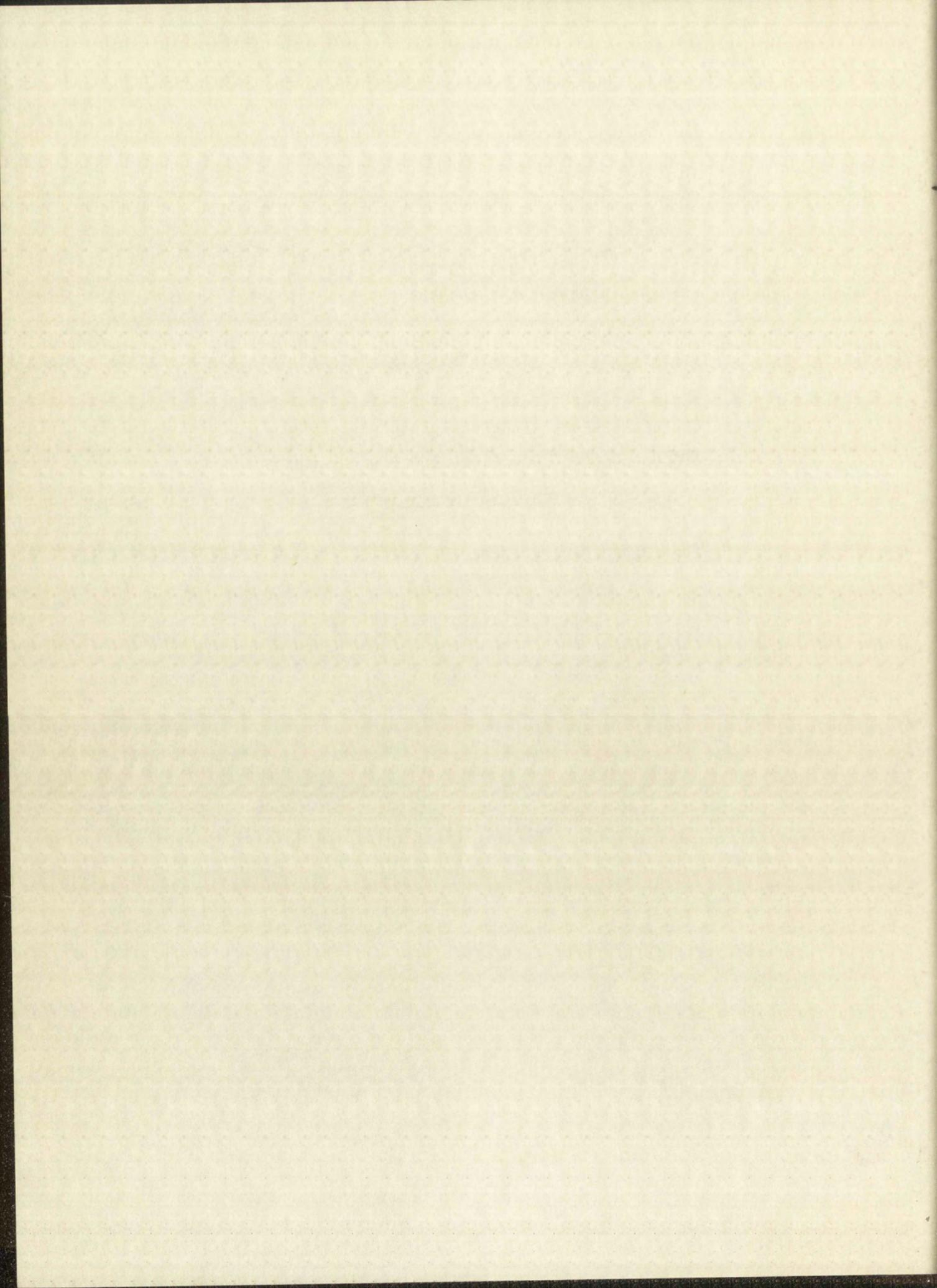
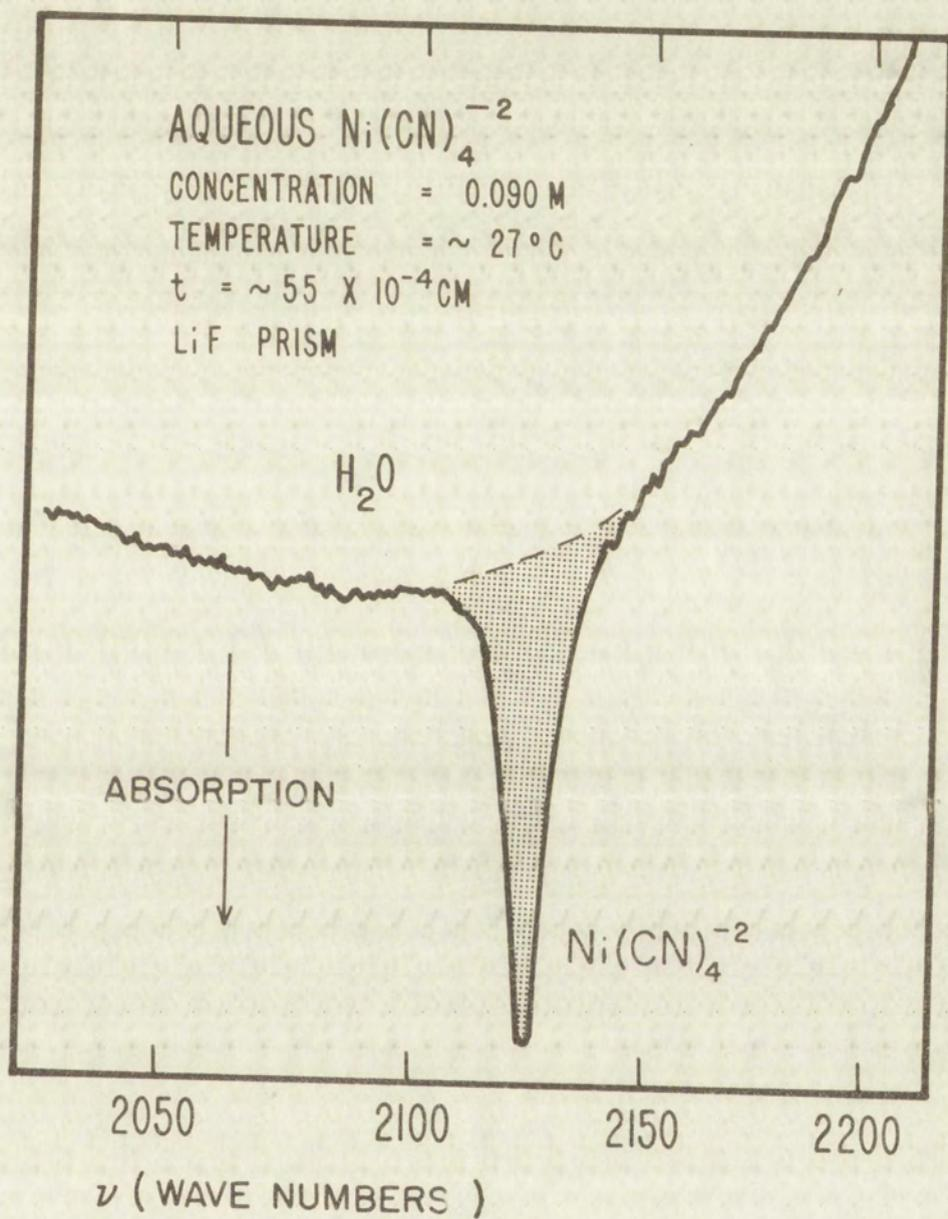


Figure 3.2.1

ABSORPTION IN THE INFRARED REGION FOR AN AQUEOUS
SOLUTION OF TETRACYANONICKELATE(II)





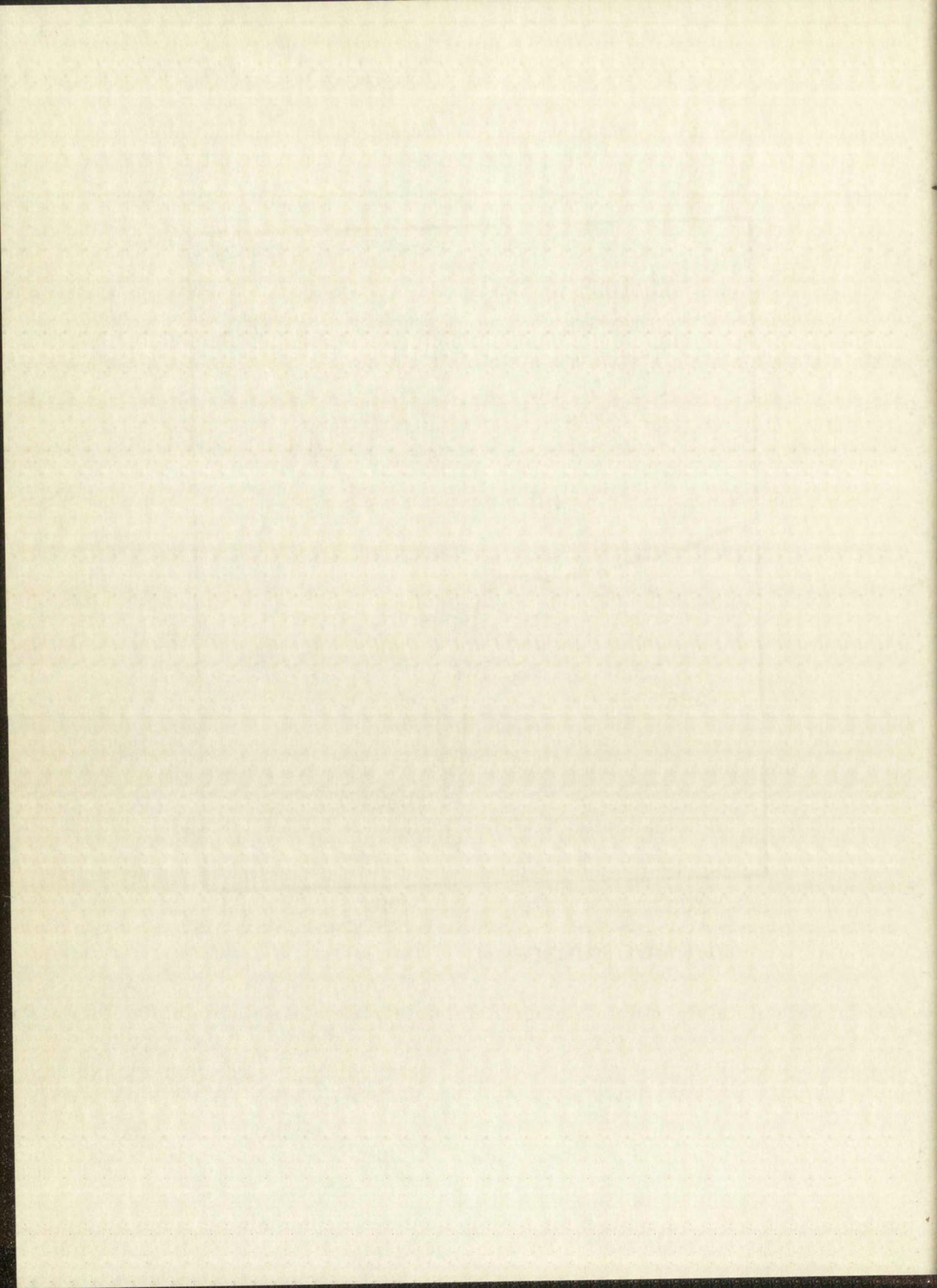


TABLE 3.2.1

THE MOLAR EXTINCTION COEFFICIENT OF THE TETRACYANONICKELATE(II) ION, $\epsilon_{a_0}^{2130 \text{ cm}^{-1}}$, AND ITS STANDARD DEVIATION, $S_{\epsilon_{a_0}^{2130 \text{ cm}^{-1}}}$, FOR THE

INFRARED REGION

$$\epsilon_{a_0}^{2130 \text{ cm}^{-1}} = \frac{A_{\text{obs}}^{2130 \text{ cm}^{-1}}}{a_0 t}$$

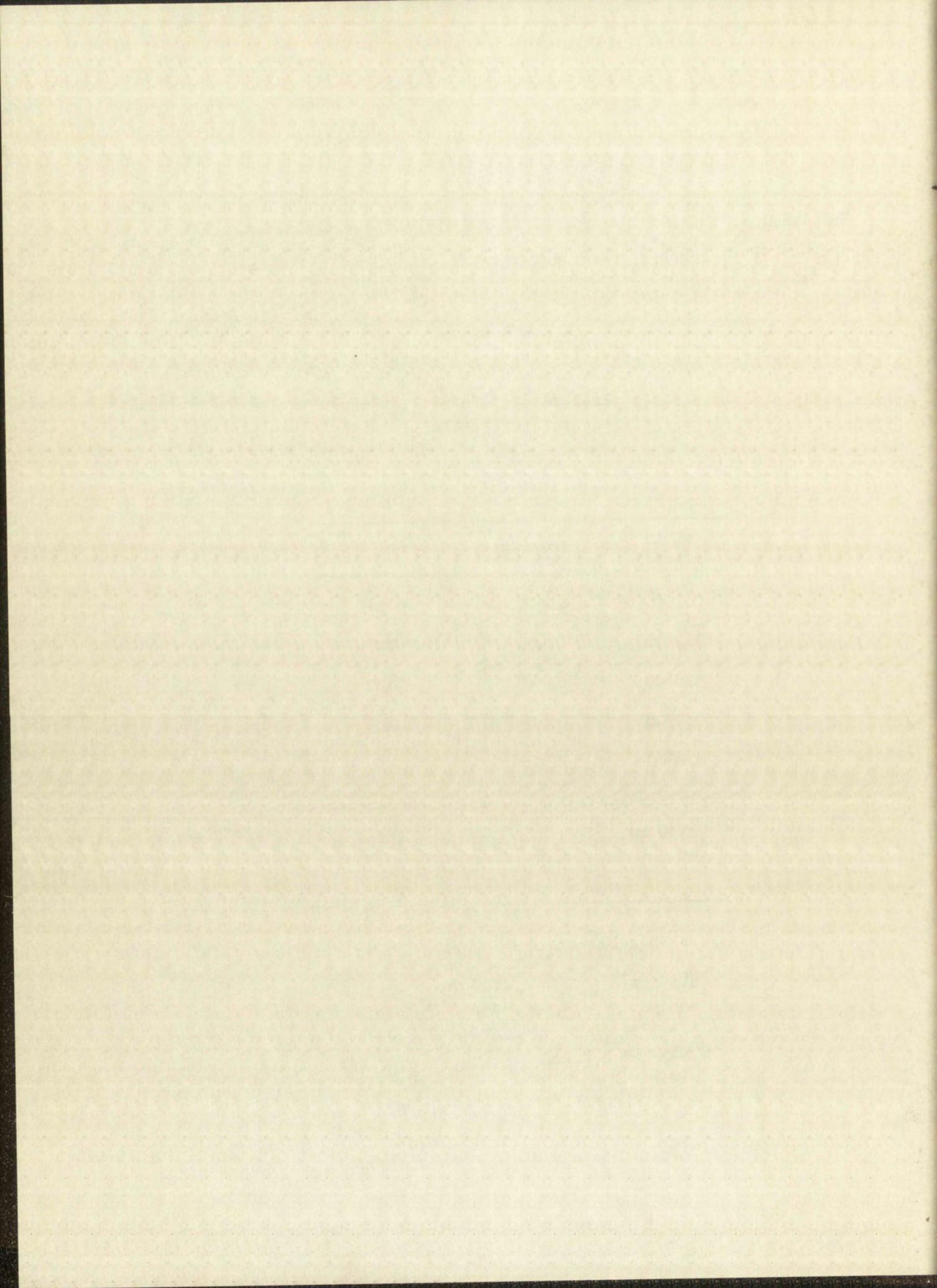
a_0 in moles/l.	$A_{\text{obs}}^{2130 \text{ cm}^{-1}}$	$\epsilon_{a_0}^{2130 \text{ cm}^{-1}}$
0.1000	0.571	1038
0.0900	0.485	978
0.0800	0.448	1020
0.0700	0.414	1075
0.0600	0.406	1231

$$\overline{\epsilon_{a_0}^{2130 \text{ cm}^{-1}}} \pm S_{\epsilon_{a_0}^{2130 \text{ cm}^{-1}}} : 1068 \pm 95$$

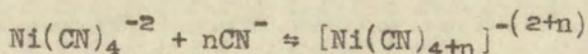
$$t = 55 \times 10^{-4} \text{ cm}$$

$$\overline{\epsilon_{a_0}^{2130 \text{ cm}^{-1}}} = \frac{1}{n} \sum \epsilon_{a_0}^{2130 \text{ cm}^{-1}}$$

$$S_{\epsilon_{a_0}^{2130 \text{ cm}^{-1}}}^2 = \frac{1}{n-1} \sum (\overline{\epsilon_{a_0}^{2130 \text{ cm}^{-1}}} - \epsilon_{a_0}^{2130 \text{ cm}^{-1}})^2$$



We assume for the reaction



that the magnitude of K is sufficiently small so that [c] is given by

$$[c] = K[a_0][b_0]^n. \quad 4.1.2$$

where the zero subscripts refer to the stoichiometric concentrations of $\text{Ni}(\text{CN})_4^{-2}$ and CN^- respectively.

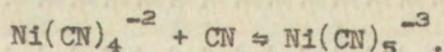
Equation 4.1.1 then becomes

$$A_c = \epsilon_c t K [a_0][b_0]^n.$$

Since the stoichiometric $[\text{Ni}(\text{CN})_4]^{-2}$ concentration, a_0 , and the path length, t , were held constant, the equation further reduces to

$$A_c = \rho [b_0]^n. \quad 4.1.3$$

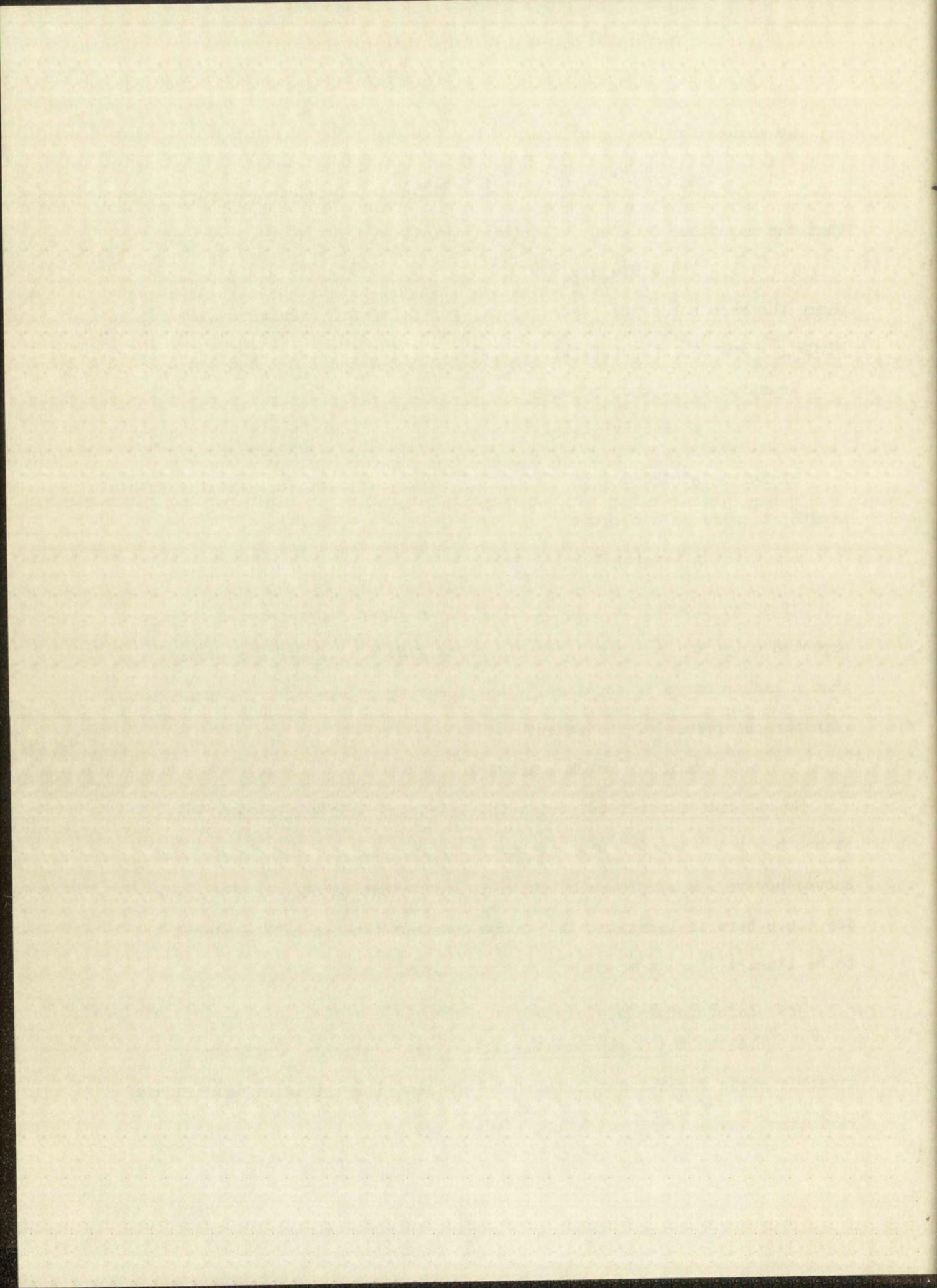
If A_c is plotted as a function of b_0 , a linear curve should be expected only for the case of $n = 1$. From Fig. 4.1, it will be noted that a linear curve is obtained. The linearity of the curve is consistent with the occurrence of the reaction



No attempt was made to obtain the exact value of K from this data since the ionic strength was not constant, nor was the path length well known; however, a simple calculation is sufficient to show that in order for the ρ term in Equation 4.1.3 to be constant (and hence Equation 4.1.3 to be linear), K must be much less than unity.

4.2 Visible Region

4.2.1 The Continuous Variation Treatment: To verify the stoichiometric formula for the assumed complex, the method of "continuous variation", as elaborated by Job,⁽⁹⁾ was used.

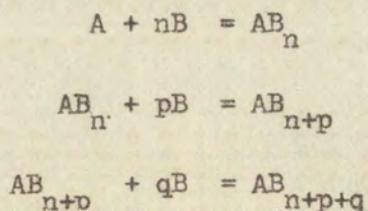


According to Job, in solutions of a fixed total formal concentration, the concentration of the product of reaction is a maximum when the concentration of the reactants are in the stoichiometric proportions in which they appear in the complex. A plot of some suitable property of the products, such as absorbance, as a function of concentration of one of the reactants should give a maximum at the ratio corresponding to the formula of the product.

The relationship between the concentration of the product and reactants is simple for systems in which only one new species is formed; however, for systems in which more than one species is found, the relationships become complicated.

Vosburgh and Cooper⁽¹⁰⁾ have described a few properties of special cases of a system forming two new species, while Katzin and Gebert⁽¹¹⁾ have extended the derivations to include a general case of formation of three new species.

As in the basic method, Katzin and Gebert considered equimolar starting solutions, of concentration N , of reactants A and B. Following Katzin and Gebert, we require that the reactants are mixed, without appreciable volume change, in the proportion of x volumes of B and $1-x$ volumes of A, where x is the ratio of the volume of B to the total volume. The following equilibria are then assumed to be established:



We then define the concentration terms as:

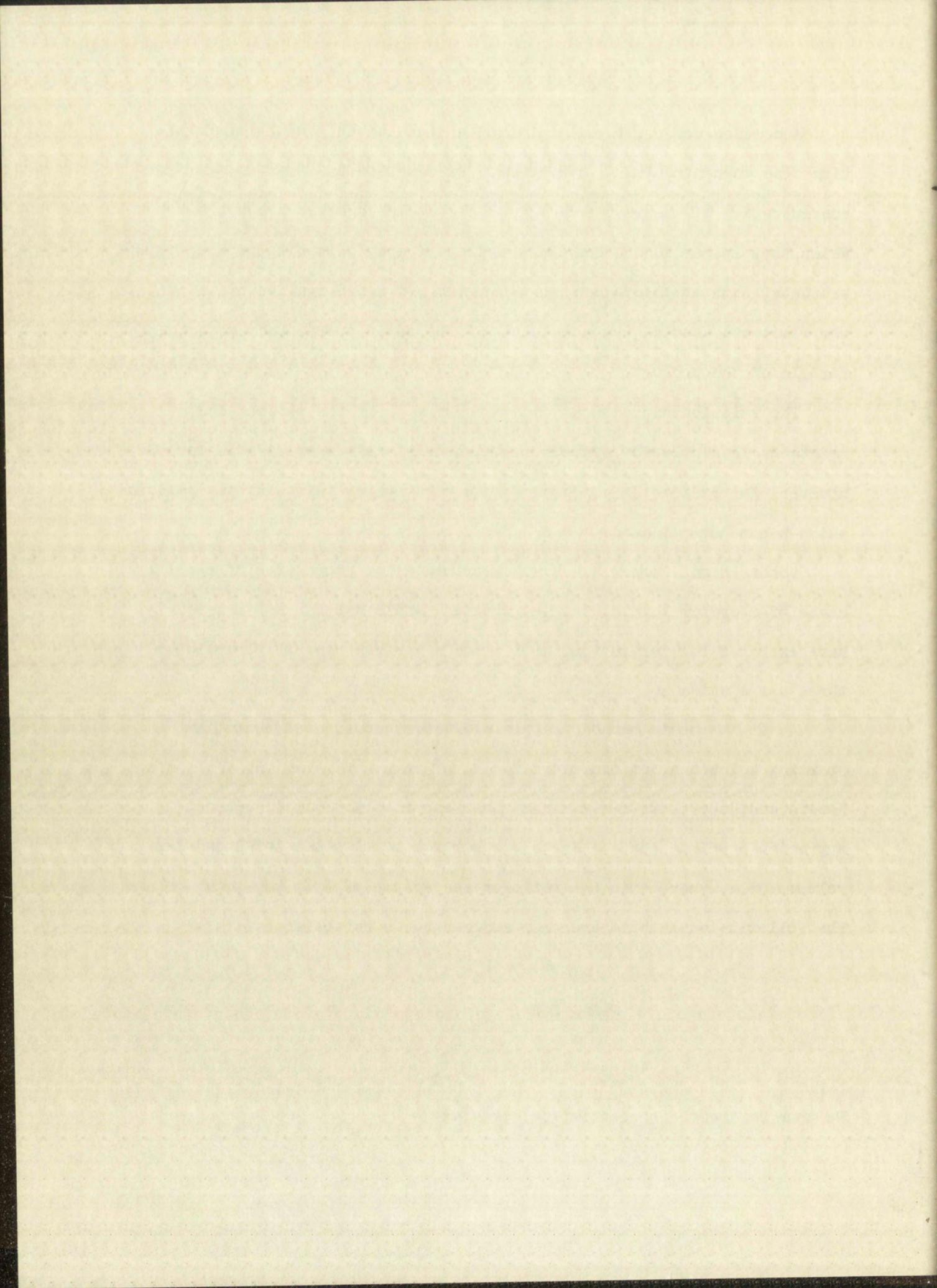
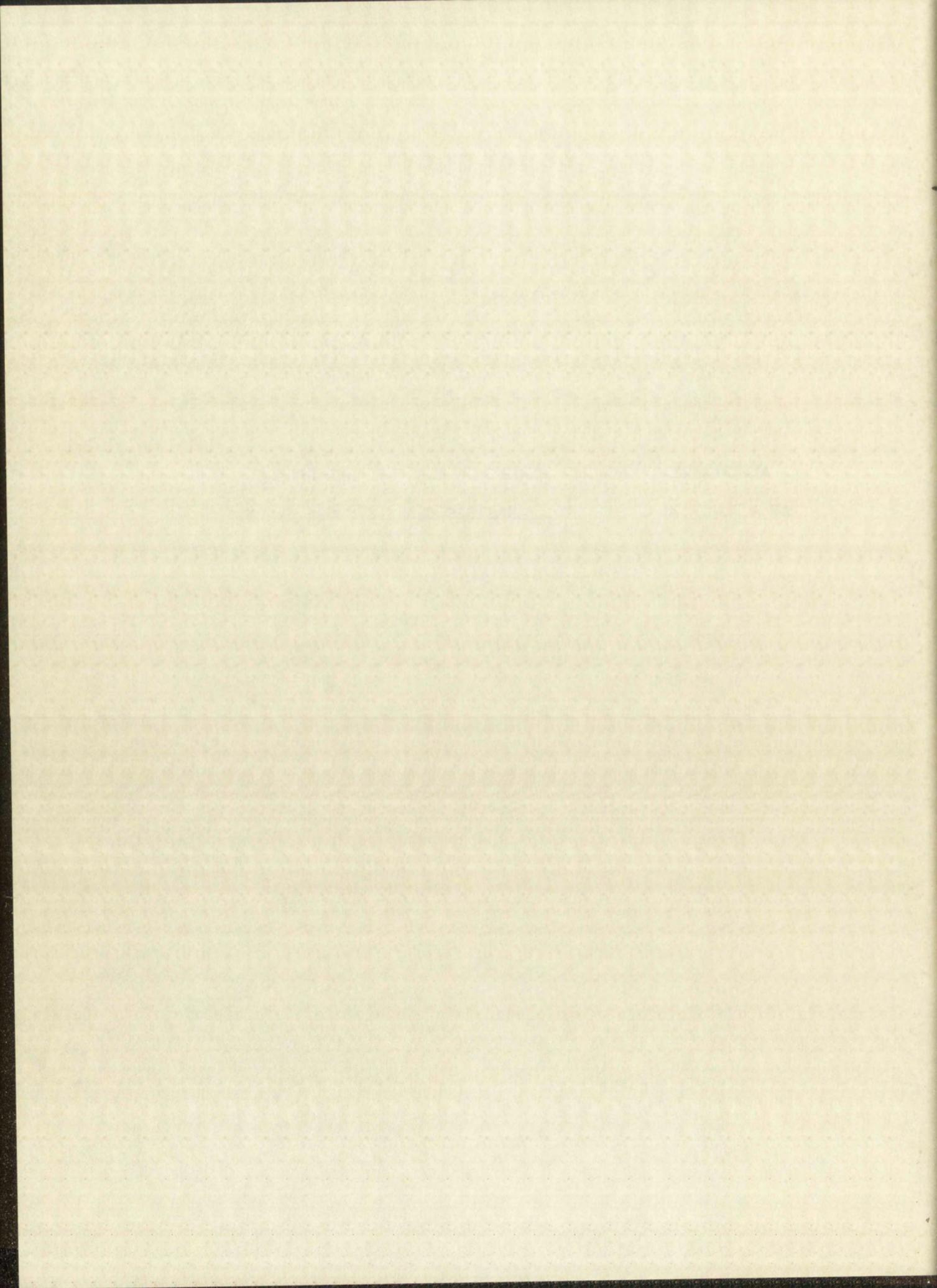
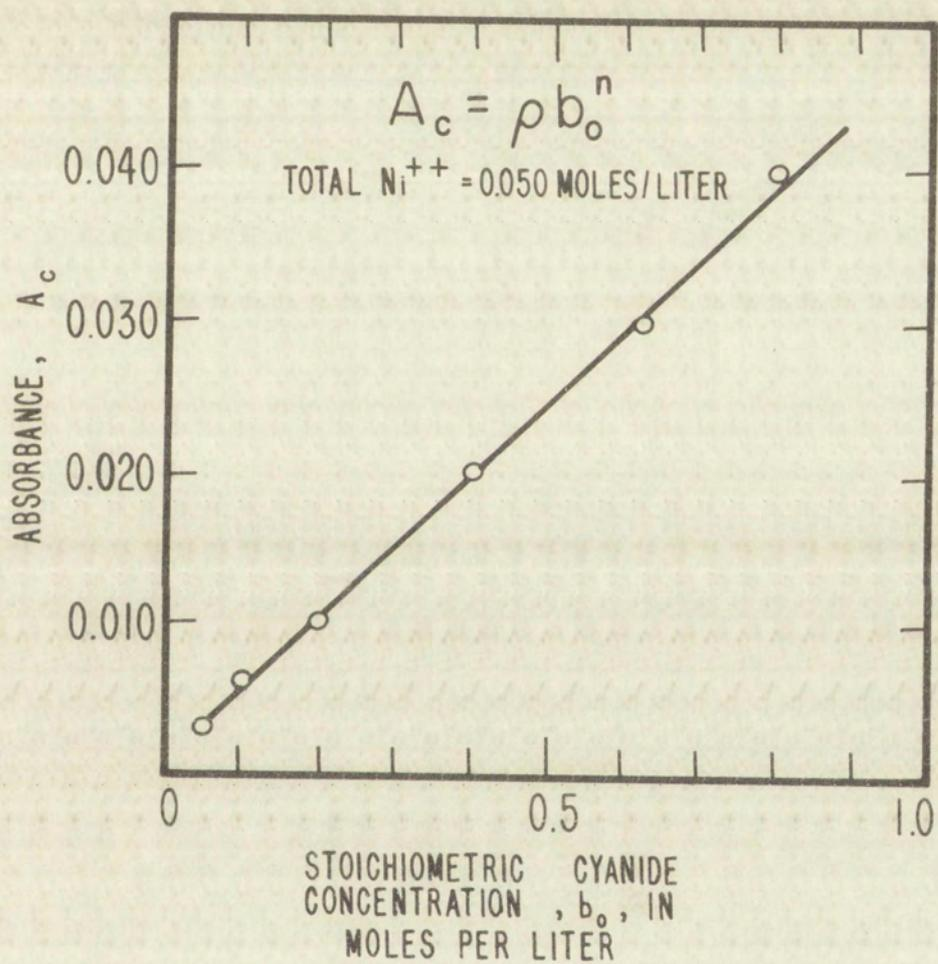
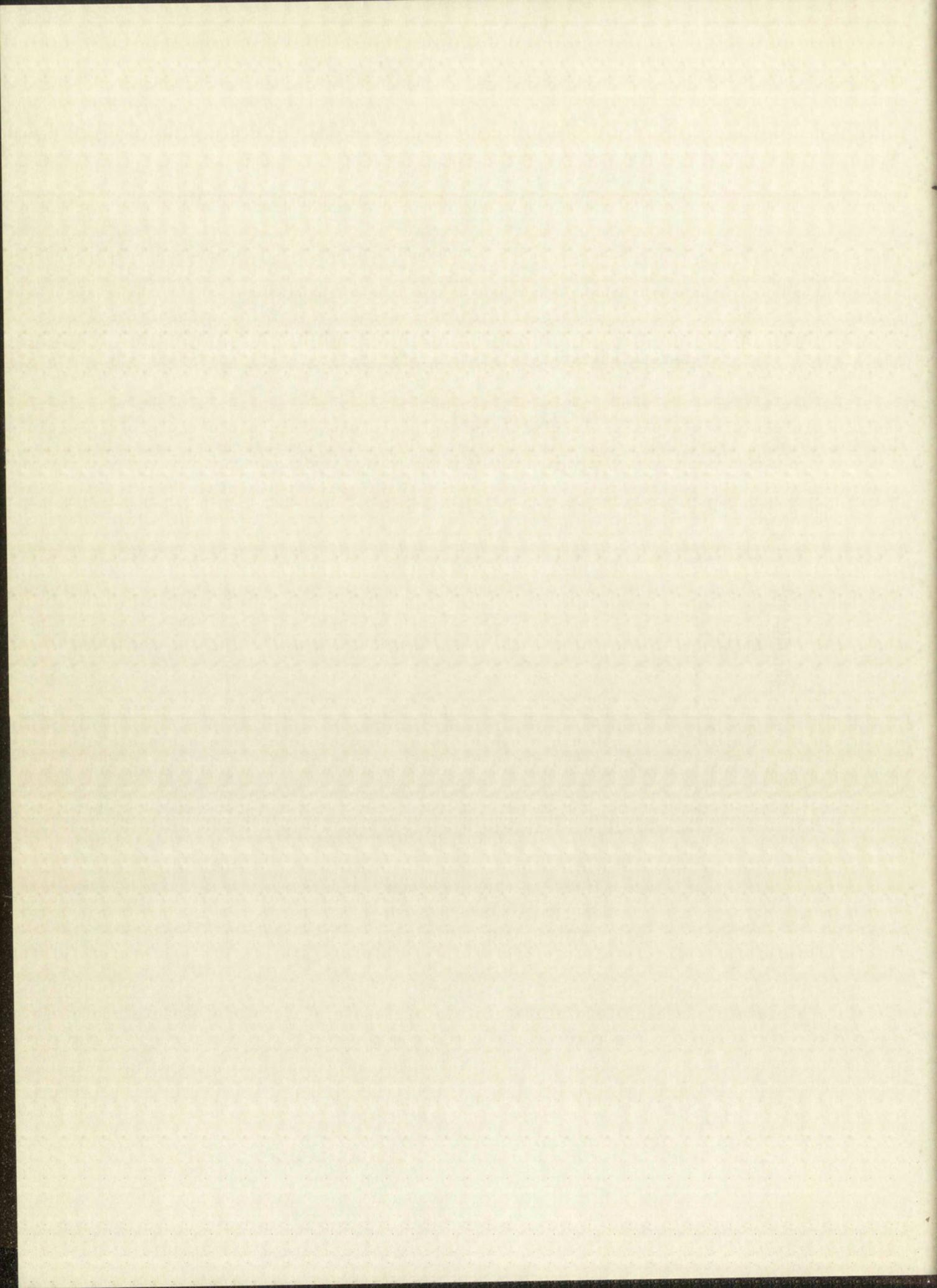


Figure 4.1.1

ABSORBANCE OF THE NEW SPECIES IN THE INFRARED REGION
AS A FUNCTION OF THE STOICHIOMETRIC CYANIDE CONCENTRATION







b = the equilibrium concentration of reactant B

a = the equilibrium concentration of A

a₀ = the initial concentration of A, in moles/liter

b₀ = the initial concentration of B, in moles/liter

N = the total initial concentration, i.e., a₀ + b₀, in moles/liter

c₁ = the equilibrium concentration of AB_n

c₂ = the equilibrium concentration of AB_{n+p}

c₃ = the equilibrium concentration of AB_{n+p+q};

the extinction coefficients as ϵ_1^λ , where the ϵ_1^λ 's correspond to the extinction coefficient for the specie, i, at wave length λ ; and a differential absorbance term as $D^\lambda = \frac{[A_{\text{obs}}^\lambda - \epsilon_a^\lambda N(1-x)]}{t}$, where t is the path length in cm.

Since a region of the spectrum is being considered in which reactant B (CN⁻) does not absorb, Katzin and Gebert's Equation (Equation 4.2.1), representing the locus of the values of $(\frac{x}{1-x})$ for which $\frac{dD^\lambda}{dx} = 0$, is valid.

$$\frac{x}{1-x} = n + \left[\frac{p[(\epsilon_{c_2} - \epsilon_a)c_2 + (\epsilon_{c_3} - \epsilon_a)c_3] + q(\epsilon_{c_3} - \epsilon_a)c_3}{(\epsilon_{c_1} - \epsilon_a)c_1 + (\epsilon_{c_2} - \epsilon_a)c_2 + (\epsilon_{c_3} - \epsilon_a)c_3} \right].$$

$$\left[1 + \frac{n(c_1 + c_2 + c_3) + p(c_2 + c_3) + qc_3}{N(1-x)} \right] -$$

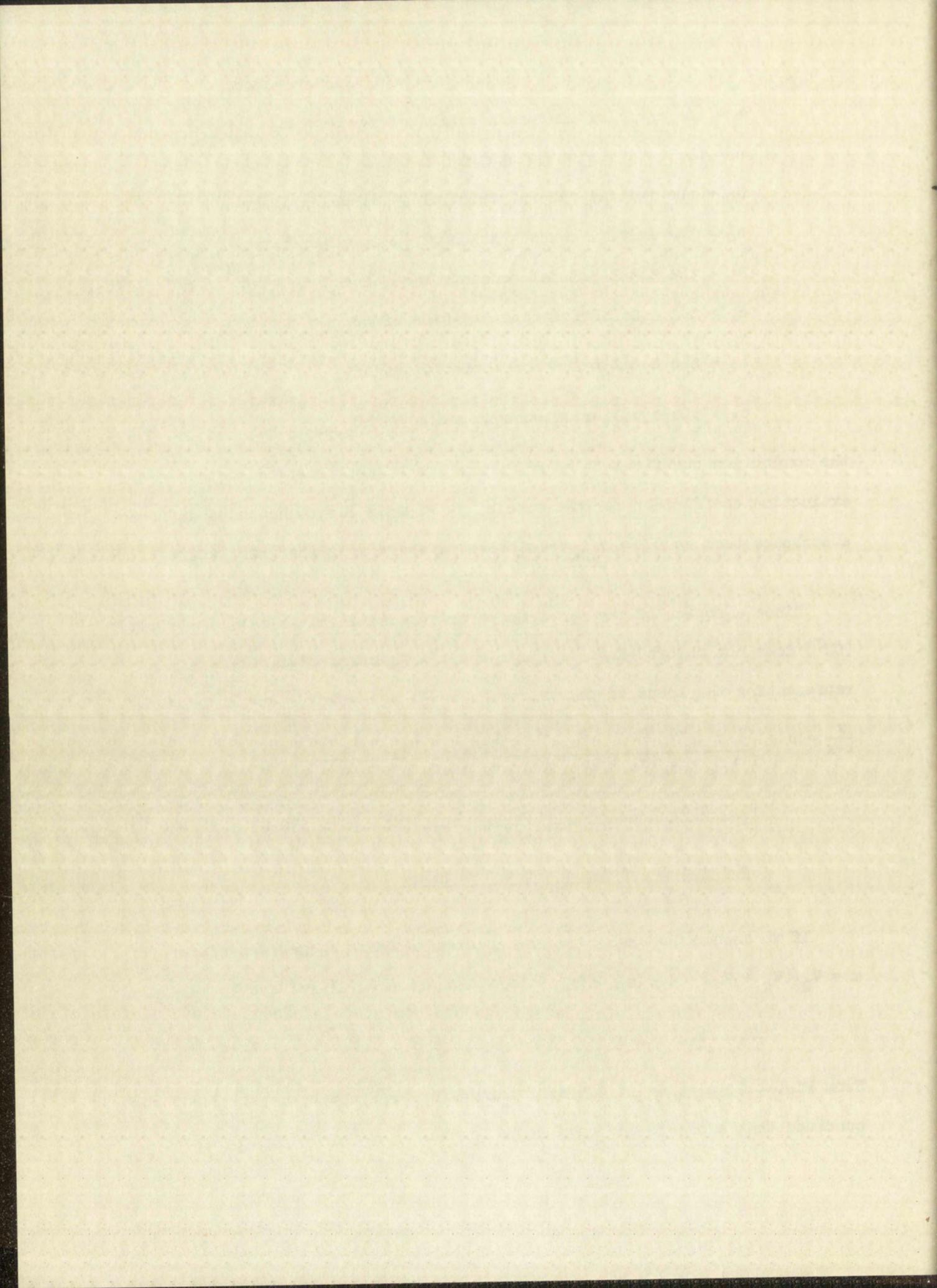
$$\frac{p(p+n)(c_2 + c_3) + q(q+n+2p)c_3}{N(1-x)}$$

4.2.1

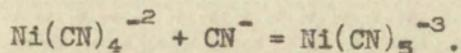
If we assume that only one new species is being formed and since $x = V_B / (V_A + V_B) = b_0 / (a_0 + b_0) = b_0 / N$, Equation 4.2.1 reduces to

$$\frac{b_0}{N} = \frac{n}{n+1}.$$

From Fig. 4.21, a value of 0.5 is obtained for b₀/N; hence n = 1. We then conclude that a one-to-one complex is formed.

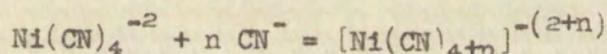


Data similar to that in Fig. 4.2.1 were collected from 3800 Å to 6000 Å at 100 Å intervals. In all cases the maximum was reached at a value of n corresponding to the reaction:



If more than one new species is formed, the position and number of maxima and minima, as determined by Equation 4.2.1, will depend upon the concentrations and extinction coefficients of the new species. Katzin and Gebert⁽¹¹⁾ discuss the situations arising from various relationships of the extinction coefficients of the new species.

4.2.2 Logarithmic Treatment: An alternate method for characterization of the new species in the visible region may be used. If one assumes the general reaction



and since the cyanide ion does not absorb in the region of the spectra being considered, then the following equations may be written:

$$[c] = [a][b]^n K \quad 4.2.2$$

$$[a] = a_0 - [c] \quad 4.2.3$$

$$\frac{A_{\text{obs}}^\lambda}{t} = [a]\epsilon_a^\lambda + [c]\epsilon_c^\lambda \quad 4.2.4$$

where the symbols are the same as used in Section 4.2.1.

Substitution of Equation 4.2.3 in Equation 4.2.4 yields:

$$D^\lambda = \left(\frac{A_{\text{obs}}^\lambda}{t} - a_0\epsilon_a^\lambda \right) = [c](\epsilon_c^\lambda - \epsilon_a^\lambda)$$

or upon substituting Equation 4.2.2

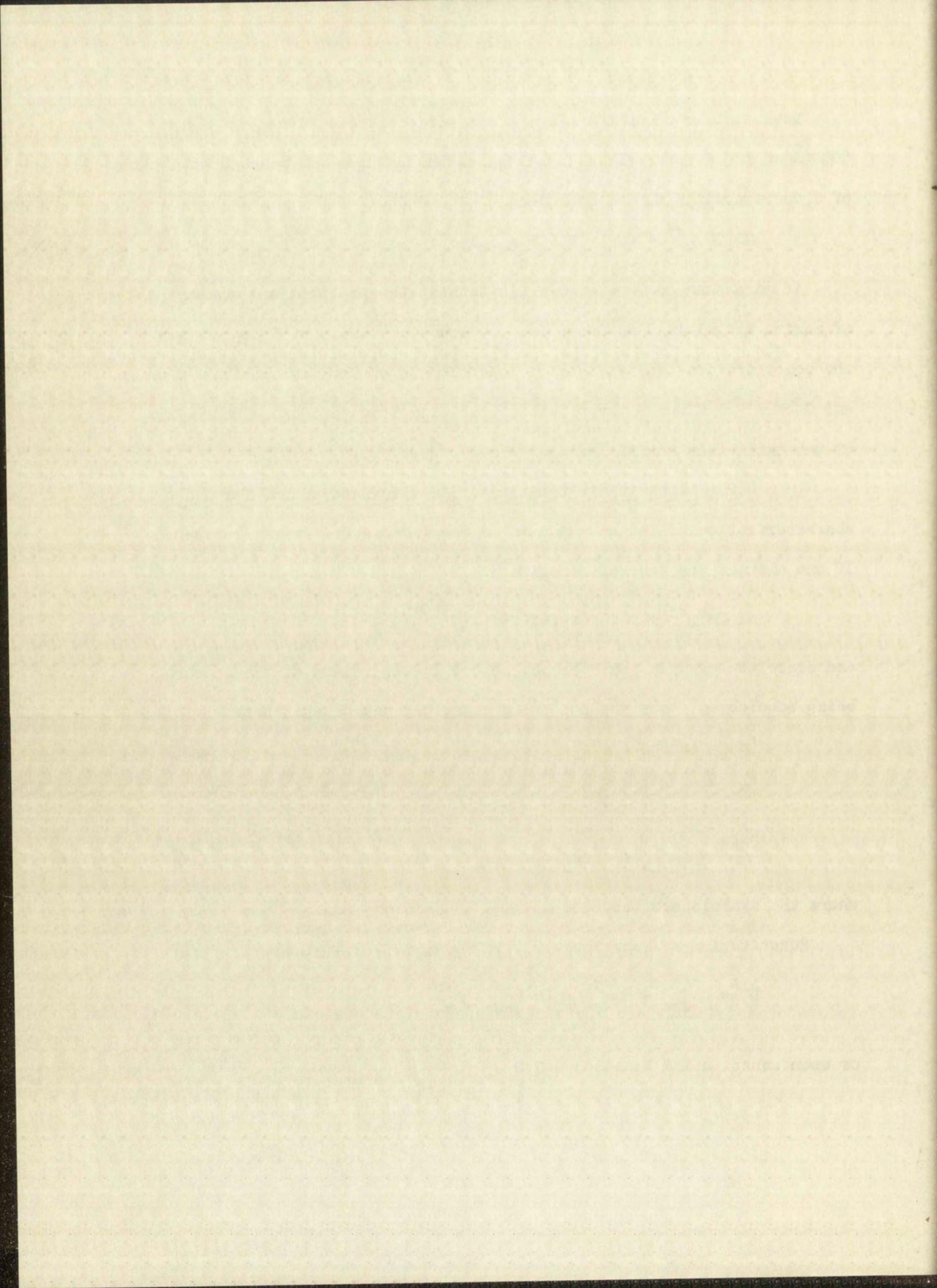
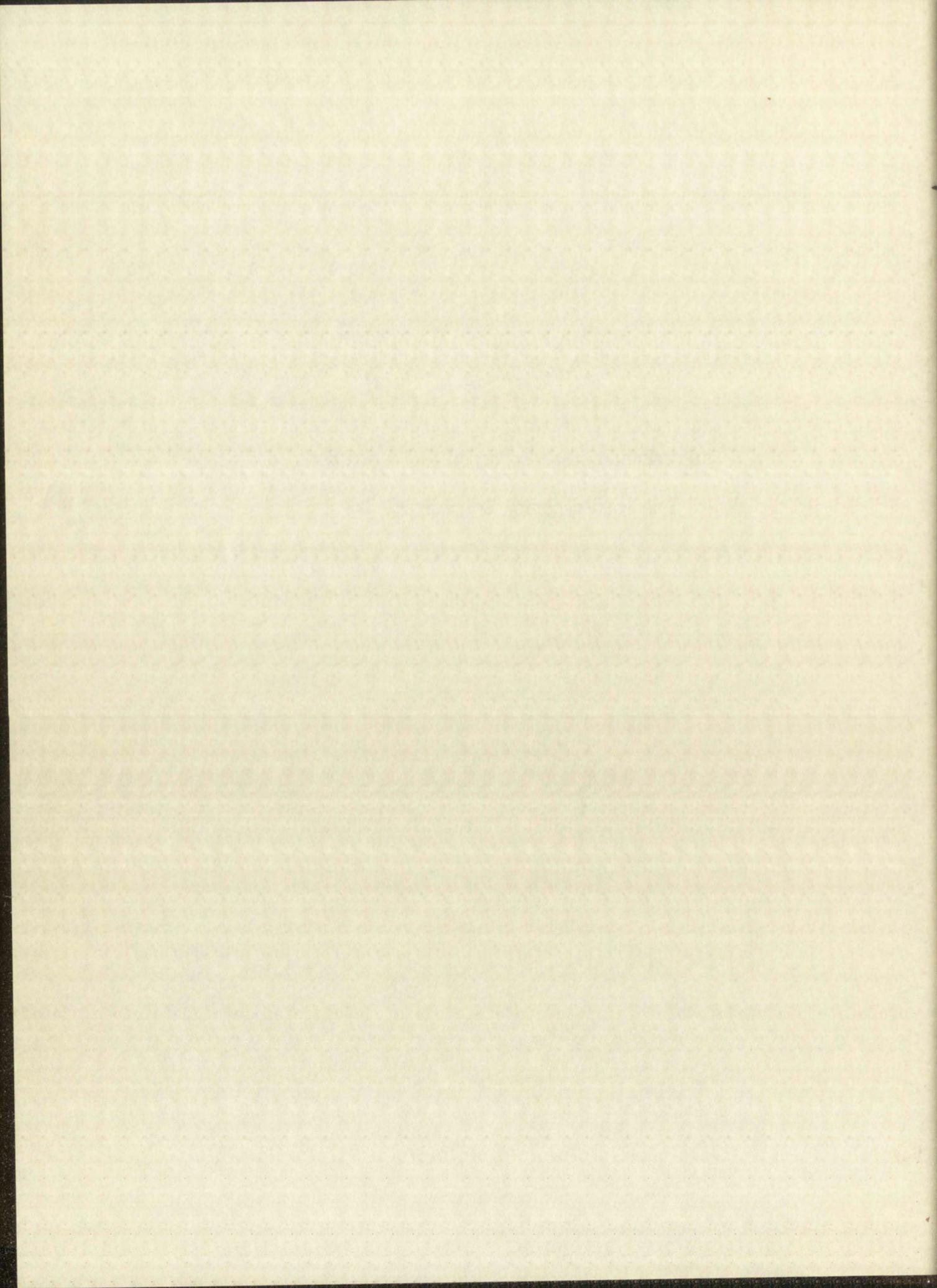
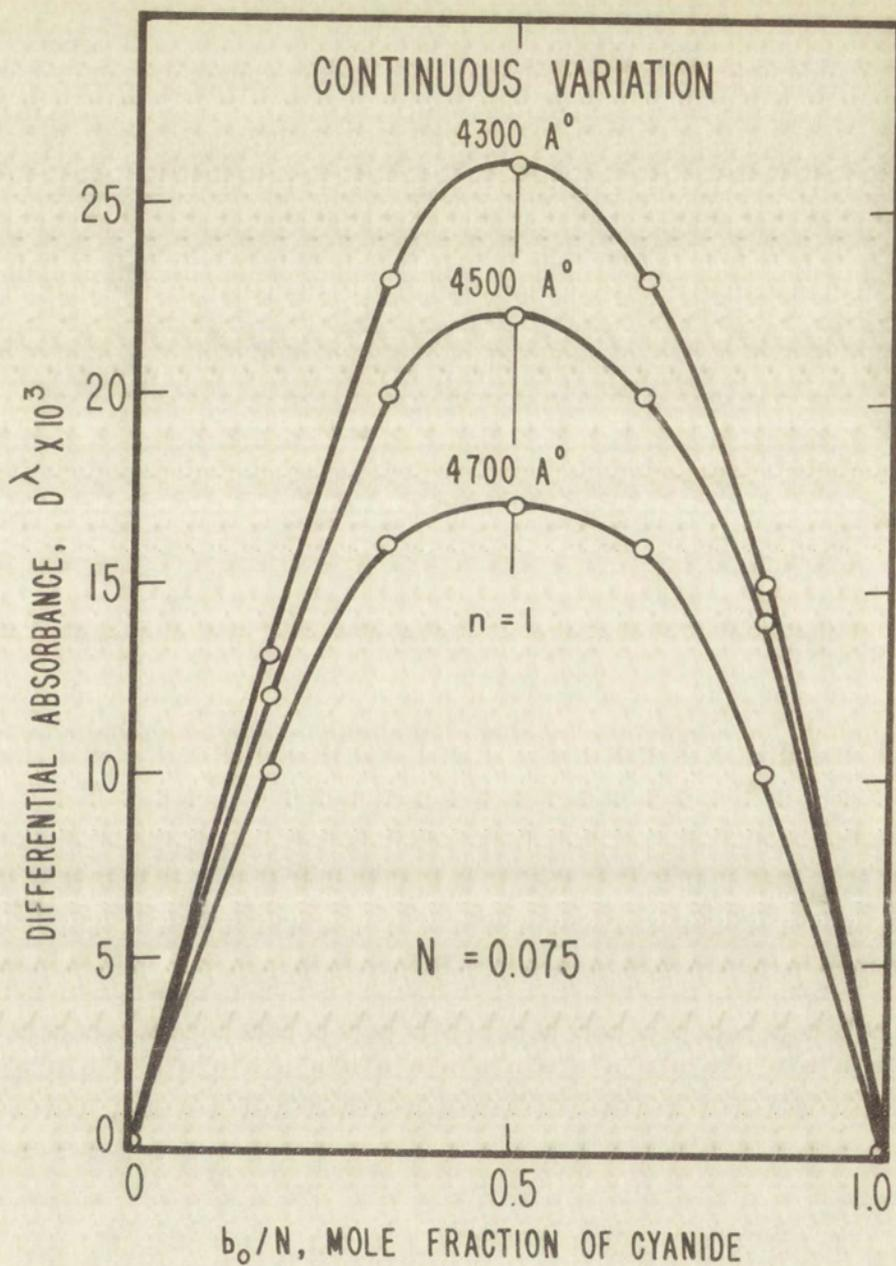
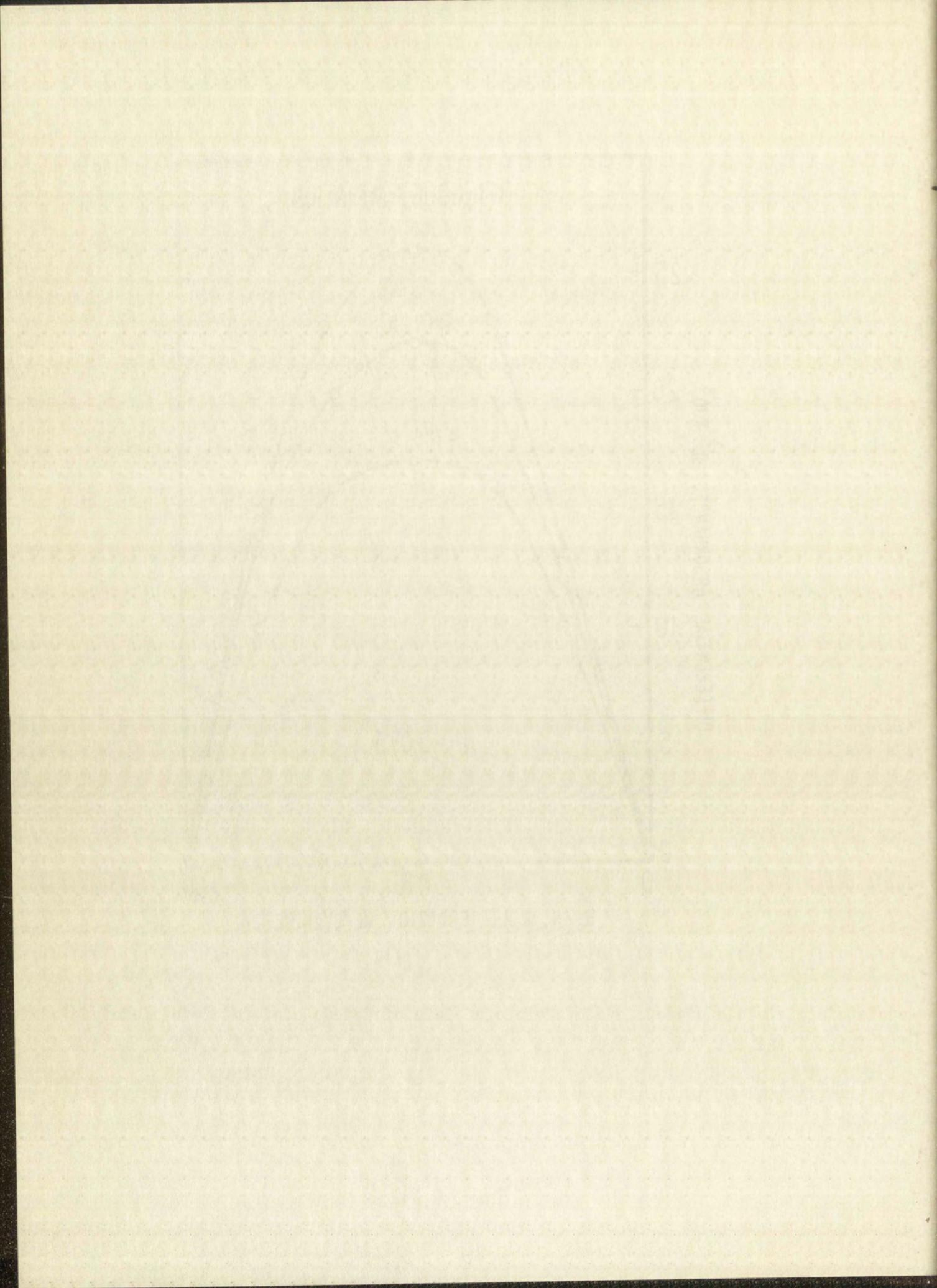


Figure 4.2.1

DIFFERENTIAL ABSORBANCE, D^λ , AS A FUNCTION
OF MOLE FRACTION OF CYANIDE, $\frac{b_0}{N}$







$$D^\lambda = [a][b]^n K(\epsilon_c^\lambda - \epsilon_a^\lambda)$$

$$\frac{D^\lambda}{[a]} = [b]^n K(\epsilon_c^\lambda - \epsilon_a^\lambda) . \quad 4.2.5$$

Taking the \log_{10} of Equation 4.2.5 yields

$$\log_{10}\left[\frac{D^\lambda}{[a]}\right] = n \log_{10}[b] + \log_{10}K(\epsilon_c^\lambda - \epsilon_a^\lambda) . \quad 4.2.6$$

Now we make two approximations,

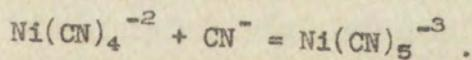
$$\log_{10}\left[\frac{D^\lambda}{[a]}\right] \approx \log_{10}\left[\frac{D^\lambda}{[a_0]}\right] \quad 4.2.7$$

and $\log_{10}(b) \approx \log_{10}(b_0) . \quad 4.2.8$

Thus $\log_{10}\left[\frac{D^\lambda}{[a_0]}\right] \approx n \log_{10}(b_0) + \log_{10}K(\epsilon_c^\lambda - \epsilon_a^\lambda) . \quad 4.2.9$

The values for eight solutions observed at three wave lengths in the visible region are tabulated in Table 4.2.2.

If $\log_{10}(b_0)$ is treated as an independent variable and $\log_{10}(D^\lambda/[a_0])$ is treated as a dependent variable, a plot of Equation 4.2.9 should yield a straight line with a slope of n and an intercept of $\log_{10}K(\epsilon_c^\lambda - \epsilon_a^\lambda)$. Fig. 4.2.2 gives such a plot at three different wave lengths. In the three cases, the slope is one, indicating once again the occurrence of the reaction:



It should be noted that the points in Fig. 4.2.2 which lie in the region of high cyanide ion concentration begin to fall away from the straight line of slope 1. This is to be expected, since the approximations involved in Equation 4.2.7 begin to break down. In this region the dependent variable should be $\log_{10}[D/a]$ instead of $\log_{10}[D/a_0]$. The proper correction may be applied by adding $\log_{10}[a_0/a]$ to $\log_{10}[D/a_0]$. The open circles on Fig. 4.2.2 represent the correction made using a value of 0.2 liters/mole for the equilibrium constant (see Section 5.0). The

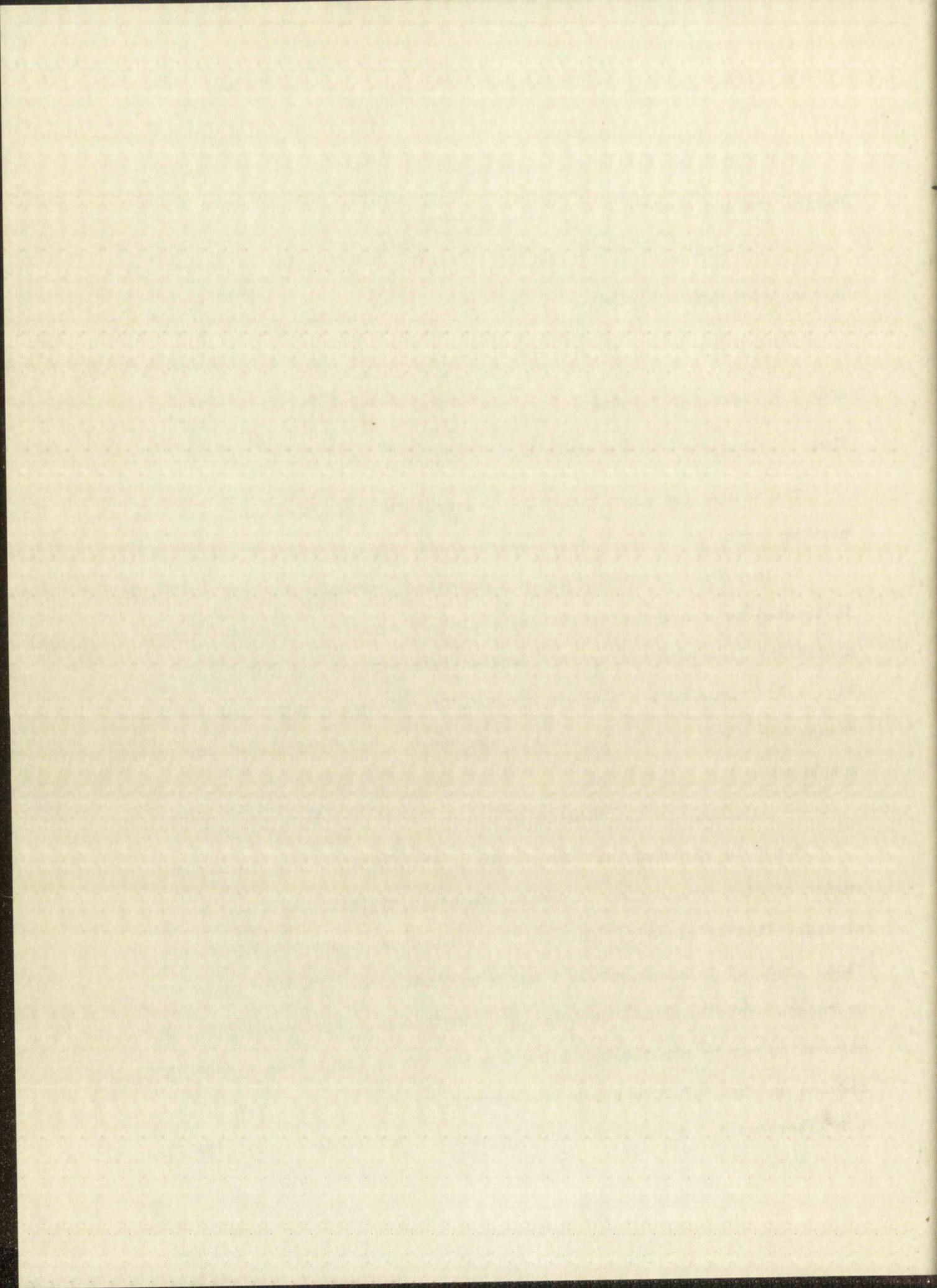


TABLE 4.2.2

LOGARITHMIC VALUES AT VARYING WAVE LENGTHS FOR THE EQUATION:

$$\log_{10}\left[\frac{D^\lambda}{a_0}\right] = n \log_{10}[b_0] + \log_{10}K(\epsilon_c^\lambda - \epsilon_a^\lambda)$$

a ₀ in moles/l.	b ₀ in moles/l.	log ₁₀ [b ₀]	log ₁₀ $\left[\frac{D^\lambda}{a_0}\right]$		
			4300 Å	4500 Å	4700 Å
0.1000	0.9653	-0.0153	-----	-----	1.4310
0.1000	0.7233	-0.1407	1.5379	1.4664	1.3160
0.1000	0.4816	-0.3175	1.3909	1.3263	1.1629
0.0800	0.03783	-1.422	0.3008	0.2317	0.1119
0.0800	0.03304	-1.481	0.2317	0.1646	0.0422
0.0800	0.02825	-1.549	0.1685	0.0990	-0.0232
0.0800	0.02348	-1.629	0.0899	0.0322	-0.0985
0.0800	0.01868	-1.729	0.0052	-0.054	-0.1762

The ionic strength was held constant at 1.33 by the addition of sodium perchlorate.

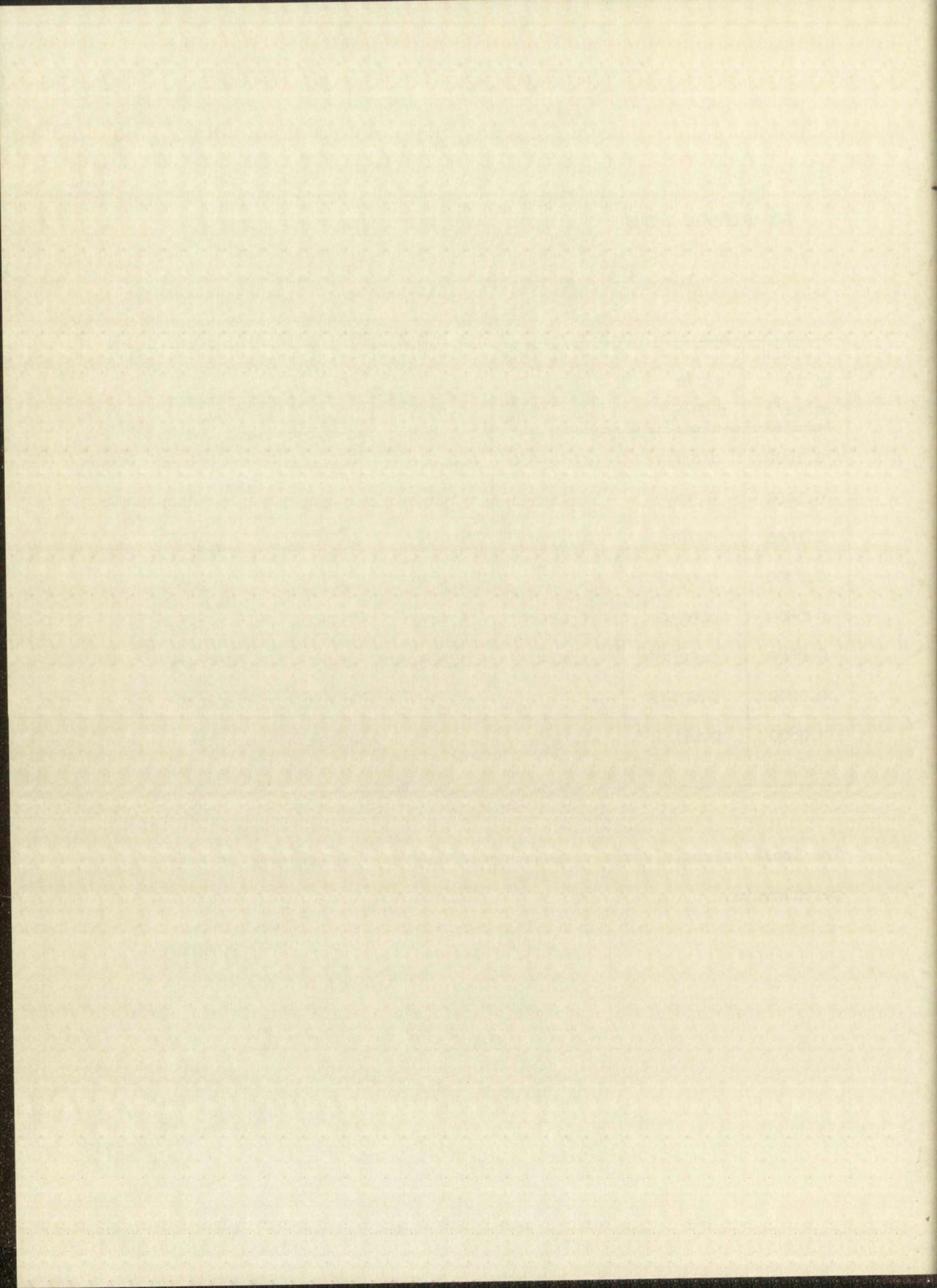
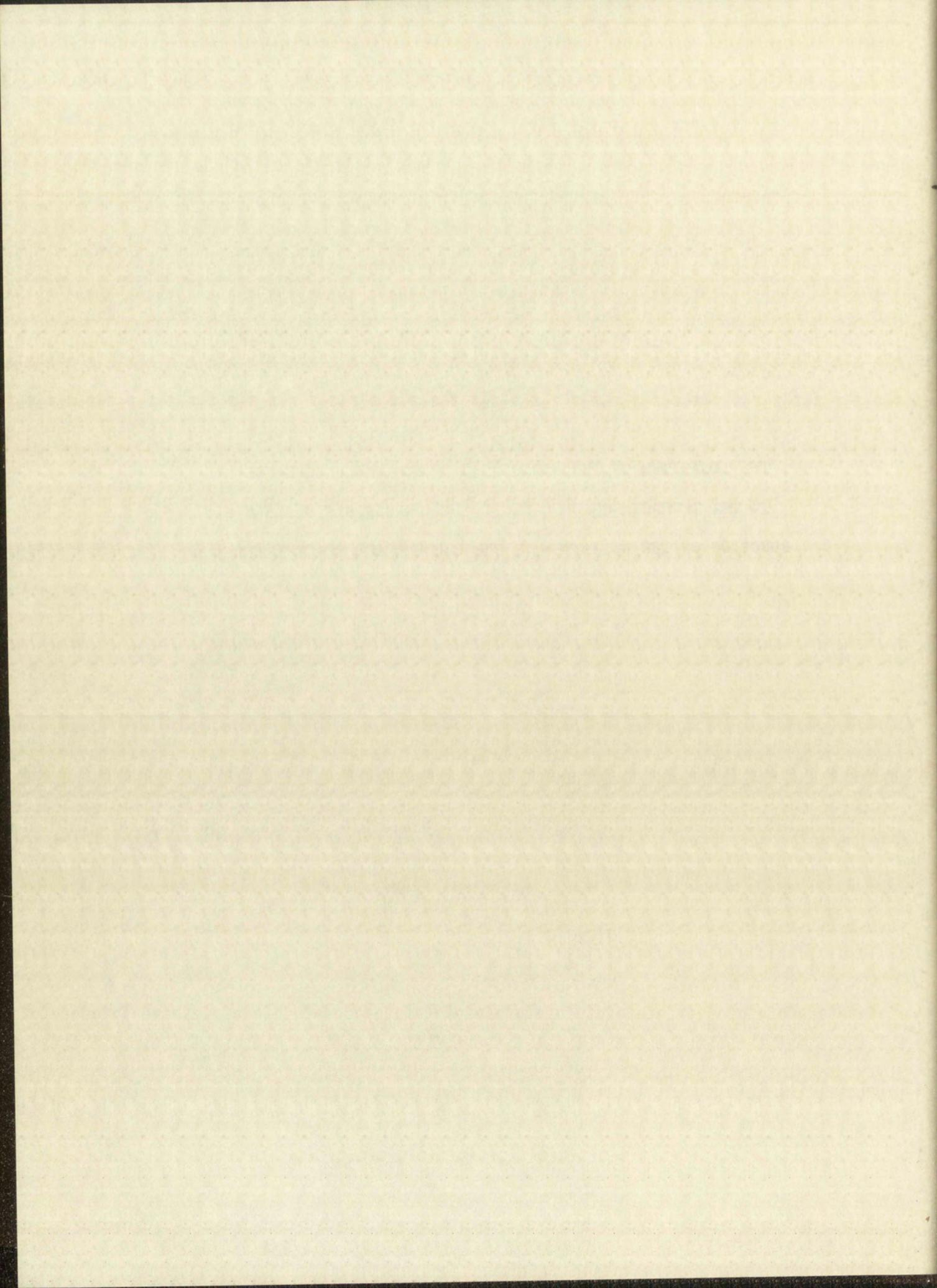
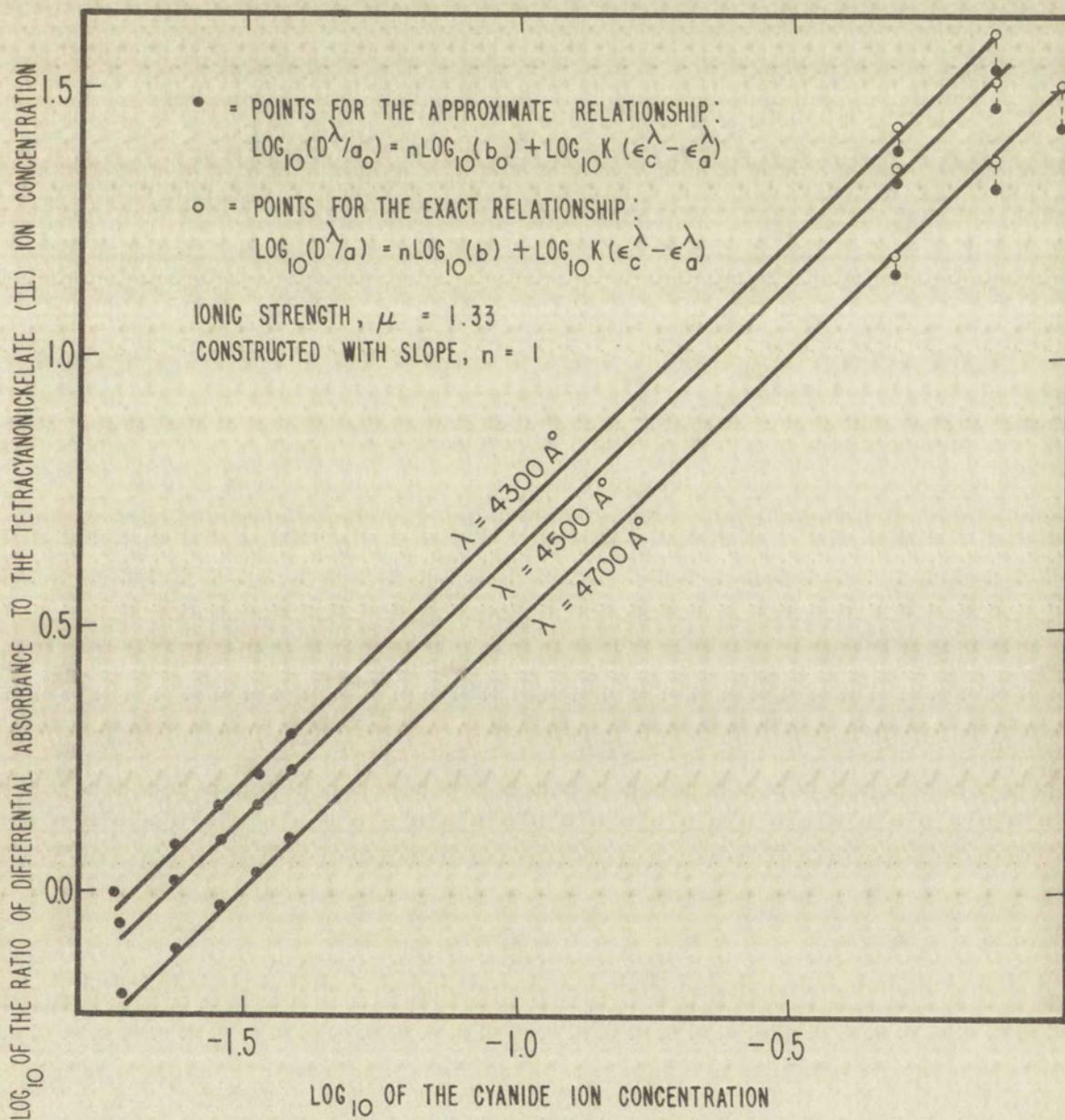
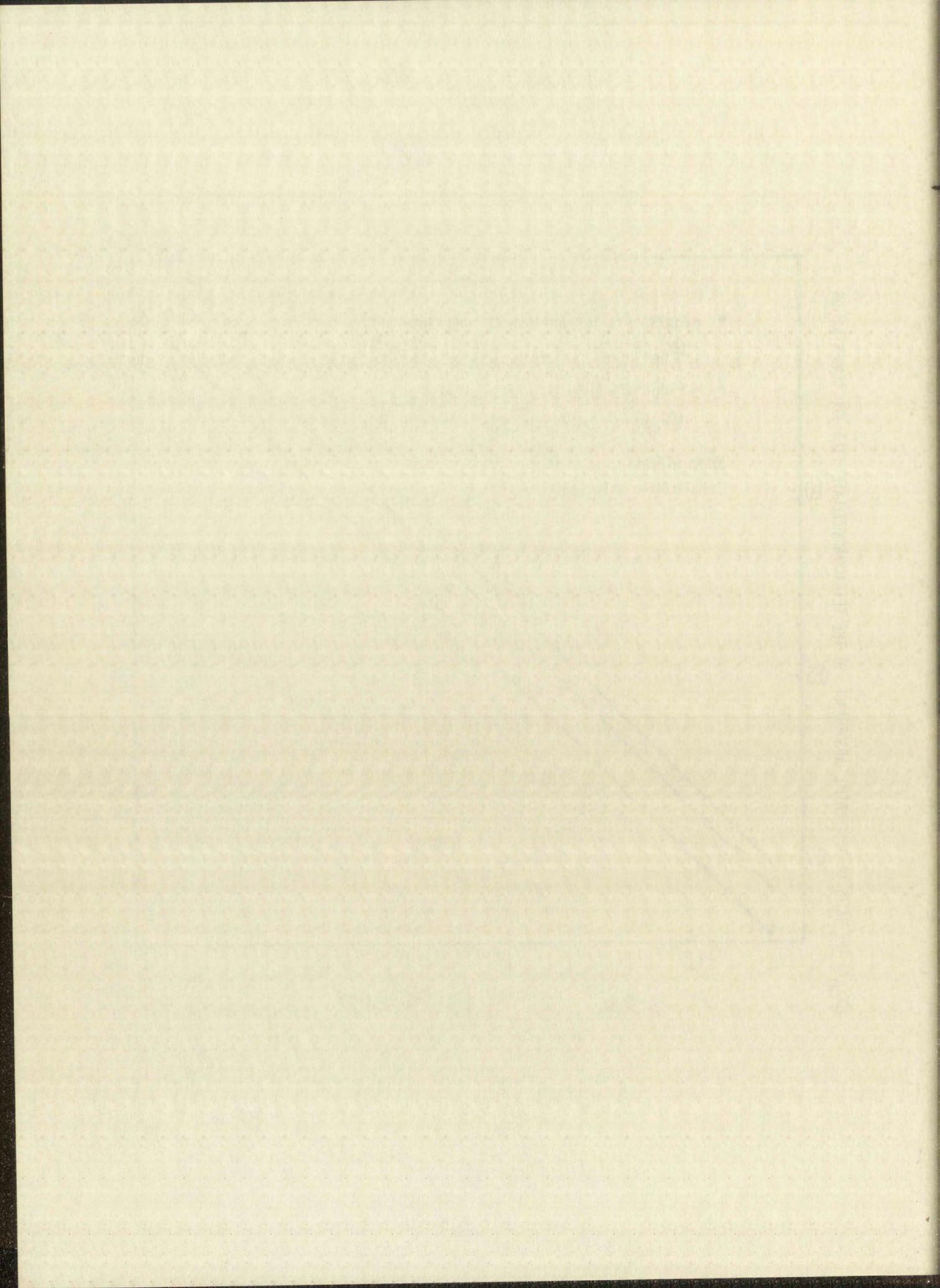


Figure 4.2.2

THE LOGARITHM OF THE RATIO OF DIFFERENTIAL ABSORBANCE
TO THE TETRACYANONICKELATE(II) ION CONCENTRATION AS A
FUNCTION OF THE LOGARITHM OF THE CYANIDE ION CONCENTRATION







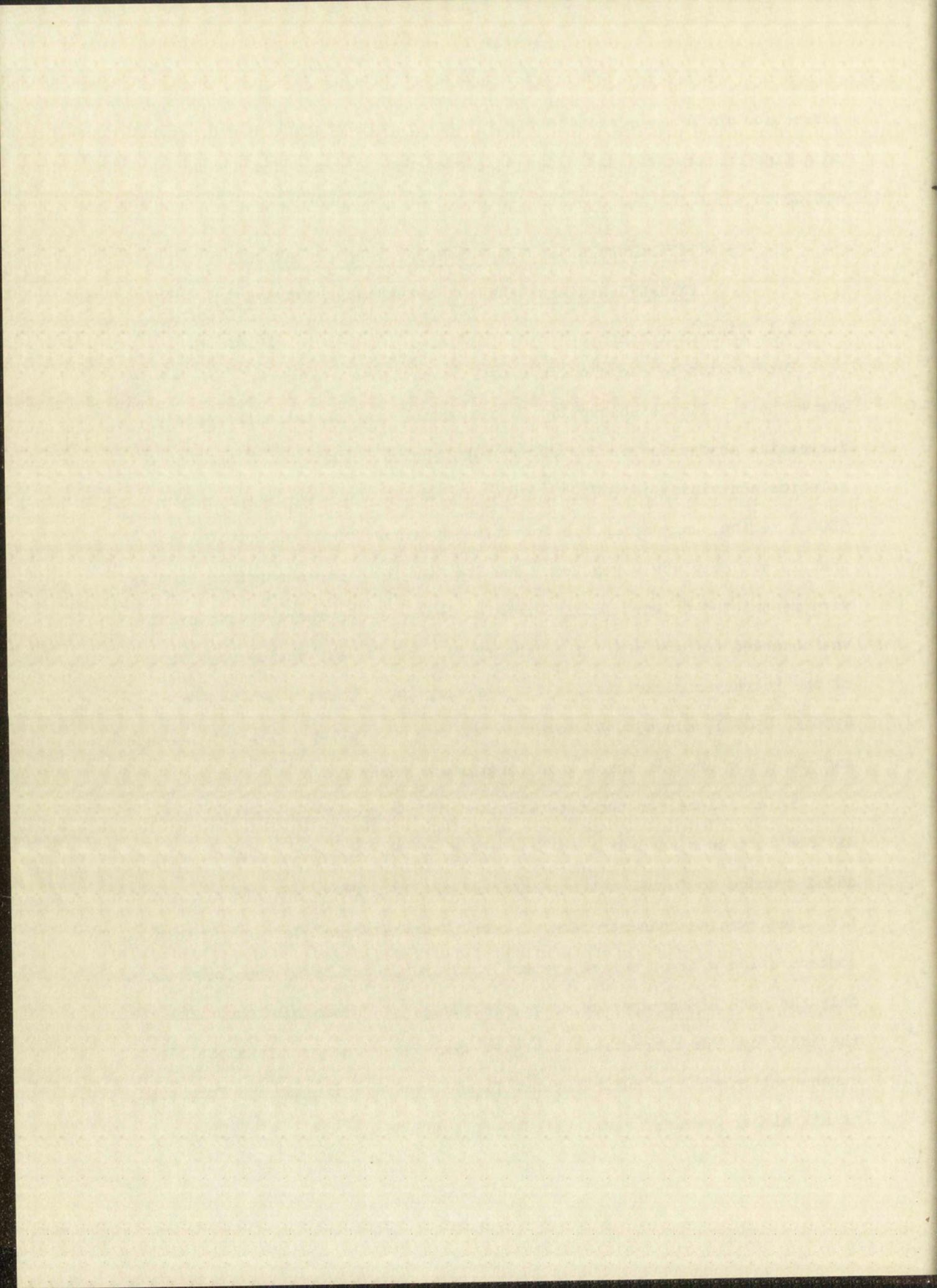
correction for $\log_{10} b_0$ term is negligible. The corrected values lie nicely on a line constructed with slope = 1, over the CN^- concentration range of ~ 0.02 to ~ 1.0 M.

5.0 DETERMINATION OF THE FORMATION CONSTANT AND MOLAR EXTINCTION COEFFICIENT OF PENTACYANONICKELATE(II)

5.1 Visible Region

Pure sodium tetracyanonickelate(II) solutions give smooth absorption curves having little absorption in the visible region but with rapidly increasing absorption in the ultraviolet region. Addition of NaCN to a solution containing $[\text{Ni}(\text{CN})_4]^{-2}$ gives an absorption hump in the 4000 - 5000 Å region, suggesting the formation of a new, broad absorption peak that is not completely resolved (see Fig. 2.3.1). The absorption studies were restricted to wave lengths greater than 4000 Å, where sodium cyanide was observed to have negligible absorption and the extinction coefficient of the tetracyanonickelate(II) ion was very low. Three wave lengths, 4700 Å, 4500 Å, and 4300 Å, covering the new absorption band, were selected and the absorbance at these wave lengths was observed.

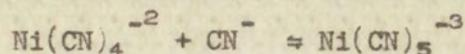
The solutions for the determination of the formation constant were divided into sets according to the ratios of the concentrations of the added cyanide to formal tetracyanonickelate(II). Those solutions in which the added cyanide concentration is less than the formal tetracyanonickelate(II) concentration will be called System I and are favorable to the formation of only the next higher species, e.g., $[\text{Ni}(\text{CN})_5]^{-3}$. Those solutions with the added cyanide concentration higher than the tetracyanonickelate(II) concentration will be called System II and are favorable to the formation of all higher species, e.g., $[\text{Ni}(\text{CN})_5]^{-3}$, $[\text{Ni}(\text{CN})_6]^{-4}$.



The equations giving the formation constant for the pentacyanonickelate(II) ion will be considered according to the ratio of the added cyanide ion concentration to the formal tetracyanonickelate(II) ion concentration, since the assumptions necessary in the derivation of the equations are dependent upon the concentration range in question.

5.1.1 System I:

For the reaction



one may write

$$[a][b]K = [c] \tag{5.1.1}$$

where

a = equilibrium concentration of $[\text{Ni}(\text{CN})_4]^{-2}$, moles/liter

b = equilibrium concentration of CN^- , moles/liter

c = equilibrium concentration of $[\text{Ni}(\text{CN})_5]^{-3}$, moles/liter

K = formation constant, liter/mole.

For System I $a_0 > b_0$, where the zero subscript refers to the formal concentration initially added. Let

$$a \approx a_0 \tag{5.1.2}$$

$$b = b_0 - c \tag{5.1.3}$$

Hence

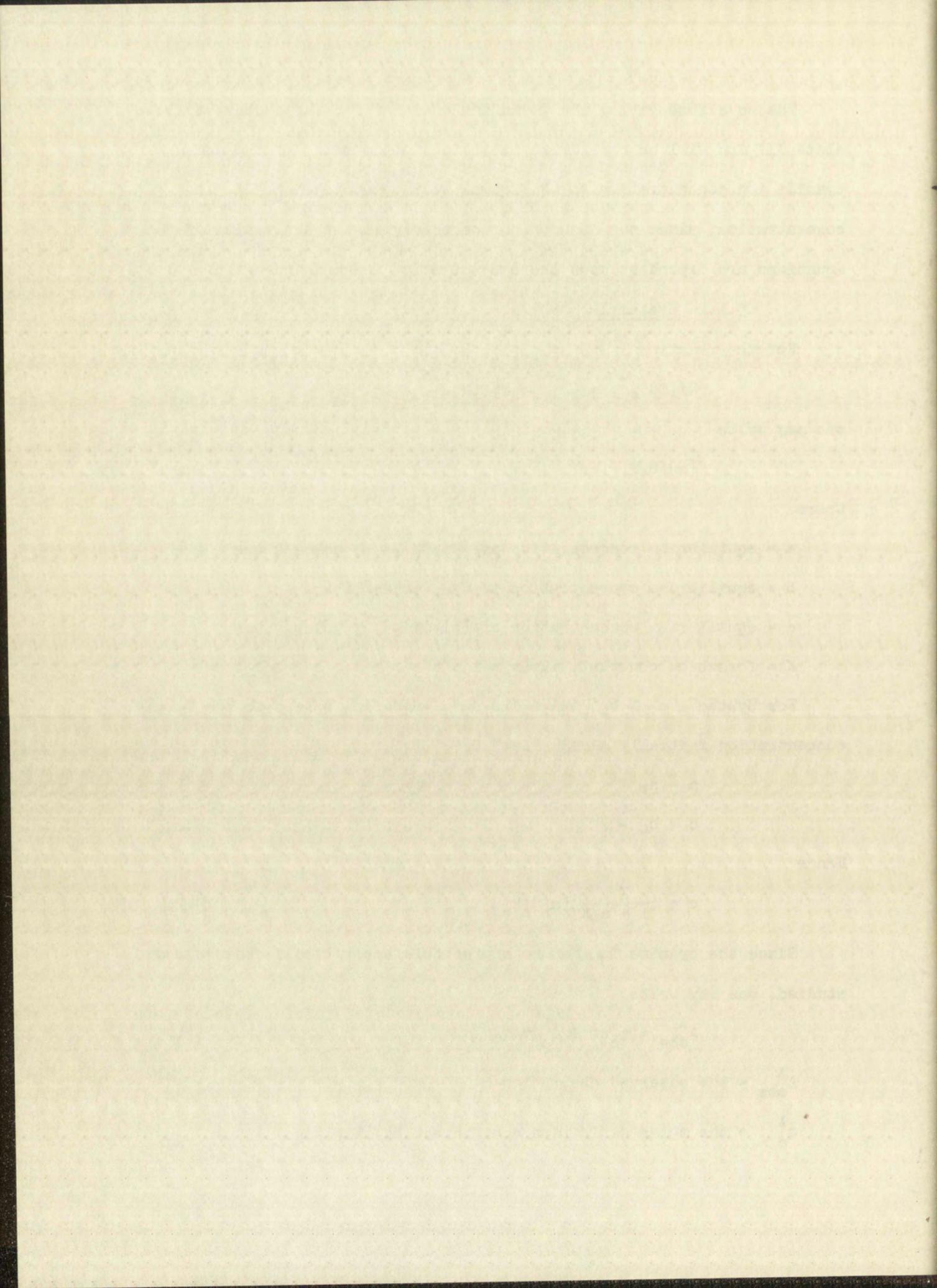
$$c \approx \left[\frac{K}{1 + a_0 K} \right] [a_0] [b_0] \tag{5.1.4}$$

Since the cyanide ion has no appreciable absorption in the regions studied, one may write

$$A_{\text{obs}}^\lambda = \epsilon_c^\lambda ct + \epsilon_a^\lambda at \tag{5.1.5}$$

A_{obs}^λ = the observed absorption at λ

ϵ_c^λ = the molar extinction coefficient of $[\text{Ni}(\text{CN})_5]^{-3}$ at λ



ϵ_a^λ = the molar extinction coefficient of $[\text{Ni}(\text{CN})_4]^{-2}$ at λ

t = the path length of the cell in cm.

Equation 5.1.5 may be rearranged to

$$\frac{A_{\text{obs}}^\lambda}{t} = \epsilon_c^\lambda c + \epsilon_a^\lambda a \quad 5.1.6$$

On substitution of Equation 5.1.2 for a and Equation 5.1.4 for c , one obtains after rearrangement

$$\left[\frac{A_{\text{obs}}^\lambda}{t} \right] - a_0 \epsilon_a^\lambda \approx \epsilon_c^\lambda \left[\frac{K}{1 + a_0 K} \right] [a_0] [b_0] \quad 5.1.7$$

If the quantity, $(A_{\text{obs}}^\lambda/t) - a_0 \epsilon_a^\lambda$, is defined as D^λ , then Equation 5.1.7 may be written as

$$\frac{D^\lambda}{a_0 b_0} \approx \epsilon_c^\lambda K - \left[\frac{K D^\lambda}{b_0} \right] = K \left[\epsilon_c^\lambda - \frac{D^\lambda}{b_0} \right] \quad 5.1.8$$

The tabulations of the quantity $\frac{D^\lambda}{a_0 b_0}$ in Tables B.5 through B.7 of the Appendix show that for System I $\frac{D^\lambda}{a_0 b_0}$ is essentially independent of the cyanide concentration, b_0 , but dependent upon the wave length. Since a_0 varies from 0.1 to 0.06, this constancy would imply that $\frac{D^\lambda}{b_0} \ll \epsilon_c^\lambda$, $\epsilon_c^\lambda - \frac{D^\lambda}{b_0} \approx \epsilon_c^\lambda$, and hence that $\frac{D^\lambda}{a_0 b_0} = \epsilon_c^\lambda K$ is a good approximation. Fig. 5.1.1 gives a typical plot of D^λ as a function of $a_0 b_0$.

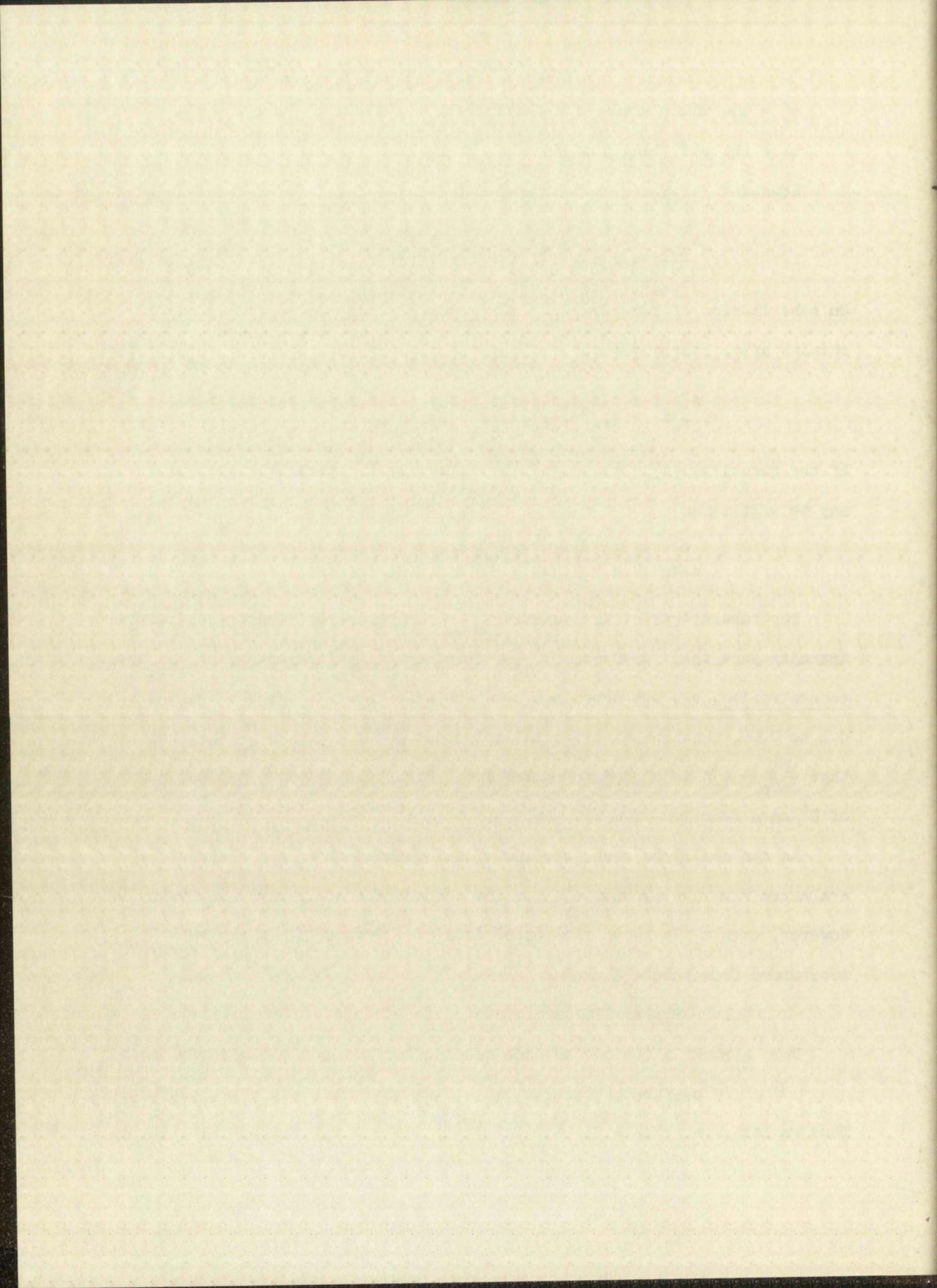
As can easily be seen, the individual values of ϵ_c^λ and K cannot be evaluated from the product $\epsilon_c^\lambda K$ for the concentrations involved in System I. However, once ϵ_c^λ is known from other data (see System II), K can be determined from this $\epsilon_c^\lambda K$ product.

5.1.2 System II:

For System II (Using the same meaning for the symbols as in System I),

$$a_0 < b_0 \quad 5.1.9$$

Thus we let $a = a_0 - c$ 5.1.10



$$b \approx b_0 \quad 5.1.11$$

$$c = \left[\frac{K}{1 + b_0 K} \right] [a_0] [b_0]. \quad 5.1.12$$

Since CN^- does not absorb in the region of the spectrum considered, Equation 5.1.5 is again valid. Substitution of Equation 5.1.10 for \underline{a} and Equation 5.1.12 for \underline{c} yields

$$\frac{A_{obs}^\lambda}{t} = (\epsilon_c^\lambda - \epsilon_a^\lambda) \left[\frac{K}{1 + b_0 K} \right] [a_0] [b_0] + \epsilon_a^\lambda a_0. \quad 5.1.13$$

Rearrangement gives

$$D^\lambda = \left(\frac{A_{obs}^\lambda}{t} - a_0 \epsilon_a^\lambda \right) = (\epsilon_c^\lambda - \epsilon_a^\lambda) \left(\frac{K}{1 + b_0 K} \right) [a_0] [b_0] \quad 5.1.14$$

or

$$\frac{a_0 b_0}{D^\lambda} = \frac{b_0}{(\epsilon_c^\lambda - \epsilon_a^\lambda)} + \frac{1}{K(\epsilon_c^\lambda - \epsilon_a^\lambda)}. \quad 5.1.15$$

Fig. 5.1.2 is a typical representation of the variables in Equation 5.1.15.

5.1.3 Statistical Treatment of the Data:

If the following identifications are made,

$$y = \frac{a_0 b_0}{D^\lambda} \quad 5.1.16$$

$$x = b_0 \quad 5.1.17$$

$$\beta = \frac{1}{(\epsilon_c^\lambda - \epsilon_a^\lambda)} \quad 5.1.18$$

$$\alpha = \frac{1}{K(\epsilon_c^\lambda - \epsilon_a^\lambda)} \quad 5.1.19$$

Equation 5.1.15 is the form of a straight line, $y = \beta x + \alpha$, with slope β and intercept α . Since the errors involved in the determination of b_0 are negligible as compared to the errors involved in the determination of $\frac{a_0 b_0}{D^\lambda}$, a linear regression analysis as discussed in Section A of the Appendix is applicable.

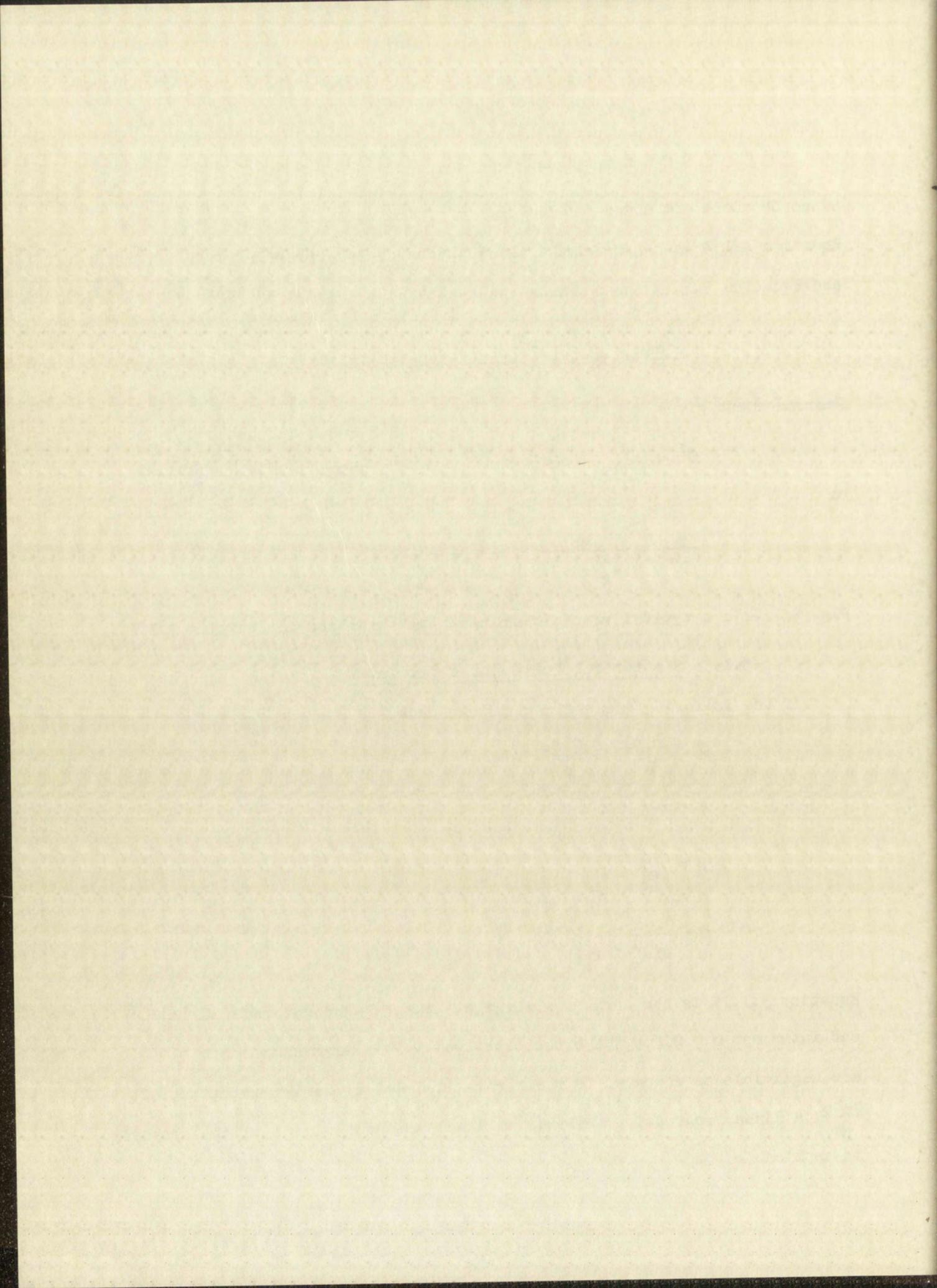
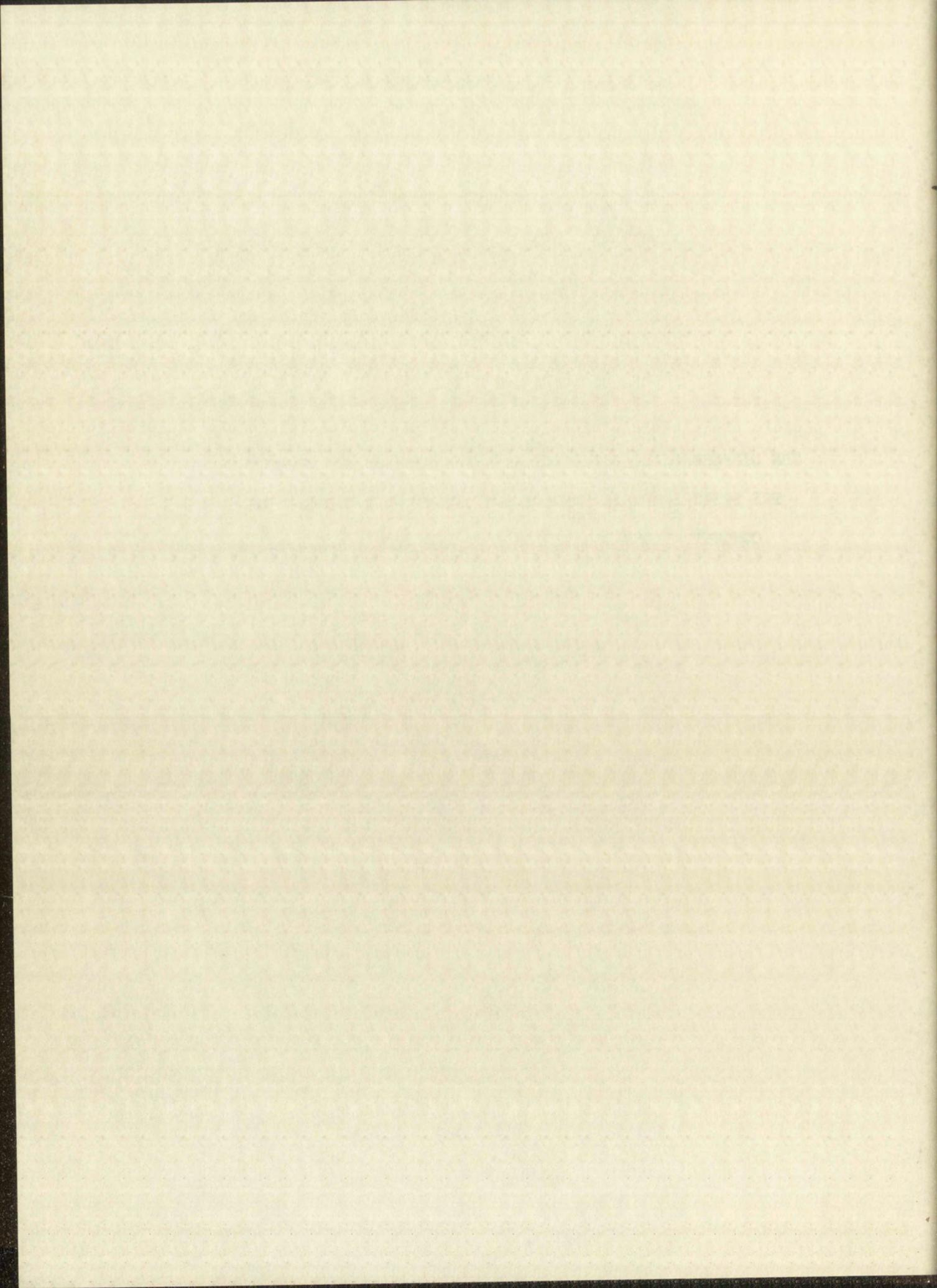
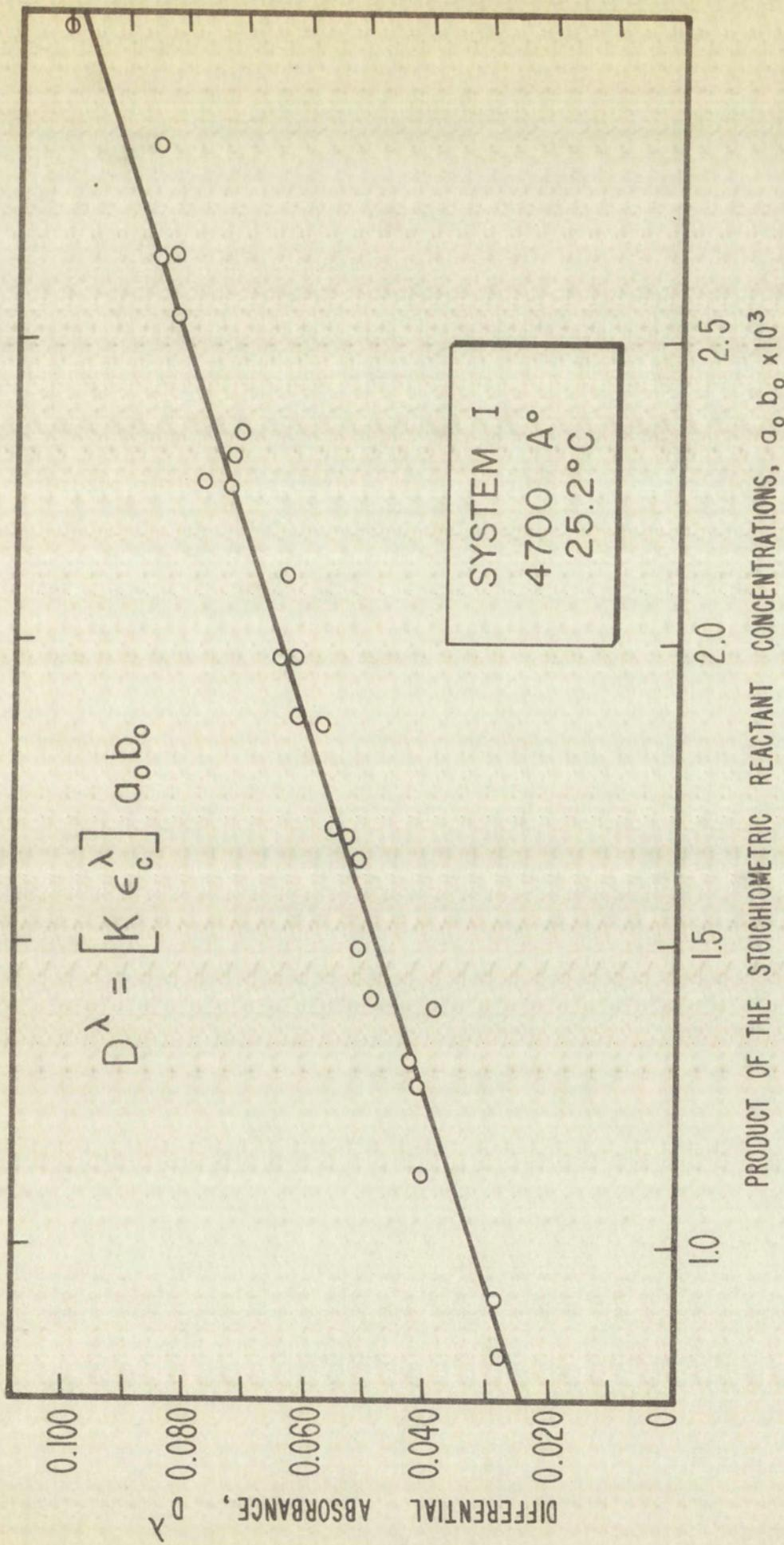


Figure 5.1.1

THE DIFFERENTIAL ABSORBANCE AS A FUNCTION OF THE PRODUCT OF
THE STOICHIOMETRIC TETRACYANONICKELATE(II) AND CYANIDE
CONCENTRATIONS FOR SYSTEM I AT $\lambda = 4700 \text{ \AA}$ AND 25.2°





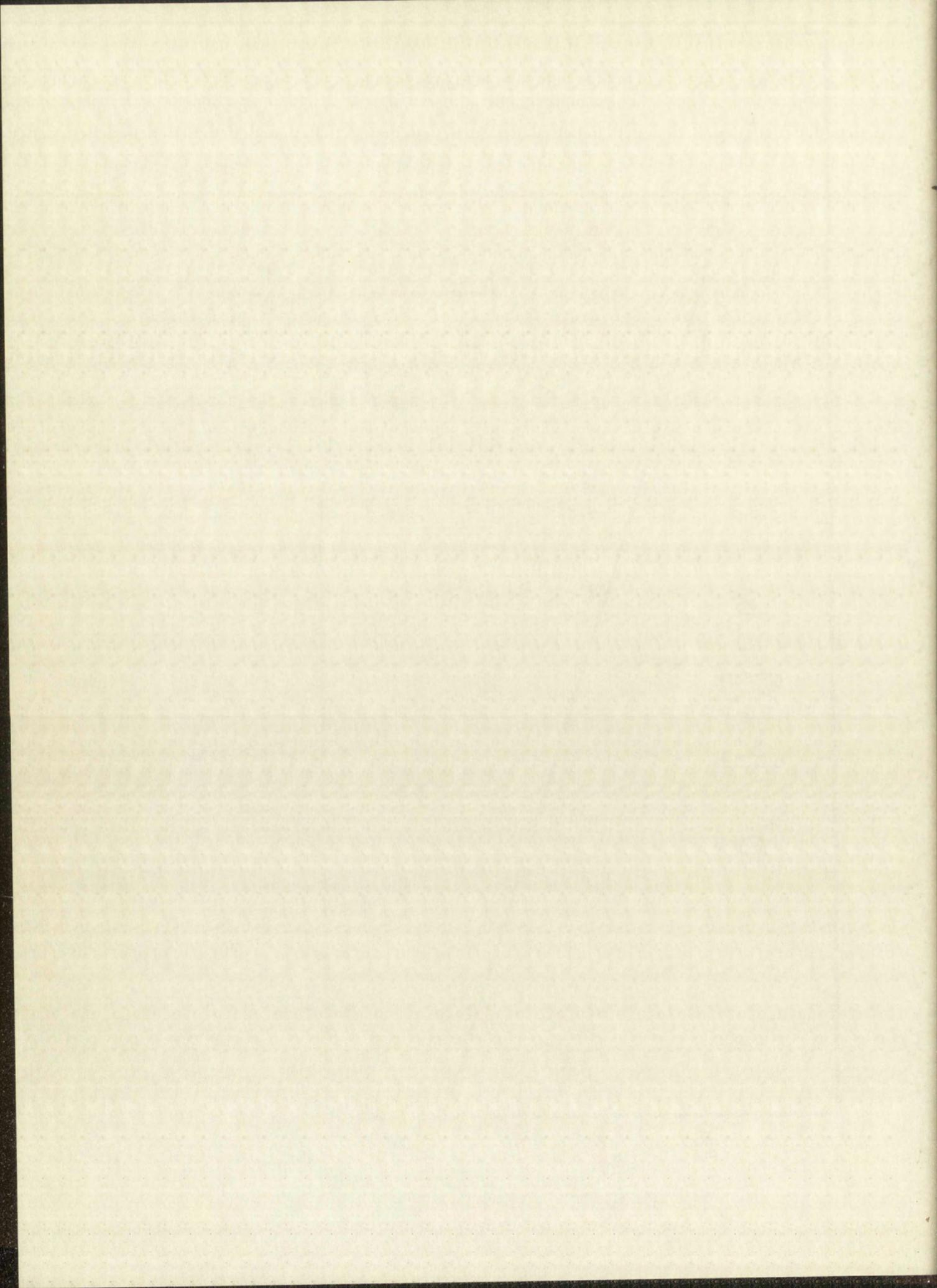
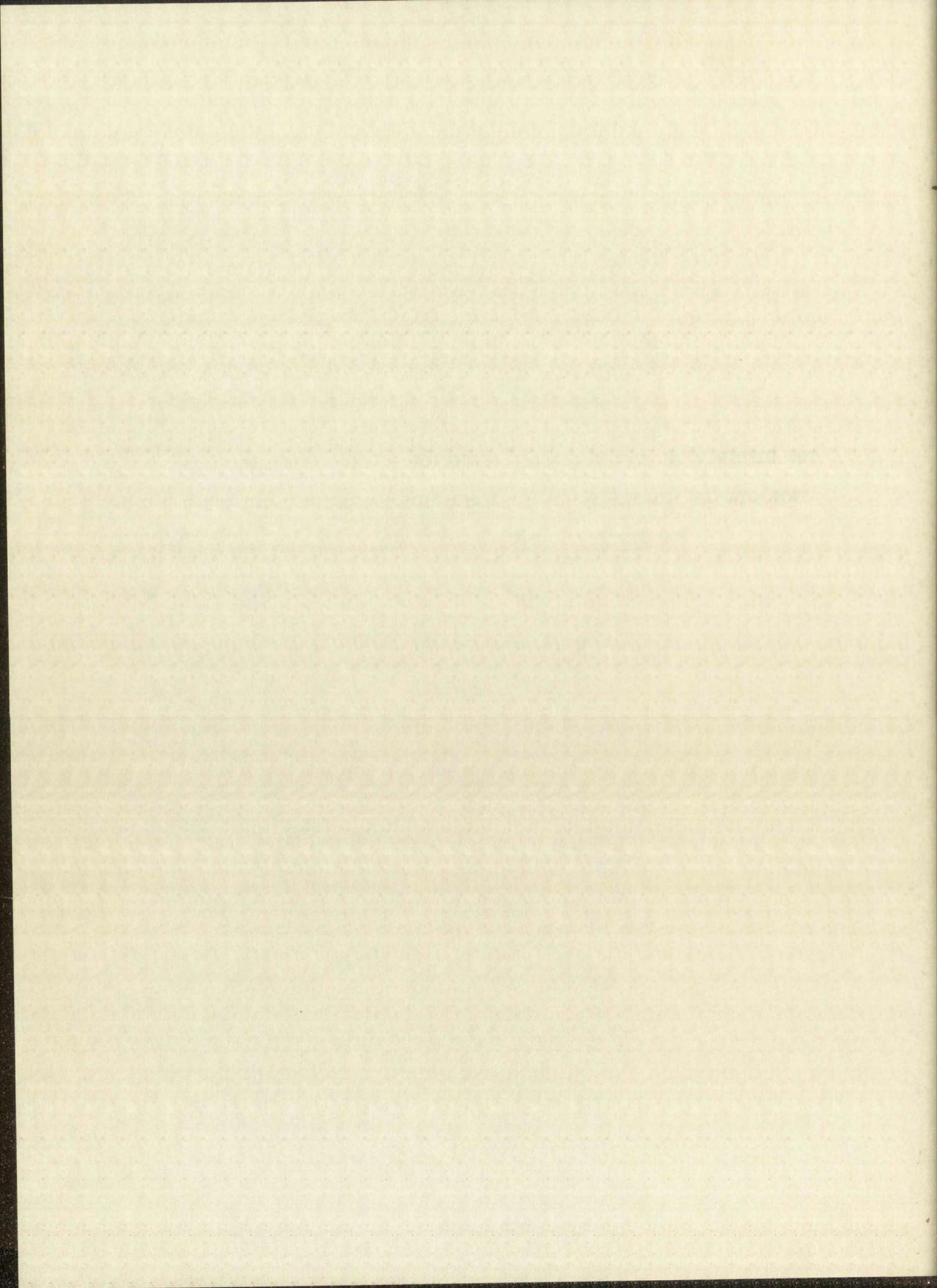
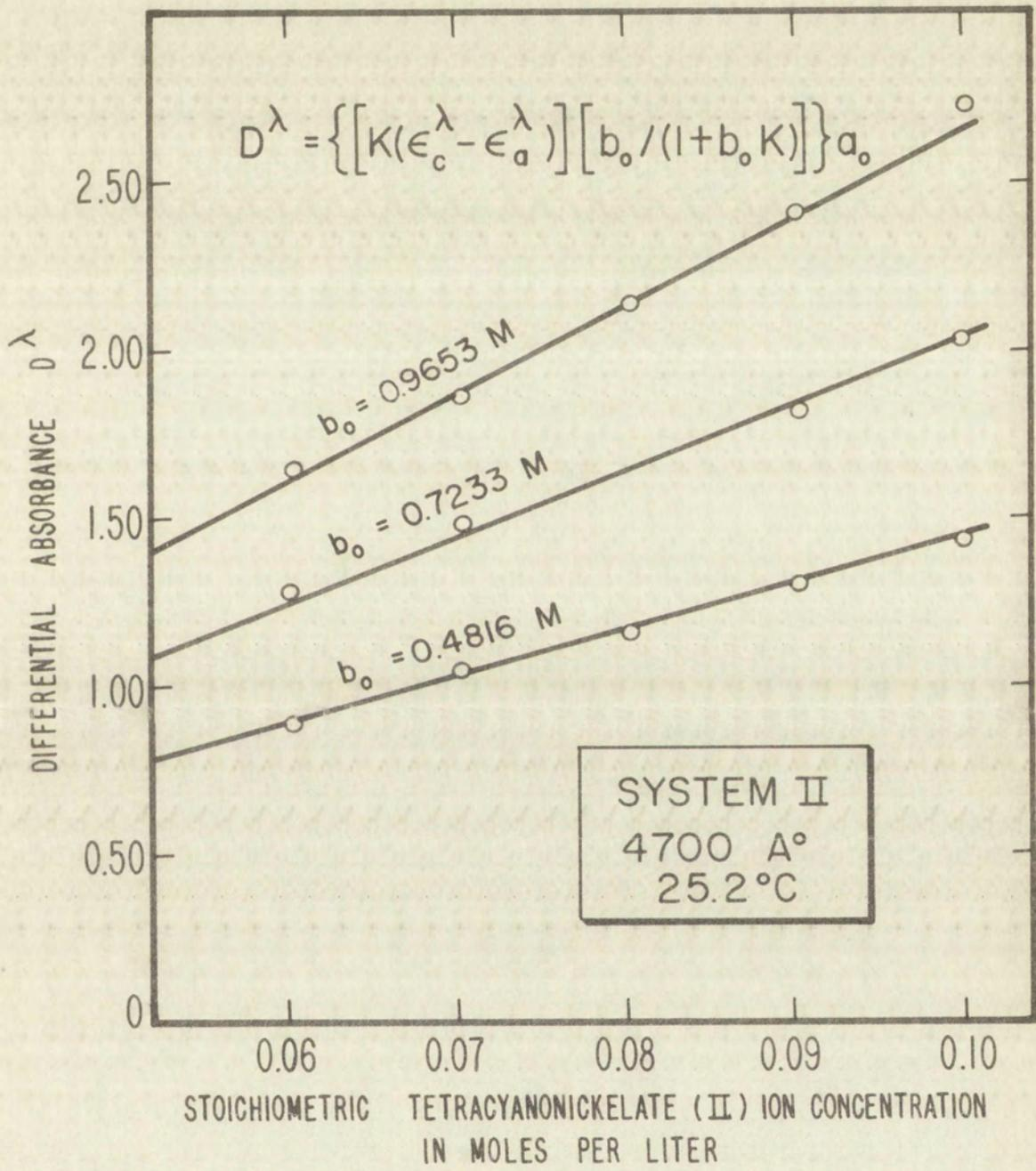


Figure 5.1.2

THE DIFFERENTIAL ABSORBANCE AS A FUNCTION OF THE STOICHIOMETRIC
TETRACYANONICKELATE(II) ION CONCENTRATION AT CONSTANT CYANIDE
FOR SYSTEM II AT $\lambda = 4700 \text{ \AA}$ AND 25.2°





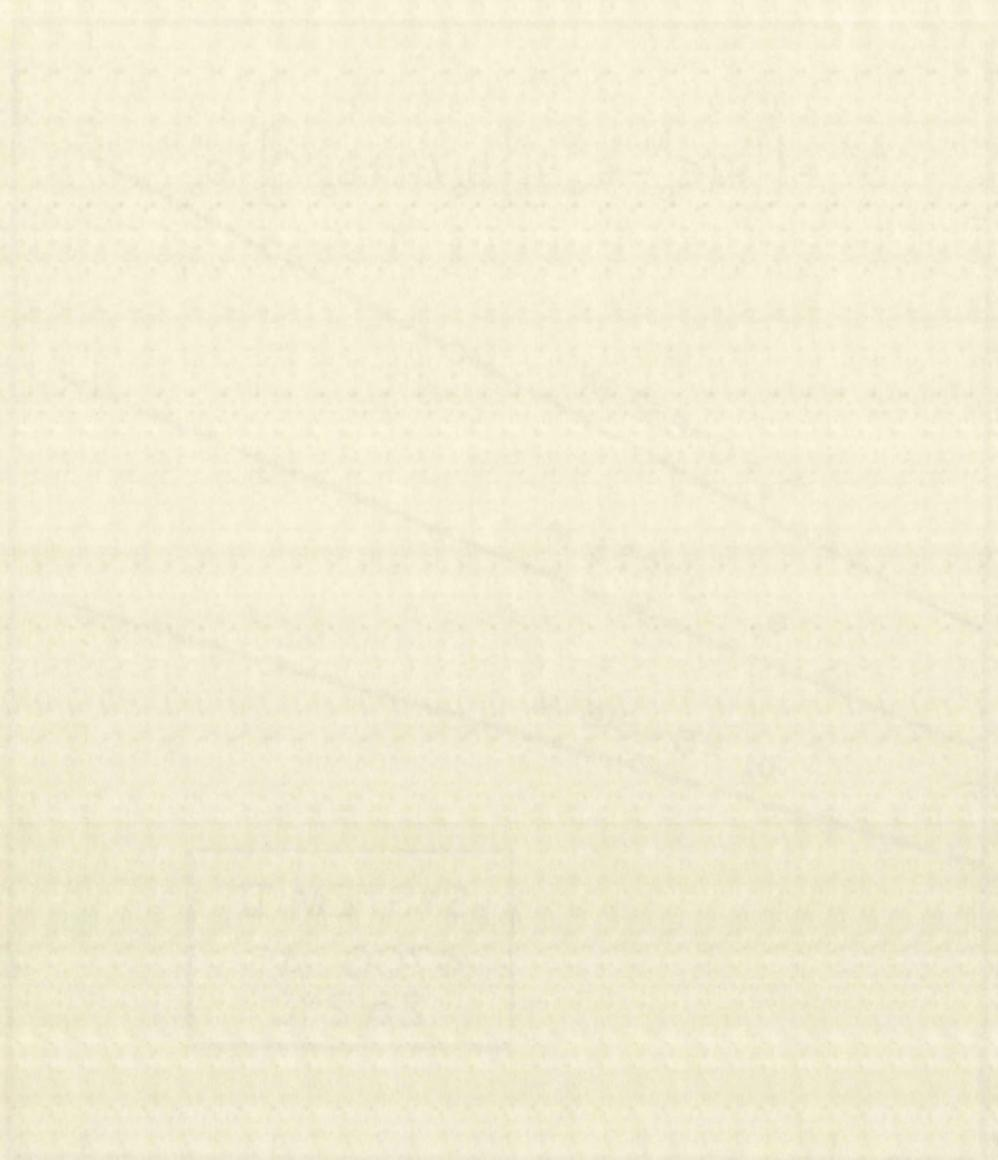


FIGURE 1. THE EFFECT OF THE INDEPENDENT VARIABLE ON THE DEPENDENT VARIABLE.

From Equations 5.1.18 and 5.1.19, one can easily verify that

$$\epsilon_c^\lambda - \epsilon_a^\lambda = \frac{1}{\beta} \quad 5.1.20$$

and
$$K = \frac{\beta}{\alpha} \quad 5.1.21$$

Since Equation 5.1.20 is a function of one variable, the variance of $\epsilon_c^\lambda - \epsilon_a^\lambda$, as given by Equation A.19 of the Appendix, is

$$S^2(\epsilon_c^\lambda - \epsilon_a^\lambda) = (\epsilon_c^\lambda - \epsilon_a^\lambda)^2 \frac{S\beta^2}{\beta^2} \quad 5.1.22$$

Equation 5.1.21, however, is a function of two variables which are not independent. Because of the dependence of α upon β , the variance of K will be given by Equation A.20 of the Appendix.

$$S_K^2 = S^2\left[\left(\frac{1}{\alpha}\right)^2 C_{11} + \left(\frac{\beta}{\alpha^2}\right) C_{22} - 2\left(\frac{\beta}{\alpha^2}\right) C_{12}\right] \quad 5.1.23$$

The variables of Equation 5.1.15 are given in Tables B.1 through B.3 of the Appendix for the wave lengths 4300 Å, 4500 Å, and 4700 Å and the temperatures 15.4°, 25.2°, and 33.6°, while the regression analysis parameters are given in Table B.4 of the Appendix. Table 5.1.2 gives typical values of K , $\epsilon_c^\lambda - \epsilon_a^\lambda$, and their standard deviation at a given temperature as obtained from Equations 5.1.20 through 5.1.23.

One will recall that for System I, $\frac{D^\lambda}{a_o b_o} = K\epsilon_c^\lambda$. If we define

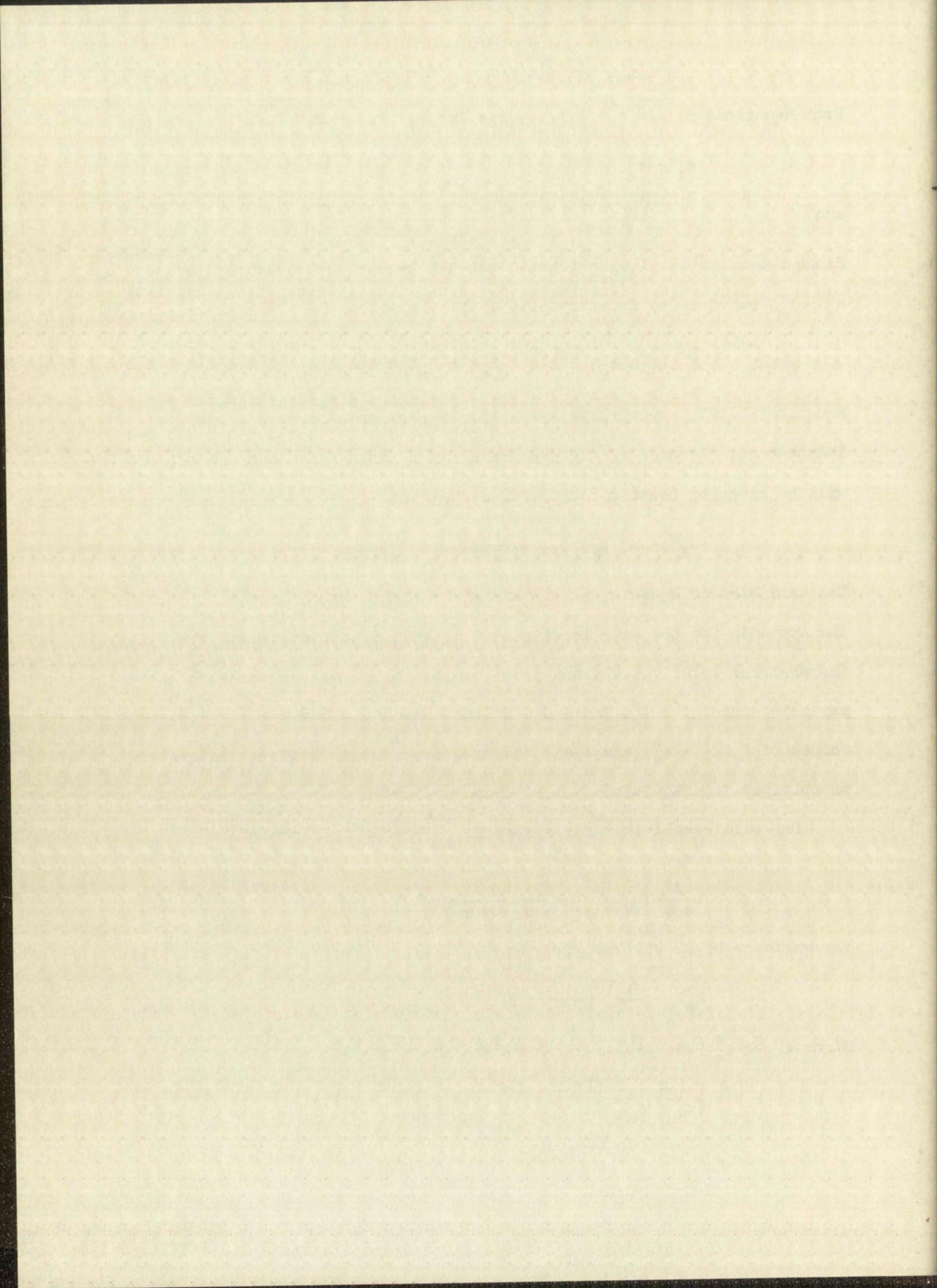
$$\left[\frac{D^\lambda}{a_o b_o}\right]_{\text{average}} = \frac{1}{n} \sum \frac{D^\lambda}{a_o b_o} = R^\lambda \quad 5.1.24$$

the variance of R^λ will be given by

$$S_{R^\lambda}^2 = \frac{1}{n-1} \sum \left(\frac{D^\lambda}{a_o b_o} - R^\lambda\right)^2 \quad 5.1.25$$

Since $\epsilon_c^\lambda \gg \epsilon_a^\lambda$ (see Tables 3.1.1 and 5.1.2),

$$\frac{1}{(\epsilon_c^\lambda - \epsilon_a^\lambda)} \approx \frac{1}{\epsilon_c^\lambda} \quad 5.1.26$$



Hence, $K = R^\lambda \beta$.

5.1.27

TABLE 5.1.2

VALUES OF K AND $(\epsilon_c^\lambda - \epsilon_a^\lambda)$ WITH THEIR STANDARD DEVIATIONS, S_K AND $S(\epsilon_c^\lambda - \epsilon_a^\lambda)$ AT 25.2° FOR THE WAVE LENGTHS, λ , AS OBTAINED FROM SYSTEM II

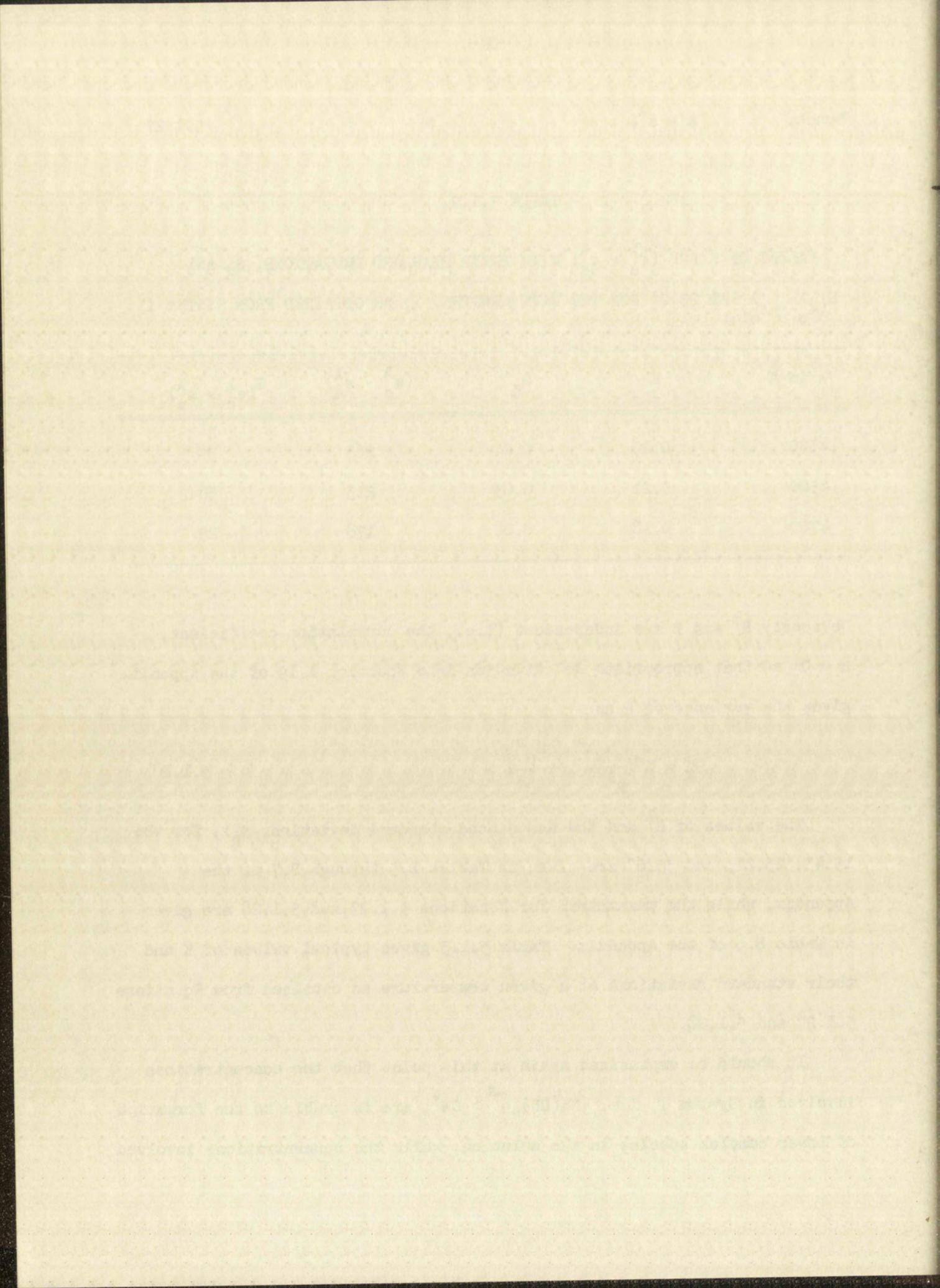
λ in Å	K	S_K	$(\epsilon_c^\lambda - \epsilon_a^\lambda)$	$S(\epsilon_c^\lambda - \epsilon_a^\lambda)$
4300	0.20	0.04	263	59
4500	0.21	0.03	213	38
4700	0.18	0.02	178	25

Obviously R^λ and β are independent (i.e., the correlation coefficient, $\rho = 0$) so that appropriate substitution into Equation A.19 of the Appendix gives the variance of K as

$$S_K^2 = K^2 \left[\frac{S_R \lambda^2}{R \lambda^2} + \frac{S_\beta^2}{\beta^2} \right] . \quad 5.1.28$$

The values of R^λ and the associated standard deviation, $S_R \lambda$, for the 15.4° , 25.2° , and 33.6° are given in Tables B.5 through B.7 of the Appendix, while the parameters for Equations 5.1.27 and 5.1.28 are given in Table B.8 of the Appendix. Table 5.1.3 gives typical values of K and their standard deviations at a given temperature as obtained from Equations 5.1.27 and 5.1.28.

It should be emphasized again at this point that the concentrations involved in System I, i.e. $[\text{Ni}(\text{CN})_4]^{2-} > \text{CN}^-$, are favorable to the formation of lower complex species in the solution, while the concentrations involved



in System II are favorable to the formation of higher complex species. The excellent correlation between the K values of Table 5.1.2 and 5.1.3 once again indicate the existence of only one new species, namely $[\text{Ni}(\text{CN})_5]^{-3}$, appearing in the concentration range studied.

TABLE 5.1.3

VALUES OF K AND S_K AT 25.2° FOR THE WAVE LENGTHS, λ , AS OBTAINED FROM SYSTEM I

λ in Å	K	S_K
4300	0.19	0.04
4500	0.21	0.04
4700	0.18	0.03

Since there seems to be no significant difference in the values of K obtained from System I and the values of K obtained from System II as well as no significant variation of K with wave length (i.e., no new species other than $[\text{Ni}(\text{CN})_5]^{-3}$ absorbing at different wave lengths) we choose to report an average value of K for the wave lengths considered and for the two systems. To accomplish this we define

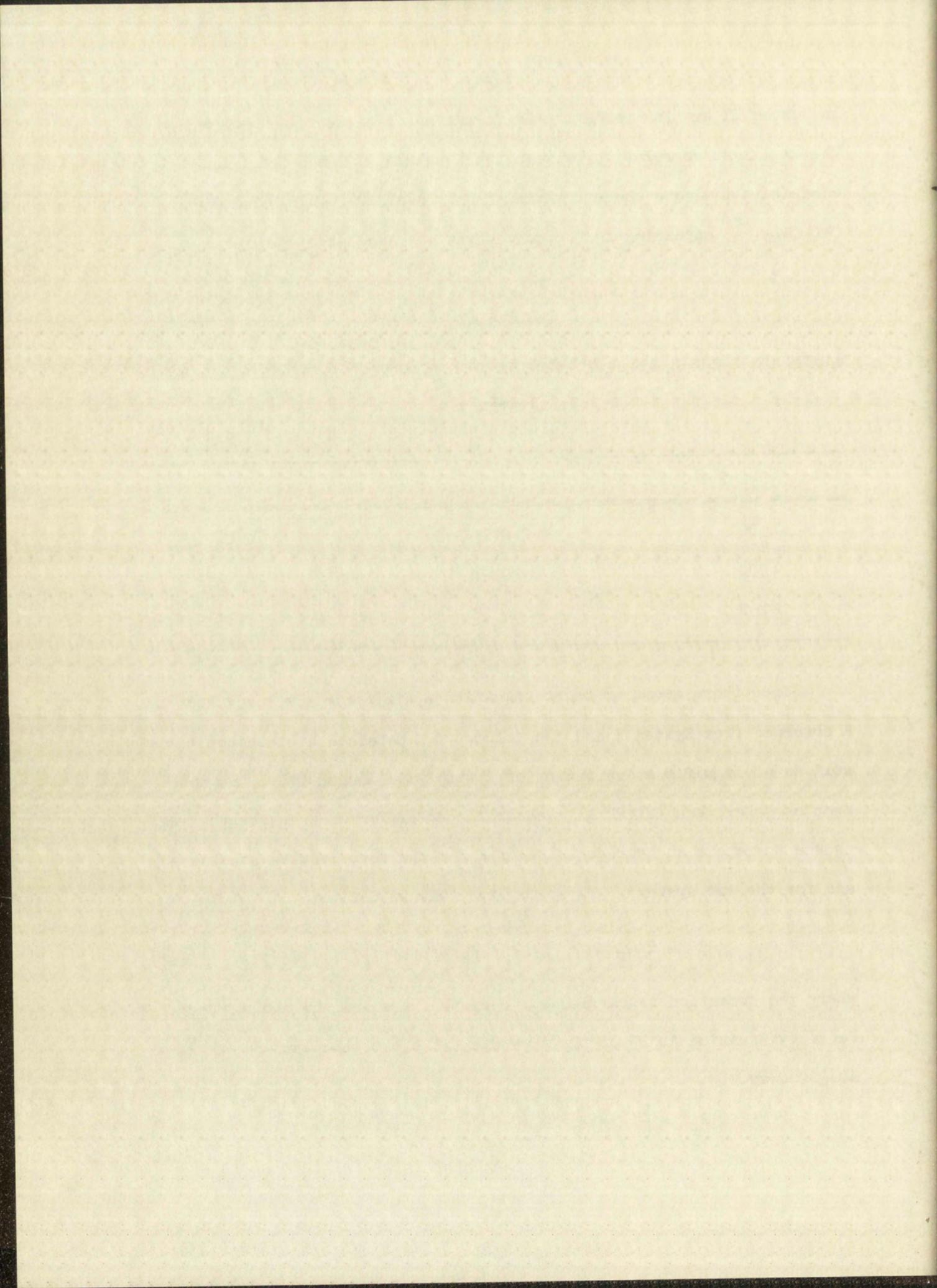
$$\bar{K} = \frac{1}{n} \sum_i \sum_j K_{ij} \quad 5.1.29$$

where the summation is carried out over the wave lengths and systems.

Hence by Equation A. 19 of the Appendix (if $\rho = 0$) the variance of \bar{K}

is given by

$$S_{\bar{K}}^2 = \frac{1}{n} \sum_i \sum_j S_{K_{ij}}^2 \quad 5.1.30$$



Appropriate substitutions into Equation 5.1.29 and 5.1.30 yields

$$\bar{K} = 0.19(S_K = 0.01) \text{ at } 25.2^\circ.$$

From this value of \bar{K} , one can show that the approximation involved in Equation 5.1.2 and Equation 5.1.11 are valid.

5.1.4 Correlation of Species Characterization Data with \bar{K} :

As has been indicated in Section 4.2.2, the experimental values could be made to fit calculated values if a K of 0.2 liters/mole were used. This correlation is in excellent agreement with the experimentally determined values of K.

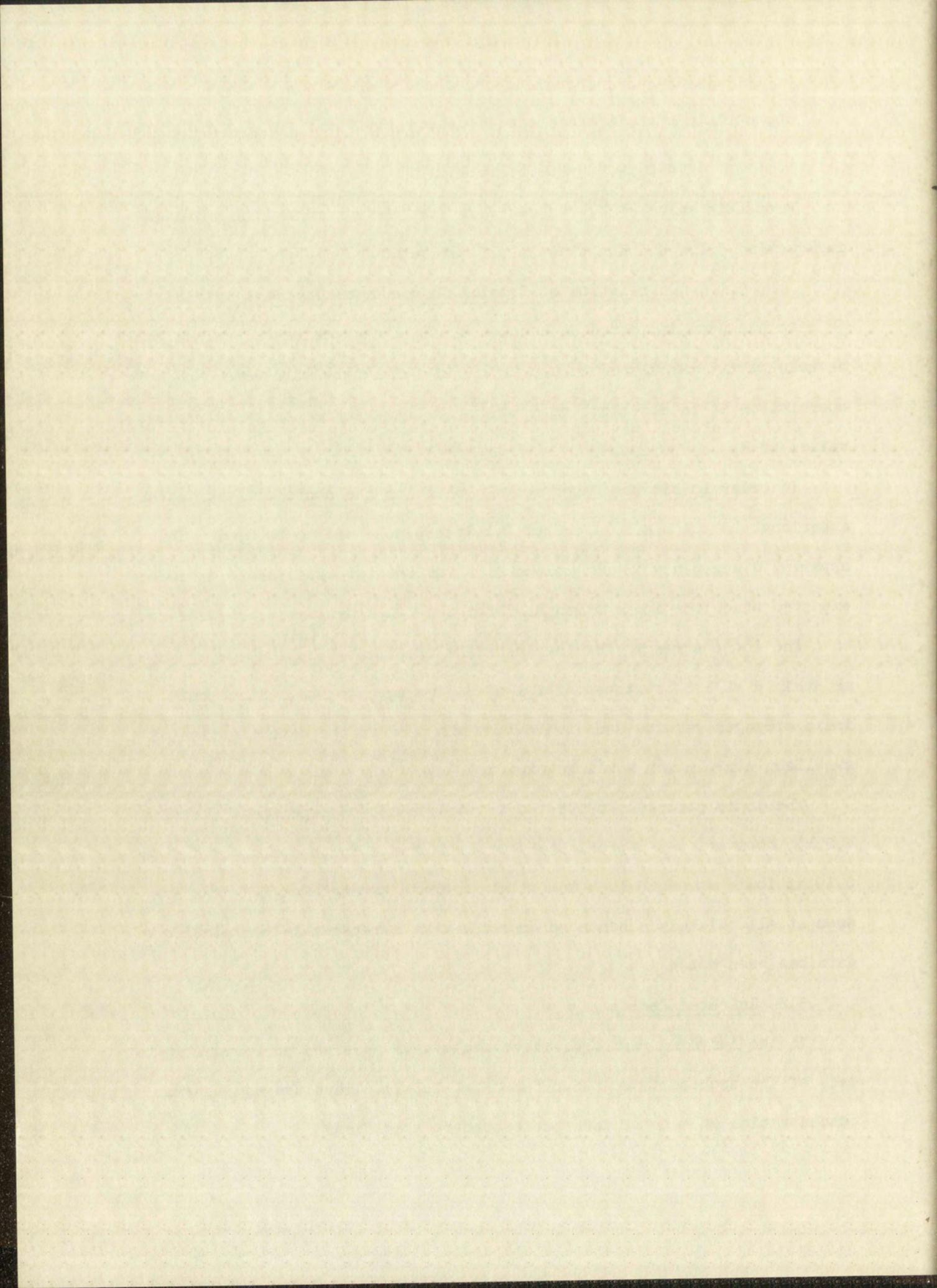
In order to fit the experimental values of the continuous variation experiment (Section 4.2.1) a K of 0.1 liters/mole had to be used. This apparent discrepancy in the values of K for the two experiments is to be expected since the ionic strengths for the two experiments are different.

The ionic strength for the logarithm treatment (Section 4.2.1) was maintained at 1.34 by the addition of sodium perchlorate. Since this ionic strength was the same ionic strength used in the determination of K, excellent correlation would be expected.

The ionic strength for the continuous variation experiment (Section 4.2.1), however, was approximately 0.3. A change in the value of K from 0.19 at ionic strength 1.34 to 0.1 at an ionic strength of 0.3 does not seem at all unlikely. Hence we conclude that a reasonable correlation of data has been established.

5.2 Infrared Region

In the infrared region distinct peaks were observed corresponding to each of the species in solution (see Fig. 2.3.2). Thus the equilibrium concentration of each of the species can be specified.



Consider that the concentration of the tetracyanonickelate(II) is given by

$$a = \frac{A_a}{\epsilon_a t} \quad 5.2.1$$

where A_a and ϵ_a refer to the absorbance and molar extinction coefficient of tetracyanonickelate(II) at maximum absorbance. Since A_a was observed, ϵ_a was obtained from solutions containing only tetracyanonickelate(II) ion (Table 3.2.1), and t is given by 55×10^{-4} cm, the equilibrium concentration, a , of the tetracyanonickelate(II) ion is known. This in turn fixes the equilibrium concentration of the cyanide and pentacyanonickelate(II) ion since

$$c = a_0 - a \quad 5.2.2$$

$$b = b_0 - c \quad 5.2.3$$

The value of K will then be given by

$$K = \frac{[c]}{[a][b]} \quad 5.2.4$$

Table 5.2.1 gives the value of K for 14 solutions. The average value of K and its standard deviation for these fourteen solutions was found to be $\bar{K} = 0.3$ ($S_K = 0.1$).

It will be noted that the \bar{K} determined from the infrared absorption data is not as well known as the \bar{K} determined from the visible absorption data. The large standard deviation arises from the large percentage errors in background corrections, the uncertainty in peak overlap, and the variance in the path length. Nevertheless, the \bar{K} obtained from the infrared data is in substantial agreement with the \bar{K} obtained in the visible region.

Since the path length can be shown to vary as much as ten percent, it would be more instructive to calculate the molar extinction coefficient

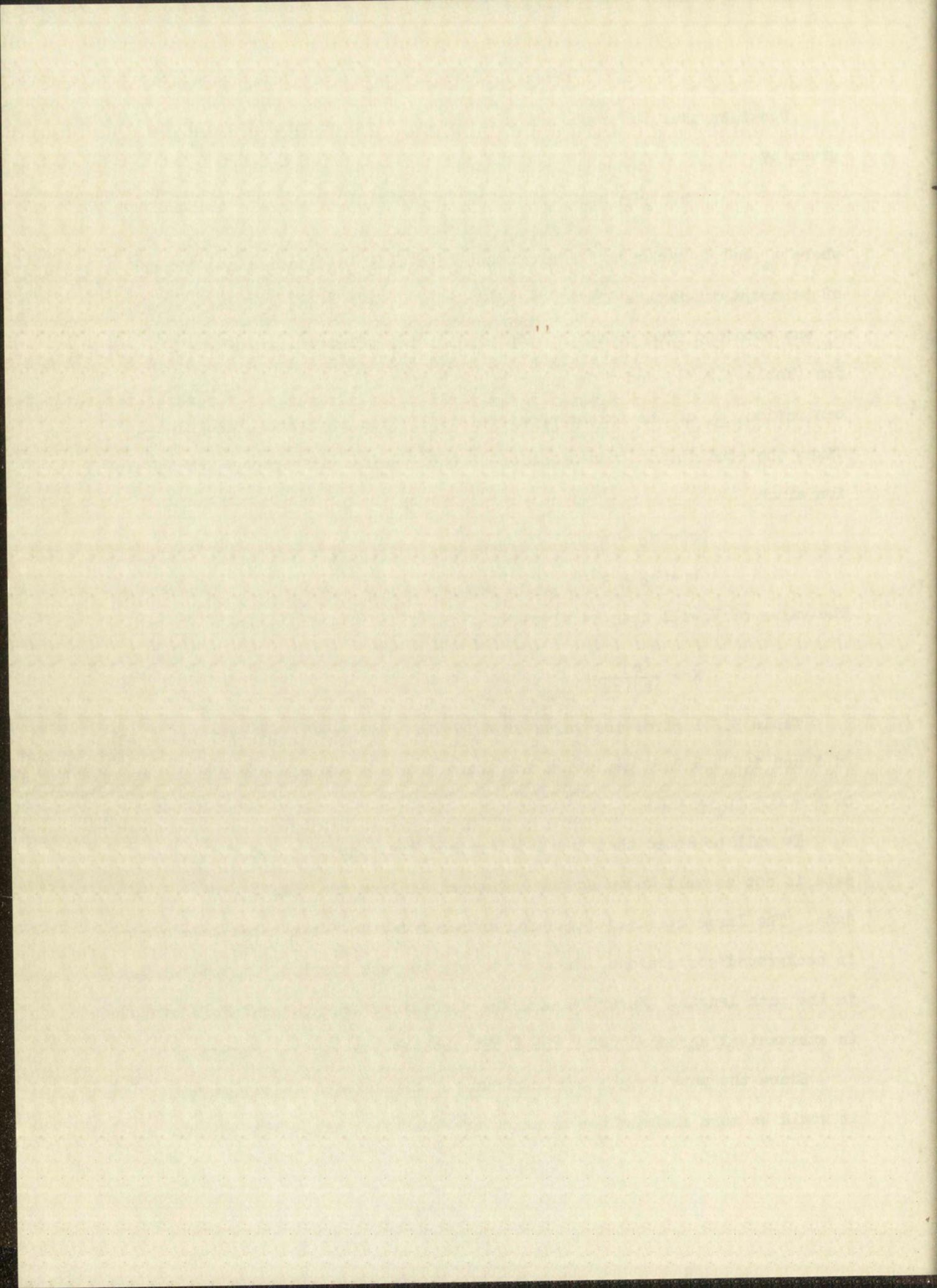


TABLE 5.2.1

CALCULATED VALUES OF K FOR THE INFRARED REGION

$$a = \frac{A^{\max} [\text{Ni}(\text{CN})_4]^{-2}}{\epsilon_a^{\max} t}$$

$$t = 55 \times 10^{-4} \text{ cm}$$

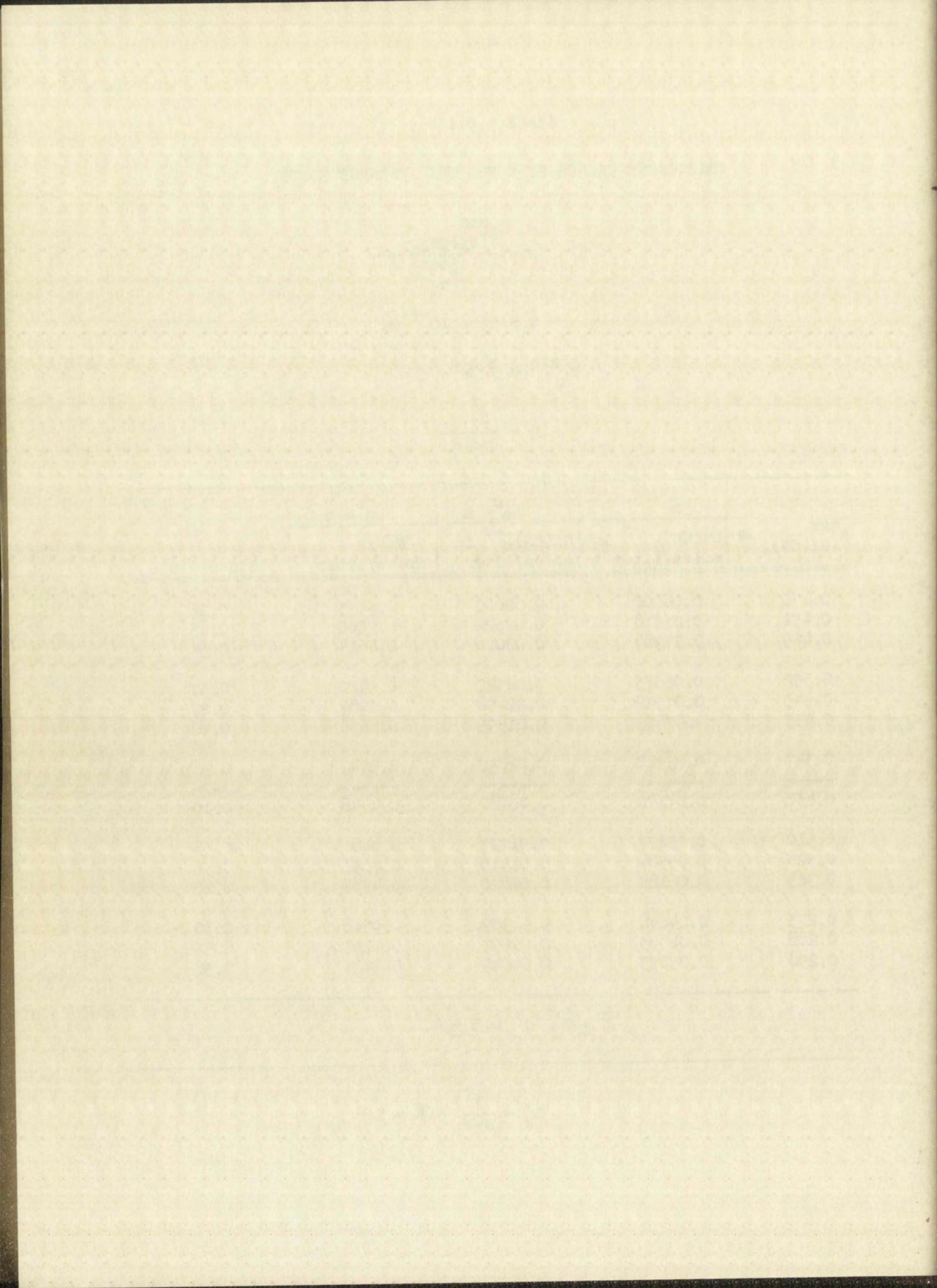
$$\epsilon_a^{\max} = 1068 \pm 95$$

$$K = \frac{[c]}{[a][b]}$$

$A^{\max} [\text{Ni}(\text{CN})_4]^{-2}$	a	$a_0^c - a$	$b_0^b - c$	K in liters/mole
	$[\text{Ni}(\text{CN})_4]^{-2}$ in moles/liter	$[\text{Ni}(\text{CN})_5]^{-3}$ in moles/liter	CN^- in moles/liter	
0.470	0.08000	0.02000	0.9453	0.26
0.451	0.07678	0.02322	0.7000	0.43
0.469	0.07984	0.02016	0.4614	0.54
0.392	0.06673	0.02327	0.9420	0.37
0.443	0.07542	0.01458	0.7087	0.27
0.435	0.07405	0.01595	0.4656	0.46
0.347	0.05910	0.02090	0.9444	0.36
-----	-----	-----	-----	-----
0.430	0.07320	0.00680	0.4748	0.19
0.310	0.05277	0.01723	0.9481	0.34
0.328	0.05584	0.01416	0.7091	0.36
0.363	0.06180	0.00820	0.4734	0.28
0.273	0.04648	0.04352	0.9518	0.30
0.288	0.04903	0.01097	0.7123	0.31
0.298	0.05073	0.00927	0.4723	0.38

$$\bar{K} \pm S_K : 0.3 \pm 0.1$$

$$S_K^2 = \frac{1}{n-1} (\bar{K} - K)^2$$



for the pentacyanonickelate(II) independent of the path length. This may be accomplished by taking the ratio of the absorbance of the pentacyanonickelate(II) ion to the absorbance of the tetracyanonickelate(II) ion for a given sample. The ratio of the respective molar extinction coefficients (at maximum absorbance) is given by

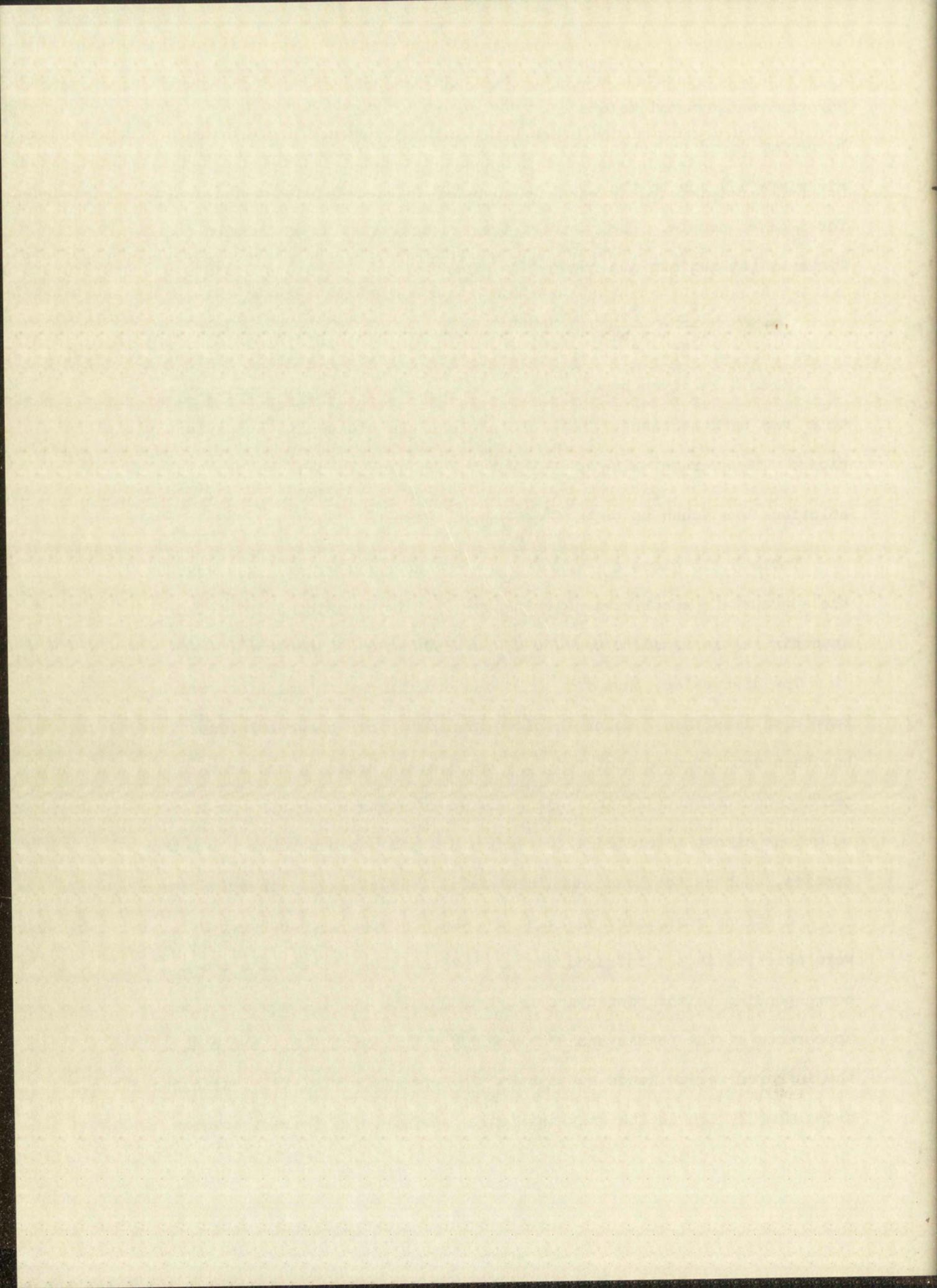
$$\frac{\epsilon_c}{\epsilon_a} = \frac{A_c}{A_a b K} \quad 5.2.5$$

Since K is given by 0.19 ($S_K = 0.01$) liters/mole, the ratio of ϵ_c to ϵ_a may be determined. Table 5.2.2 gives the value of $\frac{A_c}{A_a b}$ for 14 solutions. The average value of $\frac{A_c}{A_a b}$ and its standard deviations for these 14 solutions was found to be $0.308 \left(\frac{S_{A_c}}{A_a b} = 0.027 \right)$.

Table 3.2.1 gives $\epsilon_a = 1068 (S_{\epsilon_a} = 95)$ mole⁻¹ liter cm⁻¹, so that by the appropriate substitutions (with $\rho = 0$) into Equation A.19 of the Appendix, ϵ_c is found to be $1730 (S_{\epsilon_c} = 230)$ mole⁻¹ liter cm⁻¹.

The discussion, thus far, has been concerned with solutions which have been less than 2 molar in added cyanide. For these solutions it has been demonstrated that the only new species being formed is the pentacyanonickelate(II) ion. It would be of interest now to consider solutions almost saturated with cyanide in order to determine if another species, such as the hexacyanonickelate(II), $[\text{Ni}(\text{CN})_6]^{-4}$, is being formed.

Solutions containing as high as $\sim 0.4 \text{ M } [\text{Ni}(\text{CN})_4]^{-2}$ and $\sim 5 \text{ M } \text{CN}^-$ were observed in the infrared region. No new peak, other than the peak corresponding to the pentacyanonickelate(II) ion, was observed. This appearance of the pentacyanonickelate(II) peak as the only new peak in the infrared region lends support to the contention that the pentacyanonickelate(II) ion is the only new ionic species being formed; however, it



is not conclusive proof. The possibility exists that a species such as $[\text{Ni}(\text{CN})_6]^{-4}$ does not absorb strongly in the infrared region. Further support to the existence of the pentacyanonickelate(II) ion as the only new ionic species may be obtained from the corroboration of the value of K at these high cyanide concentrations with the value of K obtained from solutions of moderate cyanide concentrations.

TABLE 5.2.2

THE RATIO OF THE MAXIMUM ABSORBANCE OF THE PENTACYANONICKELATE(II) ION TO THE PRODUCT OF THE MAXIMUM ABSORBANCE OF THE TETRACYANONICKELATE(II) ION AND THE EQUILIBRIUM CYANIDE ION CONCENTRATION

b moles/liter	A_a	$A_a b$	A_c	$\frac{A_c}{A_a b}$
0.9501	0.470	0.446	0.130	0.271
0.7114	0.951	0.321	0.090	0.280
0.4733	0.469	0.222	0.070	0.315
0.9515	0.392	0.373	0.110	0.295
0.7126	0.443	0.316	0.093	0.294
0.4742	0.435	0.206	0.064	0.311
0.9531	0.347	0.331	0.101	0.305
0.4750	0.430	0.204	0.068	0.333
0.9545	0.310	0.296	0.080	0.270
0.7149	0.328	0.234	0.068	0.291
0.4758	0.363	0.173	0.061	0.353
0.9561	0.273	0.261	0.074	0.284
0.7161	0.288	0.206	0.070	0.340
0.4768	0.298	0.142	0.050	0.352

$$\frac{A_c}{A_a b} + \frac{S A_c}{A_a b} = 0.308 \pm 0.027$$

It is to be expected that the value of K obtained from these solutions of high cyanide concentration will not be well known for several reasons.

Faint, illegible text at the top of the page, possibly a header or introductory paragraph.

Main body of faint, illegible text, appearing to be several paragraphs of a document.

Faint, illegible text at the bottom of the page, possibly a footer or concluding paragraph.

First, since the absorbance is high, there will be a considerable overlapping of bands. Second, solutions having high cyanide concentrations will also have high pH values due to the hydrolysis of the cyanide ion. The shape of the water band (background) varies considerably with pH; hence the background will not be well known. Third, because of the high concentration involved, and hence high absorption, thin spacers, whose thicknesses were not well known, had to be used.

Attempts were made to minimize the errors introduced by these effects. The symmetry of the absorption bands was utilized to make an approximate correction for the amount of peak overlap. An aqueous solution of sodium cyanide of the approximate pH of the cyanide-tetracyanonickelate(II) solutions was observed to establish the background. The error introduced by the uncertainty in the path length was eliminated by taking the appropriate ratio of the absorbance of the tetracyanonickelate(II) ion and pentacyanonickelate(II) ion for a given sample. The value of K may then be determined from Equation 5.2.6.

$$K = \left(\frac{A_c}{A_a} \right) \left[\left(\frac{\epsilon_a}{\epsilon_c} \right) \left(\frac{1}{b_0} \right) \right] \quad 5.2.6$$

Included in Equation 5.2.6 is the assumption that the concentration of the added cyanide was not diminished by complex formation, i.e. $b = b_0$.

Table 5.2.3 gives the value of K as determined for four solutions of high cyanide concentration. For each solution the value of K is ~ 0.4 liters/mole.

Using the same argument presented in Section 5.1.4, i.e. the concentration formation may increase or decrease as the ionic strength increases and decreases, we conclude that a concentration formation constant of 0.4 at $\mu = 6$ is consistent with a concentration formation constant of 0.2 at $\mu = 1.3$.

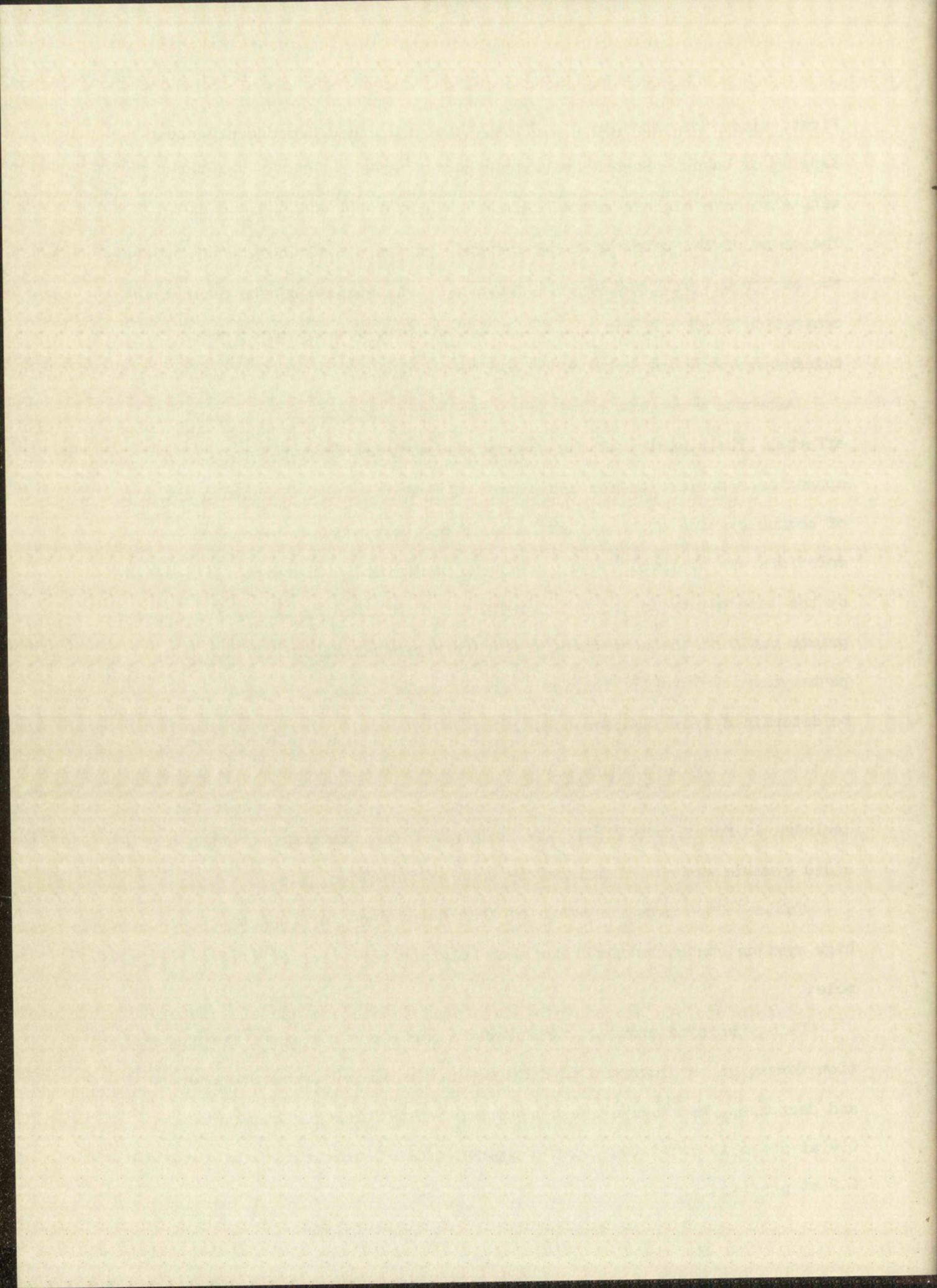


TABLE 5.2.3
THE VALUES OF K AS CALCULATED FOR SOLUTIONS WITH HIGH
CYANIDE-TO-TETRACYANONICKELATE(II) RATIOS

a_0 moles/liter	b_0 moles/liter	μ molar ionic strength	A_a	$\frac{A_c}{A_a}$	K
0.3776	4.995	6.13	0.175	2.857	0.4
0.3361	4.995	6.00	0.143	3.203	0.4
0.2741	4.995	5.82	0.130	2.985	0.4
0.1164	4.995	5.34	0.051	2.961	0.4

$$K = \left(\frac{A_c}{A_a}\right) \left[\left(\frac{\epsilon_a}{\epsilon_c}\right) \left(\frac{1}{b_0}\right) \right]$$

$$\frac{\epsilon_a}{\epsilon_c} = 1.56$$

$$t \approx 12.7 \times 10^{-4} \text{ cm}$$

The appearance of only one new ionic species ($[\text{Ni}(\text{CN})_5]^{-3}$) in aqueous solutions of cyanide and tetracyanonickelate(II) is then consistent with the data collected over a 100 fold cyanide range (i.e. $\sim .05 \text{ M}$ to $\sim 5 \text{ M}$). Notice K increases regularly with μ .

6.0 EVALUATION OF THE ENTHALPY OF REACTION

By use of Equations 5.1.8, 5.1.15, 5.1.20, 5.1.21, and the statistical technique employed in Section 5.1.3, it was possible to determine K for the temperatures 15.4°, 25.2°, and 33.6°. These values of K are given in Tables B.1, B.2, and B.3 of the Appendix. A summary of the average values of K (i.e. \bar{K}) as determined by Equation 5.1.29 and 5.1.30 is given in Table 6.0.1.

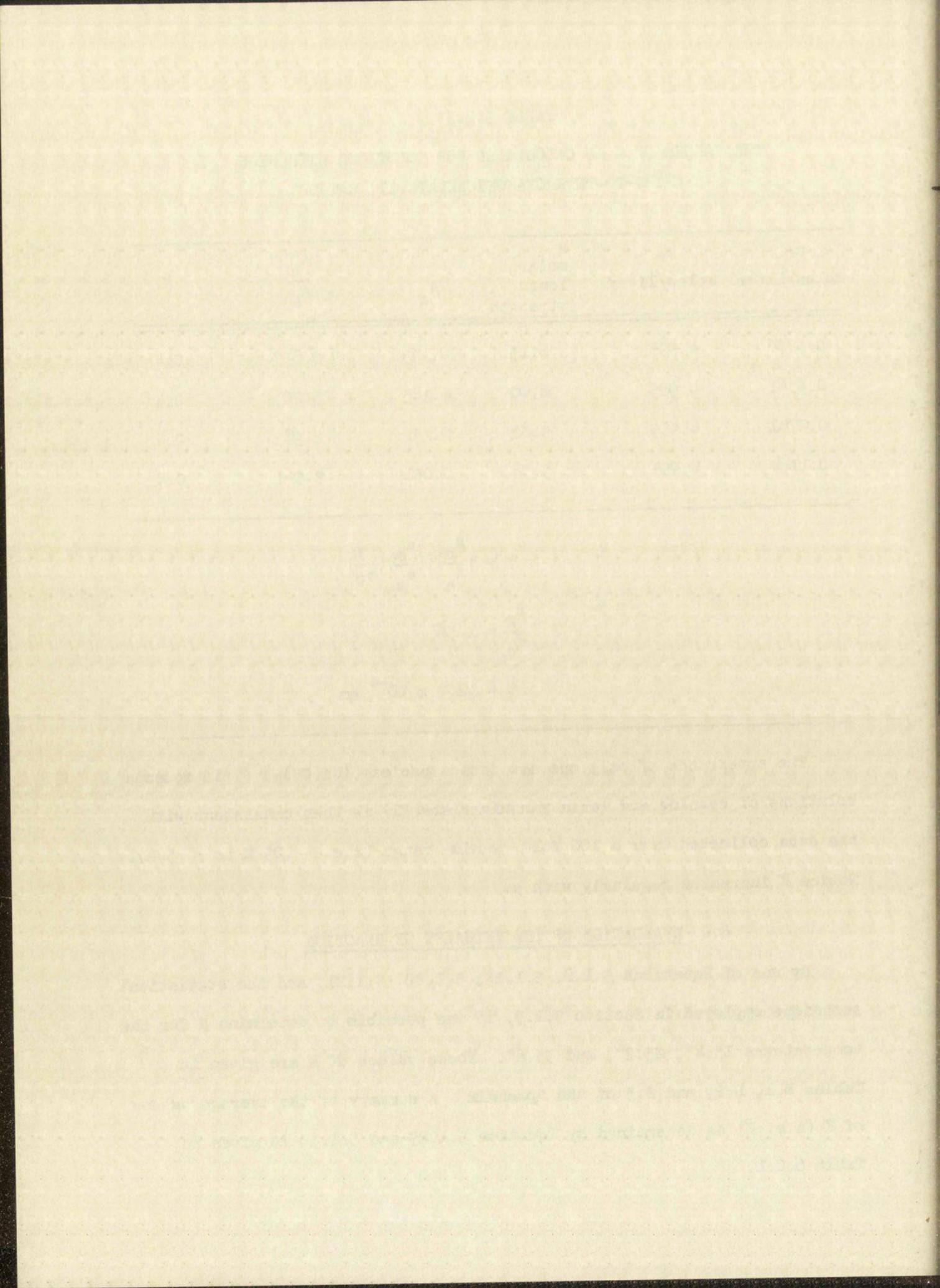


TABLE 6.0.1
AVERAGE VALUES OF K FOR THE TEMPERATURE T

T ° K	$\bar{K} \pm S_{\bar{K}}$
288.6	0.22 \pm 0.01
298.4	0.19 \pm 0.01
306.8	0.17 \pm 0.01

One will recall from elementary thermodynamics⁽¹²⁾ that the formation constant is related to the temperature by the equation

$$\log K_0 = - \left(\frac{\Delta H}{2.303 R} \right) \frac{1}{T} + C' \quad 6.0.1$$

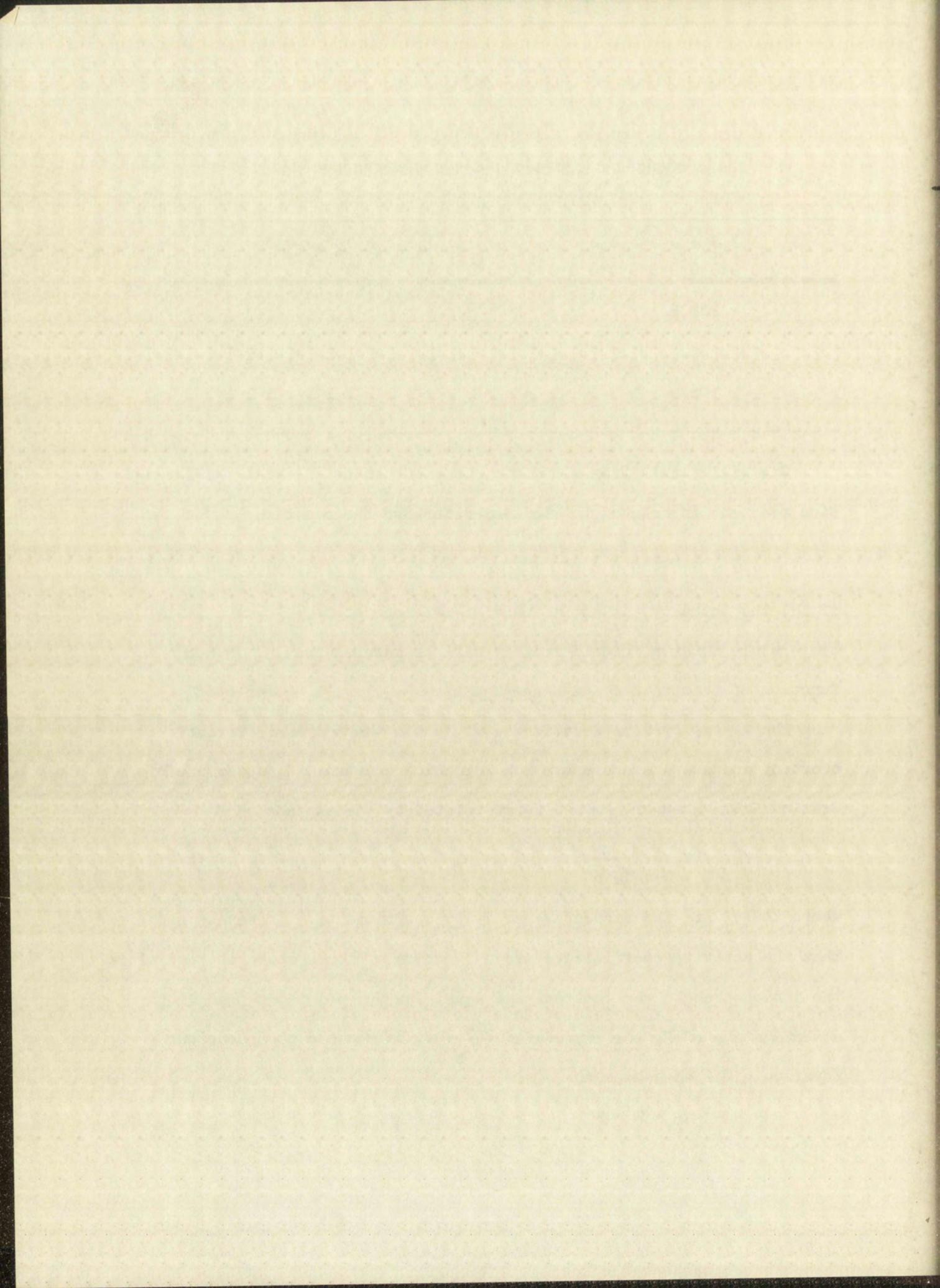
if ΔH , the enthalpy, is not a function of temperature. For the small temperature interval considered, it will be assumed that ΔH is not a function of temperature and hence Equation 6.0.1 will be employed.

The K_0 employed in Equation 6.0.1 is the thermodynamic formation constant and not the concentration formation constant, K , determined in Section 5.0. However, K_0 and K are related by the expression

$$K_0 = K \frac{\gamma_c}{\gamma_a \gamma_b} \quad 6.0.2$$

where the γ_i are the respective activity coefficients. It may be recalled that the activity coefficients are a function of ionic strength, and since the ionic strength was constant and equal for the solutions used in the determination of K , the expression $\frac{\gamma_c}{\gamma_a \gamma_b}$ may be equated to a constant K_γ . Equation 6.0.2 then becomes

$$K_0 = K \cdot K_\gamma \quad 6.0.3$$



and Equation 6.0.1 becomes

$$\log K = - \left(\frac{\Delta H}{2.303 K T} \right) \frac{1}{T} + C' - \log K_{\gamma} \quad . \quad 6.0.4$$

If we make the further assumption that K_{γ} does not vary appreciably with temperature over the temperature range in question (i.e. 15° to 35°) then Equation 6.0.4 will further reduce to

$$\log K = - \left(\frac{\Delta H}{2.303 R} \right) \frac{1}{T} + C \quad . \quad 6.0.5$$

Fig. 6.2.1 gives $\log K$ as a function of $\frac{1}{T}$. A ΔH of -3 KCal is consistent with the slope of the line in Fig. 6.2.1.

7.0 DETERMINATION OF THE MAGNETIC SUSCEPTIBILITY OF THE PENTACYANONICKELATE(II) ION

The magnetic susceptibility of the pentacyanonickelate(II) ion was determined by the Gouy⁽¹³⁾ method of observing the apparent change in weight of a solution in a magnetic field. A change in apparent weight of 0.0111 gm (balance sensitivity = 0.1 mg) for 10 ml of a solution containing ~ 0.3 M $[\text{Ni}(\text{CN})_5]^{-3}$, ~ 0.1 M $[\text{Ni}(\text{CN})_4]^{-2}$, and ~ 4.5 M CN^- was observed. The apparent changes in weight of pure solutions of $[\text{Ni}(\text{CN})_4]^{-2}$ and CN^- were observed separately, and appropriate corrections were made for the solutions containing the mixture of the species. The results showed that $[\text{Ni}(\text{CN})_5]^{-3}$ was diamagnetic. As an indication of the sensitivity of the apparatus, a dilute solution (~ 0.01 M) of $[\text{Fe}(\text{CN})_6]^{-3}$ was observed, and it was shown to be in agreement with the known paramagnetic susceptibility of $[\text{Fe}(\text{CN})_6]^{-3}$.

8.0 DISCUSSION

8.1 Comparison with Previous Work

The preceding sections demonstrate conclusively that the predominant form of any new species formed in aqueous solutions of cyanide ion and

Faint, illegible text at the top of the page, possibly a header or introductory paragraph.

THE CONSTITUTIONAL HISTORY OF THE UNITED STATES

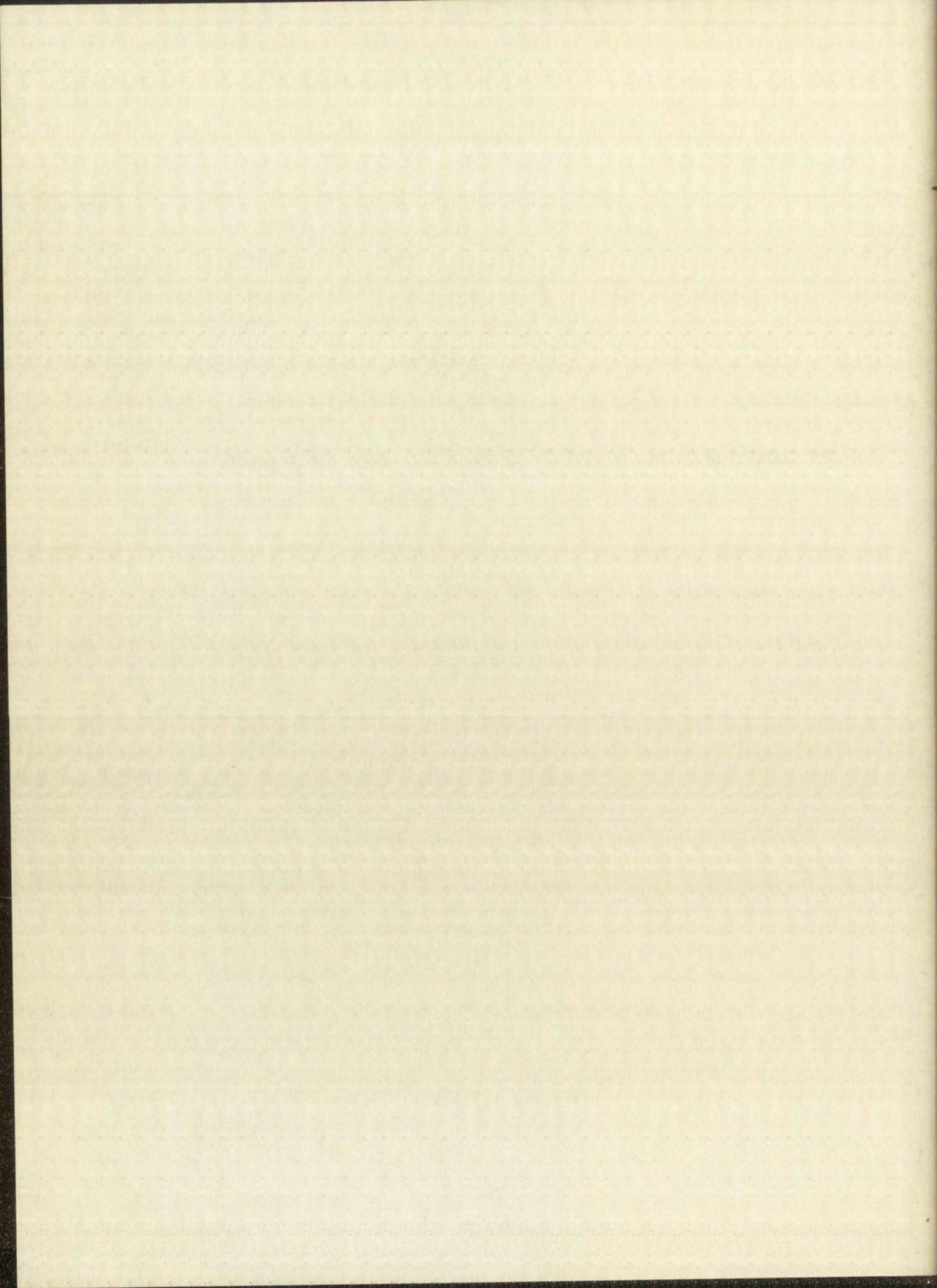
Main body of faint, illegible text, likely the beginning of a chapter or section.

CHAPTER I

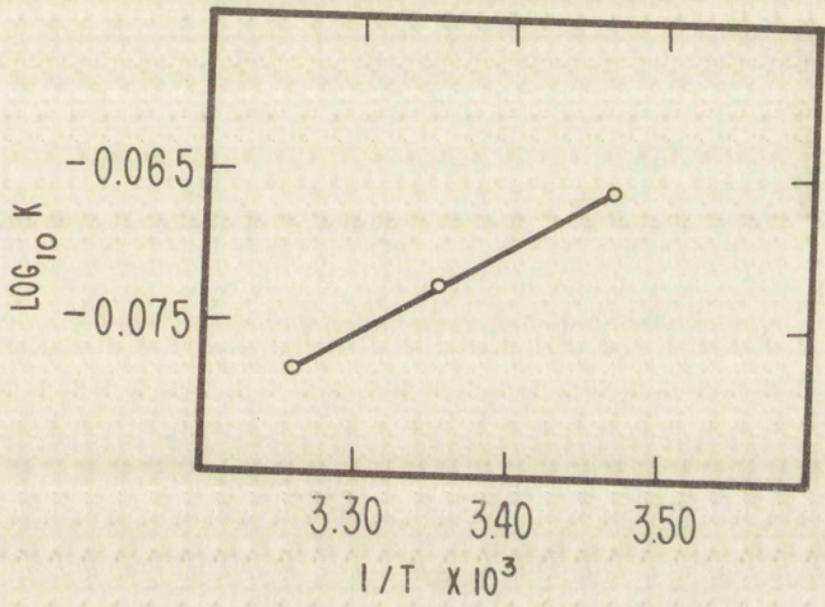
Faint, illegible text at the bottom of the page, possibly a concluding paragraph or page number.

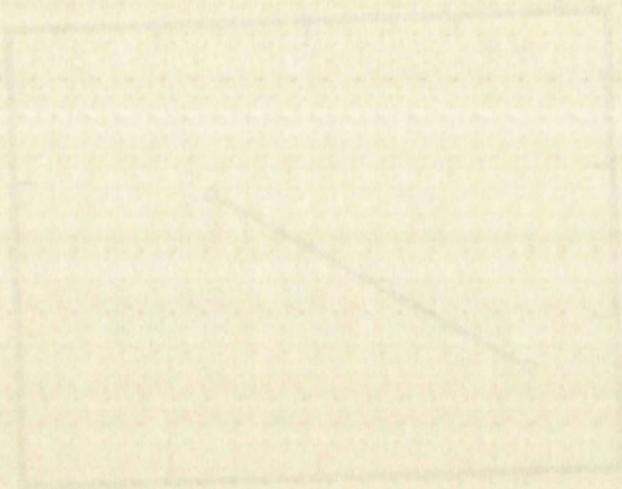
Figure 6.2.1

THE LOGARITHM OF THE FORMATION CONSTANT AS A FUNCTION OF TEMPERATURE



$$\text{LOG}_{10} K = - \left[\frac{\Delta H}{(2.303)R} \right] \frac{1}{T} + C$$





100 200 300

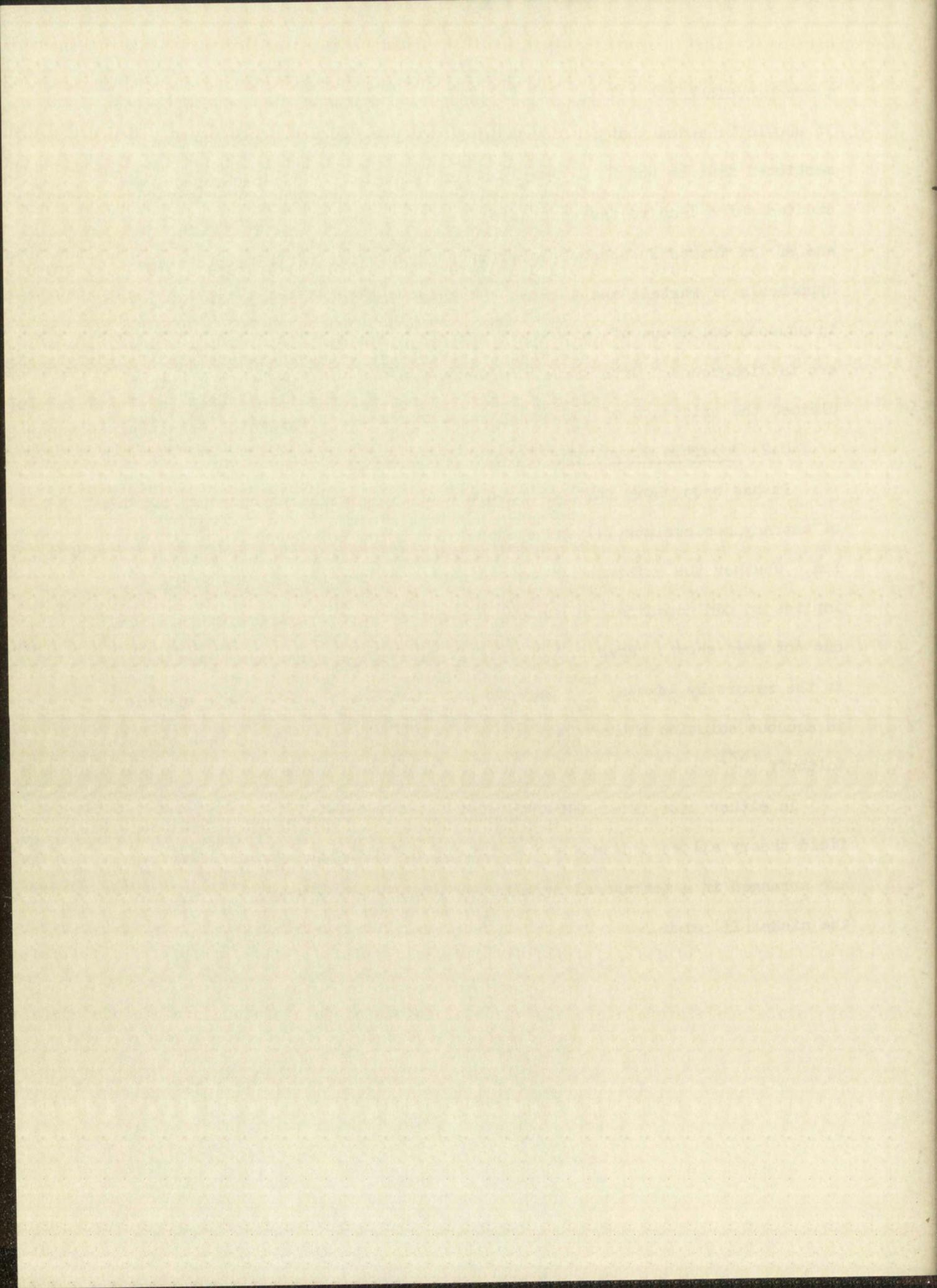
100 200

tetracyanonickelate(II) ion is the pentacyanonickelate(II) ion, $[\text{Ni}(\text{CN})_5]^{-3}$. It should be noted that R. S. Nyholm in an article in Chemical Reviews⁽¹⁴⁾ mentioned that he and B. S. Morris conducted unpublished spectrophotometric studies which lead to the conclusion that a 1:1 complex ion of $[\text{Ni}(\text{CN})_4]^{-2}$ and CN^- is formed in aqueous solutions. These observations support the hypothesis of Martell and Calvin⁽¹⁵⁾ that $[\text{Ni}(\text{CN})_5]^{-3}$ would be formed in aqueous solutions of $[\text{Ni}(\text{CN})_4]^{-2}$ and CN^- . However, these observations are in disagreement with Samuel's spectrophotometric studies from which he claimed the existence of the hexacyanonickelate(II) ion, $[\text{Ni}(\text{CN})_6]^{-4}$.

8.2 Possible Structure of the Pentacyanonickelate(II) Ion

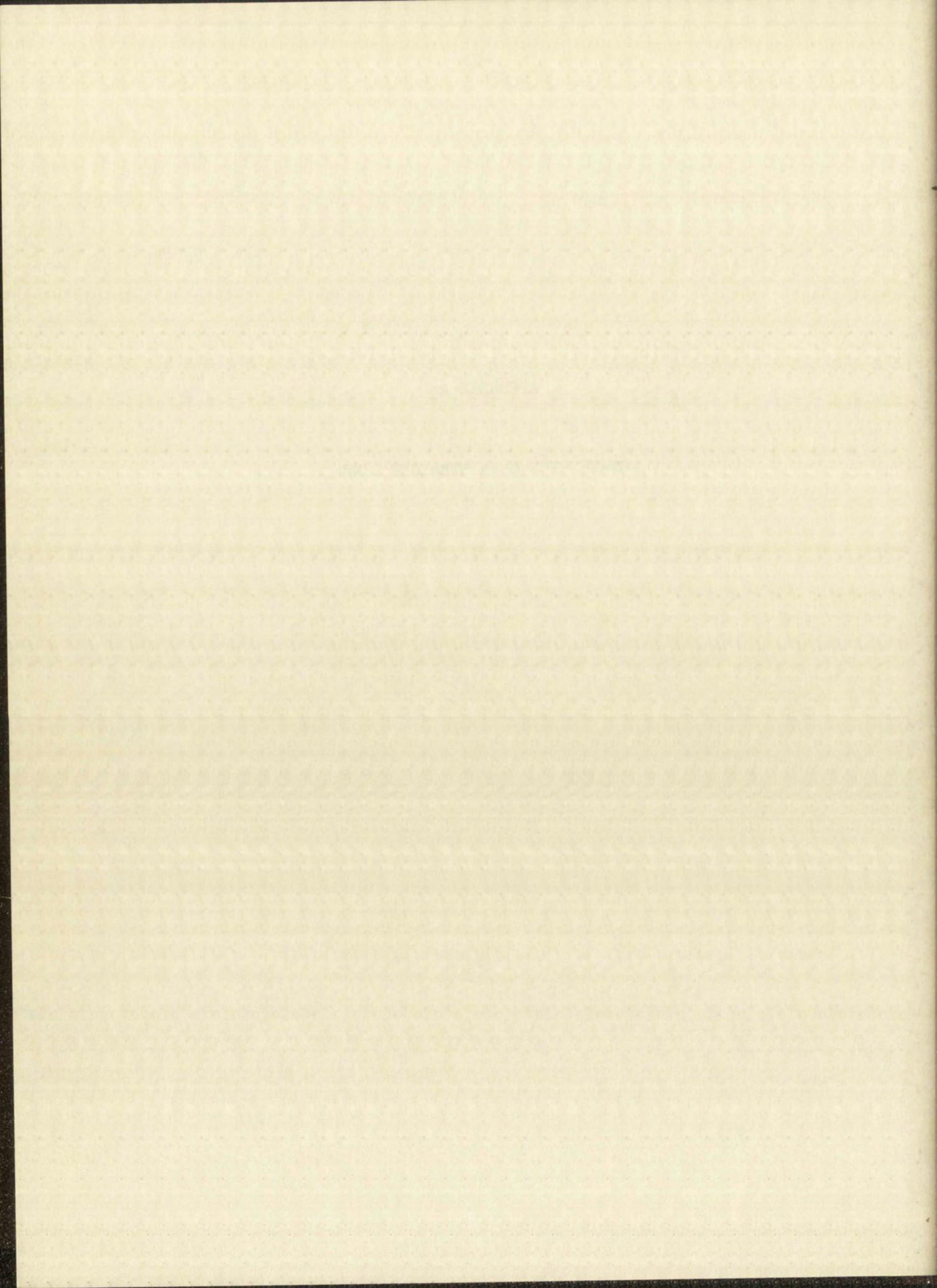
It has been shown that the predominant new species in aqueous solutions of tetracyanonickelate(II) and cyanide ion is the pentacyanonickelate(II) ion. Whether the existence of an odd number of cyanide ligands truly implies an odd coordination number, or whether an aquo complex is involved, has not been shown. However, of special interest to this consideration is the report by Adamson⁽¹⁶⁾ that the ion $[\text{Co}(\text{CN})_5]^{-3}$ is the true species in aqueous solution rather than $[\text{Co}(\text{CN})_5 \cdot \text{H}_2\text{O}]^{-3}$ as reported by Hume and Kolthoff.⁽¹⁷⁾

In either case, i.e., $[\text{Ni}(\text{CN})_5 \cdot \text{H}_2\text{O}]^{-3}$ or $[\text{Ni}(\text{CN})_5]^{-3}$, the ligand field theory allows a diamagnetic complex, in which the cyanide ligands are arranged in a tetragonal pyramid (as postulated by Nyholm⁽¹⁴⁾) around the nickel(II) atom.



APPENDIX A

STATISTICS OF A STRAIGHT LINE



APPENDIX A

For an equation of the form

$$y = \beta x + \alpha \quad \text{A.1}$$

if the assumption is made that y is normally distributed for a given value of x , a linear regression analysis may be performed in which the expression $y = \beta x + \alpha$ is an empirical regression line representing an estimate of the theoretical regression line, $Y = B(x) + A$. The quantity, α , is then an estimate of A and is distributed normally about A with an estimated variance of S_{α}^2 . Similarly, β is an estimate of B and is distributed normally about B with an estimated variance of S_{β}^2 . The variation about the empirical regression line, S^2 , is an estimate of the variations, σ^2 , about the theoretical regression line.

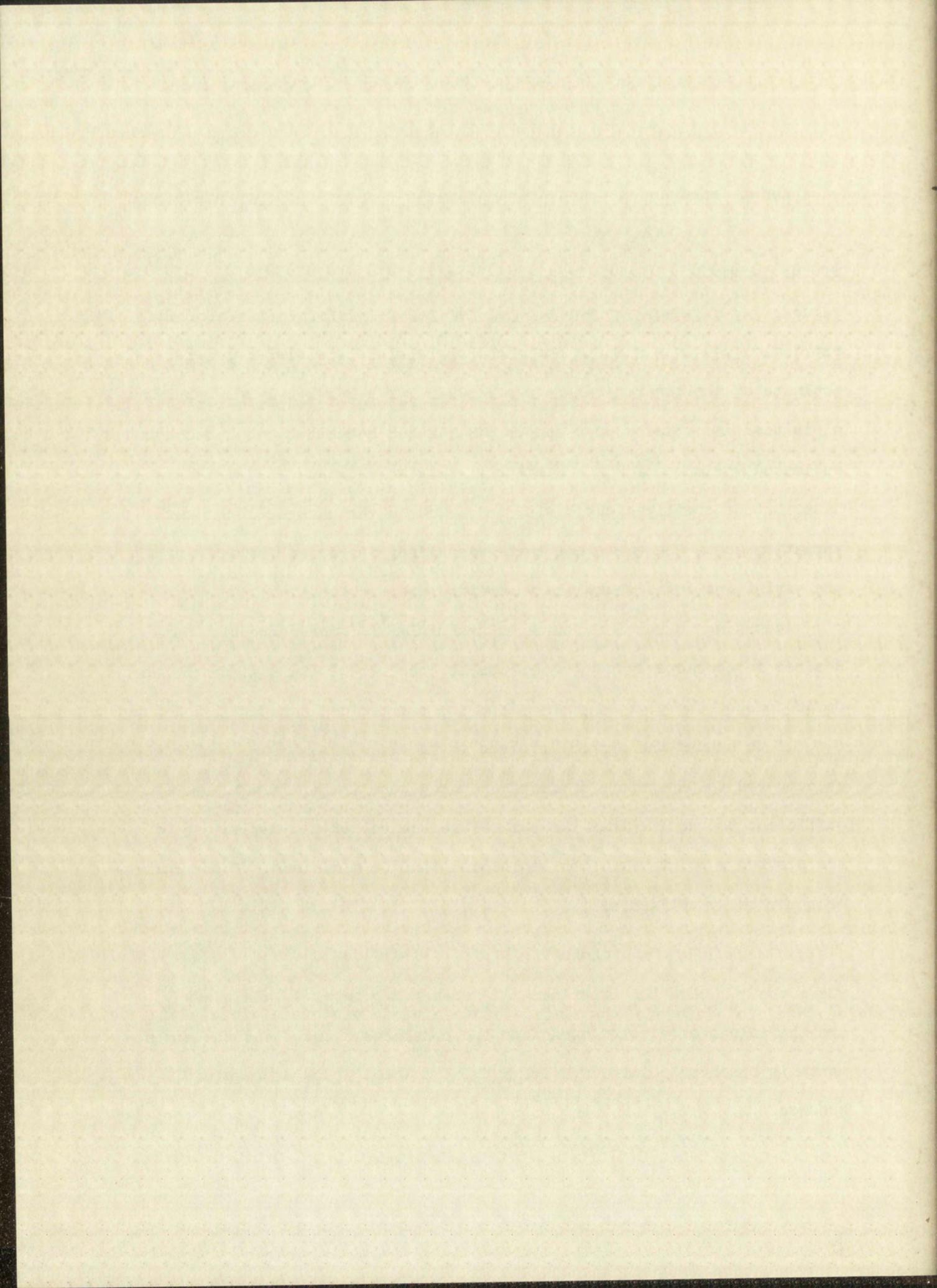
According to the least squares principle,⁽¹⁸⁾ the regression line desired is characterized by a minimum for the sum of the squares of the deviations of the plotted points from the regression line.

If we assume the errors involved in the x coordinate are negligible as compared to the errors involved in the y coordinate, it will be sufficient to require that the sum of the squares of the deviations of the plotted y points from the regression line be a minimum. This requirement may be symbolized as

$$\Sigma(y_{\text{obs}} - y_{\text{calc}})^2 = \text{Min.} \quad \text{A.2}$$

where the y_{obs} are the experimentally observed points, y , and the y_{calc} are the values of y calculated from the constants α and β and the experimentally observed points, x , i.e. $y_{\text{calc}} = \alpha + \beta x$. Thus expression A.2 becomes

$$\Sigma(y - \alpha - \beta x)^2 = \text{Min.} \quad \text{A.3}$$



To assure the condition expressed by Equation A.3, it will be necessary to minimize the quantity $(y - \alpha - \beta x)^2$ with respect to both α and β . This minimization is assured by the conditions

$$\frac{\partial}{\partial \alpha} [\Sigma(y - \alpha - \beta x)^2] = 0 \quad \text{A.4}$$

$$\frac{\partial}{\partial \beta} [\Sigma(y - \alpha - \beta x)^2] = 0 \quad \text{A.5}$$

Equations A.4 and A.5 yield the expressions

$$n\alpha + \beta \Sigma x = \Sigma y \quad \text{A.6}$$

$$\alpha \Sigma x + \beta \Sigma x^2 = \Sigma xy \quad \text{A.7}$$

where n is the number of observed points, all assumed to be determined with the same precision.

The solution of the simultaneous Equations A.6 and A.7 gives the best values for α and β in terms of Σx , Σy , and Σx^2 . The solutions yield

$$\beta = \frac{n\Sigma xy - \Sigma x \Sigma y}{n\Sigma x^2 - (\Sigma x)^2} \quad \text{A.8}$$

$$\alpha = \frac{1}{n} (\Sigma y - \beta \Sigma x) \quad \text{A.9}$$

Equations A.6 and A.7 can also be written as

$$\begin{pmatrix} n & \Sigma x \\ \Sigma x & \Sigma x^2 \end{pmatrix} \begin{pmatrix} \alpha \\ \beta \end{pmatrix} = \begin{pmatrix} \Sigma y \\ \Sigma xy \end{pmatrix} \quad \text{A.10}$$

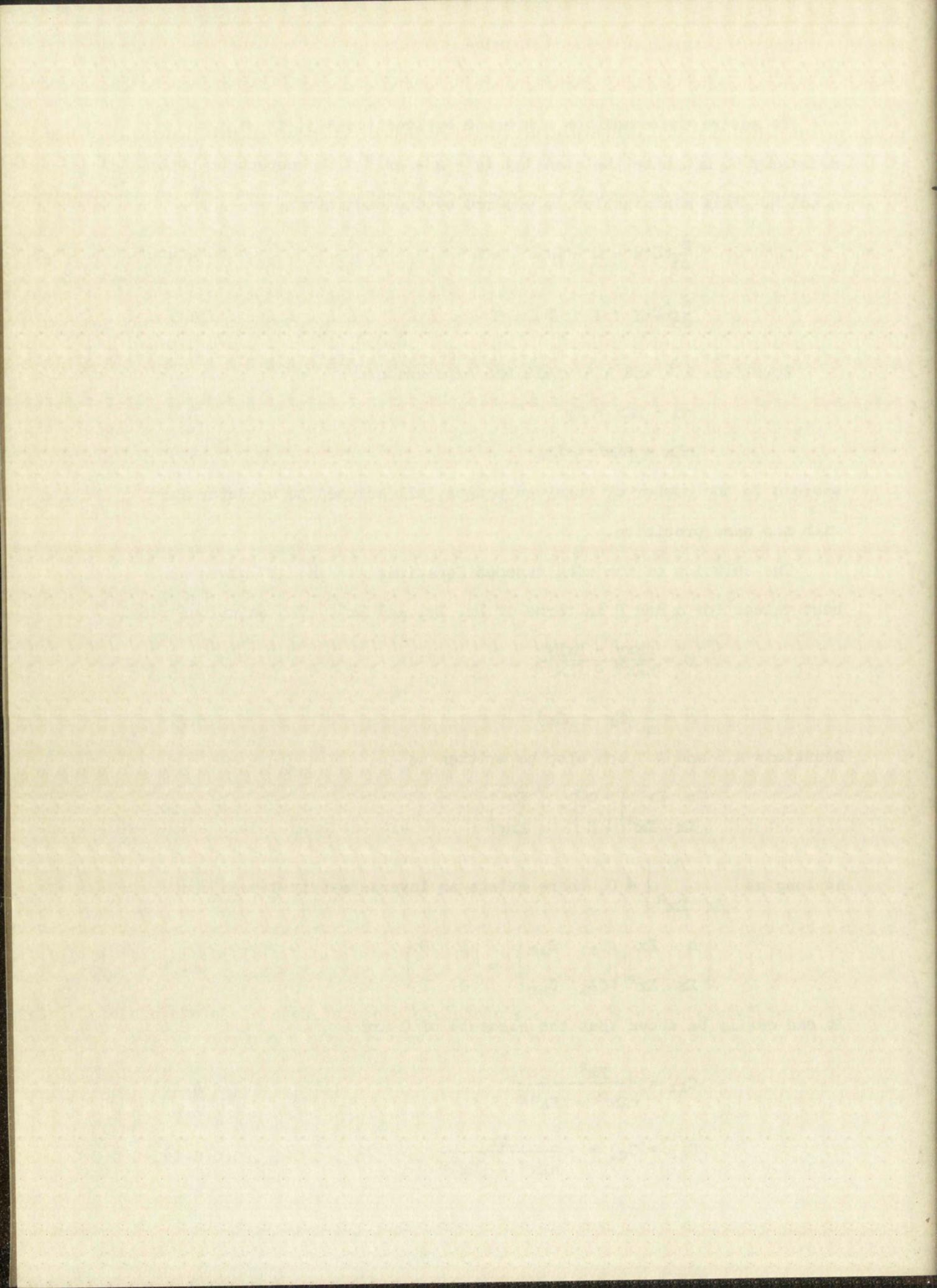
As long as $\begin{vmatrix} n & \Sigma x \\ \Sigma x & \Sigma x^2 \end{vmatrix} \neq 0$, there exists an inverse matrix \underline{C} such that

$$\begin{pmatrix} n & \Sigma x \\ \Sigma x & \Sigma x^2 \end{pmatrix} \begin{pmatrix} C_{11} & C_{12} \\ C_{21} & C_{22} \end{pmatrix} = \begin{pmatrix} 1 & 0 \\ 0 & 1 \end{pmatrix} \quad \text{A.11}$$

It can easily be shown that the elements of \underline{C} are

$$C_{11} = \frac{\Sigma x^2}{n\Sigma x^2 - (\Sigma x)^2} \quad \text{A.12}$$

$$C_{12} = C_{21} = -\frac{\Sigma x}{n\Sigma x^2 - (\Sigma x)^2} \quad \text{A.13}$$



$$C_{22} = \frac{n}{n\sum x^2 - (\sum x)^2} \quad \text{A.14}$$

Now the estimate, S^2 , of the variance, σ^2 , about the regression line is given by⁽¹⁹⁾

$$S^2 = \frac{\sum(y - \alpha - \beta x)^2}{n - 2} \quad \text{A.15}$$

while the estimate of the variance of α about A, S_α^2 , and the estimate of the variance of β about B, S_β^2 , is given by⁽¹⁹⁾

$$S_\alpha^2 = C_{11}S^2 \quad \text{A.16}$$

$$S_\beta^2 = C_{22}S^2 \quad \text{A.17}$$

Equations A.7 through A.17 completely define the parameters of the system, so that the information for the regression analysis is complete.

It will be necessary in the treatment of the data to consider functions of one or more variables in which the j th variable has associated with it a variance, S_j^2 .

In the event the variables are independent, the variance of the composite function, F, will be given by⁽²⁰⁾

$$S_F^2 = \left(\frac{\partial F}{\partial v}\right)^2 S_v^2 + \left(\frac{\partial F}{\partial w}\right)^2 S_w^2 + \dots + \left(\frac{\partial F}{\partial z}\right)^2 S_z^2 \quad \text{A.18}$$

If the function F is a function of two variables, v and w, which are dependent, the variance of the composite function will be given by⁽²¹⁾

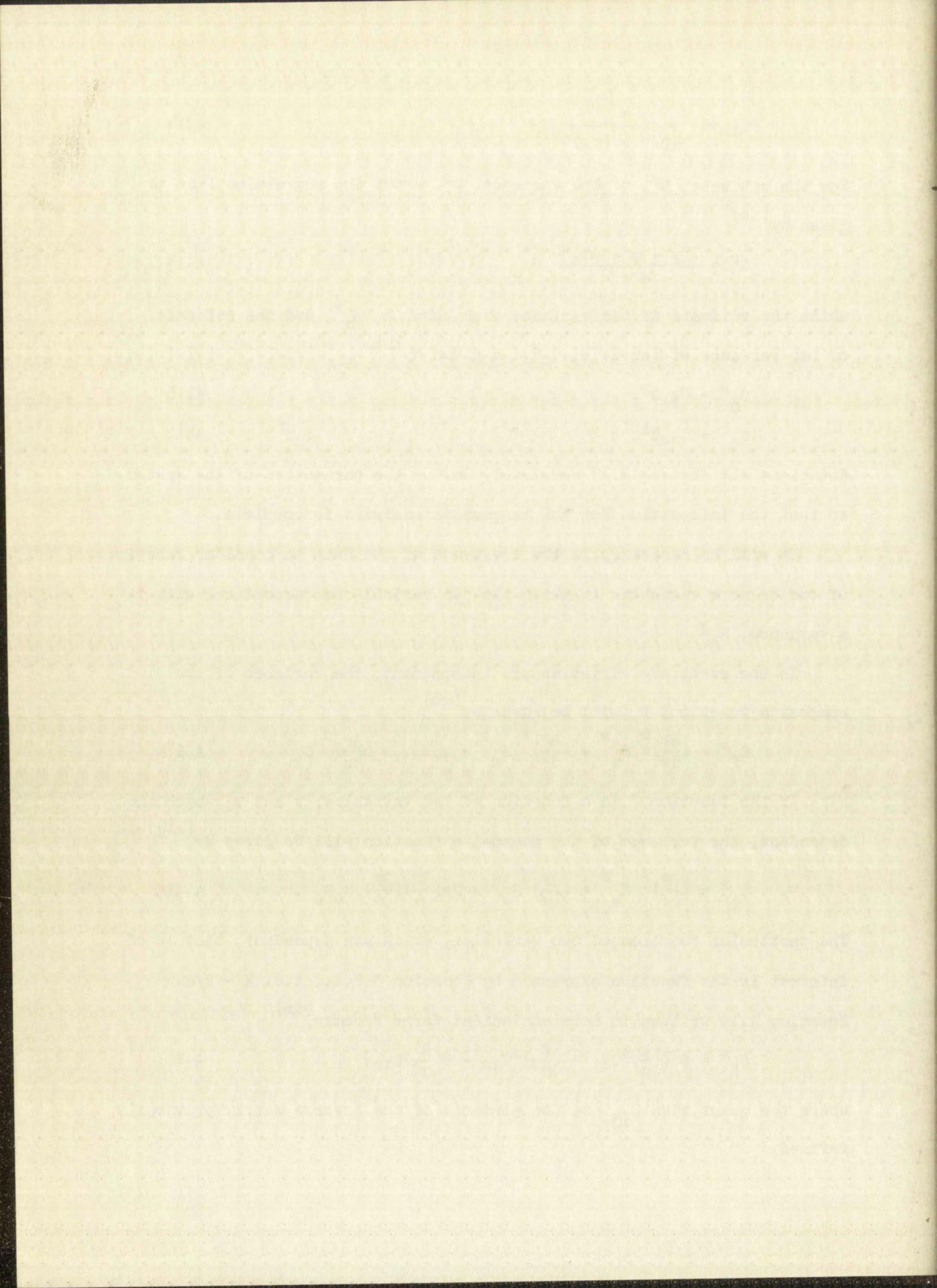
$$S_F^2 = \left(\frac{\partial F}{\partial v}\right)^2 S_v^2 + \left(\frac{\partial F}{\partial w}\right)^2 S_w^2 + 2\rho\left(\frac{\partial F}{\partial v}\right)\left(\frac{\partial F}{\partial w}\right) S_v S_w \quad \text{A.19}$$

The particular function of two variables, which are dependent, that is of interest is the function expressed by Equation 5.2.1., i.e. $K = \beta/\alpha$.

Equation A.19 written in more convenient terms becomes⁽²²⁾

$$S_K^2 = S^2\left[\left(\frac{1}{\alpha}\right)^2 C_{11} + \left(\frac{\beta}{\alpha^2}\right)^2 C_{22} - 2\left(\frac{\beta}{\alpha^3}\right) C_{12}\right] \quad \text{A.20}$$

where the quantities C_{ij} are the elements of the inverse matrix previously defined.



APPENDIX B

SUMMARY OF DATA

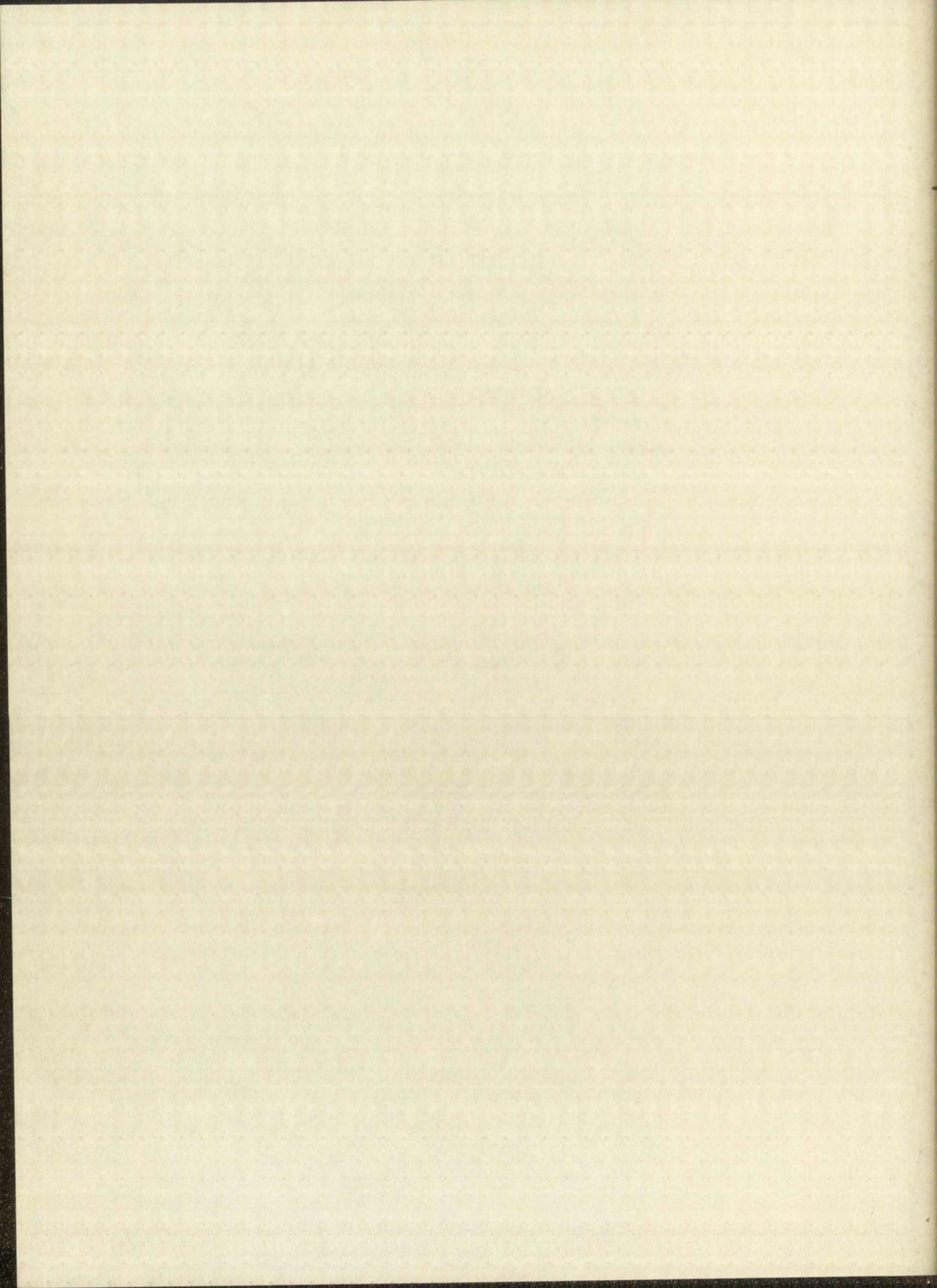


TABLE B.1

THE VARIABLES OF SYSTEM II FOR THE EQUATION $\frac{a_0 b_0}{D^\lambda} = \frac{b_0}{(\epsilon_c^\lambda - \epsilon_a^\lambda)} + \frac{1}{K(\epsilon_c^\lambda - \epsilon_a^\lambda)}$

AT WAVE LENGTH λ AND TEMPERATURE 15.2°

$$D = \left[\frac{A^\lambda}{t} - \epsilon_a^\lambda a_0 \right]$$

$$t = 1 \text{ cm}$$

$$\mu = 1.34$$

a ₀ Na ₂ Ni(CN) ₄ moles/liter	b ₀ NaCN moles/liter	P ₀ NaClO ₄ moles/liter	$\frac{a_0 b_0}{D^\lambda}$		
			4300 Å	4500 Å	4700 Å
0.1000	0.9653	0.04108	-----	-----	-----
	0.7233	0.2891	-----	-----	0.02825
	0.4816	0.5386	0.01634	0.01917	0.02426
0.09000	0.9653	0.06708	-----	-----	-----
	0.7233	0.3188	-----	0.02036	0.02822
	0.4816	0.5698	0.01633	0.01920	0.02614
0.08000	0.9653	0.1012	-----	-----	0.02615
	0.7233	0.3515	-----	-----	-----
	0.4816	0.5987	0.01618	0.01906	0.02600
0.07000	0.9653	0.1316	-----	0.02098	0.02893
	0.7233	0.3819	0.01681	0.01996	0.02718
	0.4816	0.6294	0.01602	0.01888	0.02571
0.06000	0.9653	0.1598	0.01780	0.02087	0.02857
	0.7233	0.4093	0.01710	0.01998	0.02697
	0.4816	0.6619	0.01634	0.01913	0.02581

Date	Description	Particulars	Debit	Credit	Balance
1880	To Balance				
1881	By Balance				
1882	To Balance				
1883	By Balance				
1884	To Balance				
1885	By Balance				
1886	To Balance				
1887	By Balance				
1888	To Balance				
1889	By Balance				

TABLE B.2

THE VARIABLES OF SYSTEM II FOR THE EQUATION $\frac{a_0 b_0}{D^\lambda} = \frac{b_0}{(\epsilon_c^\lambda - \epsilon_a^\lambda)} + \frac{1}{K(\epsilon_c^\lambda - \epsilon_a^\lambda)}$

AT WAVE LENGTH λ AND TEMPERATURE 25.2°

$$D^\lambda = \left[\frac{A^\lambda}{t} - \epsilon_a^\lambda a_0 \right]$$

$$t = 1 \text{ cm}$$

$$\mu = 1.34$$

a ₀ Na ₂ Ni(CN) ₄ moles/liter	b ₀ NaCN moles/liter	P ₀ NaClO ₄ moles/liter	$\frac{a_0 b_0}{D^\lambda}$		
			4300 Å	4500 Å	4700 Å
0.1000	0.9653	0.04108	-----	-----	0.03563
	0.7233	0.2891	0.02270	0.02658	0.03581
	0.4816	0.5386	0.02170	0.02491	0.03393
0.09000	0.9653	0.06708	-----	-----	0.03640
	0.7233	0.3188	0.02281	0.02671	0.03617
	0.4816	0.5698	0.02127	0.02456	0.03349
0.08000	0.9653	0.1012	-----	0.02690	0.03650
	0.7233	0.3515	-----	-----	-----
	0.4816	0.5987	0.02137	0.02464	0.03375
0.07000	0.9653	0.1316	0.02327	0.02684	0.03663
	0.7233	0.3819	0.02190	0.02541	0.03450
	0.4816	0.6294	0.02051	0.02395	0.03307
0.06000	0.9653	0.1598	0.02252	0.02627	0.03582
	0.7233	0.4093	0.02169	0.02533	0.03449
	0.4816	0.6619	0.02089	0.02427	0.03316

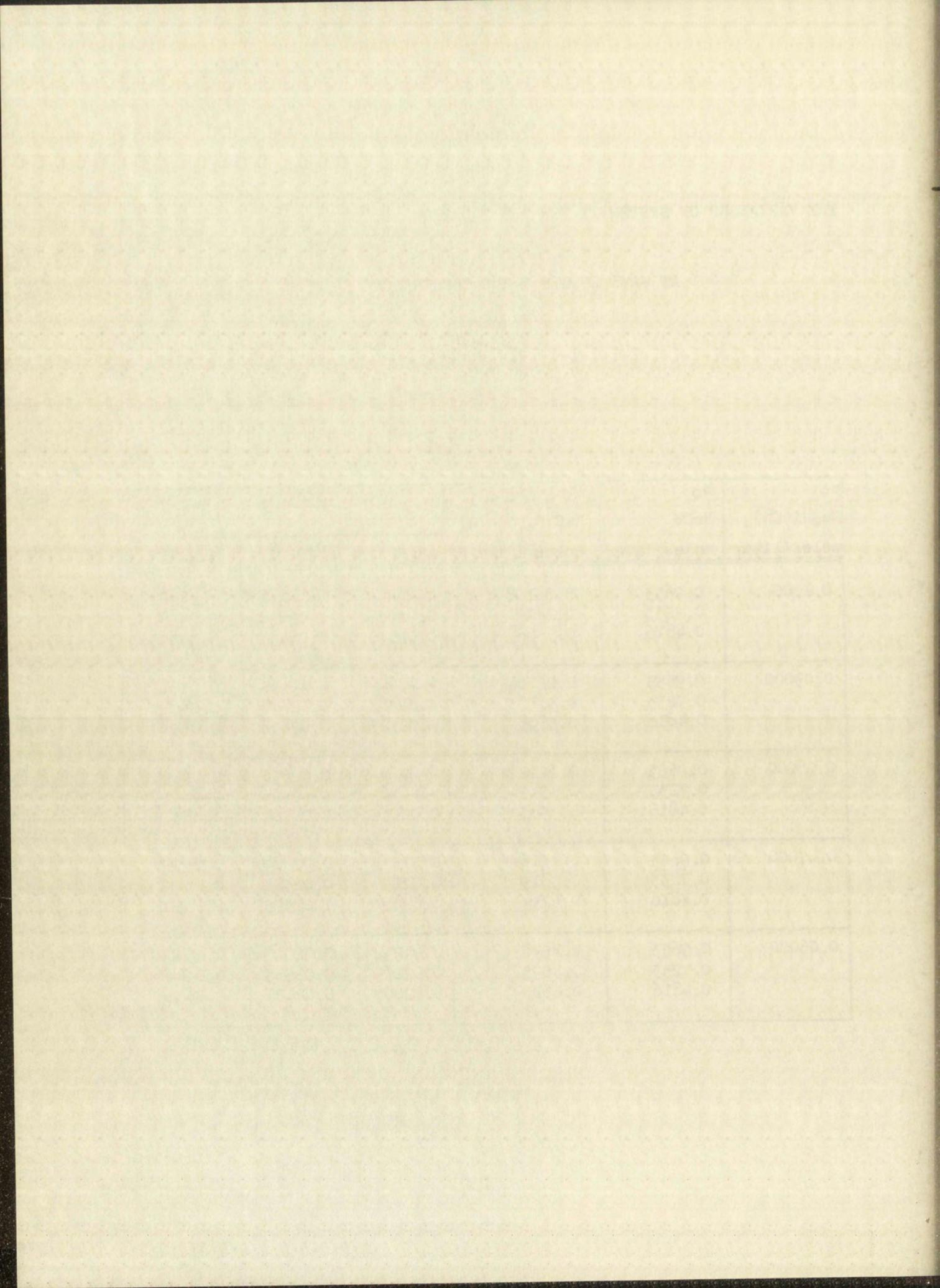


TABLE B.3

THE VARIABLES OF SYSTEM II FOR THE EQUATION $\frac{a_0 b_0}{D^\lambda} = \frac{b_0}{(\epsilon_c^\lambda - \epsilon_a^\lambda)} + \frac{1}{K(\epsilon_c^\lambda - \epsilon_a^\lambda)}$

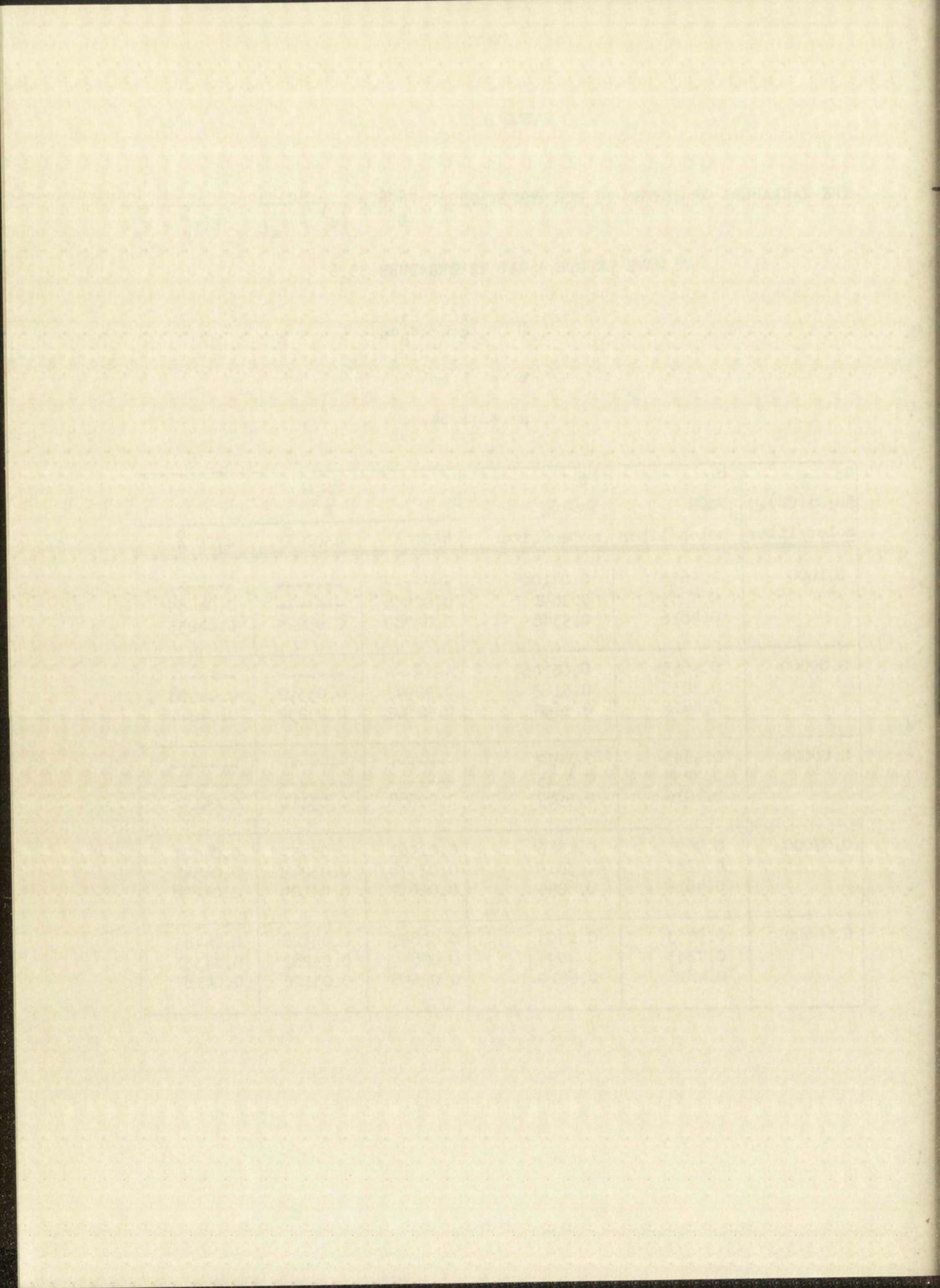
AT WAVE LENGTH λ AND TEMPERATURE 33.6°

$$D^\lambda = \left[\frac{A^\lambda}{t} - \epsilon_a^\lambda a_0 \right]$$

$$t = 1 \text{ cm}$$

$$\mu = 1.34$$

a ₀ Na ₂ Ni(CN) ₄ moles/liter	b ₀ NaCN moles/liter	P ₀ NaClO ₄ moles/liter	$\frac{a_0 b_0}{D^\lambda}$		
			4300 Å	4500 Å	4700 Å
0.1000	0.9653	0.04108	-----	-----	-----
	0.7233	0.2891	0.02934	-----	0.04485
	0.4816	0.5386	0.02789	0.03225	0.04233
0.09000	0.9653	0.06708	-----	-----	-----
	0.7233	0.3188	0.02947	0.03392	0.04508
	0.4816	0.5698	0.02802	0.03234	0.04244
0.08000	0.9653	0.1012	-----	-----	-----
	0.7233	0.3515	-----	-----	-----
	0.4816	0.5987	0.02688	0.03111	0.04172
0.07000	0.9653	0.1316	0.02961	0.03457	0.04521
	0.7233	0.3819	0.02778	0.03241	0.04341
	0.4816	0.6294	0.02677	0.03109	0.04208
0.06000	0.9653	0.1598	0.02857	0.03328	0.04485
	0.7233	0.4093	0.02857	0.03282	0.04331
	0.4816	0.6619	0.02698	0.03126	0.04187



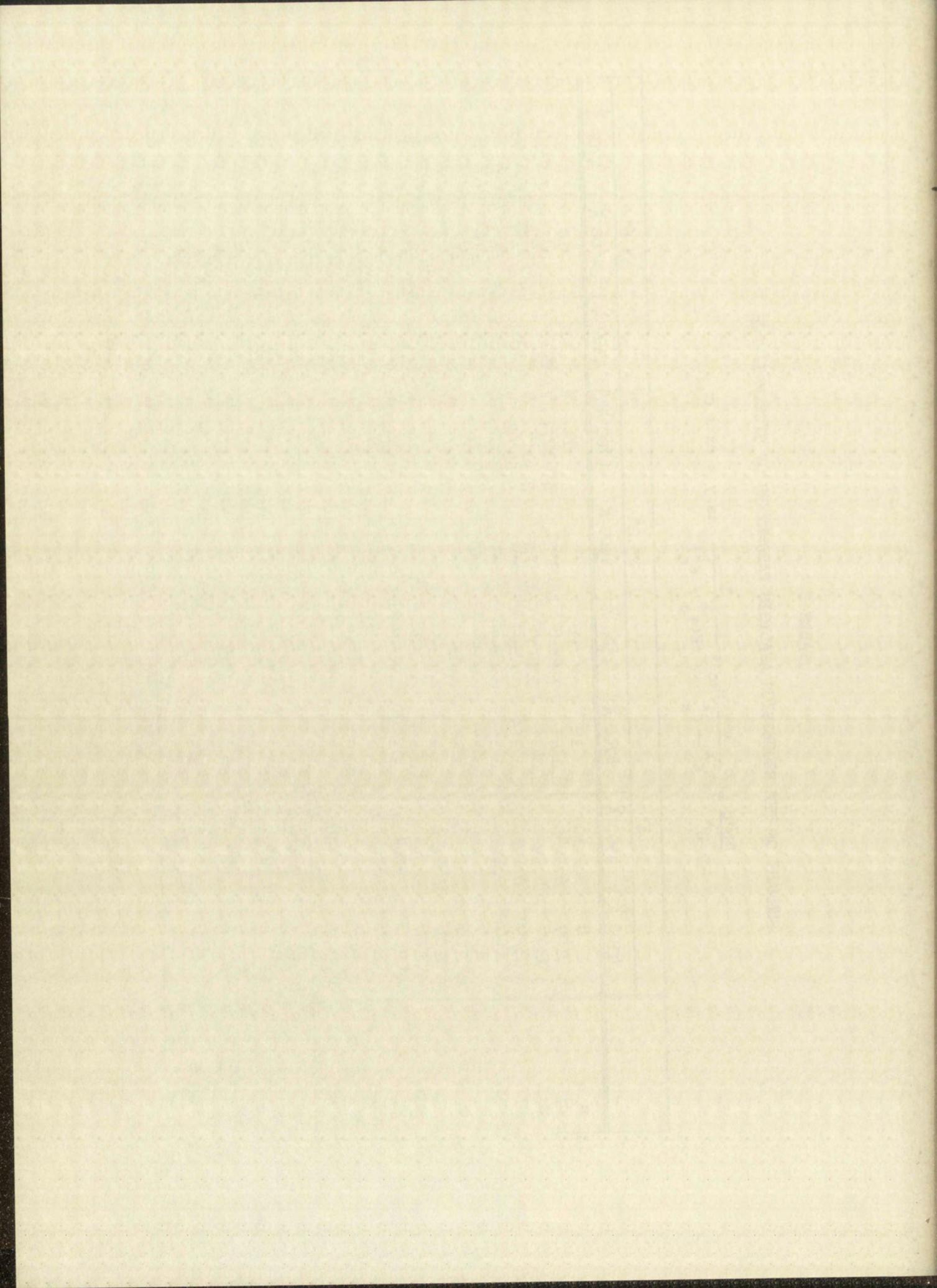


TABLE B.5

THE VARIABLES OF SYSTEM I FOR THE EQUATION $\frac{D^\lambda}{a_0 b_0} = \epsilon_c^\lambda K$

AT WAVE LENGTH λ AND TEMPERATURE 15.4°

$$D^\lambda = \left[\frac{A^\lambda}{t} - \epsilon_a^\lambda a_0 \right]$$

$$t = 5 \text{ cm}$$

$$\mu = 1.33$$

a ₀ Na ₂ Ni(CN) ₄ moles/liter	b ₀ NaCN moles/liter	P ₀ NaClO ₄ moles/liter	D ^λ a ₀ b ₀		
			4300 Å	4500 Å	4700 Å
0.1000	0.02825	1.0043	65.8	56.7	40.7
	0.02348	1.0111	67.7	57.9	41.4
	0.01868	1.0164	67.5	57.8	41.2
	0.01394	1.0209	58.8	50.2	35.1
	0.009132	1.0256	66.8	57.0	39.4
0.09000	0.02825	1.0377	69.2	59.4	44.5
	0.02348	1.0408	65.3	56.7	41.6
	0.01868	1.0446	69.0	58.9	42.8
	0.01394	1.0522	69.3	58.1	43.0
	0.009132	1.0566	64.5	54.7	40.1
0.08000	0.03783	1.0566	70.7	60.8	44.3
	0.03304	1.0606	68.5	59.4	44.3
	0.02825	1.0644	68.6	59.3	43.4
	0.02348	1.0697	68.2	57.0	42.6
	0.01868	1.0758	68.3	58.9	43.5
0.07000	0.03783	1.0857	69.0	58.9	42.3
	0.03304	1.0910	69.1	59.2	42.8
	0.02825	1.0956	70.3	59.7	44.0
	0.02348	1.0986	69.3	59.0	43.2
	0.01868	1.1039	69.4	58.9	42.8
0.06000	0.03783	1.1128	70.5	60.8	44.5
	0.03304	1.1199	68.1	59.0	43.4
	0.02825	1.1124	67.3	57.2	43.1
	0.02348	1.1131	67.4	58.9	43.3
	0.01868	1.1344	67.8	58.9	42.8
R ^λ ± S _R λ			67.9 ± 2.4	58.1 ± 2.2	42.4 ± 2.1

$$R^\lambda = \frac{1}{n} \sum \frac{D^\lambda}{a_0 b_0}$$

$$(S_R \lambda)^2 = \frac{1}{n-1} \sum \left(\frac{D^\lambda}{a_0 b_0} - R^\lambda \right)^2$$

TABLE B.6

THE VARIABLES OF SYSTEM I FOR THE EQUATION $\frac{D^\lambda}{a_0 b_0} = \epsilon_c^\lambda K$

AT WAVE LENGTH λ AND TEMPERATURE 25.2°

$$D^\lambda = \left[\frac{A^\lambda}{t} - \epsilon_a^\lambda a_0 \right]$$

$$t = 5 \text{ cm}$$

$$\mu = 1.33$$

a ₀ Na ₂ Ni(CN) ₄ moles/liter	b ₀ NaCN moles/liter	P ₀ NaClO ₄ moles/liter	$\frac{D^\lambda}{a_0 b_0}$		
			4300 Å	4500 Å	4700 Å
0.1000	0.02825	1.0043	48.2	46.7	30.4
	0.02348	1.0111	50.2	41.7	30.6
	0.01868	1.0164	50.3	42.3	31.0
	0.01394	1.0209	45.9	38.7	28.0
	0.009132	1.0256	52.6	44.9	31.8
0.09000	0.02825	1.0377	49.5	42.9	32.7
	0.02348	1.0408	48.3	40.7	30.7
	0.01868	1.0446	51.1	42.8	32.1
	0.01394	1.0522	53.3	43.1	33.4
	0.009132	1.0566	53.5	43.8	34.0
0.08000	0.03783	1.0566	51.5	43.9	33.4
	0.03304	1.0606	50.3	43.1	32.6
	0.02825	1.0644	50.9	43.4	32.8
	0.02348	1.0697	51.1	44.7	33.0
	0.01868	1.0758	52.9	46.2	34.8
0.07000	0.03783	1.0857	49.8	42.3	31.3
	0.03304	1.0910	50.1	41.9	31.6
	0.02825	1.0956	50.5	43.0	31.9
	0.02348	1.0986	50.5	43.2	31.6
	0.01868	1.1039	52.0	44.4	32.9
0.06000	0.03783	1.1138	52.9	45.4	34.3
	0.03304	1.1199	51.4	43.9	32.8
	0.02825	1.1124	51.9	44.3	33.1
	0.02348	1.1131	53.9	46.8	34.8
	0.01868	1.1344	54.4	47.3	36.6
$R^\lambda \pm S_{R^\lambda}$			51.1 ± 2.0	43.4 ± 2.1	32.5 ± 1.8

$$R^\lambda = \frac{1}{n} \sum \frac{D^\lambda}{a_0 b_0}$$

$$(S_{R^\lambda})^2 = \frac{1}{n-1} \sum \left(\frac{D^\lambda}{a_0 b_0} - R^\lambda \right)^2$$

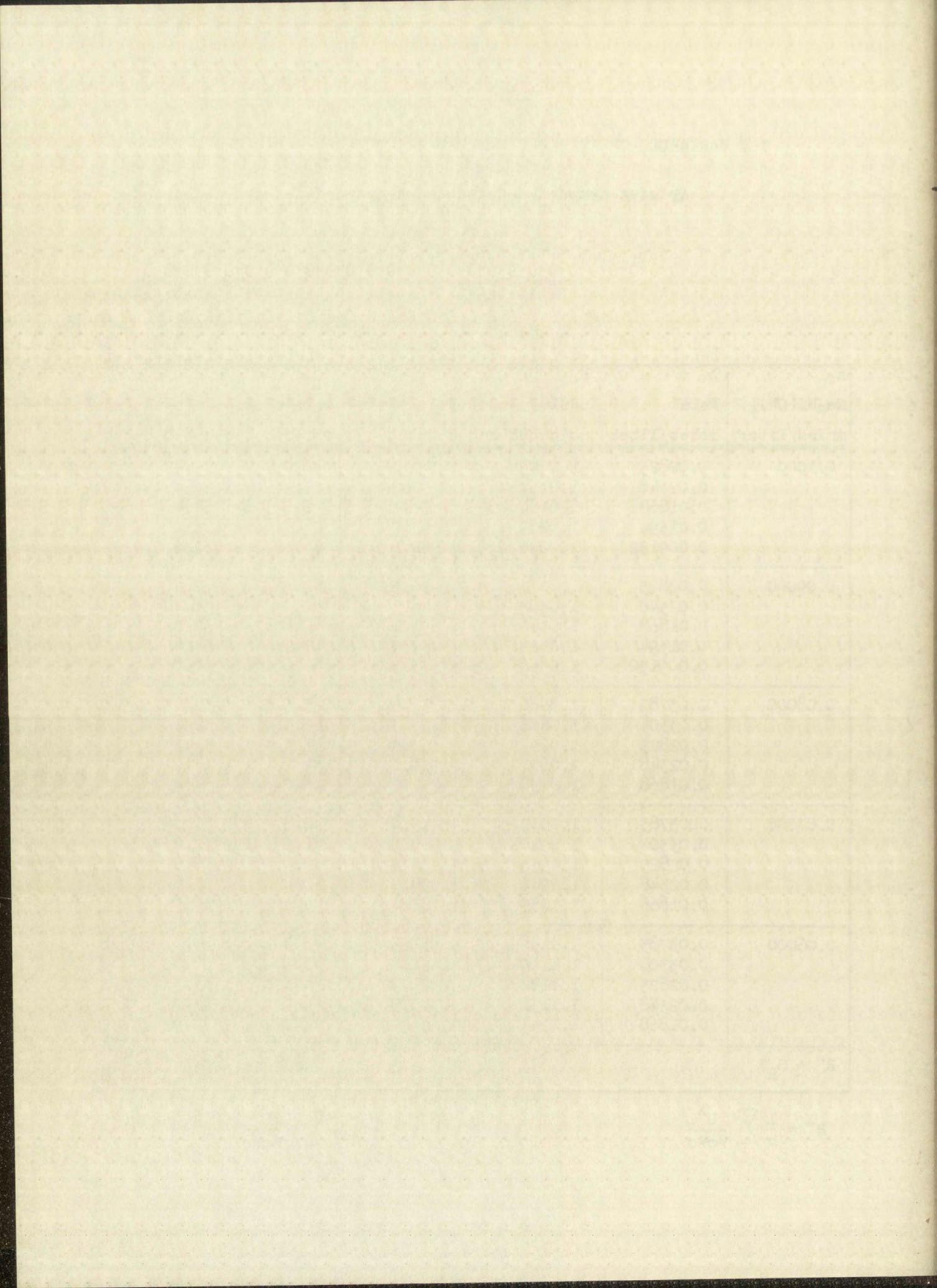


TABLE B.7

THE VARIABLES OF SYSTEM I FOR THE EQUATION $\frac{D^\lambda}{a_0 b_0} = \epsilon_c^\lambda K$

AT WAVE LENGTH λ AND TEMPERATURE 33.6°

$$D^\lambda = \left[\frac{A^\lambda}{t} - \epsilon_a^\lambda a_0 \right]$$

$$t = 5 \text{ cm}$$

$$\mu = 1.33$$

a ₀ Na ₂ Ni(CN) ₄ moles/liter	b ₀ NaCN moles/liter	P ₀ NaClO ₄ moles/liter	$\frac{D^\lambda}{a_0 b_0}$		
			4300 Å	4500 Å	4700 Å
0.1000	0.02825	1.0043	37.2	30.8	23.0
	0.02348	1.0111	38.3	32.0	24.0
	0.01868	1.0164	39.1	32.7	24.1
	0.01394	1.0209	36.6	30.1	21.6
	0.009132	1.0256	42.7	35.0	25.2
0.09000	0.02825	1.0377	38.5	32.3	24.8
	0.02348	1.0408	37.4	30.7	23.2
	0.01868	1.0446	40.5	33.3	25.0
	0.01394	1.0522	43.0	34.2	26.3
	0.009132	1.0566	41.4	31.6	25.6
0.08000	0.03783	1.0566	38.3	32.4	24.5
	0.03304	1.0606	37.8	31.8	23.8
	0.02825	1.0644	38.9	32.3	24.8
	0.02348	1.0697	38.8	32.5	24.5
	0.01868	1.0758	40.2	33.4	25.5
0.07000	0.03783	1.0857	37.7	37.7	24.2
	0.03304	1.0910	38.0	30.7	23.8
	0.02825	1.0956	38.9	32.4	24.8
	0.02348	1.0986	39.5	32.9	25.0
	0.01868	1.1039	40.6	32.1	24.5
0.06000	0.03783	1.1138	38.3	32.6	24.7
	0.03304	1.1199	37.4	31.8	23.7
	0.02825	1.1124	37.7	31.9	23.6
	0.02348	1.1131	38.3	32.0	24.1
	0.01868	1.1344	39.3	32.1	25.0
$R^\lambda \pm S_R \lambda$			39.0 ± 1.7	32.2 ± 1.1	24.4 ± 1.0

$$R^\lambda = \frac{1}{n} \sum \frac{D^\lambda}{a_0 b_0}$$

$$(S_R \lambda)^2 = \frac{1}{n-1} \sum \left(\frac{D^\lambda}{a_0 b_0} - R^\lambda \right)^2$$

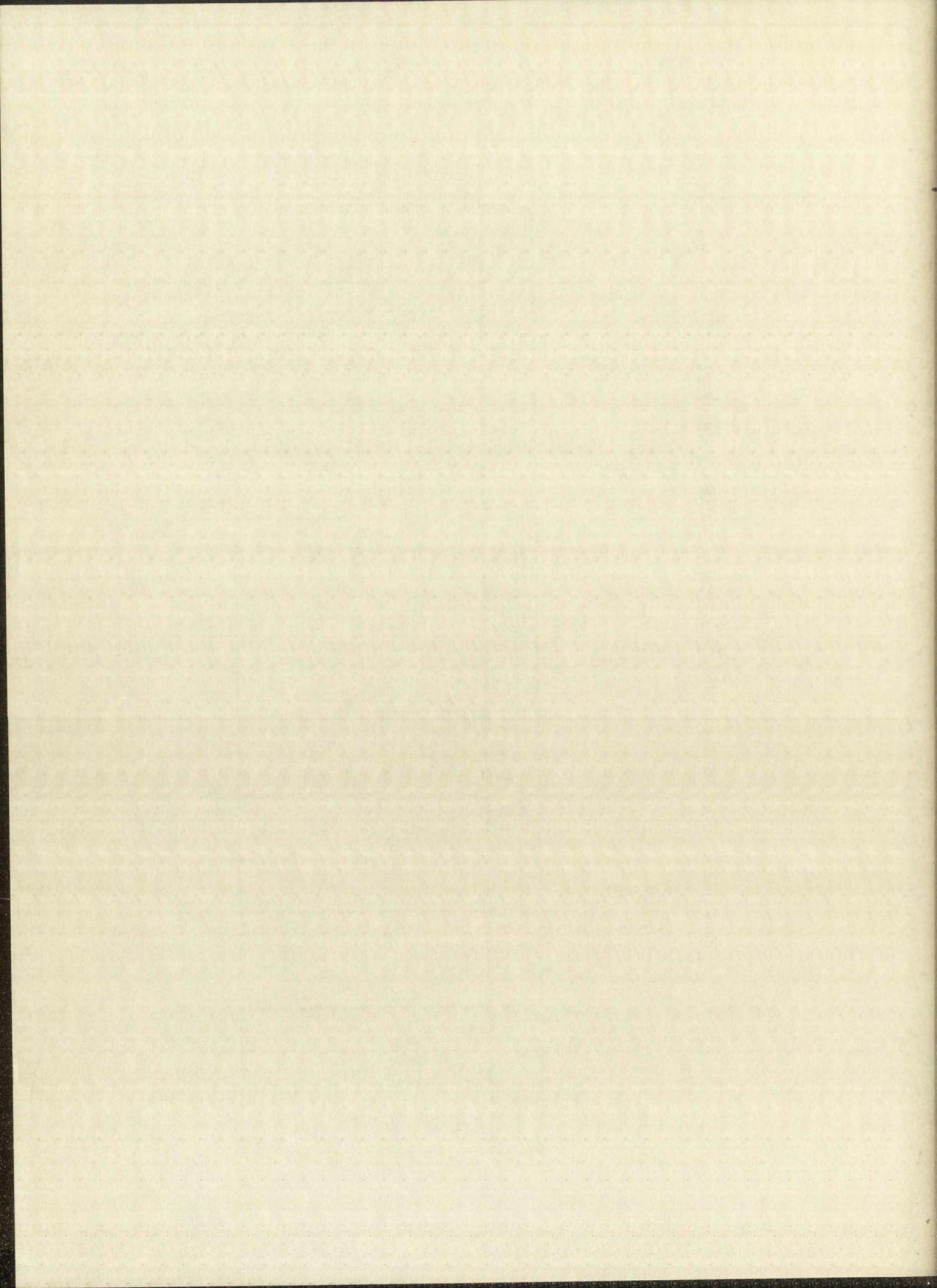
TABLE B.8

THE K VALUES FOR SYSTEM I OBTAINED FROM ϵ_c^λ VALUES FROM SYSTEM II

$$K = R^\lambda \beta$$

$$S_K^2 = R^2 \beta^2 \left[\frac{S_R^2}{R^2} \right] + \left[\frac{S_\beta^2}{\beta^2} \right]$$

	15.4°			25.2°			33.6°		
	4300 Å	4500 Å	4700 Å	4300 Å	4500 Å	4700 Å	4300 Å	4500 Å	4700 Å
R^λ	67.9	58.1	42.4	51.1	43.4	32.5	39.0	32.2	24.4
S_{R^λ}	2.4	2.2	2.1	2.0	2.1	1.8	1.7	1.1	1.0
β	0.003141	0.003834	0.005061	0.003797	0.004696	0.005598	0.004114	0.004951	0.006494
S_β	0.000299	0.000255	0.00115	0.000827	0.000808	0.000764	0.00119	0.00115	0.00110
K	0.21	0.22	0.22	0.19	0.21	0.18	0.16	0.16	0.16
S_K	0.02	0.02	0.05	0.04	0.04	0.03	0.05	0.04	0.03



BIBLIOGRAPHY

- (1) Gmelin-Friedhelm: Handbuch der Anorganischer Chemie, Vol. 5, Part I, 135, Verlag Chemie G.M.B.H., Berlin.
- (2) D. N. Hume and I. M. Kolthoff, *J. Am. Chem. Soc.*, 72, 4423 (1950).
- (3) J. Vrestal and J. Havir, *Chem listy*, 50, 1321 (1956).
- (4) A. Samuel, *J. chim. phys.*, 40, 247 (1943).
- (5) W. C. Fernelius and J. J. Burbage, Inorganic Synthesis, II p. 227, McGraw-Hill, New York, 1946.
- (6) H. Brasseur and A. De Rassenfosse, *Mem. soc. sci., Liege*, [2], 4, 397-458 (1941).
- (7) R. A. Penneman and L. H. Jones, *J. Chem. Phys.*, 24, 293 (1956).
- (8) L. H. Jones and R. A. Penneman, *J. Chem. Phys.*, 22, 965 (1954).
- (9) A. Job, *Ann. Chem.*, 10, 133 (1928).
- (10) W. C. Vosburgh and G. R. Cooper, *J. Am. Chem. Soc.*, 63, 437 (1941).
- (11) L. I. Katzin and E. Gebert, *J. Am. Chem. Soc.*, 72, 5455 (1950).
- (12) I. M. Klotz, Chemical Thermodynamics, p. 127, Prentice Hall, Inc., New York (1950).
- (13) L. G. Gouy, *Compt. rend.*, 109, 935 (1889).
- (14) R. S. Nyholm, *Chem. Revs.*, 53, 263-308 (1953).
- (15) A. E. Martell, and M. Calvin, Chemistry of the Metal Chelate Compounds, p. 226, Prentice Hall, Inc., New York (1952).
- (16) A. W. Adamson, *J. Am. Chem. Soc.*, 73, 5710 (1951).
- (17) D. N. Hume and I. M. Kolthoff, *J. Am. Chem. Soc.*, 71, 867 (1949).
- (18) A. G. Worthing, and J. Geffner, Treatment of Experimental Data, p. 240, John Wiley and Sons, Inc., New York (1943).
- (19) W. J. Youden, Statistical Methods for Chemists, p. 42, John Wiley and Sons, Inc., New York (1951).
- (20) Worthing and Geffner, op. cit., p. 213.
- (21) A. Hald, Statistical Theory with Engineering Applications, p. 118, John Wiley and Sons, Inc., New York (1952).
- (22) Private communication with R. K. Zeigler of the Los Alamos Scientific Laboratory.

SPECTROSCOPIC STUDIES OF METAL-CYANIDE COMPLEXES

PART II

AN ANALYSIS OF THE INFRARED VIBRATIONAL SPECTRA OF THE
TETRACYANONICKELATE(II) ION IN THE SOLID STATE

By

Roy L. McCullough

A Dissertation Submitted to the Graduate
Faculty in Partial Fulfillment of the
Requirements for the Degree of Doctor
of Philosophy in Chemistry

The University of New Mexico

1959

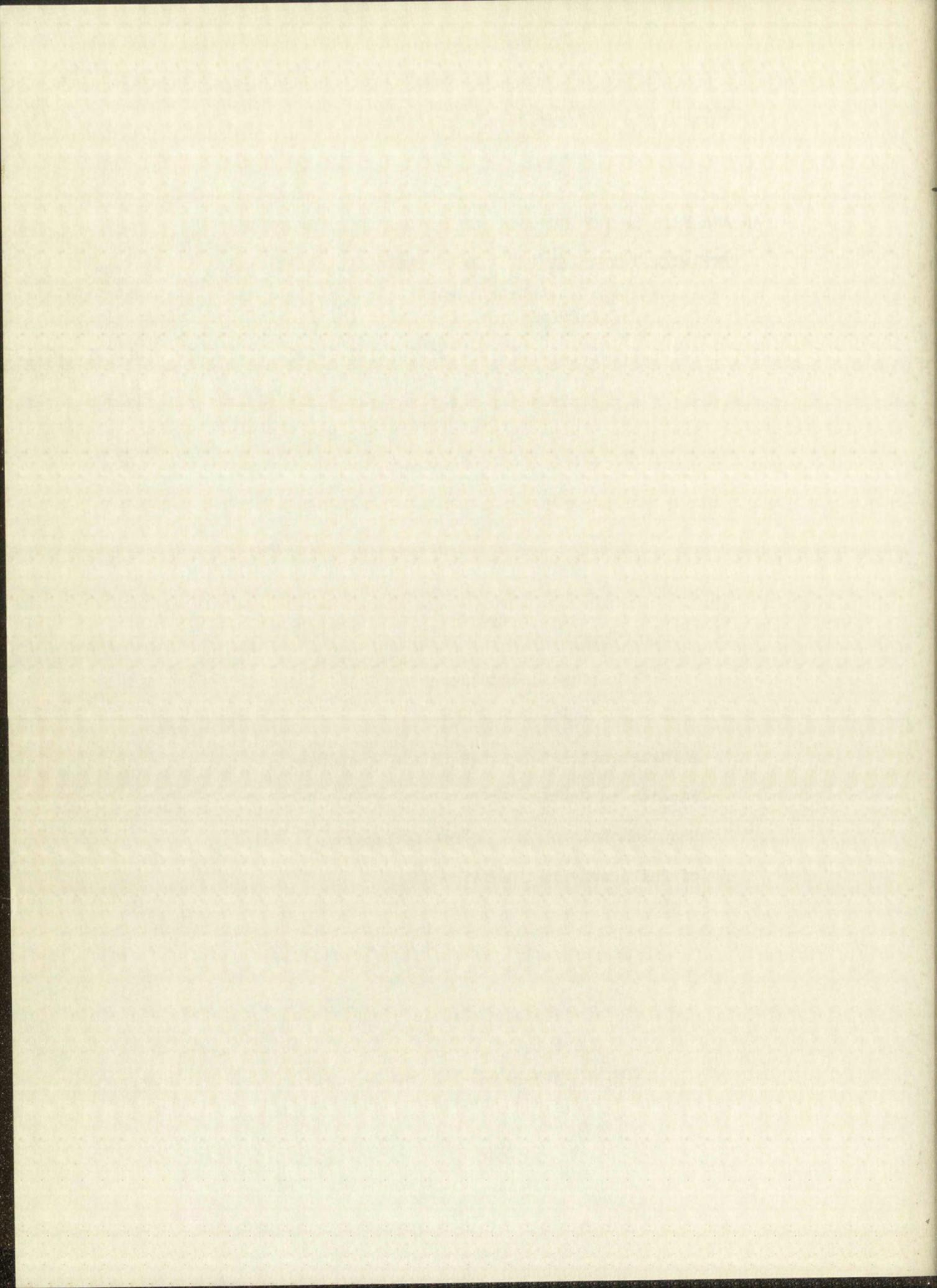
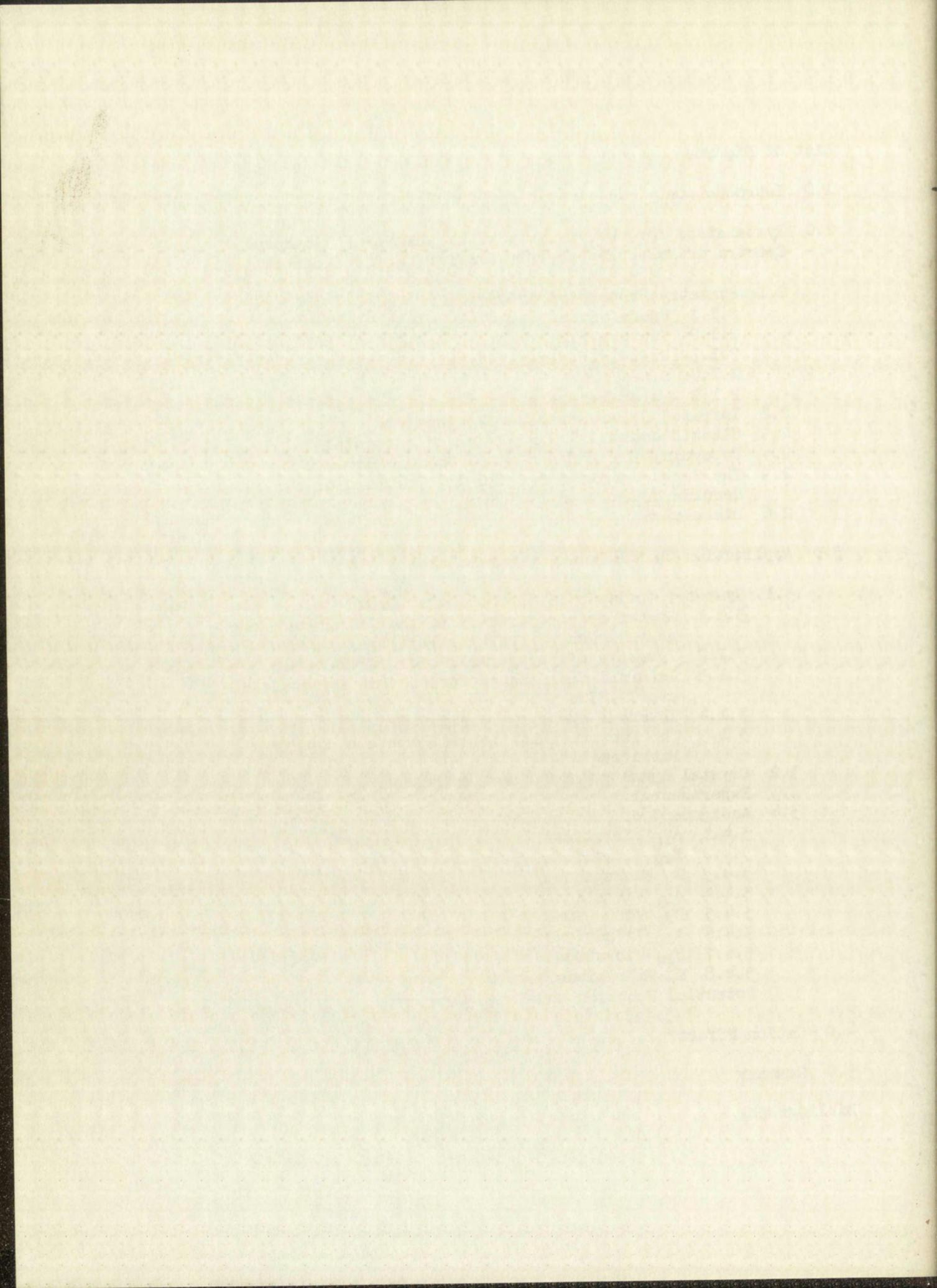


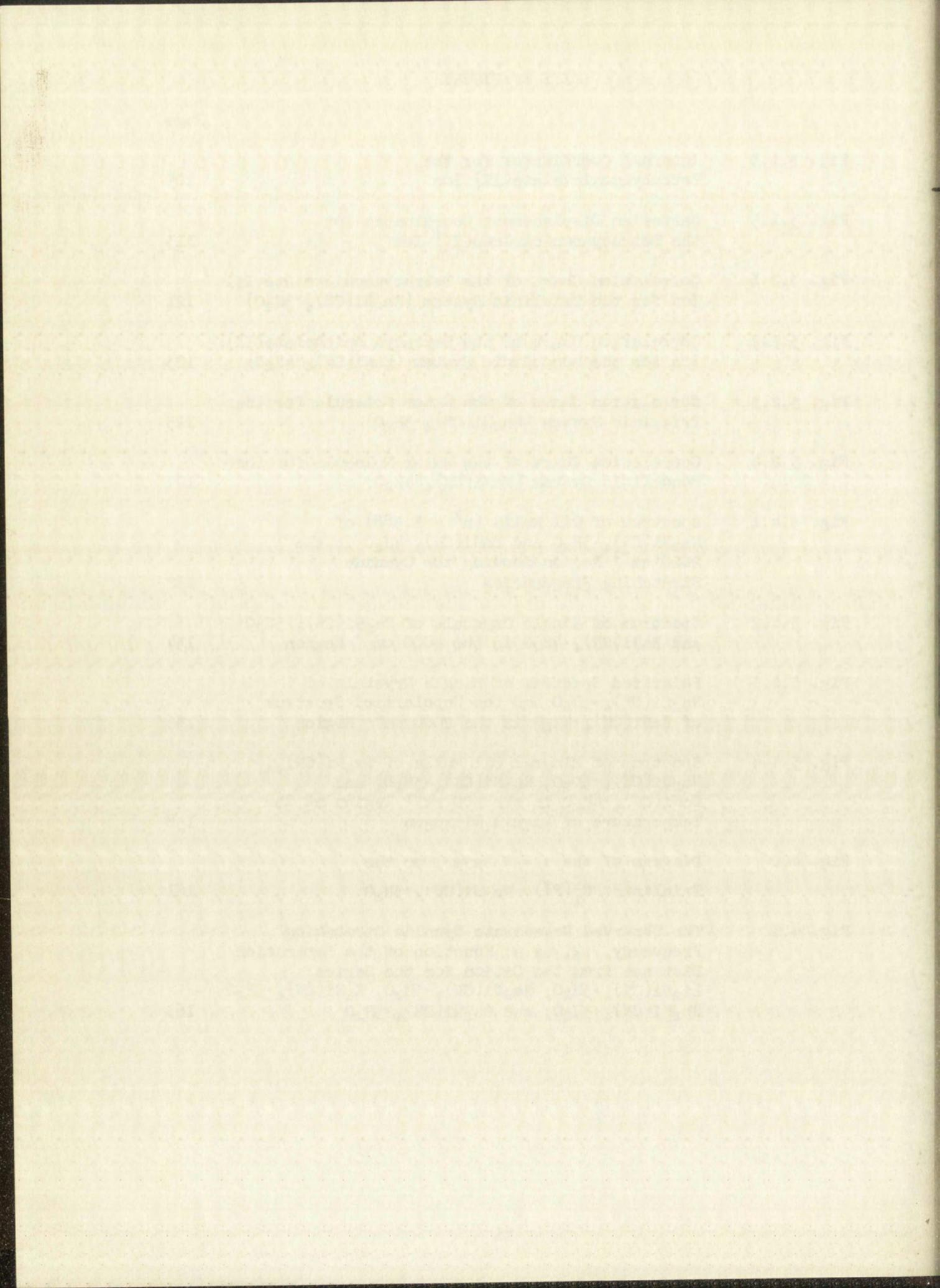
TABLE OF CONTENTS

	Page
List of Figures	ii
1.0 Introduction	66
2.0 Systematics for the Analysis of the Infrared Vibrational Spectra of Molecules and Complex Ions in the Solid State	68
2.1 Symmetry Properties of Crystals	71
2.1.1 Space Group	71
2.1.2 Factor Group	72
2.1.3 Unit Cell Group	74
2.1.4 Site Group	74
2.1.5 Molecular Group	75
2.2 Infrared Selection Rules for Crystals	75
2.3 Classification of the Motions of a Crystal	78
2.4 Determination of the \underline{G} and \underline{F} Matrix Elements	84
2.5 The Perturbation Method for the Solution of the Secular Determinant	86
2.6 Discussion	93
3.0 Application to the Tetracyanonickelate(II) Ion	98
3.1 Symmetry Analysis of the Molecular Group	100
3.1.1 Structure and Symmetry of the Tetracyanonickelate(II) Ion	100
3.1.2 Symmetry of the Normal Modes of Vibration	100
3.1.3 Internal Coordinates for the Tetracyanonickelate(II) Ion	103
3.1.4 Internal Symmetry Coordinates	109
3.1.5 The Factored Kinetic and Potential Energy Matrices	110
3.2 Crystal Symmetry and Selection Rules	119
3.3 Experimental	120
3.4 Assignment of Frequencies	130
3.4.1 A_{1g} Vibrations	130
3.4.2 B_{1g} Vibrations	131
3.4.3 E_u Vibrations	142
3.4.4 A_{2g} Vibrations	143
3.4.5 B_{2g} Vibrations	143
3.4.6 A_{2u} Vibrations	143
3.4.7 B_{2u} Vibrations	144
3.4.8 E_g Vibrations	144
3.5 Potential Function and Force Constants	146
4.0 Cation Effect	158
5.0 Summary	165
Bibliography	166



LIST OF FIGURES

	Page	
Fig. 3.1.3	Internal Coordinates for the Tetracyanonickelate(II) Ion	105
Fig. 3.1.5	Cartesian Displacement Coordinates for the Tetracyanonickelate(II) Ion	113
Fig. 3.2.1	Correlation Chart of the Tetracyanonickelate(II) Ion for the Triclinic System (Na ₂ Ni(CN) ₄ ·3H ₂ O)	121
Fig. 3.2.2	Correlation Chart of the Tetracyanonickelate(II) Ion for the Monoclinic System (BaNi(CN) ₄ ·4H ₂ O)	123
Fig. 3.2.3	Correlation Chart of the Water Molecule for the Triclinic System (Na ₂ Ni(CN) ₄ ·3H ₂ O)	125
Fig. 3.2.4	Correlation Chart of the Water Molecule for the Monoclinic System (BaNi(CN) ₄ ·4H ₂ O)	127
Fig. 3.4.1	Spectrum of Oil Mulls (n ^y = 1.588) of Na ₂ Ni(CN) ₄ ·3H ₂ O and BaNi(CN) ₄ ·4H ₂ O in the 2000 cm ⁻¹ Region Showing the Cyanide Stretching Frequencies	132
Fig. 3.4.2	Spectrum of Single Crystals of Na ₂ Ni(CN) ₄ ·3H ₂ O and BaNi(CN) ₄ ·4H ₂ O in the 4000 cm ⁻¹ Region	134
Fig. 3.4.3	Polarized Spectrum of Single Crystals of Na ₂ Ni(CN) ₄ ·3H ₂ O and the Unpolarized Spectrum of BaNi(CN) ₄ ·4H ₂ O in the 2000 cm ⁻¹ Region	136
Fig. 3.4.4	Spectrum of Mineral Oil Mulls of Na ₂ Ni(CN) ₄ , Na ₂ Ni(CN) ₄ ·3D ₂ O, Na ₂ Ni(CN) ₄ ·3H ₂ O, and BaNi(CN) ₄ ·4H ₂ O in the 500 cm ⁻¹ Region at the Temperature of Liquid Nitrogen	138
Fig. 4.0	Diagram of the z = 0 Layer for the Triclinic, C ₁ ⁱ (P1), Na ₂ Ni(CN) ₄ ·3H ₂ O	161
Fig. 4.1	The Observed Degenerate Cyanide Stretching Frequency, ν ₈ , as a Function of the Separation Distance from the Cation for the Series: Li ₂ Ni(CN) ₄ ·3H ₂ O, Na ₂ Ni(CN) ₄ ·3H ₂ O, K ₂ Ni(CN) ₄ ·3H ₂ O, Rb ₂ Ni(CN) ₄ ·3H ₂ O, and Cs ₂ Ni(CN) ₄ ·3H ₂ O	163

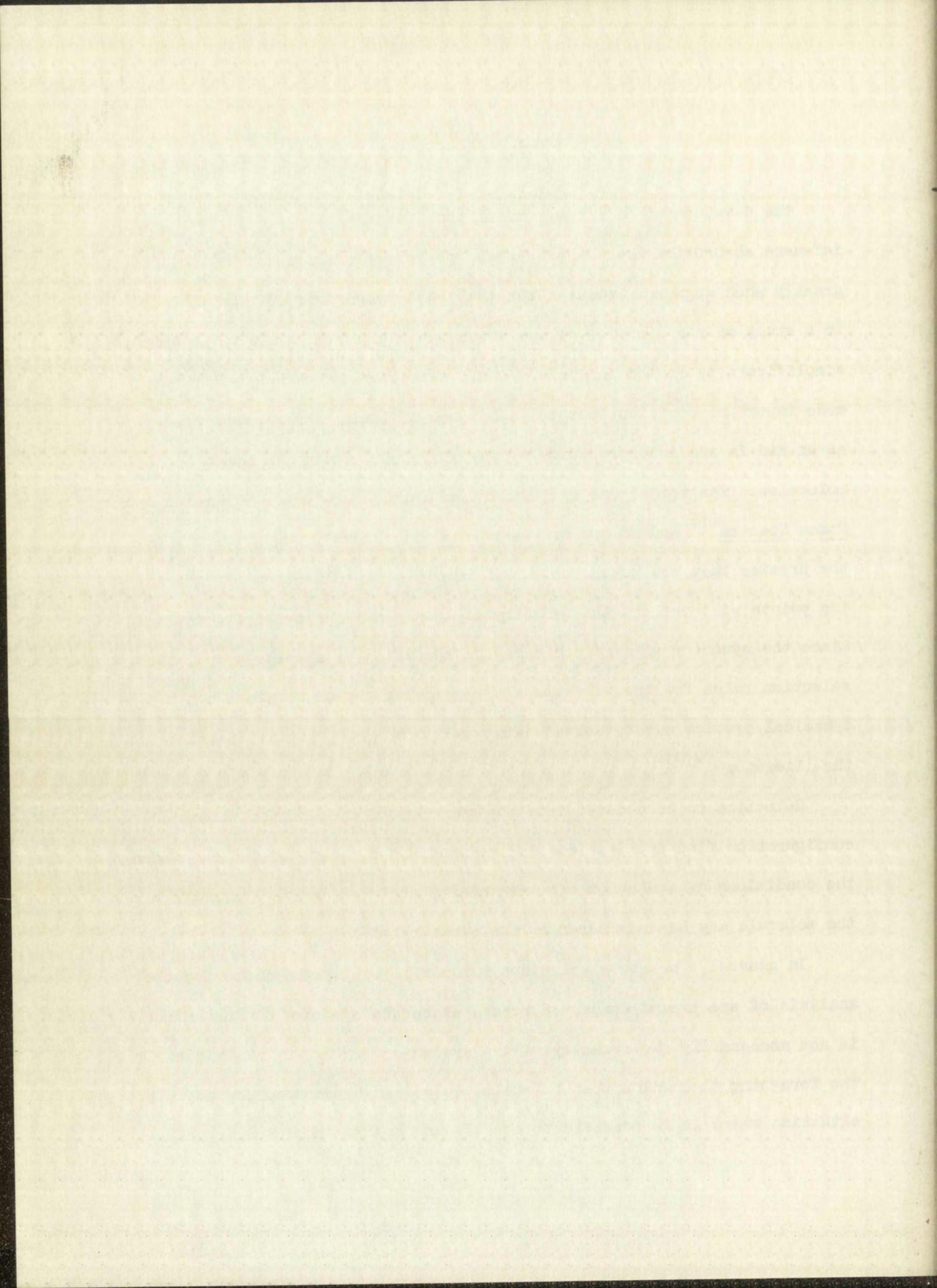


1.0 INTRODUCTION

The development of a theoretical tool for the analysis of the infrared absorption spectra of gaseous polyatomic molecules was facilitated greatly when Wigner⁽¹⁾ pointed out that the application of group theory to a study of the dynamics of the molecular vibrations would yield some simplifications in the analysis. Other investigators subsequently have made important contributions to techniques utilizing point group theory as an aid in the interpretation of the infrared spectra of gaseous molecules. The techniques are summarized in the two texts: Infrared and Raman Spectra⁽²⁾ and Molecular Vibrations⁽³⁾. These procedures rely on the premise that the mutual potential energy of a collection of interacting points will reflect the symmetry of their equilibrium configuration. Since the symmetry of a molecule may be specified by a point group, the selection rules for the vibrational frequencies may be obtained and the dynamical problem may be solved using the point group theory described in the literature^(2,3).

Selection rules deduced from the symmetry of an isolated molecular configuration find applications in the analysis of gaseous spectra, where the conditions of isolation are very nearly achieved and the symmetry of the molecule may be considered as the symmetry of the system.

In general, the above selection rules will be inappropriate for the analysis of spectra of condensed phases since the symmetry of the molecule is not necessarily the symmetry of the system. However, it is evident from the foregoing discussion that selection rules can be deduced for any situation where it is possible to specify and analyze the symmetry of a



suitable configuration of interacting points. A prerequisite, then, to the treatment of any molecular crystal is a suitable knowledge of the crystal structure. Once the crystal structure is known, procedures may be developed which will give the selection rules for the vibrations associated with the individual molecules. Of necessity these procedures must be based on space group theory since the symmetry of a crystal is specified by a given space group. The application of space group theory is not as straightforward as the utilization of point group theory; hence, specialized techniques are required.

Bhagavantum and Venkatarayudu⁽⁴⁾ have taken the lead in developing methods to permit deduction of selection rules for molecules in crystals. They propose that all the spectroscopically important frequencies can be discovered and classified by examination of the related crystallographic unit cell (the unit cell group analysis). Halford⁽⁵⁾, however, proposed to treat the motions of one molecule of the crystal moving in a potential field which reflects the symmetry of the surrounding crystal environment (the site group analysis).

Hornig⁽⁶⁾ was able to show that the approach of Halford was rigorous for the calculations of observed fundamental modes.

Later, Winston and Halford⁽⁷⁾ were able to show that both the Bhagavantum-Venkatarayudu procedure and the Halford procedure are special cases of a treatment which considers the motions of a crystal segment composed of an arbitrary number of unit cells (the factor group analysis). They were able to demonstrate that both the site group analysis and the unit cell group analysis were rigorous for the determination of the selection rules for fundamentals.

In this work we propose to unify the different techniques from the existing methods and, in so doing, develop a simplified approach for the analysis of the vibrational spectra of molecules and complex ions in a crystal lattice. The techniques developed will then be applied to the analysis of the vibrational spectra of the tetracyanonickelate(II) ion in a crystal lattice.

2.0 SYSTEMATICS FOR THE ANALYSIS OF THE INFRARED VIBRATIONAL SPECTRA OF MOLECULES AND COMPLEX IONS IN THE SOLID STATE

For the crystal system, as in the case for the isolated molecule, the kinetic and potential energies may be expressed by the harmonic oscillator approximations for small oscillations as: ^(e)

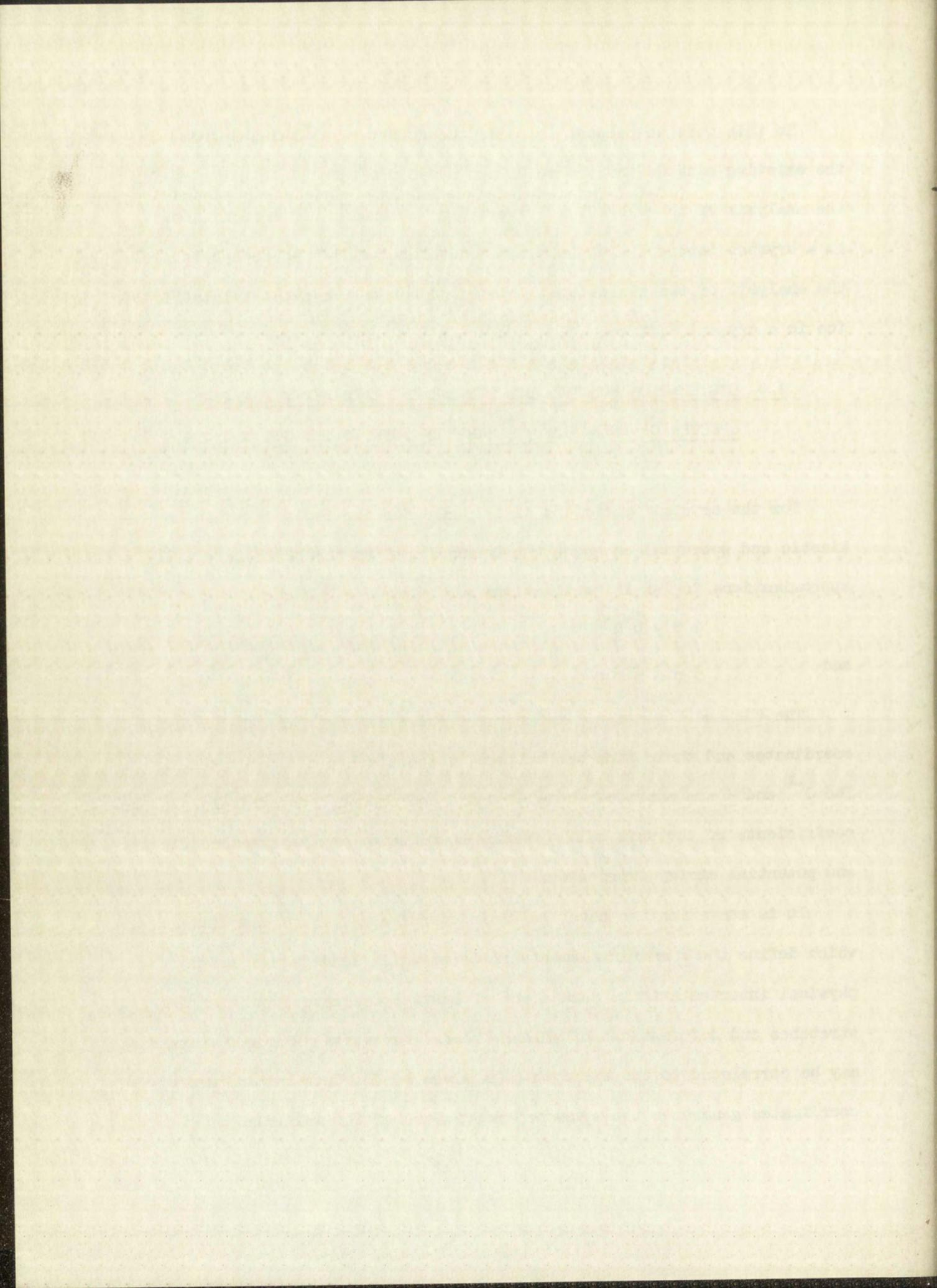
$$2 T = \underline{\dot{U}}^\dagger \underline{G}^{-1} \underline{\dot{U}} \quad 2.1$$

and

$$2 V = \underline{U}^\dagger \underline{F} \underline{U} \quad 2.2$$

The \underline{U} 's and $\underline{\dot{U}}$'s are column matrices whose elements are the symmetry coordinates and their time derivatives, respectively, of the crystal. The \underline{G}^{-1} and \underline{F} are matrices whose elements correspond, respectively, to the coefficients of the unit cell symmetry coordinates in the expanded kinetic and potential energy expressions.

It is convenient to have, as basis coordinates, those coordinates which define the \underline{F} matrix elements in terms which lend themselves to physical interpretation. Such a set of basis coordinates would be the stretches and deformations of valence bonds; hence, the \underline{F} matrix elements may be correlated to the strength of a given bond. This set of basis coordinates generates the symmetry coordinates of the molecule.



We wish to consider the molecules as units in the crystal lattice; hence, we will define the symmetry coordinates of the crystal in terms of the symmetry coordinates of the molecules. The symmetry coordinates of the molecules will then be basis coordinates for the crystal in the same sense that the valence bond coordinates are basis coordinates for the molecules. The \underline{G}^{-1} and \underline{F} matrix elements then may be expressed in terms of the \underline{g}^{-1} and \underline{f} matrix elements for the molecules.

The normal coordinates of the crystal, Q , are related to the U 's by a linear transformation.

Substitution of Equations 2.1 and 2.2 into the Lagrangian equations of motion, and the assumption of a harmonic oscillator solution, yields the following secular determinant as a solution for the vibrational frequencies: ^(s)

$$| \underline{GF} - \underline{E}\lambda | = 0 . \quad 2.3$$

The λ 's are related to the vibrational frequencies, ν (in cm^{-1}), by the equation

$$\lambda = 4\pi^2 c^2 \nu^2 \quad 2.4$$

where c is the speed of light in cm sec^{-1} . \underline{E} is the unit matrix.

The use of the symmetry coordinates of the crystal guarantees that the secular determinant is factored to the maximum extent. Each one of these factored "blocks" of the secular determinant is associated with a given irreducible representation of the system. Since the frequency of a normal mode is associated with a given irreducible representation, the normal coordinate itself is associated with the same irreducible representation. Hence, certain sets of the symmetry coordinates of the crystal (those symmetry coordinates whose linear combinations give the normal coordinates)

The first part of the paper is devoted to the general theory of the problem. It is shown that the problem is equivalent to a certain boundary value problem for a system of partial differential equations. The second part is devoted to the construction of the Green's function for the problem. It is shown that the Green's function can be expressed in terms of certain special functions. The third part is devoted to the asymptotic expansion of the Green's function for large values of the parameter. It is shown that the asymptotic expansion is valid in the sense of distributions. The fourth part is devoted to the application of the results to the problem of the scattering of waves by a half-plane. It is shown that the asymptotic expansion of the Green's function can be used to obtain the asymptotic expansion of the scattering amplitude. The fifth part is devoted to the conclusion. It is shown that the results of the paper are valid for a wide class of problems.

will be associated with the given irreducible representation. These irreducible representations (sometimes referred to as symmetry species) may be visualized as non-equivalent bases of a given symmetry. The possible motions of the crystal system are the composite sum of all motions belonging to an irreducible representation extended over all irreducible representations.

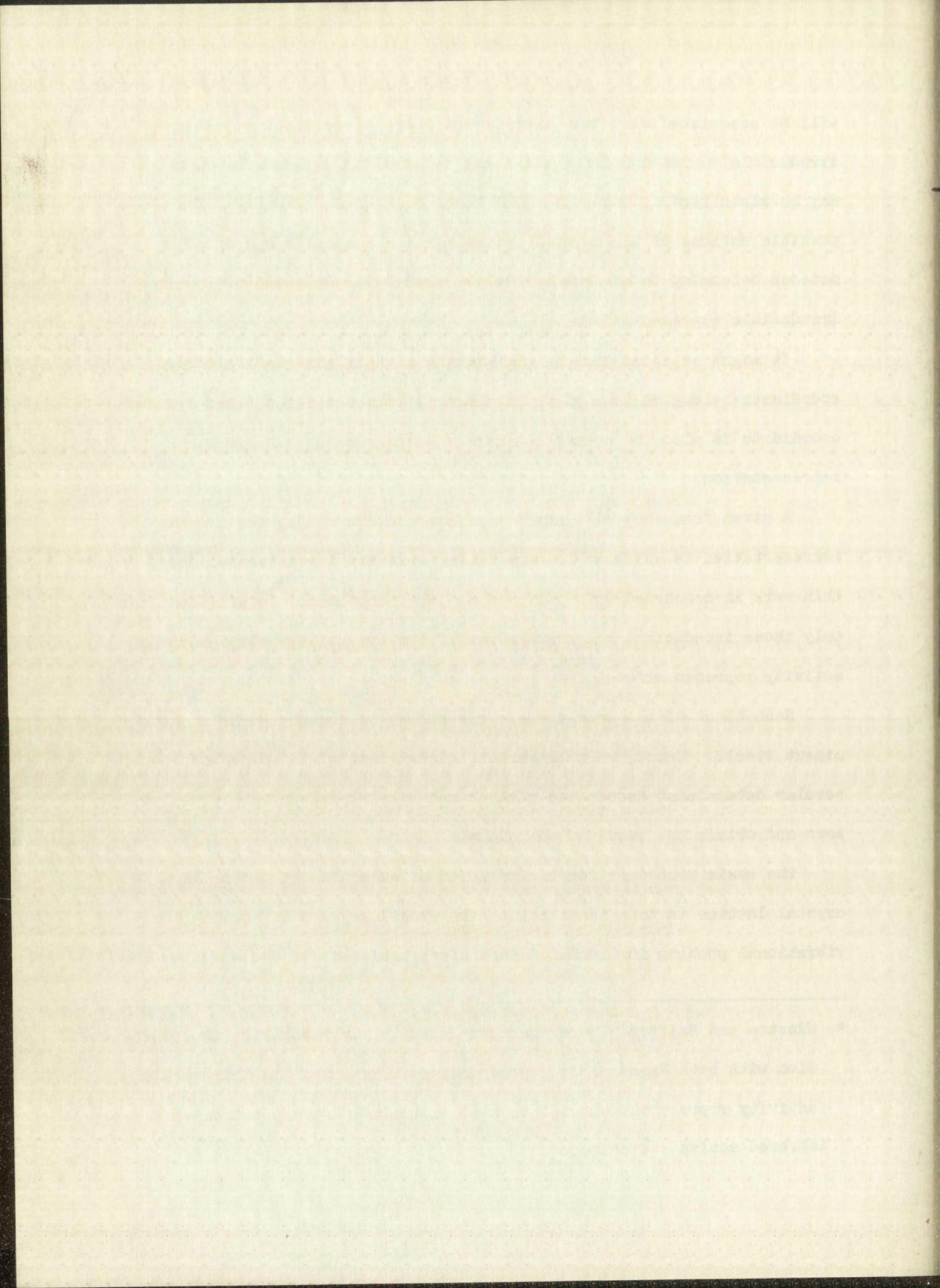
It might be added that in the special case of only one symmetry coordinate belonging to a given irreducible representation, that symmetry coordinate is also the normal coordinate belonging to that irreducible representation.

A given frequency will not be infrared active unless the irreducible representation to which it belongs is an "activity" representation.* Since this work is concerned with infrared active frequencies, we will consider only those irreducible representations of the crystal symmetry which are activity representations.

Each block of the secular determinant may be considered as a determinant itself. Hence, we will set the determinant of the block of the secular determinant associated with an activity representation equal to zero and obtain the required solutions.

The basic procedure for the solution of molecules vibrating in a crystal lattice is then identical to the procedure used in solving the vibrational problem for isolated molecules; the steps of the solution are

* Winston and Halford⁽⁷⁾ use the term activity representation in connection with both Raman and Infrared active vibrations. In this work an activity representation will be used exclusively in connection with an infrared active vibration.



as follows:

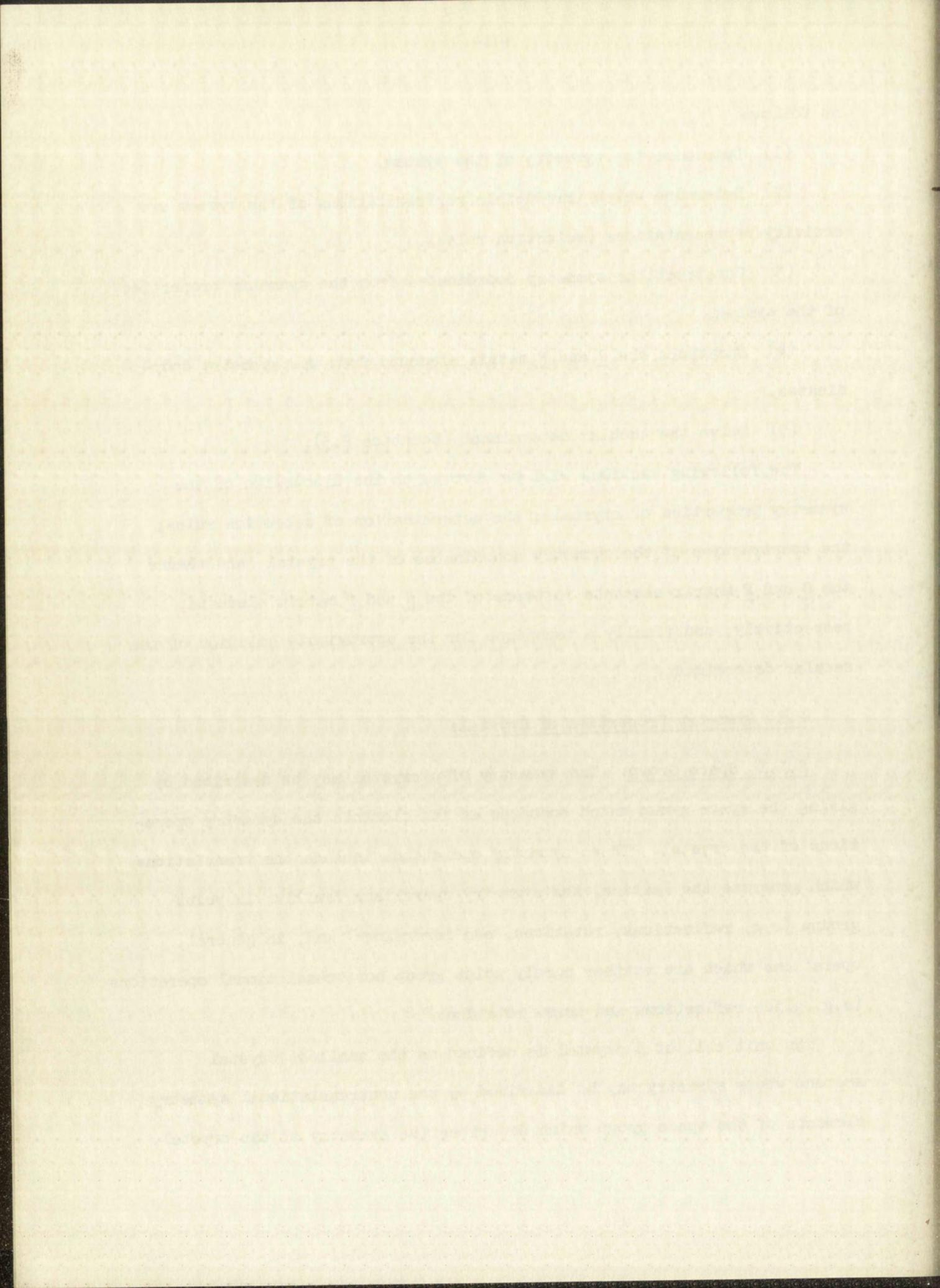
- (1) Determine the symmetry of the system.
- (2) Determine which irreducible representations of the system are activity representations (selection rules).
- (3) Construct the symmetry coordinates from the symmetry properties of the system.
- (4) Construct the \underline{G} and \underline{F} matrix elements from the symmetry coordinates.
- (5) Solve the secular determinant (Equation 2.3).

The following sections will be devoted to the discussion of the symmetry properties of crystals; the determination of selection rules; the construction of the symmetry coordinates of the crystal, and thence the \underline{G} and \underline{F} matrix elements in terms of the \underline{g} and \underline{f} matrix elements, respectively; and finally a technique for the approximate solution of the secular determinant.

2.1 Symmetry Properties of Crystals

2.1.1 Space Group: The symmetry of a crystal may be described by giving the space group which contains as its elements the symmetry operations of the crystal. These symmetry operations include the translations which generate the lattice, the symmetry operations familiar in point groups (e.g. reflections, rotations, and inversions) and, in general, operations which are neither purely point group nor translational operations (e.g. glide reflections and screw rotations).

The unit cell of a crystal is defined as the smallest crystal segment whose symmetry may be described by the nontranslational symmetry elements of the space group which describes the symmetry of the crystal.



The crystal lattice is constructed from the unit cell by the translations which carry any unit cell into any other unit cell. The complete set of symmetry operations of the crystal is obtained by combining the operations within the unit cell with the translations which carry one unit cell into the other cells.

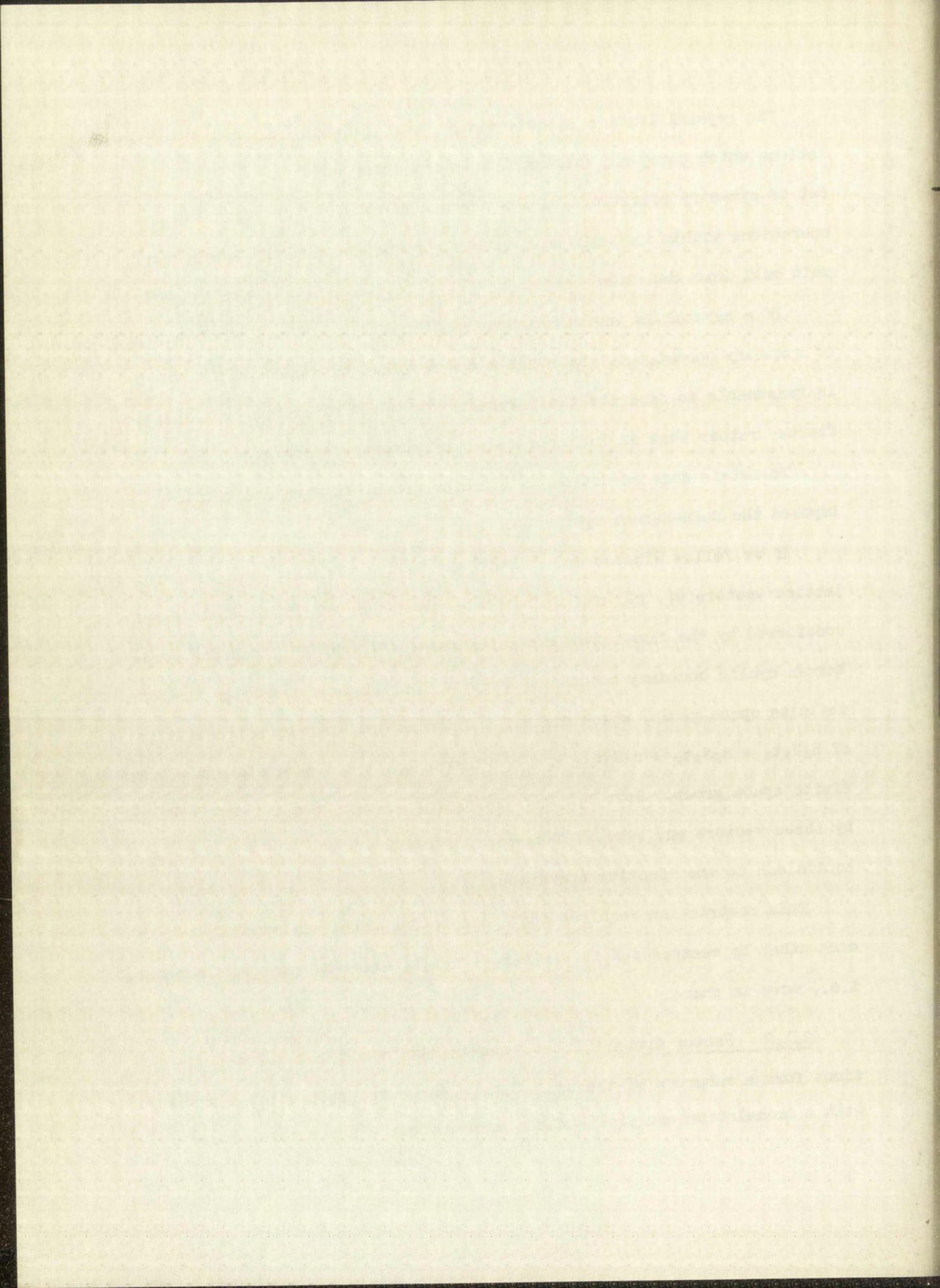
If a crystal is infinite in extent, it will allow an infinite number of symmetry operations. However, since physical crystals are finite, it is reasonable to describe their symmetry in terms of groups containing a finite rather than an infinite number of symmetry operations.

To obtain this reduction to a finite group, Winston and Halford⁽⁷⁾ imposed the Born-Karman cyclic boundary conditions⁽¹⁰⁾.

If we follow Winston and Halford and define the unit cell by the lattice vectors t_1 , t_2 , and t_3 , and the dimensions of the crystal segment considered by the fixed positive integers N_1 , N_2 , and N_3 , then the Born-Karman cyclic boundary conditions require that those elements of the infinite space group, which differ in their affect only by a translation of $n_1N_1t_1 + n_2N_2t_2 + n_3N_3t_3$, are considered to be the same element of the finite space group. Here n_1 , n_2 , and n_3 may be any integer. Translations by these vectors and sums of them carry a lattice into itself and so are equivalent to the identity operation.

This restriction requires that those atoms which are separated from each other by vectors $n_1N_1t_1 + n_2N_2t_2 + n_3N_3t_3$ have the same displacement, i.e., move in phase.

2.1.2 Factor Group: It is apparent that the translational operations form a subgroup of the space group, since the product of a translation with a translation can yield only a translation. Furthermore, since



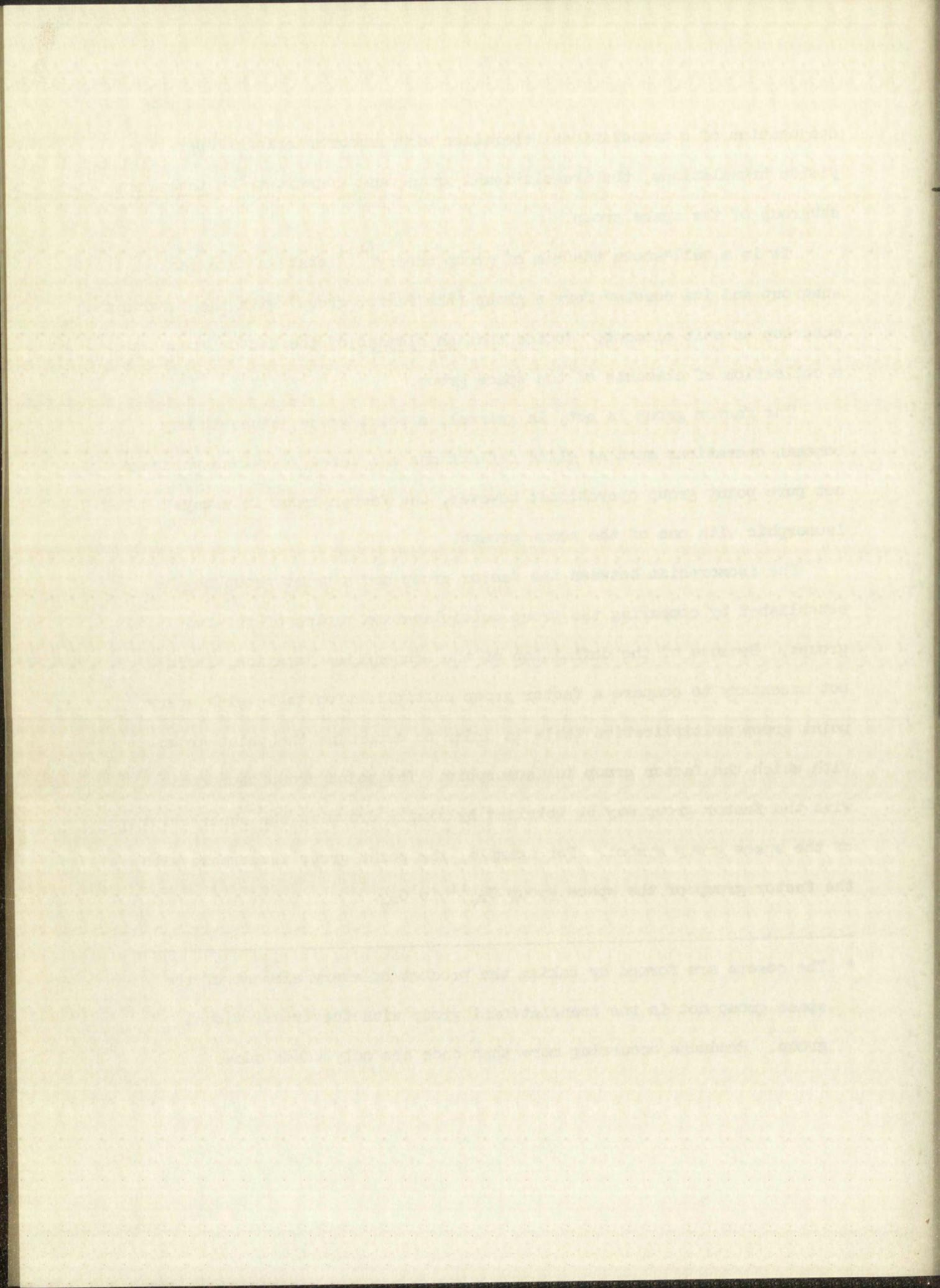
conjugation of a translational operation with nontranslational operations yields translations, the translational group must constitute an invariant subgroup of the space group.

It is a well-known theorem of group theory⁽¹¹⁾ that an invariant subgroup and its cosets* form a group (the factor group) with the invariant subgroup as unit element. Notice that an element of the factor group is a collection of elements of the space group.

The factor group is not, in general, a point group, since it may contain operations such as glide reflections and screw rotations which are not pure point group operations; however, the factor group is always isomorphic with one of the point groups.

The isomorphism between the factor group and a point group may be established by comparing the group multiplication tables of the two groups. Because of the definition of the Schoenflies Notation, it is not necessary to compare a factor group multiplication table with every point group multiplication table in order to determine the point group with which the factor group is isomorphic. The point group isomorphic with the factor group may be obtained by simply dropping the superscript of the space group symbol. For example, the point group isomorphic with the factor group of the space group C_{2v}^{11} is C_{2v} .

* The cosets are formed by taking the product of every element of the space group not in the translational group with the translational group. Products occurring more than once are only taken once.

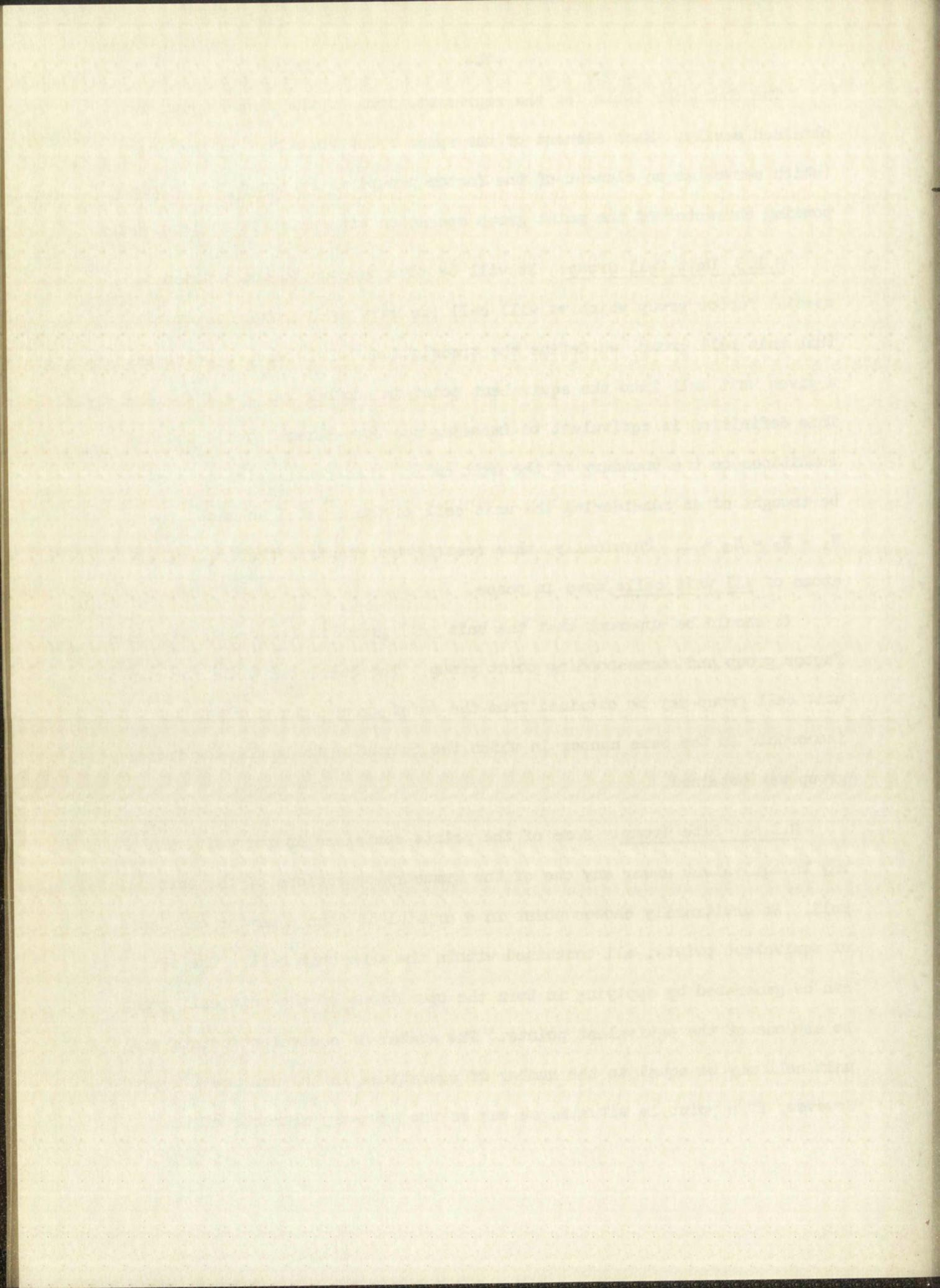


The character table for the representations of the factor group is obtained easily. Each element of the space group contained in the coset (which serves as an element of the factor group) is assigned the corresponding character of the point group operation with which it is isomorphic.

2.1.3 Unit Cell Group: It will be advantageous to construct a special factor group which we will call the unit cell group. To obtain this unit cell group, we define the translations which carry a point in a given unit cell into the equivalent point in another unit cell as identity. This definition is equivalent to imposing the Born-Karman cyclic boundary conditions on the boundary of the unit cell. This restriction also may be thought of as considering the unit cell as the crystal segment, i.e., $N_1 = N_2 = N_3 = 1$. Physically, this restriction requires that equivalent atoms of all unit cells move in phase.

It should be apparent that the unit cell group is isomorphic with the factor group and corresponding point group. The character table for the unit cell group may be obtained from the point group with which it is isomorphic in the same manner in which the character table for the factor group was obtained.

2.1.4. Site Group: Some of the points contained in the unit cell may be equivalent under any one of the symmetry operations of the unit cell. An arbitrarily chosen point in a crystal is then a member of a set of equivalent points, all contained within the same unit cell. The set can be generated by applying in turn the operations of the unit cell group to any one of the equivalent points. The number of equivalent points per unit cell may be equal to the number of operations in the unit cell group. However, if a point is situated on one of the symmetry elements of the



unit cell group, then the point remains invariant under those symmetry operations associated with that symmetry element. (Such a point is designated as a site.) This is the definition of a point group (the site group). Furthermore, since the operations which left the site invariant are also operations contained in the unit cell group, the site group must be a subgroup of the unit cell group. Since the unit cell group is isomorphic with the factor group, the site group is also a subgroup of the factor group.

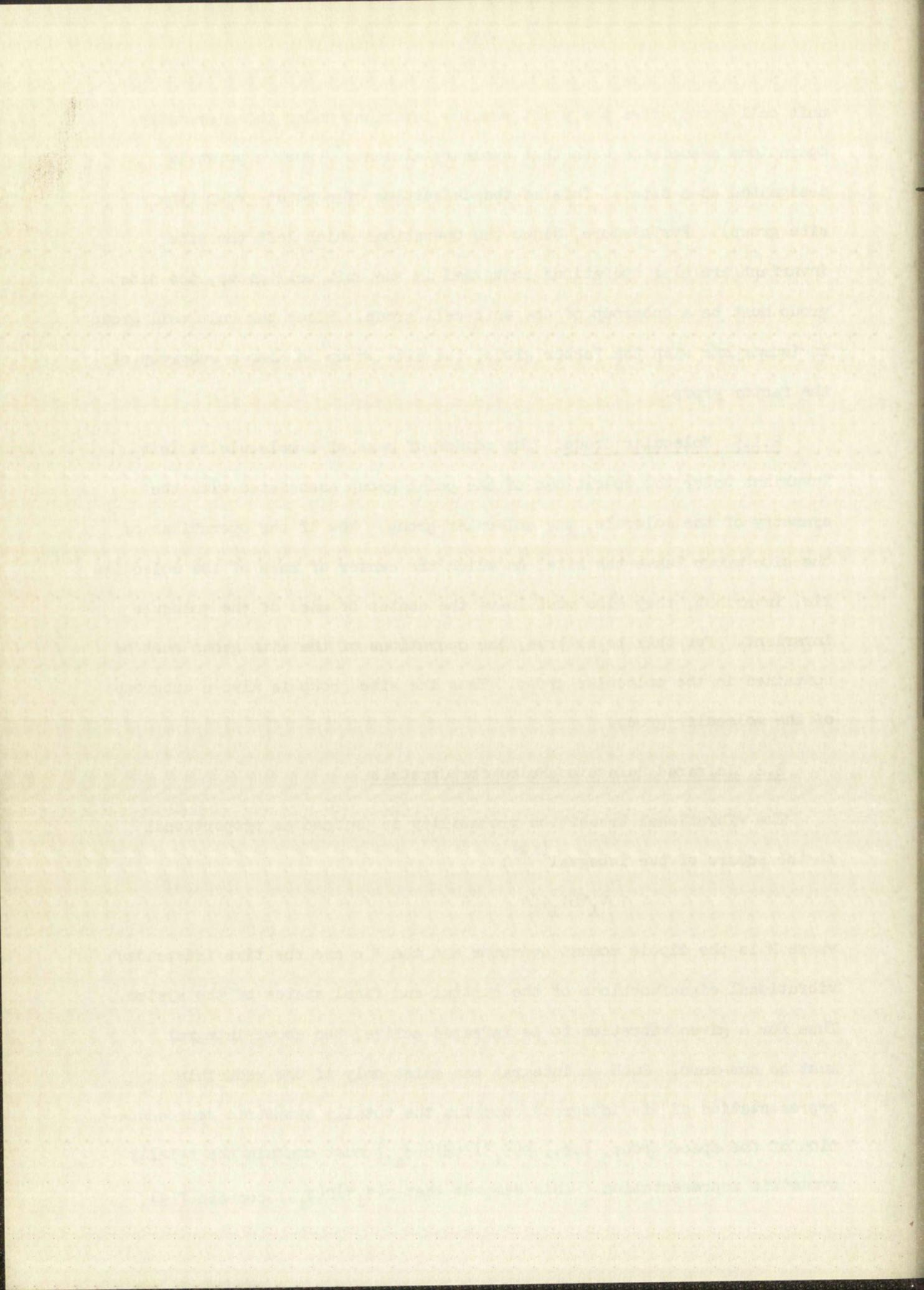
2.1.5 Molecular Group: The center of mass of a molecule is left invariant under the operations of the point group associated with the symmetry of the molecule, the molecular group. Now if the operations of the site group leave the site, on which the center of mass of the molecules lie, invariant, they also must leave the center of mass of the molecule invariant. For this to be true, the operations of the site group must be contained in the molecular group. Thus the site group is also a subgroup of the molecular group.

2.2 Infrared Selection Rules for Crystals

The vibrational transition probability is defined as proportional to the square of the integral⁽¹²⁾:

$$\int \psi_1^* M \psi_1' d\tau$$

where M is the dipole moment operator and the ψ 's are the time independent vibrational eigenfunctions of the initial and final states of the system. Thus for a given vibration to be infrared active, the above integral must be non-zero. Such an integral can exist only if the reducible representation of its integrand contains the totally symmetric representation of the space group, i.e., $\Gamma(\psi_1^*)\Gamma(M)\Gamma(\psi_1')$ must contain the totally symmetric representation. This demands that $\Gamma(\psi_1^*)\Gamma(\psi_1')$ contain $\Gamma(M)$.



The representation of the ground state is totally symmetric; hence, $\Gamma(\psi_1^*)\Gamma(\psi_1) = \Gamma(\psi_1)$. Since translation leaves any vector invariant, it follows that the representation of the dipole moment operator (a vector) must belong to the same representation as the translation. (These representations have been very conveniently noted for point groups and are easily identified from the character tables in that a T_x , T_y , or a T_z appears by the representation.) We call those irreducible representations which occur in the representations of vectors, activity representations.

From the definition of the ψ 's for the first excited states, it can be shown that they possess the same symmetry as the symmetry coordinate,⁽¹³⁾ i.e., ψ_1 , belongs to the same representations as U_1 . Hence, from the above discussion, it is apparent that the criterion for infrared activity is that $\Gamma(U_1)$ contain an activity representation. Similarly, it will be required of composite transitions that $\Gamma(U_1)\Gamma(U_j)$ contain an activity representation.

Since most spectra are observed at room temperature, not all of the molecules will be in the ground state because of the Boltzman distribution. These higher initial states will not necessarily be totally symmetric, and hence the selection rules should be suitably modified. The effect of transitions involving these higher initial states is a broadening of the observed bands. This problem has been discussed in detail by Hornig⁽⁸⁾, who emphasizes, however, that the previously mentioned criteria are usually sufficient.

Certain directional properties also may be obtained from these rules, since in a crystal it is possible to distinguish directions. If, for example,

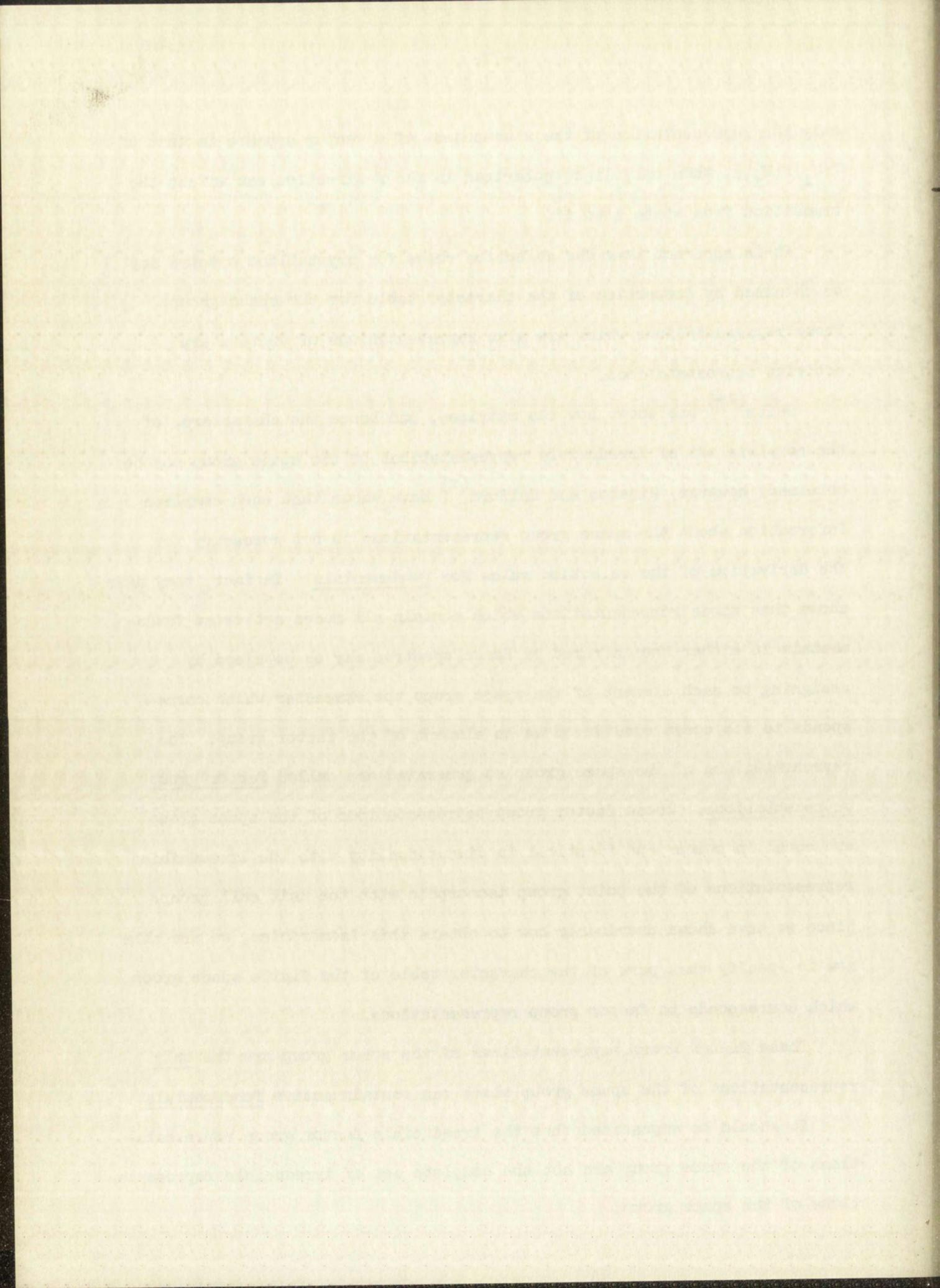
only the representation of the x component of a vector appears in that of $\Gamma(U_1)\Gamma(U_1')$, then only light polarized in the x direction can effect the transition from state i to i'.

It is apparent that the selection rules for crystalline spectra may be obtained by inspection of the character table for the space group. Those representations which are also representations of vectors are activity representations.

Seitz⁽¹⁴⁾ has shown how the matrices, and hence the characters, of the complete set of irreducible representations of the space group may be obtained; however, Winston and Halford⁽⁷⁾ have shown that such complete information about the space group representations is not necessary for the derivation of the selection rules for fundamentals. In fact, they have shown that those representations which contain all modes active as fundamentals in either the infrared or Raman spectrum may be obtained by assigning to each element of the space group the character which corresponds to its coset considered as an element of the factor group. The representations of the space group so generated are called factor group representations. These factor group representations of the space group are equal in number and identical in dimensionality with the irreducible representations of the point group isomorphic with the unit cell group. Since we have shown previously how to obtain this isomorphism, we are able now to specify that part of the character table of the finite space group which corresponds to factor group representations.

These factor group representations of the space group are the only representations of the space group which can contain active fundamentals.

It should be emphasized that the irreducible factor group representations of the space group are not the complete set of irreducible representations of the space group.



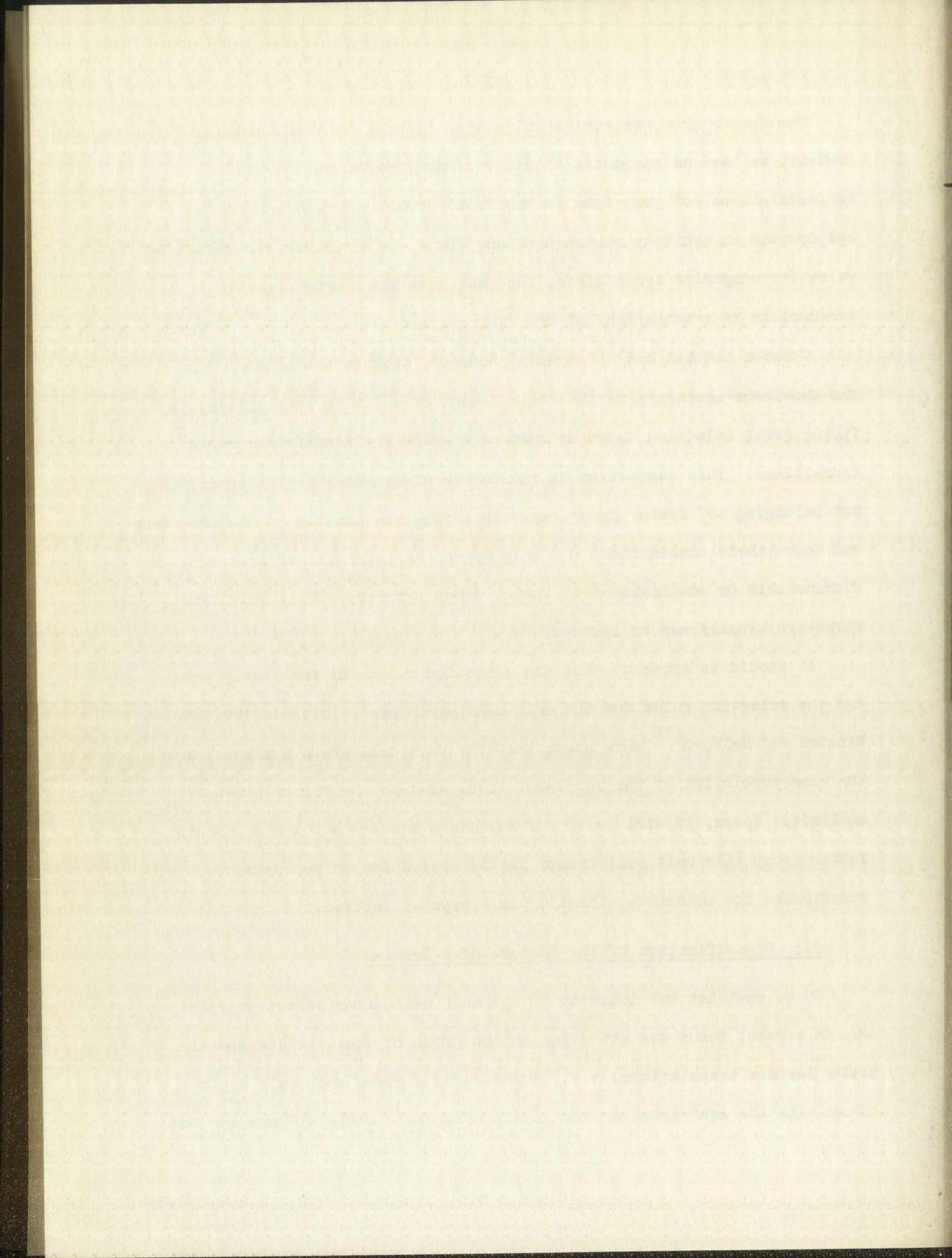
The factor group selection rules are rigorous for fundamentals; however, we have no guarantee that the direct product of irreducible representations not contained in the factor group representations may not contain an activity representation. Thus, to determine the selection rules for composite transitions, one must have the complete set of irreducible representations of the finite space group.

Winston and Halford⁽⁷⁾ suggest, however, that in the absence of the knowledge necessary for the calculation of relative intensities, the factor group selection rules be used as a guide in identifying composite transitions. This suggestion is reasonable since modes having symmetries not belonging to factor group representations are usually of low frequency, and hence their combinations may only appear as satellite structure on the fundamentals or combinations of factor group symmetry. This satellite structure usually may be ignored.

It should be apparent that the selection rules for the factor group and the selection rules for the unit cell group are identical. Further, Winston and Halford⁽⁷⁾ have shown that the unit cell group analysis gives the same population of the representations as does the factor group analysis. Hence, it will be to our advantage to use the simpler special factor group (the unit cell group) in the derivation of the symmetry coordinates for molecules vibrating in a crystal lattice.

2.3 Classification of the Motions of a Crystal

If we restrict our interest to the unit cell group selection rules, we, in effect, focus our attention on the group of vibrations symmetric under lattice translations, i.e., a motion in a given unit cell is in phase with the equivalent motion in all other unit cells. These are the



only fundamental modes which belong to irreducible activity representations of the factor group. Because of the symmetry of these unit cell modes under lattice translations, each such crystal mode can be specified by the appropriate set of motions of the atoms in a single unit cell.

As in the case of an isolated molecule, the next step after determining the symmetry group exemplified by the system is to find out how the representations of the motions of the system are reduced among the irreducible representations of this group. Again, as in the case of an isolated molecule, we begin by assigning the appropriate "internal coordinates"⁽¹⁵⁾.

It will be convenient to assign these coordinates under two types of motion: (1) lattice modes, which are approximately the motions of rigid molecules and (2) molecular modes, which are approximately the distortions of molecules whose centers of mass and principal axes of inertia are at rest.

The displacement of the center of gravity of each ion or molecule will be designated by the coordinates l_{ij}^a . The symbol "a" refers to the kind of molecule or ion, j takes on the values of 1, 2, 3. . . up to the population of ions or molecules of type "a" per unit cell, n_a , and i refers to the Cartesian coordinate relative to a fixed set of axes in the crystal. The displacement of the angles which define the orientations of a set of axes fixed to each molecule with respect to axes fixed in the crystal will be designated by the coordinate π_{ij}^a . The symbol "a" refers to the kind of molecule, j once again takes on the values of 1, 2, 3. . . up to the population of molecules of type "a" per unit cell, n_a , and i denotes



Faint, illegible text covering the majority of the page, appearing to be a document or report.

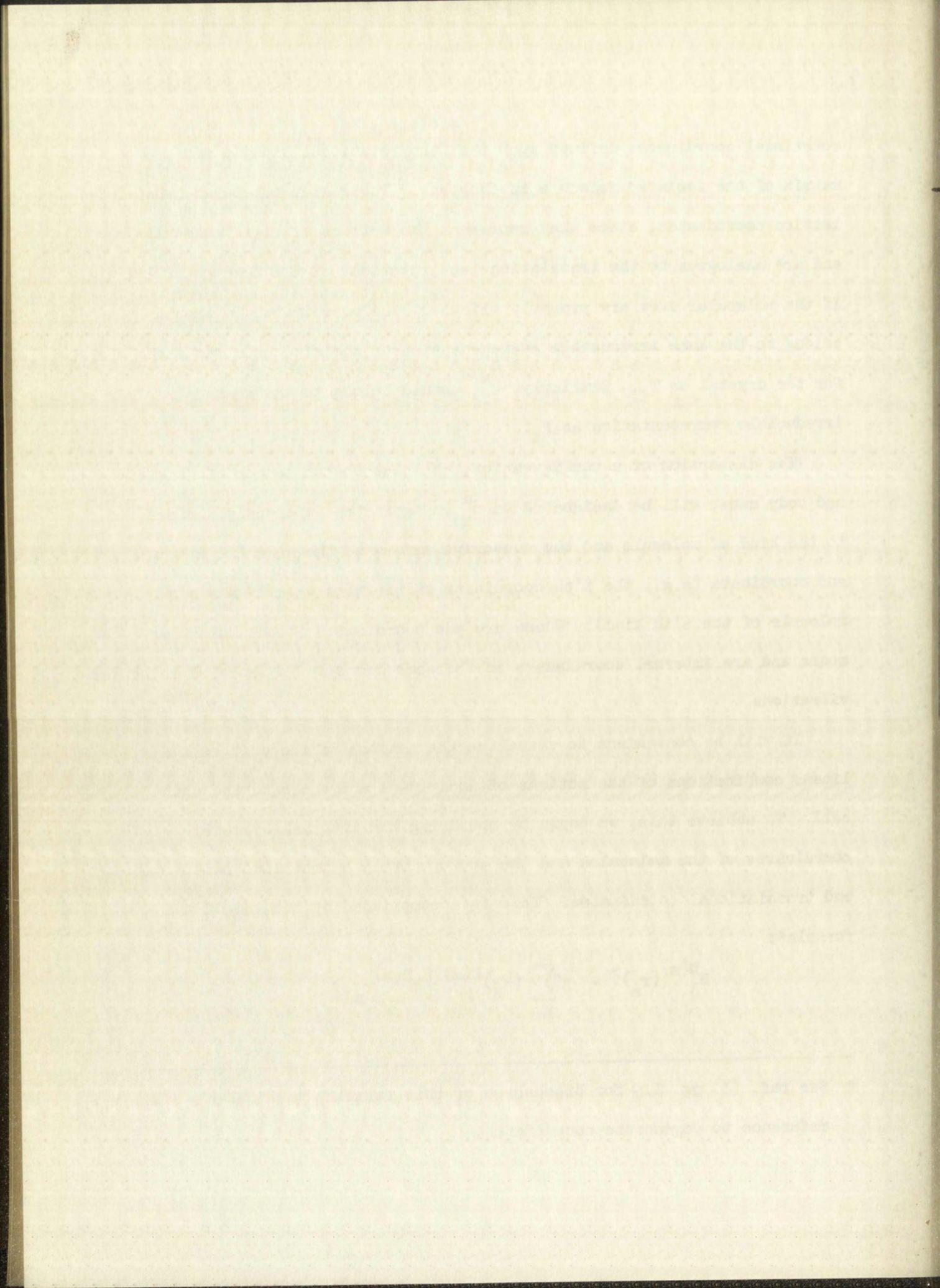
rotational coordinates defined such that the rotational kinetic energy matrix of the isolated molecule is diagonal. These are, of course, the lattice coordinates, since they represent the motions of rigid molecules and are analogous to the translations and rotations of the free molecule. If the molecular axes are properly oriented, the coordinate l_{ij}^a should belong to the same irreducible representation of the site group defined for the crystal as T_i . Similarly, π_{ij}^a should belong to the same irreducible representation as R_i .

The distortion of a configuration, relative to the center of gravity and body axes, will be designated as m_{ij}^a . Again the superscript refers to the kind of molecule and the subscript refers to the specific molecule and coordinate (e.g., the i 'th coordinate of the m 'th type of the j 'th molecule of the a 'th kind). These are the coordinates of the molecular modes and are internal coordinates in the same sense as in isolated molecular vibrations.

It will be convenient to visualize the motions of the unit cell as linear combinations of the motions of individual molecules in the unit cell. To achieve this, we begin by obtaining the internal symmetry coordinates of the molecules and the appropriately symmetrized rotational and translational coordinates. This is accomplished by the use of the formula*:

$$S_j^{D(m)}(r_a)^\gamma = \eta'' \sum_R (X_R)^{D(m)} [R^{D(m)} r_{aj}] \quad . \quad 2.3.1$$

* See ref. (3) pg. 119 for discussion of this formula, particularly with reference to degenerate coordinates.



Here $S_j^{D(m)}(r_a)^\gamma$ is the symmetry coordinate of the m'th representation of the point group D generated by the r'th coordinate $(m_{ij}^a, i_{ij}^a, \text{ or } \pi_{ij}^a)$ for the j'th molecule of type a. If m is a degenerate representation, the γ superscript denotes which degenerate set of the r's to which we refer. Obviously $S_j^{D(m)}(r_a)^\gamma = S_1^{D(m)}(r_a)^\gamma = \dots = S_{n_a}^{D(m)}(r_a)^\gamma$, where n_a is the population of molecules of type a in a unit cell. η is a normalizing factor. $(\chi_R)^{D(m)}$ is the character of the R'th operation for the m'th representation of the point group D. The notation, $\left[R^{D(m)}_{r_{aj}} \right]$, stands for the coordinate of the j'th molecule of type a to which the coordinate r_{aj} is transferred by the operation $R^{D(m)}$.

We now take these $S_j^{D(m)}(r_a)^\gamma$ coordinates as "internal coordinates" for the site group and reduce them on the site group symmetry by:

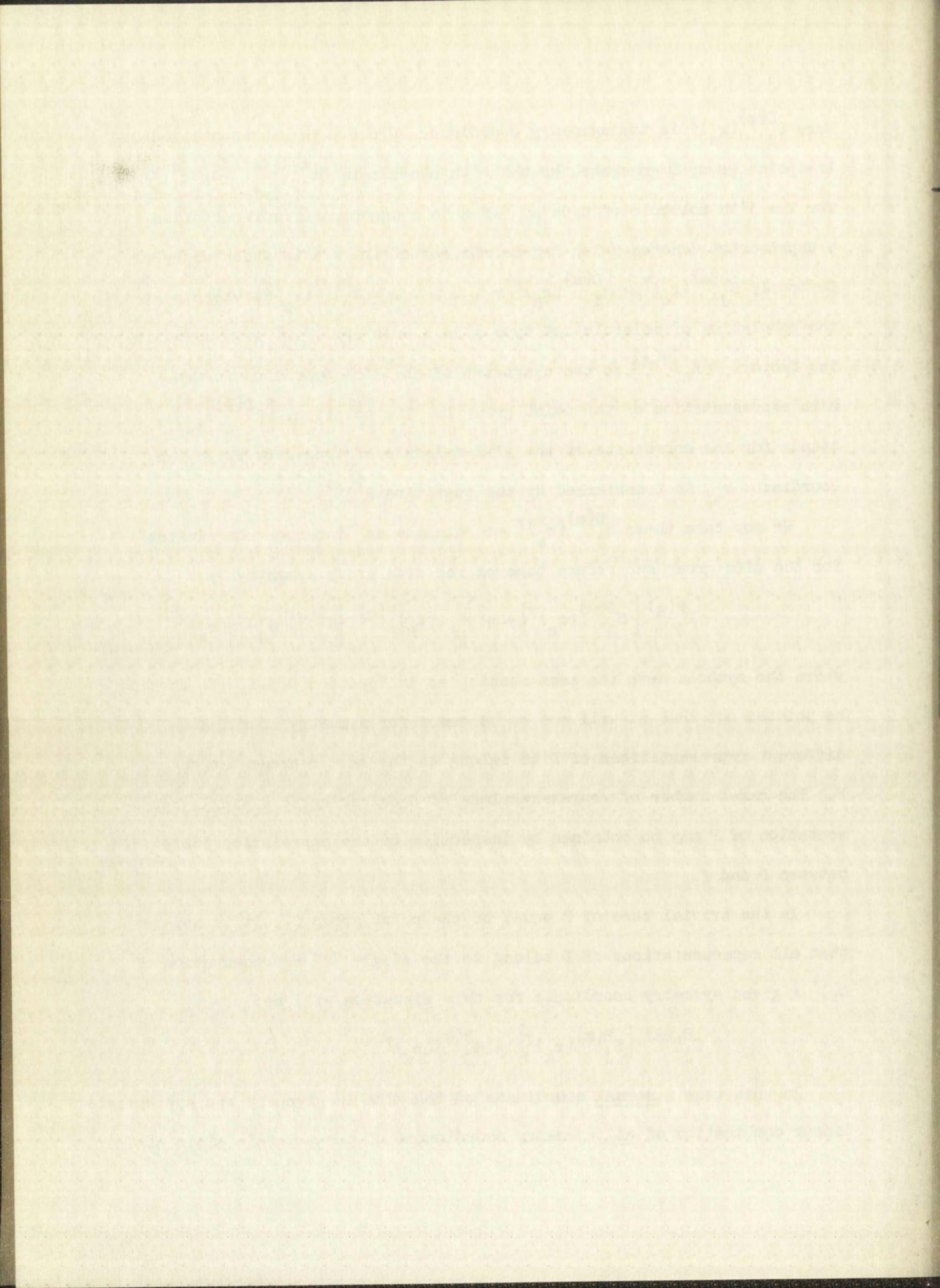
$$T_j^{P(q)} \left[S_j^{D(m)}(r_a)^\gamma \right] = \eta' \sum_R (\chi_R)^{P(q)} \left[R^{P(q)} \left(S_j^{D(m)}(r_a)^\gamma \right) \right] \quad 2.3.2$$

where the symbols have the same meaning as in Equation 2.3.1. It should be pointed out that it will not be uncommon for symmetry coordinates of different representations of D to belong to the same representations of P. The exact number of representations of D belonging to a single representation of P may be obtained by inspection of the correlation table between D and P.

In the trivial case of P equal to the point group C_1 , it is apparent that all representations of D belong to the single "A" representation of C_1 . A given symmetry coordinate for this situation will be:

$$T_j^{C_1(A)} \left[S_j^{D(m)}(r_a)^\gamma \right] = S_j^{D(m)}(r_a)^\gamma.$$

In this case a normal coordinate of the site is given by the appropriate linear combination of all symmetry coordinates of the molecule since all



representations of D correlate with the single representation of C_1 .

The process of "coordinate building" is taken into its final form by considering these $T_j^{P(q)} [S_j^{D(m)}(r_a)\gamma]$ coordinates as "internal coordinates" of the unit cell. If the $T_j^{P(q)} [S_j^{D(m)}(r_a)\gamma]$ coordinates are nondegenerate, the usual case, they are symmetrized on the unit cell group by:

$$U^{C(n)} \left(T_j^{P(q)} [S_j^{D(m)}(r_a)\gamma] \right) = \eta \sum_R (\chi_R)^{C(n)} \left[R^{C(n)} \left(T_j^{P(q)} [S_j^{D(m)}(r_a)\gamma] \right) \right] \quad 2.3.3$$

Here the $U^{C(n)} \left(T_j^{P(q)} [S_j^{D(m)}(r_a)\gamma] \right)$ are the symmetry coordinates of the unit cell and are the matrix elements of the U matrix in Equations 2.1 and 2.2. The $(\chi_R)^{C(n)}$ are the characters of the point group isomorphic with the unit cell group. The notation, $\left[R^{C(n)} \left(T_j^{P(q)} [S_j^{D(m)}(r_a)\gamma] \right) \right]$, stands for the coordinate to which $T_j^{P(q)} [S_j^{D(m)}(r_a)\gamma]$ is transferred by the operation $R^{C(n)}$ of the unit cell group. The operations $R^{C(n)}$ will not necessarily be pure point group operations. It should be apparent that the operations $R^{C(n)}$ transform a given molecule of type "a" either into itself or another molecule of type "a".

The U symmetry coordinates may be written as functions of the symmetry coordinates of the molecules, the $S_j^{D(m)}(r_a)\gamma$.

$$U^{C(n)} [S_j^{D(m)}(r_a)\gamma] = \eta^o \sum_{R^{C(n)}} (\chi_R)^{C(n)} \left[R^{C(n)} \sum_{P(q)} (\chi_R)^{P(q)} [R^{P(q)} S_j^{D(m)}(r_a)\gamma] \right] \quad 2.3.4$$

where there will be as many $U^{C(n)} [S_j^{D(m)}(r_a)\gamma]$ as there are inequivalent sets of molecules of type a in the unit cell. We may also define

$$U_k^{C(n)} [S^{D(m)}(r_a)^\gamma] = \sum_j^{n_a} A[C(n),k,j] S_j^{D(m)}(r_a)^\gamma \quad 2.3.5$$

where the $U_k^{C(n)} [S^{D(m)}(r_a)^\gamma]$'s are related to the $U^{C(n)} [S_j^{D(m)}(r_a)^\gamma]$'s by a unitary transformation. The coefficients $A[C(n),k,j]$ may be obtained by comparing the linear combinations of the U's with Equation 2.3.5.

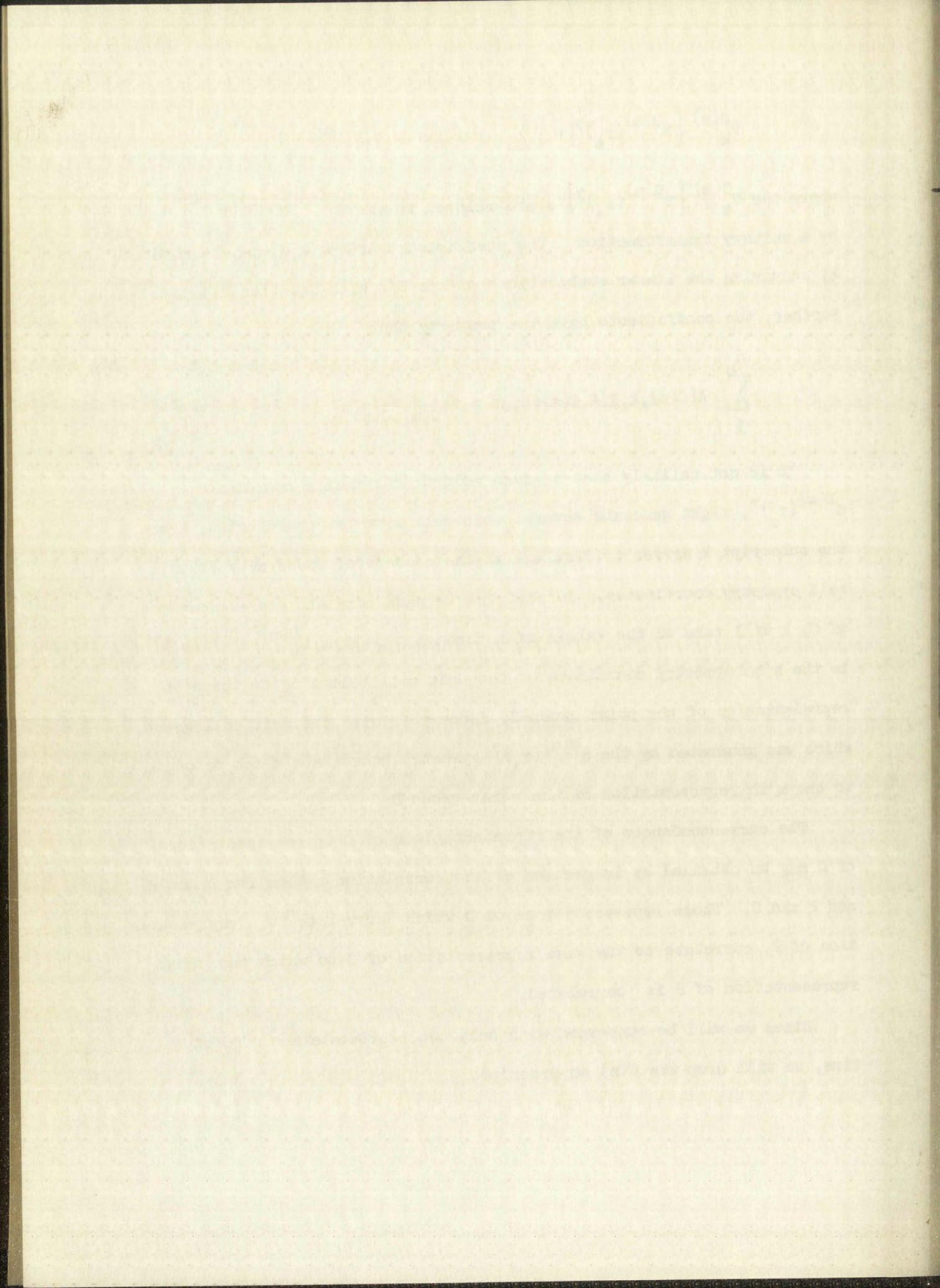
Further, the coefficients have the property that

$$\sum_j^{n_a} A[C(n),k,j] A[C(m),h,j] = \delta_{C(m),C(n)} \delta_{hk} \quad 2.3.6$$

It is not unlikely that a given molecular symmetry coordinate, $S^{D(m)}(r_a)^\gamma$, might generate several unit cell symmetry coordinates; hence, the subscript k serves to distinguish the members of these sets of unit cell symmetry coordinates. In fact, as we pass over all representations of C, k will take on the values of 1 through n_a . Thus $U_k^{C(n)} [S^{D(m)}(r_a)^\gamma]$ is the k'th symmetry coordinate of the unit cell belonging to the n'th representation of the point group C, isomorphic with the unit cell group, which was generated by the $S^{D(m)}(r_a)^\gamma$ symmetry coordinate which belongs to the m'th representation of the point group D.

The correspondences of the representations of D to representations of C may be obtained by inspection of the correlation tables for D and P, and P and C. Those representations of D which correlate to a representation of P, correlate to the same representation of C to which the given representation of P is correlated.

Since we will be concerned with only one representation of C at a time, we will drop the C(n) superscript.



2.4 Determination of the G and F Matrix Elements

It should be recalled that the molecular symmetry coordinate may be expressed also in terms of Cartesian displacement coordinates:

$$S_j^{D(m)}(r_a)^\gamma = \sum_{t_j}^{3m_a} b[S_j^{D(m)}(r_a)^\gamma; t_j] \xi_{t_j} \quad 2.4.1$$

Here m_a is the number of atoms in a given molecule (j) of type a . The Cartesian displacement coordinates are given by ξ_{t_j} , where t labels the coordinate belonging to molecule j . The b 's are transformation coefficients, and their values may be obtained by expressing $r_{a,j}$, in Equation 2.3.1, in terms of Cartesian displacement coordinates and comparing coefficients in Equations 2.3.1 and 2.4.1.

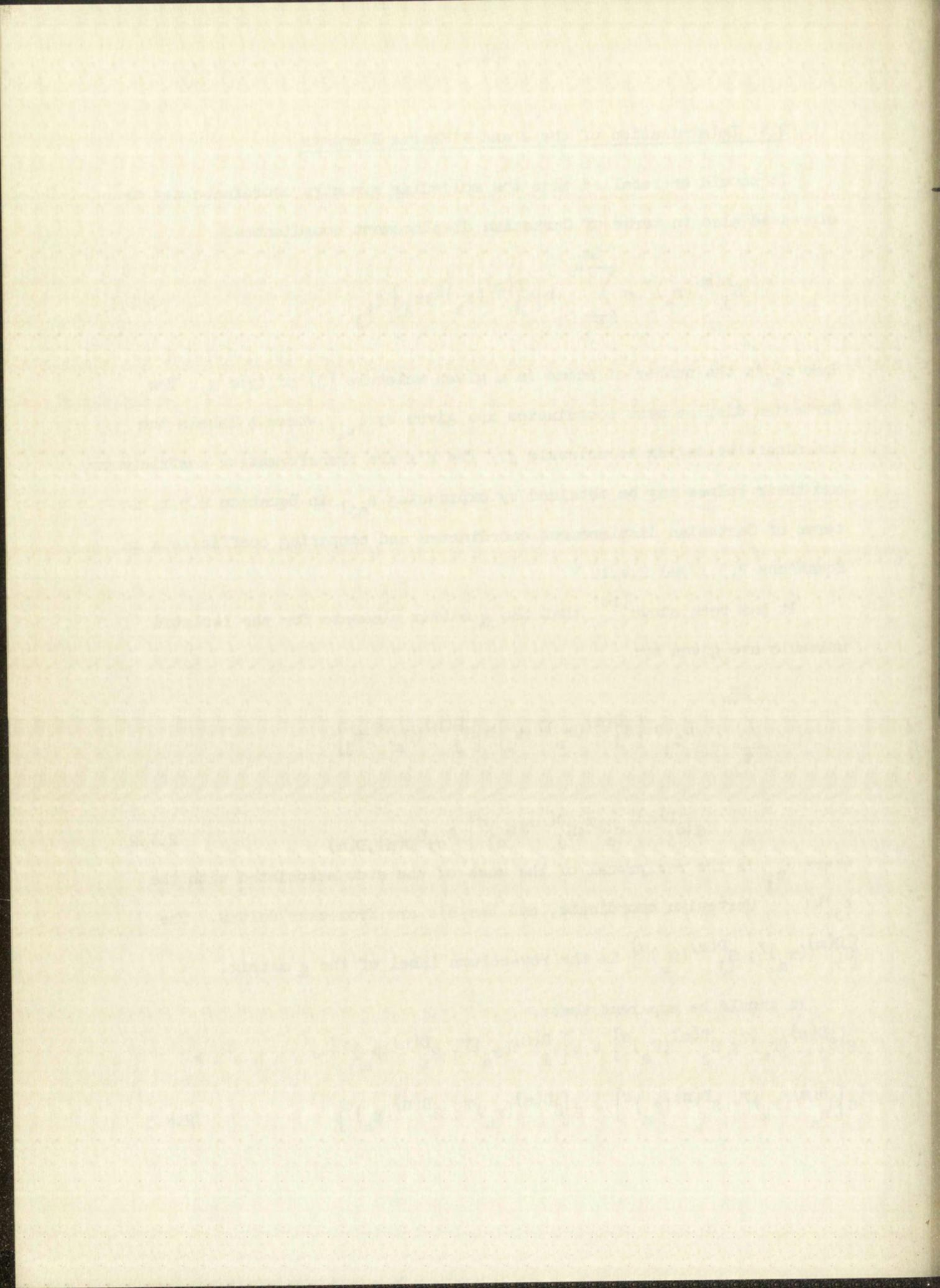
It has been shown⁽¹⁶⁾ that the g matrix elements for the isolated molecule are given by:

$$\sum_{t_j}^{3m_a} \mu_{t_j} b[S_j^{D(m)}(r_a)^\gamma; t_j] b[S_j^{D(n)}(R_a)^\sigma; t_j] = g[S_j^{D(m)}(r_a)^\gamma; S_j^{D(n)}(R_a)^\sigma] \delta_{\sigma\gamma} \delta_{D(n), D(m)} \quad 2.4.2$$

where μ_{t_j} is the reciprocal of the mass of the atom associated with the t_j 'th Cartesian coordinate, and the δ 's are Kronecker deltas. The $[S_j^{D(m)}(r_a)^\gamma; S_j^{D(n)}(R_a)^\sigma]$ is the row-column label of the g matrix.

It should be apparent that:

$$g[S_j^{D(m)}(r_a)^\gamma; S_j^{D(n)}(R_a)^\sigma] = g[S_i^{D(m)}(r_a)^\gamma; S_i^{D(n)}(R_a)^\sigma] = \dots = g[S_{n_a}^{D(m)}(r_a)^\gamma; S_{n_a}^{D(n)}(R_a)^\sigma] \quad 2.4.3$$



If we substitute Equation 2.4.1 into Equation 2.3.5, we have:

$$U_k \left[S^{D(m)}(r_a)^\gamma \right] = \sum_j^{n_a} \sum_{t_j}^{3m_a} A(k,j) b \left[S_j^{D(m)}(r_a)^\gamma, t_j \right] \xi_{t_j} \quad 2.4.4$$

so that

$$G \left(U_k \left[S^{D(m)}(r_a)^\gamma \right]; U_h \left[S^{D(n)}(R_a)^\sigma \right] \right) = \sum_j^{n_a} \sum_{t_j}^{3m_a} A(k,j) A(h,j) \mu_{t_j} b \left[S_j^{D(m)}(r_a)^\gamma; t_j \right] b \left[S_j^{D(n)}(R_a)^\sigma; t_j \right] \quad 2.4.5$$

Substitution of Equations 2.4.2, 2.4.3, and 2.3.6 into 2.4.5 yields:

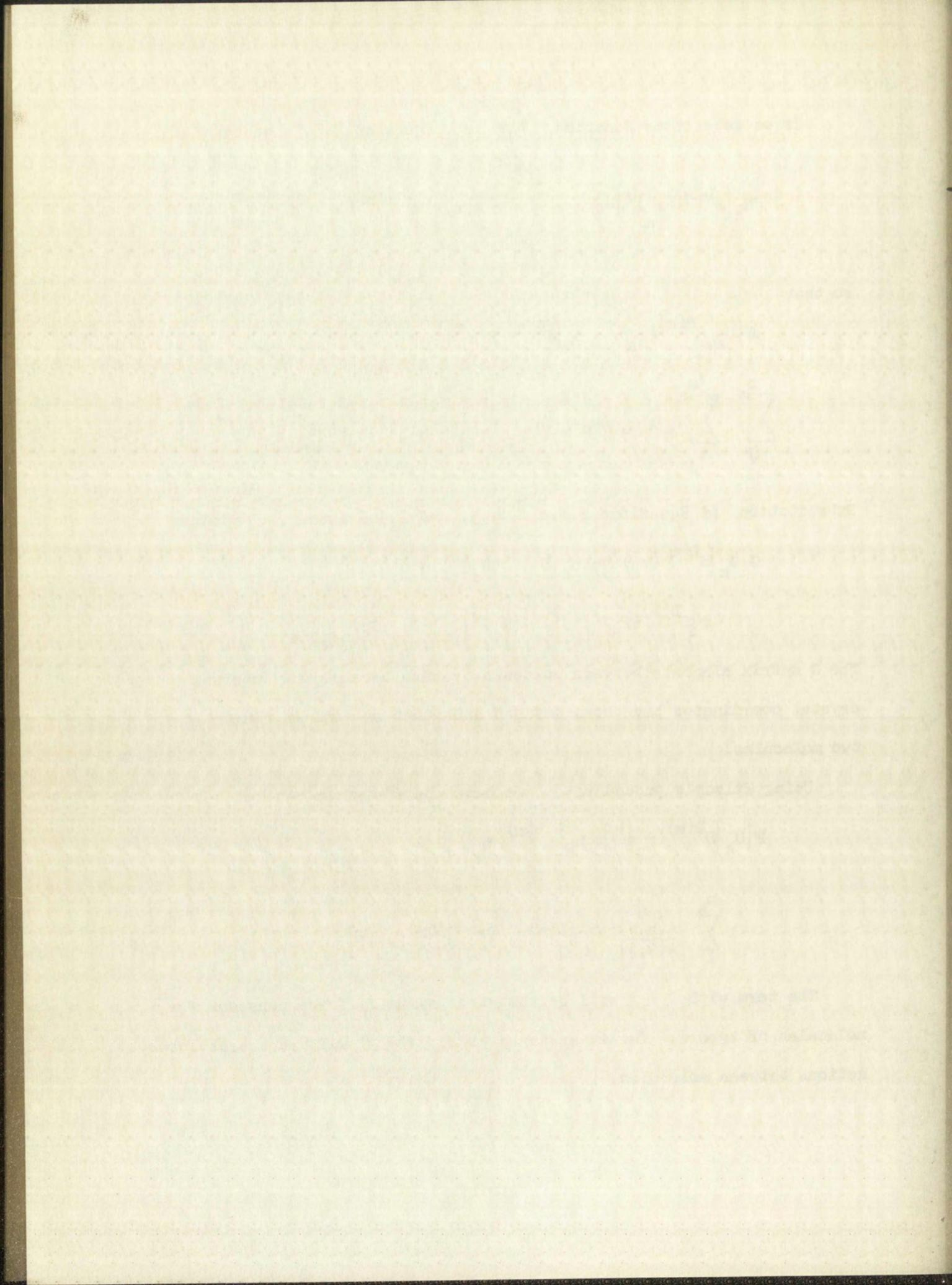
$$G \left(U_k \left[S^{D(m)}(r_a)^\gamma \right]; U_h \left[S^{D(n)}(R_a)^\sigma \right] \right) = g \left[S^{D(m)}(r_a)^\gamma; S^{D(n)}(R_a)^\sigma \right] \delta_{hk} \delta_{\sigma\gamma} \delta_{D(n),D(m)} \quad 2.4.6$$

The G matrix elements between molecules vanish because the internal crystal coordinates have been defined such that no bond is common to two molecules.

Using Wilson's procedure⁽¹⁷⁾ we have the F's given by:

$$F \left(U_k \left[S^{D(m)}(r_a)^\gamma \right]; U_h \left[S^{D(m)}(R_a)^\sigma \right] \right) = \sum_l^{n_a} \frac{A(h,l)}{A(k,j)} f \left[S_j^{D(m)}(r_a)^\gamma; S_l^{D(m)}(R_a)^\sigma \right] \quad 2.4.7$$

The term with $l = j$ will be the given symmetry force constant for molecules of type a. The other terms (i.e., $l \neq j$) will represent interactions between molecules.



2.5 The Perturbation Method for the Solution of the Secular Determinant

Equation 2.3 may be expressed as

$$|\underline{H} - \underline{E}\lambda| = 0 \quad 2.5.1$$

where

$$\underline{H} \equiv \underline{G} \underline{F} . \quad 2.5.2$$

Also

$$|\underline{H} - \underline{E}\lambda|^{C(n)} = 0 \quad 2.5.3$$

where the superscript, C(n), denotes that the determinant is that part of the secular determinant which belongs to the n'th representation of C.

We will be interested only in those determinants which belong to activity representations of C.

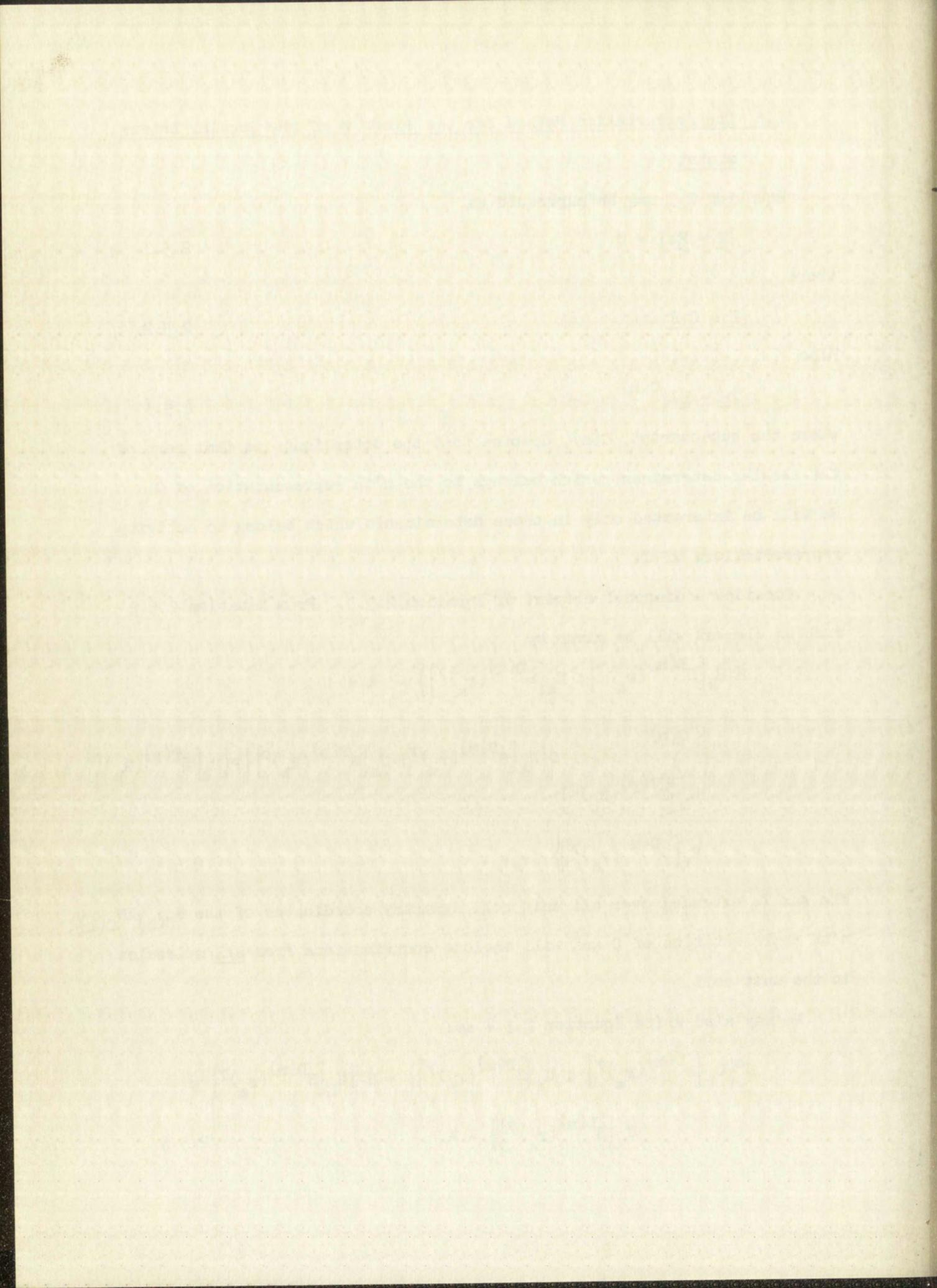
Consider a diagonal element of Equation 2.5.3. From Equation 2.5.2 such an element will be given by

$$\begin{aligned} & H \left(U_k \left[S^{D(m)}(r_a)^\gamma \right] ; U_k \left[S^{D(m)}(r_a)^\gamma \right] \right) - \lambda = \\ & \left\{ \sum_{U_h \left[S^{T(p)}(R_b)^\rho \right]}^{N_{C(n)}} G \left(U_k \left[S^{D(m)}(r_a)^\gamma \right] ; U_h \left[S^{T(p)}(R_b)^\rho \right] \right) F \left(U_h \left[S^{T(p)}(R_b)^\rho \right] ; \right. \\ & \left. U_k \left[S^{D(m)}(r_a)^\gamma \right] \right) \right\} - \lambda . \quad 2.5.4. \end{aligned}$$

The sum is extended over all unit cell symmetry coordinates of the $N_{C(n)}^{XN_{C(n)}}$, n'th representation of C and will include contributions from all molecules in the unit cell.

We may also write Equation 2.5.4 as:

$$\begin{aligned} & H^0 \left(U_k \left[S^{D(m)}(r_a)^\gamma \right] ; U_k \left[S^{D(m)}(r_a)^\gamma \right] \right) + H' \left(U_k \left[S^{D(m)}(r_a)^\gamma \right] ; \right. \\ & \left. U_k \left[S^{D(m)}(r_a)^\gamma \right] \right) - \lambda \quad 2.5.5 \end{aligned}$$



where

$$\begin{aligned}
 H^0(U_k[S^{D(m)}(r_a)^\gamma]; U_k[S^{D(m)}(r_a)^\gamma]) = \\
 G(U_k[S^{D(m)}(r_a)^\gamma]; U_k[S^{D(m)}(r_a)^\gamma]) F(U_k[S^{D(m)}(r_a)^\gamma]; \\
 U_k[S^{D(m)}(r_a)^\gamma]) \quad 2.5.6
 \end{aligned}$$

and

$$\begin{aligned}
 H'(U_k[S^{D(m)}(r_a)^\gamma]; U_k[S^{D(m)}(r_a)^\gamma]) = \\
 \sum_{U_h[S^{T(p)}(R_b)^\rho]} \left[G(U_k[S^{D(m)}(r_a)^\gamma]; U_h[S^{T(p)}(R_b)^\rho]) \right. \\
 \left. F(U_h[S^{T(p)}(R_b)^\rho]; U_k[S^{D(m)}(r_a)^\gamma]) \cdot (1 - \delta(U_h[S^{T(p)}(R_b)^\rho]; \right. \\
 \left. U_k[S^{D(m)}(r_a)^\gamma])) \right] \quad 2.5.7
 \end{aligned}$$

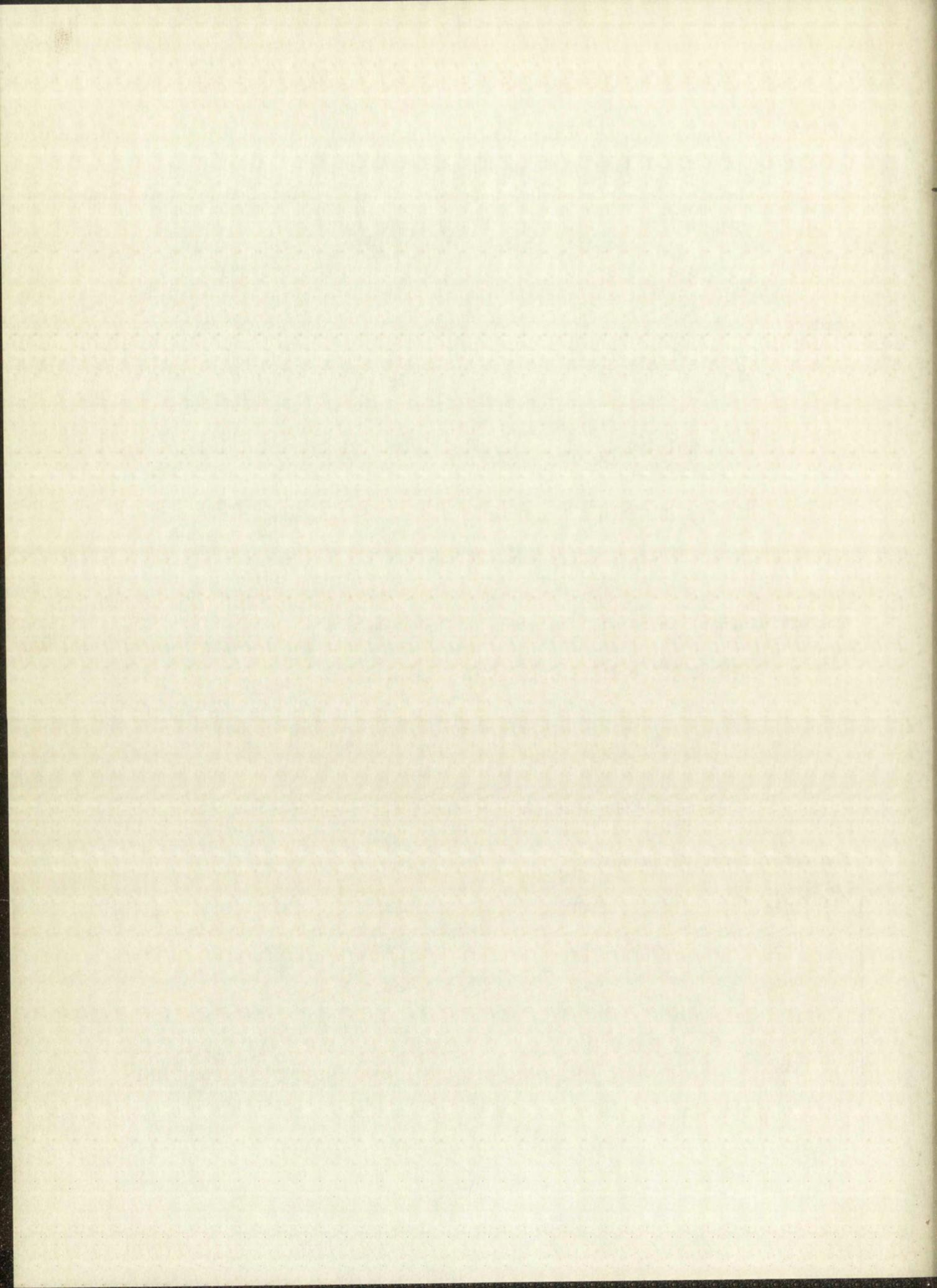
The off diagonal terms will be given by Equation 2.5.3 as:

$$\begin{aligned}
 H(U_k[S^{D(m)}(r_a)^\gamma]; U_q[S^{Q(t)}(w_c)^\rho]) = \\
 \sum_{U_h[S^{T(p)}(R_b)^\rho]} \left[G(U_k[S^{D(m)}(r_a)^\gamma]; U_h[S^{T(p)}(R_b)^\rho]) \right. \\
 \left. F(U_h[S^{T(p)}(R_b)^\rho]; U_q[S^{Q(t)}(w_c)^\rho]) \right] \quad 2.5.8
 \end{aligned}$$

The determinant which belongs to C(n) now takes on the form:

$H_{11}^0 + H_{11}' - \lambda$	H_{12}	H_{13}	\dots	H_{1n}	$C(n)$
H_{21}	$H_{22}^0 + H_{22}' - \lambda$	H_{23}	\dots	H_{2n}	
H_{31}	H_{32}	$H_{33}^0 + H_{33}' - \lambda$	\dots	H_{3n}	
\dots	\dots	\dots	\dots	\dots	
H_{n1}	H_{n2}	H_{n3}	\dots	$H_{nn}^0 + H_{nn}' - \lambda$	

2.5.9



Here the row and column labels have been replaced by subscript numbers for simplicity in notation.

Equation 2.5.9 can be rearranged to:

$$\begin{array}{cccccc}
 H'_{11} - (\lambda - H^0_{11}) & H_{12} & H_{13} & \dots & H_{1n} & \\
 H_{21} & H'_{22} - (\lambda - H^0_{22}) & H_{23} & \dots & H_{2n} & \\
 H_{31} & H_{32} & H'_{33} - (\lambda - H^0_{33}) & \dots & H_{3n} & \\
 \dots & \dots & \dots & \dots & \dots & \\
 H_{n1} & H_{n2} & H_{n3} & \dots & H'_{nn} - (\lambda - H^0_{nn}) &
 \end{array} \quad C(n)$$

2.5.10

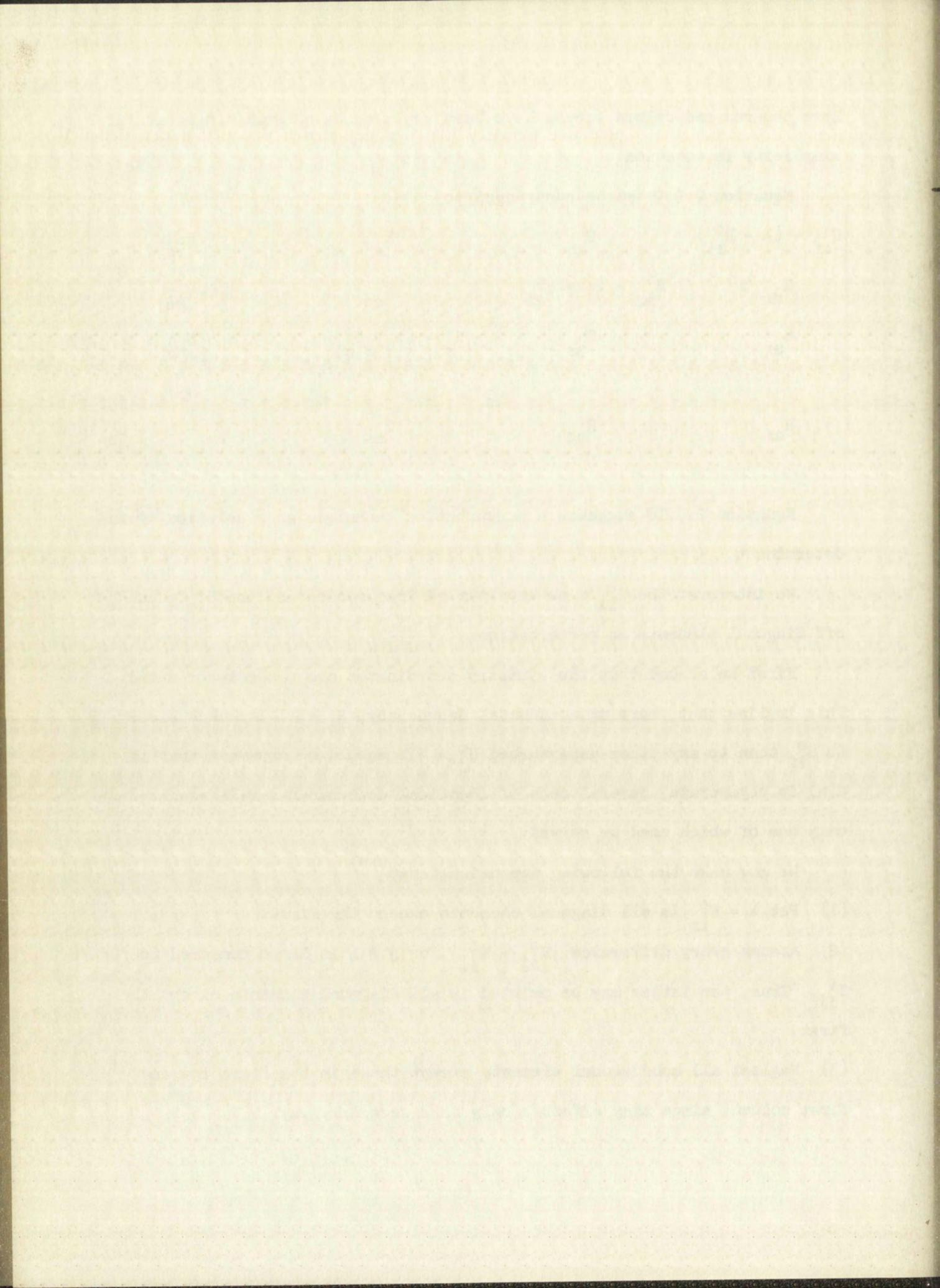
Equation 2.5.10 suggests a perturbation technique as a solution to the determinant.

We interpret the H^0_{ii} 's as unperturbed frequencies and the H'_{ii} 's and off diagonal elements as perturbations.

First we assume that the symmetry coordinates are properly oriented. This implies that, barring accidental degeneracy, λ_1 will lie much closer to H^0_{11} than to any other unperturbed H^0_{jj} . It should be apparent that if $C(n)$ is degenerate, several sets of identical determinants will result, only one of which need be solved.

We now make the following approximations: ⁽¹⁸⁾

- (1) Put $\lambda = H^0_{11}$ in all diagonal elements except the first.
- (2) Assume every difference $|H^0_{jj} - H^0_{11}|$ for $j \neq 1$ is large compared to H'_{jj} . Thus, the latter may be omitted in all diagonal elements except the first.
- (3) Neglect all nondiagonal elements except those in the first row and first column, since they effect λ only in a secondary way.



The determinant now becomes:

$$\begin{vmatrix}
 H'_{11} - (\lambda - H^0_{11}) & H_{12} & H_{13} & 0 & \dots & H_{1n} \\
 H_{21} & H^0_{22} - H^0_{11} & 0 & 0 & \dots & 0 \\
 H_{31} & 0 & H^0_{33} - H^0_{11} & 0 & \dots & 0 \\
 \dots & \dots & \dots & \dots & \dots & \dots \\
 H_{n1} & 0 & 0 & 0 & \dots & H^0_{nn} - H^0_{11}
 \end{vmatrix}$$

2.5.11

the solution of which is

$$\left[H'_{11} - (\lambda - H^0_{11}) \right] - \sum_{j=1}^n \left[\frac{H_{1j} H_{j1}}{H^0_{jj} - H^0_{11}} (1 - \delta_{j1}) \right] \prod_{j=2}^n (H^0_{jj} - H^0_{11}) = 0. \quad 2.5.12$$

Since $H^0_{11} \neq H^0_{jj}$, the only term that can be zero is the first, hence

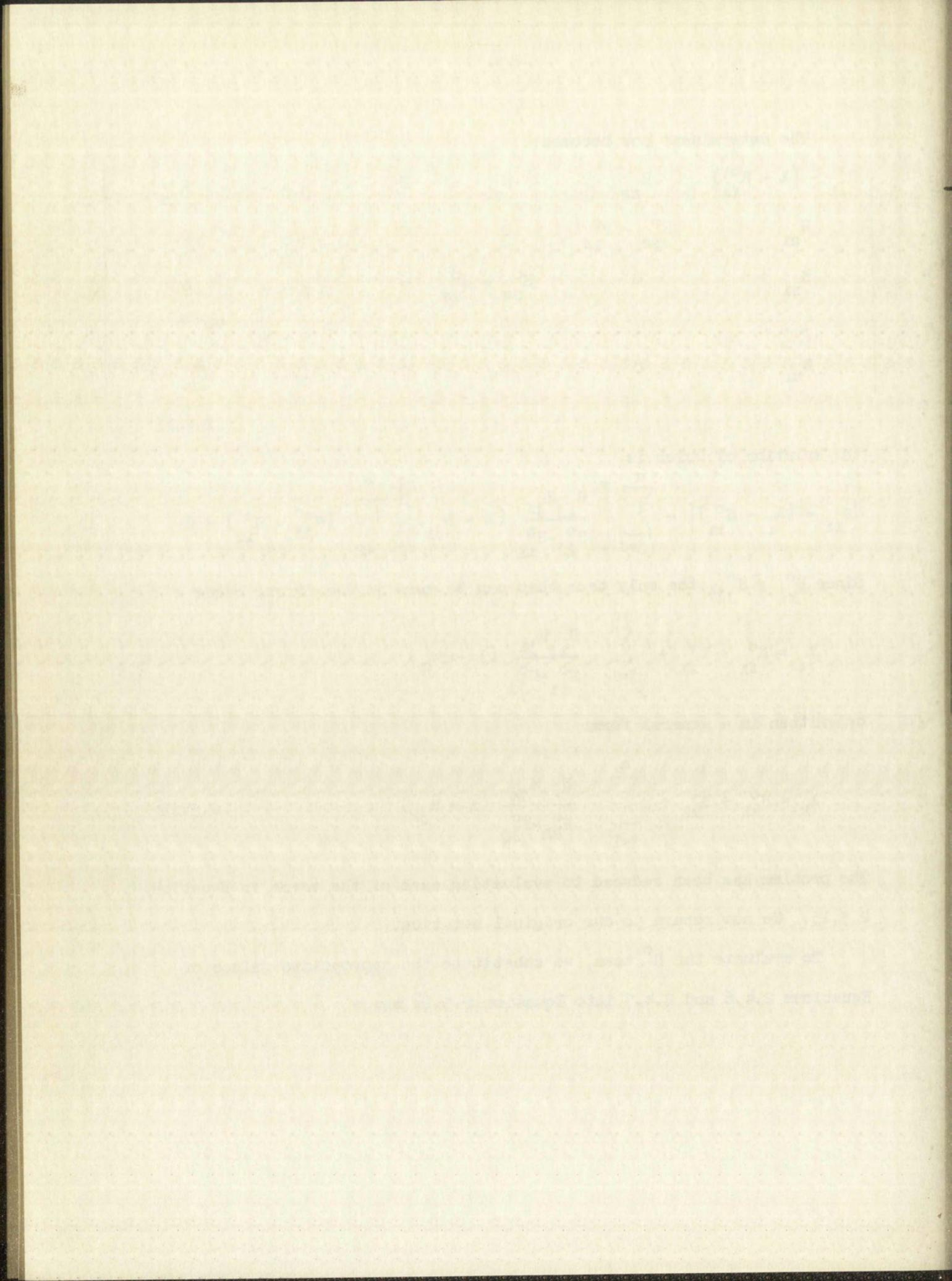
$$\lambda_1 = H^0_{11} + H'_{11} + \sum_{j=1}^n \frac{H_{1j} H_{j1}}{H^0_{jj} - H^0_{11}} (1 - \delta_{j1})$$

or written in a general form:

$$\lambda_k = H^0_{kk} + H'_{kk} + \sum_{j=1}^n \frac{H_{kj} H_{jk}}{H^0_{kk} - H^0_{jj}} (1 - \delta_{jk}) \quad 2.5.13$$

The problem has been reduced to evaluating each of the terms in Equation 2.5.13. We now return to our original notation.

To evaluate the H^0 term, we substitute the appropriate values of Equations 2.4.6 and 2.4.7 into Equation 2.5.6; hence



$$\begin{aligned}
 H^0 \left(U_k \left[S^{D(m)}(r_a)^\gamma \right] ; U_k \left[S^{D(m)}(r_a)^\gamma \right] \right) = \\
 g \left[S^{D(m)}(r_a)^\gamma ; S^{D(m)}(r_a)^\gamma \right] f \left[S^{D(m)}(r_a)^\gamma ; S^{D(m)}(r_a)^\gamma \right] + \\
 g \left[S^{D(m)}(r_a)^\gamma ; S^{D(m)}(r_a)^\gamma \right] \sum_l^{n_a} \frac{A(k,l)}{A(k,j)} \cdot \\
 f \left[S_j^{D(m)}(r_a)^\gamma ; S_l^{D(m)}(r_a)^\gamma \right] (1 - \delta_{lj}) \quad . \quad 2.5.14
 \end{aligned}$$

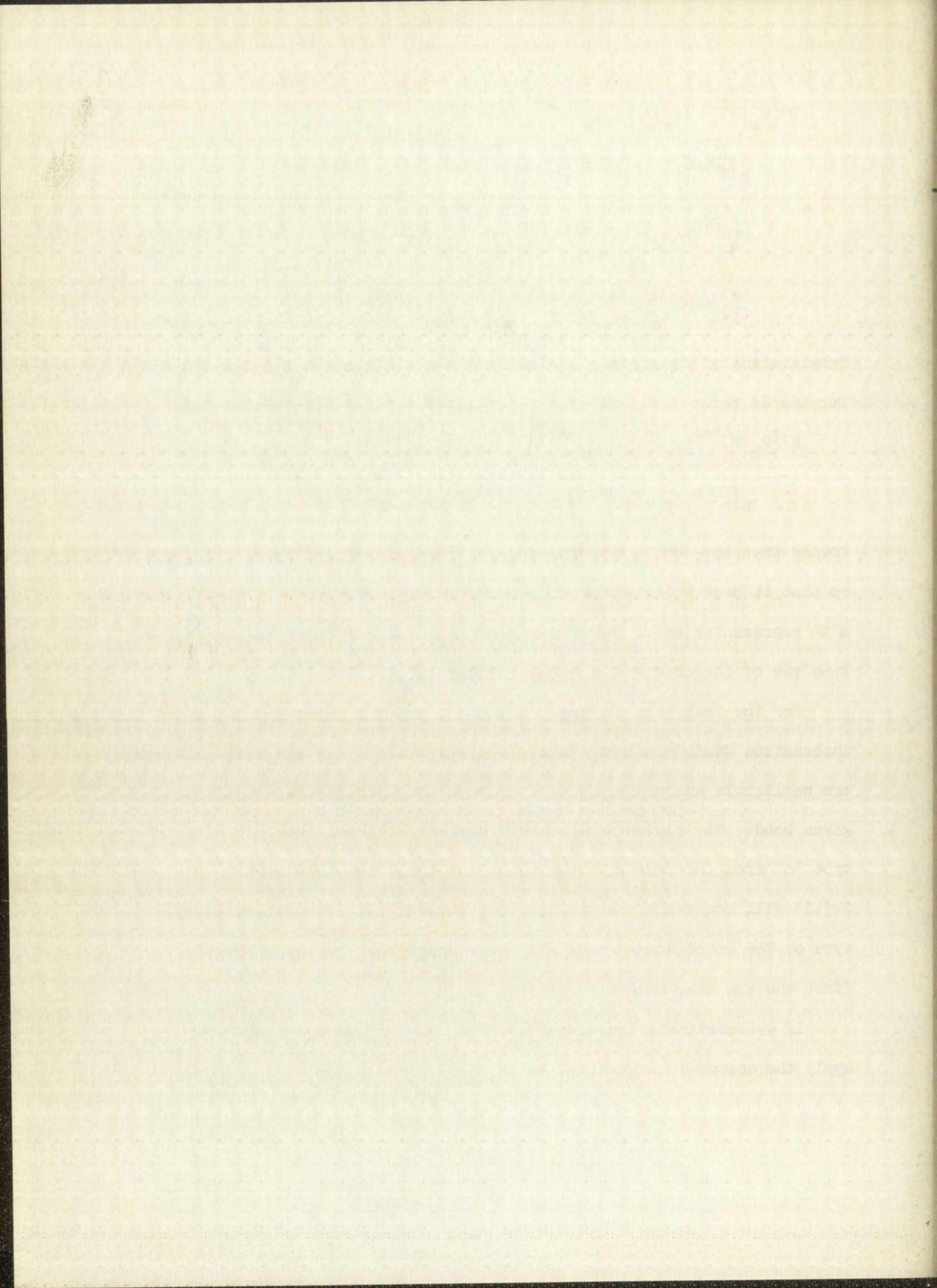
Substitution of Equations 2.4.6 and 2.4.7 into Equation 2.5.7 yields for the H' term:

$$\begin{aligned}
 H' \left(U_k \left[S^{D(m)}(r_a)^\gamma \right] ; U_k \left[S^{D(m)}(r_a)^\gamma \right] \right) = \\
 \sum_R g \left[S^{D(m)}(r_a)^\gamma ; S^{D(m)}(R_a)^\gamma \right] f \left[S^{D(m)}(R_a)^\gamma ; S^{D(m)}(r_a)^\gamma \right] (1 - \delta_{Rr}) \quad . \quad 2.5.15
 \end{aligned}$$

Notice that the sum in Equation 2.5.15 has been reduced by Equation 2.4.6 so that it need be extended only over those symmetry coordinates in the m 'th representation of D and then only over those R which belong to the same row of the degenerate representation as r .

For the last term in Equation 2.5.13, we will make the assumption that interaction force constants between different bonds in the same molecule are negligible as compared to the valence bond force constants for a given bond. For convenience we will separate the sum over molecules of type "a" from the rest of the expression; thus, the last term in Equation 2.5.13 will consist of two parts: one summed just over molecules of type a; the other summed over all other molecules. We will consider first the sum over molecules of type a.

If we substitute Equations 2.4.6 and 2.4.7 into Equation 2.5.8 and apply the assumptions we made, we have:



$$H \left(U_k \left[S^{D(m)}(r_a)^\gamma \right]; U_h \left[S^{D(p)}(R_a)^\rho \right] \right) =$$

$$\sum_{S_l^{D(n)}(q_a)^\rho} g \left[S_j^{D(m)}(r_a)^\gamma; S_l^{D(n)}(q_a)^\rho \right] f \left[S_l^{D(n)}(q_a)^\rho; S_i^{D(p)}(R_a)^\rho \right] \cdot$$

$$\delta_{D(m), D(n)} \delta_{\rho\gamma} \delta_{lj} \delta_{qR}$$

and

$$H \left(U_h \left[S^{D(p)}(R_a)^\rho \right]; U_k \left[S^{D(m)}(r_a)^\gamma \right] \right) =$$

$$\sum_{S_l^{D(n)}(q_a)^\rho} g \left[S_i^{D(p)}(R_a)^\rho; S_l^{D(n)}(q_a)^\rho \right] f \left[S_l^{D(n)}(q_a)^\rho; S_j^{D(m)}(r_a)^\gamma \right] \cdot$$

$$\delta_{D(n), D(p)} \delta_{li} \delta_{\rho\gamma} \delta_{qr}$$

Since the g's are hermitian, the product of the H's is:

$$g \left[S^{D(m)}(r_a)^\gamma; S^{D(m)}(R_a)^\gamma \right]^2 f \left[S^{D(m)}(r_a)^\gamma; S^{D(m)}(r_a)^\gamma \right] f \left[S^{D(m)}(R_a)^\gamma; S^{D(m)}(R_a)^\gamma \right]$$

so that the sum term is given by:

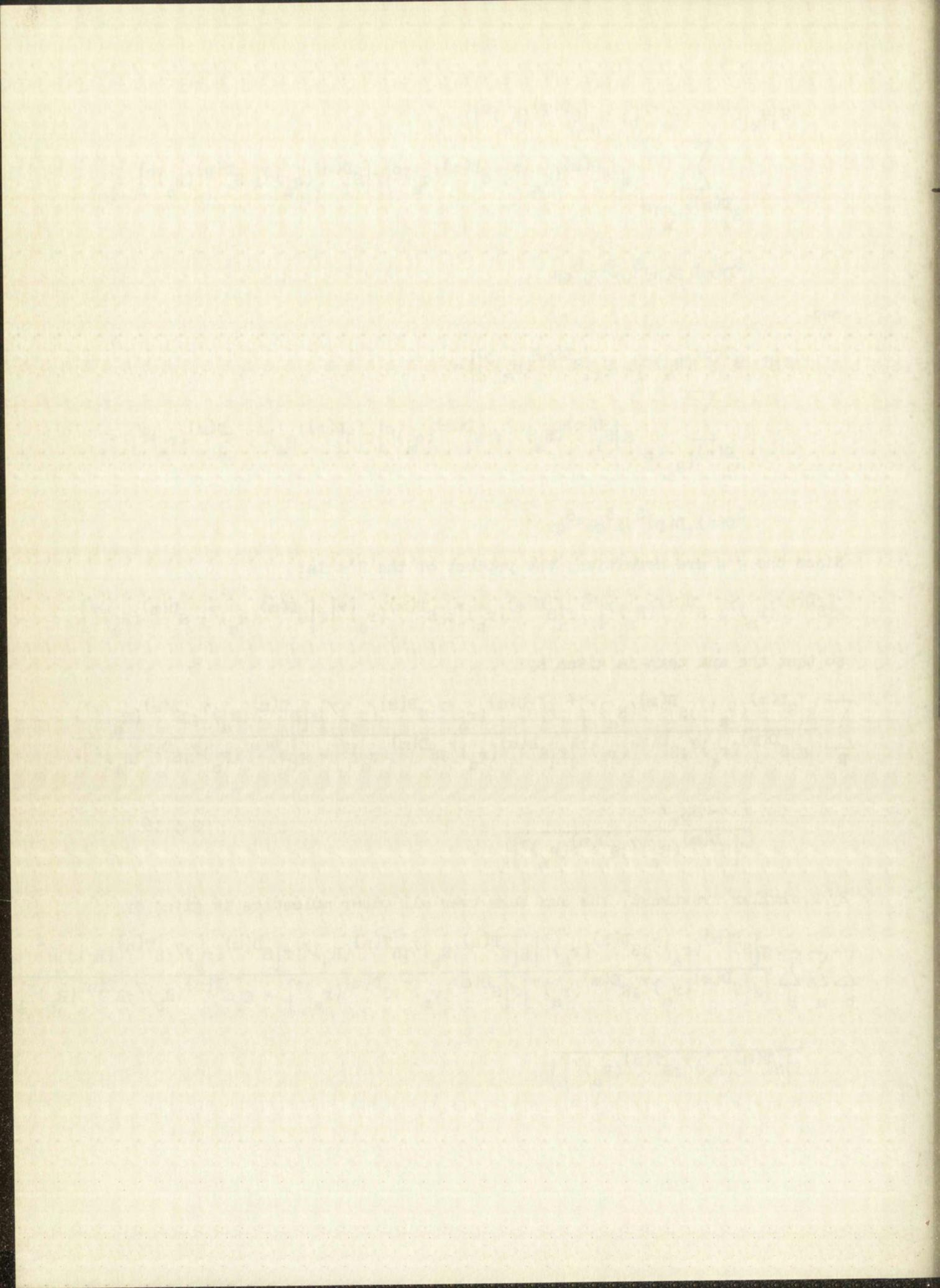
$$\sum_R \frac{g \left[S^{D(m)}(r_a)^\gamma; S^{D(m)}(R_a)^\gamma \right]^2 f \left[S^{D(m)}(r_a)^\gamma; S^{D(m)}(r_a)^\gamma \right] f \left[S^{D(m)}(R_a)^\gamma; S^{D(m)}(R_a)^\gamma \right]}{\left(g \left[S^{D(m)}(r_a)^\gamma; S^{D(m)}(r_a)^\gamma \right] f \left[S^{D(m)}(r_a)^\gamma; S^{D(m)}(r_a)^\gamma \right] - g \left[S^{D(m)}(R_a)^\gamma; S^{D(m)}(R_a)^\gamma \right] \right)}$$

$$\frac{(1 - \delta_{Rr})}{f \left[S^{D(m)}(R_a)^\gamma; S^{D(m)}(R_a)^\gamma \right]} \quad 2.5.16$$

By a similar treatment, the sum term over all other molecules is given by

$$\sum_b \sum_n \sum_R \frac{g \left[S^{D(m)}(r_a)^\gamma; S^{D(m)}(r_a)^\gamma \right] g \left[S^{T(n)}(R_b)^\gamma; S^{T(n)}(R_b)^\gamma \right] f \left[S^{D(m)}(r_a)^\gamma; S^{T(n)}(R_b)^\gamma \right]^2}{\left(g \left[S^{D(m)}(r_a)^\gamma; S^{D(m)}(r_a)^\gamma \right] f \left[S^{D(m)}(r_a)^\gamma; S^{D(m)}(r_a)^\gamma \right] - g \left[S^{T(n)}(R_b)^\gamma; S^{T(n)}(R_b)^\gamma \right] \right)}$$

$$\frac{1}{f \left[S^{T(n)}(R_b)^\gamma; S^{T(n)}(R_b)^\gamma \right]}$$

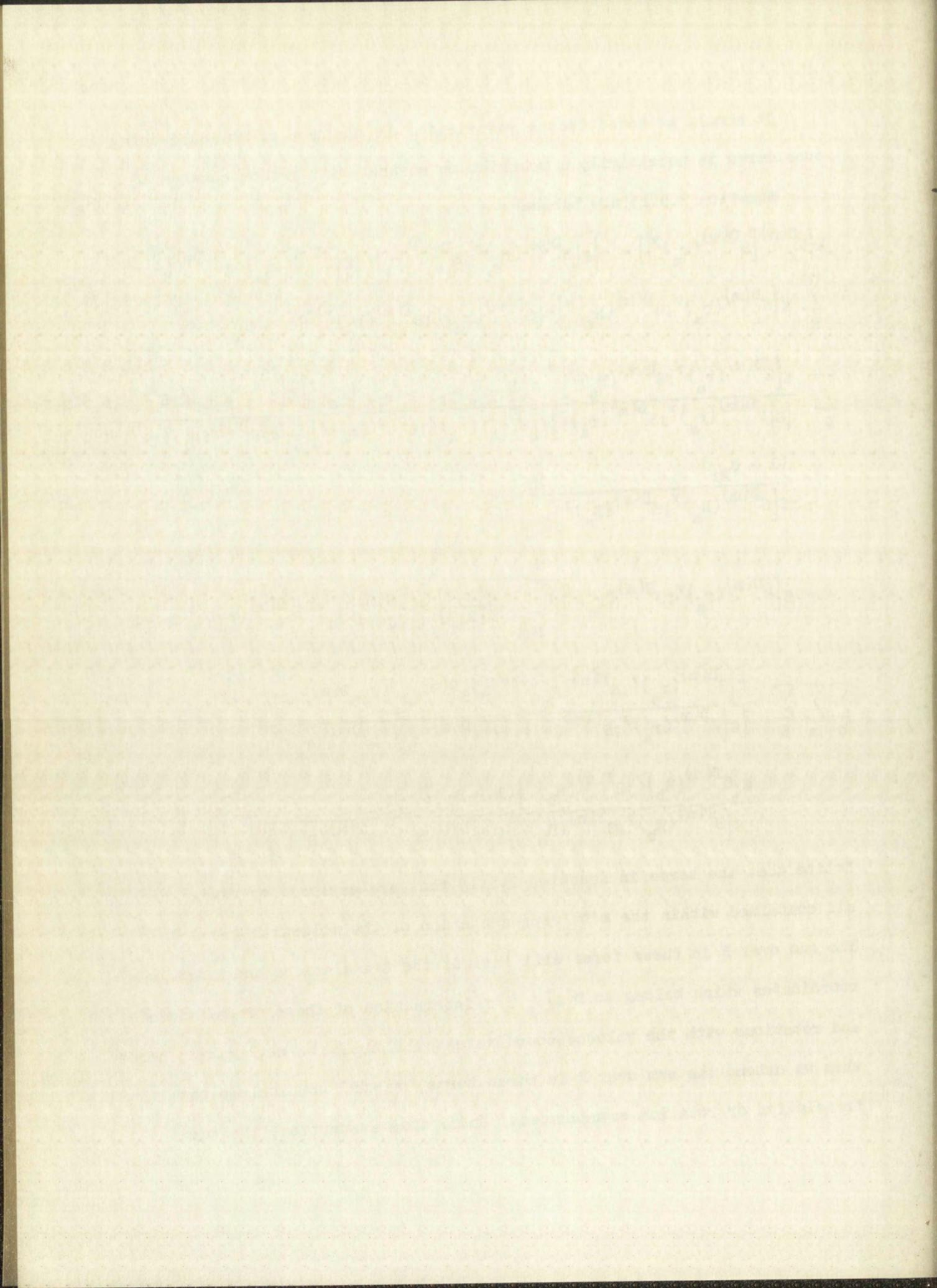


It should be noted that a restriction on the type of molecule being considered is necessarily a restriction on the point groups considered.

Equation 2.5.13 now becomes:

$$\begin{aligned} \lambda \left(U_k^{C(n)} \left[S^{D(m)}(r_a)^\gamma \right] \right) &= \left\{ g \left[S^{D(m)}(r_a)^\gamma; S^{D(m)}(r_a)^\gamma \right] f \left[S^{D(m)}(r_a)^\gamma; S^{D(m)}(r_a)^\gamma \right] + \right. \\ &\sum_R g \left[S^{D(m)}(r_a)^\gamma; S^{D(m)}(R_a)^\gamma \right] f \left[S^{D(m)}(r_a)^\gamma; S^{D(m)}(r_a)^\gamma \right] (1 - \delta_{Rr}) + \\ &\sum_R \frac{g \left[S^{D(m)}(r_a)^\gamma; S^{D(m)}(R_a)^\gamma \right]^2 f \left[S^{D(m)}(r_a)^\gamma; S^{D(m)}(r_a)^\gamma \right] f \left[S^{D(m)}(R_a)^\gamma; S^{D(m)}(R_a)^\gamma \right]}{\left(g \left[S^{D(m)}(r_a)^\gamma; S^{D(m)}(r_a)^\gamma \right] f \left[S^{D(m)}(r_a)^\gamma; S^{D(m)}(r_a)^\gamma \right] - g \left[S^{D(m)}(R_a)^\gamma; S^{D(m)}(R_a)^\gamma \right] \right)} \cdot \\ &\left. \frac{(1 - \delta_{Rr})}{f \left[S^{D(m)}(R_a)^\gamma; S^{D(m)}(R_a)^\gamma \right]} \right\} + \\ &g \left[S^{D(m)}(r_a)^\gamma; S^{D(m)}(r_a)^\gamma \right] \sum_{l=j}^n \frac{A(k,l)}{A(k,j)} f \left[S_j^{D(m)}(r_a)^\gamma; S_l^{D(m)}(r_a)^\gamma \right] (1 - \delta_{lj}) + \\ &\sum_b \sum_n \sum_R \frac{f \left[S^{D(m)}(r_a)^\gamma; S^{T(n)}(R_b)^\gamma \right]^2 g \left[S^{D(m)}(r_a)^\gamma; S^{D(m)}(r_a)^\gamma \right]}{\left(g \left[S^{D(m)}(r_a)^\gamma; S^{D(m)}(r_a)^\gamma \right] f \left[S^{D(m)}(r_a)^\gamma; S^{D(m)}(r_a)^\gamma \right] - \right.} \\ &\left. \frac{g \left[S^{T(n)}(R_b)^\gamma; S^{T(n)}(R_b)^\gamma \right] (1 - \delta_{ba})}{g \left[S^{T(n)}(R_b)^\gamma; S^{T(n)}(R_b)^\gamma \right] f \left[S^{T(n)}(R_b)^\gamma; S^{T(n)}(R_b)^\gamma \right]} \right). \end{aligned} \quad 2.5.17$$

Notice that the terms in Equation 2.5.17 that are enclosed by braces are all contained within the m'th representation of the molecular group D. The sum over R in these terms will include the translations and rotation coordinates which belong to D(m). The interaction of these translations and rotations with the valence coordinates will surely be negligible; hence, when we extend the sum over R in these terms, we will not include the translation or rotation coordinates. Under this assumption, the terms



enclosed in braces become identical to the terms which define $\lambda \left\{ S^{D(m)}(r_a)^\gamma \right\}$ if the determinant of the m'th representation of D is solved by the preceding perturbation technique. $\lambda \left\{ S^{D(m)}(r_a)^\gamma \right\}$ is the frequency associated with the isolated molecule. Further, for the last term in Equation 2.5.17 we may set:

$$g \left[S^{D(m)}(r_a)^\gamma; S^{D(m)}(r_a)^\gamma \right] f \left[S^{D(m)}(r_a)^\gamma; S^{D(m)}(r_a)^\gamma \right] = \lambda \left\{ S^{D(m)}(r_a)^\gamma \right\}$$

and

$$g \left[S^{T(n)}(R_b)^\gamma; S^{T(n)}(R_b)^\gamma \right] f \left[S^{T(n)}(R_b)^\gamma; S^{T(n)}(R_b)^\gamma \right] = \lambda \left\{ S^{T(n)}(R_b)^\gamma \right\}$$

so that Equation 2.5.17 may be expressed as:

$$\lambda \left\{ U_k^{C(n)} \left[S^{D(m)}(r_a)^\gamma \right] \right\} = \lambda \left\{ S^{D(m)}(r_a)^\gamma \right\} +$$

$$g \left[S^{D(m)}(r_a)^\gamma; S^{D(m)}(r_a)^\gamma \right] \sum_{l=j}^n \frac{A(k,l)}{A(k,j)} f \left[S_j^{D(m)}(r_a)^\gamma; S_l^{D(m)}(r_a)^\gamma \right] (1 - \delta_{lj}) +$$

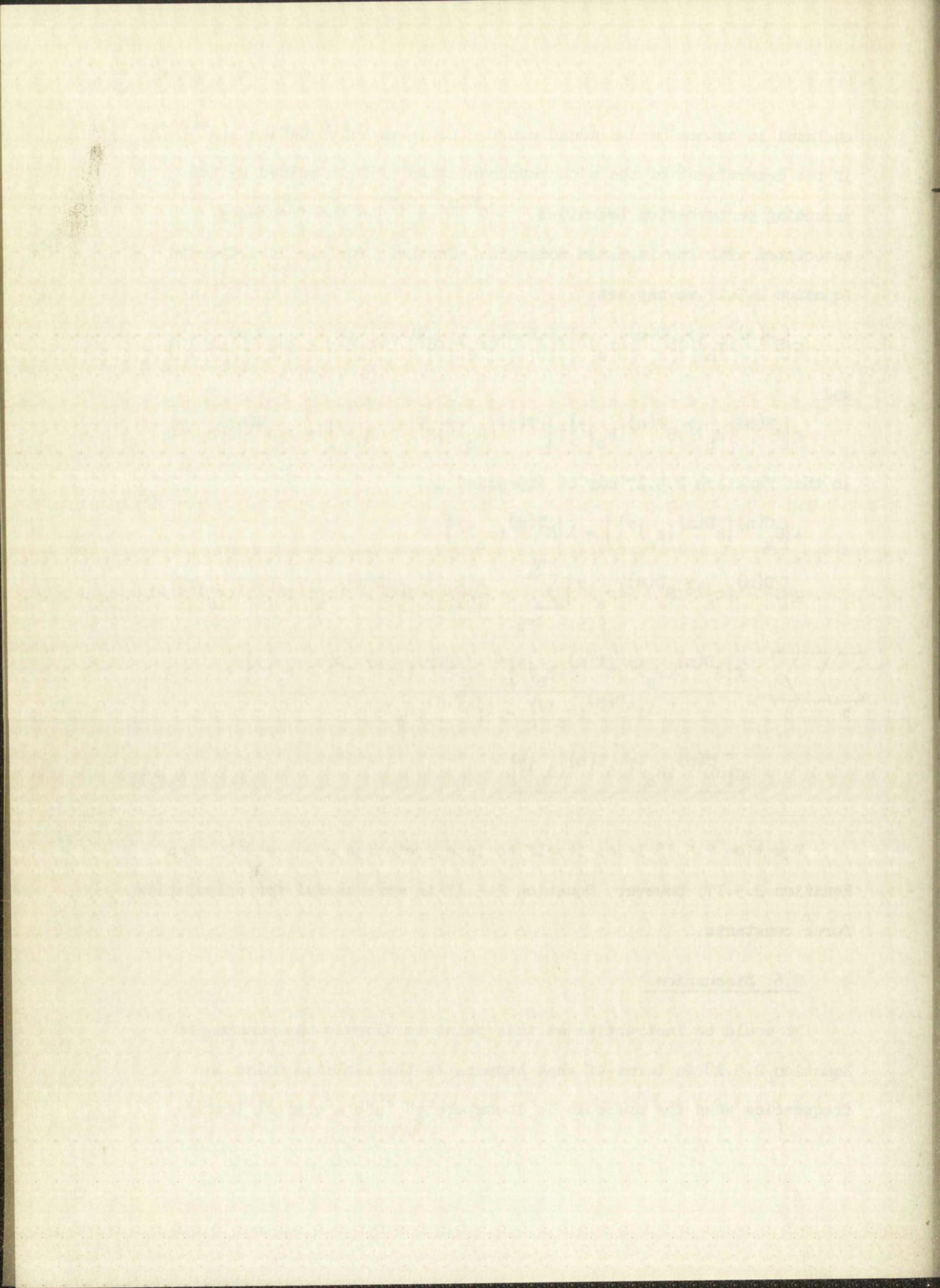
$$\sum_b \sum_n \sum_R \frac{f \left[S^{D(m)}(r_a)^\gamma; S^{T(n)}(R_b)^\gamma \right]^2 g \left[S^{D(m)}(r_a)^\gamma; S^{D(m)}(r_a)^\gamma \right]}{\lambda \left\{ S^{D(m)}(r_a)^\gamma \right\} - \lambda \left\{ S^{T(n)}(R_b)^\gamma \right\}} \cdot$$

$$\frac{g \left[S^{T(n)}(R_b)^\gamma; S^{T(n)}(R_b)^\gamma \right]}{\lambda \left\{ S^{T(n)}(R_b)^\gamma \right\}} \cdot \quad 2.5.18$$

Equation 2.5.18 lends itself to interpretation more readily than Equation 2.5.17; however, Equation 2.5.17 is more useful for calculating force constants.

2.6 Discussion

It would be instructive at this point to discuss the meaning of Equation 2.5.18 in terms of what happens to the isolated molecular frequencies when the molecule is incorporated into a crystal lattice.



Equation 2.5.18 tells us that we should expect a shift in frequencies as we go from gaseous molecules to a crystal lattice. The magnitude and direction of the shift will be dependent upon all the molecules contained in the unit cell (the 2nd and 3rd terms in Equation 2.5.18).

Secondly, Equation 2.5.18 tells us that degenerate frequencies will be split.* The magnitude of the separation of these split degenerate frequencies will be a function of the intermolecular interaction constants in the second and third terms of Equation 2.5.18.

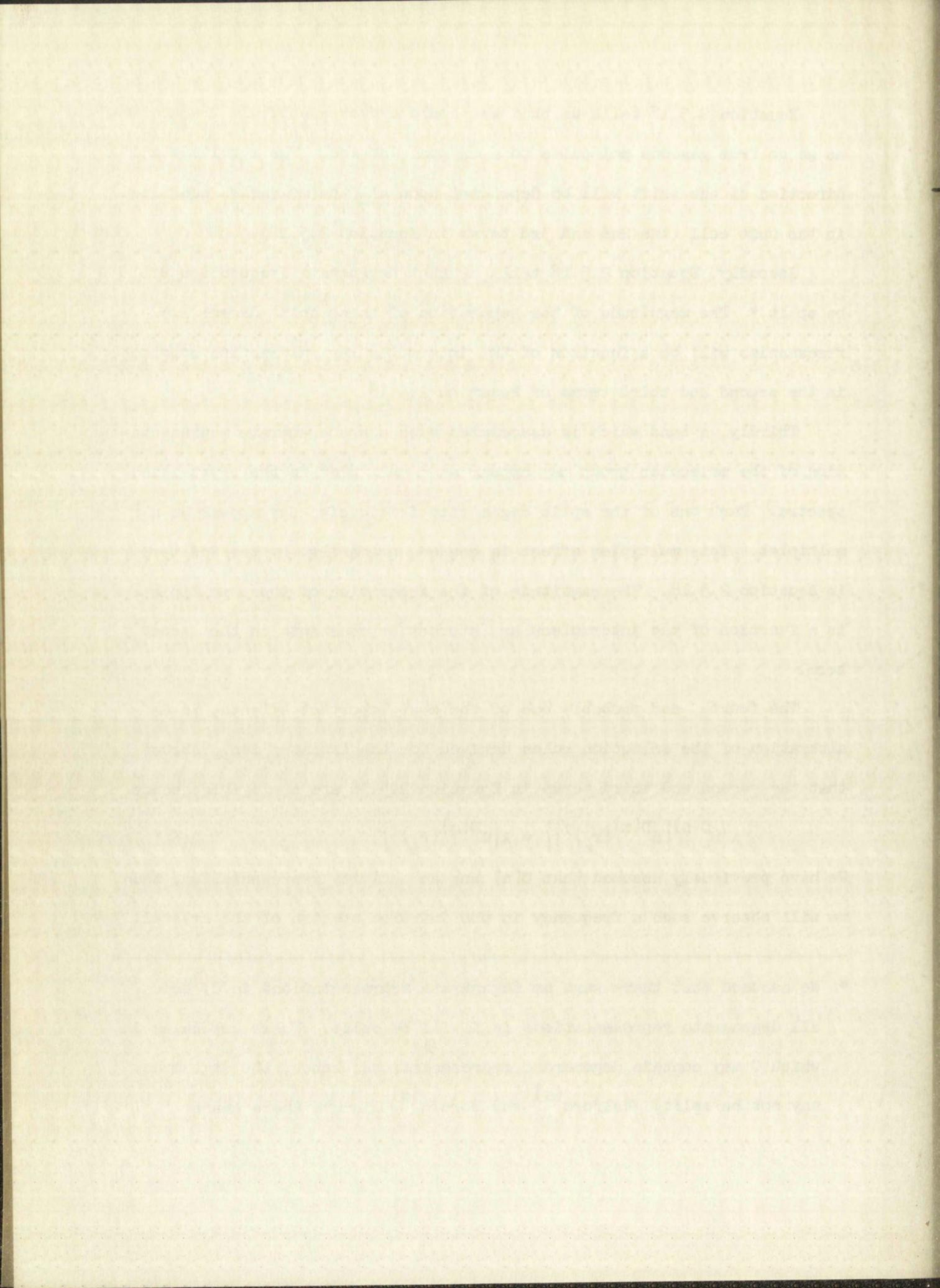
Thirdly, a band which is associated with a nondegenerate representation of the molecular group may appear as a multiplet in the crystalline spectra. Each one of the split degenerate frequencies may appear as a multiplet. This multiplet effect is caused, primarily, by the 2nd term in Equation 2.5.18. The magnitude of the separation of these multiplets is a function of the intermolecular interaction constants in the second term.

The fourth, and probably one of the most important effects, is an alteration of the selection rules derived for the isolated ion. Assume that the second and third terms in Equation 2.5.18 are negligible; hence

$$\lambda \left(U_k^{C(n)} \left[S^{D(m)}(r_a)^\gamma \right] \right) = \lambda \left(S^{D(m)}(r_s)^\gamma \right). \quad 2.6.1$$

We have previously assumed that C(n) was an activity representation; thus, we will observe such a frequency in the infrared spectra of the crystal.

* We assumed that there were no degenerate representations in C; hence, all degenerate representations in D will be split. There are cases in which C may contain degenerate representations; hence, the degeneracy may not be split. Halford⁽⁵⁾ and Hornig⁽⁶⁾ discuss these cases.



Further assume that $D(m)$ was not an activity representation for the molecular group; hence, we would not observe such a frequency in the infrared spectra of the gas. Since $D(m)$ belongs to $C(n)$, however, the frequency has attained infrared activity in the crystal spectra. Some insight as to the mechanism giving rise to this phenomena may be gained by considering the following hypothetical situation. Consider that the nuclei of the atoms comprising the molecule (or complex ion) are arranged in a pattern representative of the symmetry of the molecule. Next we assume that, under conditions of isolation, the electrons are distributed with some symmetry around the skeletal structure of the nuclei. Certain vibrations of these nuclei in this electron atmosphere give rise to a change of dipole moment and, hence, a mechanism is present for the exchange of energy which gives rise to the infrared absorption (or emission) phenomena. As we incorporate the molecule into a crystal lattice, we assume that the symmetry of the skeletal structure remains unchanged; however, the symmetry of the electron cloud may change and hence alter the selection rules. The symmetry of this "warped" (or polarized) electron cloud then must be taken into account in the derivation of the selection rules.

It would seem advisable at this point in the discussion to summarize the assumptions and approximations used in the derivation of Equation 2.5.18. The approximations and assumptions were as follows:

- (1) The criteria for infrared active transitions from the ground state (i.e. at 0°K) hold for transitions observed at room temperature.
- (2) Factor Group selection rules are rigorous for composite transitions.
- (3) The approximations for the perturbation solution outlined on page 88 are valid.

The first part of the document discusses the importance of maintaining accurate records of all transactions. It emphasizes that every entry should be supported by a valid receipt or invoice. This ensures transparency and allows for easy verification of the data.

The second section details the various methods used to collect and analyze the data. It includes a list of the different types of transactions recorded, such as sales, purchases, and transfers. Each method is described in detail, including the steps involved in the process.

The third part of the document provides a summary of the findings. It highlights the key trends and patterns observed in the data. This information is crucial for making informed decisions and identifying areas for improvement.

The final section concludes the report and offers recommendations for future actions. It suggests ways to enhance the data collection process and improve the overall accuracy of the records. The document is intended to serve as a guide for anyone responsible for managing financial data.

(4) Interaction force constants between different bonds in the same molecule are small as compared to the valence bond force constants for a given molecule.

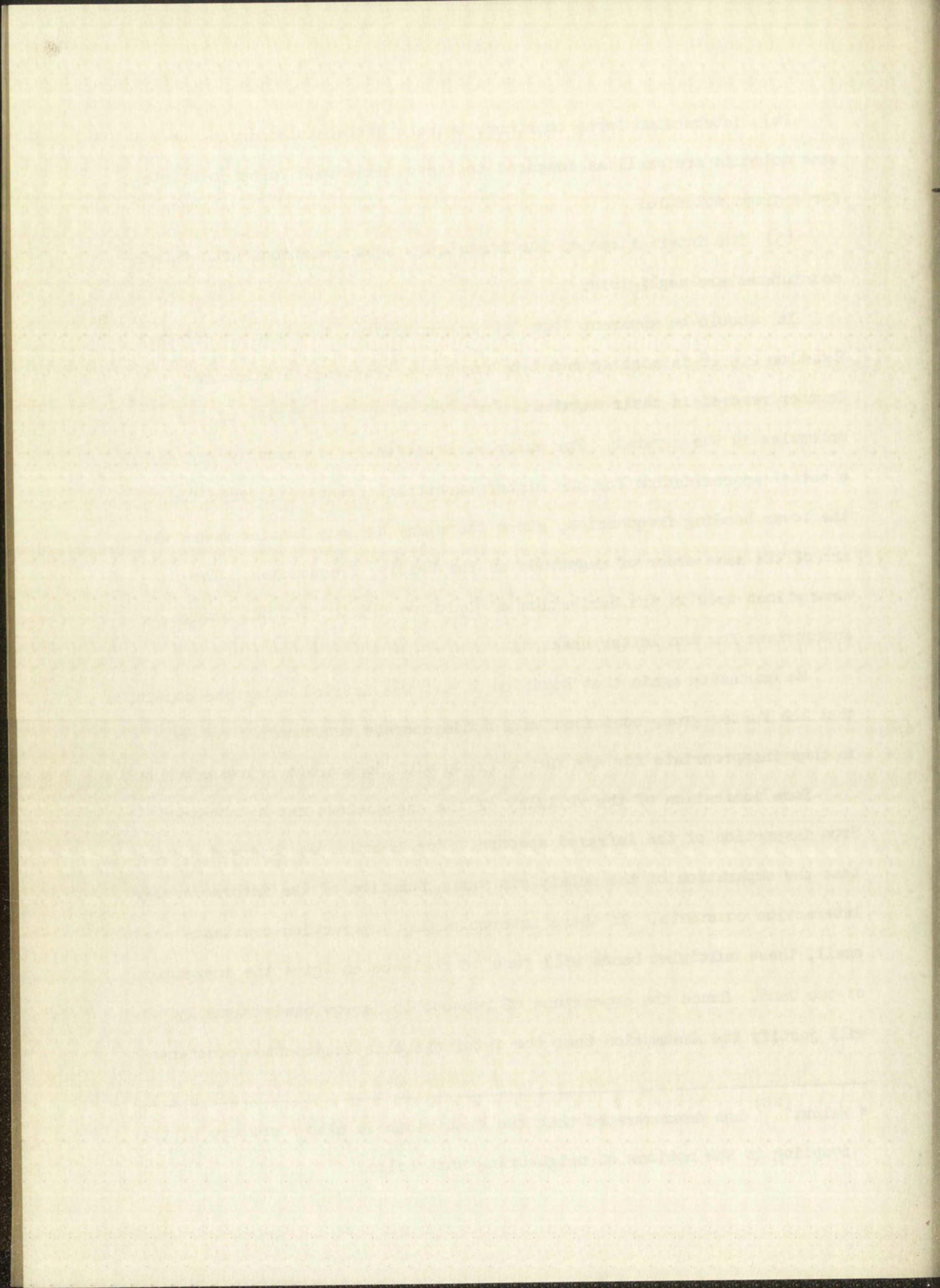
(5) The interactions of the translations and rotations with valence coordinates are negligible.

It should be apparent from the approximations involved in (3) that Equation 2.5.18 is more appropriate for those frequencies which are further removed in their magnitude from the other frequencies of the molecules in the crystal. For example, Equation 2.5.18 usually represents a better approximation for the higher stretching frequencies than for the lower bending frequencies, since there may be some lattice modes which are of the same order of magnitude as the bending frequencies. The assumptions used in the derivation of Equation 2.5.18 will not always be appropriate for the latter case.

We emphasize again that Equation 2.5.18 was derived under the condition that the factor group contained only nondegenerate representations and is thus inappropriate for any factor group with degenerate representations.

Some indication of the validity of the assumptions may be obtained from inspection of the infrared spectra. For example, we observed previously that the separation of the multiplets was a function of the intermolecular interaction constants. If these intermolecular interaction constants are small, these multiplet bands will tend to coalesce and give the impression of one band. Hence the appearance of reasonable narrow bands* usually will justify the assumption that the intermolecular interaction constants

* Walnut⁽¹⁹⁾ has demonstrated that the band width is also a measure of the coupling in the motions of neighboring unit cells.



are negligible. Another indication as to the validity of assuming small intermolecular interaction constants will be the magnitude of the separation of the split degenerate frequencies. A separation of low magnitude indicates that the intermolecular forces are weak.

If it is possible to estimate the magnitude of the frequency shift in going from the gaseous molecules to the crystal lattice, some insight can be gained as to the validity of Equation 2.6.1. In some cases (e.g., complex ions) this information will not be available. We propose in these cases that Equation 2.6.1 represents a good approximation.

In the event that Equation 2.6.1 is used, it should be apparent that it is not necessary to determine the symmetry coordinates of the unit cell in order to determine the selection rules. Inspection of the correlation tables or charts for the molecular group, site group, and factor group will give information concerning the selection rules and polarization properties.

A procedure which will normally be adequate is then one in which the activity of the representation of the factor group is assigned to the representation of the molecular group which is correlated to the given representation of the factor group through the site group. The observed frequencies of the crystalline spectra are assigned to the appropriate representations of the molecular group. The force constants then may be calculated as if the molecules were under conditions of isolation. Force constants calculated by this procedure will have strict meaning only for the particular crystal lattice for which the frequencies were observed.

Perhaps the most important ramification of the preceding sections is the ability to alter selection rules for a given molecule. For example, if a given complex anion crystallizes in different crystal systems which

The first part of the report deals with the general situation of the country and the progress of the work done during the year. It is followed by a detailed account of the various projects and the results achieved. The report concludes with a summary of the work done and a list of the names of the staff members who have been engaged in the work.

The work done during the year has been of a very satisfactory nature and has resulted in the completion of a number of important projects. The progress made has been due to the co-operation and hard work of the staff members who have been engaged in the work.

The following are the names of the staff members who have been engaged in the work during the year:

Mr. A. B. C. D. E. F. G. H. I. J. K. L. M. N. O. P. Q. R. S. T. U. V. W. X. Y. Z.

are dependent upon the cations employed, it is apparent that a different factor group, and hence different selection rules, may be obtained with each cation employed in the formation of a compound with the complex anion. This variation of the selection rules serves as an additional powerful tool in the assignment of frequencies.

3.0 APPLICATION TO THE TETRACYANONICKELATE(II) ION

The chemical nature of the tetracyanonickelate(II) ion will not permit the ion to exist in the gaseous or liquid state. (The compounds of the ion decompose before transition from the solid to liquid state can occur.) One then must be content with spectra of the species obtained from crystalline specimens, or from solutions.

Since the symmetry of the surroundings of an ion in the crystalline state usually is known explicitly, while the symmetry of the surroundings in a solution is not well defined, it follows a priori that the spectra observed for the crystalline state will be more informative. We restrict our attention, then, to the crystalline spectra of the tetracyanonickelate(II) ion.

Preliminary observations of the crystalline spectra of the tetracyanonickelate(II) ion demonstrate that the degenerate frequencies are split only slightly and that multiplet structure is absent. From the arguments presented in Section 2.6, we conclude that Equation 2.6.1 will adequately explain the crystalline spectra.

The procedure we will follow is one in which the activity of the factor group representation is assigned to the representation of the molecular group with which it is correlated (through the site group).

The first part of the document discusses the importance of maintaining accurate records of all transactions. It emphasizes that every entry should be supported by a valid receipt or invoice. This ensures transparency and allows for easy verification of the data.

In the second section, the author outlines the various methods used to collect and analyze the data. This includes both primary and secondary data collection techniques. The analysis focuses on identifying trends and patterns over time, which is crucial for making informed decisions.

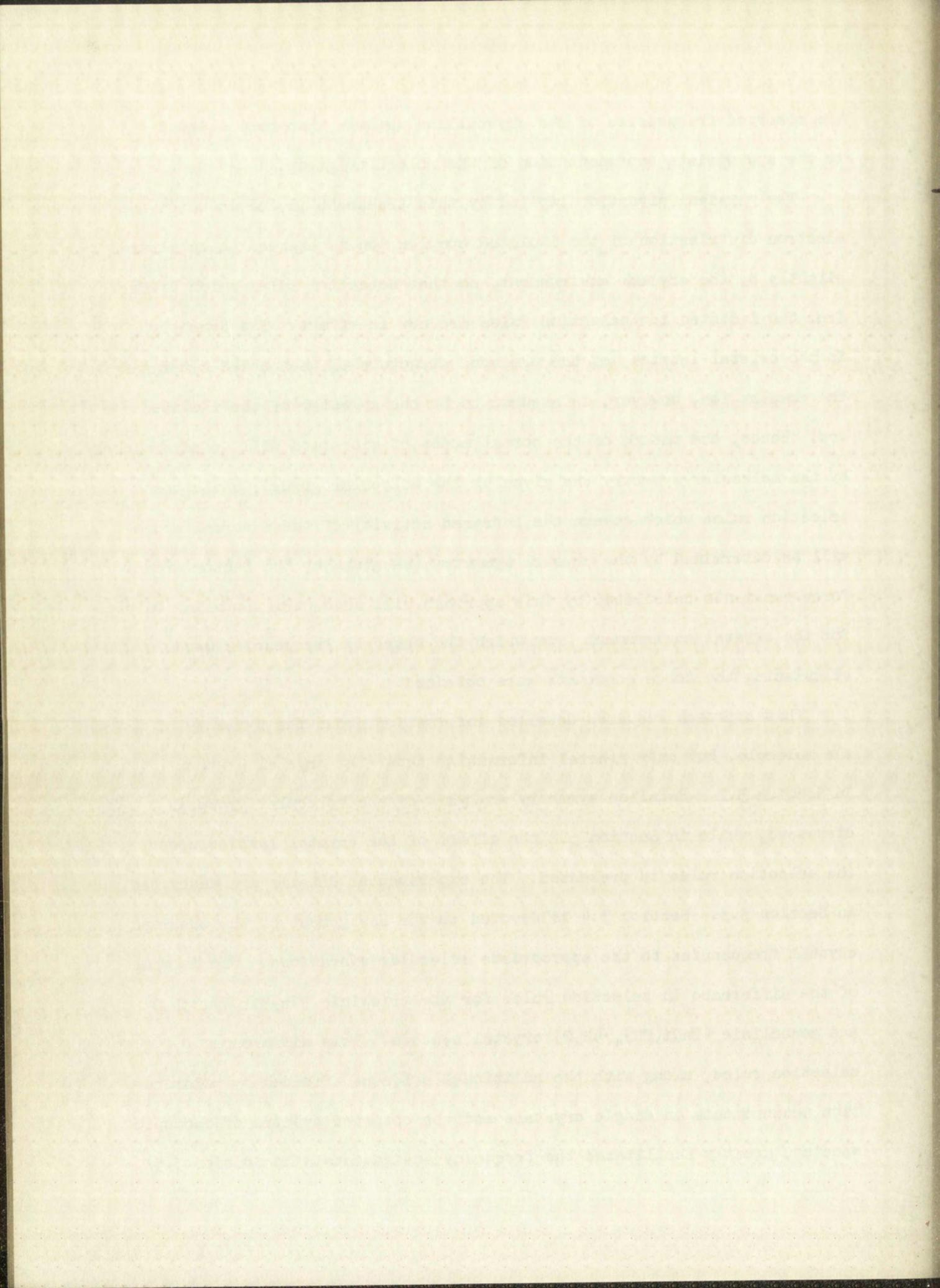
The third part of the report details the results of the data analysis. It shows a clear upward trend in sales over the period studied, with a significant increase in the latter half of the year. This is attributed to several factors, including improved marketing strategies and a strong economic environment.

Finally, the document concludes with a series of recommendations for future actions. It suggests continuing the current marketing efforts while also exploring new channels to reach a wider audience. The author also recommends regular monitoring of the market to stay ahead of potential competitors.

The observed frequencies of the crystalline spectra then are assigned to the appropriate representation of the molecular group.

The physical situation implied by this treatment is one in which the electron distribution of the isolated complex ion is assumed to be altered slightly by the crystal environment, so that selection rules which differ from the isolated ion selection rules are now in effect. The symmetry, in the crystal lattice, of the skeletal structure of the nuclei comprising the complex ion, however, is assumed to be the symmetry of the isolated ion. Hence, the nature of the normal modes of vibration will be determined by the molecular symmetry (as given by the molecular group), while the selection rules which govern the infrared activity of these normal modes will be determined by the crystal symmetry (as given by the factor group). Force constants calculated by this approach will have strict meaning only for the crystal environment from which the observed frequencies used in calculating the force constants were obtained.

This approach requires detailed information about the symmetry of the molecule, but only general information about the crystal system. In Section 3.1 a detailed symmetry analysis of the molecular group is discussed, while in Section 3.2 the effect of the crystal lattice upon the selection rules is presented. The experimental details are described in Section 3.3. Section 3.4 is devoted to the assignment of the observed crystal frequencies to the appropriate molecular vibrations. Use is made of the difference in selection rules for the triclinic ($\text{Na}_2\text{Ni}(\text{CN})_4 \cdot 3\text{H}_2\text{O}$) and monoclinic ($\text{BaNi}(\text{CN})_4 \cdot 4\text{H}_2\text{O}$) crystal systems. This difference in selection rules, along with the additional evidence afforded by polarization measurements on single crystals and the observed spectra of isotopic species, greatly facilitates the frequency assignments. In Section 3.5



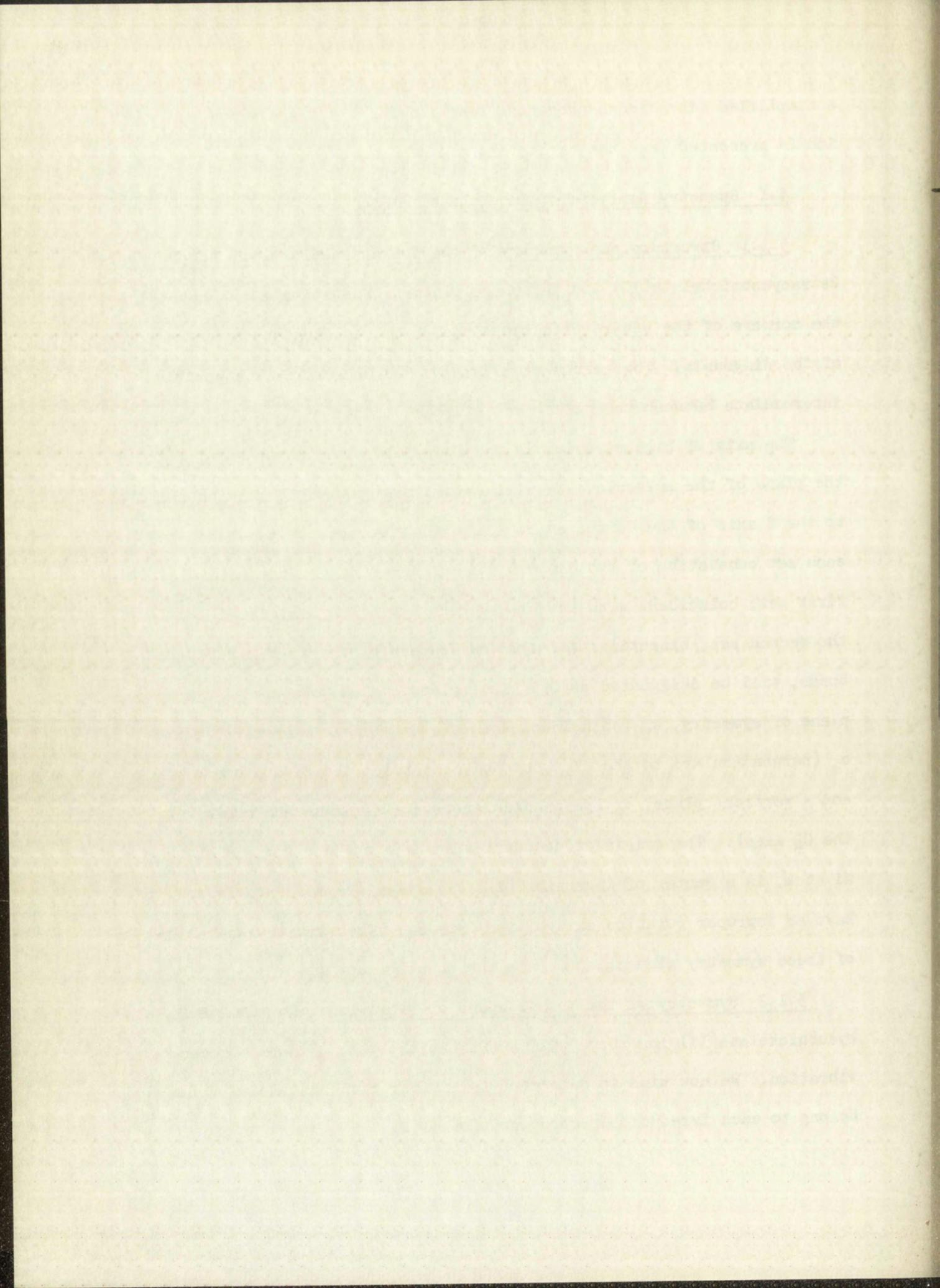
a simplified vibrational potential function for the tetracyanonickelate(II) ion is presented, and the parameters are evaluated.

3.1 Symmetry Analysis of the Molecular Group

3.1.1 Structure and Symmetry of the Tetracyanonickelate(II) Ion: The tetracyanonickelate(II) ion is square planar. The nitrogen atoms are at the corners of the square with the nickel atom residing at the intersection of the diagonals. The carbon atoms are on the diagonals at a position intermediate between the nickel and nitrogen atoms⁽²⁰⁾ (see Fig. 3.1.3).

The axis of highest order is the four-fold axis, perpendicular to the plane of the molecule. We will regard this four-fold axis as parallel to the Z axis of the Cartesian coordinates. Two sets of two-fold axes, each set consisting of two members, lie in the plane of the molecule. The first set, coincident with the Ni-C-N bonds, will be designated as C_2' ; the second set, bisecting the right angle made by the in-plane N-C-Ni-C-N bonds, will be designated as C_2'' . The molecule also possesses a horizontal plane of symmetry, σ_h (coincident with the XY plane); a vertical plane, σ_v (perpendicular) to the XY plane and containing the Ni-C-N bonds); and a vertical plane, σ_d (perpendicular to the XY plane and containing the C_2'' axes). The origin of the Cartesian axis system, located at the Ni atom, is a center of inversion "i". Finally, the molecule is seen to have an improper rotation axis of the type S_4 . The symmetry operations of these symmetry elements generate the point group D_{4h} .

3.1.2 Symmetry of the Normal Modes of Vibration: For the tetracyanonickelate(II) ion there will be $21 (= 3N - 6)$ ⁽²¹⁾ normal modes of vibration. We now wish to determine the number of normal modes which belong to each irreducible representation of D_{4h} .



The three Cartesian displacement coordinates, (see Fig. 3.1.5) x_j, y_j, z_j , of each nucleus j ($j = 1, 2, \dots, N$) together form a $3N$ -dimensional basis of a completely reducible representation. In this completely reducible representation defined by the Cartesian coordinates, the character of any operation, R , is given by⁽²²⁾:

$$(\chi_R) = w_R (\pm 1 + 2 \cos \theta_R)$$

where w_R is the number of invariant atoms under the operation R , and θ_R is the angle through which operation R takes a given atom. The + sign is used if the operation is a pure rotation (proper rotation), and the - sign is used if the operation is a rotation-reflection (improper rotation). From a knowledge of the group characters in any representation γ of D_{4h} , we find n_c^γ , the number of times a particular irreducible representation of D_{4h} is contained in the reducible representation, by means of the reduction formula⁽²³⁾:

$$n_c^\gamma = \frac{1}{g} \sum_R (\chi_R)^\gamma (\chi_R)$$

where $(\chi_R)^\gamma$ is the character of R in D_{4h} . The number of operations in the group is given by g .

Table 3.1.2 contains, in addition to the character table for the group D_{4h} , the analysis of the Cartesian coordinate representation into the irreducible representations of D_{4h} . The column headed by n_c^γ gives the number of times the irreducible representation, γ , of D_{4h} appears in the

[†] The actual value of n_c^γ is obtained when $(\chi_R)^\gamma$ is replaced by its complex conjugate. As we are dealing with real characters, this distinction is of no significance.



reduced Cartesian coordinate representation. The columns headed by n_T^γ and n_R^γ give the number of representations corresponding to translation and rotation of the molecule as a whole. The column headed by n^γ gives the number of genuine vibrations, which is given by $n_C^\gamma - (n_T^\gamma + n_R^\gamma)$.

TABLE 3.1.2

SYMMETRY ANALYSIS OF THE REDUCIBLE CARTESIAN REPRESENTATION
OF THE TETRACYANONICKELATE(II) ION

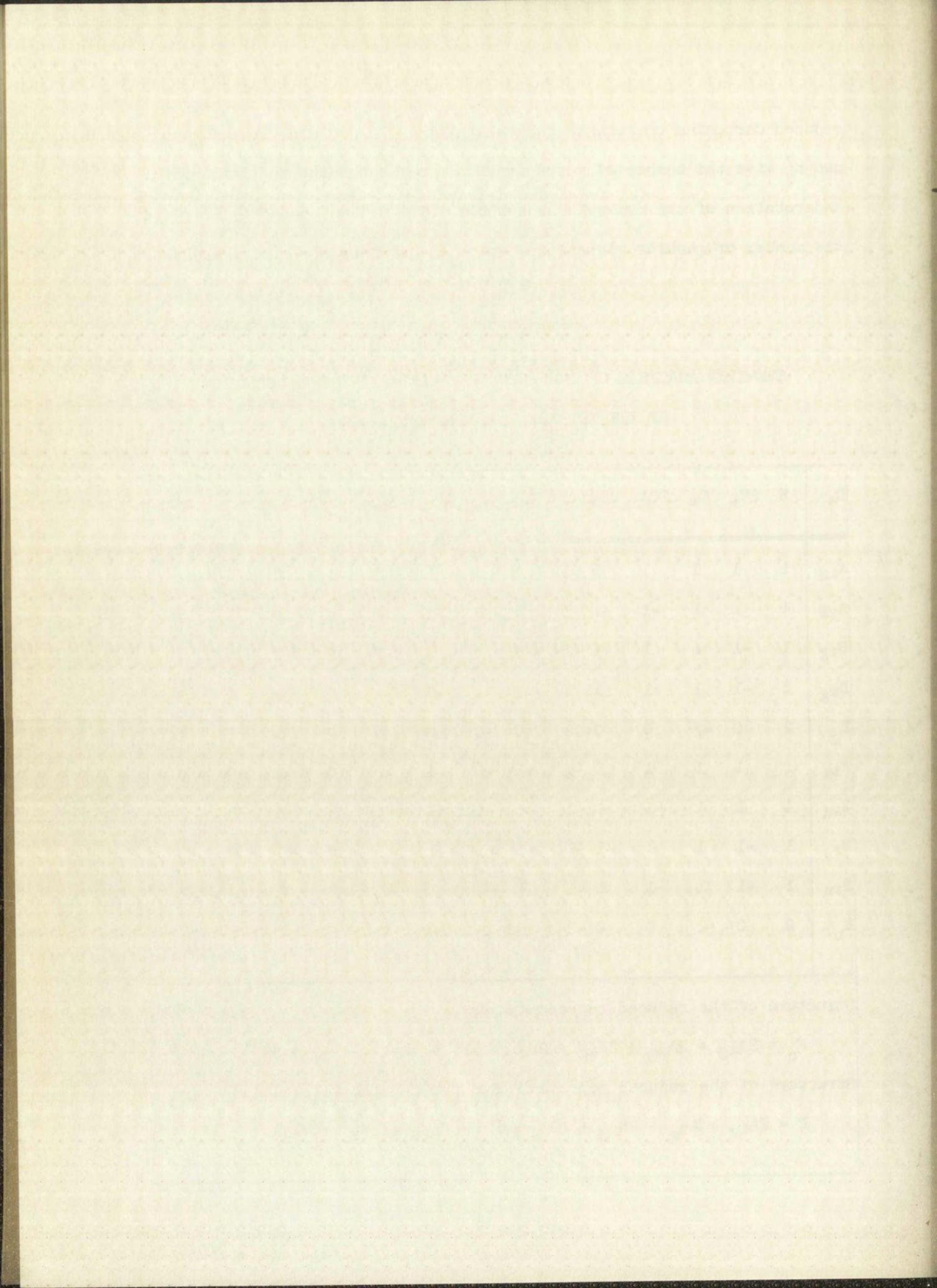
D _{4h}	E	2C ₄	C ₂	2C ₂ '	2C ₂ "	i	2S ₄	σ_h	2 σ_v	2 σ_d	n_C^γ	n_T^γ	n_R^γ	n^γ
A _{1g}	1	1	1	1	1	1	1	1	1	1	2	0	0	2
A _{2g}	1	1	1	-1	-1	1	1	1	-1	-1	2	0	1	1
B _{1g}	1	-1	1	1	-1	1	-1	1	1	-1	2	0	0	2
B _{2g}	1	-1	1	-1	1	1	-1	1	-1	1	2	0	0	2
E _g	2	0	-2	0	0	2	0	-2	0	0	2	0	1	1
A _{1u}	1	1	1	1	1	-1	-1	-1	-1	-1	0	0	0	0
A _{2u}	1	1	1	-1	-1	-1	-1	-1	1	1	3	1	0	2
B _{1u}	1	-1	1	1	-1	-1	1	-1	-1	1	0	0	0	0
B _{2u}	1	-1	1	-1	1	-1	1	-1	1	-1	2	0	0	2
E _u	2	0	-2	0	0	-2	0	2	0	0	5	1	0	4

Structure of the reduced representation:

$$\Gamma_c = 2A_{1g} + 2A_{2g} + 2B_{1g} + 2B_{2g} + 2E_g + 3A_{2u} + 2B_{2u} + 5E_u .$$

Structure of the reduced representation for genuine vibrations:

$$\Gamma = 2A_{1g} + A_{2g} + 2B_{1g} + 2B_{2g} + E_g + 2A_{2u} + 2B_{2u} + 4E_u .$$



Notice that if we multiply each of the coefficients of the representations in the above expressions by the dimensions of the representation and sum, we obtain $27 (= 3N)$ modes for the reduced representation and $21 (= 3N - 6)$ modes for the reduced representation for genuine vibrations.

In the further analysis of the vibrational motions, it will be convenient to consider the in-plane and out-of-plane modes separately. The in-plane and out-of-plane modes are distinguished readily by reference to the character of σ_h , which should be positive in the first case and negative in the second. Thus the structure of the reduced representation of the in-plane normal modes of vibration is

$$\Gamma_1 = 2A_{1g} + A_{2g} + 2B_{1g} + 2B_{2g} + 4E_u,$$

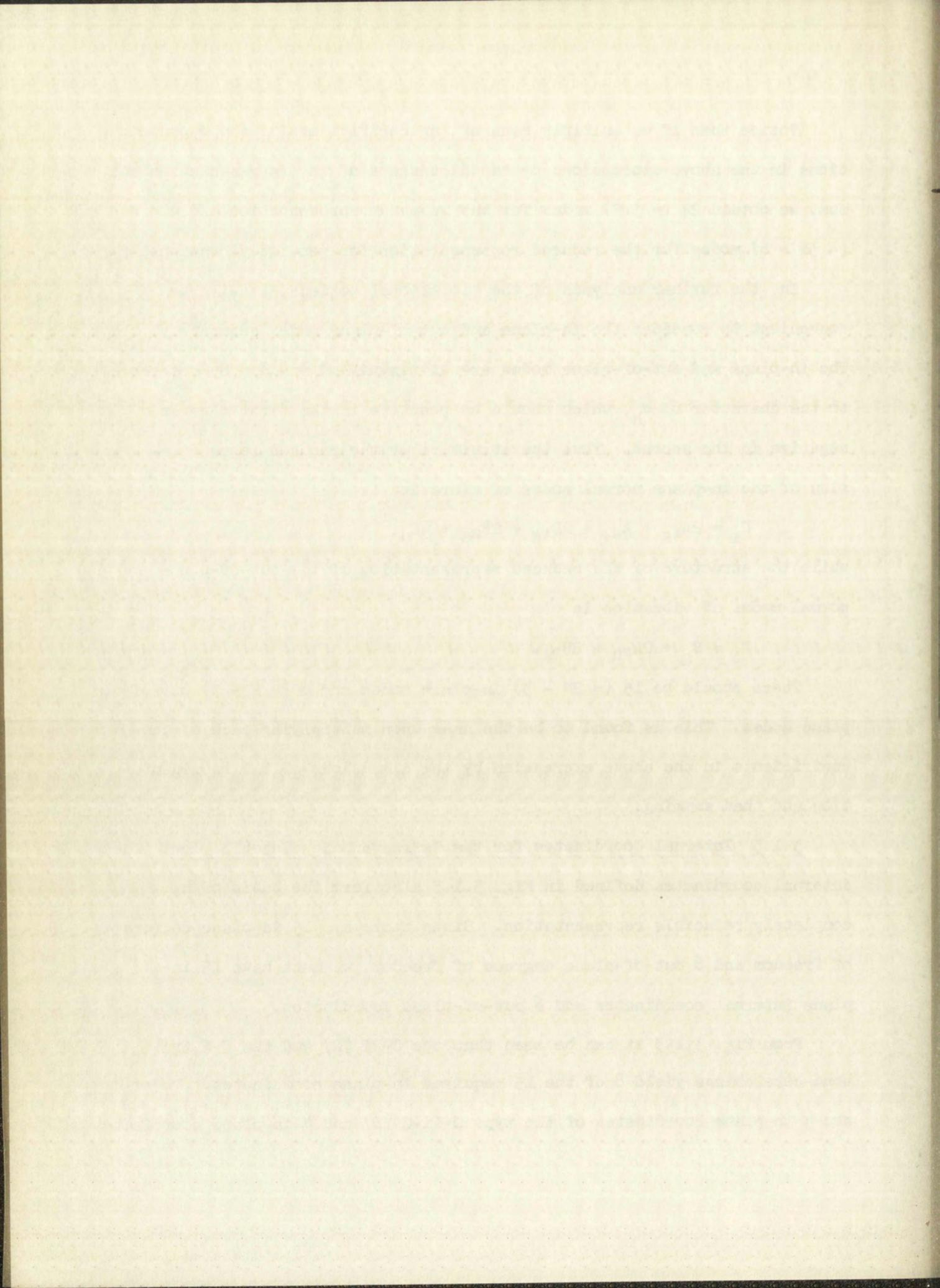
while the structure of the reduced representation of the out-of-plane normal modes of vibration is

$$\Gamma_0 = E_g + 2A_{2u} + 2B_{2u}.$$

There should be $15 (= 2N - 3)$ in-plane modes and $6 (= N - 3)$ out-of-plane modes. This is found to be the case upon multiplying each of the coefficients in the above expression by the dimensions of the representation and then summing.

3.1.3 Internal Coordinates for the Tetracyanonickelate(II) Ion: The internal coordinates defined in Fig. 3.1.3 also form the basis of a completely reducible representation. Since there are 15 in-plane degrees of freedom and 6 out-of-plane degrees of freedom, we must have 15 in-plane internal coordinates and 6 out-of-plane coordinates.

From Fig. 3.1.3 it can be seen that the C-Ni (R) and the C-N (r) bond stretchings yield 8 of the 15 required in-plane coordinates. There are 4 in-plane coordinates of the type C-Ni-C (β) and 4 in-plane coordinates



of the type Ni-C-N (α) bending vibrations. This gives a total of 16 in-plane coordinates; hence a redundancy exists.

Two sets of out-of-plane coordinates are introduced. The first set consists of the two equivalent bendings of the C-Ni-C angle (θ), while the second set consists of the four equivalent Ni-C-N bendings (ϕ). Since there are two of the former and 4 of the latter, no redundancy is present in the out-of-plane internal coordinates.

As was the case for the Cartesian coordinates, we now wish to determine the number of times a particular irreducible representation of D_{4h} is contained in the reducible representation defined by the internal coordinates. This enumeration may be achieved by means of the reduction formula*:

$$n^\gamma = \frac{1}{g} \sum_j g_j (\chi_R)_j^\gamma (\chi_R)_j$$

where, as before, g is the number of operations in the group, $(\chi_R)_j$ refers to the reducible representation, $(\chi_R)_j^\gamma$ refers to the γ th irreducible representation, and n^γ is the number of times the irreducible representation appears in the reduced representation. The term g_j refers to the number of operations in the j th class, and the $(\chi_R)_j$'s refer to the character of each operation in that class. The character $(\chi_R)_j$ may be obtained in terms of the internal coordinate representation if the improper operations are treated exactly as they were treated in obtaining (χ_R) (see Section 3.1.2). The character of the proper operations must be

* This reduction formula is equivalent to the reduction formula given in Section 3.1.2. It is convenient to sum over the classes rather than the operations.

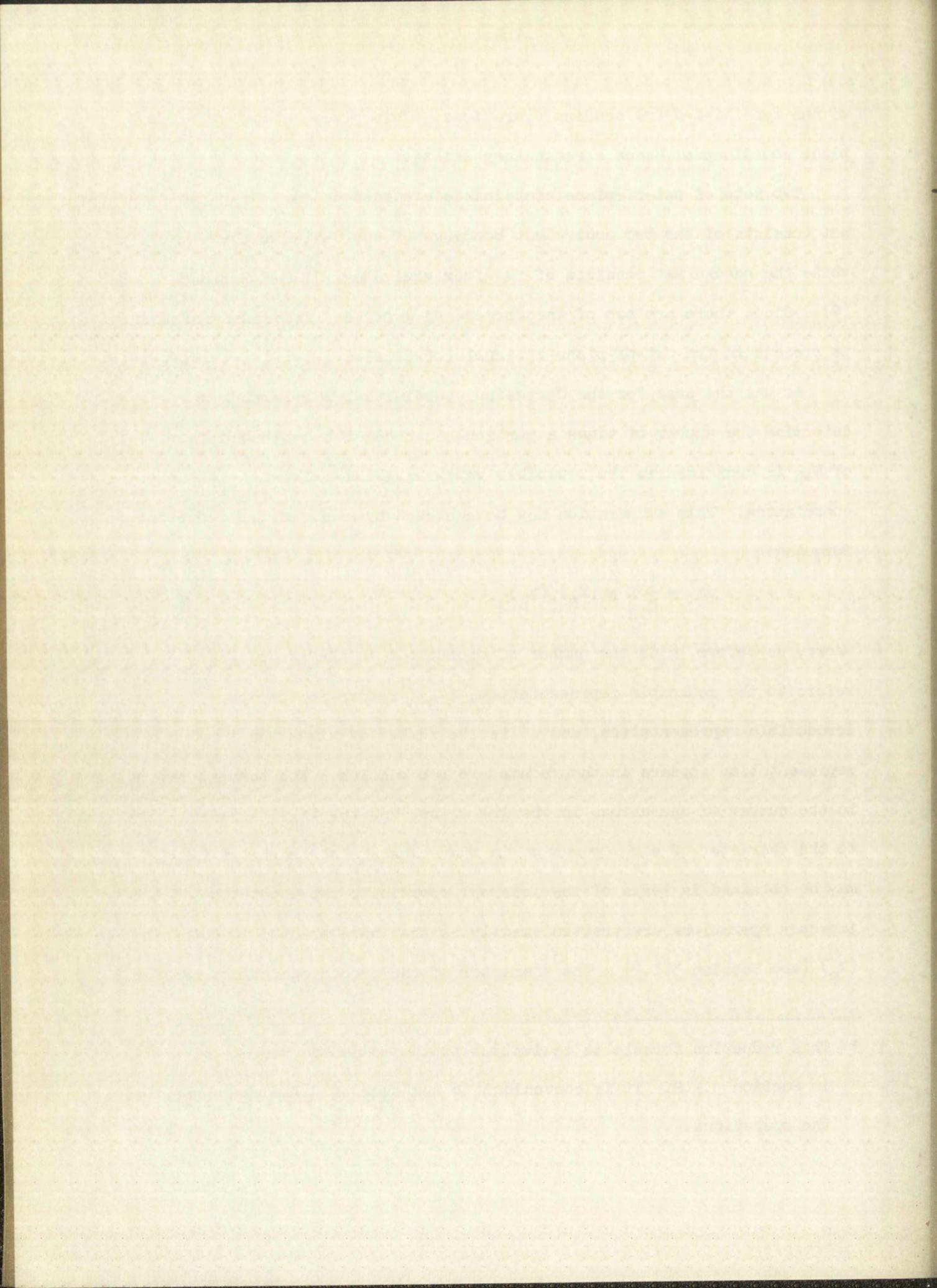
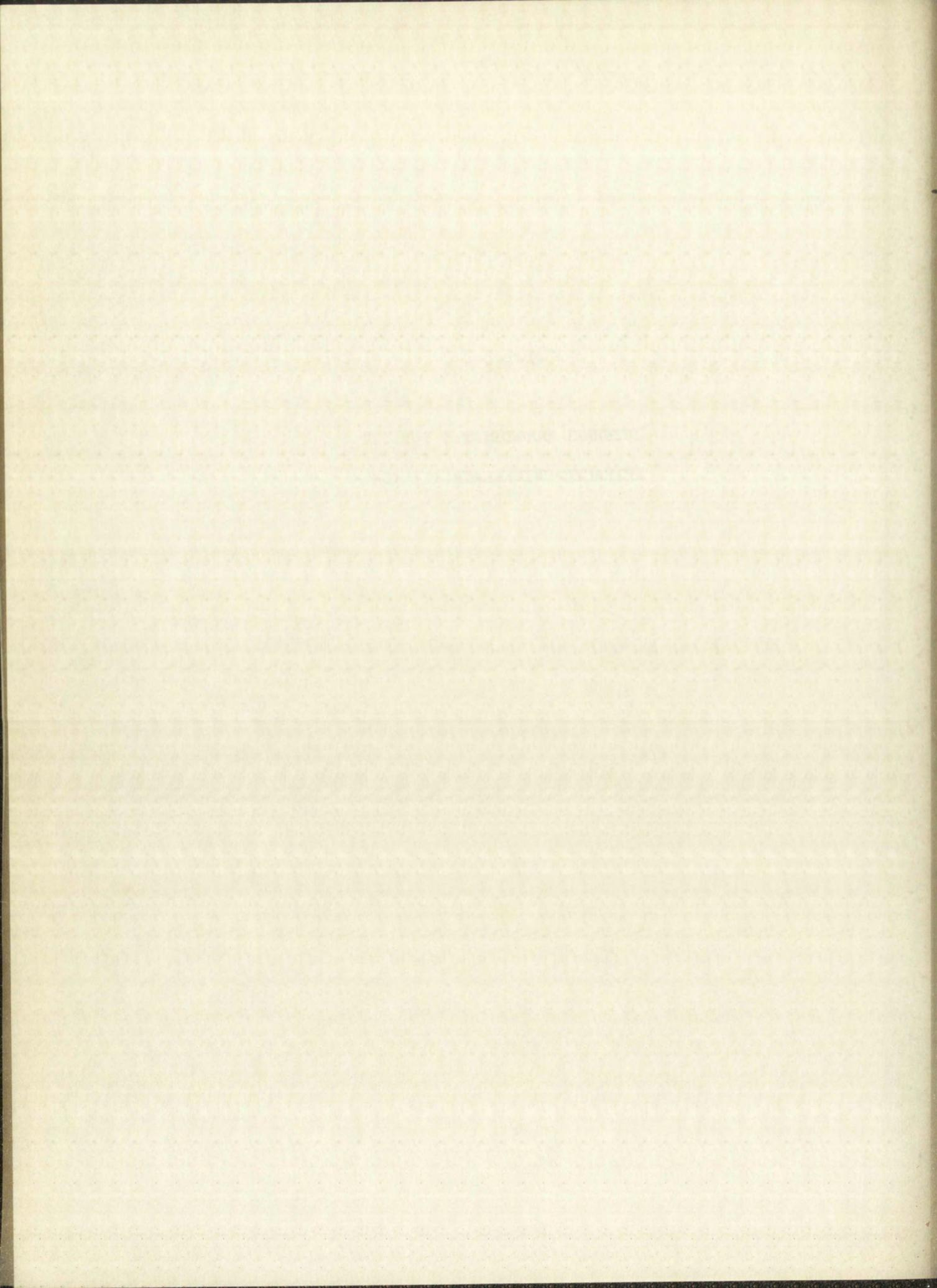
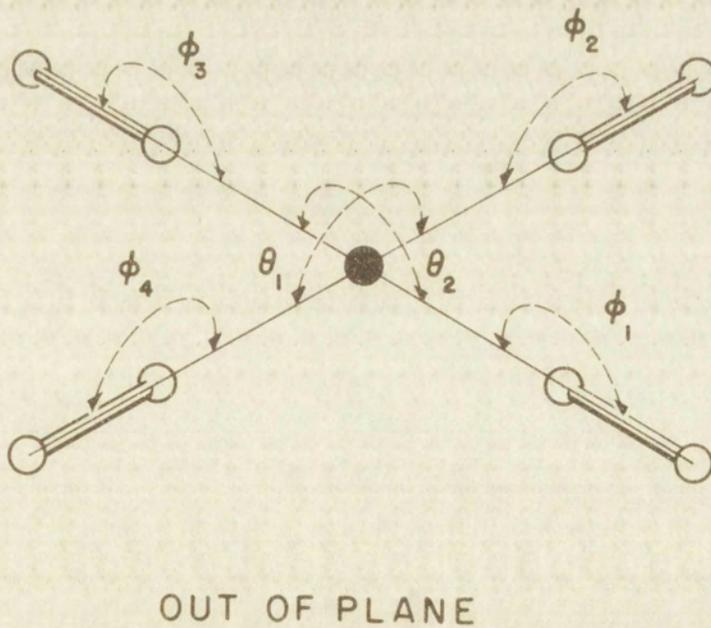
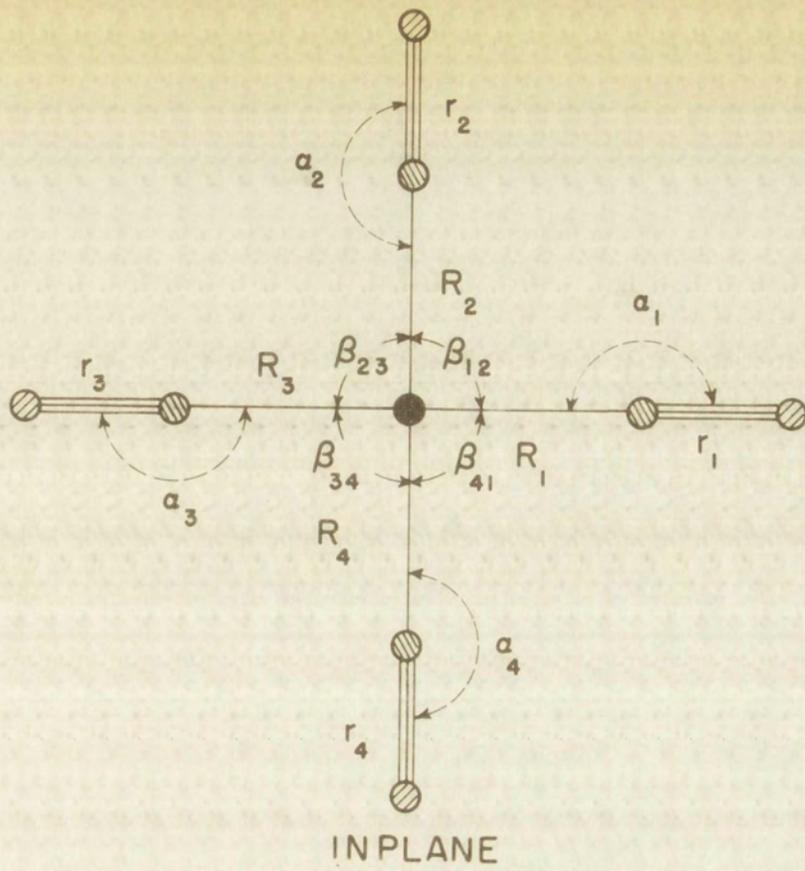
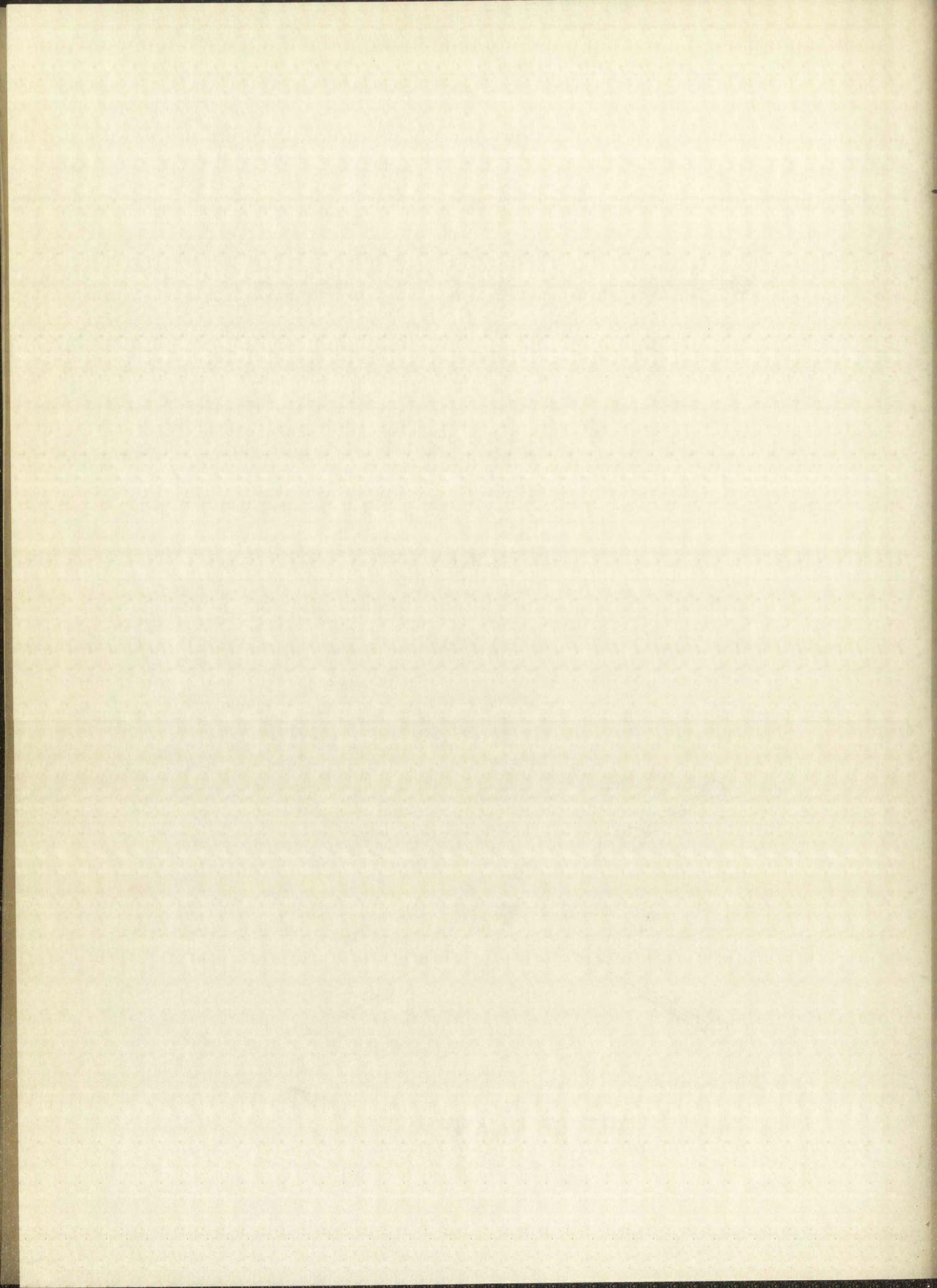


Figure 3.1.3

INTERNAL COORDINATES FOR THE
TETRACYANONICKELATE(II) ION







obtained by multiplying the term $(1 + \cos \theta_R)$ by two less than the number of unshifted atoms, w_R . The quantities, g , ϵ_j , and $(\chi_R)_j^{\gamma}$ are given in Table 3.1.2. The values for $(\chi_R)_j$, as well as the structure of the reduced representation based on equivalent sets of internal coordinates, are tabulated in Table 3.1.3^a.

From Table 3.1.3^a we notice the occurrence of $3A_{1g}$ representations. In Section 3.1.2 we discovered only $2A_{1g}$ representations; hence, the expected redundant coordinate must be of A_{1g} symmetry. Since neither the C-N (r) nor the Ni-C (R) coordinates can be redundant, the redundancy must occur in the C-Ni-C (β) coordinates, as is obvious from Fig. 3.1.3.

TABLE 3.1.3^a

STRUCTURE OF THE REDUCED REPRESENTATION OF THE TETRACYANONICKELATE(II)
ION IN TERMS OF INTERNAL COORDINATES

	E	$2C_4$	C_2	$2C_2$	$2C_2''$	1	$2S_4$	σ_h	$2\sigma_v$	$2\sigma_d$	Structure
r	4	0	0	2	0	0	0	4	2	0	$A_{1g} + B_{1g} + E_u$
R	4	0	0	2	0	0	0	4	2	0	$A_{1g} + B_{1g} + E_u$
β	4	0	0	0	2	0	0	4	0	2	$A_{1g} + B_{2g} + E_u$
α	4	0	0	-2	0	0	0	4	-2	0	$A_{2g} + B_{2g} + E_u$
ϕ	4	0	0	-2	0	0	0	-4	2	0	$A_{2u} + B_{2u} + E_g$
θ	2	0	2	-2	0	-2	0	-2	2	0	$A_{2u} + B_{2u}$

The 21 normal vibrations then may be grouped into nine representations as shown in Table 3.1.3^b.

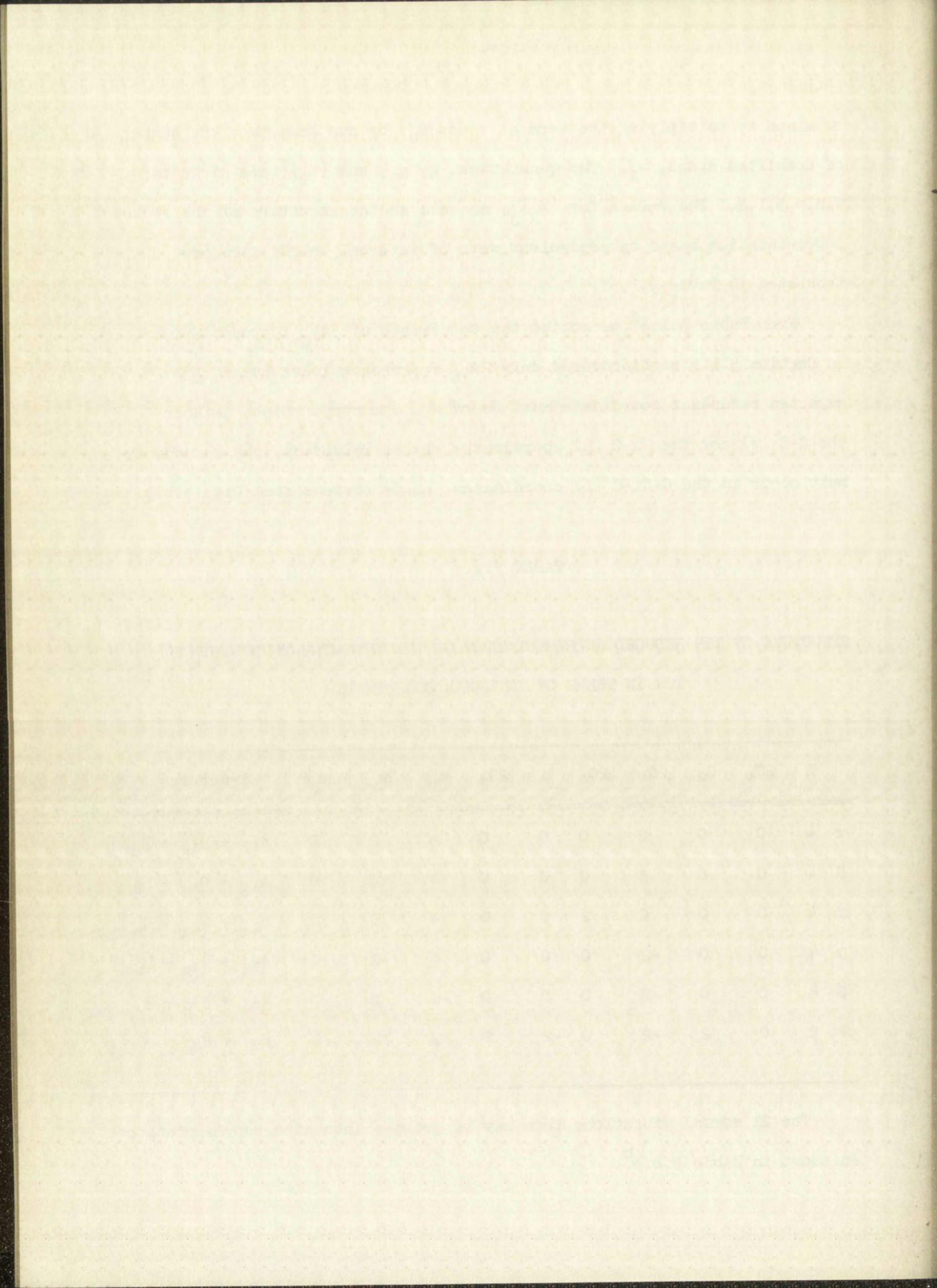
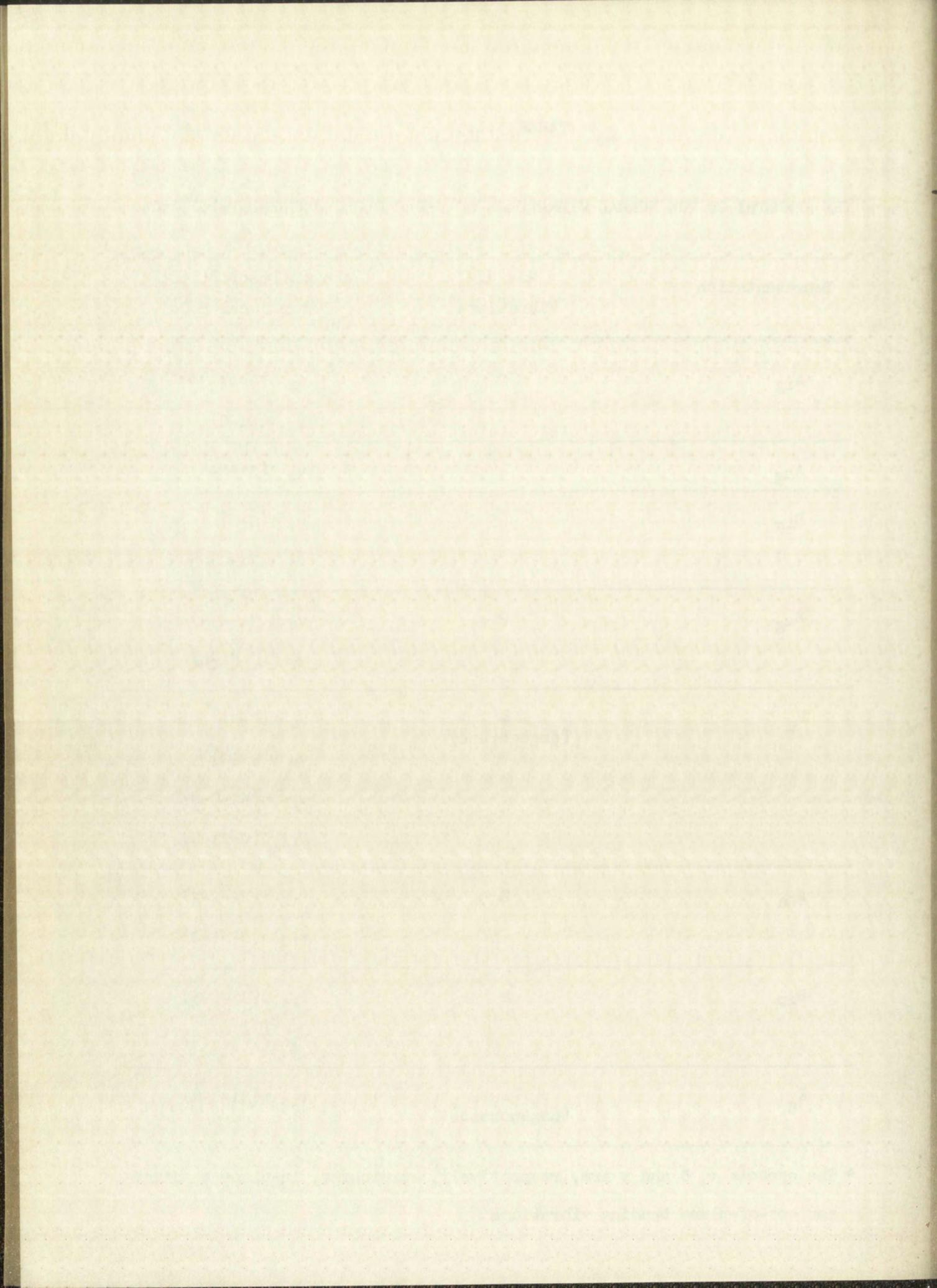


TABLE 3.1.3^b

THE SYMMETRY OF THE NORMAL VIBRATIONS OF THE TETRACYANONICKELATE(II) ION

Representation	No. of Vibrations	Approx. Description of Vibrational Mode*
A_{1g}	2	ν_1 $\nu(\text{C-N})$
		ν_2 $\nu(\text{Ni-C})$
A_{2g}	1	ν_3 $\delta(\text{Ni-C-N})$
B_{1g}	2	ν_4 $\nu(\text{C-N})$
		ν_5 $\nu(\text{Ni-C})$
B_{2g}	2	ν_6 $\delta(\text{Ni-C-N})$
		ν_7 $\delta(\text{C-Ni-C})$
E_u	4 (degenerate)	ν_8 $\nu(\text{C-N})$
		ν_9 $\nu(\text{Ni-C})$
		ν_{10} $\delta(\text{Ni-C-N})$
		ν_{11} $\delta(\text{C-Ni-C})$
A_{2u}	2	ν_{12} $\pi(\text{Ni-C-N})$
		ν_{13} $\pi(\text{C-Ni-C})$
B_{2u}	2	ν_{14} $\pi(\text{Ni-C-N})$
		ν_{15} $\pi(\text{C-Ni-C})$
E_g	1 (degenerate)	ν_{16} $\pi(\text{Ni-C-N})$

* The symbols ν , δ and π are, respectively, stretching, in-plane bending, and out-of-plane bending vibrations.



3.1.4 Internal Symmetry Coordinates: Certain linear combinations of the internal coordinates exist, which, when used as the basis for a representation, factor the secular determinant to the maximum extent possible by symmetry.⁽²⁴⁾ These linear combinations of the internal coordinates are called internal symmetry coordinates.

The nondegenerate symmetry coordinates may be obtained directly from the expression:

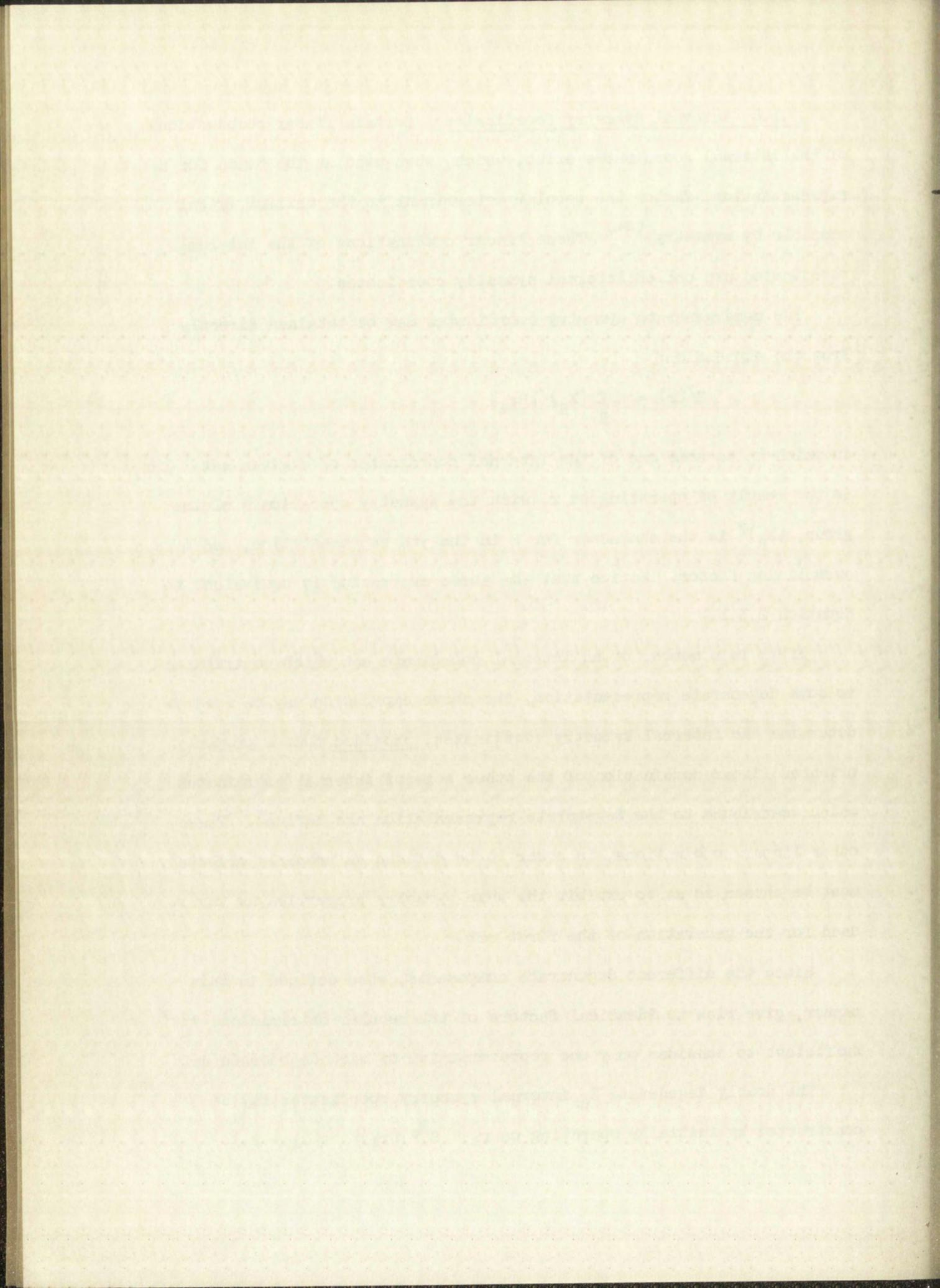
$$S^{\gamma}(r) = \eta \sum_R (\chi_R)^{\gamma} [Rr_l]$$

in which r_l is some one of the internal coordinates of a given set. $[Rr_l]$ is the result of operating on r_l with the symmetry operation R of the group, $(\chi_R)^{\gamma}$ is the character for R in the γ th representation, and η is a normalizing factor. Notice that the above expression is equivalent to Equation 2.3.1.

If r_l is a member of an internal coordinate set which contributes to some degenerate representation, the above expression may be used to determine the internal symmetry coordinates, provided that a properly oriented linear combination of the other sets of internal coordinates which contribute to the degenerate representation are defined. These other linear combinations, in order to be defined as properly oriented, must be chosen so as to exhibit the same symmetry properties as the r_l used for the generation of the first set.

Since the different degenerate components, when defined in this manner, give rise to identical factors of the secular determinant, it is sufficient to consider only one representative of each degenerate set.

The doubly degenerate E_u internal symmetry coordinates may be constructed by initially operating on r_1 : $S^{E_u}(r_1) = \eta(r_1 - r_3)$.



It is seen easily that E , C_2^1 , σ_h , and σ_v leave r_1 invariant. These are the same operations that leave R_1 invariant; hence, $S^{Eu}(R) = \eta(R_1 - R_3)$.

To obtain the coordinate $S^{Eu}(\alpha)$, one cannot operate simply upon α_1 , since α_1 is symmetric with respect to E and σ_h but is not symmetric with respect to C_2^1 and σ_v . However, the linear combination $(\alpha_2 - \alpha_4)$ has the desired property of being invariant under E , C_2^1 , σ_h , and σ_v . Hence one should operate on $(\alpha_2 - \alpha_4)$ to give a properly oriented set: $S^{Eu}(\alpha) = \eta(\alpha_2 - \alpha_4)$.

Likewise, a linear combination of $(\beta_{12} + \beta_{41})$ is invariant under the same E , C_2^1 , σ_h and σ_v operations. Operating on this linear combination yields: $S^{Eu}(\beta) = \eta(\beta_{12} - \beta_{23} - \beta_{34} + \beta_{41})$.

In the case of the degenerate E_g representation, only one internal coordinate contributes to the degenerate species; hence ϕ may be symmetrized directly.

The normalized symmetry coordinates are summarized in Table 3.1.4.

3.1.5 The Factored Kinetic and Potential Energy Matrices: Fig. 3.1.5 defines a set of Cartesian displacement coordinates for the tetracyanonickelate(II) ion. By a detailed comparison of Fig. 3.1.3 and Fig. 3.1.5, one may express the internal coordinates, defined in Section 3.1.3, as a function of Cartesian displacement coordinates. These functions are summarized in Table 3.1.5. Appropriate substitution for the internal coordinates in terms of the functions given in Table 3.1.4 defines the internal symmetry coordinates in terms of Cartesian displacement coordinates. The internal symmetry coordinates, as functions of Cartesian displacement coordinates, are summarized in Table 3.1.6.

We see from Table 3.1.6 that the internal symmetry coordinates, written as a function of Cartesian displacement coordinates, are all of

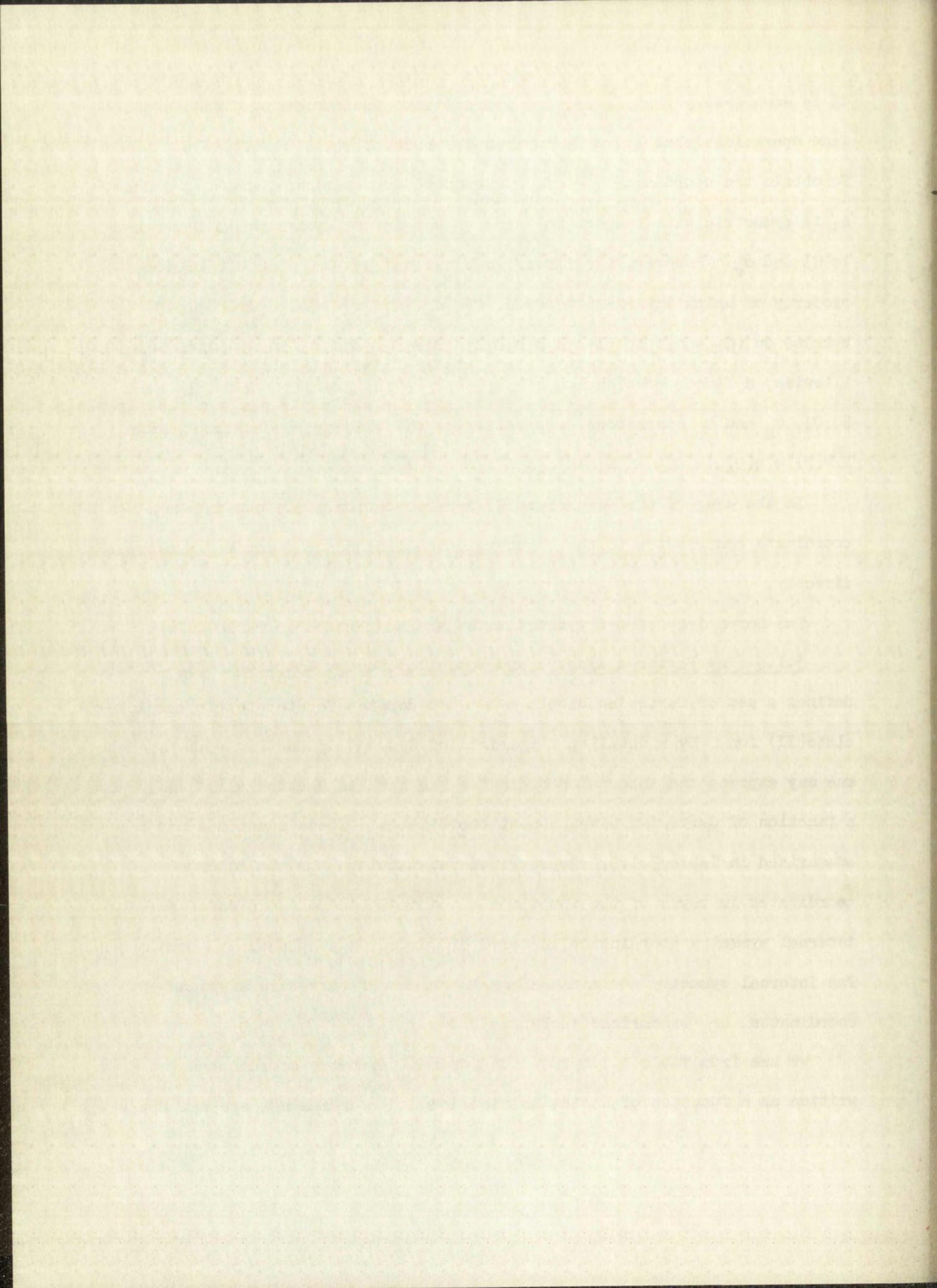


TABLE 3.1.4

THE NORMALIZED INTERNAL SYMMETRY COORDINATES

FOR THE TETRACYANONICKELATE(II) ION

$$S^{A_{1g}}(r) = \frac{1}{2} \Delta(r_1 + r_2 + r_3 + r_4)$$

$$S^{A_{2u}}(\theta) = \frac{1}{\sqrt{2}} \Delta(\theta_1 + \theta_2)$$

$$S^{A_{1g}}(R) = \frac{1}{2} \Delta(R_1 + R_2 + R_3 + R_4)$$

$$S^{A_{2u}}(\phi) = \frac{1}{2} \Delta(\phi_1 + \phi_2 + \phi_3 + \phi_4)$$

$$S^{B_{1g}}(r) = \frac{1}{2} \Delta(r_1 - r_2 + r_3 - r_4)$$

$$S^{B_{2u}}(\theta) = \frac{1}{\sqrt{2}} \Delta(\theta_1 - \theta_2)$$

$$S^{B_{1g}}(R) = \frac{1}{2} \Delta(R_1 - R_2 + R_3 - R_4)$$

$$S^{B_{2u}}(\phi) = \frac{1}{2} \Delta(\phi_1 - \phi_2 + \phi_3 - \phi_4)$$

$$S^{E_u}(r) = \frac{1}{\sqrt{2}} \Delta(r_1 - r_3)$$

$$S^{B_{2g}}(\alpha) = \frac{1}{2} \Delta(\alpha_1 - \alpha_2 + \alpha_3 - \alpha_4)$$

$$S^{E_u}(R) = \frac{1}{\sqrt{2}} \Delta(R_1 - R_3)$$

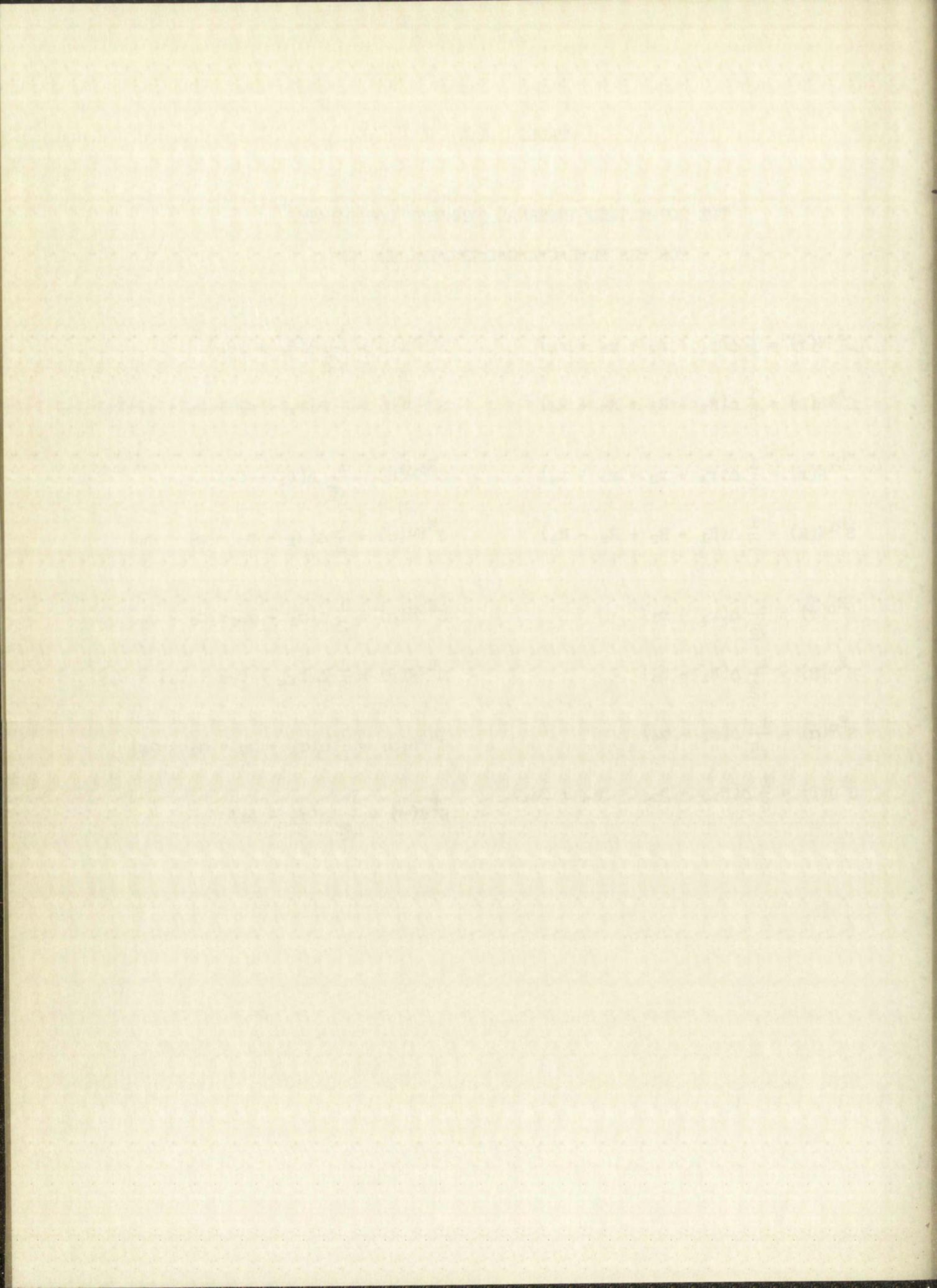
$$S^{B_{2g}}(\beta) = \frac{1}{2} \Delta(\beta_{12} - \beta_{23} + \beta_{34} - \beta_{41})$$

$$S^{E_u}(\alpha) = \frac{1}{\sqrt{2}} \Delta(\alpha_2 - \alpha_4)$$

$$S^{A_{2g}}(\alpha) = \frac{1}{2} \Delta(\alpha_1 + \alpha_2 + \alpha_3 + \alpha_4)$$

$$S^{E_u}(\beta) = \frac{1}{2} \Delta(\beta_{12} - \beta_{23} - \beta_{34} + \beta_{41})$$

$$S^{E_g}(\phi) = \frac{1}{\sqrt{2}} \Delta(\phi_1 - \phi_3)$$



the form: $S^\gamma(r) = \sum_{i=1}^{3N} B^\gamma(r)_i \xi_i$ where the ξ_i are the Cartesian displacement coordinates, and the $B^\gamma(r)_i$ are the linear transformation coefficients.

The $g^\gamma(r;r')$ element of the matrix \underline{g}^γ is defined as⁽¹⁶⁾:

$$g^\gamma(r;r') = \sum_{i=1}^{3N} \mu_i B^\gamma(r)_i B^\gamma(r')_i$$

where μ_i is the reciprocal of the mass of the atom to which the subscript i refers. Hence, from the enumeration of the $B^\gamma(r)_i$ given in Table 3.1.6, one is able to construct the \underline{g} matrices. The $g^\gamma(r;r')$ matrix elements belonging to the matrix \underline{g}^γ are summarized in Table 3.1.7.

The symbols ρ and σ in Table 3.1.7 are the reciprocals of the equilibrium bond length of the C-N (1.15 Å)⁽²⁵⁾ and the Ni-C (1.82 Å)⁽²⁶⁾ bonds, respectively. The in-plane g matrix elements are similar to the g matrix elements reported by Sweeney et.al.⁽²⁷⁾

It has been shown⁽¹⁷⁾ that the rule for getting the potential energy coefficient of the square of the symmetry coordinate is as follows: "Multiply the force constant in the first row and in the column labeled by a given internal coordinate by the coefficient with which that internal coordinate appears in the symmetry coordinate. Then divide by the coefficient of the first internal coordinate (row label). Do this for each column and add the results."

Similarly, it has been shown that the off-diagonal terms are given as follows: "Multiply the force constant in the first row and in the column labeled by a given internal coordinate by the coefficient with which that internal coordinate appears in the symmetry coordinate. Then divide by the coefficient of the first internal coordinate of the other set (row label). Do this for each column and add."

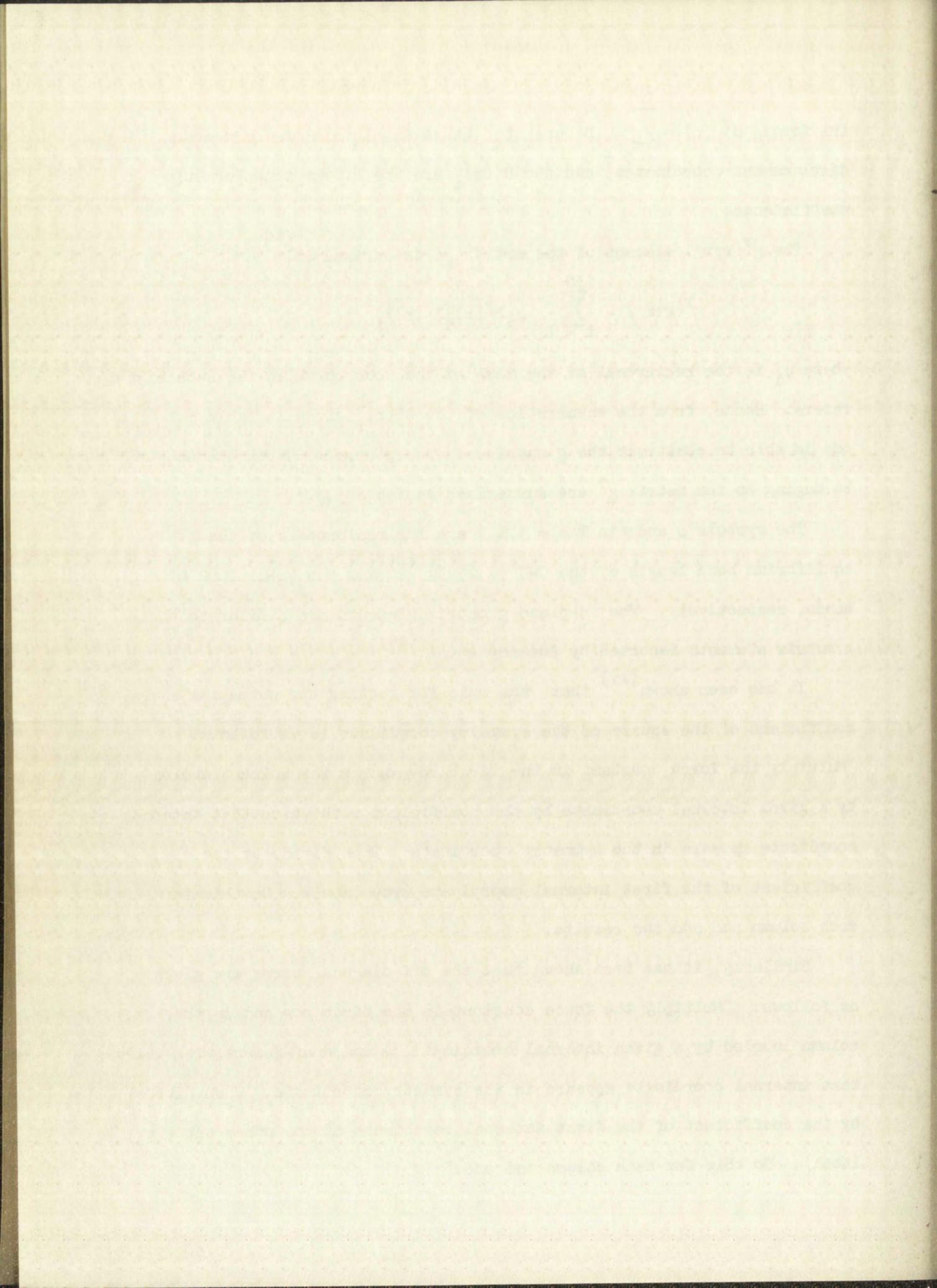
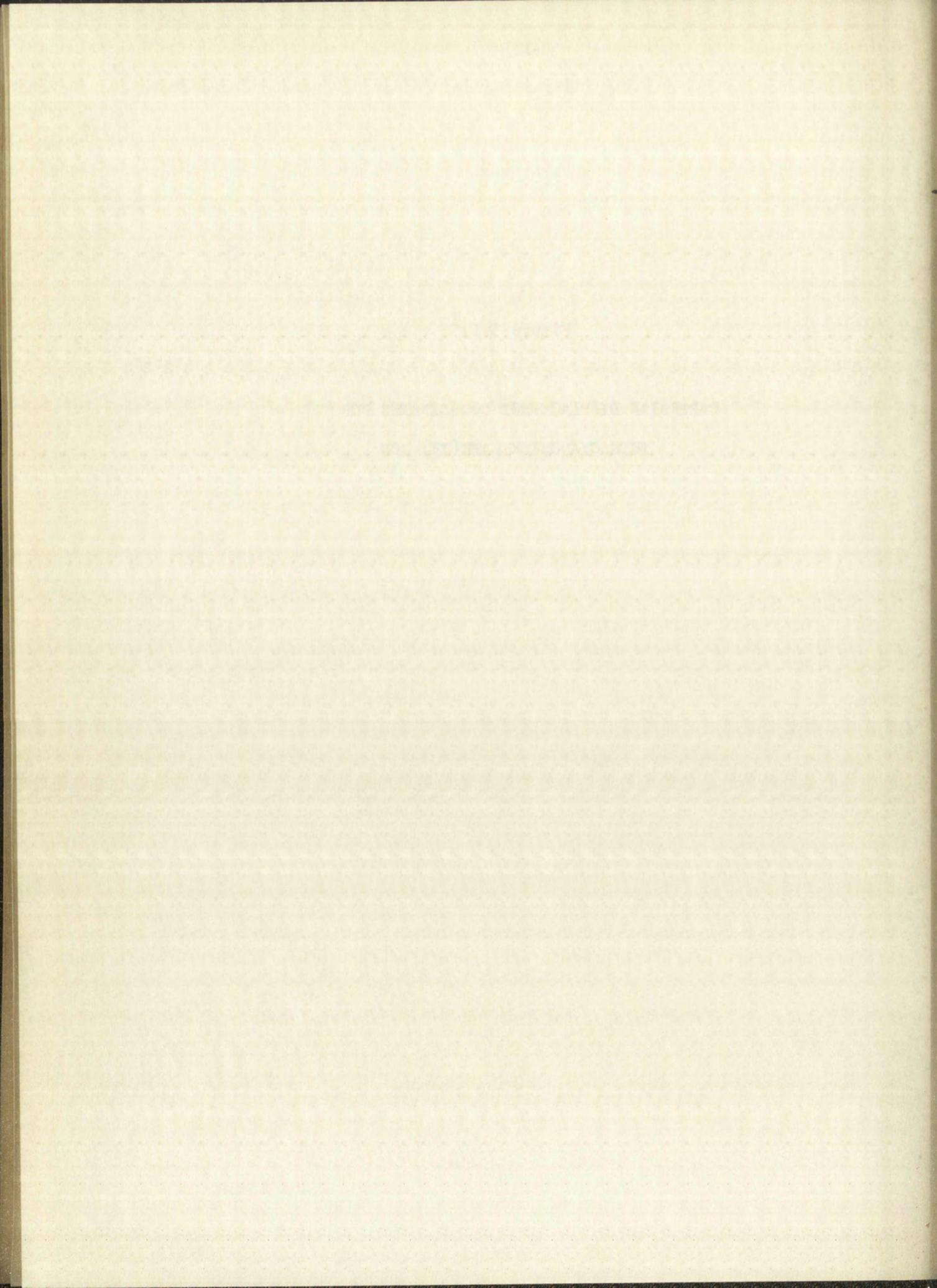
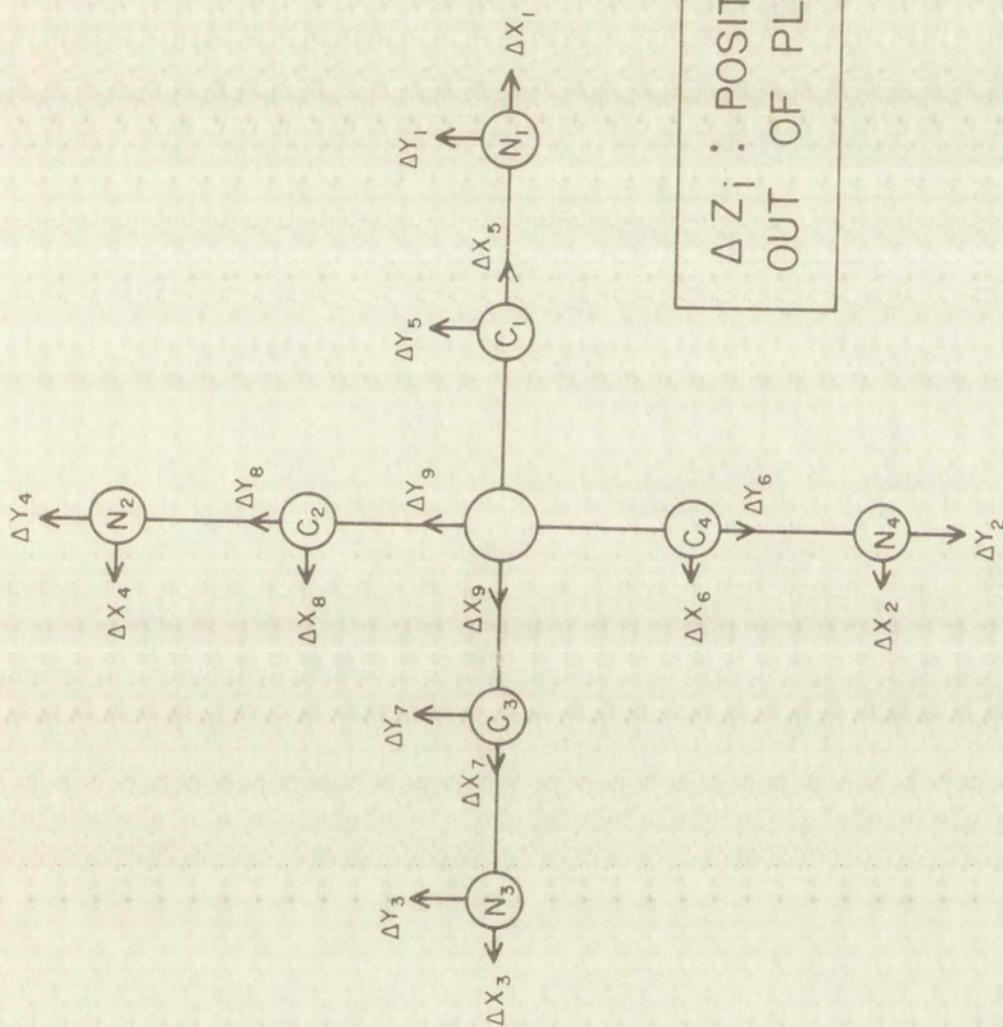


Figure 3.1.5

CARTESIAN DISPLACEMENT COORDINATES FOR THE
TETRACYANONICKELATE(II) ION





ΔZ_i : POSITIVE
OUT OF PLANE

CARTESIAN COORDINATES OF THE TETRACYANONICKELATE
(II) ION

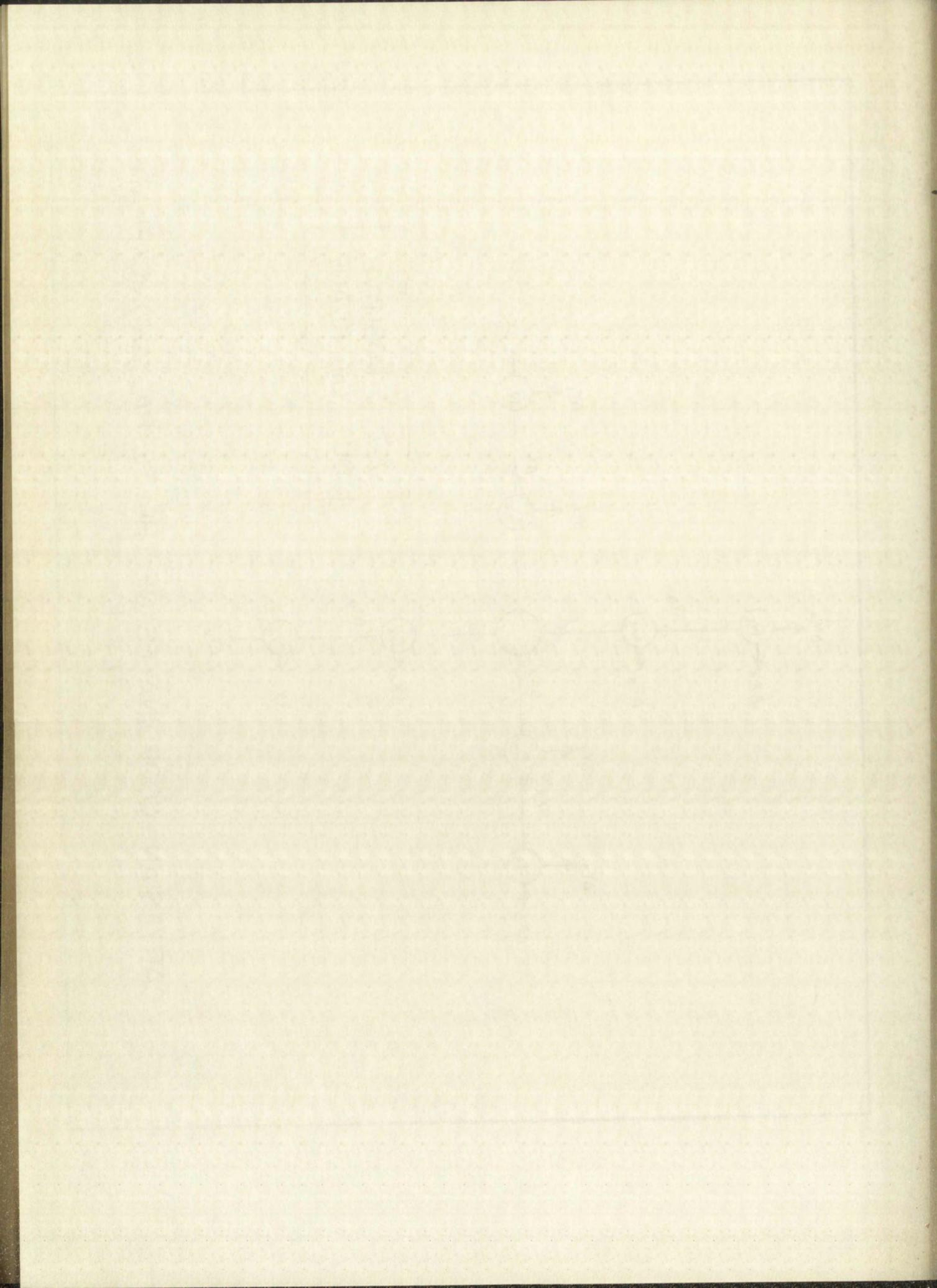


TABLE 3.1.5

INTERNAL COORDINATES AS A FUNCTION OF CARTESIAN DISPLACEMENT COORDINATES

$$\Delta R_1 = \Delta X_5 + \Delta X_9$$

$$\Delta R_2 = \Delta Y_8 - \Delta Y_9$$

$$\Delta R_3 = \Delta X_7 - \Delta X_9$$

$$\Delta R_4 = \Delta Y_6 + \Delta Y_9$$

$$\Delta \alpha_1 = -\sigma \Delta Y_9 + (\sigma + \rho) \Delta Y_5 - \rho \Delta Y_1$$

$$\Delta \alpha_2 = -\sigma \Delta X_9 + (\sigma + \rho) \Delta X_3 - \rho \Delta X_4$$

$$\Delta \alpha_3 = \sigma \Delta Y_9 - (\sigma + \rho) \Delta Y_7 + \rho \Delta Y_3$$

$$\Delta \alpha_4 = \sigma \Delta X_9 - (\sigma + \rho) \Delta X_6 + \rho \Delta X_2$$

$$\Delta r_1 = \Delta X_1 - \Delta X_5$$

$$\Delta r_2 = \Delta Y_4 - \Delta Y_8$$

$$\Delta r_3 = \Delta X_3 - \Delta X_7$$

$$\Delta r_4 = \Delta Y_2 - \Delta Y_6$$

$$\Delta \beta_{12} = \sigma \Delta X_8 + \sigma \Delta Y_9 - \sigma \Delta X_9 - \sigma \Delta Y_5$$

$$\Delta \beta_{23} = -\sigma \Delta Y_7 + \sigma \Delta X_9 + \sigma \Delta Y_9 - \sigma \Delta X_3$$

$$\Delta \beta_{34} = -\sigma \Delta X_6 - \sigma \Delta Y_9 + \sigma \Delta X_9 + \sigma \Delta Y_7$$

$$\Delta \beta_{41} = \sigma \Delta Y_5 - \sigma \Delta X_9 - \sigma \Delta Y_9 + \sigma \Delta X_6$$

$$\Delta \theta_1 = -\sigma \Delta Z_8 + 2\sigma \Delta Z_9 - \sigma \Delta Z_6$$

$$\Delta \theta_2 = -\sigma \Delta Z_7 + 2\sigma \Delta Z_9 - \sigma \Delta Z_5$$

$$\Delta \phi_1 = -\sigma \Delta Z_9 + (\sigma + \rho) \Delta Z_5 - \rho \Delta Z_1$$

$$\Delta \phi_2 = -\sigma \Delta Z_9 + (\sigma + \rho) \Delta Z_3 - \rho \Delta Z_4$$

$$\Delta \phi_3 = -\sigma \Delta Z_9 + (\sigma + \rho) \Delta Z_7 - \rho \Delta Z_8$$

$$\Delta \phi_4 = -\sigma \Delta Z_9 + (\sigma + \rho) \Delta Z_6 - \rho \Delta Z_2$$

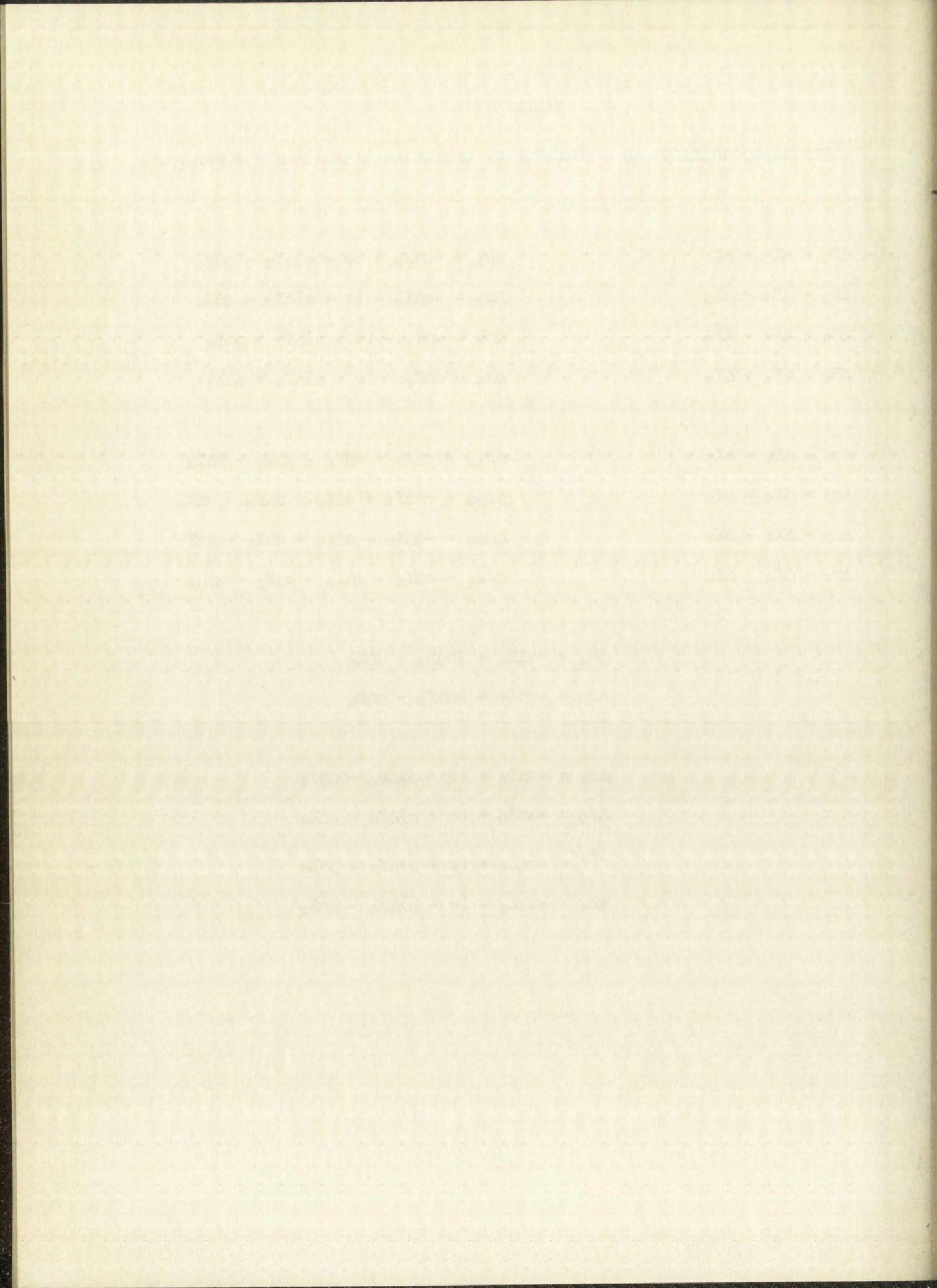


TABLE 3.1.6

INTERNAL SYMMETRY COORDINATES IN TERMS OF CARTESIAN DISPLACEMENT COORDINATES

$$S^{A1g}(r) = \frac{1}{2} \Delta(X_1 + Y_2 + X_3 + Y_4 - X_5 - Y_6 - X_7 - Y_8)$$

$$S^{A1g}(R) = \frac{1}{2} \Delta(X_5 + Y_6 + X_7 + Y_8)$$

$$S^{A2g}(\alpha) = \frac{1}{2} \Delta[\rho(-Y_1 + X_2 + Y_3 - X_4) + (\sigma + \rho)(Y_5 - X_6 - Y_7 + X_8)]$$

$$S^{B1g}(r) = \frac{1}{2} \Delta(X_1 - Y_2 + X_3 - Y_4 - X_5 + Y_6 - X_7 + Y_8)$$

$$S^{B1g}(R) = \frac{1}{2} \Delta(X_5 - Y_6 + X_7 - Y_8)$$

$$S^{B2g}(\alpha) = \frac{1}{2} \Delta[\rho(-Y_1 - X_2 + Y_3 + X_4) + (\sigma + \rho)(Y_5 + X_6 - Y_7 - X_8)]$$

$$S^{B2g}(\beta) = -\sigma \Delta(Y_5 + Y_6 - Y_7 - X_8)$$

$$S^{Eu}(r) = \frac{1}{\sqrt{2}} \Delta(X_1 - X_3 - X_5 + X_7)$$

$$S^{Eu}(R) = \frac{1}{\sqrt{2}} \Delta(X_5 - X_7 + 2X_9)$$

$$S^{Eu}(\alpha) = \frac{1}{\sqrt{2}} \Delta[\rho(-X_2 - X_4) + (\sigma + \rho)(X_6 + X_8) + 2\sigma X_9]$$

$$S^{Eu}(\beta) = \Delta(X_6 + X_8 - 2X_9)$$

$$S^{A2u}(\theta) = \frac{1}{\sqrt{2}} \sigma \Delta(-Z_5 - Z_6 - Z_7 - Z_8 + 4Z_9)$$

$$S^{A2u}(\phi) = \frac{1}{2} \Delta[\rho(-Z_1 - Z_2 - Z_3 - Z_4) + (\sigma + \rho)(Z_5 + Z_6 + Z_7 + Z_8) - 4\sigma Z_9]$$

$$S^{B2u}(\theta) = \frac{1}{\sqrt{2}} \sigma \Delta(Z_5 - Z_6 + Z_7 - Z_8)$$

$$S^{B2u}(\phi) = \frac{1}{2} \Delta[\rho(-Z_1 + Z_2 - Z_3 + Z_4) + (\sigma + \rho)(Z_5 - Z_6 + Z_7 - Z_8)]$$

$$S^{Eg}(\phi) = \frac{1}{\sqrt{2}} \Delta[\rho(-Z_1 + Z_3) + (\sigma + \rho)(Z_5 - Z_7)]$$

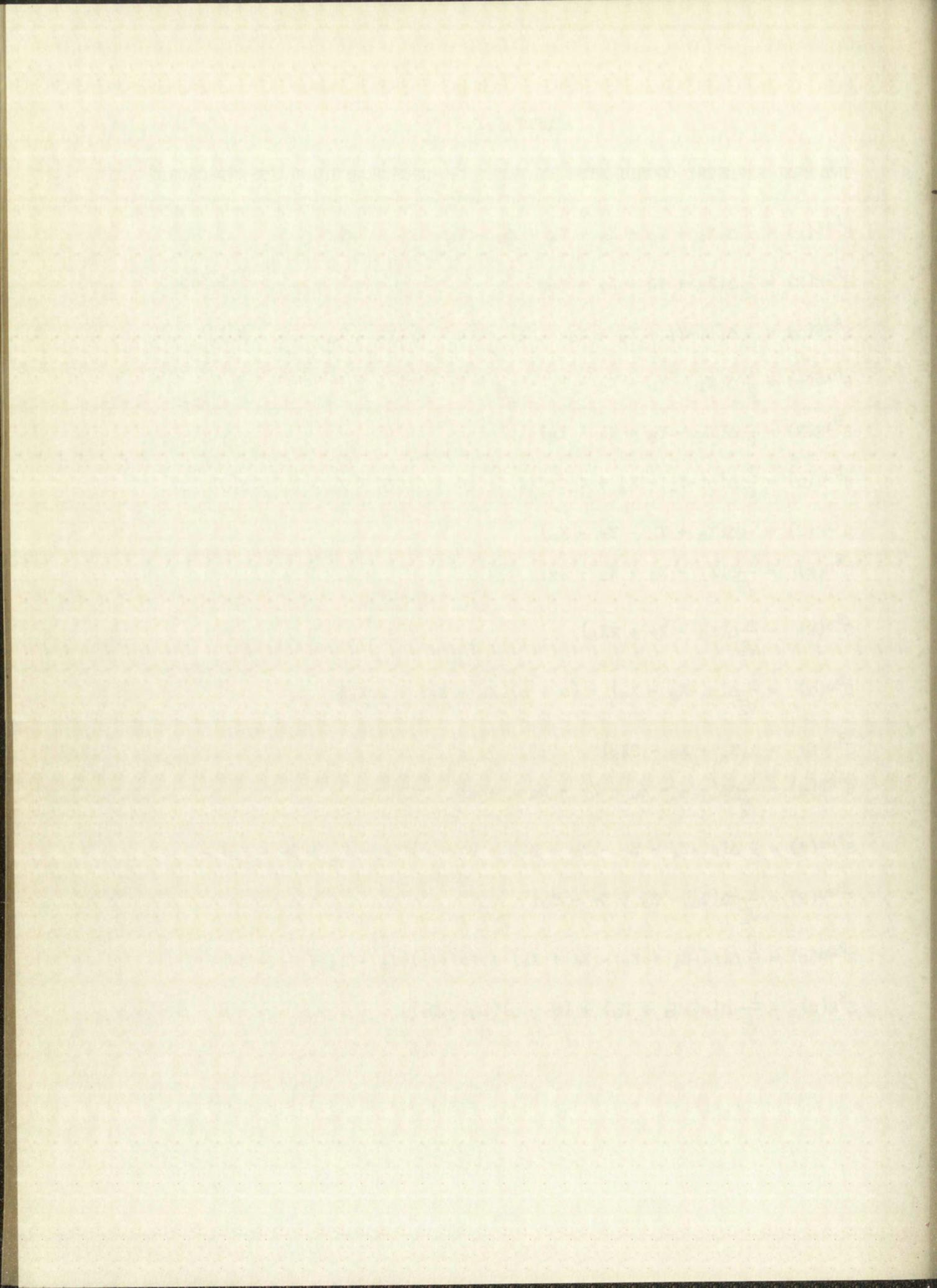


TABLE 3.1.7

THE $g^{\gamma}(r;r')$ MATRIX ELEMENTS

$$g^{A1g}(r;r) = \mu_N + \mu_C$$

$$g^{A1g}(R;R) = \mu_C$$

$$g^{A1g}(r;R) = -\mu_C$$

$$g^{A2g}(\alpha;\alpha) = \rho^2 \mu_N + (\sigma^2 + 2\rho\sigma + \rho^2) \mu_C$$

$$g^{B1g}(r;r) = \mu_N + \mu_C$$

$$g^{B1g}(R;R) = \mu_C$$

$$g^{B1g}(r;R) = -\mu_C$$

$$g^{B2g}(\alpha;\alpha) = \rho^2 \mu_N + (\sigma^2 + 2\rho\sigma + \rho^2) \mu_C$$

$$g^{B2g}(\beta;\beta) = 4\sigma^2 \mu_C$$

$$g^{B2g}(\alpha;\beta) = -2(\sigma^2 + \rho\sigma) \mu_C$$

$$g^{A2u}(\theta;\theta) = 2\sigma^2 \mu_C + 8\sigma^2 \mu_{N1}$$

$$g^{A2u}(\varnothing;\varnothing) = \rho^2 \mu_N + (\sigma^2 + 2\sigma\rho + \rho^2) \mu_C + 4\sigma^2 \mu_{N1}$$

$$g^{A2u}(\theta;\varnothing) = -\sqrt{2} [(\sigma^2 + \sigma\rho) \mu_C + 4\sigma^2 \mu_{N1}]$$

$$g^E g(\varnothing;\varnothing) = \rho^2 \mu_N + (\sigma^2 + 2\sigma\rho + \rho^2) \mu_C$$

$$g^{Eu}(r;r) = \mu_N + \mu_C$$

$$g^{Eu}(R;R) = \mu_C + 2\mu_{N1}$$

$$g^{Eu}(\alpha;\alpha) = \rho^2 \mu_N + (\sigma^2 + 2\rho\sigma + \rho^2) \mu_C + 2\sigma^2 \mu_{N1}$$

$$g^{Eu}(\beta;\beta) = 2\sigma^2 \mu_C + 4\sigma^2 \mu_{N1}$$

$$g^{Eu}(r;R) = -\mu_C$$

$$g^{Eu}(r;\alpha) = 0$$

$$g^{Eu}(r;\beta) = 0$$

$$g^{Eu}(R;\alpha) = -2\sigma \mu_{N1}$$

$$g^{Eu}(R;\beta) = -2\sqrt{2} \sigma \mu_{N1}$$

$$g^{Eu}(\alpha;\beta) = \sqrt{2} [\mu_C(\sigma^2 + \rho\sigma) + 2\sigma^2 \mu_{N1}]$$

$$g^{B2u}(\theta;\theta) = 2\sigma^2 \mu_C$$

$$g^{B2u}(\varnothing;\varnothing) = \rho^2 \mu_N + (\sigma^2 + 2\sigma\rho + \rho^2) \mu_C$$

$$g^{B2u}(\theta;\varnothing) = \sqrt{2} [(\sigma^2 + \sigma\rho) \mu_C]$$

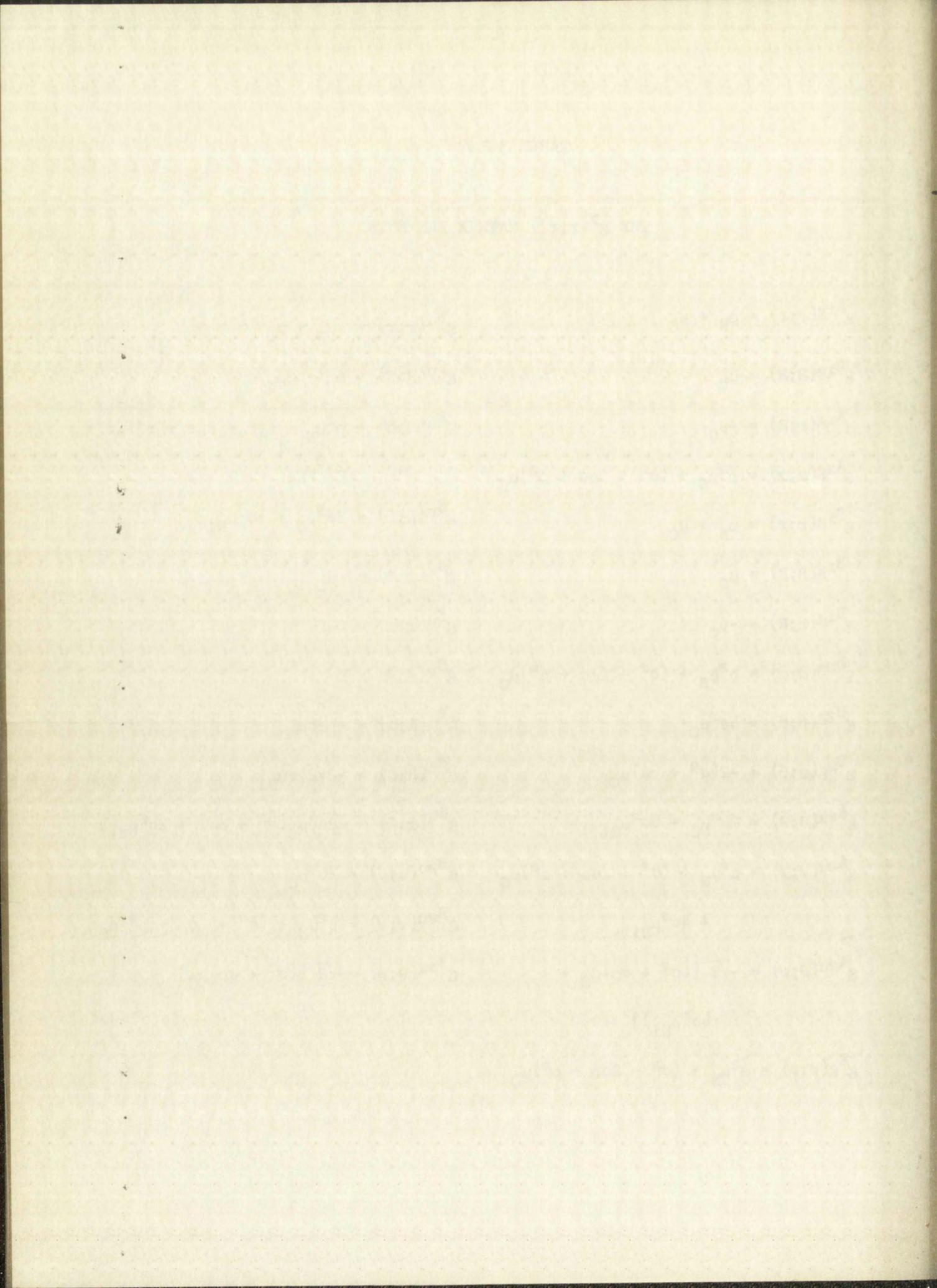
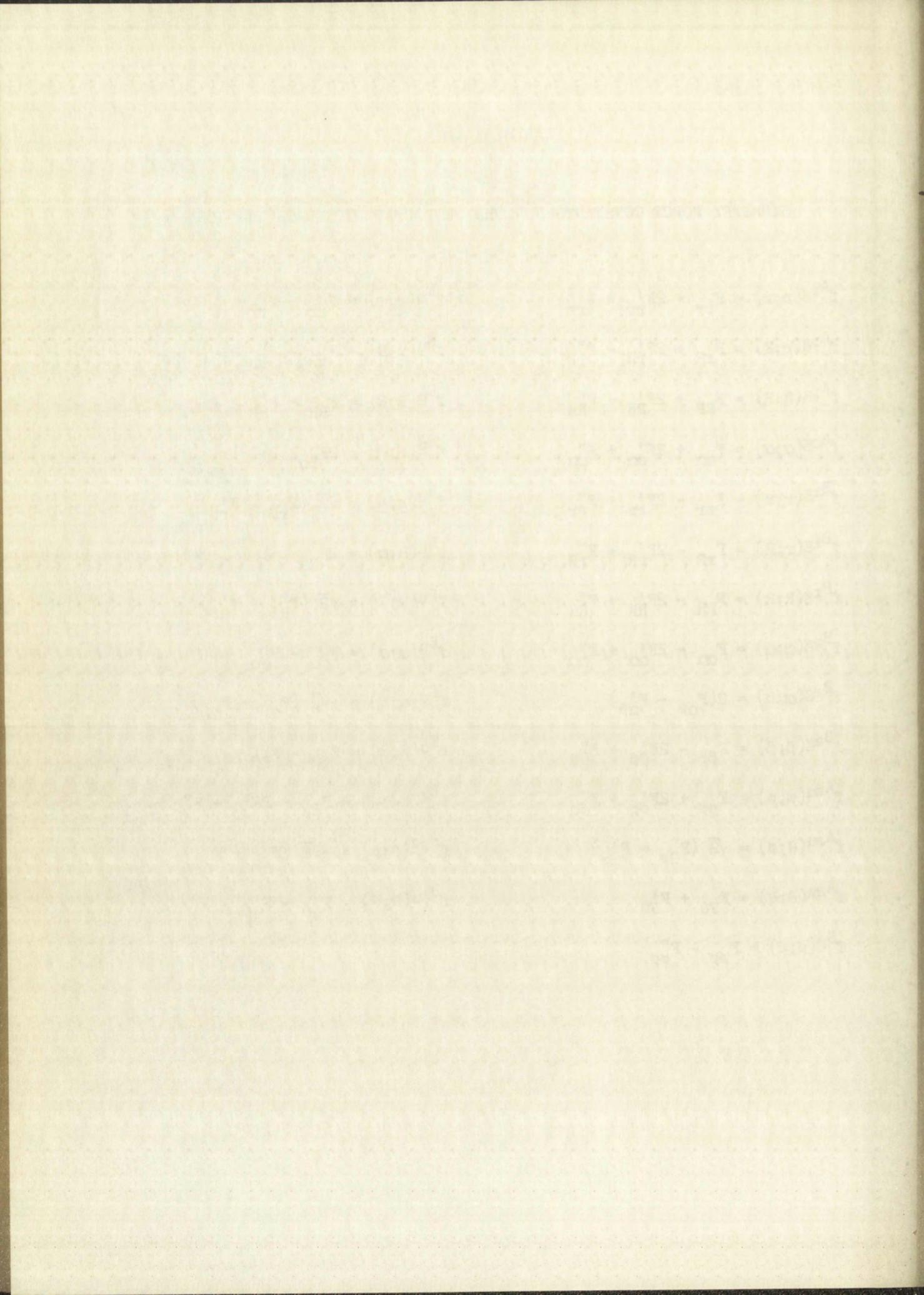


TABLE 3.1.8

SYMMETRY FORCE CONSTANTS FOR THE TETRACYANONICKELATE(II) ION

$$\begin{array}{ll}
 f^{A_{1g}}(r;r) = F_{rr} + 2F'_{rr} + F''_{rr} & f^{E_u}(r;r) = F_{rr} - F''_{rr} \\
 f^{A_{1g}}(r;R) = F_{rR} + 2F'_{rR} + F''_{rR} & f^{E_u}(r;R) = F_{rR} - F''_{rR} \\
 f^{A_{1g}}(R;R) = F_{RR} + 2F'_{RR} + F''_{RR} & f^{E_u}(R;R) = F_{RR} - F''_{RR} \\
 f^{A_{2g}}(\alpha;\alpha) = F_{\alpha\alpha} + 2F'_{\alpha\alpha} + F''_{\alpha\alpha} & f^{E_u}(r;\alpha) = 2F'_{r\alpha} \\
 f^{B_{1g}}(r;r) = F_{rr} - 2F'_{rr} + F''_{rr} & f^{E_u}(r;\beta) = \sqrt{2} (F_{r\beta} - F'_{r\beta}) \\
 f^{B_{1g}}(r;R) = F_{rR} - 2F'_{rR} + F''_{rR} & f^{E_u}(R;\alpha) = 2F'_{R\alpha} \\
 f^{B_{1g}}(R;R) = F_{RR} - 2F'_{RR} + F''_{RR} & f^{E_u}(R;\beta) = \sqrt{2} (F_{R\beta} - F'_{R\beta}) \\
 f^{B_{2g}}(\alpha;\alpha) = F_{\alpha\alpha} - 2F'_{\alpha\alpha} + F''_{\alpha\alpha} & f^{E_u}(\alpha;\alpha) = F_{\alpha\alpha} - F''_{\alpha\alpha} \\
 f^{B_{2g}}(\alpha;\beta) = 2(F_{\alpha\beta} - F'_{\alpha\beta}) & f^{E_u}(\alpha;\beta) = -\sqrt{2} (F_{\alpha\beta} + F'_{\alpha\beta}) \\
 f^{B_{2g}}(\beta;\beta) = F_{\beta\beta} - 2F'_{\beta\beta} + F''_{\beta\beta} & f^{E_u}(\beta;\beta) = F_{\beta\beta} - F''_{\beta\beta} \\
 f^{A_{2u}}(\phi;\phi) = F_{\phi\phi} + 2F'_{\phi\phi} + F''_{\phi\phi} & f^{B_{2u}}(\phi;\phi) = F_{\phi\phi} - 2F'_{\phi\phi} + F''_{\phi\phi} \\
 f^{A_{2u}}(\theta;\phi) = \sqrt{2} (F_{\theta\phi} + F'_{\theta\phi}) & f^{B_{2u}}(\theta;\phi) = -\sqrt{2} (F_{\theta\phi} - F'_{\theta\phi}) \\
 f^{A_{2u}}(\theta;\theta) = F_{\theta\theta} + F'_{\theta\theta} & f^{B_{2u}}(\theta;\theta) = F_{\theta\theta} - F'_{\theta\theta} \\
 f^{E_g}(\phi;\phi) = F_{\phi\phi} - F''_{\phi\phi} &
 \end{array}$$



The application of these rules yields the symmetry force constants summarized in Table 3.1.8. The F_i 's and the F_{ij} 's are valence force constants. The ij subscripts refer to the i th valence coordinate interacting with the j th valence coordinate. The prime and double prime refer to the interaction with an adjacent or opposite valence coordinate, respectively.

3.2 Crystal Symmetry and Selection Rules

X-ray studies have shown that $\text{Na}_2\text{Ni}(\text{CN})_4 \cdot 3\text{H}_2\text{O}$ has the triclinic symmetry of the space group $C_1^{\bar{1}}$ ($P\bar{1}$)⁽²⁰⁾, while $\text{BaNi}(\text{CN})_4 \cdot 4\text{H}_2\text{O}$ has the monoclinic symmetry of the space group C_{2h}^6 ($C2/c$)⁽²⁸⁾. Both of these crystals contain four molecules per unit cell. In the case of the $\text{Na}_2\text{Ni}(\text{CN})_4 \cdot 3\text{H}_2\text{O}$ crystals, the tetracyanonickelate(II) ions and the water molecules are located in general positions of site symmetry C_1 . In the case of the $\text{BaNi}(\text{CN})_4 \cdot 4\text{H}_2\text{O}$ crystals, the water molecules are located in general positions of site symmetry C_1 , but the tetracyanonickelate(II) ions are located on special positions of site symmetry C_1 . The sodium atoms are located on sites of symmetry C_1 , and the barium atoms are located on sites of symmetry C_1 .

The tetracyanonickelate(II) ions are arranged in planes perpendicular, or very nearly perpendicular, to the c axis of the crystal. Hence we expect in-plane modes to absorb radiation polarized perpendicularly to the c axis of the crystal, while the out-of-plane modes should absorb radiation polarized parallel to the c axis of the crystal. The orientation of the water molecules has not been determined by x-ray studies, but the lack of any obvious polarization characteristics indicates that they are neither perpendicular nor parallel to the c axis.

Figures 3.2.1 through 3.2.4 relate the representations of the indicated molecular group, site group, and the point group isomorphic with the factor group of the crystal. The appearance of a T by a representation denotes infrared activity.

From Fig. 3.2.1 it is seen easily that for the triclinic crystal, $\text{Na}_2\text{Ni}(\text{CN})_4 \cdot 3\text{H}_2\text{O}$, all representations of the molecular group for the tetracyanonickelate(II) ion are correlated to an infrared active representation of the factor group; hence, all its molecular frequencies can be infrared active in the triclinic crystal. Similarly, Fig. 3.2.2 shows that only the "u" representations of the molecular group for the tetracyanonickelate(II) ion may be infrared active in the monoclinic crystal, $\text{BaNi}(\text{CN})_4 \cdot 4\text{H}_2\text{O}$. Hence, only fundamental and combination modes of "u" symmetry will be allowed for the monoclinic crystal, but all fundamental and combination modes will be allowed for the triclinic crystal. Thus, one can distinguish many of the "u" vibrations from the "g" vibrations by comparing the spectra of the triclinic and monoclinic salts.

It is apparent from Fig. 3.2.3 and Fig. 3.2.4 that all representations of the molecular group for water may be activity representations for both the triclinic and monoclinic crystals.

3.3 Experimental

Sodium tetracyanonickelate(II) was prepared⁽²⁹⁾ by the precipitation of nickel dicyanide from a nickel nitrate solution and the subsequent dissolution of the nickel dicyanide with a stoichiometric quantity of aqueous sodium cyanide. Recrystallization yielded yellow needle-like

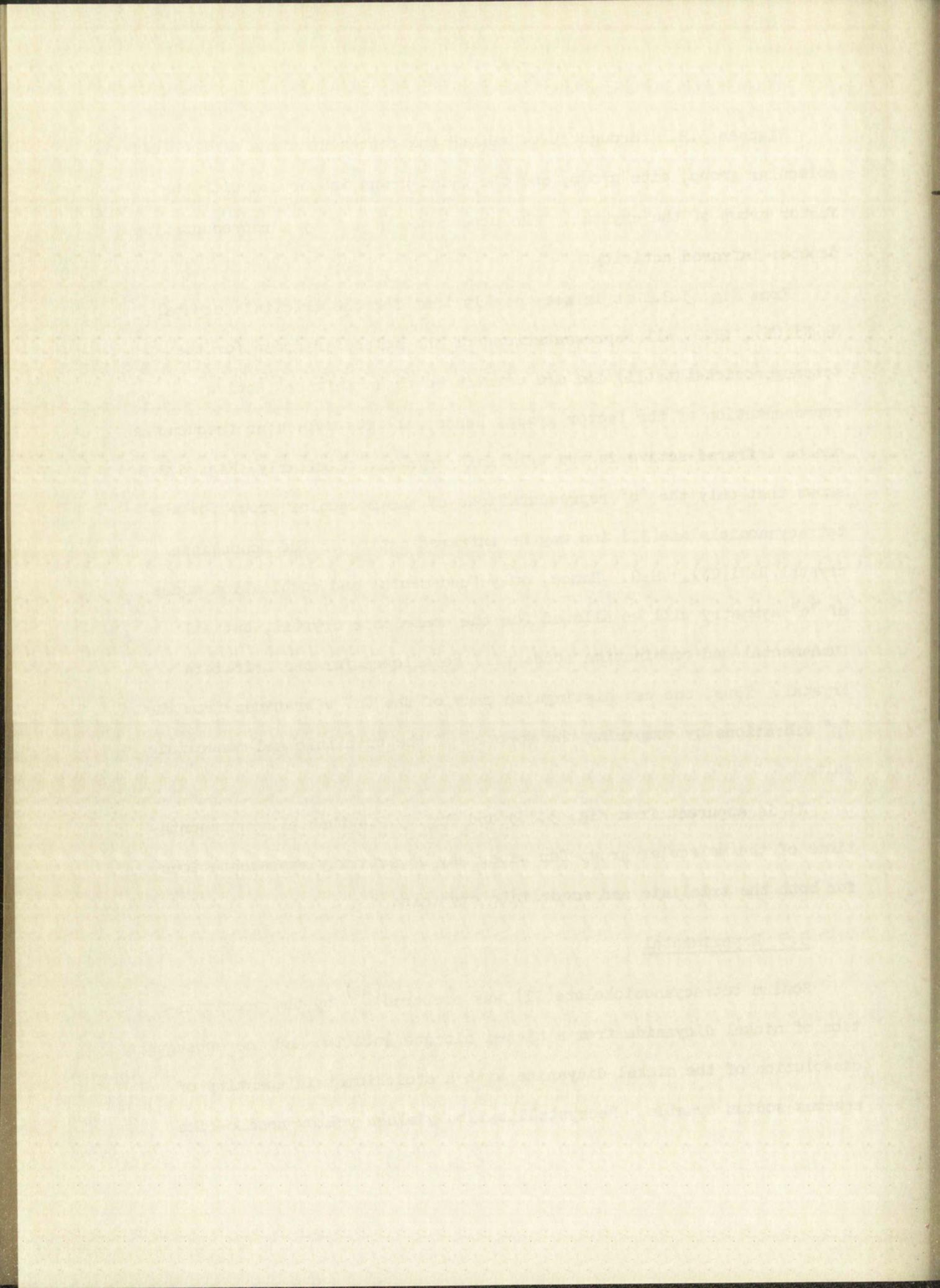
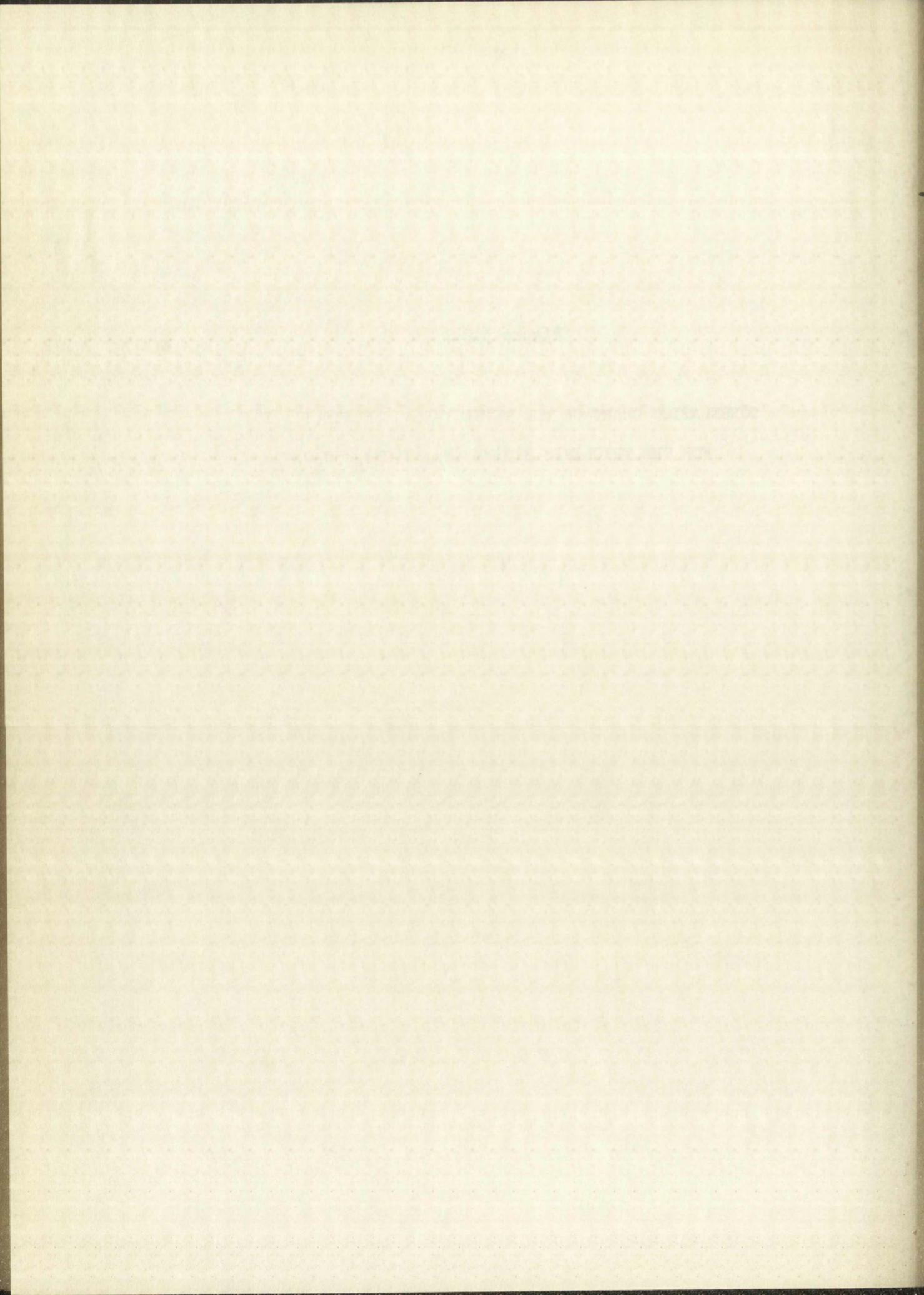
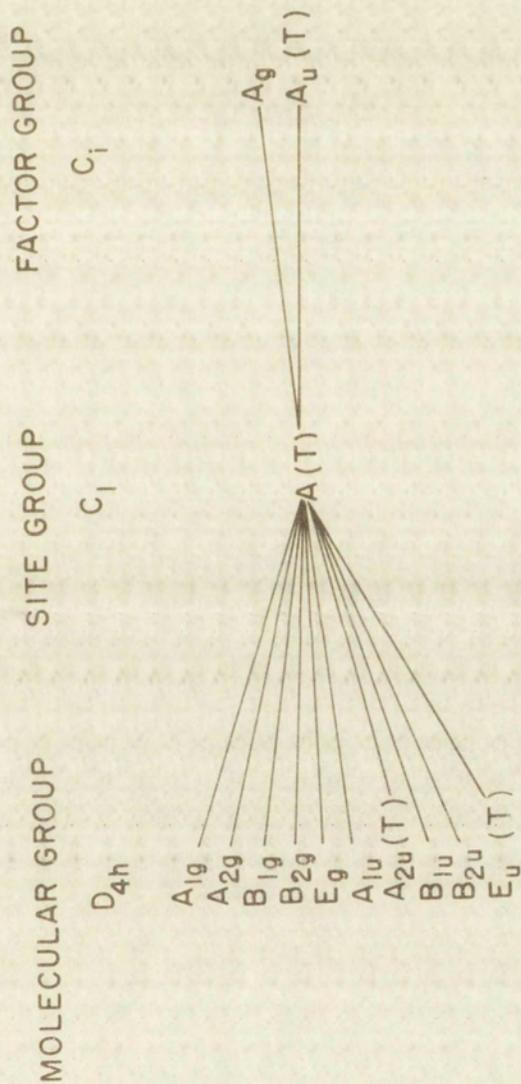


Figure 3.2.1

CORRELATION CHART OF THE TETRACYANONICKELATE(II) ION
FOR THE TRICLINIC SYSTEM ($\text{Na}_2\text{Ni}(\text{CN})_4 \cdot 3\text{H}_2\text{O}$)





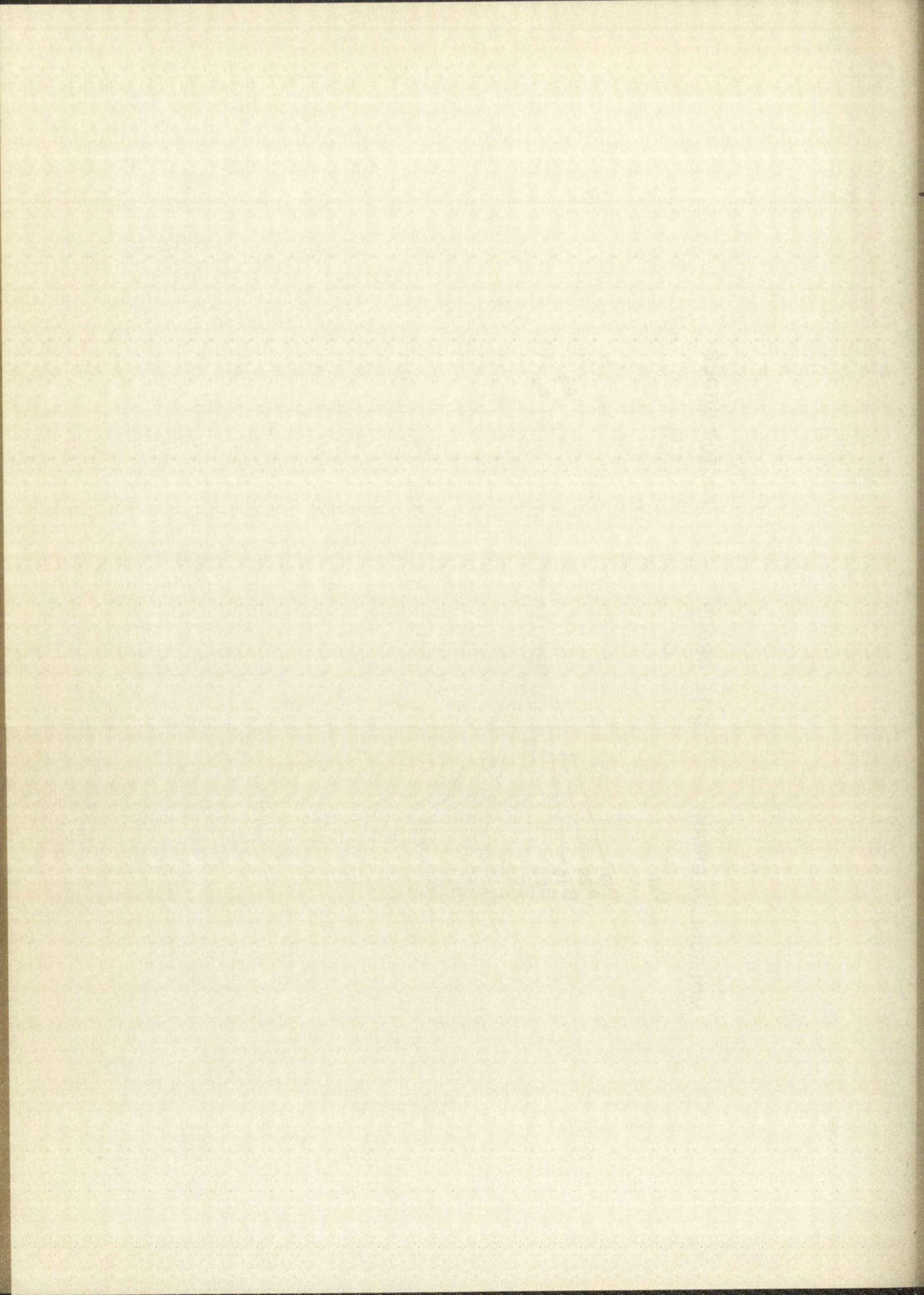
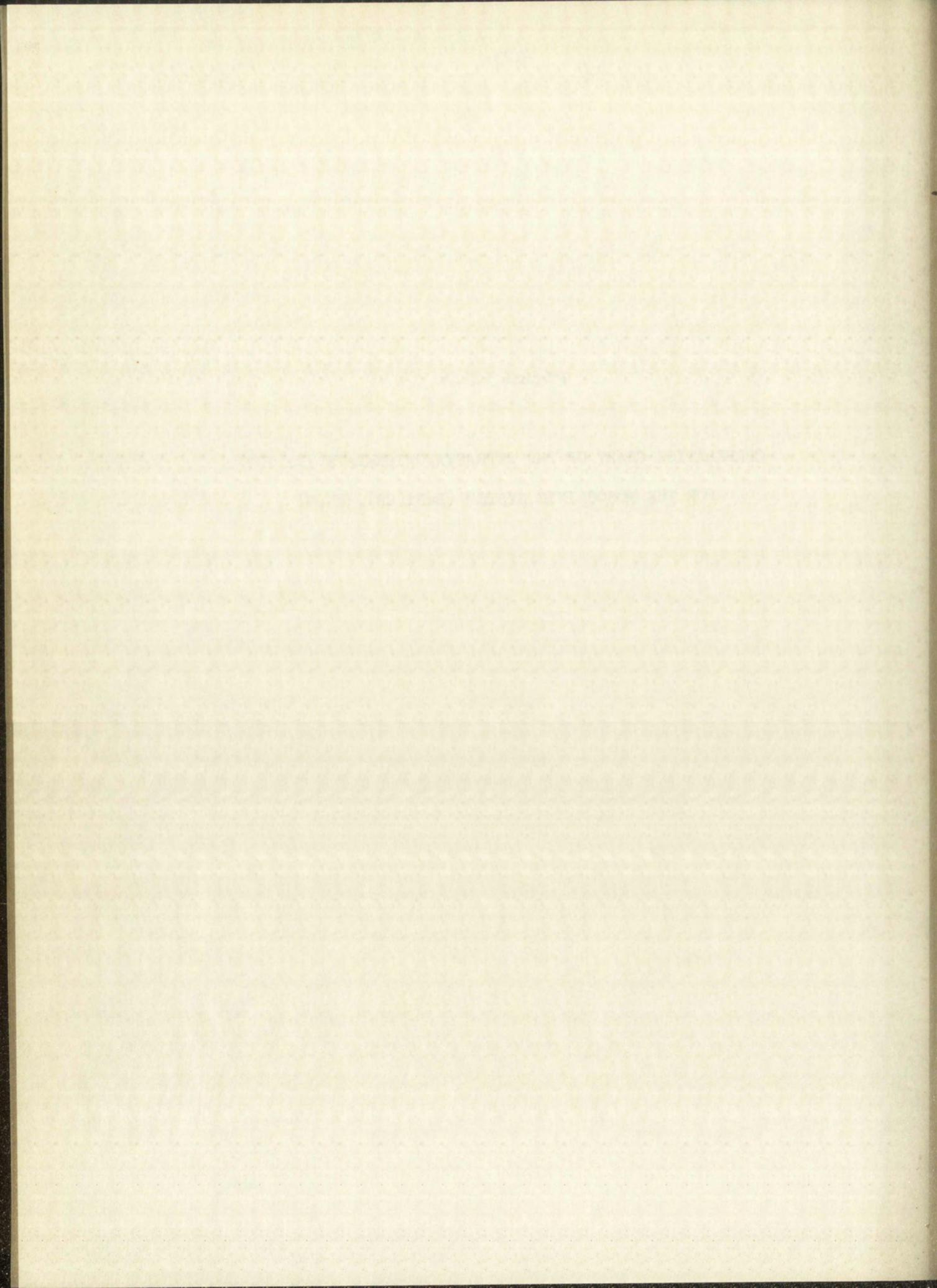
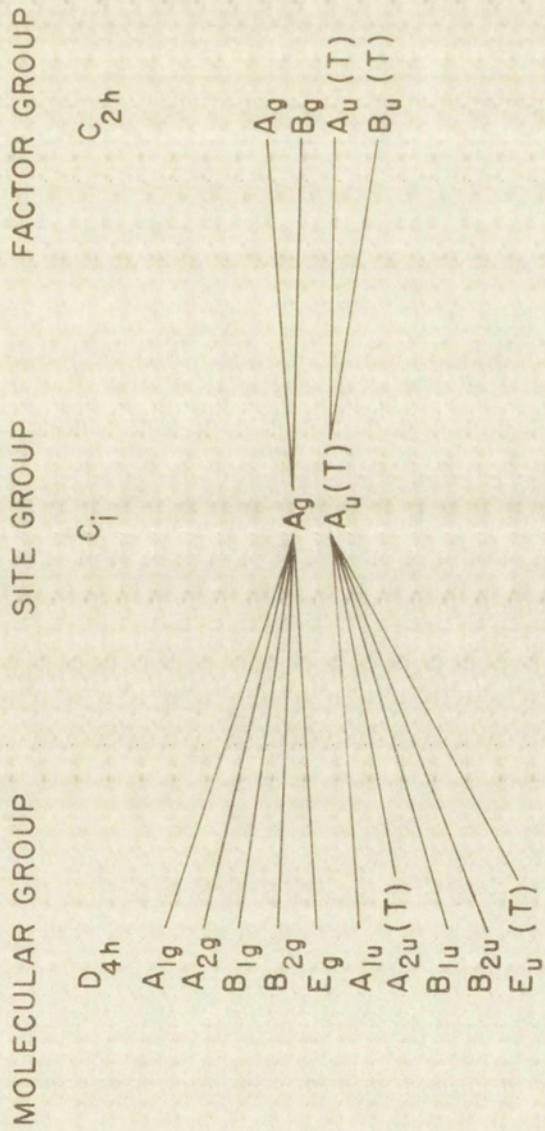


Figure 3.2.2

CORRELATION CHART OF THE TETRACYANONICKELATE(II) ION
FOR THE MONOCLINIC SYSTEM $(\text{BaNi}(\text{CN})_4 \cdot 4\text{H}_2\text{O})$





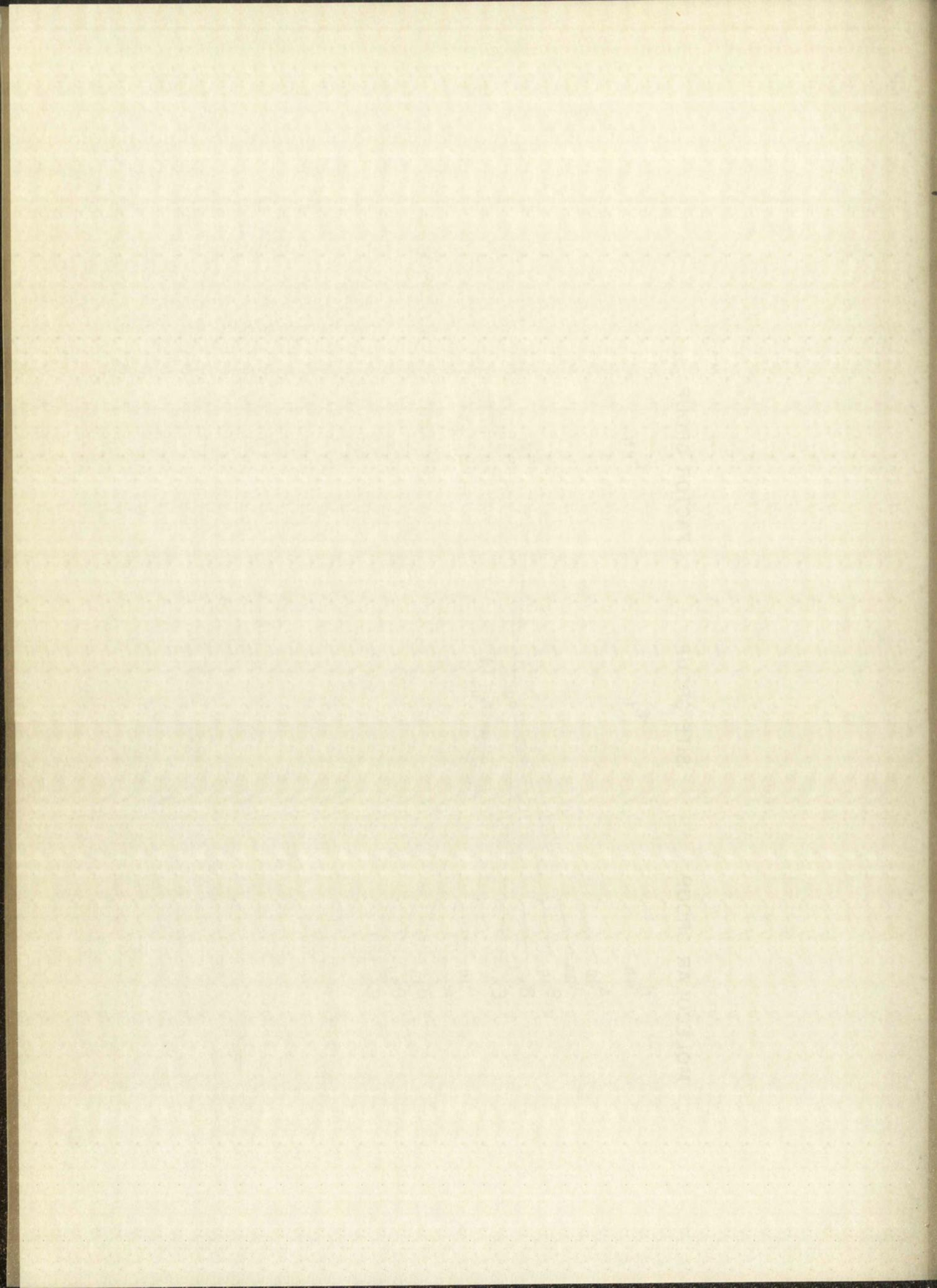
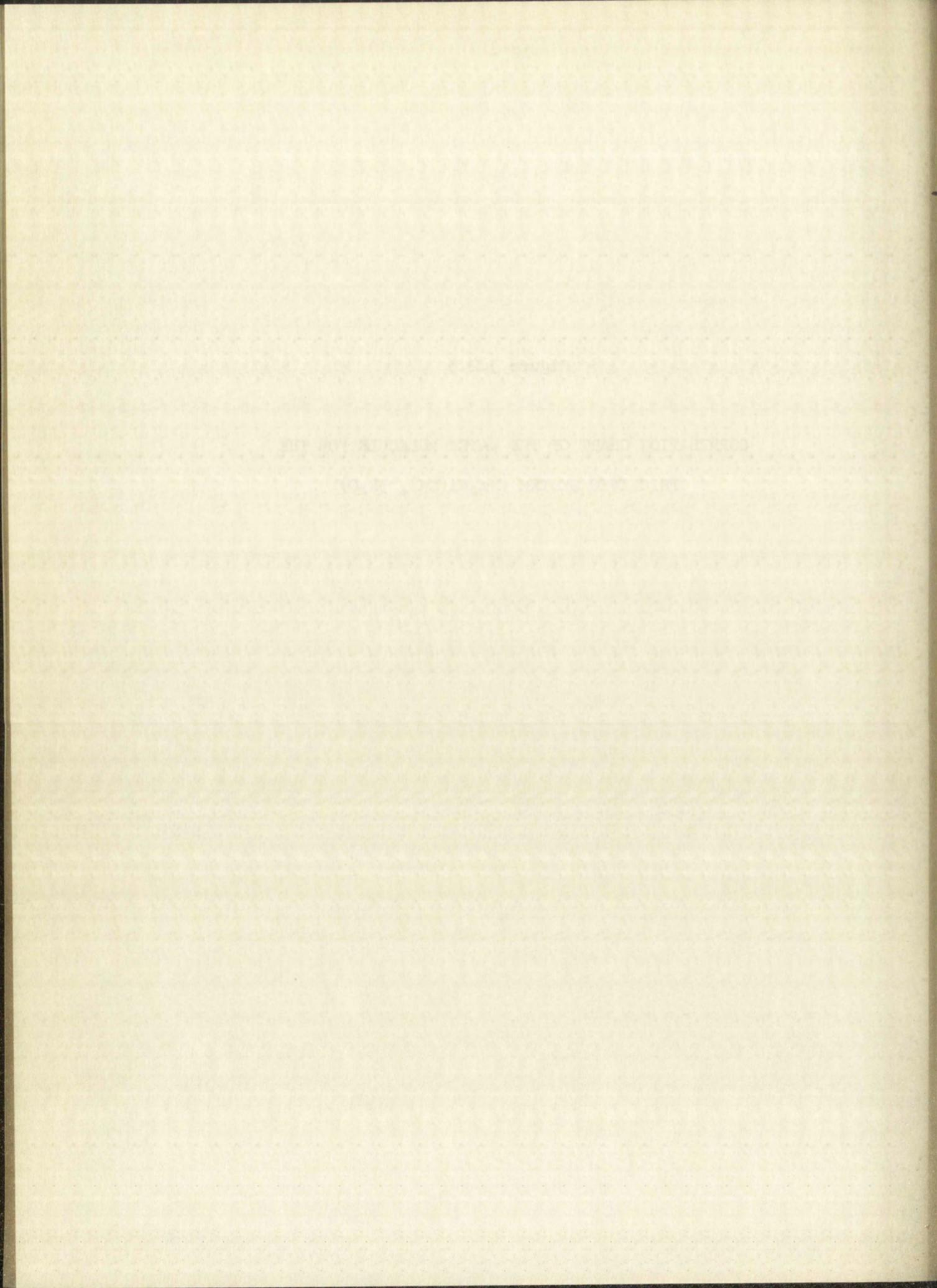


Figure 3.2.3

CORRELATION CHART OF THE WATER MOLECULE FOR THE
TRICLINIC SYSTEM ($\text{Na}_2\text{Ni}(\text{CN})_4 \cdot 3\text{H}_2\text{O}$)



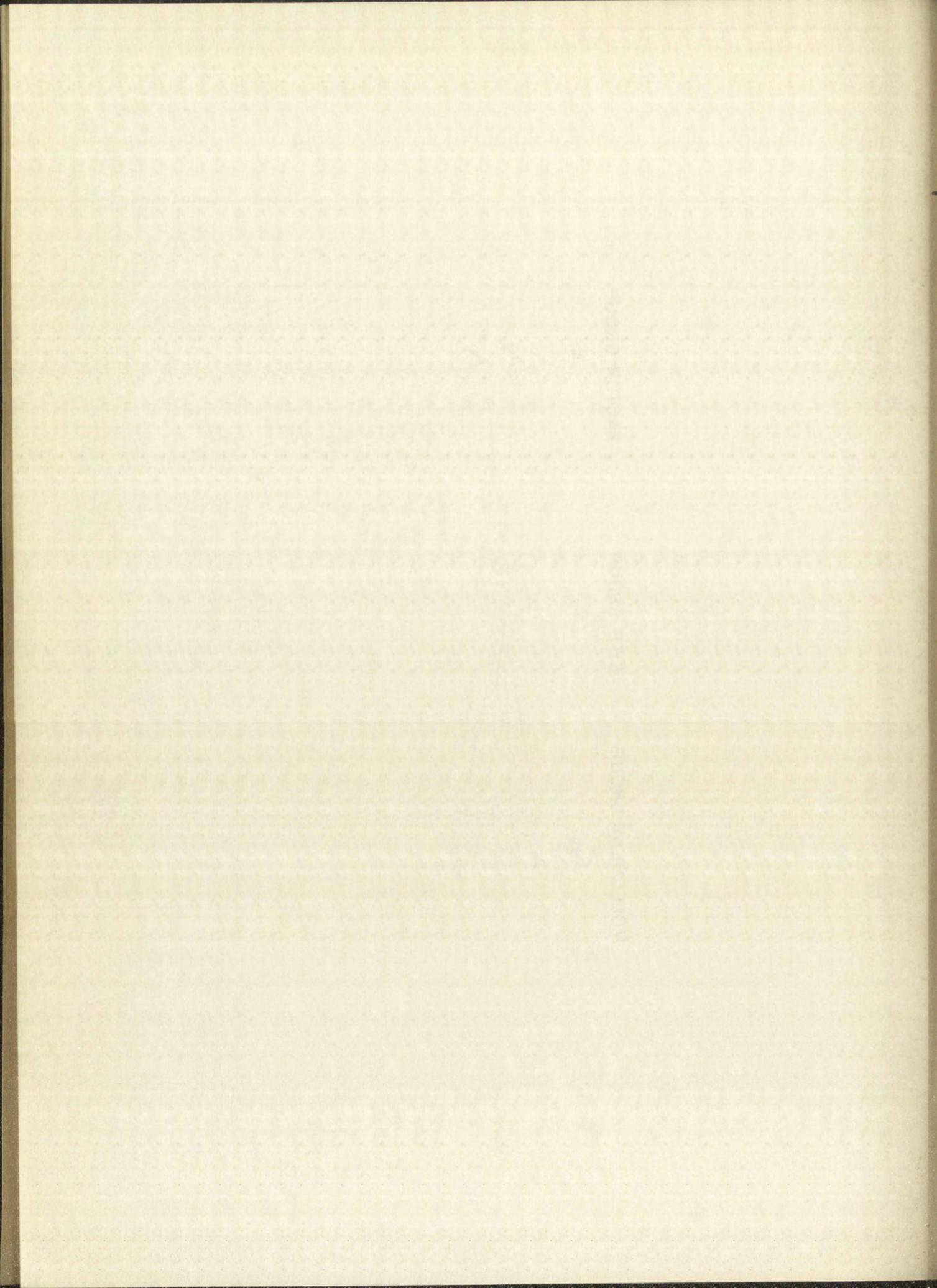
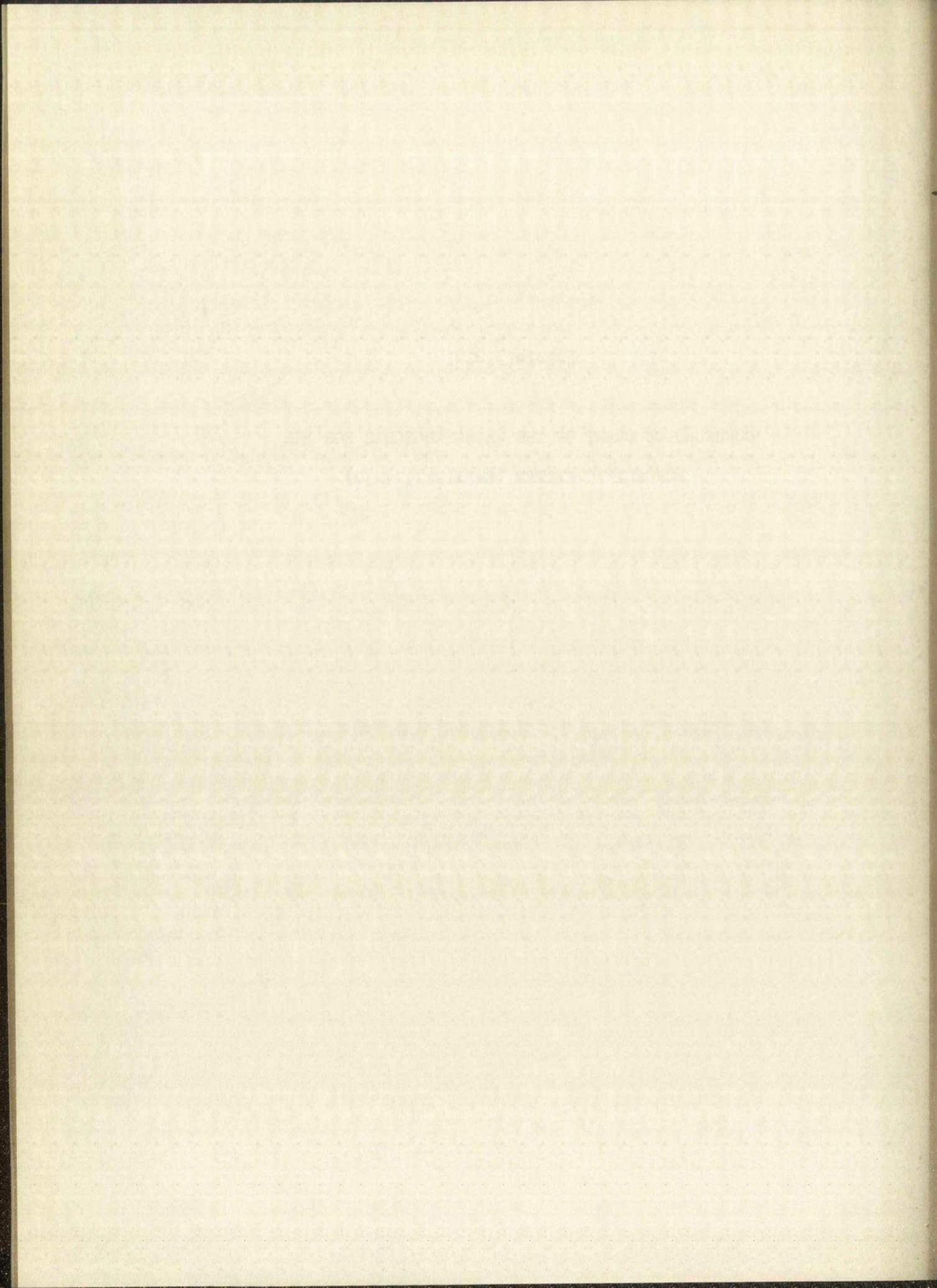
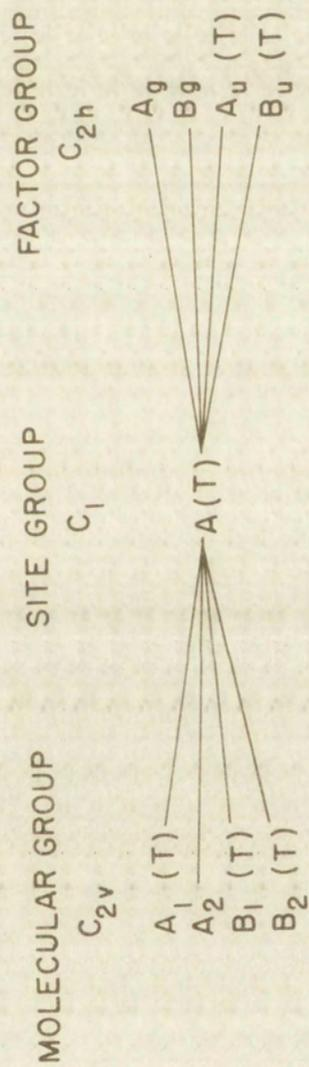
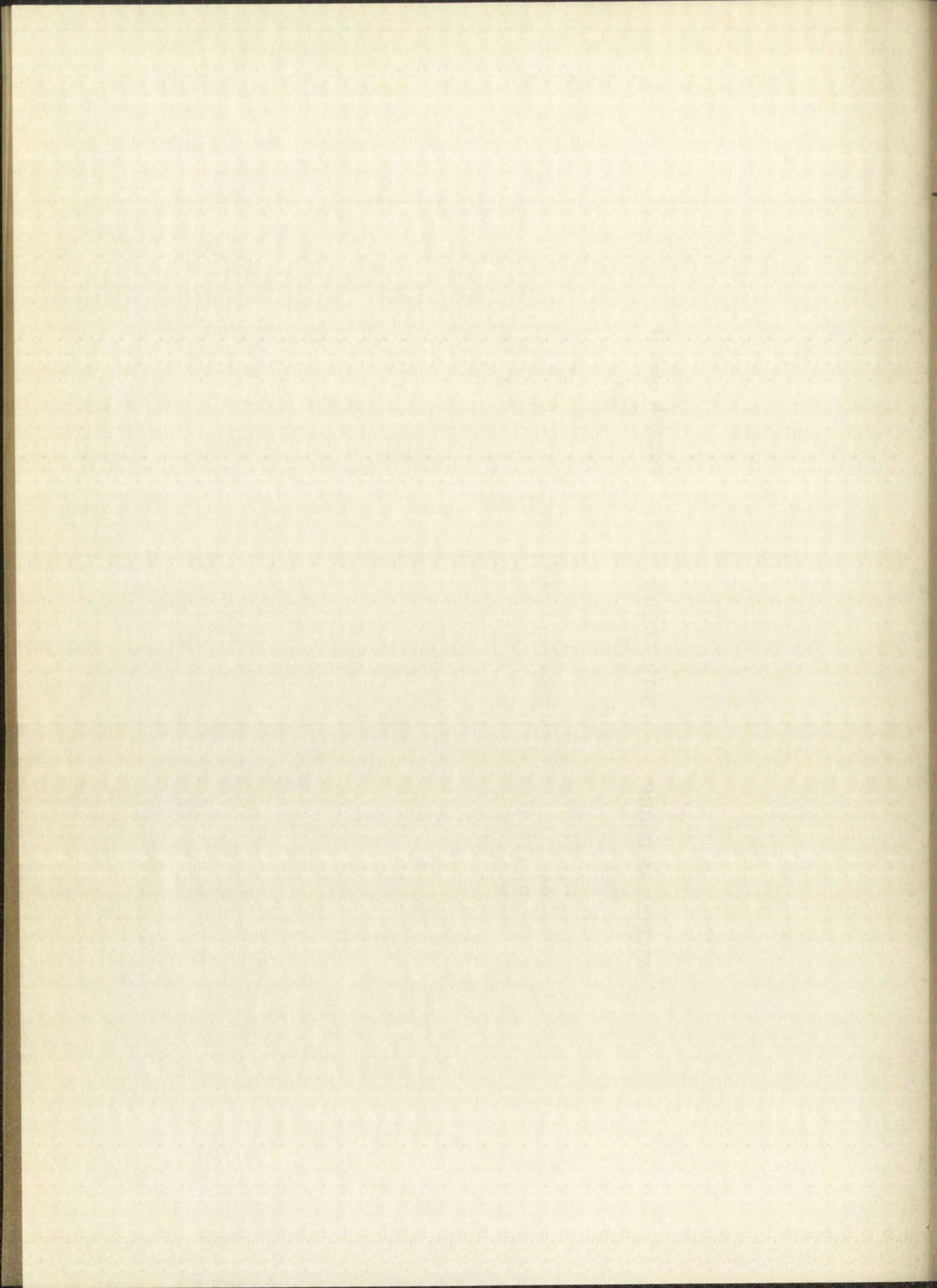


Figure 3.2.4

CORRELATION CHART OF THE WATER MOLECULE FOR THE
MONOCLINIC SYSTEM ($\text{BaNi}(\text{CN})_4 \cdot 4\text{H}_2\text{O}$)







crystals of sodium tetracyanonickelate(II) with three waters of crystallization.

The same procedure was used to prepare $\text{Na}_2\text{Ni}(\text{CN}^{15})_4 \cdot 3\text{H}_2\text{O}$ with the substitution of 95% NaCN^{15} for NaCN .

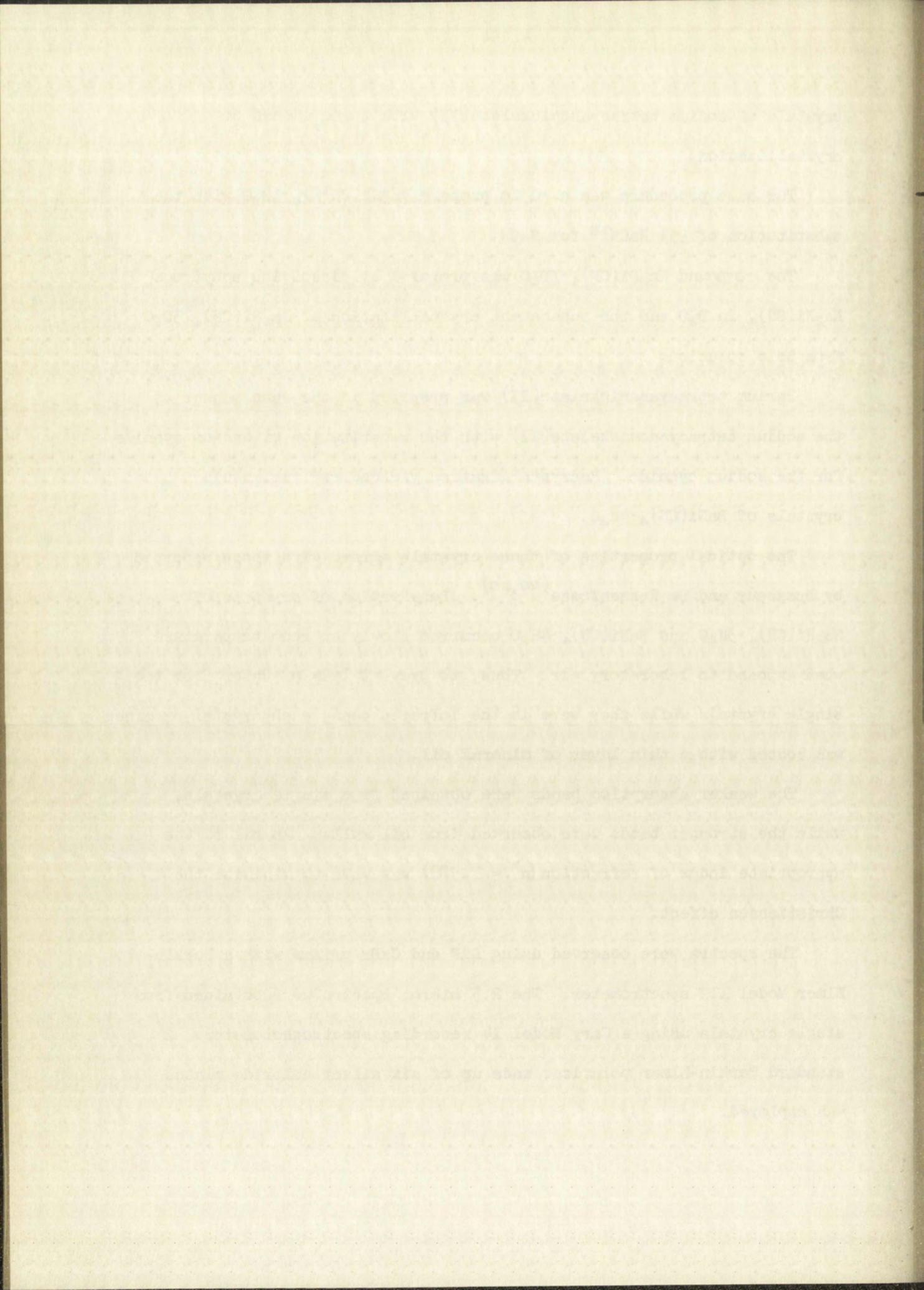
The compound $\text{Na}_2\text{Ni}(\text{CN})_4 \cdot 3\text{D}_2\text{O}$ was prepared by dissolving anhydrous $\text{Na}_2\text{Ni}(\text{CN})_4$ in D_2O and the subsequent crystallization of $\text{Na}_2\text{Ni}(\text{CN})_4 \cdot 3\text{D}_2\text{O}$ from this solution.

Barium tetracyanonickelate(II) was prepared in the same manner as the sodium tetracyanonickelate(II) with the substitution of barium cyanide for the sodium cyanide. Recrystallization yielded red rectangular crystals of $\text{BaNi}(\text{CN})_4 \cdot 4\text{H}_2\text{O}$.

The optical properties of these crystals agreed with those reported by Brasseur and De Rassenfosse^(20,28). Dehydration of crystals of $\text{Na}_2\text{Ni}(\text{CN})_4 \cdot 3\text{H}_2\text{O}$ and $\text{BaNi}(\text{CN})_4 \cdot 4\text{H}_2\text{O}$ occurred slowly at room temperature when exposed to laboratory air. Thus, to prevent loss of water from the single crystals while they were in the infrared beam, each crystal examined was coated with a thin layer of mineral oil.

The weaker absorption bands were obtained from single crystals, while the stronger bands were observed from oil mulls. An oil of the appropriate index of refraction ($n^y = 1.588$) was used to minimize the Christiansen effect.

The spectra were observed using LiF and CsBr prisms with a Perkin-Elmer Model 112 spectrometer. The 2.5 micron spectra were obtained from single crystals using a Cary Model 14 recording spectrophotometer. A standard Perkin-Elmer polarizer made up of six silver chloride plates was employed.

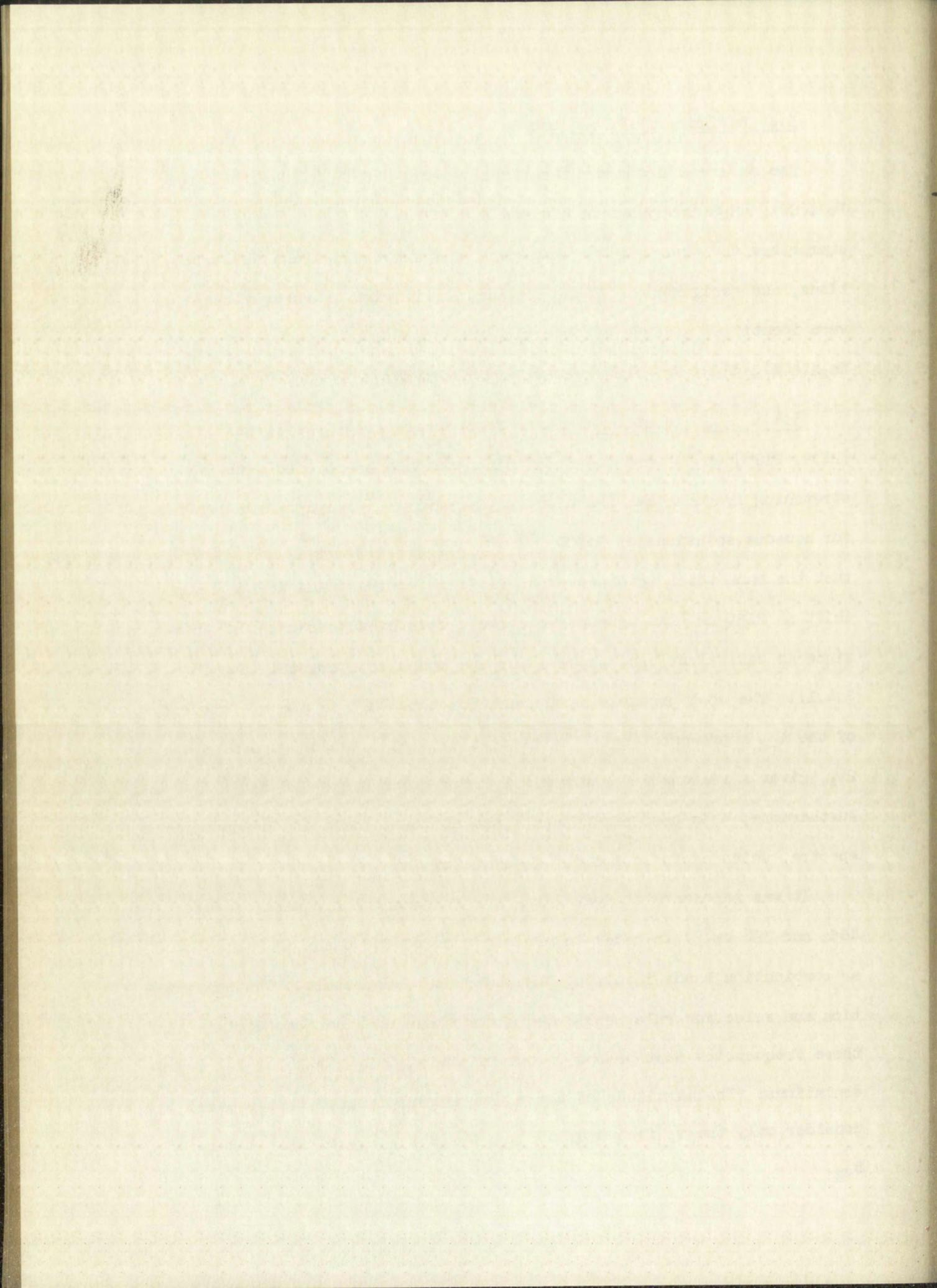


3.4 Assignment of Frequencies

The observed infrared vibrational spectra of $\text{Na}_2\text{Ni}(\text{CN})_4 \cdot 3\text{H}_2\text{O}$ and $\text{BaNi}(\text{CN})_4 \cdot 4\text{H}_2\text{O}$ are given in Figures 3.4.1 through 3.4.4. Table 3.4.0 summarizes the observed frequencies, their representations, polarizations, and assignments. Those frequencies labeled as water vibrations were identified as such by observing the spectra of crystals of $\text{Na}_2\text{Ni}(\text{CN})_4 \cdot 3\text{H}_2\text{O}$, $\text{Na}_2\text{Ni}(\text{CN})_4 \cdot 3\text{D}_2\text{O}$, and $\text{Na}_2\text{Ni}(\text{CN})_4$.

3.4.1 A_{1g} Vibrations: Three frequencies (2149, 2141, and [2132, 2129] cm^{-1}) were observed which could be associated with C-N stretching frequencies. Mathieu and Cornevin⁽³⁰⁾ report Raman shifts for aqueous solutions of $\text{Ni}(\text{CN})_4^{2-}$ at 2159 and 2149 cm^{-1} . We propose that the band which we observed at 2149 cm^{-1} corresponds to the Raman shift at 2159 cm^{-1} in aqueous solution. This band possesses "g" symmetry, since no equivalent band appears for the monoclinic crystal (see Fig. 3.4.1). The most probable assignment for this band is the ν_1 frequency of the A_{1g} representation. The band at 4279 cm^{-1} , which we assign as $2\nu_1$, gives a reasonable anharmonicity correction of $\sim -20 \text{ cm}^{-1}$ ⁽³¹⁾. Furthermore, this band at 4279 cm^{-1} has no counterpart in the monoclinic spectra, which again indicates "g" symmetry.

It was necessary to postulate four fundamental frequencies (488, 416, 405, and 326 cm^{-1}) in order to explain some of the bands in Table 3.4.0 as combination bands involving the observed fundamentals. The polarization and selection rule requirements for these combinations dictate that these frequencies must belong to one of the A_{1g} , B_{1g} , A_{2g} , or B_{2g} representations. The magnitude of these frequencies is such that we need consider only the ν_2 frequency of A_{1g} , ν_5 of B_{1g} , ν_3 of A_{2g} , and ν_6 of B_{2g} .



Since the bands at 2535 and 2455 cm^{-1} were the most intense combination bands which we observed, we conclude that 416 cm^{-1} and 405 cm^{-1} must be associated with Ni-C stretching frequencies (ν_2 and ν_5). In all cyanides studied⁽³¹⁾ the most intense combinations were $\nu_{\text{CN}} \pm \nu_{\text{MC}}$.

By using the low-frequency approximation⁽³²⁾ for the A_{1g} and B_{1g} determinants, we have:

$$\frac{\lambda_2}{\lambda_5} = \frac{f^{A_{1g}}(R;R)}{f^{B_{1g}}(R;R)}$$

Jones has demonstrated that the metal-carbon interaction constants for $\text{Ni}(\text{CO})_4$ are positive⁽³³⁾. Assuming that the metal-carbon force constants for the tetracyanonickelate(II) ion are analogous to the metal-carbon force constants for $\text{Ni}(\text{CO})_4$, we have (from the definitions of $f^{A_{1g}}(R;R)$ and $f^{B_{1g}}(R;R)$ given in Table 3.1.8) the following inequality:

$$\frac{\lambda_2}{\lambda_5} > 1.$$

The assignment of ν_2 as 416 cm^{-1} and ν_5 as 405 cm^{-1} is consistent with this inequality.

3.4.2 B_{1g} Vibrations: We conclude a priori that the band at 2141 cm^{-1} corresponds to the Raman shift at 2149 cm^{-1} as reported by Mathieu and Cornevin⁽³⁰⁾. This band possesses "g" symmetry, since no equivalent band appears for the monoclinic crystal. The most probable assignment for this band is the ν_4 fundamental of B_{1g} symmetry.

The appearance of a band at 2535 cm^{-1} possessing in-plane polarization character in the triclinic crystal, and the appearance of a similar band for the monoclinic crystal, may be explained by the combination of a band of 405 cm^{-1} with ν_8 . The arguments presented in Section 3.4.1 lead to the conclusion that this is the ν_5 fundamental of B_{1g} symmetry.

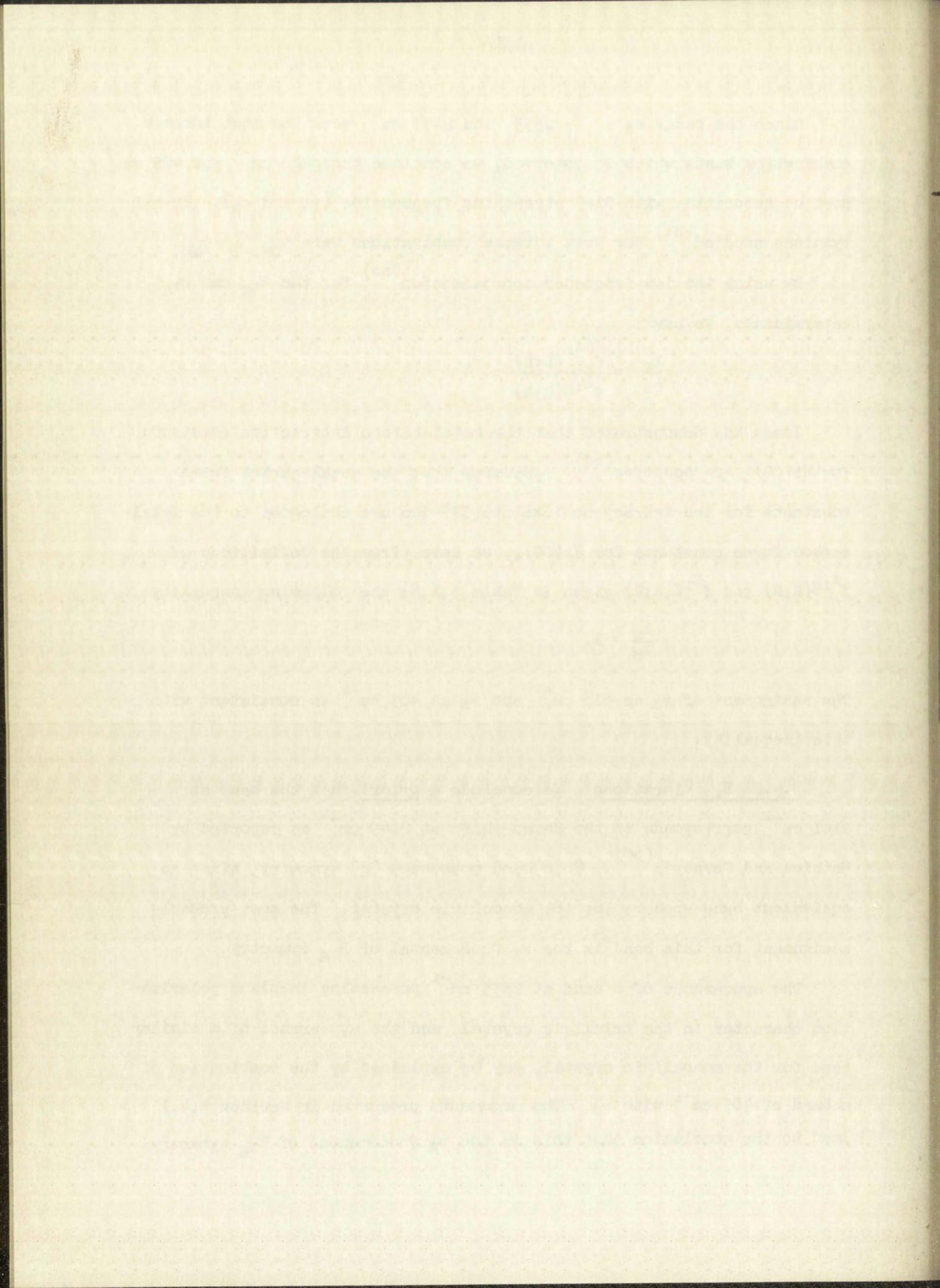
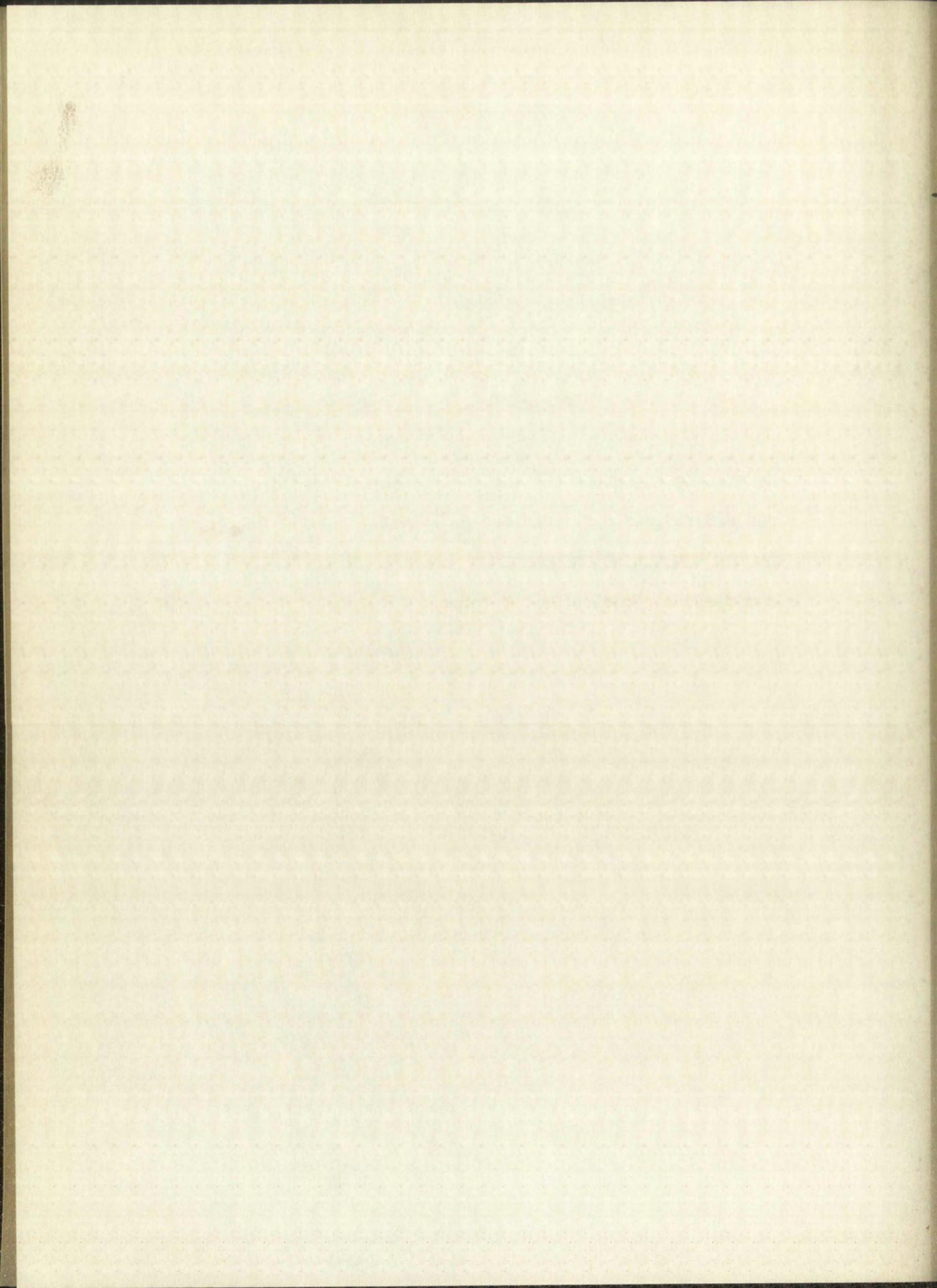
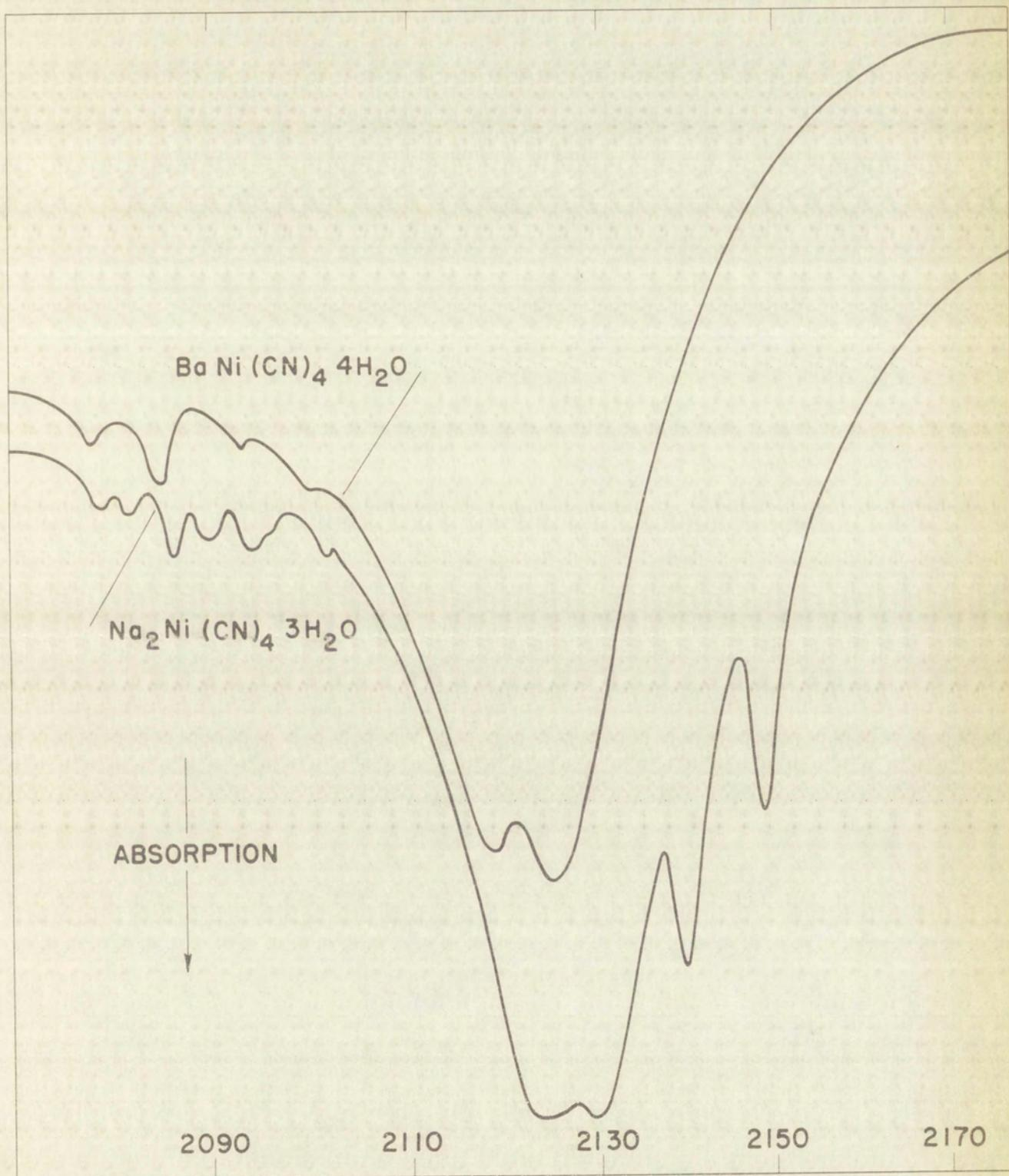


Figure 3.4.1

SPECTRUM OF OIL MULLS ($n^{\gamma} = 1.588$) OF $\text{Na}_2\text{Ni}(\text{CN})_4 \cdot 3\text{H}_2\text{O}$
AND $\text{BaNi}(\text{CN})_4 \cdot 4\text{H}_2\text{O}$ IN THE 2000 cm^{-1} REGION SHOWING THE
CYANIDE STRETCHING FREQUENCIES. Abscissa in cm^{-1} .
(Perkin-Elmer Model 112--LiF Prism)





Be W. 1000

HEMLOCK, B.C.

ABSTRACT

1905

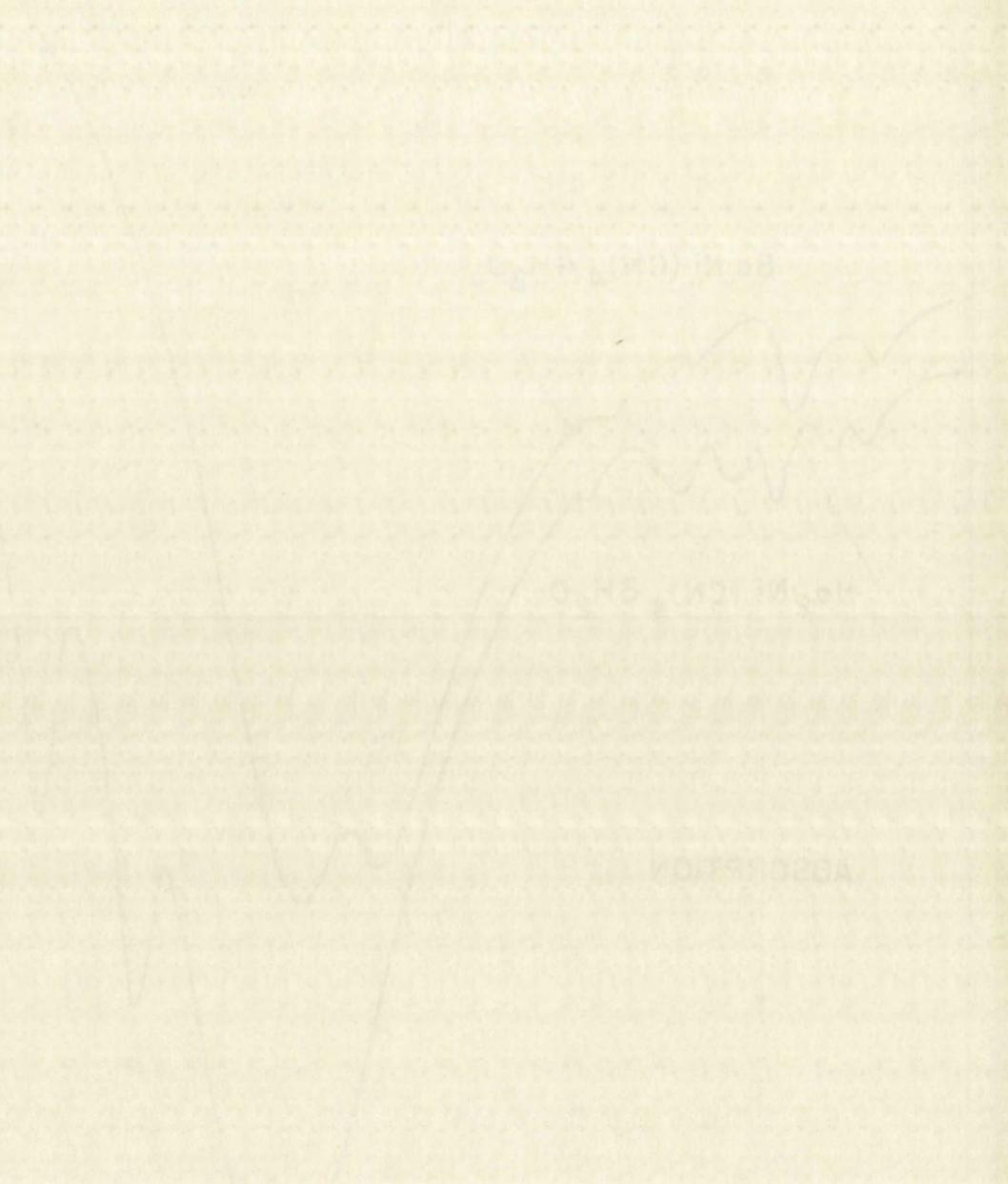
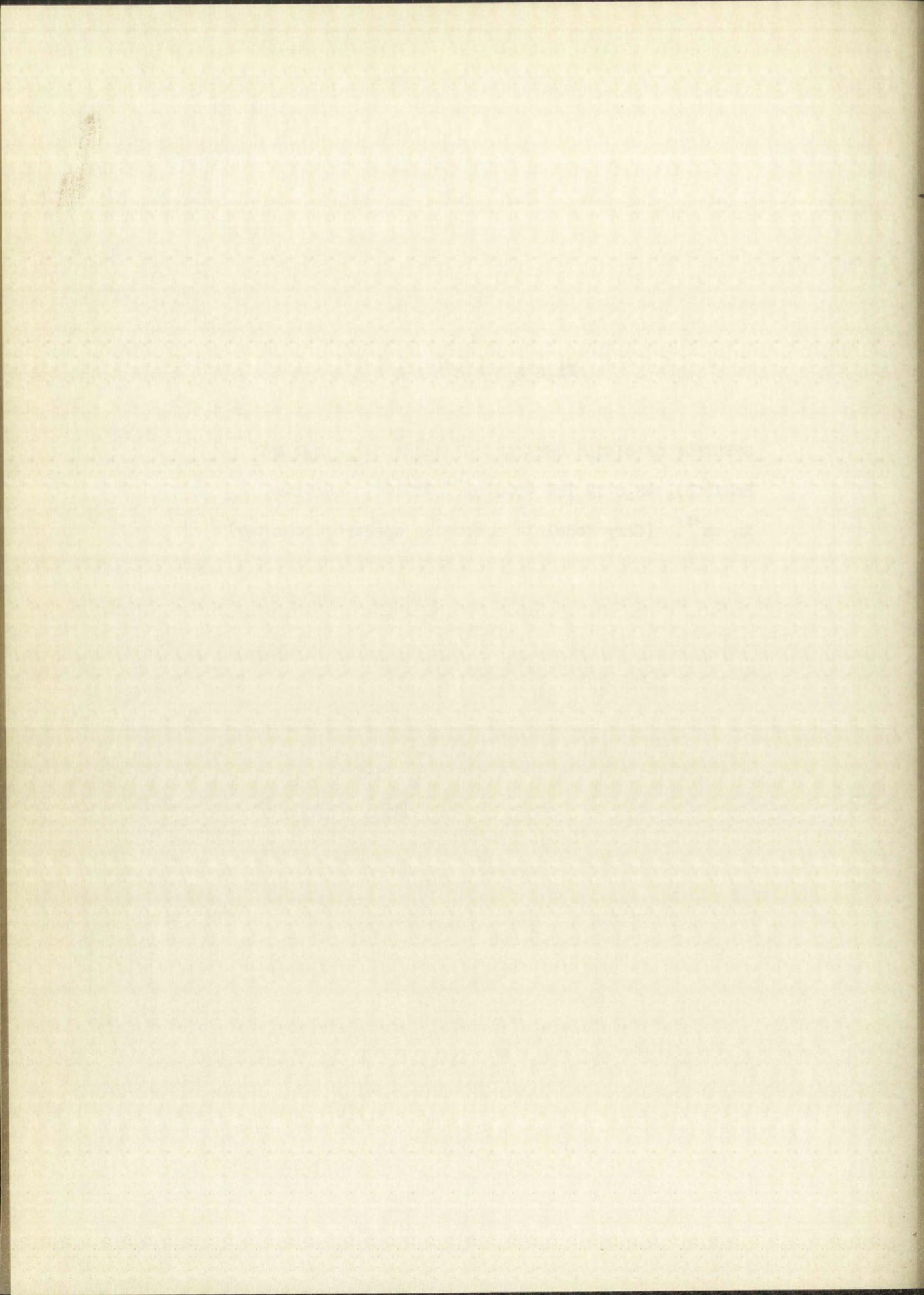
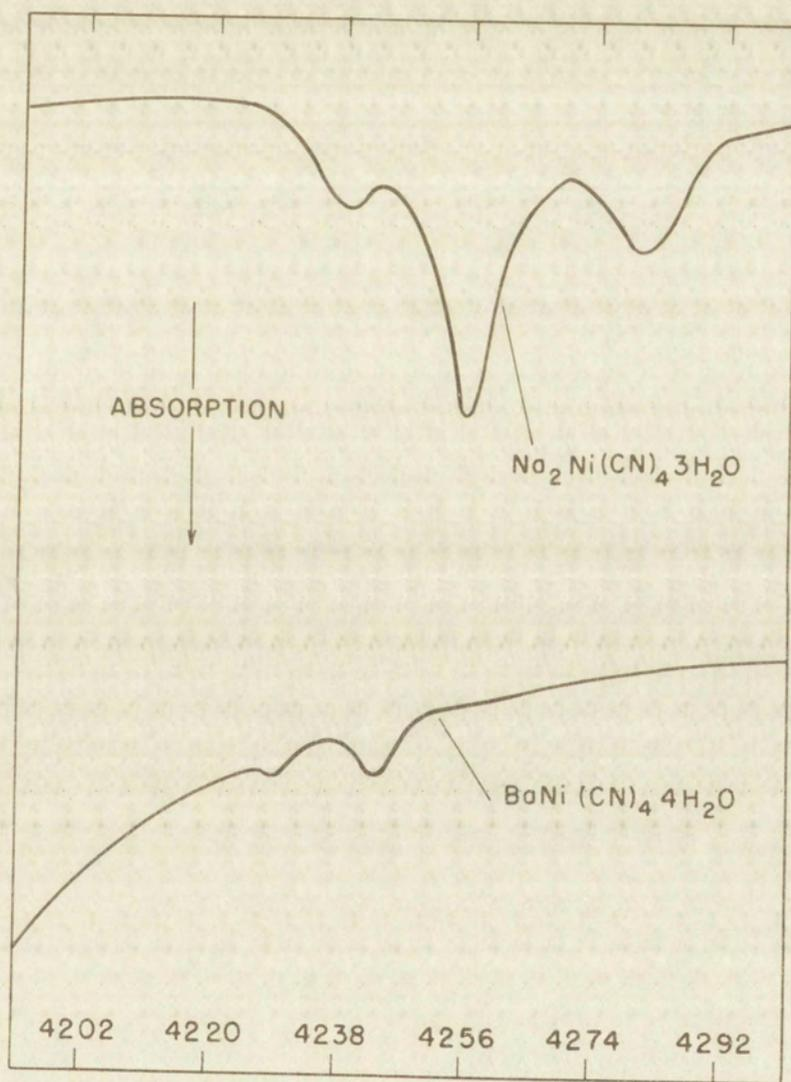


Figure 3.4.2

SPECTRUM OF SINGLE CRYSTALS OF $\text{Na}_2\text{Ni}(\text{CN})_4 \cdot 3\text{H}_2\text{O}$ AND
 $\text{BaNi}(\text{CN})_4 \cdot 4\text{H}_2\text{O}$ IN THE 4000 cm^{-1} REGION. Abscissa
in cm^{-1} . (Cary Model 14 recording spectrophotometer)





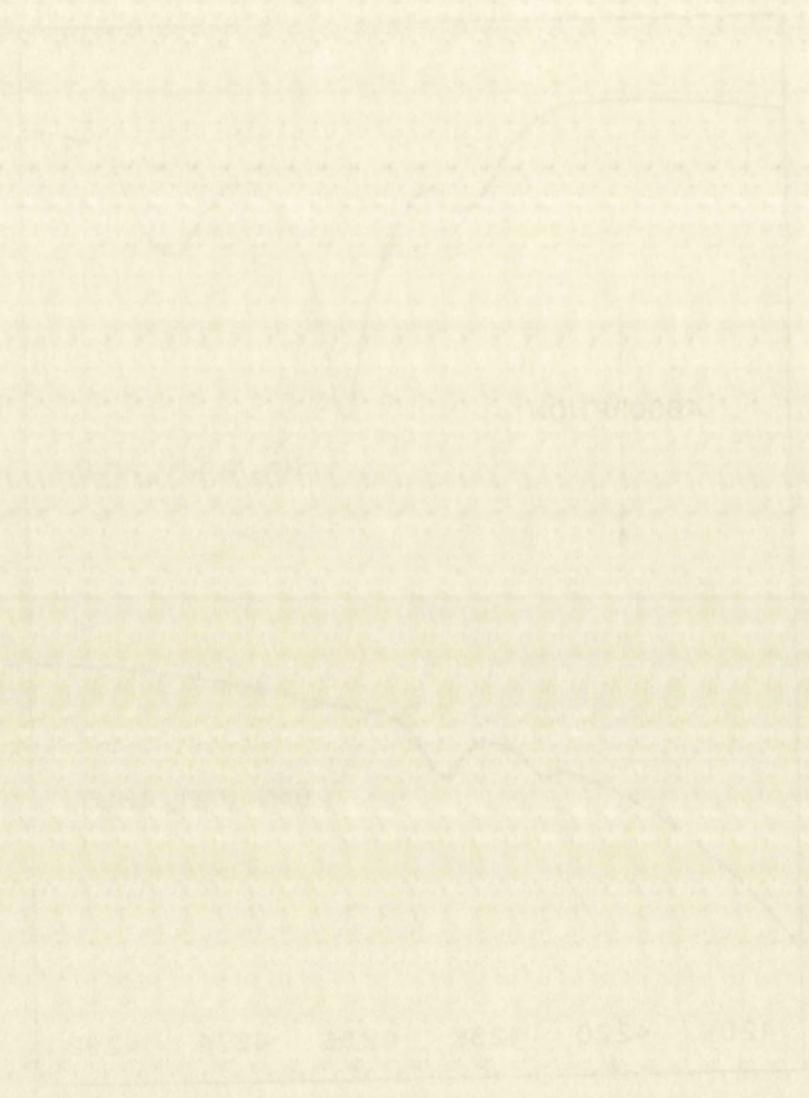
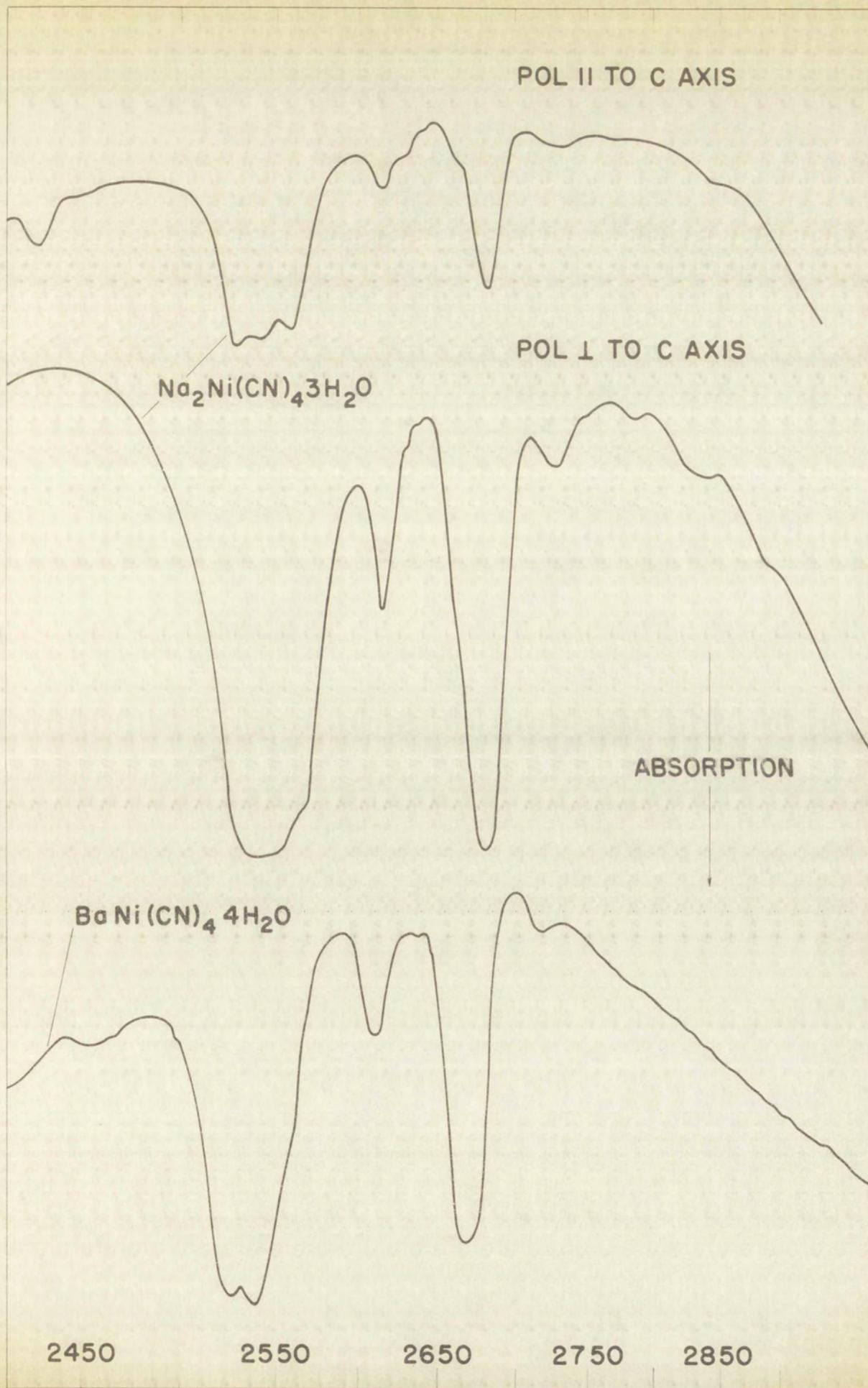


Figure 3.4.3

POLARIZED SPECTRUM OF SINGLE CRYSTALS OF $\text{Na}_2\text{Ni}(\text{CN})_4 \cdot 3\text{H}_2\text{O}$
AND THE UNPOLARIZED SPECTRUM OF $\text{BaNi}(\text{CN})_4 \cdot 4\text{H}_2\text{O}$ IN THE
2000 cm^{-1} region. Abscissa in cm^{-1} . (Perkin-Elmer
Model 112--LiF prism)

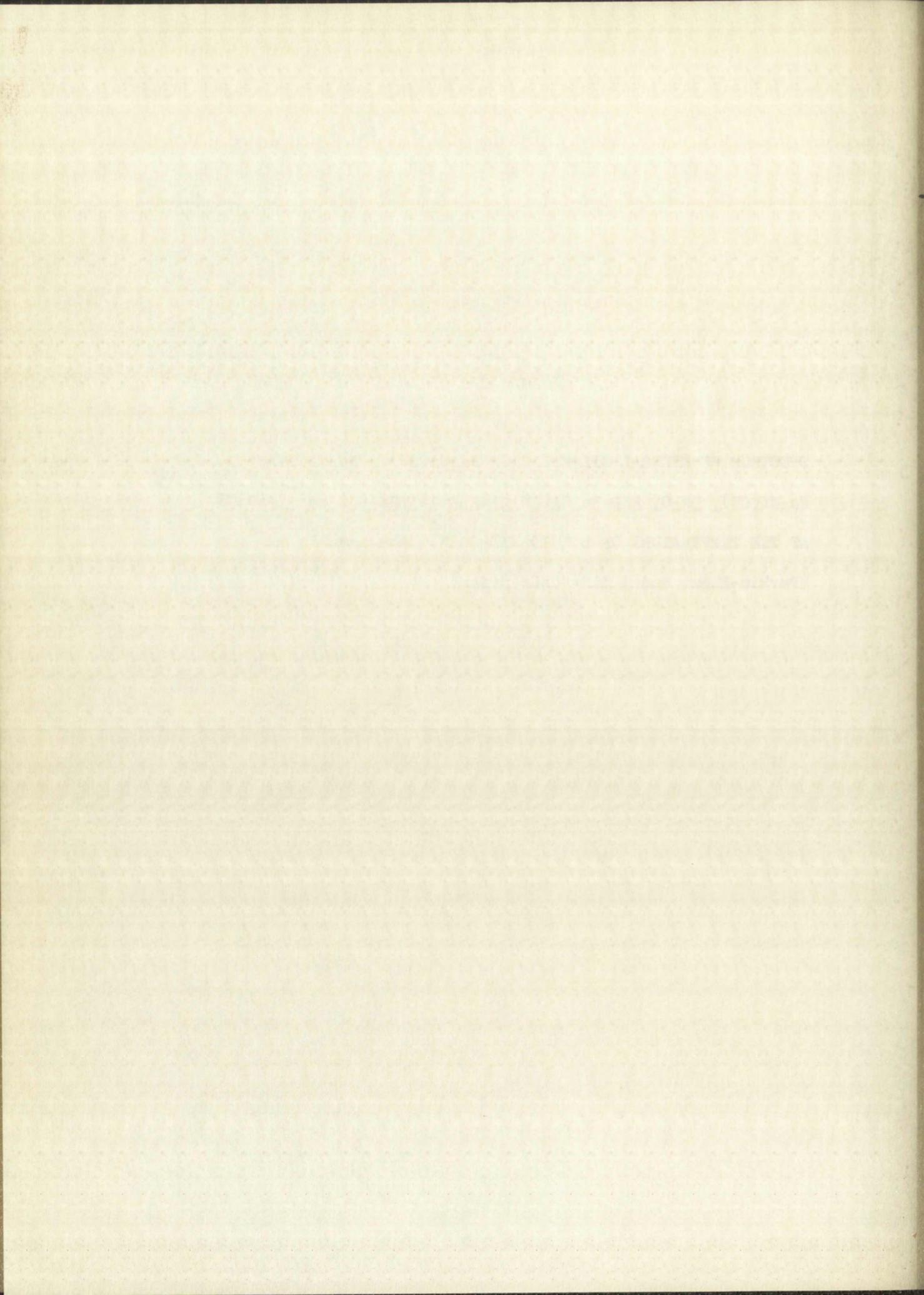


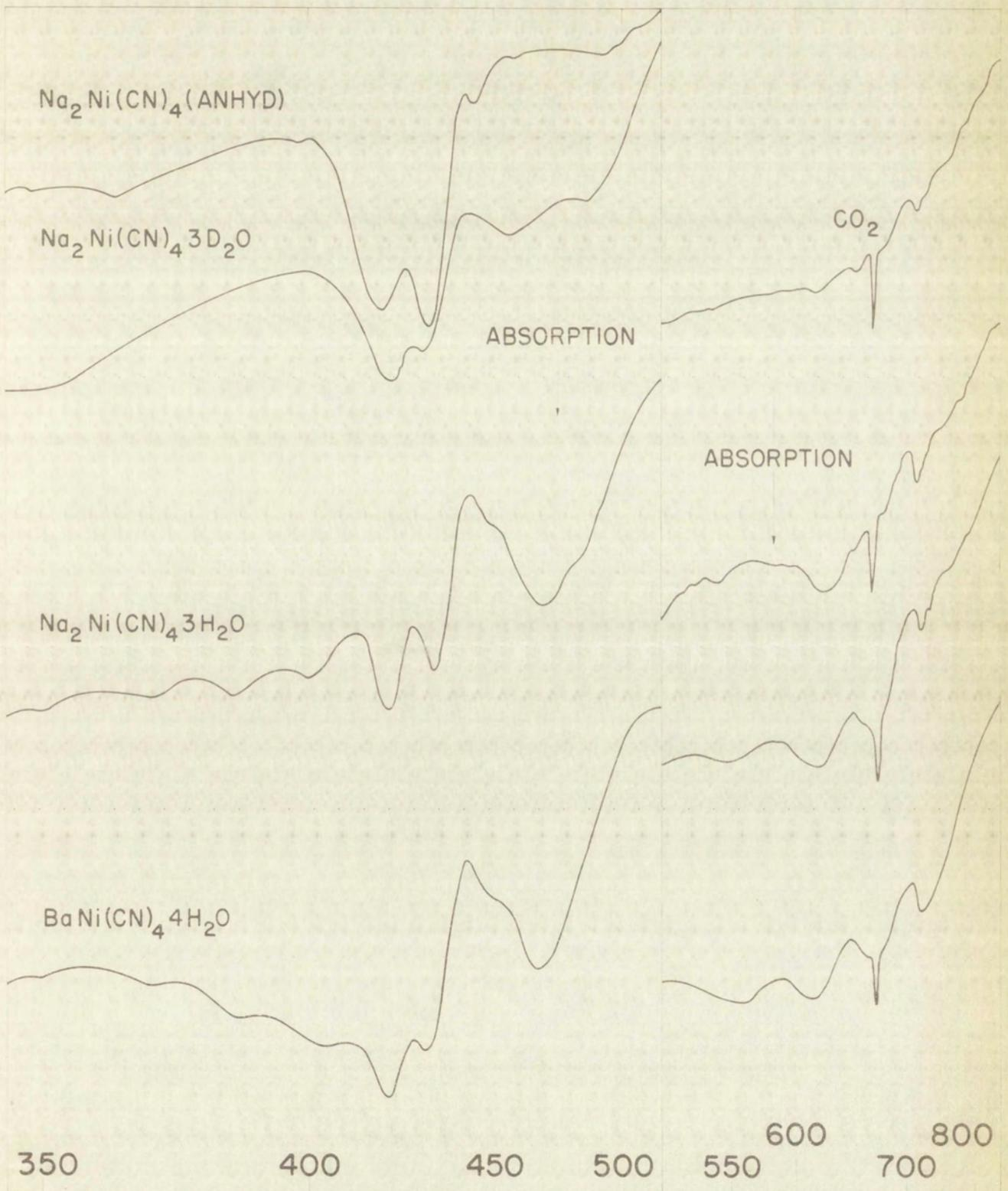
100

THE UNIVERSITY OF CHICAGO
LIBRARY

Figure 3.4.4

SPECTRUM OF MINERAL OIL MULLS OF $\text{Na}_2\text{Ni}(\text{CN})_4$, $\text{Na}_2\text{Ni}(\text{CN})_4 \cdot 3\text{D}_2\text{O}$,
 $\text{Na}_2\text{Ni}(\text{CN})_4 \cdot 3\text{H}_2\text{O}$, AND $\text{Ba Ni}(\text{CN})_4 \cdot 4\text{H}_2\text{O}$ IN THE 500 cm^{-1} REGION
AT THE TEMPERATURE OF LIQUID NITROGEN. Abscissa in cm^{-1} .
(Perkin-Elmer Model 112--CsBr prism)





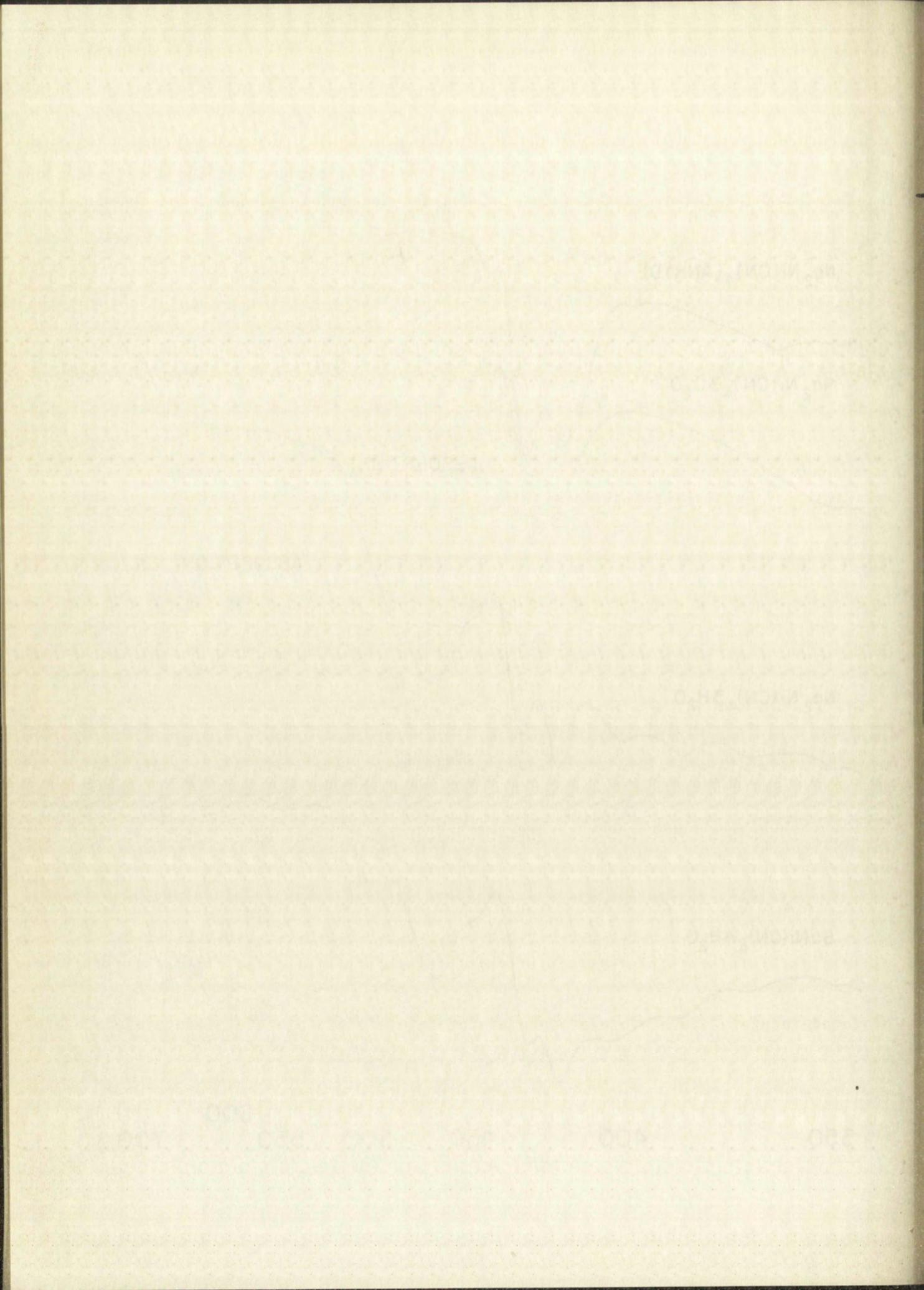


TABLE 3.4.0

OBSERVED VIBRATIONAL FREQUENCIES OF $\text{Na}_2\text{Ni}(\text{CN})_4 \cdot 3\text{H}_2\text{O}$ AND $\text{BaNi}(\text{CN})_4 \cdot 4\text{H}_2\text{O}$

ν_{Na} cm^{-1}	ν_{Ba} cm^{-1}	Approx. Ext. Coef. (d) $\text{moles}^{-1} \text{cm}^2$	Pol. (e)	Assignment	Representation
4279 (a)		30		$2\nu_1$	A_{1g}
4254 (a)	4243 (a)	40		$\nu_1 + \nu_8$	E_u
4237 (a)	4229 (a)	20		$\nu_4 + \nu_8$	E_u
3595 (b,c)	3595 (b)			$\nu(\text{H}_2\text{O})$	
3535 (b,c)	3540 (b)			$\nu(\text{H}_2\text{O})$	
3440 (b,c)	3435 (b)			$\nu(\text{H}_2\text{O})$	
3250 (b,c)	3240 (b)			$\nu(\text{H}_2\text{O})$	
2792 (a)		8	ip	$\nu_4 + 2\nu_3$	B_{1g}
2683 (a,b)	2674 (a,b)	130	ip	$\nu_4 + \nu_5$	E_u
2618 (a,b)	2617 (a,b)	35	ip	$\nu_6 + \nu_8$	E_u
2563 (a,b)		150	ip	$\nu_8 + \nu_{10}$	$A_{1g} + B_{1g} +$ $E_u^{A_{2g} + B_{2g}}$
2549 (a,b)	2547 (a,b)	150	ip	$\nu_2 + \nu_8$	E_u
2535 (a,b)	2533 (a,b)	150	ip	$\nu_5 + \nu_8$	E_u
2455 (a)	2458 (a)	8	ip	$\nu_3 + \nu_8$	E_u
2429 (a)		8	op	$\nu_1 + \nu_{16}$	E_g
2207 (a)		8	op	$\nu_1 + \nu_{15}$	B_{2u}
2149 (a,b,c)		140	ip	ν_1	A_{1g}
2141 (a,b,c)		115	ip	ν_4	B_{1g}
2132 (a,b,c)	2126 (b)	1070	ip	ν_8	E_u
2128 (a,b,c)	2120 (b)	1035	ip	ν_8	E_u

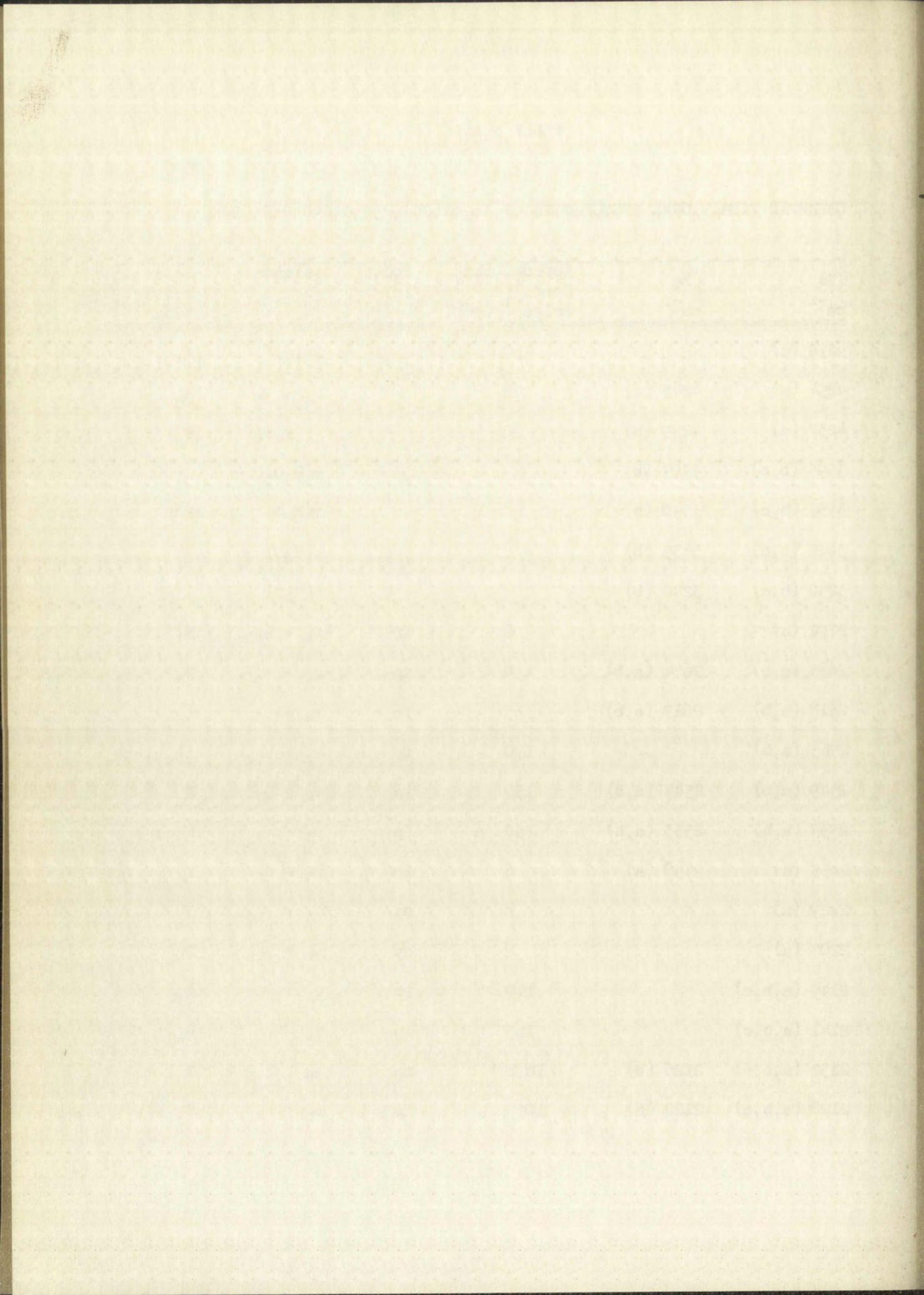
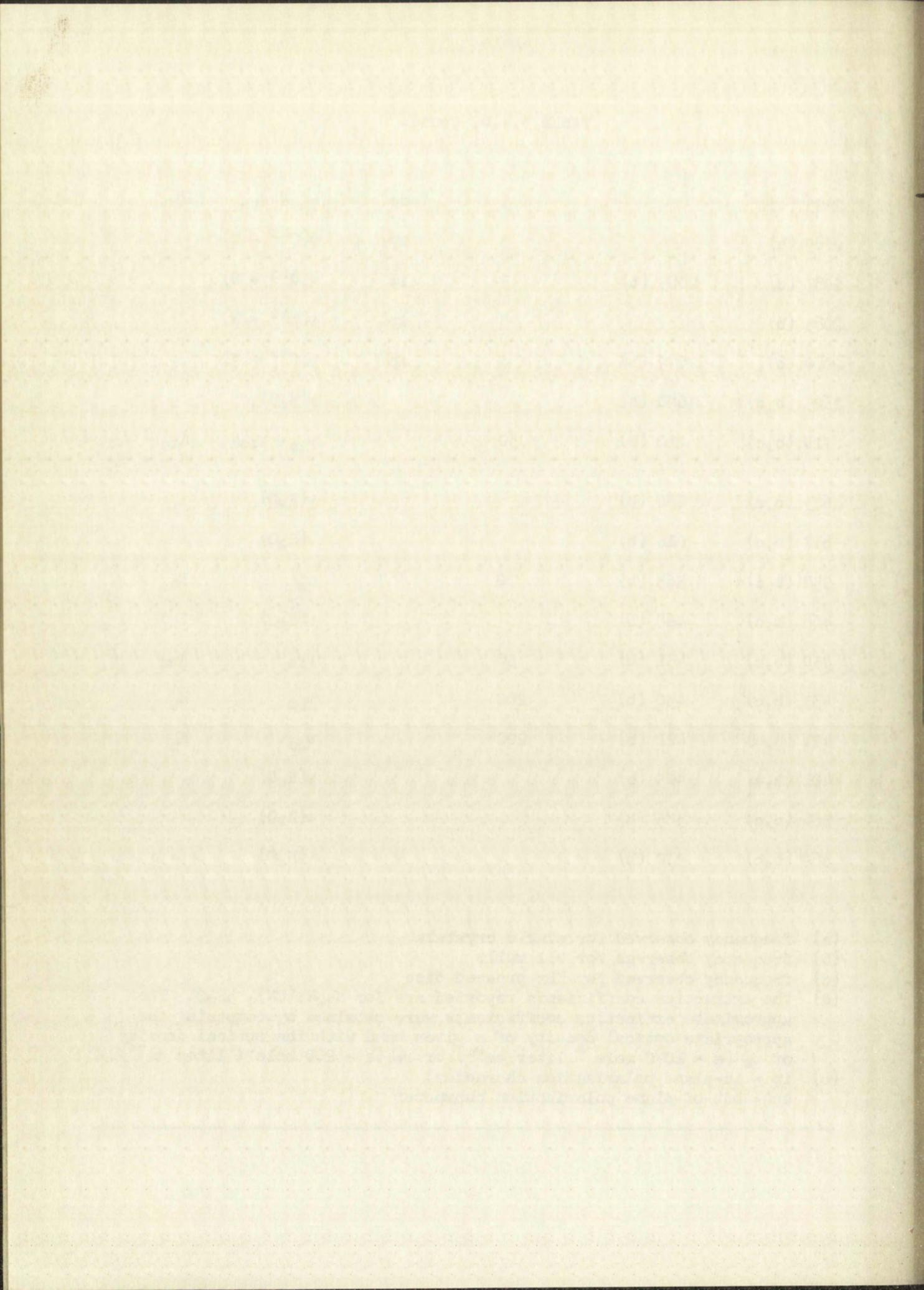


TABLE 3.4.0, Contd.

2095 (b)		5	op	$\nu_1 - \nu_{15}$	B_{2u}
2089 (b)		3	ip	$\nu(C^{13} - N)$	
2087 (b)	2085 (b)	5	ip	$\nu(C^{13} - N)$	
2083 (b)		3	ip	$\nu(C^{13} - N)$	
2080 (b)	2079 (b)	3	ip	$\nu(C^{13} - N)$	
1625 (b,c)	1620 (b)			$\nu(H_2O)$	
710 (b,c)	710 (b)	30		$\nu_{10} + \nu_{16}$	$A_{1u} + A_{2u} + B_{1u} + B_{2u}$
673 (b,c)	680 (b)			$\nu(H_2O)$	
617 (b,c)	616 (b)			$\nu(H_2O)$	
552 (b,c)	563 (b)	70		ν_9	E_u
468 (b,c)	468 (b)			$\nu(H_2O)$	
450 (b,c)	451 (b)	30		ν_{12}	A_{2u}
433 (b,c)	430 (b)	200		ν_{10}	E_u
421 (b,c)	421 (b)	200		ν_{10}	E_u
401 (b,c)	405 (b)			$\nu(H_2O)$	
386 (b,c)	385 (b)			$\nu(H_2O)$	
369 (b,c)	370 (b)			$\nu(H_2O)$	

- (a) frequency observed for single crystals
 (b) frequency observed for oil mulls
 (c) frequency observed for KBr pressed disc
 (d) The extinction coefficients reported are for $Na_2Ni(CN)_4 \cdot 3H_2O$. The approximate extinction coefficients were obtained by comparing the appropriate optical density of a given band with the optical density of ν_8 ($\epsilon = 1070 \text{ mole}^{-1} \text{ liter cm}^{-1}$) or ν_9 ($\epsilon = 200 \text{ mole}^{-1} \text{ liter cm}^{-1}$).
 (e) ip = in-plane polarization character;
 op = out-of-plane polarization character



3.4.3 E_u Vibrations: There is little doubt that the frequency pair (2132, 2128) cm⁻¹ belongs to the ν₈ vibration of the degenerate E_u representation. The bands at 4254 and 4237 cm⁻¹, which appear in the spectra of the triclinic and the monoclinic crystals, can be explained by a combination of ν₈ with ν₁ and ν₄, respectively. These assignments yield anharmonic constants X₁₈ and X₄₈ of 25 and 34 cm⁻¹, respectively.

Three frequencies, (433, 421), 552, and 450 cm⁻¹, appear in the 400-600 cm⁻¹ region of the spectra for both crystal systems. Only two of these can belong to the E_u representation.

The appearance of a band at 2563 cm⁻¹ possessing in-plane polarization character in the triclinic crystal, and the absence of such a band for the monoclinic crystal, may be explained by the combination of a band of ~ 430 cm⁻¹ with ν₈. This low frequency vibration must belong to the E_u representation in order to satisfy the polarization and selection rule requirements for the observed peak.

The band at 2683 cm⁻¹ may be explained by the combination of ν₈ with a frequency of ~ 550 cm⁻¹. The selection rule and polarization requirements for the observed peak dictate that this low frequency must belong to the E_u representation.

These considerations lead us to the conclusion that the frequency at 450 cm⁻¹ must belong to either A_{2u} or B_{2u}.

The distinction as to which kind of motion of E_u symmetry is involved in the frequencies (433, 421) and 552 cm⁻¹ is not obvious. As will be shown later, both (433, 421) and 552 cm⁻¹ involve the Ni-C(R) and Ni-C-N(α) coordinates to a large extent.

The first part of the report deals with the general situation of the country and the progress of the work done during the year. It is followed by a detailed account of the various projects undertaken and the results achieved. The report concludes with a summary of the work done and a list of the names of the staff members who have been engaged in the work.

The second part of the report deals with the financial statement of the year. It shows the total amount of the grant received from the Government and the total amount of the grant received from other sources. It also shows the total amount of the grant expended and the balance carried forward to the next year.

The third part of the report deals with the accounts of the various projects undertaken. It shows the total amount of the grant received for each project and the total amount of the grant expended for each project. It also shows the progress of each project and the results achieved.

The fourth part of the report deals with the accounts of the staff members who have been engaged in the work. It shows the total amount of the grant received for each staff member and the total amount of the grant expended for each staff member. It also shows the progress of each staff member and the results achieved.

The fifth part of the report deals with the accounts of the various committees and sub-committees which have been formed to deal with the various aspects of the work. It shows the total amount of the grant received for each committee and the total amount of the grant expended for each committee. It also shows the progress of each committee and the results achieved.

The sixth part of the report deals with the accounts of the various conferences and meetings which have been held during the year. It shows the total amount of the grant received for each conference and the total amount of the grant expended for each conference. It also shows the progress of each conference and the results achieved.

The seventh part of the report deals with the accounts of the various publications which have been produced during the year. It shows the total amount of the grant received for each publication and the total amount of the grant expended for each publication. It also shows the progress of each publication and the results achieved.

The eighth part of the report deals with the accounts of the various exhibitions and displays which have been held during the year. It shows the total amount of the grant received for each exhibition and the total amount of the grant expended for each exhibition. It also shows the progress of each exhibition and the results achieved.

The ninth part of the report deals with the accounts of the various lectures and talks which have been given during the year. It shows the total amount of the grant received for each lecture and the total amount of the grant expended for each lecture. It also shows the progress of each lecture and the results achieved.

The tenth part of the report deals with the accounts of the various courses and classes which have been held during the year. It shows the total amount of the grant received for each course and the total amount of the grant expended for each course. It also shows the progress of each course and the results achieved.

The eleventh part of the report deals with the accounts of the various research projects which have been undertaken during the year. It shows the total amount of the grant received for each project and the total amount of the grant expended for each project. It also shows the progress of each project and the results achieved.

The twelfth part of the report deals with the accounts of the various publications which have been produced during the year. It shows the total amount of the grant received for each publication and the total amount of the grant expended for each publication. It also shows the progress of each publication and the results achieved.

The thirteenth part of the report deals with the accounts of the various exhibitions and displays which have been held during the year. It shows the total amount of the grant received for each exhibition and the total amount of the grant expended for each exhibition. It also shows the progress of each exhibition and the results achieved.

The fourteenth part of the report deals with the accounts of the various lectures and talks which have been given during the year. It shows the total amount of the grant received for each lecture and the total amount of the grant expended for each lecture. It also shows the progress of each lecture and the results achieved.

The fifteenth part of the report deals with the accounts of the various courses and classes which have been held during the year. It shows the total amount of the grant received for each course and the total amount of the grant expended for each course. It also shows the progress of each course and the results achieved.

The sixteenth part of the report deals with the accounts of the various research projects which have been undertaken during the year. It shows the total amount of the grant received for each project and the total amount of the grant expended for each project. It also shows the progress of each project and the results achieved.

The seventeenth part of the report deals with the accounts of the various publications which have been produced during the year. It shows the total amount of the grant received for each publication and the total amount of the grant expended for each publication. It also shows the progress of each publication and the results achieved.

The eighteenth part of the report deals with the accounts of the various exhibitions and displays which have been held during the year. It shows the total amount of the grant received for each exhibition and the total amount of the grant expended for each exhibition. It also shows the progress of each exhibition and the results achieved.

The nineteenth part of the report deals with the accounts of the various lectures and talks which have been given during the year. It shows the total amount of the grant received for each lecture and the total amount of the grant expended for each lecture. It also shows the progress of each lecture and the results achieved.

The twentieth part of the report deals with the accounts of the various courses and classes which have been held during the year. It shows the total amount of the grant received for each course and the total amount of the grant expended for each course. It also shows the progress of each course and the results achieved.

No fundamental, difference, or summation band was observed which we could associate with ν_{11} .

3.4.4 A_{2g} Vibrations: From the arguments presented in Section 3.4.1 we conclude that the ν_3 vibration of A_{2g} may be either 488 cm^{-1} or 326 cm^{-1} .

By using the high-frequency approximation for B_{2g} we have: ⁽³⁴⁾

$$\frac{\lambda_3}{\lambda_6} = \frac{f^{A_{2g}}(\alpha; \alpha)}{f^{B_{2g}}(\alpha; \alpha)}$$

Jones has shown that the Ni-C-O interaction constants for $\text{Ni}(\text{CO})_4$ are negative. Assuming then that the Ni-C-N force constants for the tetracyanonickelate(II) ion are analogous to the Ni-C-O force constants for $\text{Ni}(\text{CO})_4$, we have (from the definition of $f^{A_{2g}}(\alpha; \alpha)$ and $f^{B_{2g}}(\alpha; \alpha)$ given in Table 3.1.8) the following inequality:

$$\frac{\lambda_3}{\lambda_6} < 1 .$$

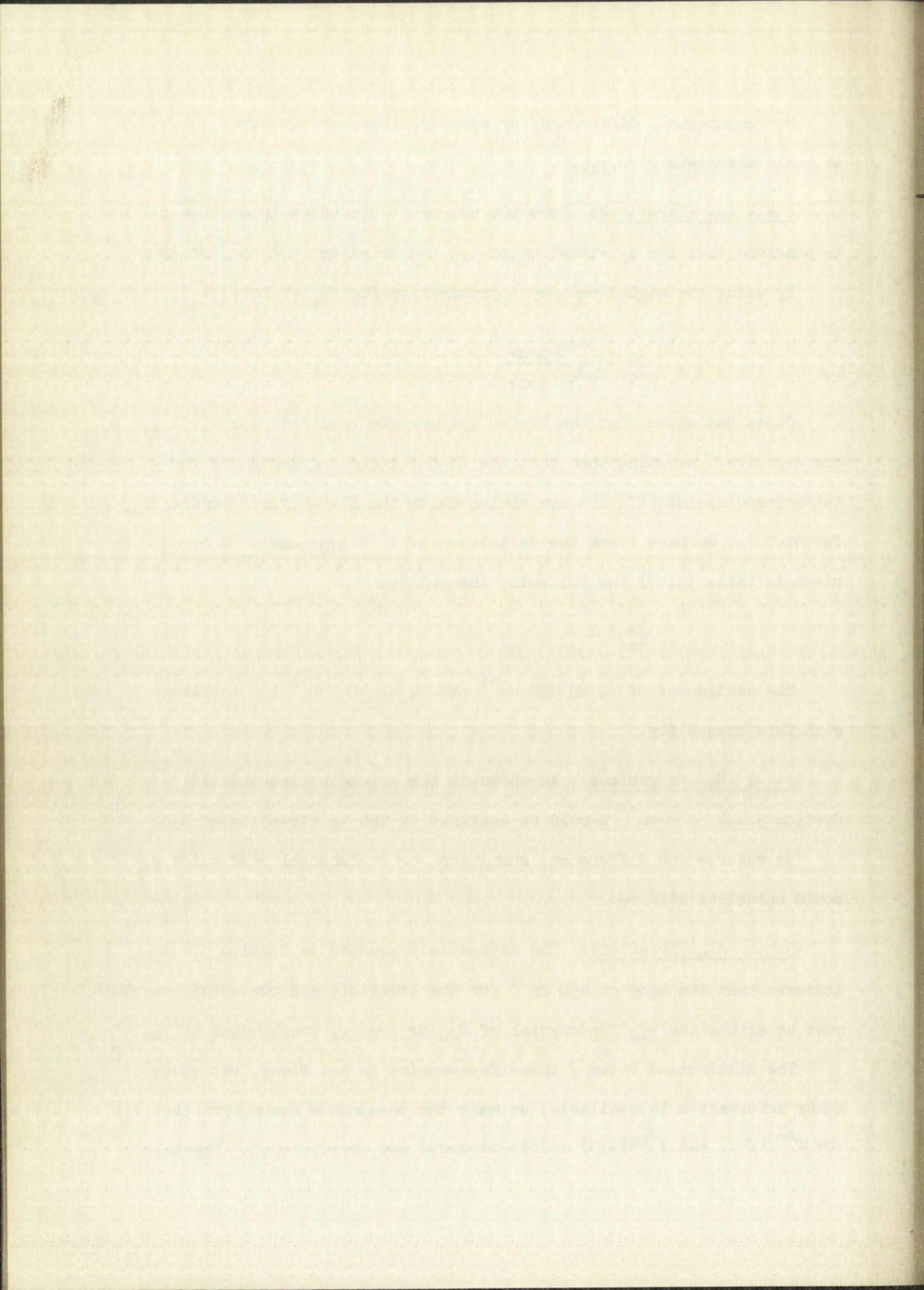
The assignment of ν_3 as 326 cm^{-1} and ν_6 as 488 cm^{-1} is consistent with this inequality.

3.4.5 B_{2g} Vibrations: As shown in the argument presented in Section 3.4.4, 488 cm^{-1} should be assigned to the ν_6 vibration of B_{2g} .

We observed no difference, summation, or fundamental band which we could associate with ν_7 .

3.4.6 A_{2u} Vibrations: The arguments presented in Section 3.4.3 indicate that the band at 450 cm^{-1} for the triclinic and monoclinic crystals must be either the ν_{12} fundamental of A_{2u} or the ν_{14} fundamental of B_{2u} .

The distinction between these frequencies is not clear, but since no other information is available, we make the reasonable assumption that the $f^{A_{2u}}(\beta; \beta)$ and $f^{B_{2u}}(\beta; \beta)$ matrix elements are nearly equal. The high



frequency approximation then indicates that $\nu_{12} > \nu_{14}$. We conclude that the band at 450 cm^{-1} is ν_{12} and that the ν_{14} vibration either is below our range of observation or is masked by other fundamentals (e.g., ν_{10}).

We observed no frequency which we could assign to ν_{13} .

3.4.7 B_{2u} Vibrations: No fundamental or combination bands were observed which we could correlate to the ν_{14} vibration of B_{2u} . However, from the arguments presented in Section 3.4.6, we conclude that $\nu_{14} < 450 \text{ cm}^{-1}$.

The difference band at 2095 cm^{-1} and the summation band at 2207 cm^{-1} , both observed only for the triclinic system, indicate that a frequency of "g" symmetry at 54 cm^{-1} is combining with ν_1 . Both of these bands have out-of-plane polarization character. However, there is no "g" frequency with out-of-plane polarization character which may be of the magnitude of 54 cm^{-1} .

Since the monoclinic system approaches D_{4h} symmetry, it would seem reasonable to assume that the B_{2u} frequencies are either very weak or absent in the spectra of $\text{BaNi}(\text{CN})_4 \cdot 4\text{H}_2\text{O}$. This low frequency could be the ν_{15} vibration of B_{2u} symmetry or possibly a lattice vibration. Since $\sim 50 \text{ cm}^{-1}$ is about the right magnitude for this out-of-plane bending frequency, we conclude that this frequency at 54 cm^{-1} is the ν_{15} vibration of B_{2u} .

3.4.8 E_g Vibration: The appearance only for the triclinic crystal of a band at 2429 cm^{-1} with out-of-plane polarization character, and the appearance of a band at 710 cm^{-1} for oil mulls of both the triclinic and monoclinic crystals indicates strongly that a frequency of 282 cm^{-1} is combining with ν_1 and ν_9 , respectively. The polarization and selection

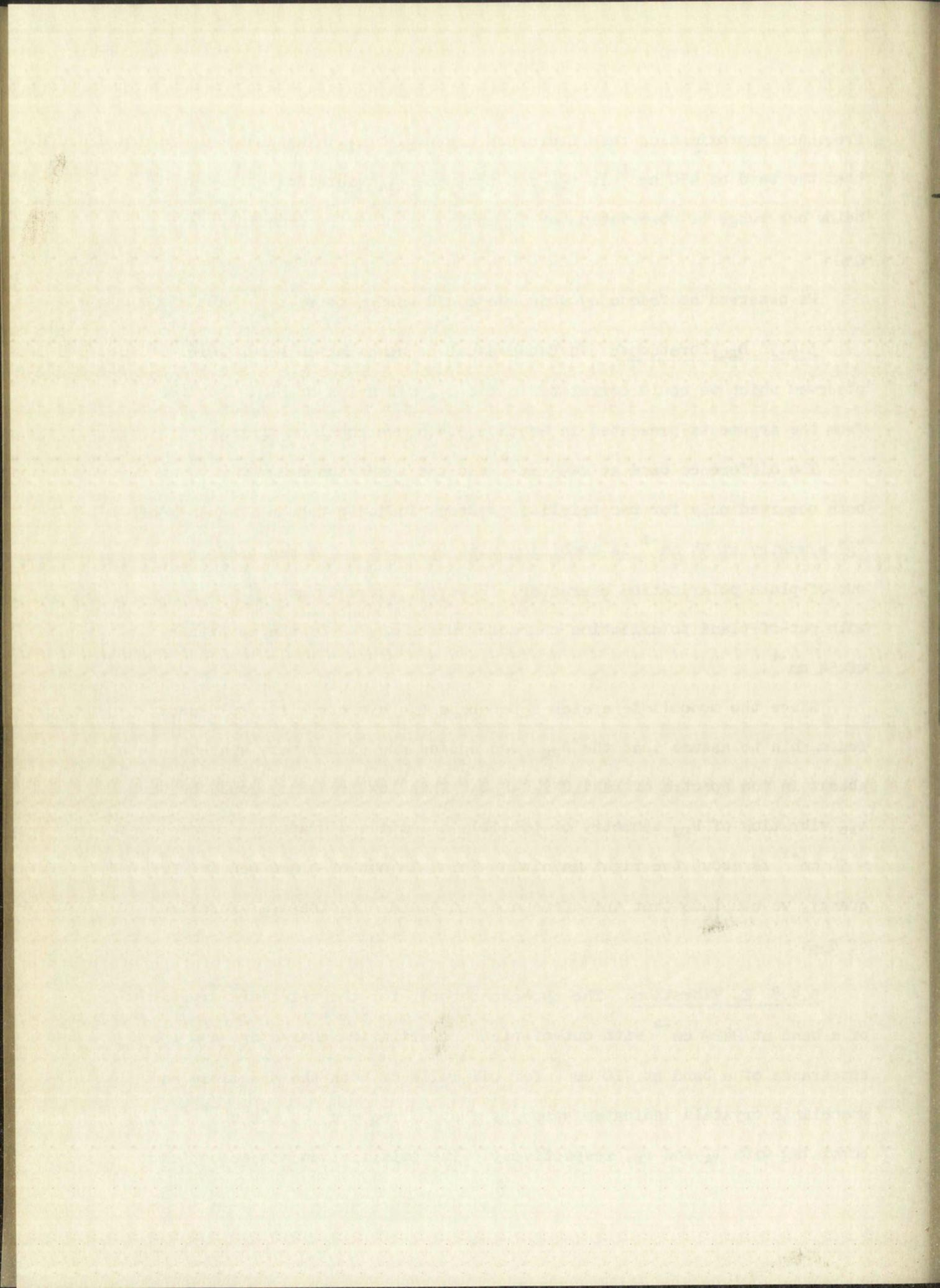


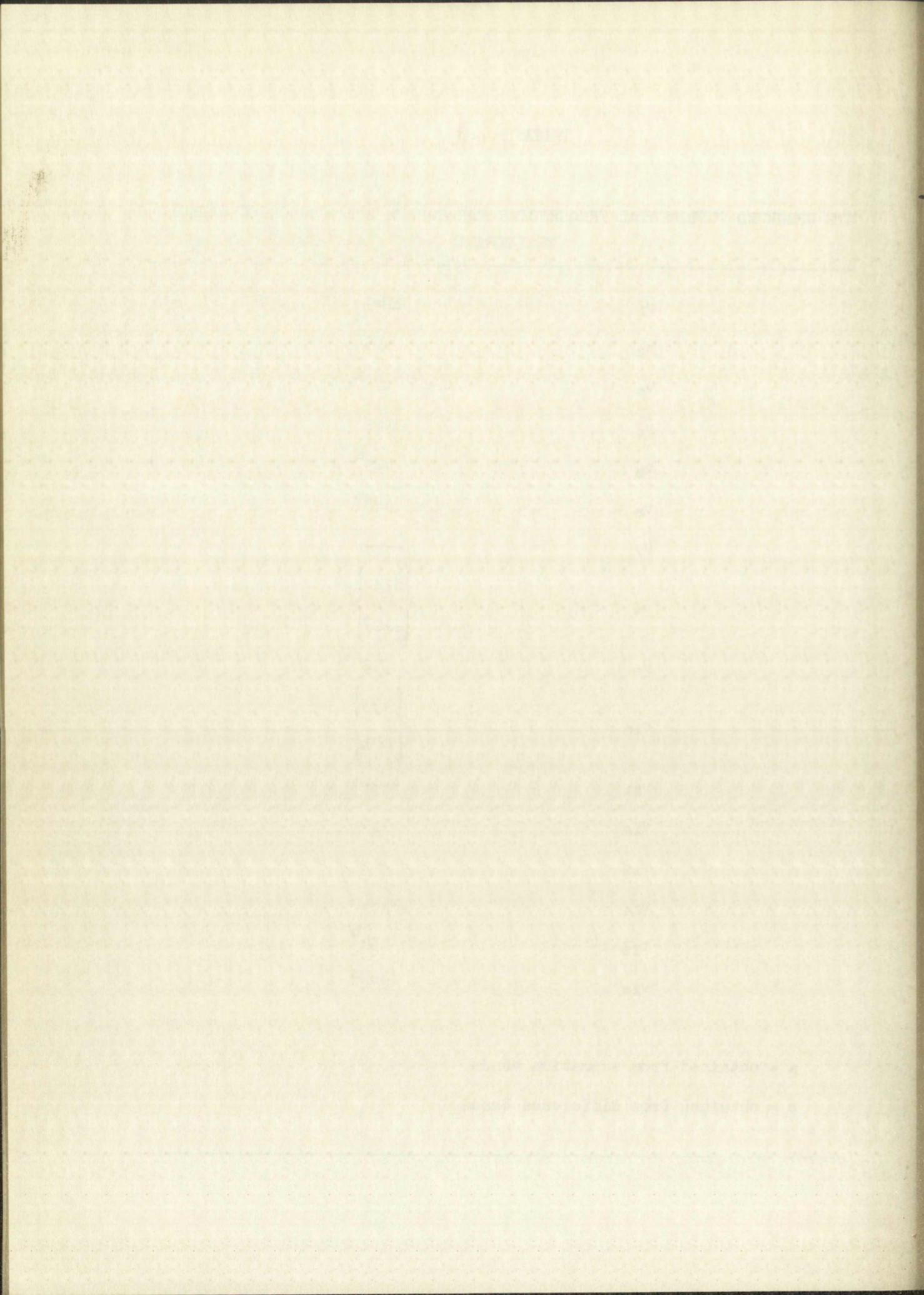
TABLE 3.4.8

THE OBSERVED FUNDAMENTAL FREQUENCIES FOR SODIUM TETRACYANONICKELATE(II)
TRIHYDRATE

ν_1	2149
ν_2	416 ^a
ν_3	326 ^a
ν_4	2141
ν_5	405 ^a
ν_6	488 ^a
ν_7	----
ν_8	$\left\{ \begin{array}{l} 2132 \\ 2128 \end{array} \right\}$
ν_9	552
ν_{10}	$\left\{ \begin{array}{l} 433 \\ 421 \end{array} \right\}$
ν_{11}	----
ν_{12}	450
ν_{13}	----
ν_{14}	----
ν_{15}	54 ^b
ν_{16}	282 ^a

a = obtained from summation bands

b = obtained from difference bands



rule requirements dictate that this frequency is the ν_{1g} fundamental of E_g .

The assignments of the fundamental frequencies are summarized in Table 3.4.8.

3.5 Potential Function and Force Constants

From Table 3.1.8 it can be seen that the general quadratic valence potential function contains many more force constants than there are observed fundamental frequencies. No solution, in terms of the defined valence bond force constants, will be obtainable unless we follow the usual practice and arbitrarily assign values to some of the force constants and or neglect some of the interaction terms.

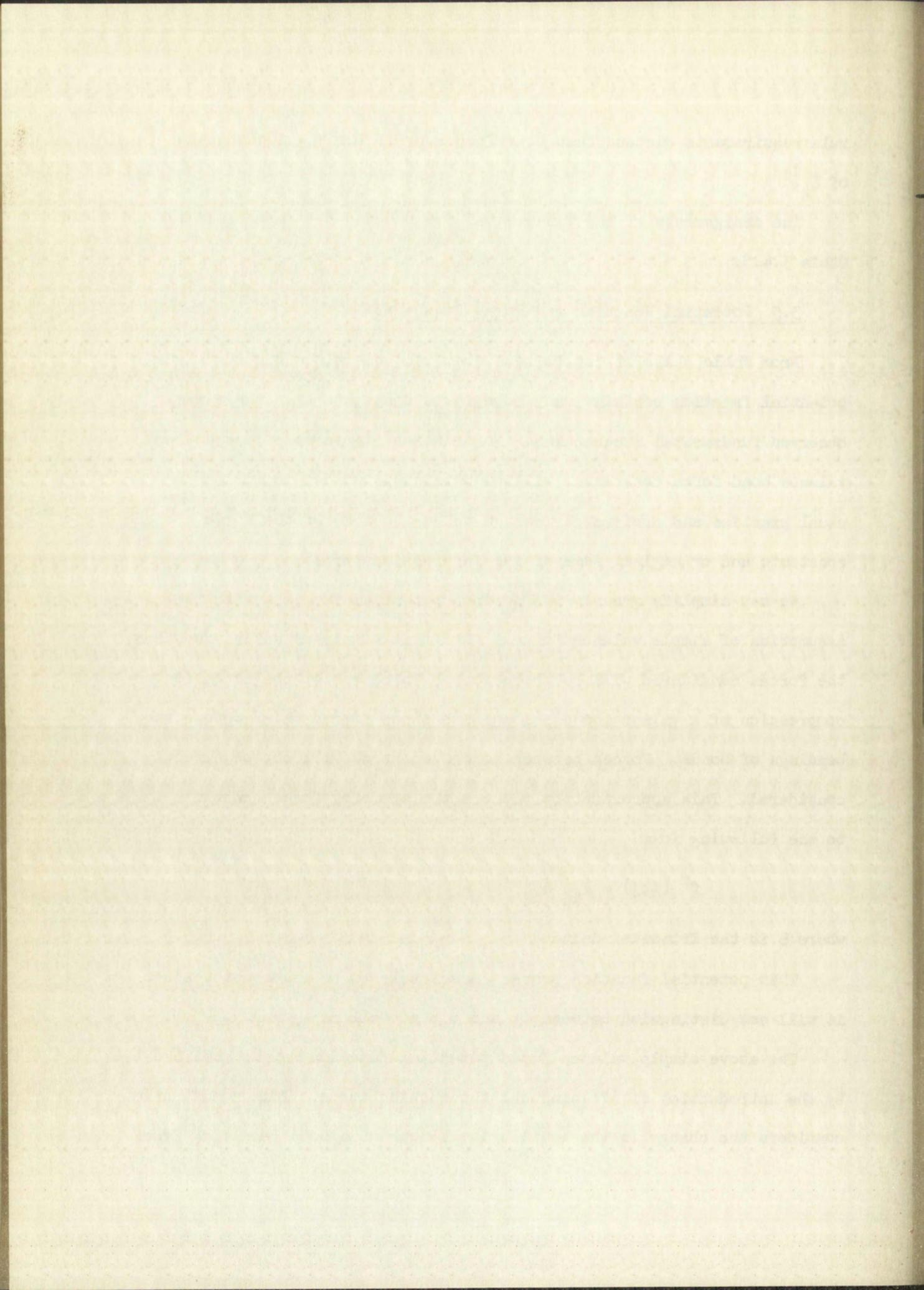
We may simplify greatly the defined potential function with the assumption of simple valence forces. For this simple potential function, the forces considered will be those forces which resist the extension or compression of a valence bond, along with those forces which oppose the bendings of bonds. Forces between nonbonded atoms will not be directly considered. This approximation reduces the symmetry force constants to the following form:

$$f^{\gamma}(i;j) = F_{ij} \delta_{ij}$$

where δ is the Kronecker delta.

This potential function proves immediately to be inadequate, since it will not distinguish between ν_1 and ν_4 , as well as ν_2 and ν_5 .

The above simple valence force potential function may be modified by the introduction of off-diagonal interaction terms. This modification considers the change in the equilibrium length of a bond resulting from



the distortion of an adjacent bond. The symmetry force constants now take on the following form:

$$f^{\gamma}(i;j) = F_{ij} \cdot$$

This potential function also proves to be inadequate since it, too, will not distinguish between v_1 and v_4 as well as v_2 and v_5 .

We were able to obtain an adequate potential function in terms of the defined valence force constants by making the following approximations:

$$f^{\gamma}(i;j) = [F_{ij} + a(\gamma)F'_{ij} + b(\gamma)F''_{ij}] \delta_{ij}$$

$$F'_{\phi\phi} = F''_{\phi\phi}$$

$$F'_{\beta\beta} = F''_{\beta\beta} = 0$$

$$F'_{\theta\theta} = F''_{\theta\theta} = 0$$

where the coefficients $a(\gamma)$ and $b(\gamma)$ are given in Table 3.1.8.

The values of these potential function parameters are given in Table 3.5.1.

Even though this potential function will explain the observed frequencies adequately, the interpretation of the physical significance of the valence bond force constants is far from satisfactory. It would seem unreasonable to assume simultaneously that the deformation of a cyanide bond would affect another cyanide bond to the extent indicated by this potential function and that the deformation of an adjacent nickel-carbon bond would have no effect on a cyanide bond (see Figure 3.1.3). We conclude that this potential function is a mathematical artifice with only slight physical significance.

Recently, L. H. Jones⁽³⁵⁾ has suggested a simplified potential function which not only reduces the number of potential function parameters,



TABLE 3.5.1

NUMERICAL EVALUATION OF THE APPROXIMATE VALENCE FORCE
POTENTIAL FUNCTION PARAMETERS

$$F_{rr} = 16.66 \text{ md}/\text{\AA}$$

$$F_{RR} = 2.55 \text{ md}/\text{\AA}$$

$$F'_{rr} = 0.02 \text{ md}/\text{\AA}$$

$$F'_{RR} = 0.05 \text{ md}/\text{\AA}$$

$$F''_{rr} = 0.04 \text{ md}/\text{\AA}$$

$$F''_{RR} = 0.15 \text{ md}/\text{\AA}$$

$$F_{\alpha\alpha} = 0.43 \text{ md } \text{\AA}/\text{radian}^2$$

$$F_{\phi\phi} = 0.28 \text{ md } \text{\AA}/\text{radian}^2$$

$$F'_{\alpha\alpha} = -0.06 \text{ md } \text{\AA}/\text{radian}^2$$

$$F'_{\phi\phi} = 0.06 \text{ md } \text{\AA}/\text{radian}^2$$

$$F''_{\alpha\alpha} = -0.02 \text{ md } \text{\AA}/\text{radian}^2$$

$$F''_{\phi\phi} = 0.06 \text{ md } \text{\AA}/\text{radian}^2$$

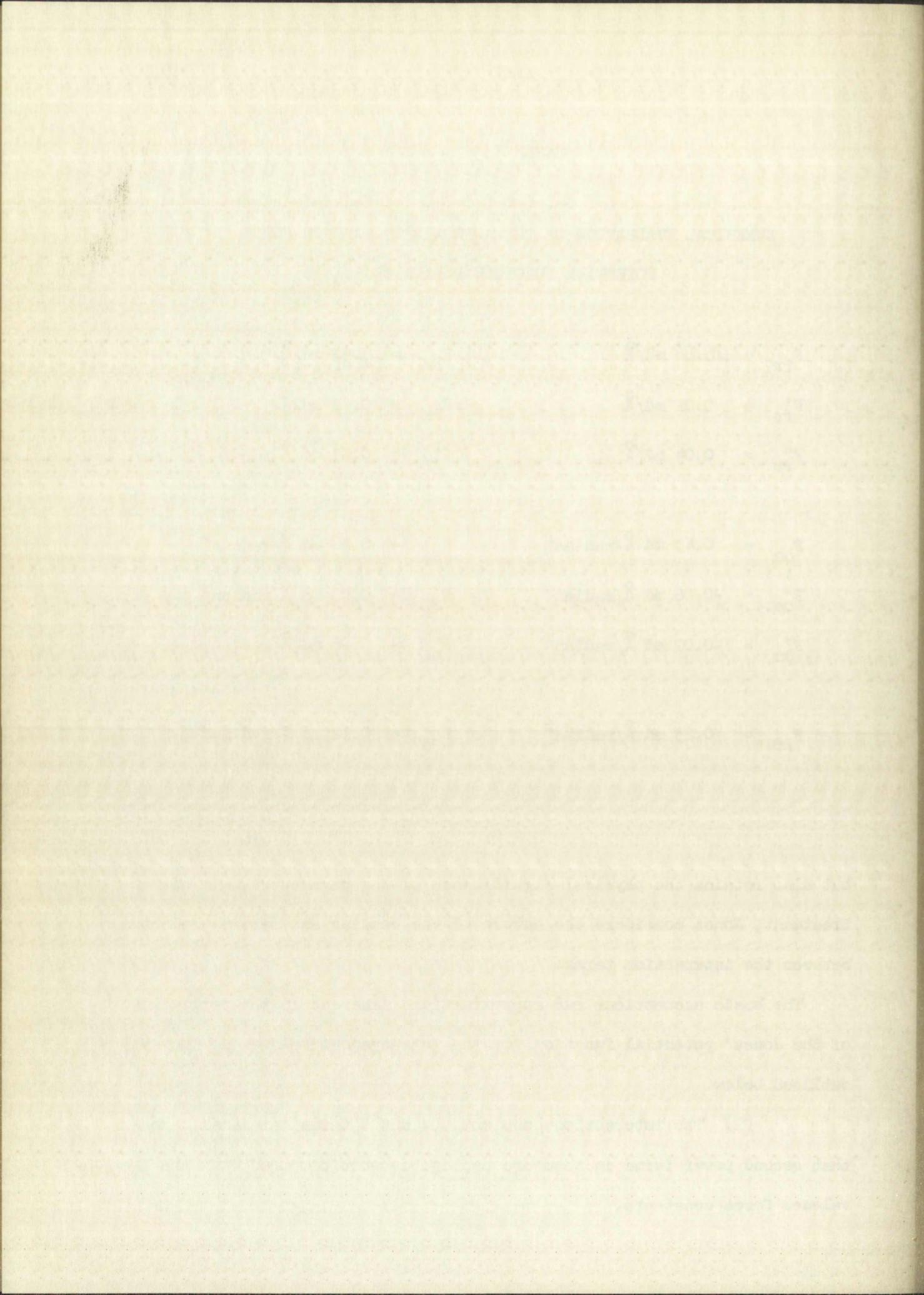
$$F_{\beta\beta} = 0.23 \text{ md } \text{\AA}/\text{radian}^2$$

$$F_{\theta\theta} = 0.12 \text{ md } \text{\AA}/\text{radian}^2$$

but also retains the physical significance of the parameters. In his treatment, Jones considers the nature of the bonding and derives relations between the interaction terms.

The basic assumptions and approximations inherent in the derivation of the Jones' potential function for the tetracyanonickelate(II) ion are outlined below.

(1) The interaction constants (' and '' terms) are small, so that second power terms in them are negligible when compared with the primary valence force constants.



(2) The stretch-stretch interaction constants arise mainly from changes in the d_{Ni-P_C} pi bonding and p_C-p_N pi bonding accompanying displacements of the internal coordinates. The change in the d_{Ni-P_C} pi bonding is proportional (and of opposite sign) to the change in Ni-C distance. The change in p_C-p_N pi bonding is proportional (and of opposite sign) to the change in C-N distance.

(3) The bend-bend interaction constants arise mainly from orbital "following"^(3e).

(4) The stretch-bend interaction constants are negligible.

(5) The d_{xz} , d_{yz} , and d_{xy} orbitals of Ni exhibit the same total amount of pi bonding among the favorably oriented carbon atoms, and this total amount of pi bonding is conserved.

The application of these considerations to the tetracyanonickelate(II) ion yields the following definitions of the valence bond interaction constants in terms of the Jones' potential function parameters:

$$\begin{array}{lll}
 F'_{rr} = (1/9)B & F'_{\alpha\alpha} = -H & F'_{\beta\beta} = 0 \\
 F''_{rr} = (7/9)B & F''_{\alpha\alpha} = -H & F''_{\beta\beta} = P \\
 \\
 F'_{RR} = (1/9)(D^2/B) & F'_{\beta\beta} = (1/3)F_{\beta\beta} & F'_{\theta\theta} = 0 \\
 F''_{RR} = (7/9)(D^2/B) & F''_{\beta\beta} = (1/3)F_{\beta\beta} & \\
 & & F_{\theta\theta} = Q \\
 \\
 F_{rR} = D & F_{\alpha\beta} = K & F'_{\theta\theta} = 0 \\
 F'_{rR} = -(1/9)D & F'_{\alpha\beta} = (1/3)K & \\
 F''_{rR} = -(7/9)D & &
 \end{array}$$

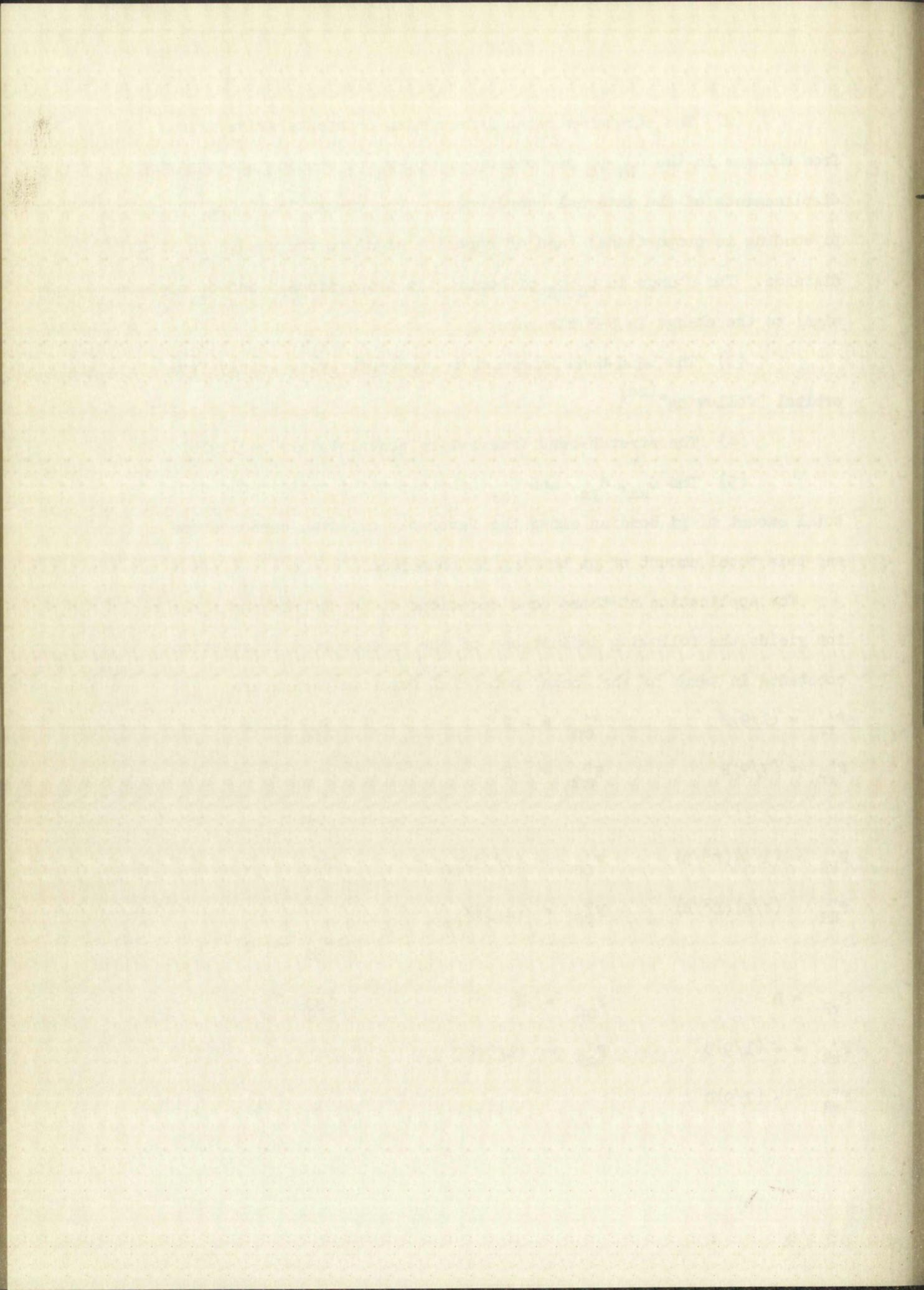


Table 3.5.2 defines the symmetry force constants in terms of the Jones' potential function parameters.

TABLE 3.5.2

SYMMETRY FORCE CONSTANTS FOR THE TETRACYANONICKELATE(II) ION
IN TERMS OF THE JONES' SIMPLIFIED POTENTIAL FUNCTION PARAMETERS

$$f^{A_1g}(r;r) = F_{rr} + B$$

$$f^{A_1g}(r;R) = 0$$

$$f^{A_1g}(R;R) = F_{RR} + D^2/B$$

$$f^{B_1g}(r;r) = F_{rr} + (5/9)B$$

$$f^{B_1g}(r;R) = (4/9)D$$

$$f^{B_1g}(R;R) = F_{RR} + (5/9)(D^2/B)$$

$$f^{A_2g}(\alpha;\alpha) = F_{\alpha\alpha} - 3H$$

$$f^{B_2g}(\alpha;\alpha) = F_{\alpha\alpha} + H$$

$$f^{B_2g}(\alpha;\beta) = (4/3)K$$

$$f^{B_2g}(\beta;\beta) = (2/3)F_{\beta\beta}$$

$$f^{A_{2u}}(\theta;\theta) = F_{\theta\theta}$$

$$f^{A_{2u}}(\theta;\phi) = \sqrt{2}(Q)$$

$$f^{A_{2u}}(\phi;\phi) = F_{\phi\phi} + P$$

$$f^{E_g}(\phi;\phi) = F_{\phi\phi} - P$$

$$f^{E_u}(r;r) = F_{rr} - (7/9)B$$

$$f^{E_u}(r;R) = (2/9)D$$

$$f^{E_u}(R;R) = F_{RR} - (7/9)(D^2/B)$$

$$f^{E_u}(r;\alpha) = 0$$

$$f^{E_u}(r;\beta) = 0$$

$$f^{E_u}(R;\alpha) = 0$$

$$f^{E_u}(R;\beta) = 0$$

$$f^{E_u}(\alpha;\alpha) = F_{\alpha\alpha} + H$$

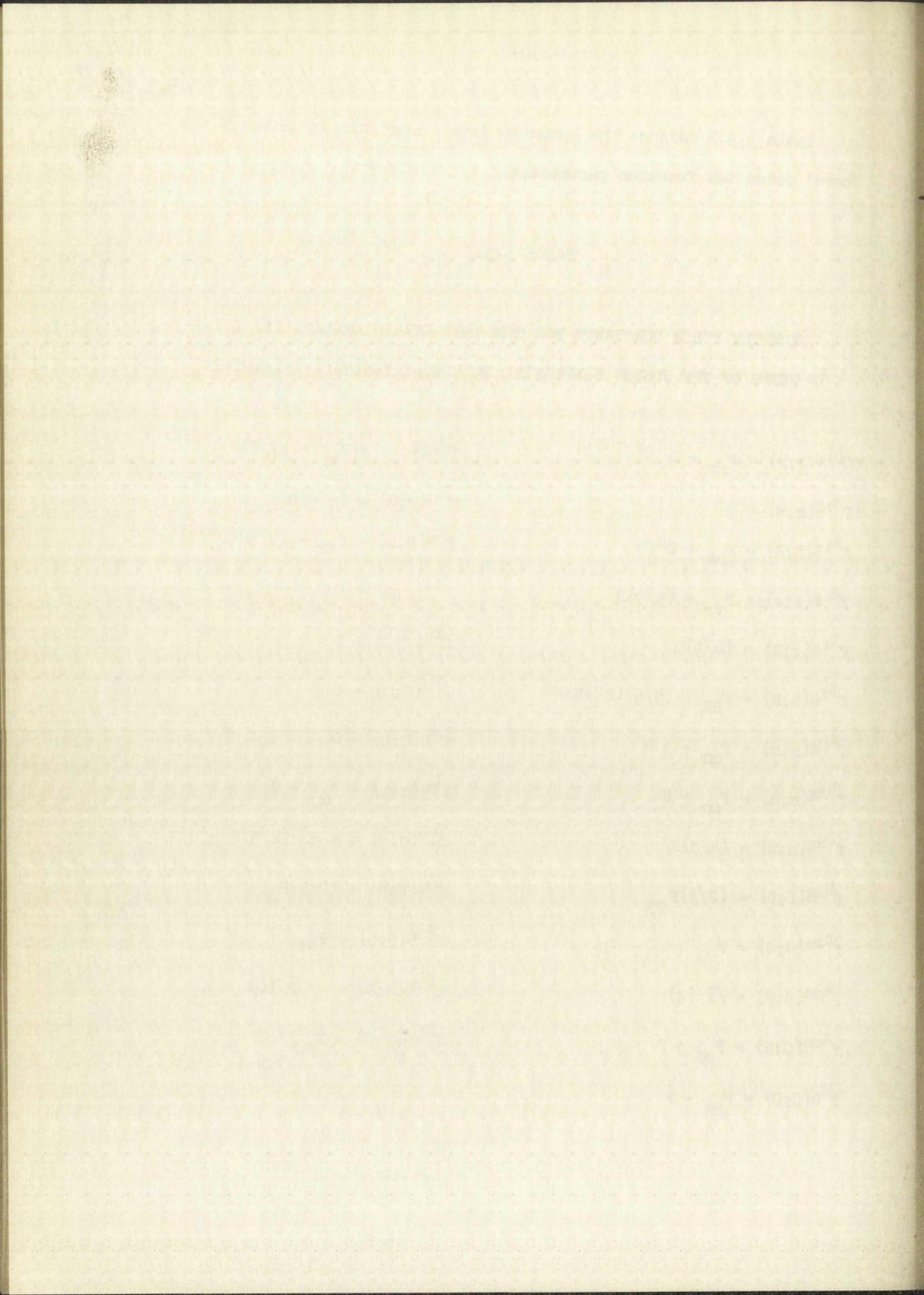
$$f^{E_u}(\alpha;\beta) = -\sqrt{2}(4/3)K$$

$$f^{E_u}(\beta;\beta) = (2/3)F_{\beta\beta}$$

$$f^{B_{2u}}(\theta;\theta) = F_{\theta\theta}$$

$$f^{B_{2u}}(\theta;\phi) = -\sqrt{2}(Q)$$

$$f^{B_{2u}}(\phi;\phi) = F_{\phi\phi} + P$$



Test solutions indicated that the best fit of the data may be obtained by assigning a negative value of $-0.095 \text{ md } \text{\AA} / \text{radians}^2$ to K . A negative value for K , however, is incompatible with accepted bonding concepts. Hence we choose to set $K = 0$ and to report the potential function so generated. Since only two out-of-plane frequencies were observed, it was necessary also to assume $Q = 0$.

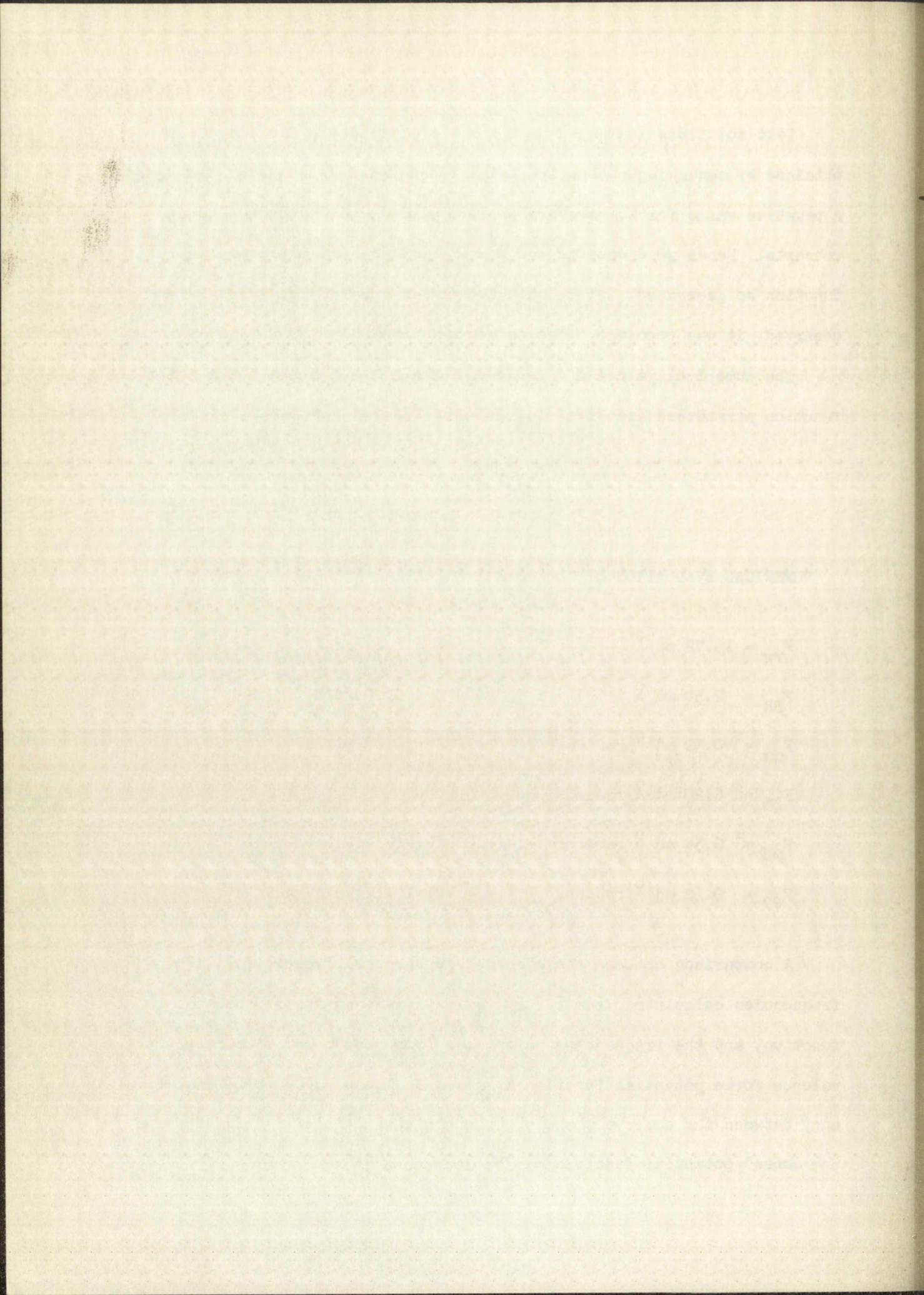
The numerical values of the Jones' simplified valence force potential function parameters are given in Table 3.5.3.

TABLE 3.5.3

NUMERICAL EVALUATION OF THE JONES' POTENTIAL FUNCTION PARAMETERS

$F_{rr} = 16.72 \text{ md}/\text{\AA}$	$B = 0.02 \text{ md}/\text{\AA}$
$F_{RR} = 2.30 \text{ md}/\text{\AA}$	$D = 0.10 \text{ md}/\text{\AA}$
$F_{\alpha\alpha} = 0.52 \text{ md } \text{\AA} / \text{radians}^2$	$H = 0.08 \text{ md}/\text{\AA}$
$F_{\beta\beta} = 0.20 \text{ md } \text{\AA} / \text{radians}^2$	$K = 0$
$F_{\beta\beta} = 0.34 \text{ md } \text{\AA} / \text{radians}^2$	$Q = 0$
$F_{\theta\theta} = 0.12 \text{ md } \text{\AA} / \text{radians}^2$	$P = 0.12 \text{ md } \text{\AA} / \text{radians}^2$

A comparison between the observed fundamental frequencies, the frequencies calculated from the approximate valence force potential function, and the frequencies calculated from the Jones' simplified valence force potential function is given in Table 3.5.4. The discrepancy between the observed bending frequencies and those calculated from the Jones' potential function may be decreased by arbitrarily



distinguishing between $F'_{\alpha\alpha}$ and $F''_{\alpha\alpha}$. However, some discrepancy for these bending frequencies is to be expected because of the relative magnitude of the bend-bend interaction terms and primary bending force constants. Because the bend-bend interaction terms are of the same order of magnitude as the primary bending force constants, the approximation that the second-order terms are negligible when compared with the primary valence force constants is not completely valid.

These results reflect the approximate nature of the Jones' simplified valence force potential function and indicate that further refinements in the potential function are necessary. However, before further refinements can be introduced, a detailed study of the nature of the pi-bond will be required. A thorough analysis of the spectra of the $\text{Pd}(\text{CN})_4^{=}$ and $\text{Pt}(\text{CN})_4^{=}$ vibrations will be helpful in refining the potential function.

In order to gain some insight as to the nature of the fundamental modes of vibration, we have determined the relative amplitude for each of the internal symmetry coordinates in a given normal mode of vibration.

It may be recalled that the internal symmetry coordinates, S , are related to the normal coordinates, Q , through the expression⁽³⁷⁾:

$$S(j) = \sum_{k=1}^n L_{S(j),k} Q_k,$$

where the $L_{S(j),k}$ satisfy the matrix equation:

$$(\underline{GF} - \underline{E}\lambda_k)\underline{L}_k = 0.$$

The $L_{S(j),k}$'s are related by a normalizing factor to the amplitudes of vibration, so that the ratio $L_{S(j),k}/L_{S(i),k}$ gives the relative amplitude of internal symmetry coordinate $S(j)$ to $S(i)$ for the vibration ν_k . These ratios are given in Table 3.5.5.



TABLE 3.5.4

OBSERVED AND CALCULATED FUNDAMENTAL FREQUENCIES FOR
SODIUM TETRACYANONICKELATE(II) TRIHYDRATE

ν_k cm^{-1}	Observed	Calculated from Jones' Simplified VFPF (Table 3.5.3)	Calculated from Approximate VFPF (Table 3.5.1)
ν_1	2149	2149	2150
* ν_1	2118	2120	2120
ν_2	416	417	417
ν_3	326	325	330
ν_4	2141	2141	2141
* ν_4	2112	2112	2108
ν_5	405	402	403
ν_6	488	503	480
ν_7	----	86	91
ν_8	$\left\{ \begin{array}{l} 2132 \\ 2128 \end{array} \right\}$	2129	2136
* ν_8	$\left\{ \begin{array}{l} 2100 \\ 2096 \end{array} \right\}$	2099	2106
ν_9	552	532	549
* ν_9	545	528	544
ν_{10}	$\left\{ \begin{array}{l} 433 \\ 421 \end{array} \right\}$	446	425
* ν_{10}	$\left\{ \begin{array}{l} 430 \\ 416 \end{array} \right\}$	442	422

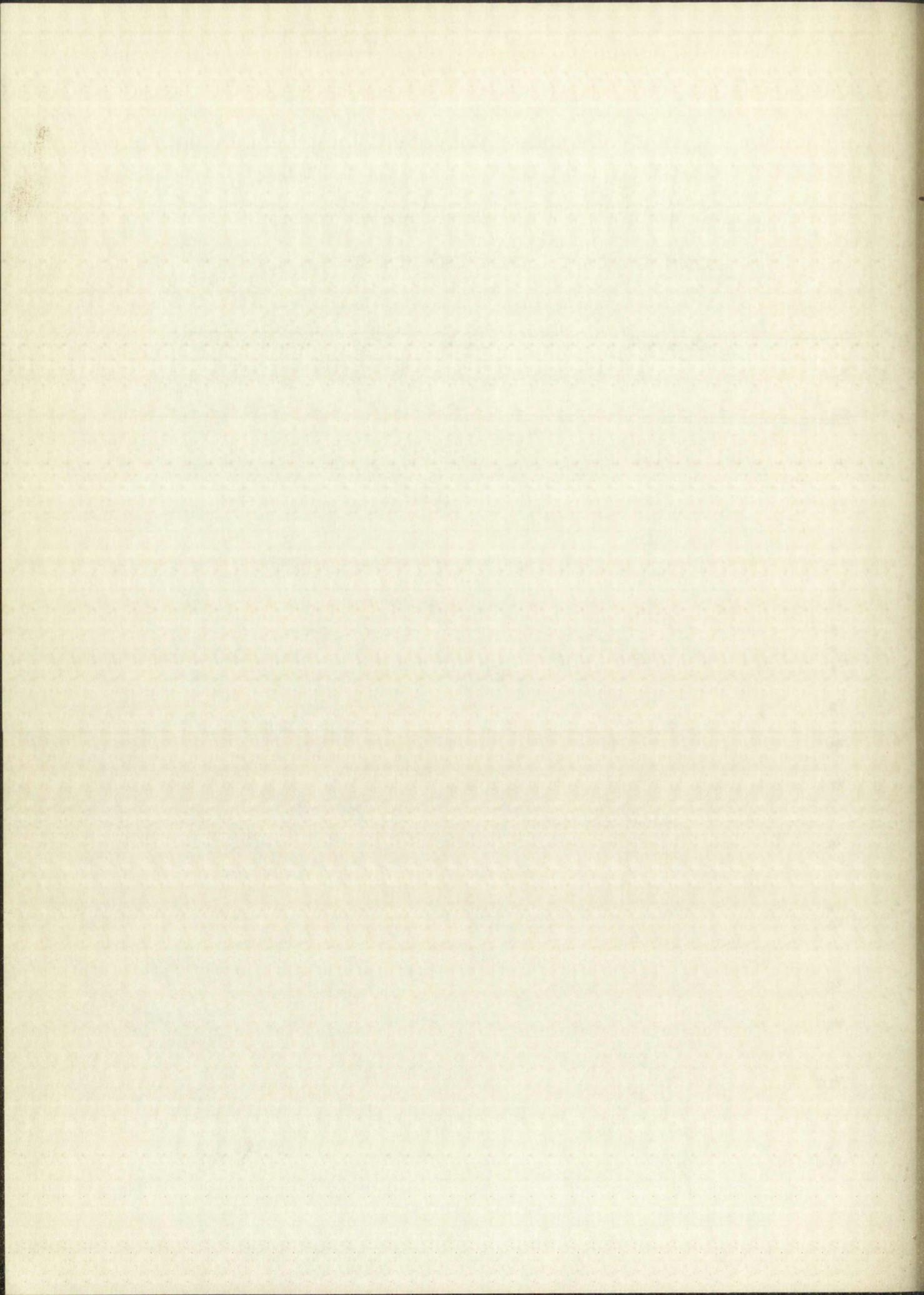


TABLE 3.5.4, contd

ν_{11}	----	74	78
*			
ν_{11}	----	72	76
ν_{12}	450	450	446
*			
ν_{12}	448	447	442
ν_{13}	----	77	77
ν_{14}	----	425	303
ν_{15}	54	55	42
ν_{16}	282	282	282

* These frequencies are the frequencies for the isotopic species $\text{Na}_2\text{Ni}(\text{CN}^{15})_4 \cdot 3\text{H}_2\text{O}$.

It can be shown from Equation 2.2 that:

$$2V = \sum_k^n \lambda_k Q_k^2,$$

so that the potential energy $V(\nu_k)$ associated with the fundamental mode of vibration ν_k is given by

$$2V(\nu_k) = \lambda_k Q_k^2.$$

However,

$$\lambda_k = \sum_{j,l} r^{\gamma} [s(j); s(l)] L_{S(j),k} L_{S(l),k}$$

so that

$$2V(\nu_k) = (L_{S(i),k} Q_k)^2 \sum_{j,l} r^{\gamma} [s(j); s(l)] \left(\frac{L_{S(j),k}}{L_{S(i),k}} \right) \left(\frac{L_{S(l),k}}{L_{S(i),k}} \right).$$

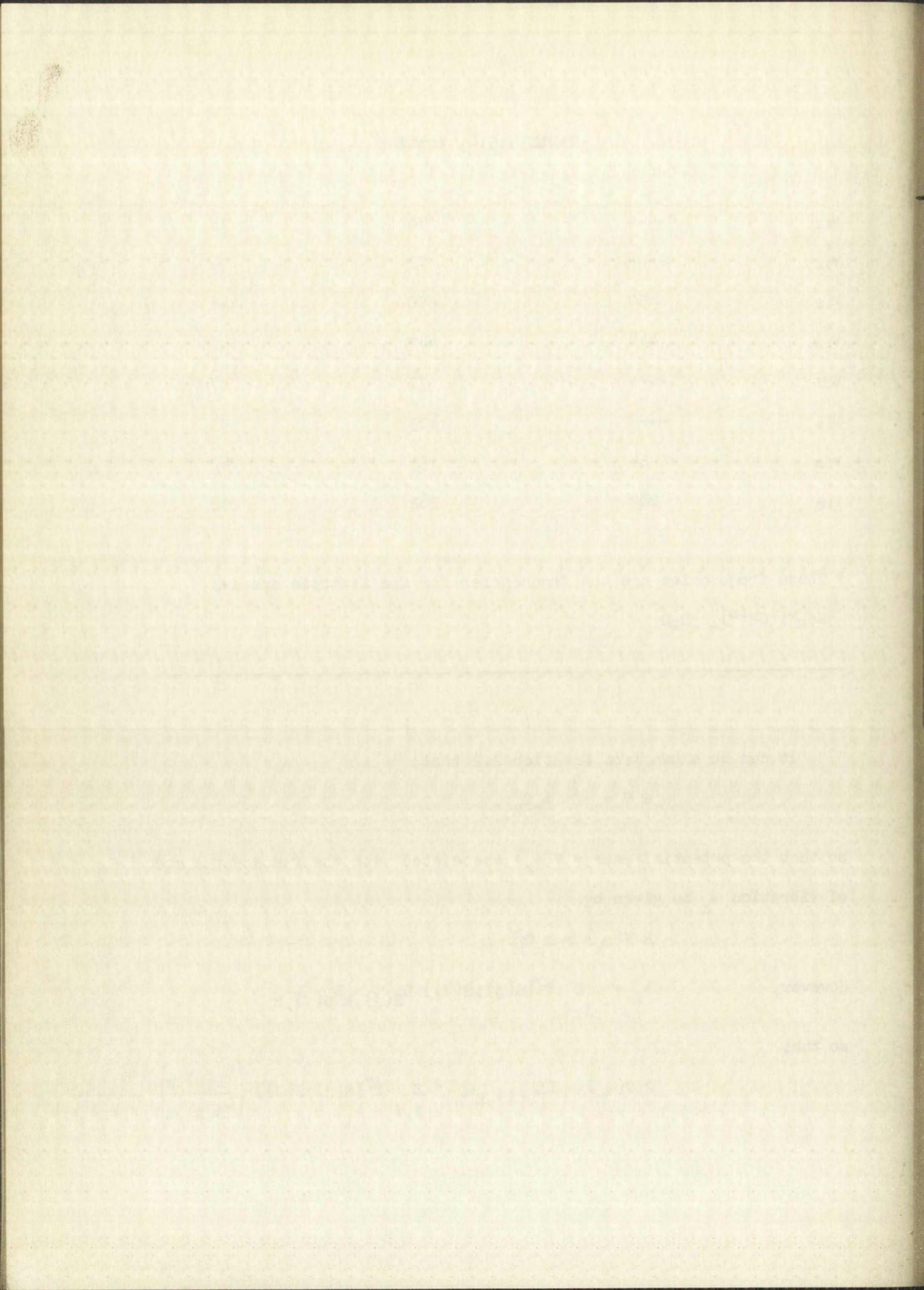


TABLE 3.5.5

THE NORMALIZED EIGENVECTORS FOR THE JONES' POTENTIAL FUNCTION

$$Q_k = L_{S(i),k} \sum_j \frac{L_{S(j),k}}{L_{S(i),k}} s(j)$$

	$\frac{L_{S(j),k}}{L_{S(i),k}}$					
	r	R	α	β	ϕ	θ
A _{1g} : Q ₁	1	-0.561	0	0	0	0
Q ₂	0.0938	1	0	0	0	0
A _{2g} : Q ₃	0	0	1	0	0	0
B _{1g} : Q ₄	1	-0.526	0	0	0	0
Q ₅	0.0836	1	0	0	0	0
B _{2g} : Q ₆	0	0	1	-0.606	0	0
Q ₇	0	0	0.202	1	0	0
E _u : Q ₈	1	-0.567	0.00800	0.0109	0	0
Q ₉	0.0642	1	-2.366	-1.330	0	0
Q ₁₀	0.0475	0.754	1	0.248	0	0
Q ₁₁	0.00163	0.0271	-0.150	1	0	0
A _{2u} : Q ₁₂	0	0	0	0	1	-0.516
Q ₁₃	0	0	0	0	0.135	1

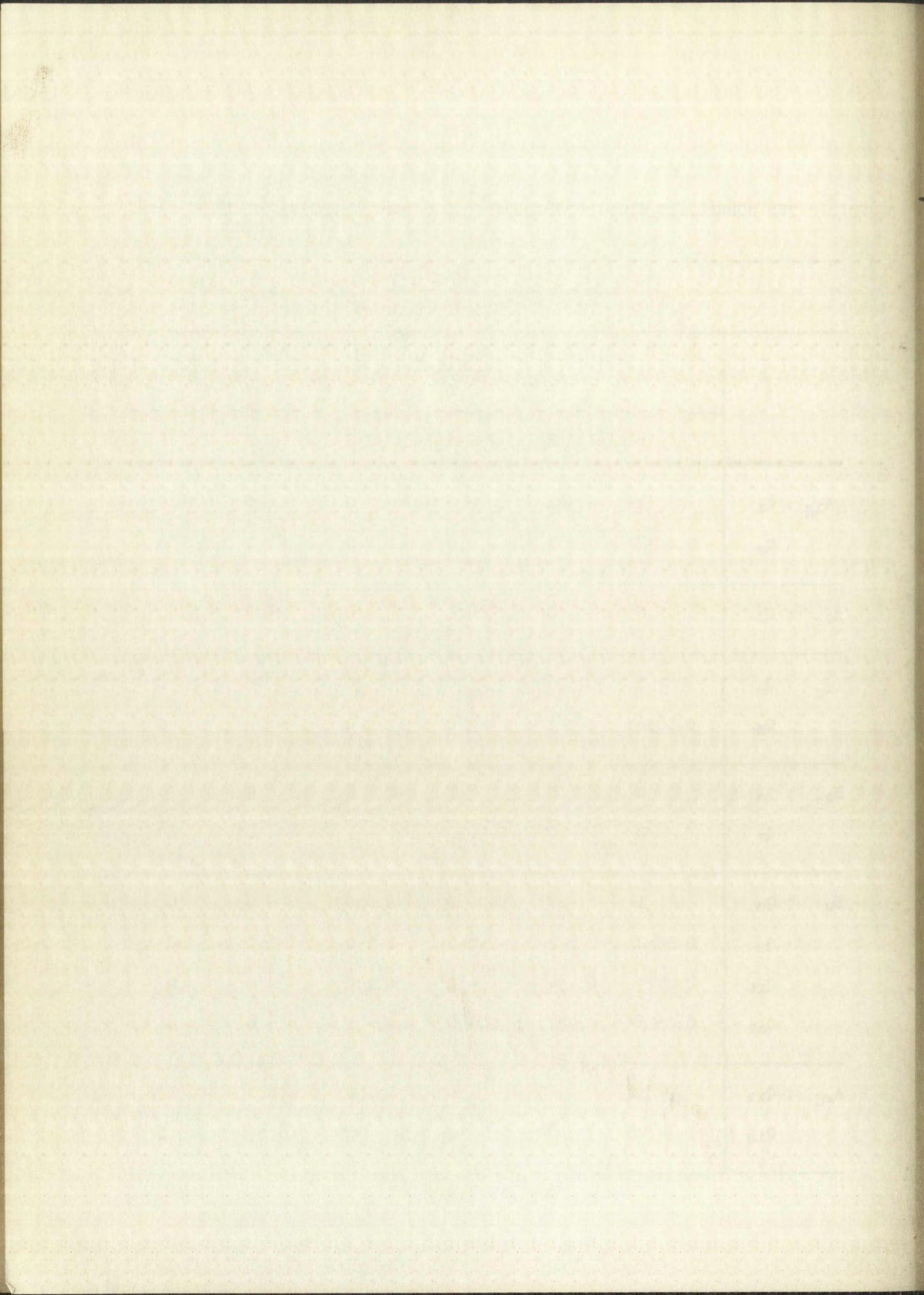


TABLE 3.5.5, contd.

B _{2u} : Q ₁₄	0	0	0	0	1	0.386
	Q ₁₅	0	0	0	0	-0.110
<hr/>						
E _g : Q ₁₆	0	0	0	0	1	0

The dimensions of L for the stretching coordinates is different from that for the deformation coordinates. The L's for the α and ϕ coordinates may be converted to the units of the stretch L's by multiplication by $(\sigma\rho)^{-\frac{1}{2}}$, while the L's for the β and θ coordinates may be converted to the units of the stretch L's by division by ρ .

The symmetry coordinates of r, R, α , β , ϕ and θ are given in Table 3.1.4.

We define

$$v_k^{\gamma}(i|j, l) = r^{\gamma}[S(j); S(l)] \frac{\left(\frac{L_{S(j),k}}{L_{S(i),k}} \right) \left(\frac{L_{S(l),k}}{L_{S(i),k}} \right)}{\left(\frac{L_{S(i),k}}{L_{S(i),k}} \right)},$$

so that

$$\frac{v_k(i|j, l)}{\sum_{j, l} v_k(i|j, l)}$$

is the fraction of potential energy in the coordinate product, $S_j S_l$, for the vibration v_k .

The potential energy distribution is given in Table 3.5.6. Notice, in particular, that the distinction as to which kind of motion of E_u symmetry (i.e. stretching or bending) is involved in v_9 and v_{10} is ambiguous, though v_9 is more bending and v_{10} is more stretching.

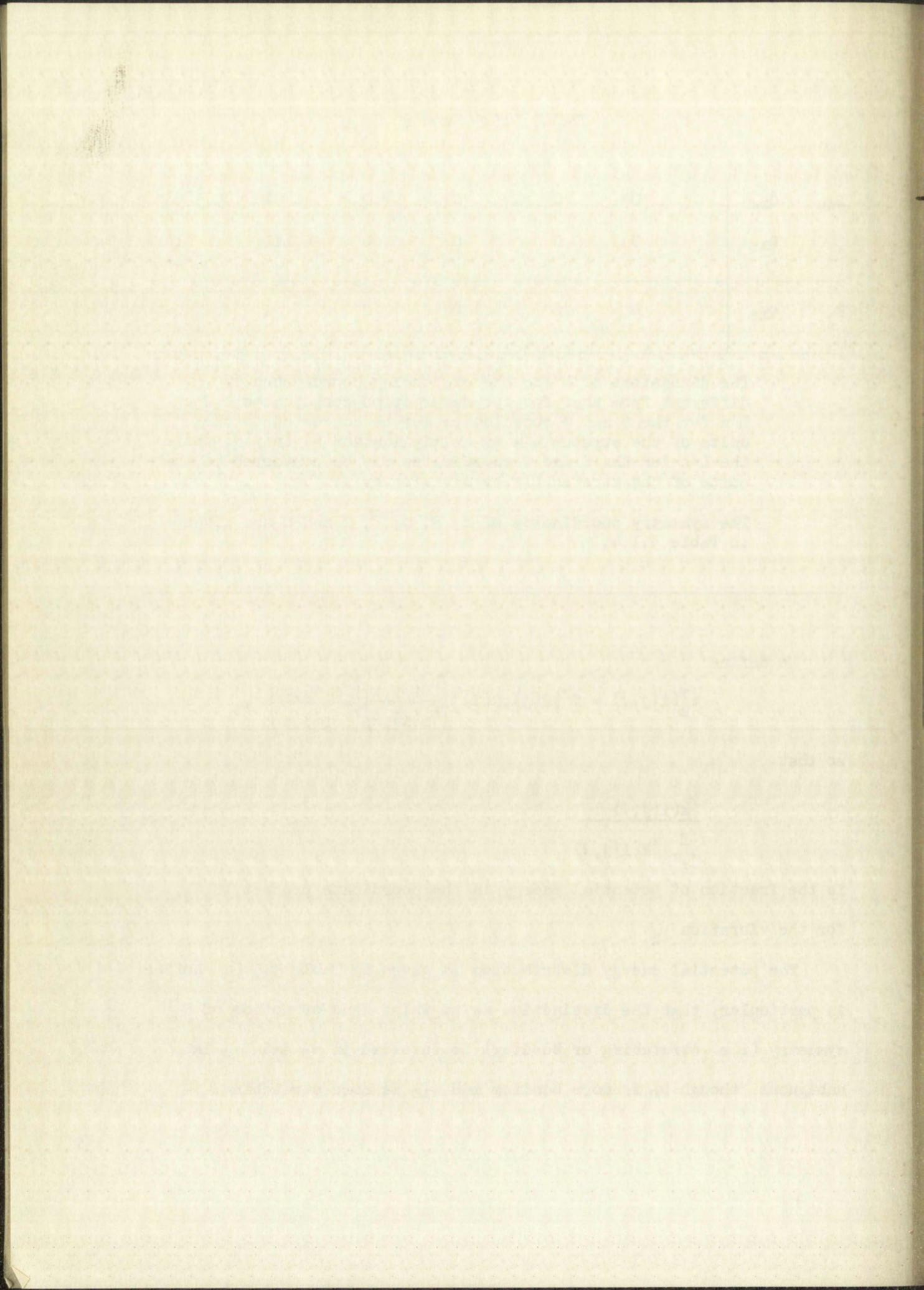


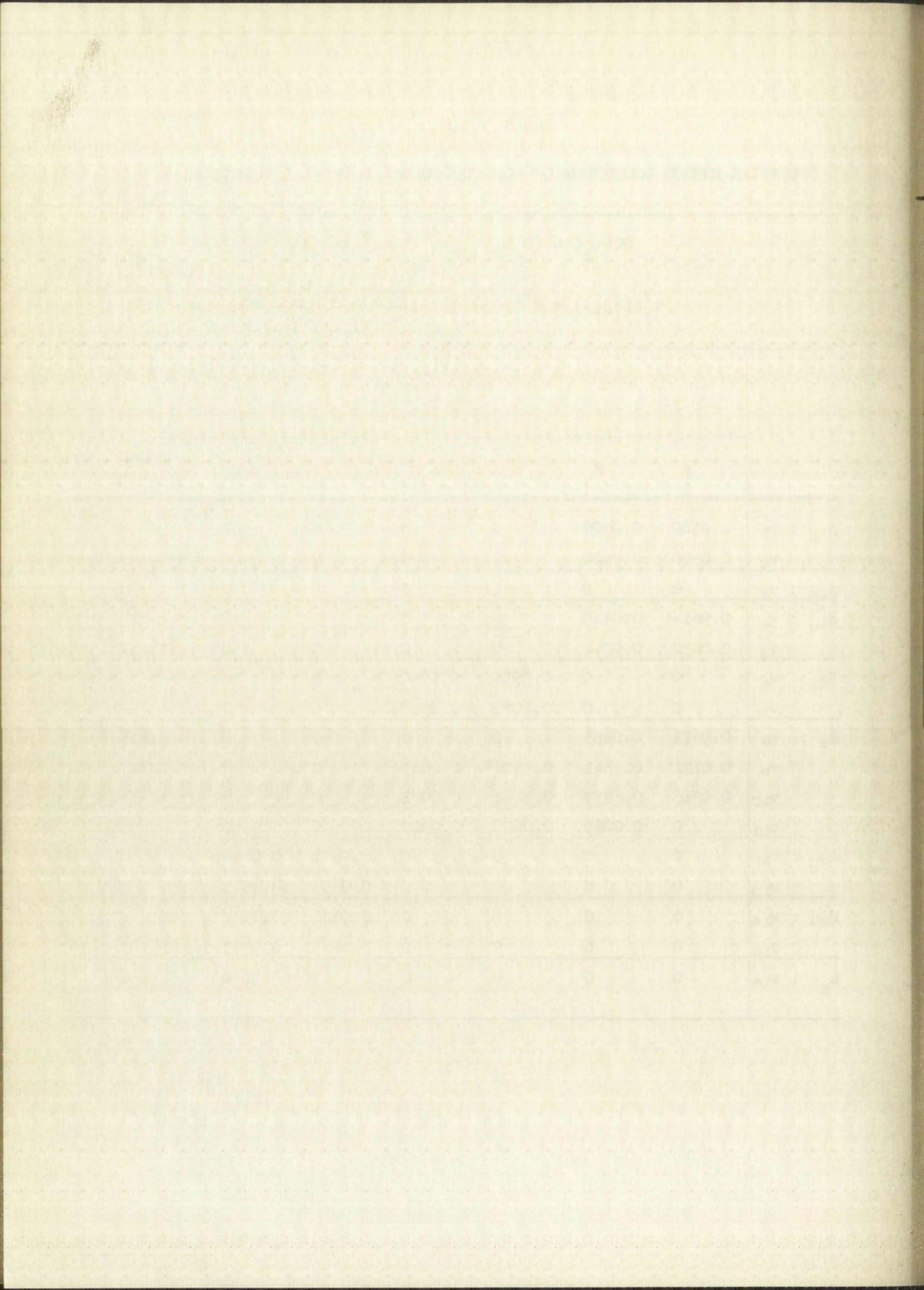
TABLE 3.5.6

POTENTIAL ENERGY DISTRIBUTION FOR THE JONES' POTENTIAL FUNCTION

$$2V(v_k) = (Q_k L_{S(1)k})^2 \sum_{j,l} v_k^\gamma(i|j,l)$$

$$v_k^\gamma(i|j,l) = f^\gamma[S(j);S(l)] \left(\frac{L_{S(j),k}}{L_{S(i),k}} \right) \left(\frac{L_{S(l),k}}{L_{S(i),k}} \right)$$

	$\frac{v_k^\gamma(i j,l)}{\sum_{j,l} v_k^\gamma(i j,l)}$						
	r	R	α	β	ϕ	θ	Interaction energy
A _{1g} : v ₁	0.9500	0.0500	0	0	0	0	0
v ₂	0.0500	0.9500	0	0	0	0	0
A _{2g} : v ₃	0	0	1	0	0	0	0
B _{1g} : v ₄	0.9614	0.0410	0	0	0	0	-0.0024
v ₅	0.0432	0.9544	0	0	0	0	0.0024
B _{2g} : v ₆	0	0	0.8910	0.1090	0	0	0
v ₇	0	0	0.1072	0.8928	0	0	0
E _u : v ₈	0.9671	0.0353	0	0	0	0	-0.0024
v ₉	0.0121	0.3341	0.5906	0.0623	0	0	0.0009
v ₁₀	0.0216	0.6237	0.3461	0.0071	0	0	0.00015
v ₁₁	0	0.0065	0.0628	0.9307	0	0	0
A _{2u} : v ₁₂	0	0	0	0	0.9351	0.0649	0
v ₁₃	0	0	0	0	0.0653	0.9347	0
B _{2u} : v ₁₄	0	0	0	0	0.9626	0.0374	0
v ₁₅	0	0	0	0	0.0443	0.9557	0
E _g : v ₁₆	0	0	0	0	1	0	0



4.0 CATION EFFECT

The alkali metal salts of the tetracyanonickelate(II) ion represent an excellent series of compounds with which to study the perturbing influence of the cation upon the molecular vibrations of the tetracyanonickelate(II) ion. The series of compounds⁽²⁰⁾, $\text{Li}_2\text{Ni}(\text{CN})_4 \cdot 3\text{H}_2\text{O}$, $\text{Na}_2\text{Ni}(\text{CN})_4 \cdot 3\text{H}_2\text{O}$, $\text{K}_2\text{Ni}(\text{CN})_4 \cdot 3\text{H}_2\text{O}$, $\text{Rb}_2\text{Ni}(\text{CN})_4 \cdot 3\text{H}_2\text{O}$, and presumably $\text{Cs}_2\text{Ni}(\text{CN})_4 \cdot 3\text{H}_2\text{O}$, all have the triclinic symmetry of the space group C_1^1 (P1) and the same number of molecules per unit cell. Hence, the compounds all have the same selection rules, and Equation 2.5.18 should hold for the series.

The series of compounds, $\text{Li}_2\text{Ni}(\text{CN})_4 \cdot 3\text{H}_2\text{O}$, $\text{Rb}_2\text{Ni}(\text{CN})_4 \cdot 3\text{H}_2\text{O}$, and $\text{Cs}_2\text{Ni}(\text{CN})_4 \cdot 3\text{H}_2\text{O}$, was prepared by passing a dilute solution of $\text{BaNi}(\text{CN})_4$ over a cation exchange column converted to the appropriate cation. Evaporation of the effluent yielded crystals of the appropriate salts. The compound $\text{K}_2\text{Ni}(\text{CN})_4 \cdot 3\text{H}_2\text{O}$ was prepared in the same manner as the $\text{Na}_2\text{Ni}(\text{CN})_4 \cdot 3\text{H}_2\text{O}$ with the substitution of KCN for NaCN. Optical and analytical data confirmed the presence of the correct cation in each of the compounds.

Oil mulls ($n^y = 1.588$) of these compounds were examined in the 2000 cm^{-1} region of the spectra. The observed ν_8 cyanide stretching vibrations of E_u symmetry are given in Table 4.0. Table 4.0 also gives the distance separating the centers of the cation and nitrogen atom, as well as the radius of the cation.

The observed shift in this frequency for the different salts obviously is influenced by the cation. We now must correlate the observed frequency shift with the change in the system brought about by the change of cations.



The terms in Equation 2.5.18 that are influenced directly by a change in the cation are the interaction constant between the cation motions and the molecular motions $(f[S^{D(m)}(r_a)^\gamma; S^{T(n)}(R_b)^\gamma])^2$, and the g matrix element for the cation $(g[S^{T(n)}(R_b)^\gamma; S^{T(n)}(R_b)^\gamma])$. The other terms may be affected in a secondary way, but for the sake of simplicity, we will assume that they remain constant. Thus, if we consider only one frequency of the tetracyanonickelate(II) ion (e.g. the degenerate cyanide stretching frequency, ν_8), Equation 2.5.18 reduces to

$$\lambda_8^1(M) = C + B \mu_M f_{C-N,M}^2,$$

where $\lambda_8^1(M)$ is related to the observed frequency associated with the degenerate cyanide stretching vibration ν_8 for the crystal $M_2Ni(CN)_4 \cdot 3H_2O$, C and B are constants of the system, μ_M is the reciprocal of the mass of the cation, and $f_{C-N,M}$ represents the interaction of the cation with the degenerate cyanide stretching frequency. We now wish to determine upon which variable of the system $f_{C-N,M}$ is dependent.

Examination of Fig. 4.0 will indicate that the distance of separation of the effective boundaries of the cation and the nitrogen atoms might be a strong factor in influencing the cyanide vibrations. If we define the distance of nearest approach between the centers of the cation and the nitrogen atoms as m and the radius of the cation as r (see Table 4.0), then $\lambda_8^1(M)$ should be some function of $(m - r)$.

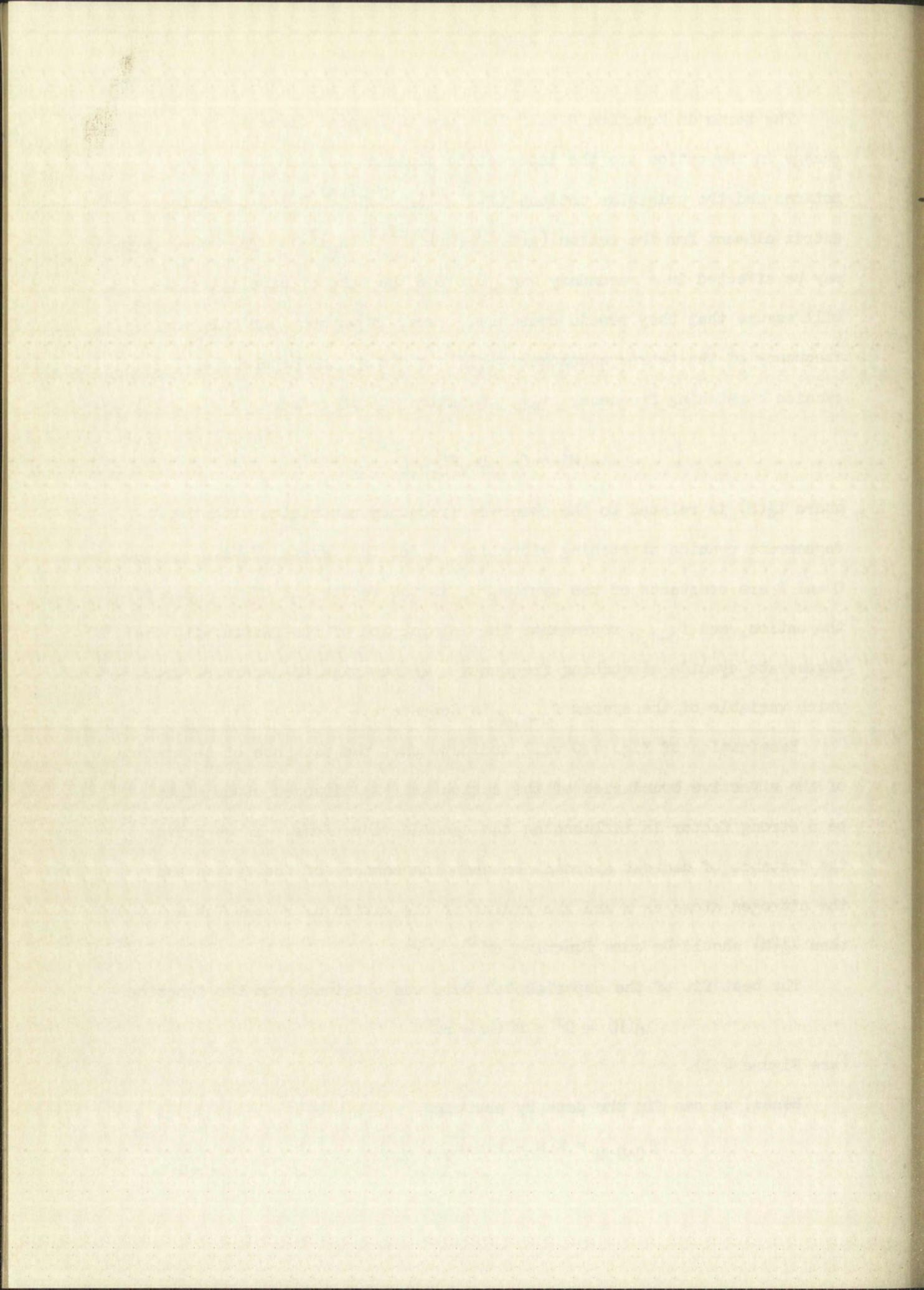
The best fit of the experimental data was obtained from the function

$$\lambda_8^1(M) = C' + B'(m - r)^2,$$

(see Figure 4.1).

Hence, we can fit the data by assuming

$$f_{C-N,M} = K(m - r) / \sqrt{\mu_M},$$



where K is a proportionality constant. In view of the approximations involved we cannot conclude that $f_{C-N,M}$ has been defined unambiguously.

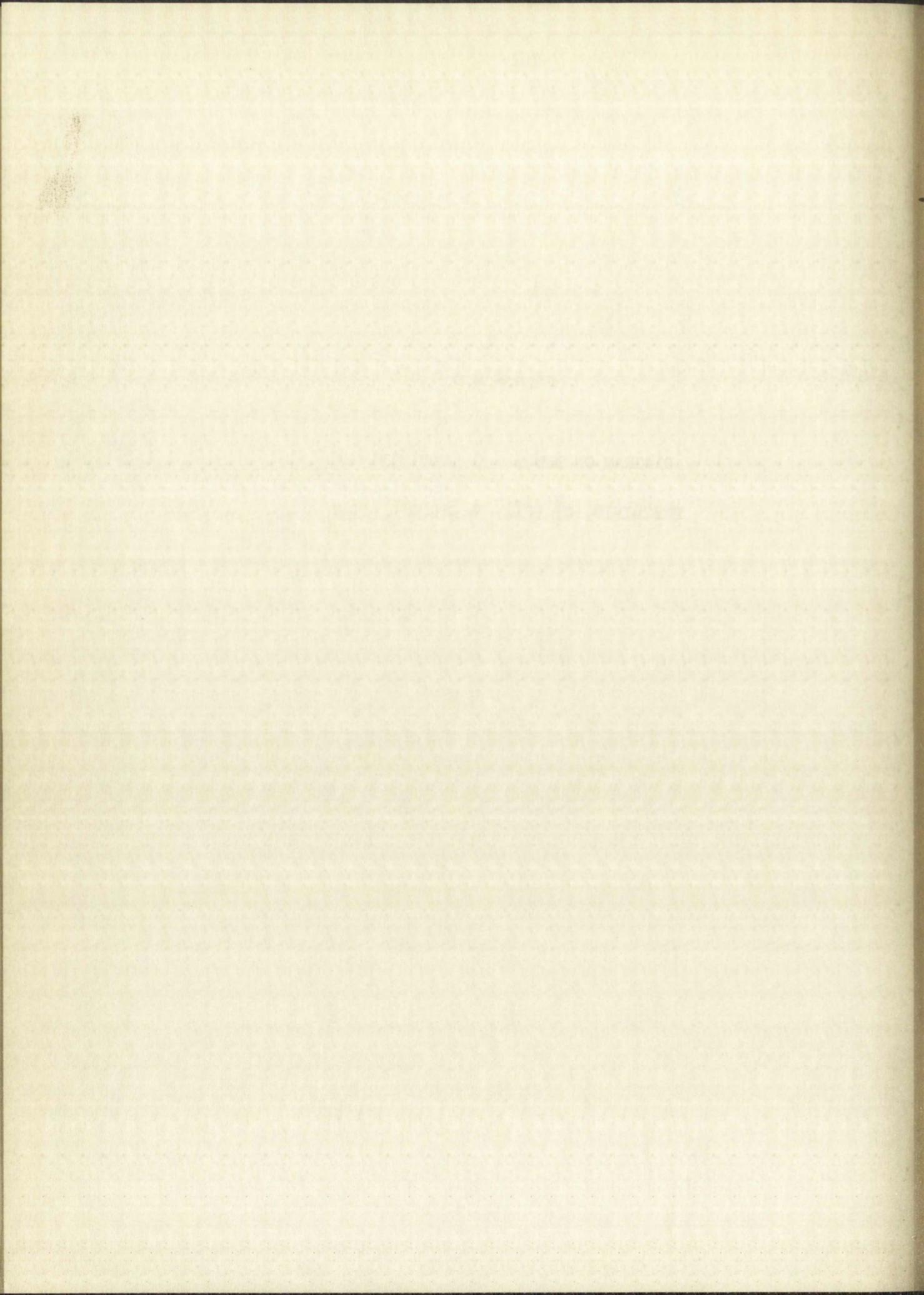
TABLE 4.0

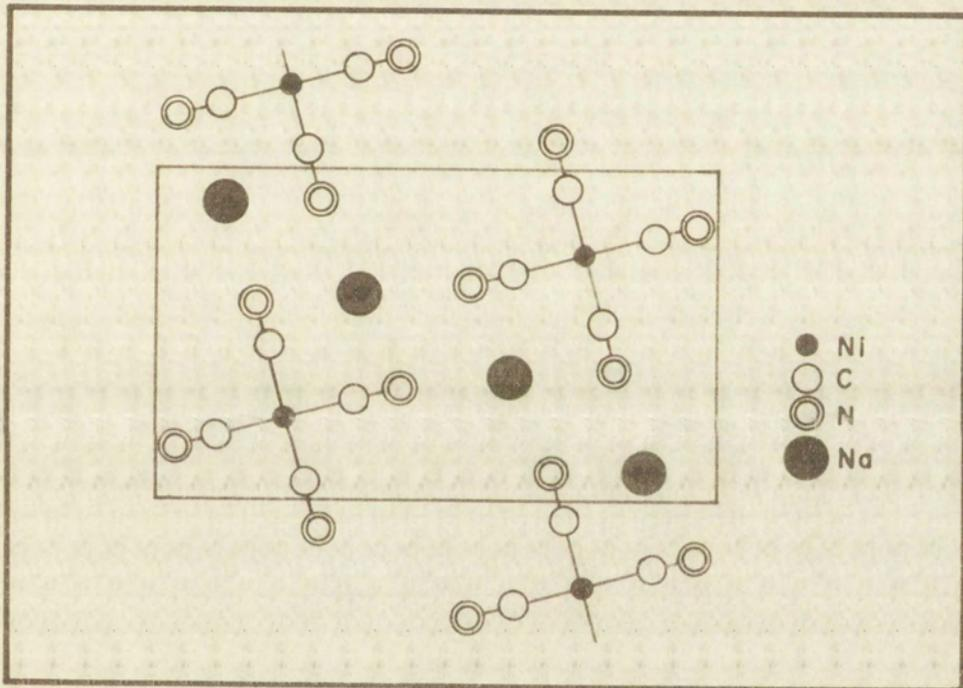
VARIABLES OF INTEREST FOR THE COMPOUNDS $M_2Ni(CN)_4 \cdot 3H_2O$

M	ν_B, cm^{-1}	$\lambda_B^1, \text{sec}^{-1}$	$M, \text{\AA}^{(20)}$	$r, \text{\AA}^{(38)}$	$(m - r), \text{\AA}$
Li	2138	2.692	2.67	0.60	2.07
Na	2128	2.667	2.67	0.95	1.72
K	2120	2.646	2.71	1.33	1.38
Rb	2117	2.640	2.72	1.48	1.24
Cs	2114	2.632	2.73	1.69	1.04

Figure 4.0

DIAGRAM OF THE $z = 0$ LAYER FOR THE
TRICLINIC, $C_{1i}^{\bar{1}}$ ($P\bar{1}$), $Na_2Ni(CN)_4 \cdot 3H_2O$





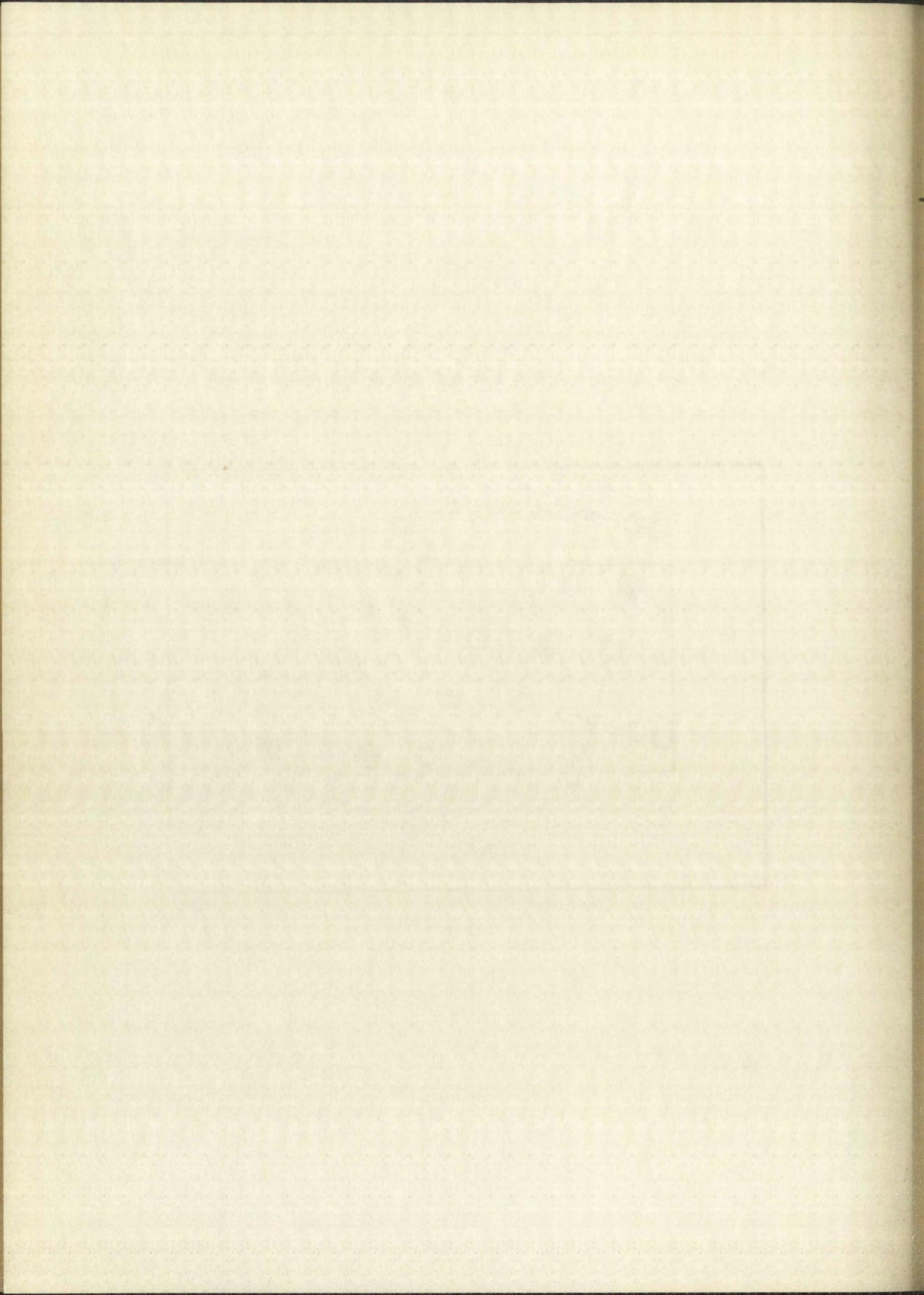
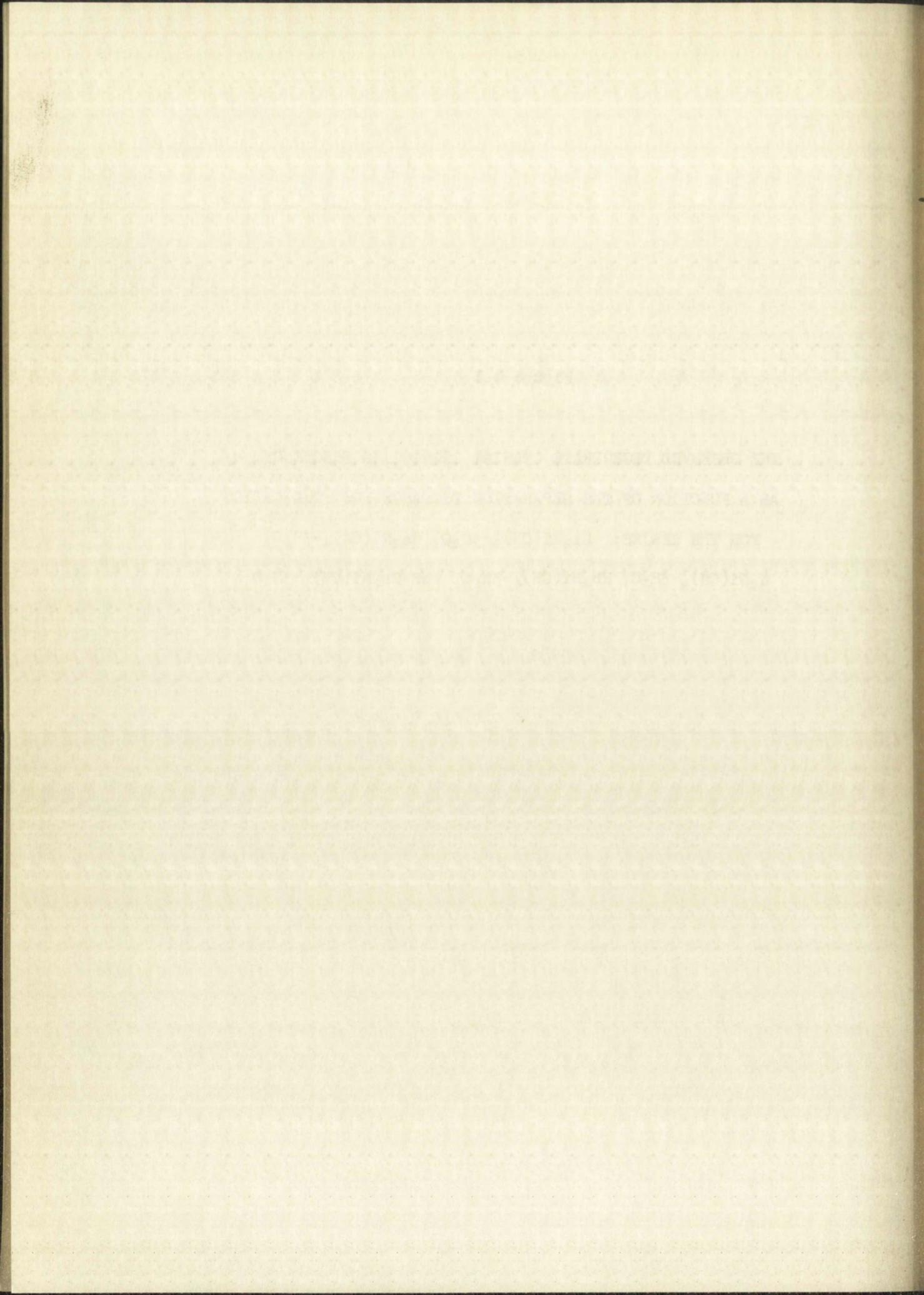
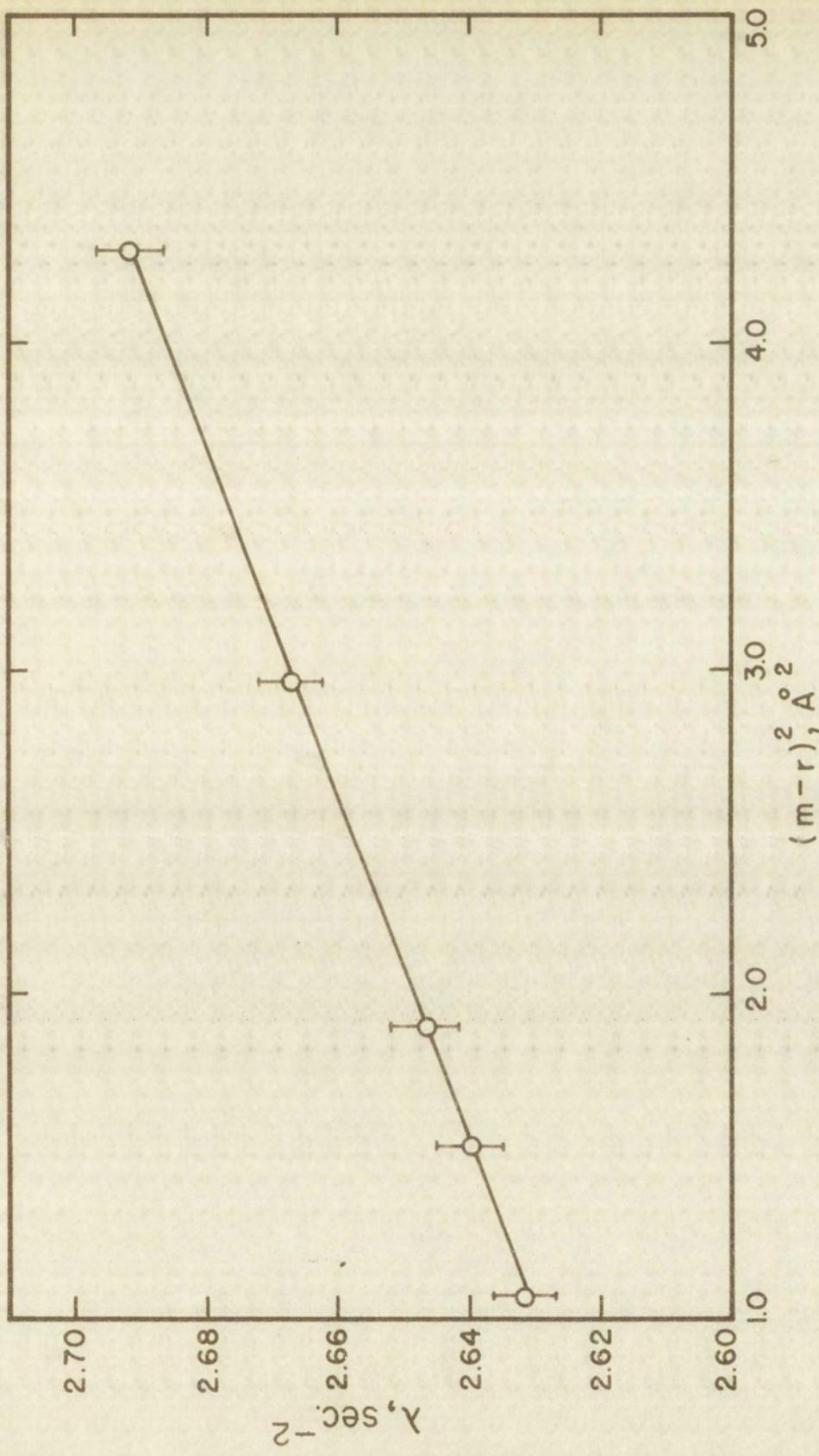
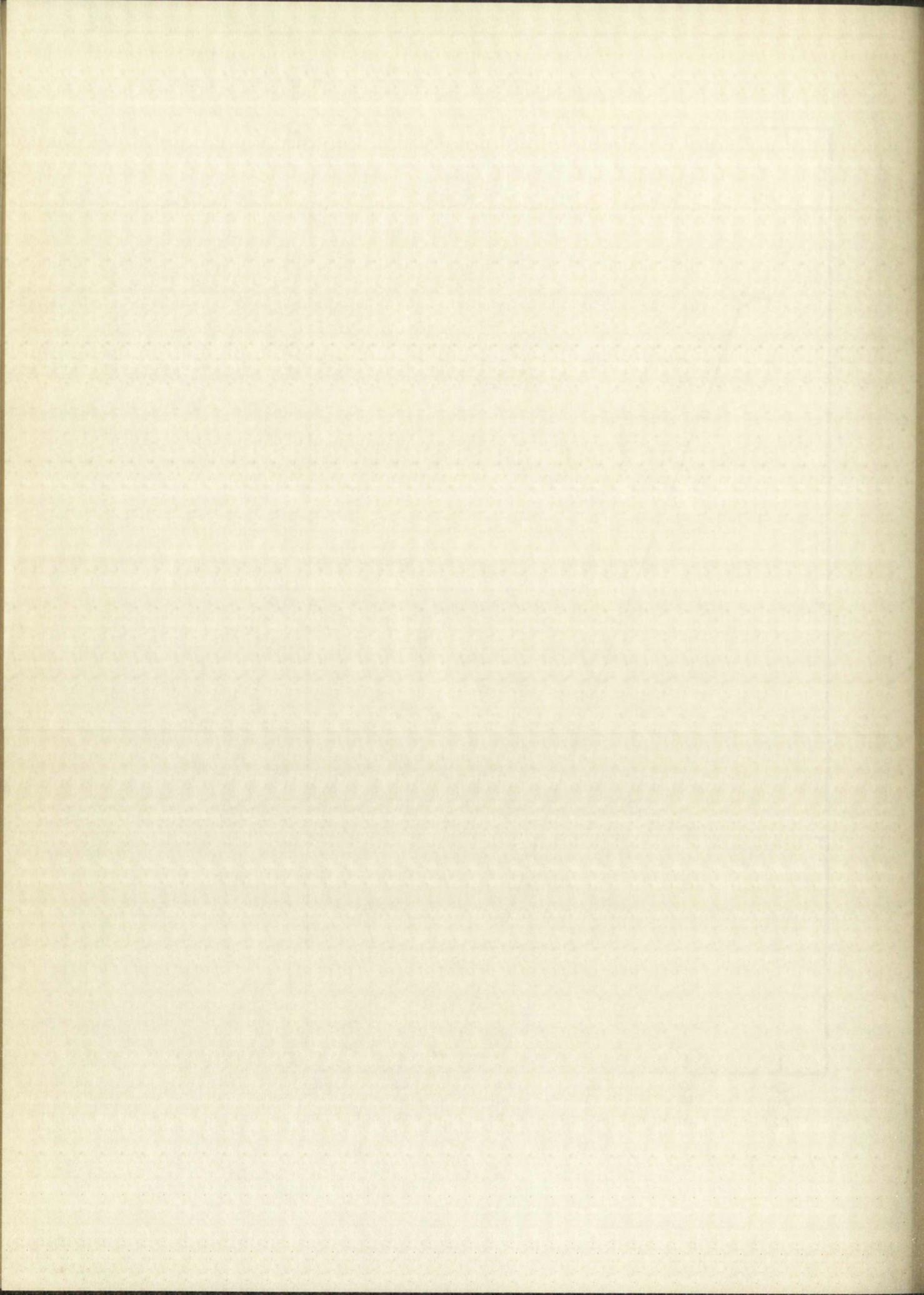


Figure 4.1

THE OBSERVED DEGENERATE CYANIDE STRETCHING FREQUENCY, ν_8 ,
AS A FUNCTION OF THE SEPARATION DISTANCE FROM THE CATION
FOR THE SERIES: $\text{Li}_2\text{Ni}(\text{CN})_4 \cdot 3\text{H}_2\text{O}$, $\text{Na}_2\text{Ni}(\text{CN})_4 \cdot 3\text{H}_2\text{O}$,
 $\text{K}_2\text{Ni}(\text{CN})_4 \cdot 3\text{H}_2\text{O}$, $\text{Rb}_2\text{Ni}(\text{CN})_4 \cdot 3\text{H}_2\text{O}$, and $\text{Cs}_2\text{Ni}(\text{CN})_4 \cdot 3\text{H}_2\text{O}$







5.0 SUMMARY

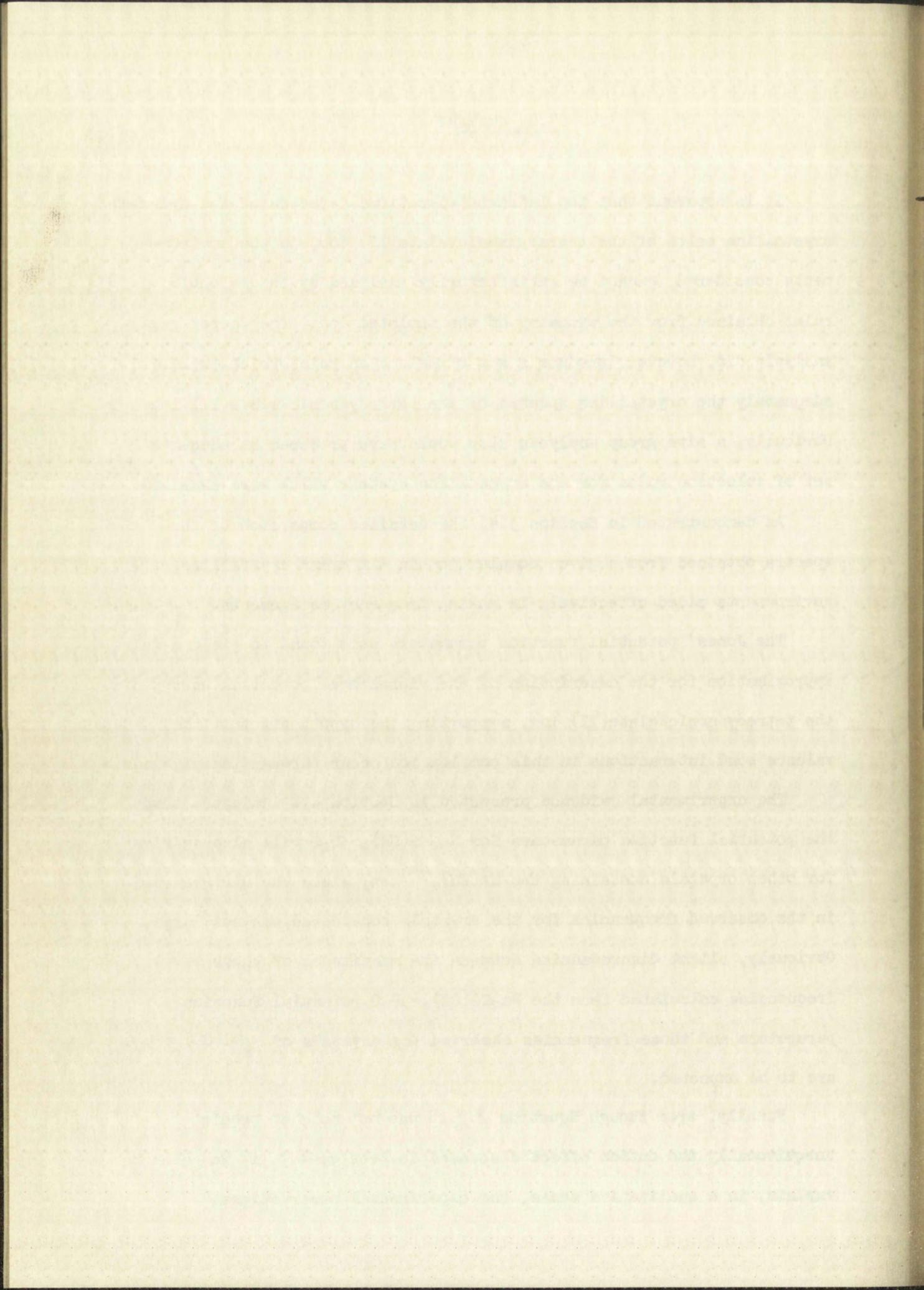
It is apparent that the infrared vibrational spectra of the hydrated crystalline salts of the tetracyanonickelate(II) ion, in the environments considered, cannot be satisfactorily analyzed by the selection rules obtained from the symmetry of the isolated ion. The factor group analysis did, however, produce a set of selection rules which explained adequately the crystalline spectra of the tetracyanonickelate(II) ion. Obviously, a site group analysis also would have produced an adequate set of selection rules for the crystalline systems which were examined.

As demonstrated in Section 3.4, the detailed comparison of the spectra obtained from a given complex ion in different crystalline environments aided effectively in making frequency assignments.

The Jones' potential function parameters were found to yield a fair approximation for the description of the vibrational potential energy of the tetracyanonickelate(II) ion, supporting the hypothesis that the valence bond interactions in this complex ion occur through the pi bonds.

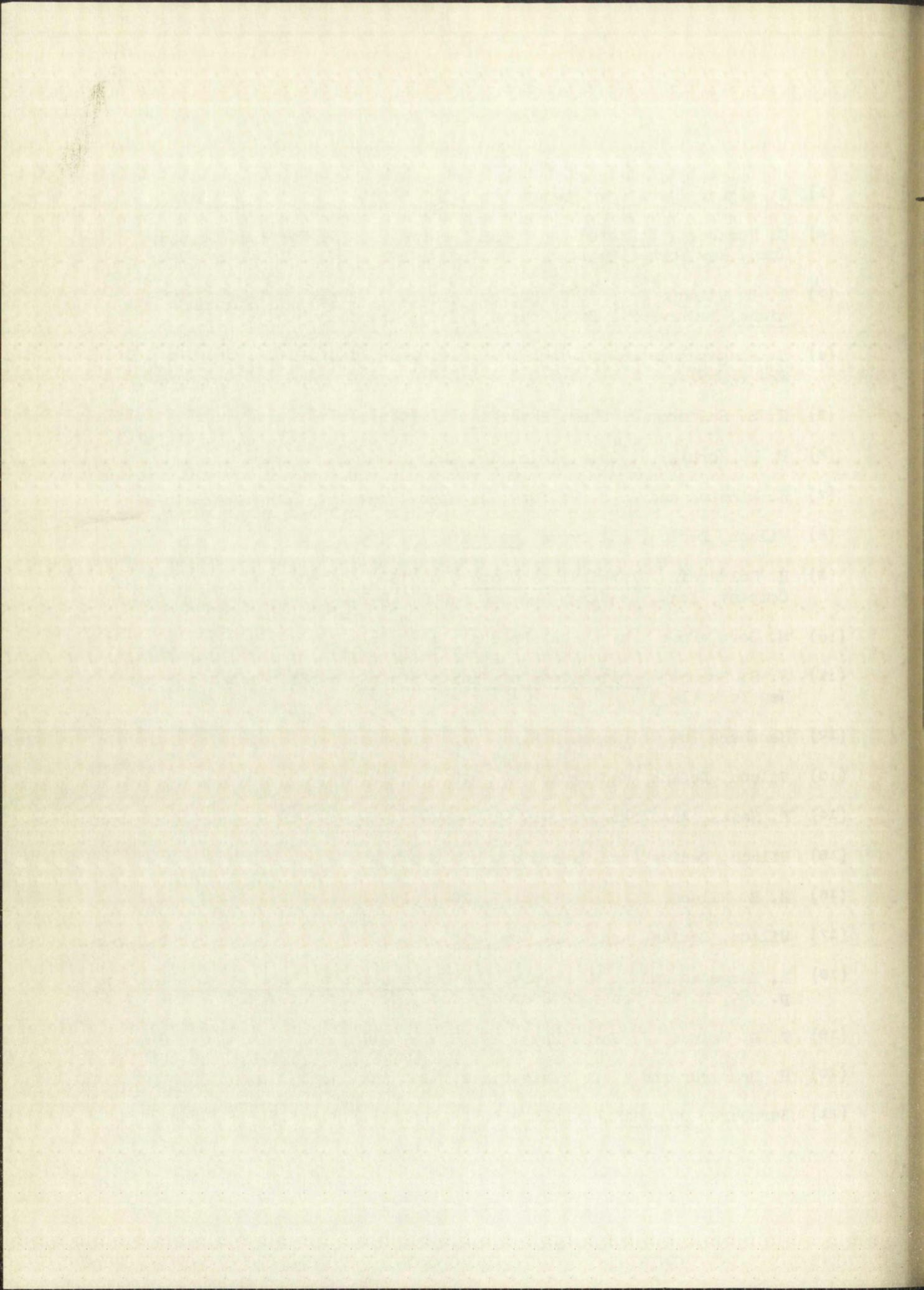
The experimental evidence presented in Section 4.0 indicates that the potential function parameters for $\text{Na}_2\text{Ni}(\text{CN})_4 \cdot 3\text{H}_2\text{O}$ will also suffice for other crystals containing the $\text{Ni}(\text{CN})_4^{2-}$ ion, since the differences in the observed frequencies for the crystals considered was not large. Obviously, slight discrepancies between the magnitudes of those frequencies calculated from the $\text{Na}_2\text{Ni}(\text{CN})_4 \cdot 3\text{H}_2\text{O}$ potential function parameters and those frequencies observed for crystals of $\text{M}_x\text{Ni}(\text{CN})_4 \cdot \text{yH}_2\text{O}$ are to be expected.

Finally, even though Equation 2.5.18 was not able to predict unequivocally the cation effect discussed in Section 4.0, it was able to explain, in a qualitative sense, the experimental observations.



BIBLIOGRAPHY

- (1) E. Wigner, Göttinger Nachrichten, 133 (1930).
- (2) G. Herzberg, Infrared and Raman Spectra, D. Van Nostrand Company, Inc., New York (1945).
- (3) E. B. Wilson, Jr., J. C. Decius, and P. C. Cross, Molecular Vibrations, McGraw-Hill Book Company, Inc., New York (1955).
- (4) S. Bhagavantam and T. Venkatarayudu, Proc. Indian Acad. Sci. 9A, 224 (1939).
- (5) R. S. Halford, J. Chem. Phys. 14, 8 (1946).
- (6) D. F. Hornig, J. Chem. Phys. 16, 1063 (1948).
- (7) H. Winston and R. S. Halford, J. Chem. Phys. 17, 607 (1949).
- (8) Wilson, Decius, and Cross, op. cit., p. 309.
- (9) H. Goldstein, Classical Mechanics, p. 320, Addison-Wesley Publishing Company, Inc., Reading, Massachusetts (1957).
- (10) M. Born, Proc. Phys. Soc. London 54, 362 (1942).
- (11) J. S. Lomont, Applications of Finite Groups, p. 21, Academic Press, New York (1959).
- (12) Herzberg, op. cit., p. 252.
- (13) Wilson, Decius, and Cross, op. cit., p. 147.
- (14) F. Seitz, Ann. Math. 37, 17 (1936).
- (15) Wilson, Decius, and Cross, op. cit., p. 54.
- (16) E. B. Wilson, J. Chem. Phys. 7, 1047 (1939).
- (17) Wilson, Decius, and Cross, op. cit., p. 132.
- (18) H. Margenau and G. M. Murphy, The Mathematics of Physics and Chemistry, p. 389, D. Van Nostrand Company, Inc., New York (1943).
- (19) T. H. Walnut, J. Chem. Phys. 20, 58 (1952).
- (20) H. Brasseur and A. De Rassenfosse, Mem. soc. sci., Liege, 2, 4 397 (1941).
- (21) Herzberg, op. cit., p. 61.



- (22) Wilson, Decius, and Cross, op. cit., p. 105.
- (23) Ibid., p. 99.
- (24) Ibid., p. 347.
- (25) L. Pauling, The Nature of the Chemical Bond, p. 168, Cornell University Press, Ithaca (1948).
- (26) L. O. Brockway and P. C. Cross, J. Chem. Phys., 3, 828 (1935).
- (27) D. M. Sweeney, I. Nakagawa, San-Ichiro Mizushima, and I. V. Quagliano, J. Am. Chem. Soc. 78, 889 (1956).
- (28) H. Brasseur and A. De Rassenfosse, Bull. soc. franc. mineral, 61, 129 (1938).
- (29) W. C. Fernelius and J. J. Burbage, Inorganic Syntheses, II p. 227, McGraw-Hill, New York (1946).
- (30) J. P. Mathieu and Suzanne Cornevin, J. chim. phys., 56, 271 (1939).
- (31) L. H. Jones, J. Chem. Phys., 27, 468 (1957).
- (32) Wilson, Decius, and Cross, op. cit., p. 311.
- (33) L. H. Jones, J. Chem. Phys., 28, 1215 (1958).
- (34) Wilson, Decius, and Cross, op. cit., p. 74.
- (35) L. H. Jones, Paper to be published on Simplified Valence Force Potential Function.
- (36) J. W. Linnett and P. J. Wheatley, Trans. Faraday Soc. 45, 33 (1949).
- (37) Wilson, Decius, and Cross, op. cit., p. 73.
- (38) Pauling, op. cit., p. 358.

